FACTORS AFFECTING THE DISTRIBUTION OF CETACEANS IN EUROPEAN ATLANTIC WATERS

Claire Lacey

A Thesis Submitted for the Degree of PhD
at the
University of St Andrews

2023

Identifiers to use to cite or link to this thesis:

DOI: https://doi.org/10.17630/sta/523
http://hdl.handle.net/10023/27845

Factors affecting the distribution of cetaceans in European Atlantic Waters

Claire Lacey

This thesis is submitted in partial fulfilment for the degree of

Doctor of Philosophy (PhD)

at the University of St Andrews

August 2022

Candidate's declaration

I, Claire Lacey, do hereby certify that this thesis, submitted for the degree of PhD, which is approximately 60,000 words in length, has been written by me, and that it is the record of work carried out by me, or principally by myself in collaboration with others as acknowledged, and that it has not been submitted in any previous application for any degree. I confirm that any appendices included in my thesis contain only material permitted by the 'Assessment of Postgraduate Research Students' policy.

I was admitted as a research student at the University of St Andrews in September 2015.

I received funding from an organisation or institution and have acknowledged the funder(s) in the full text of my thesis.

6 Aug 2022

Date Signature of candidate

Supervisor's declaration

I hereby certify that the candidate has fulfilled the conditions of the Resolution and Regulations appropriate for the degree of PhD in the University of St Andrews and that the candidate is qualified to submit this thesis in application for that degree. I confirm that any appendices included in the thesis contain only material permitted by the 'Assessment of Postgraduate Research Students' policy.

6 Aug 2022

Date Signature of supervisor

Permission for publication

In submitting this thesis to the University of St Andrews we understand that we are giving permission for it to be made available for use in accordance with the regulations of the University Library for the time being in force, subject to any copyright vested in the work not being affected thereby. We also understand, unless exempt by an award of an embargo as requested below, that the title and the abstract will be published, and that a copy of the work may be made and supplied to any bona fide library or research worker, that this thesis will be electronically accessible for personal or research use and that the library has the right to migrate this thesis into new electronic forms as required to ensure continued access to the thesis.

I, Claire Lacey, confirm that my thesis does not contain any third-party material that requires copyright clearance.

The following is an agreed request by candidate and supervisor regarding the publication of this thesis:

Printed copy.

No embargo on print copy.

Electronic copy

No embargo on electronic copy.

6 Aug 2022

Date Signature of candidate

6 Aug 2022

Date Signature of supervisor

Underpinning Research Data or Digital Outputs

Candidate's declaration

I, Claire Lacey, hereby certify that no requirements to deposit original research data or digital outputs apply to this thesis and that, where appropriate, secondary data used have been referenced in the full text of my thesis.

"Whenever I find myself growing grim about the mouth; whenever it is a damp, drizzly November in my soul…—then, I account it high time to get to sea as soon as I can."

- Herman Melville, Moby Dick

Bottlenose dolphins. Photograph by C. Lacey

Contents

Abstract

The waters of the European North Atlantic are subject to an increasing amount of anthropogenic pressure. Much of the environmental legislation designed to protect cetaceans requires detailed knowledge of the abundance and distribution of cetaceans within these waters. This data often comes from large scale surveys. Data from two such series of surveys, spanning two time periods: the SCANS-II and CODA surveys in 2005/07 and the SCANS-III and ObSERVE surveys in 2016 were analysed using Generalised Additive Models to describe relationships between cetacean density and static and remotely accessed dynamic environmental features.

Predictive models using spatial covariates as well as environmental predictors were created for the full survey area using the most recently available data. This was done to conduct a “baseline” snapshot, representing the best possible picture of cetacean distribution for the summer of 2016. Subsequent chapters focus in on specific ecoregions. These regions of relatively homogeneous habitat were selected with an aim of finding the best environmental predictors of genuine ecological relationships.

In the North Sea ecoregion, models for harbour porpoise, minke whale, and white-beaked dolphin were also constructed using additional prey data, which were available only for this region. This was found to be no better than modelling only environmental covariates. Depth was one of the most commonly retained covariates for all three species in this ecoregion.

White-sided, bottlenose, common and striped dolphins and fin whale were investigated in the Celtic Seas, and Bay of Biscay and Iberian Peninsula ecoregions. Despite these two ecoregions being quite different, in most cases, model fits did not improve with the inclusion of ecoregion as a factor covariate, suggesting that relationships between species and their environment were similar across both regions.

General acknowledgements

This PhD would most definitely not have been possible without the help and support of a large group of amazing people. First and foremost, I'd like to thank my supervisor Professor Philip Hammond. I first met Phil during my undergraduate degree more years ago than I care to admit, and he has been an incredible mentor supervisor and PI ever since. When poor Phil took me on as a research assistant to organise the SCANS-III surveys, I'm not sure he fully anticipated that he was getting saddled with another future PhD student but I'm incredibly grateful for how things worked out – even if things did take rather longer than anticipated. It's been a real pleasure working with, and, more importantly learning from you, Phil!

Phil also built an amazing lab group, and I am lucky enough to have made very dear friends amongst my colleagues from the old Bute office, notably Nadya, Emily and Janneke. You are brilliant, wonderful humans, all three of you – and one day we will definitely make that joint paper happen! I loved sharing coffee, code, maps, support and cake with you all.

The SCANS projects are, by their very nature, collaborative. As well as providing the data used in this thesis, it was a real pleasure working with all the national representatives on planning team, particularly Anita Giles, Meike Scheidat and Emer Rogan. This was a great opportunity to learn about the work that goes into organising and implementing a project of this scale, and to learn from the best. Thank you all for your patience and generosity throughout!

I am very much a field biologist at heart, so I'd also like to thank all the people who offered me fieldwork during this time. Anna Moscrop & Richard Mclanaghan from Song of the Whale, Sophie Fielding and Jen Jackson of British Antarctic Survey, Ewan Wakefield for the Discovery Cruise and Monica Arso Civil for the Tay dolphin surveys. Whilst not part of my PhD work itself, these pockets of boat time very much helped maintain motivation, provide much needed thinking time and helped keep me focussed and give me a (sometimes extended, I admit) break from my screen.

Outside of the work – well, the Friday Coffee group (Monica, Becci, Theoni, Danielle, Lindesay, Esther) were a wonderful support, particularly during the long months of COVID lockdown and continue to be so even now I'm living in an awkward time zone and can't join as often. The wonderful people of the Fife bat group, for teaching me about a different kind

of echolocating creature, introducing me to some wonderful secret places in Fife, and making some of the best baked goods and friendships a person could wish for.

Thanks also to Lars and the other wonderful people at MMRP who took me on as a post-doc despite me not having finished my PhD yet; were incredibly patient through tiresome COVID-delayed visa issues and made me feel instantly at home once I finally arrived, despite Kaneohe being very different from rural Fife!

Thank you, Kate, Rachel, Emma and Mairi for dog walks, horse adventures and your wonderful company. Thank you Anni, for the fabulous drawings I've used in my data chapters – I love them. Thanks to Andy for the confidence boosts and the reality checks and finally to my family for not asking too often when I was going to get a "real job". The answer remains the same – hopefully not anytime soon!

Funding

This work was supported by the Department for Environment, Food and Rural Affairs, UK as part of the SCANS-III project.

Research Data/Digital Outputs access statement

Research data underpinning this thesis will be made available on the SCANS-III project web pages following completion of the SCANS-III project.

Provision of data

Data used in this thesis were from the SCANS series of surveys, the ObSERVE surveys in Irish waters, and the T-NASS/NASS in Faroese wates.

SCANS-II 2005, CODA 2007, and SCANS-III 2016 data are curated at SMRU, University of St Andrews on behalf of the SCANS series of projects. Acoustic beaked whale data used in Chapter 6 were collected as part of the SCANS series of surveys and analysed and processed by Claudia Quintana as part of her MSc thesis (see also Quintana 2017). Processed data were made available by Doug Gillespie.

Permission to use the ObSERVE data was granted by the Department of Communications, Climate Action and Environment and the National Parks and Wildlife Service, Department of Culture, Heritage and the Gaeltacht, Ireland (see also Rogan et al. 2018); processed data were made available by Ana Cañadas.

1 General Introduction

> *IT IS SPECIALLY THE PROVINCE OF MODERN SCIENCE TO EXPLAIN THE PHENOMENA OF NATURE ON KNOWN NATURAL LAWS AND FORCES, AND WITH THIS VIEW NO PHENOMENA ARE MORE INTERESTING THAN THOSE OF THE GEOGRAPHICAL DISTRIBUTION OF SPECIES.(Smith, 1868)*

1.1 Context

Knowledge of where species exist, and where they do well, is one of the fundaments of ecology and conservation (Begon et al., 2006; O'Hara et al., 2017). In times of increasing anthropogenic pressure on marine ecosystems (Halpern et al., 2019, 2015), conservation and management efforts requiring spatially explicit estimates of density and distribution to assess impacts (CIEEM, 2018), can be hampered by a lack of knowledge and understanding about the ecology of populations. As such there is a growing need for information on the distribution of marine mammal species (Forney et al., 2015; Redfern et al., 2006).

One such management mechanism, which is active across a large proportion of the region of interest in this thesis is the European Union Marine Strategy Framework Directive (MSFD) (E.U. 2008). Under this directive, EU member states describe what they consider to be a healthy and productive sea, defined as Good Environmental Status (GES). Using descriptor species, they then monitor and assess their marine habitats against the criteria for Good Environmental Status, and ensure they take appropriate action to maintain or achieve GES (E.U. 2008). Within MSFD, there are four functional groups of marine mammals included for assessment and reporting. These are seals, baleen whales, small odontocetes and deep diving cetaceans (Authier et al., 2017). To fulfil international obligations under this framework, routine monitoring of the species in question must be undertaken. This monitoring work can be expensive and is logistically challenging particularly in offshore areas.

1.2 Filing the data gap - the initiation of large-scale cetacean surveys

Considerable amounts of effort have been put into the investigation of cetacean abundance and distribution over the past 40 years or more (Kaschner et al., 2012). Surveys have covered a diverse range of habitats and target species, ranging from the Arctic to the Antarctic. One of the first such examples was initiated by the International Whaling

Commission (IWC), which commenced cetacean surveys in 1978 in the Southern Ocean. These targeted minke whales (Branch and Butterworth, 2001a), but recorded all cetaceans seen, and resulted in abundance estimates for eight other species over a twenty year period (Branch and Butterworth, 2001b; Kasamatsu and Joyce, 1995).

In the U.S.A., a range of work has been carried out, covering both large-scale multi-species surveys and more targeted species-specific survey programmes. By 1986 in the Eastern Tropical Pacific, the U.S. National Marine Fisheries Service initiated a programme of large-scale surveys to monitor trends in the abundance of dolphin populations, some of which were being affected by tuna purse-seining operations (Wade and Gerrodette, 1993).

1.2.1 Large scale cetacean surveys in the Atlantic

1.2.1.1 The Western North Atlantic

In the western North Atlantic, the Cetacean and Turtle Assessment Program (CETAP 1982) ran between 1978-1982 investigating the distribution of cetaceans within the U.S. Exclusive Economic Zone (EEZ). In addition, 1981 saw the initiation of five surveys of Baffin Bay conducted for bowhead whale (*Balaena mysticetus*), beluga whale (*Delphinapterus leucas*) and narwhal (*Monodon monoceros*) which were repeated in 1982, 1991, 1993 and 1994 (Heide-Jørgensen et al. 1993), (Heide-Jørgensen and Reeves 1996).

Subsequent years saw considerable amounts of further survey work along the east coast of both Canada and the U.S.A. In 1991, shipboard surveys were conducted in the Gulf of Maine to estimate the abundance of harbour porpoises (*Phocoena phocoena*) (Palka, 1995) and aerial surveys of beluga whales were conducted in James Bay, Hudson Bay and Ungava Bay (Canada) in 1993 (Kingsley, 2000).

Amendments to the U.S. Marine Mammal Protection Act (MMPA) in 1994 (Section 117) require the production of annual stock assessment reports for all marine mammal species occurring in waters under U.S.A. jurisdiction (Waring et al., 2013). Consequently, activity increased in the following years and no less than 37 surveys were conducted between 1995 and 2012 (Waring et al., 2015).

The Atlantic Marine Assessment Program for Protected Species (AMAPPS) was set up in 2010 to estimate the abundance, distribution, ecology and behaviour of marine mammals, turtles, and seabirds throughout the U.S. Atlantic Outer Continental Shelf, covering waters from Maine to the Florida Keys. These surveys collect shipboard and aerial line transect data, as well as environmental data for 18 different species of marine mammals (Palka et al., 2017). The programme is now in its third phase, and scheduled to run until at least 2024 (NMFS 2021).

1.2.1.2 The Eastern and Central North Atlantic

The North Atlantic Sightings Surveys (NASS), now coordinated by the North Atlantic Marine Mammal Commission (NAMMCO), took place in 1987, 1989, 1995, 2001, 2007 (known as Trans-NASS – T-NASS) and 2015. These surveys aimed to obtain quantitative information on the abundance and distribution of all cetacean species within the survey area (Lockyer and Pike, 2009). Surveys took place over a large geographical region, with data collection during NASS-87 taking place in the waters of Greenland, Norway, Iceland, and the Faroe Islands as well as extending down the west coast of the UK and Ireland, and down to northern Spain. Abundance estimates from these surveys have been published in reports to the International Whaling Commission (Buckland & Cattanach 1992a, Buckland and Cattanach 1992a, 1992b, Cattanach et al. 1993) and a NAMMCO Scientific Publication series Special Issue (Lockyer and Pike, 2009). An additional aerial survey of Icelandic shelf and territorial waters was conducted in 2016 (Pike et al., 2020). Since 1995, Norwegian Independent Line Transect Surveys (NILS) have covered waters of the central and eastern Northeast Atlantic, primarily to estimate the abundance of minke whale (*Balaenoptera acutorostrata*) (Bøthun et al., 2009)

In addition to NASS and NILS, a series of surveys has been conducted in European Atlantic waters focussing on the North Sea and European Continental Shelf waters. The Small Cetacean Abundance in the North Sea (SCANS) survey was conducted in summer 1994. Comprised of concurrent shipboard and aerial surveys, this was designed to generate precise and unbiased abundance estimates for the main species in this area. The surveys were initiated in response to concerns surrounding large levels of cetacean by-catch from fisheries. In the absence of baseline population size, it was very difficult to provide context for the reported mortalities. During the first survey, around 20,000 km of shipboard transects were covered in an area of 890,000 km^2, alongside 7,000 km of aerial transects in an area of 150,000 km^2 (Hammond et al., 2002) (Figure 1.2-1).

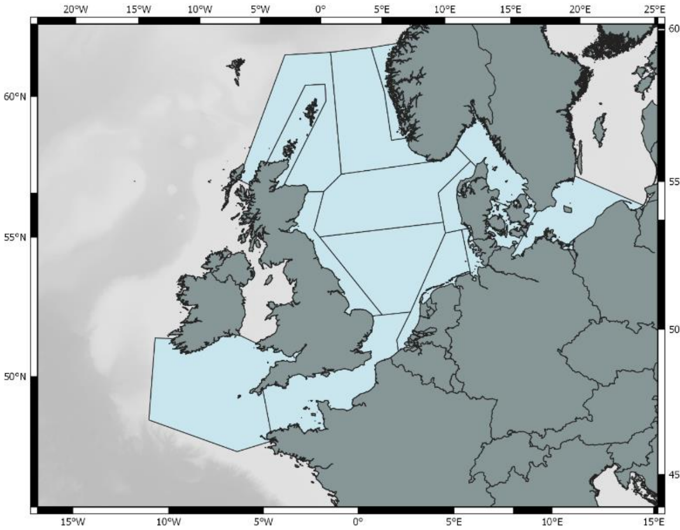

Figure 1.2-1:Survey blocks for the SCANS survey which took place in 1995 (Hammond et al., 1994). All blocks were surveyed using ships.

In July 2005, a second survey – SCANS-II – was conducted over a larger area, encompassing the entire EU Atlantic continental shelf. Overall coverage by the shipboard survey was 19,725 km transects in an area of 1,005,743 km^2, and 15,802 km aerial survey transects in an area of 364,371 km^2 (Hammond et al., 2013) (Figure 1.2-2).

The 2005 survey produced abundance estimates for five of the 13 species seen during the survey: harbour porpoise, bottlenose dolphin (*Tursiops truncatus*), white-beaked dolphin, common dolphin (*Dephinus delphis*) and minke whale.

The Cetacean Offshore Distribution and Abundance in the European Atlantic (CODA) project was conducted to expand coverage in European Atlantic waters beyond the continental shelf. The survey was conducted by ship in July 2007 and covered 9,651 km of transects within a 968,000 km^2 survey area (Figure 1.2-2). This survey yielded abundance estimates for common dolphin, striped dolphin (*Stenella coeruleoalba*), bottlenose dolphin, long-finned pilot whale (*Globicephala melas*), minke whale, sperm whale (*Physeter macrocephalus*), fin whale (*Balaenoptera physalus*) and beaked whales (Z*iphidae Sp.*) (Hammond et al., 2009).

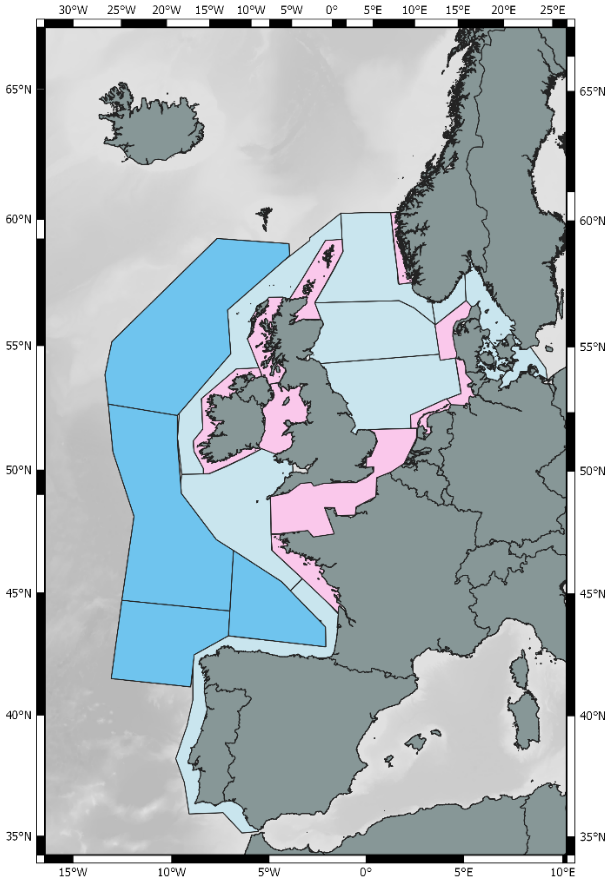

Figure 1.2-2 The survey blocks for the SCANS-II and CODA surveys. Areas coloured in pink were surveyed using aircraft, areas in blue were surveyed using ships. The CODA area is designated by a darker blue.

The third SCANS project – SCANS-III – took place in 2016, with survey effort again centred around July. This project covered the waters previously covered by the SCANS-II and CODA surveys combined (but not in Irish waters – see ObSERVE below), as well as extending north to include coastal waters of Norway as far as Vestfjorden. A total of 51,287 km of aerial survey transects was completed, along with 9,800 km of shipboard survey effort (Hammond et al., 2021).

The ObSERVE project was one of the first initiatives to include winter data collection as well as summer. It took place during 2015 and 2016 and conducted aerial surveys of Ireland's offshore and coastal waters. Over 37,000 km were flown during the combined surveys (Rogan et al., 2018). ObSERVE and SCANS-III were designed in parallel so that the two survey areas would join, and the methods between the two surveys were compatible for joint analysis. Survey blocks for both the ObSERVE and SCANS-III survey are shown in Figure 1.2-3. Data from the SCANS-II, SCANS-III and ObSERVE are analysed as part of this thesis.

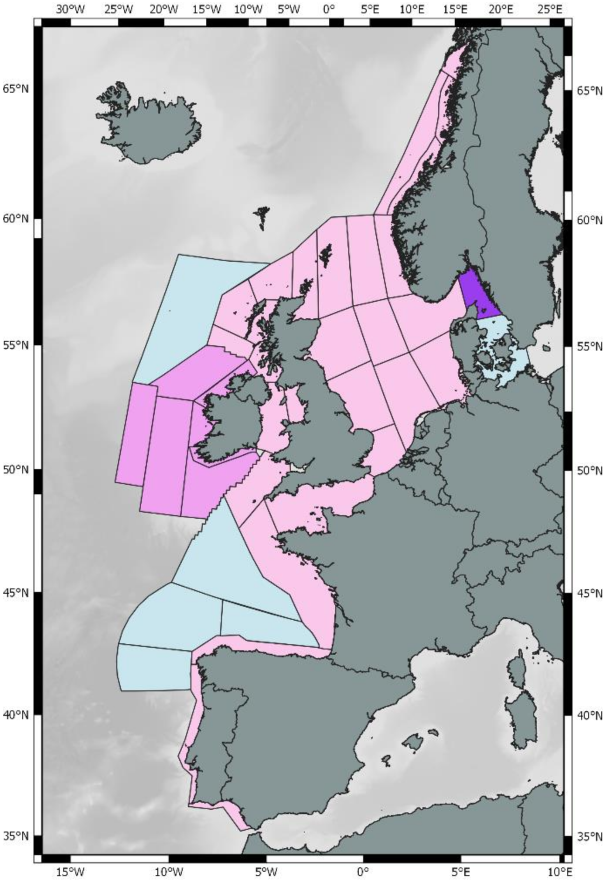

Figure 1.2-3 The survey blocks for the SCANS-III and ObSERVE surveys. Areas coloured in pink were surveyed using aircraft, areas in blue were surveyed using ships. The ObSERVE area is designated by a darker pink. The purple area of the Skagerrak to the north of Denmark was surveyed using both plane and ship.

1.3 Estimating abundance from line transect surveys.

A great deal has been written on line transect methodologies for cetaceans. Buckland, (2001); Buckland et al., (2015) and Hammond et al., (2021) provide detailed information; an overview is provided below.

Line transect surveys are a way of estimating animal density. When undertaken for cetaceans they are generally conducted using ships, small boats or aircraft and involve surveying defined areas, often termed “strata”, by following defined transect lines, prepared in advance as part of a design to ensure each stratum is covered representatively.

Survey teams typically consist of two observers, each searching one side of the ship or the plane, and a data recorder. Observers record sightings of animals. Details noted typically include the time of the sighting, location as GPS coordinates, species, and number of animals at a minimum. Additional information may include notes on behaviour of the animals or the cue for the sightings.

In traditional strip transect surveys, it is assumed that all animals on the survey trackline, and to a known distance to either side (the survey strip), are seen. The density can then be estimated by dividing the total number of animals (or groups) seen by the total area surveyed, calculated by adding all the lengths of the transect lines, multiplied by the width visible on either side of the trackline. For cetaceans, which spend large amounts of their time under the water when they are not available at the surface to be seen, the assumption that all animals in the survey strip are seen, is clearly violated. This leads to an underestimate of density and subsequently abundance.

In a line transect (also known as distance sampling) survey, the assumption that all animals within the defined strip are detected is relaxed. This methodology only requires that all animals on the trackline are seen. When conducting the survey, additional data on the perpendicular distance of the animal from the trackline are collected. Perpendicular distance is measured directly on aerial survey. On a ship, perpendicular distance is calculated from estimated distance from the observer to the detected animal or group of animals, and the angle subtended to the animal/group.

These perpendicular distances are used to fit a detection function (Thomas et al., 2010), which provides an estimate of the average probability of detection within the strip. The *effective strip width* (ESW) is the result of multiplying the survey strip width by the average detection probability. Conventionally, this refers only to one half of the transect line, so in reality is the effective strip half-width.

Although this method accounts for animals missed in the strip, it does not account for animals that may be missed on the transect line. The method still assumes that all animals on the trackline are seen to avoid under-estimating the true density. The term conventionally used for the probability of detection on the trackline is g(0).

One way of estimating g(0) is to use double platform surveys. In this methodology, two independent teams of observers search for cetaceans. The “primary” observers operate as they would in a single platform survey, looking close to the ship and recording animals when they are encountered. The second team, often referred to as “trackers’, look much further ahead of the vessel, often with the aid of powerful binoculars. They search for animals far ahead of the vessel, which they then track as they come closer to the ship, until they come into range for the primary observers, thus setting up “trials” to see whether these animals are seen by the primary team. This methodology was implemented for the surveys analysed in this thesis. For full details of the methods, see Hammond et al., (2021, 2013).

1.4 Modelling analyses: adding value.

Many cetacean species are wide-ranging and respond to changes in their environment by changing their distribution (Forney, 2000). Considering this, and the fact that data are expensive and difficult to obtain, any technique that allows predictions as well as presenting the status quo is a valuable management tool for informing decision making (Cañadas et al., 2005; Gilles et al., 2016; Guisan and Thuiller, 2005; Redfern et al., 2006). Spatial modelling analyses fill the management need for spatial information at a management level.

Habitat modelling is one example of this type of spatial modelling. It is a method that allows prediction of species distributions and, from the resulting models, an understanding of the ecological processes which might be driving these distributions (Hedley and Buckland, 2004; Redfern et al., 2006). Models relate species distribution data to information on environmental conditions at the same locations through statistical functions, and use these to map species distribution across a study region (Elith and Leathwick, 2009).

Many modelling studies of this sort have been conducted for cetaceans. These vary by species, by geographic area, and by methodology used, but all aim to examine associations between the study species and different environmental parameters. For example, in northern California Current System (CCS) Tynan et al., (2005) used a multiple logistic regression model to examine occurrence patterns for several species. Humpback whale August distribution was linked to temperature, depth, and distance to the upwelling front. Harbour porpoise distribution was associated with high chlorophyll concentrations and Pacific white-sided dolphin (*Lagenorhynchus obliquidens*) distribution was explained by distance to the upwelling front, and an acoustic backscatter parameter.

Large scale surveys, like the SCANS surveys in scope, have been conducted over the entire Hawaiian Islands Exclusive Economic Zone. These have generated habitat models for nine different species of cetacean, including spatially explicit density predictions (Becker, 2021). These models allow updated information on density to be provided to individual species assessment reports, one of the fundamental components of the management aspects of the Marine Mammal Protection Act, the cornerstone of U.S. marine mammal conservation (Roman et al., 2013).

These kinds of models can also be used to combined data from multiple different platforms and years, again linking these to environmental covariates. One such set of models was completed by Roberts et al., (2016), and included information from 23 years of survey, resulting in models for 26 species. These were centred around the U.S. Atlantic, and the Gulf of Mexico, and represented the first density maps produced for this region to be published.

The eastern Atlantic has also been the focus of such studies, including those on hard-to-study beaked whales (Rogan et al., 2017; Virgili et al., 2019); and those with the ambitious scope of the Joint Cetacean Protocol (JCP), which worked with a dataset combining 38 different data sources, spanning a 17 year period (Paxton et al., 2016).

Practical applications of these types of studies include, but are not limited to, the development of marine protected areas (Ana Cañadas et al., 2002; Embling et al., 2010), understanding the impacts of anthropogenic activities (Purdon et al., 2020), or predicting the potential impacts of climate change (Becker et al., 2019).

Density surface modelling (DSM) is a type of habitat modelling that uses data specifically collected on line transect surveys, allowing the resulting models to be corrected for uncertain detection via distance sampling methodology (Miller et al., 2013).

To make models as useful as possible some careful consideration must be made to the covariates that are used, not least because predictors may be acting in either parallel or interactive ways, and over different spatial and temporal scales (Wagner and Fortin, 2005).

Generalised Additive Models (GAMs) are a well-established regression method, commonly used to investigate the relationships between species and their environments (Baines et al., 2021; Becker et al., 2020; Booth et al., 2013; Redfern et al., 2006; Wood, 2006). They are extremely flexible, which makes them suitable for capturing relationships between study species and environmental predictors that may be non-linear, via the use of smoothing functions (Redfern et al., 2006).

A variety of studies have compared the performance of GAMS with that of other methodologies. These include boosted regression trees (BRTs) (Becker et al., 2020) and hierarchical Bayesian Models using integrated Nested Laplace Approximations (HBM-INLA) (Williamson et al., 2022). GAMs have been found in these cases to perform at least as well at the geospatial scale used in this thesis (Williamson et al., 2022), or better (Becker et al., 2020). GAMS are therefore considered an appropriate method for this analysis and have been used throughout this thesis.

1.5 Building ecologically meaningful models

Distribution of a species can be affected both directly and indirectly (Austin, 2002; Guisan and Thuiller, 2005; Guisan and Zimmermann, 2000). Austin (2002) describes three types of idealised environmental predictor in a study on plants:

Indirect predictors may have no particular effect on the species of interest *per se*, but they correlate with species distribution, due to a location-dependent correlation with other variables which do have a direct influence on a species, for example longitude with fin whales (Azzellino et al., 2012). Resource predictors are those consumed by the species of interest. Direct predictors are those which have a direct physiological influence on a species but are not consumed directly – for example, temperature. Tropical delphinids, for example, may be restricted to warmer waters due to limitations on their thermoregulatory ability (Learmonth et al., 2006).

The distribution of different species will be influenced in different ways. Prey predictors, for example, are likely to have stronger effects on some species compared to others. It has been suggested that harbour porpoises (*Phocoena phocoena*) need to feed almost continuously (Wisniewska et al., 2016), thus it seems plausible that distribution of prey would have a direct effect on the distribution of harbour porpoises, as proximity is required at all times. This is less likely to hold true for many baleen whale species that have distinct breeding and feeding grounds (Chivers, 2009), where direct effect of prey may be expected on the feeding grounds, but would not be expected in the breeding grounds.

Position of a predictor in the “chain” may also cause a variation in the effect it may have on a species (Austin, 2002). For example, the depth of the mixed layer in the North Sea has been linked to the presence of herring (*Clupea harengus*) (Maravelias, 1997). When considered as a predictor mixed layer depth may have a comparatively proximal influence on the presence of predators of herring, including marine mammal species. Looking at chlorophyll as a predictor however, there would be a more distal influence on predators of herring, as chlorophyll concentrations drive zooplankton concentrations, which are in turn preyed upon by herring, which are in turn preyed upon by marine mammals (Dalpadado, 2000). Thus, chlorophyll would have a more distal effect.

To build a model that is useful over large scales, both proximal and direct predictors are desirable (Guisan and Zimmermann, 2000). However, they are not always available, requiring the use instead, of more indirect measures (Austin, 2002).

Prey availability and distribution can be particularly difficult to measure, and consequently modelling studies of cetaceans do not often include prey density as a covariate (C. Lambert et al., 2014). The problem is exacerbated because many cetacean species feed on a wide range of different prey species, and so reduction of one species may simply mean they switch to an alternative or may mean a change in distribution. Studies which were able to include prey data have had mixed results. Lambert *et al* (2014) examined cetacean density in relation to modelled distributions of potential prey species generated by the SEAPODYM model. They split cetacean species into three guilds, namely sperm and beaked whales (low energy requirement cetaceans), *Globicephalinae* (medium energy requirement cetaceans) and *Delphininae* (high energy requirement cetaceans). In this study, both *Delphininae* and *Globicephalinae* were shown to select habitat where high levels or prey biomass was available at shallow depths, and thus within easier foraging range. (Benoit-Bird and Au, 2003) also found a close overlap between spinner dolphins (*Stenella longirostris*) and prey species, but this work was done at a much finer scale than is possible using large-scale survey data. Studies of seabirds and pinnipeds found no spatial overlap between predators and areal biomass, density, of numerical abundance of prey (Benoit-Bird et al., 2013).

This commonly results in the use of indirect variables instead, which are often easier to measure, although they may show a more distal influence on cetacean distribution. Chapter 4 makes use of some rarely available prey energy surfaces (Ransijn et al., 2019) to compare whether models including these perform better than those based only on indirect predictors.

1.5.1 Environmental covariates used.

As discussed above, this is not the first study to attempt to predict cetacean distribution using environmental covariates. Each study will use its own suite of variables which have been selected based on their species of interest, their area of interest and the data that may be available to match the time period and resolution at which the cetacean data have been collected. Not only is the environment highly variable, but the factors that may be influencing the distribution of cetaceans are also varied. These include prey distribution, location of breeding and calving areas, likely prevalence of predators and also anthropogenic activity (Davis et al., 2002). The study region encompasses habitat which, during the period the data were collected, all the species of interest are known to feed, even the two rorqual whale species for which feeding and calving is often separated. As a consequence, the covariates chosen to model their distribution within the study region primarily relate to factors which may be driving prey availability or foraging ability. Further information on covariates is provided in Chapter 2, and maps of covariates are provided for specific modelling regions in Chapters 3-5. The following brief descriptions provide information on why different variables were included.

1.5.1.1 Depth

Cetaceans live in a 3-dimensional environment, and depth is crucial to defining the habitat a species is found in. If a predator is known to feed on bottom-dwelling prey species, such as sand-eels, then the predator species is unlikely to be found in waters with depths that exceed their diving abilities. Similarly, if a species is feeding primarily on deep water prey species, such as many squid species, then that predator species is unlikely to be found routinely in a shallow water habitat. Many studies have found depth to be an important covariate in models examining distribution of cetaceans. Examples include, but are by no means limited to, the Gully in Nova Scotia, for which seven species were found to have depth as a significant predictor (Hooker et al., 2011); harbour porpoises in the North Sea (Gilles et al., 2016)and studies of delphinid distribution in the Mediterranean (A Cañadas et al., 2002).

1.5.1.2 Seabed rugosity

In this thesis, this is modelled as both slope and as the standard deviation of depth (See chapter 2), but both are looking at changes in elevation of the seafloor. Areas of steep slopes are often associated with nutrient rich waters as a result of upwelling processes, in which nutrient rich waters are brought closer to the surface. As a result, areas with steep slopes are often found to be good predictors for different species of cetacean. As with depth, this is a staple covariate, and relationships between slope and density have been found for nine species in the Gulf of Mexico (Davis et al., 2002), odontocetes in the Ligurian Sea (Azzellino et al., 2008), as well as a variety of species in the Bay of Biscay (Laran et al., 2017).

1.5.1.3 Mixed Layer Depth

Mixed layer depth is the depth that separates the well mixed surface layer from the denser, stratified water below. It thought to influence cetacean distribution via influence on prey species directly as described for herring in the North Sea in the previous section and to have influence at a finer scale than some physiographic variables, such as depth (Stephenson et al., 2020).

1.5.1.4 Sea surface temperature
Sea surface temperature may work on cetacean species in two different ways. Sea surface temperature may also influence the distribution of different prey species, but it may also influence the distribution of the animals themselves.

Cetaceans have evolved considerable insulation by way of a thick blubber layer. This primarily serves the purpose of insulating the animal and keeping them warm (Ryg et al., 1993). When excess heat is generated, for example via exercise, then heat can be lost to the environment via the less well insulated extremities – the pectoral fins, dorsal fin and fluke (Kanwisher and Ridgway, 1983). Some species are better adapted to cooler waters, and others to more tropical habitats (section 1.7.1 below); these adaptations limit the thermal window in which a species may comfortably exist (E. Lambert et al., 2014; Lambert et al., 2011). Consequently, sea surface temperatures may be used to predict the distribution of a species. White-beaked dolphins, for example, are particularly associated with sea surface temperatures of 14^0C or lower (MacLeod et al., 2008).

1.5.1.5 Salinity
Areas of lower salinity are often associated with having higher levels of nutrients, due to run-off from land. These are usually very close to the coast and may form as plumes at river estuaries where the fresh and saline water mix. These more productive waters may prove to be good areas for different prey species. It is also possible within this study region that the areas of low salinity are acting in the model as a proxy for very shallow coastal waters. Nevertheless, salinity has been shown to contribute to describing cetacean distribution in other studies, for example white-beaked dolphins (Breen et al., 2016).

1.5.1.6 Proximity to depth contours
Depth contours are included in the list of potential modelling covariates, as they are a good proxy for changes in overall habitat. The 200m isobath demarcates the continental shelf break, as well as the approximate ending of the euphotic zone. In waters that exceed this depth, there is a change in habitat from a water column which is fully able to photosynthesise. The euphotic zone should be more productive waters (Khanna et al., 2009)

1.5.1.7 Proximity to seabed features
Rather than modelling the seabed as a combination of different proxy variables, such as depth and slope, it is sometimes possible to use the actual seafloor geomorphic features themselves as predictors. For example, it may be more appropriate to model “distance to seamount” than it is to model a combination of depth or slope. This was shown to be successful with striped dolphin by Claro et al., (2020).A selection of different seabed features

have been included in the models for chapter 5. The were not included for the models of chapter 4, as the features do not occur within the North Sea region.

1.5.1.8 Measures of mesoscale activity

Predator abundance and diversity is driven by oceanographic conditions (Scales et al., 2014). Whilst marine biodiversity at a global scale is regulated by sea surface temperature (Worm et al., 2005), at ocean-basin scale (mesoscale activity refers to changes in flows at a 10s to 100s of km scale) biodiversity is generally higher in the productive zones associated with currents, upwellings and changes in bathymetry. Eddies create movement throughout the water column, which redistributes nutrients and other biomass creating areas of increased productivity, and persistent aggregation of low-trophic-level prey. Fish then feed along density structures in these eddies, which in turn then attracts predators (Godø et al., 2012; Pardo et al., 2015).

The location of eddies and other oceanographic processes, such as fronts, which may indicate areas of higher productivity can be shown using remotely sensed variables. absolute dynamic topography (ADT) as well as sea surface height (SSH) and sea level anomaly (SLA), from which ADT is derived (Figure 1.5-1). As eddies and other processes cause changes in density of water, the volume of the water will also decrease slightly. This will result in a corresponding decline in the hight of ADT. ADT, SSH and SLA can therefore be used as indicators of mesoscale activity when modelling cetacean distribution. Previous studies using these variables include an examination of links between common dolphins and blue whales and ADT in the Northeast Pacific Ocean (Pardo et al., 2015) and between nine different cetacean species and SSH and SLA (Correia et al., 2021).

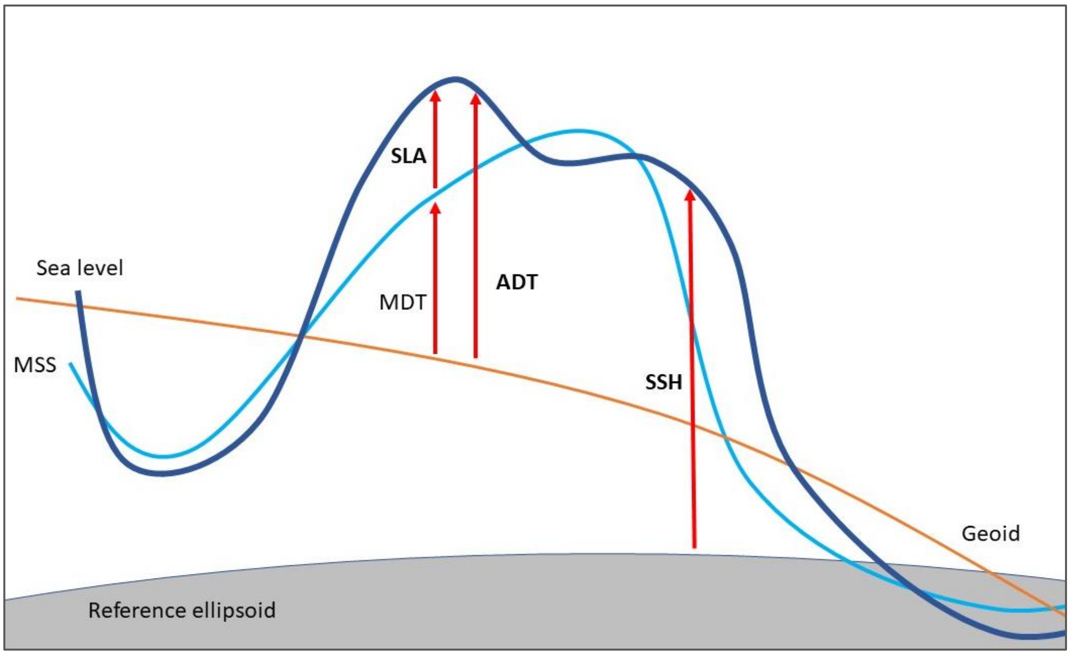

Reference ellipsoid: smoothed mathematical representation of Earth's sea level surface, ignoring the effects of tides, seasonal currents, and waves.
Geoid: the shape that the ocean surface would take under the influence of gravity and the earth's rotation, assuming other influences such as tide and wind were absent.
MSS: 20-year Mean Sea Surface above the ellipsoid
SLA: Sea level anomaly (difference between MSS and sea level at time of measurement)
MDT: Mean Dynamic Topography: mean departure of the sea surface from the geoid due to ocean dynamics.
ADT: Absolute Dynamic Topography: departure of the sea surface from the geoid due to ocean dynamics. ADT = MDT+SLA
SSH: Sea Surface Height: height of the sea surface above the ellipsoid.

Figure 1.5-1: Schematic showing the differences between the different measures of mesoscale activity SLA, ADT and SSH with reference to the geoid. Adapted from (Fernandez and Lellouche, 2021)

1.5.2 Spatial scale

Marine ecosystems are highly variable. The scale of variation can be anything from a single tidal cycle to multi-year processes and spatially can range from meters to many thousands of kilometres (Becker et al., 2019; Forney et al., 2015; Redfern et al., 2006). The scale at which modelling can be conducted is determined by the resolution of the data. The data used in this study were collected at a very large spatial scale. Whilst these data are not sufficiently detailed to conduct fine scale modelling, it is possible to split the survey region into areas of more similar habitat, with the objective of isolating predictors which may work better at predicting animal distribution. The regions selected for this thesis are the International Council for the Exploration of the Sea (ICES) marine ecoregions.

1.5.2.1 ICES marine Ecoregions

Ecoregions are defined based on similarity of biogeographic and oceanographic features (ICES, 2020a). Twelve ecoregions for the Northeast Atlantic were proposed in 2015 and are now used for all ICES-based advice. Of these 12 ecoregions (Figure 1.5-2), three are primarily used in this thesis; the Greater North Sea ecoregion (Chapter 4) and the Celtic Seas, and Bay of Biscay & Iberian Coast ecoregions (Chapter 5). Details of the oceanographic characteristics are provided in the introductions to the chapters in which they are used.

Figure 1.5-2 The 12 ICES ecoregions. Figure taken from ICES 2020, p1.

1.6 The study region

The study region for this thesis spans approximately 2,447,300 km^2 and more than 30^0 of latitude, from northern Norway to the Straits of Gibraltar (Figure 1.6-1). Such a large area encompasses a wide range of habitats and includes parts of seven different ICES ecoregions (although the focus is primarily on three of these). Water depths extend from the coast to more than 5000m. The deeper parts of the region are heavily influenced by oceanic inputs, as well as by prevailing strong westerly winds which can cause the build-up of large swells leading to the surface layers being well mixed (McMahon, 1995). Along with the North East Trade Winds these drive the North Atlantic Gyre which is a system of comparatively warm waters which flows northwards from Portugal and up past the coast of Ireland (Gonzalez-Pola et al., 2018). By contrast, the North Sea region is a temperate shelf sea with permanently mixed water in the south and east, and seasonally stratified layers to the north (ICES, 2020b).

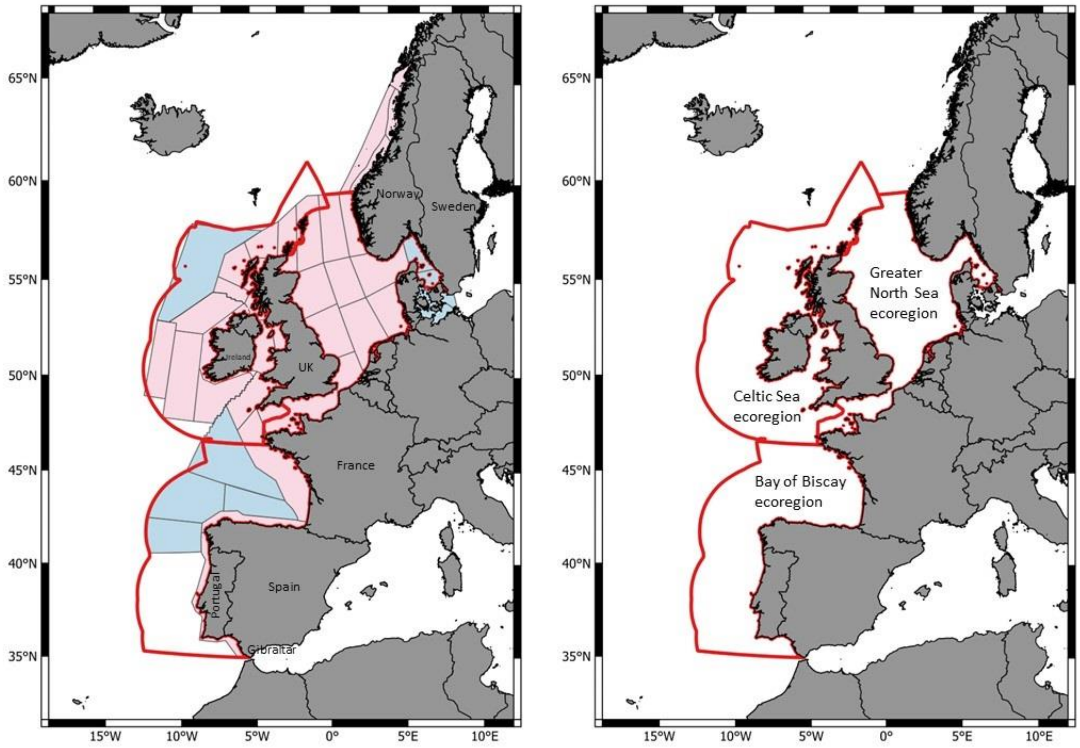

Figure 1.6-1 LEFT: Map of the study region in the north-east Atlantic. Blue areas were surveyed in 2016 by ship, pink areas by air. Red lines denote the three ecoregions which are used in chapters 4 and 5. RIGHT: the three ecoregions labelled.

1.7 The Northeast Atlantic Cetacean Community

The considerable variation in habitat in the study region results in a diverse cetacean community. At least 25 different species (Hammond et al., 2009; P. S. Hammond et al., 2013; Reid et al., 2003; Rogan et al., 2018; Wall et al., 2013) and maybe as many as 36 species (Evans, 2020) have been recorded in these waters. Of these, at least 15 are considered to be resident (Reid et al., 2003; Wall et al., 2013). This thesis looks at 8 of these species. These are harbour porpoise – *Phocoena phocoena*, minke whale – *Balaenoptera acutorostrata*, white-beaked dolphin – *Lagenorhynchus albirostris*, (chapters 3 & 4) white-sided dolphin – *Lagenorhynchus acutus*, bottlenose dolphin – *Tursiops truncatus*, common dolphin – *Delphinus delphis*, striped dolphin – *Stenella coeruleoalba*, fin whale – *Balaenoptera physalus*) (chapters 3 & 5). Due to the number of species, an extensive review of the literature for each is not provided, however relevant background material is presented in detail in the introduction sections to the chapters in which their density has been modelled. The following brief sections outline the key features of the distribution of each study species within the region, as well as the habitat in which they are most frequently sighted.

1.7.1 Harbour porpoise – *Phocoena phocoena*

The harbour porpoise is the most commonly abundant cetacean species in the region, and is sighted most commonly on the continental shelf, with an estimated 504,829 animals within the study region (Hammond et al., 2021; Rogan et al., 2018, see also chapter 3). The species is distributed throughout the shelf waters of the study region, from the Barents Sea and Iceland in the north, to the coasts of France and Spain in the south (Evans, 2020; Reid et al., 2003). There is also a discrete West African population, with sightings and acoustic detections recorded in Moroccan waters (Boisseau et al., 2007), showing the species is capable of inhabiting both sup-polar waters.

Whilst they do occasionally form large aggregations, they are usually found in smaller groups of 1-3 animals. The SCANS-III survey reported a mean group size of 1.53 individuals (Hammond et al., 2021).

Harbour porpoises are small; adult females are around 150cm long on average and males slightly smaller. They are well adapted to living in cold water (11^0C – 14^0C) (Bjørge and Tolley, 2018), with a selection of different adaptations to this environment. These include extremely thick blubber relative to body size and blubber which has the lowest thermal conductivity recorded for any cetacean species. In comparison with the Pantropical spotted dolphins (*Stenella attenuata*), which is a similar size, but inhabits tropical waters, harbour porpoise was found to have twice the blubber thickness (1.5 ± 0.3cm) compared to (0.8 ± 0.1cm), and conductivity of 0.1 ± 0.01 Wm^{-1}, compared with 0.2 ± 0.01 Wm^{-1} in the spotted dolphin (Worthy and Edwards, 1990). This blubber layer is energetically expensive to maintain, and so harbour porpoises require the ability to locate predictable, high densities of prey in order to maintain their insulation (Wisniewska et al., 2016). They feed on many prey species, and some studies have shown that their choice of prey may be dependent on calorie content (Andreasen et al., 2017; Heide-Jørgensen et al., 2011; Spitz et al., 2012). This species is known to eat both pelagic and demersal prey (Leopold et al., 2015)

Harbour porpoises are typically noted to be a species found on the continental shelf, in waters shallower than 200m. Animals tagged in Danish waters, to the far east of the study region of this thesis, were found to conduct multiple short dives - between 29 and 43 per hour depending on the season. Dive depth was found to correspond to the depth of the water column itself, usually not exceeding 50m, although the maximum recorded was 132m (Teilmann et al., 2023). Harbour porpoises are physically able to dive deeper and longer, however, with studies of tagged animals in Greenland waters revealing movements into waters well past the continental shelf, and an average dive depth of 248m, with the deepest reaching 410m (Nielsen et al., 2018). Models for this species are explored in chapter 4. Locations of sightings within the study region are shown in Figure 1.7-1.

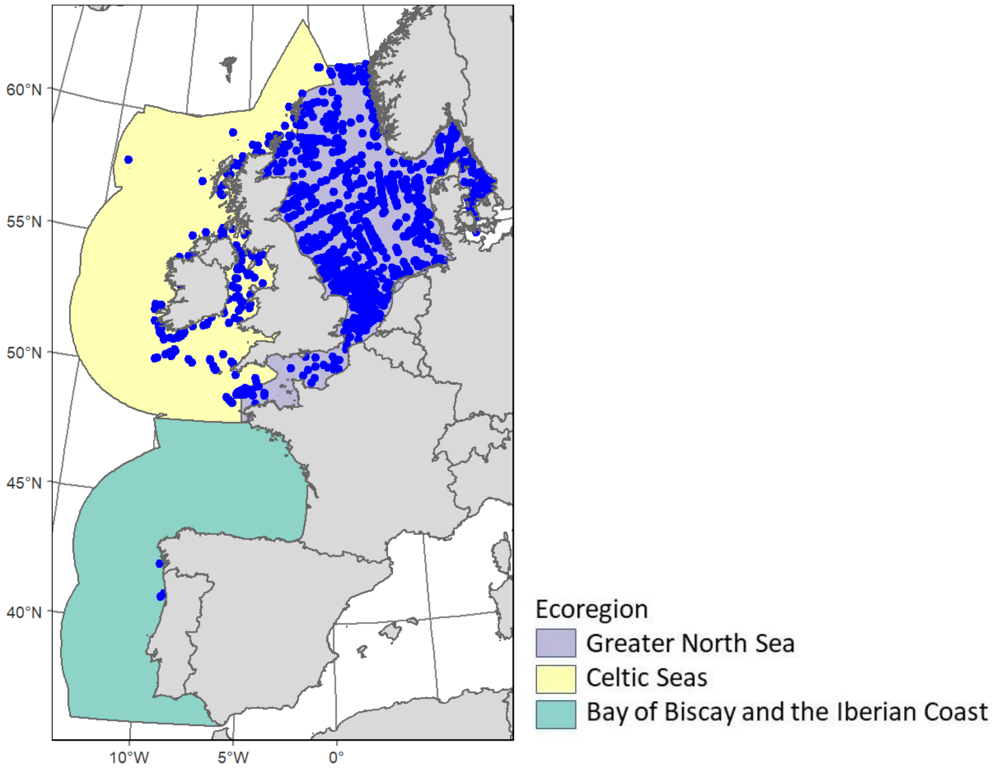

Figure 1.7-1 Locations of the combined harbour porpoise sightings (blue dots) seen during the surveys analysed in this thesis (SCANS-II, CODA, SCANS-III and ObSERVE), showing where they were most commonly recorded in relation to the three ecoregions modelled in chapters 4 and 5.

1.7.2 White-beaked dolphin – *Lagenorynchus albirostris*

White-beaked dolphins are generally a sub-polar species, associated with sea surface temperatures of 2^0C to 13^0C (Evans, 2020). Their northeast Atlantic distribution ranges from southwest Greenland, Svalbard and the Barents sea to the Bay of Biscay (Evans, 2020; Reid et al., 2003; Wall et al., 2013). Described by Kinze (2018) as a facultative coastal species, within the study region, they are found almost entirely in waters shallower 200m, but do also occur in deeper waters in other parts of their range (Hansen and Heide-Jørgensen, 2013). Within the study region they are known to prey upon demersal and pelagic fish (Canning et al., 2008; Jansen et al., 2010). The diving capabilities of this species have not been extensively studied, but two tags applied to individuals caught in Iceland recorded dives to the bottom of the bay in which the animals were swimming – a depth of 45m. Dolphins were noted to conduct both U and V shaped dives, with more time and more acoustic activity expended in U shaped dives (Rasmussen et al., 2013).

The SCANS-III survey reported a mean group size of 3.86 individuals and an abundance of 36,287 animals (95% C.I. 20,790 – 63,334) (Hammond et al., 2021, see also chapter 3) within the study region. Models for this species are explored in chapter 4. Locations of sightings within the study region are shown in Figure 1.7-2.

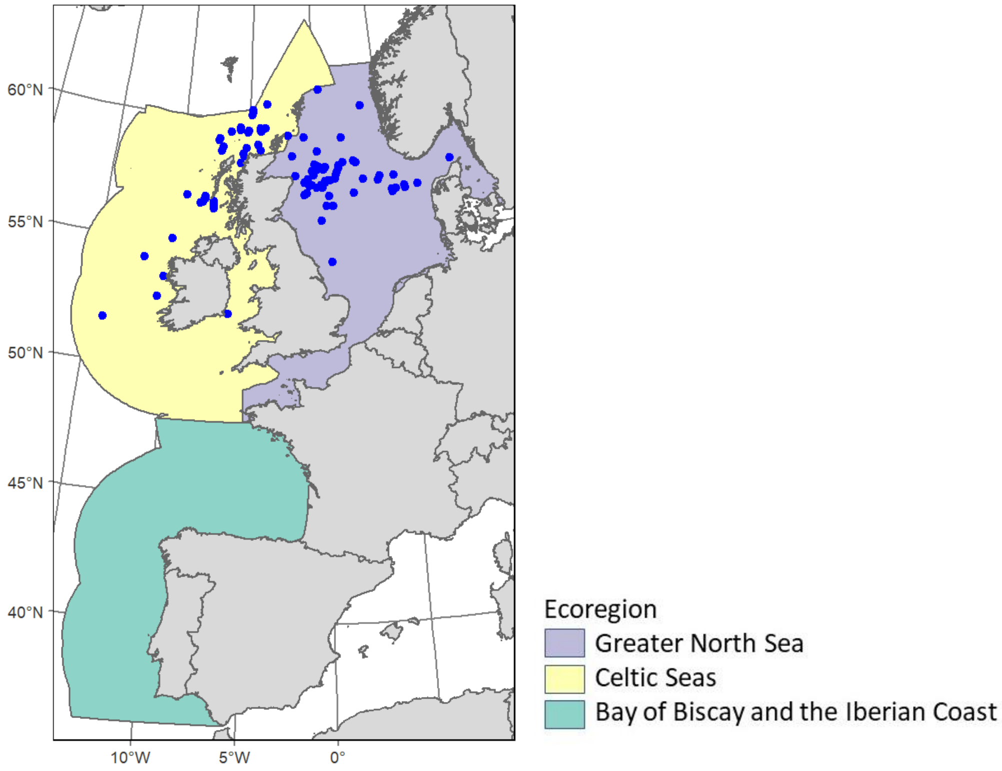

Figure 1.7-2 Locations of the combined white-beaked dolphin sightings (blue dots) seen during the surveys analysed in this thesis (SCANS-II, CODA, SCANS-III and ObSERVE), showing where they were most commonly recorded in relation to the three ecoregions modelled in chapters 4 and 5.

1.7.3 Minke whale – *Balaenoptera acutorostrata*

Minke whales have a widespread distribution, ranging from the tropics to the ice-edge, and are widespread throughout the study region as well as the wider North Atlantic in general. The species can be found in both coastal and offshore waters (Perrin et al., 2018). Most baleen whales conduct a seasonal migration from high latitude summer feeding grounds to lower latitude winter breeding grounds and it is thought that minke whales do the same, with the study region representing summer feeding habitat for this species (Risch et al., 2014; Víkingsson and Heide-Jørgensen, 2015). Records of minke whales have, however, been made within the study region all year round including some of adults accompanied by “young calves” which has led to speculation that some females at least may calve in more northerly waters (Anderwald and Evans, 2007; Evans, 2020; Kavanagh et al., 2018).

Telemetry studies of minke whales tagged in Norway and California have shown minke whales to rarely diver deeper than 120m, with most dives being much shorter (Kvadsheim et al., 2017). Like other rorqual whales, minke whales are obligate lunge filter feeders. This technique involves engulfing large volumes of water, ideally also including a high density of prey. This process incurs significant drag and energy expenditure which can limit diving ability, resulting in a trade-off between foraging efficiency and prey density. Spitz et al., (2012) demonstrated that minke whales have a high metabolic cost of living, and as such need to target prey patches with high calorie densities. Within the study area this species has been reported feeding on both demersal and pelagic species (Meier et al., 2016; Pierce et al., 2004; Víkingsson et al., 2014).

The SCANS-III survey reported a mean group size of 1.05 individuals (Hammond et al., 2021). The most recent abundance estimate across 21,338 animals (Hammond et al., 2021; Rogan et al., 2018, see also Chapter 3). Models for this species are explored in chapter 4. Locations of sightings within the study region are shown in Figure 1.7-3.

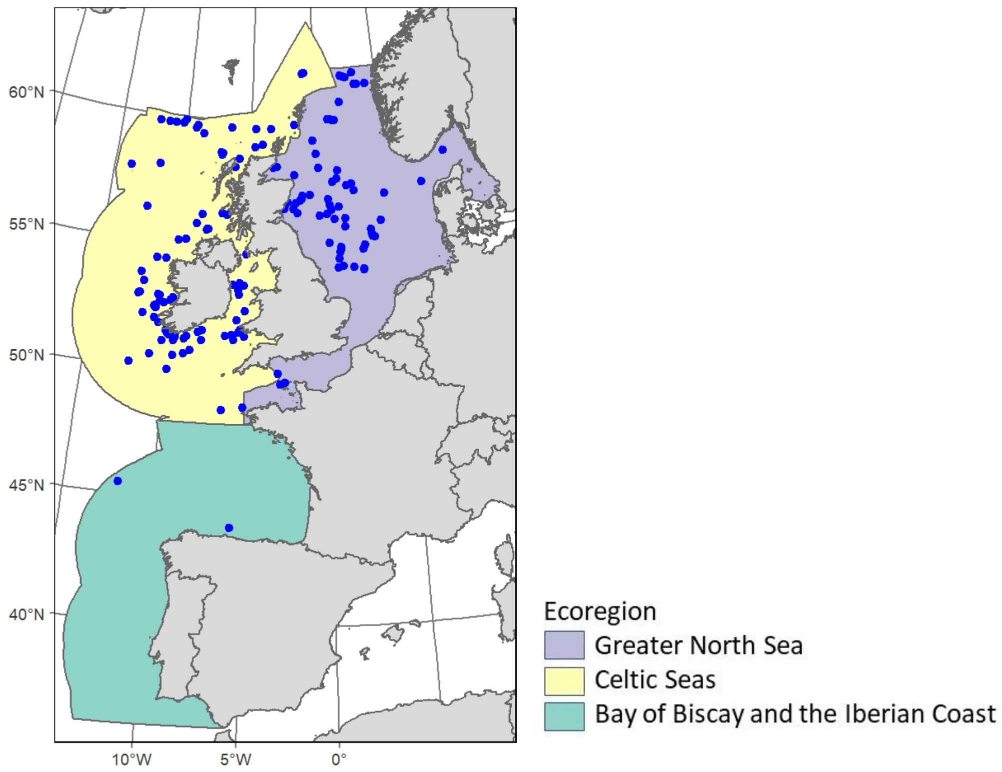

Figure 1.7-3 Locations of the combined minke whale sightings (blue dots) seen during the surveys analysed in this thesis (SCANS-II, CODA, SCANS-III and ObSERVE), showing where they were most commonly recorded in relation to the three ecoregions modelled in chapters 4 and 5.

1.7.4 Atlantic white-sided dolphin – *Lagenorynchus acutus*

Atlantic white-sided dolphins are a temperate and sub-polar species, found predominantly in waters of 5^{0}C to 16^{0}C (Cipriano, 2018). The northeast Atlantic distribution of this species extends from Iceland and the Barents Sea down to Ireland, and occasionally into the Bay of Biscay (Evans, 2020; Reid et al., 2003; Wall et al., 2013). This species is frequently sighted in large schools (Reid et al., 2003; Wall et al., 2013), but the SCANS-III survey reported a low mean group size of 3.02 individuals (Hammond et al., 2021).Abundance estimates for white-sided dolphins from the SCANS-III and ObSERVE surveys sum to 18,416 individuals (Hammond et al., 2021; Rogan et al., 2018, see also chapter 3).

This species is not well studied within the survey region. In the northwest Atlantic, analysis of stomach contents revealed a wide range of prey species, including cephalopods, lanternfish species, cod (*Gadus morhua*, haddock (*Melanogrammus aeglefinus*), sand eels (*Ammodytes spp*) and other pelagic and demersal species (Craddock et al., 2009). In the northeast Atlantic, stomach contents analyses determined the diet to be comprised mainly by teleost fish, comprising mostly of Gadiformes. The most important species by weight was blue whiting (*Micromesistius poutassou)*, contributing 36.8% of the overall weight, along with Atlantic mackerel (*Scomber scombrus*) which also contributed 20.6% of the total reconstructed mass. Mesopelagic fish were also found to be important. Notably, these are prey species which for the most part are species found primarily in shelf waters (Hernandez-Milian et al., 2016).

Models for this species are explored in chapter 4. Locations of sightings within the study region are shown in Figure 1.7-4.

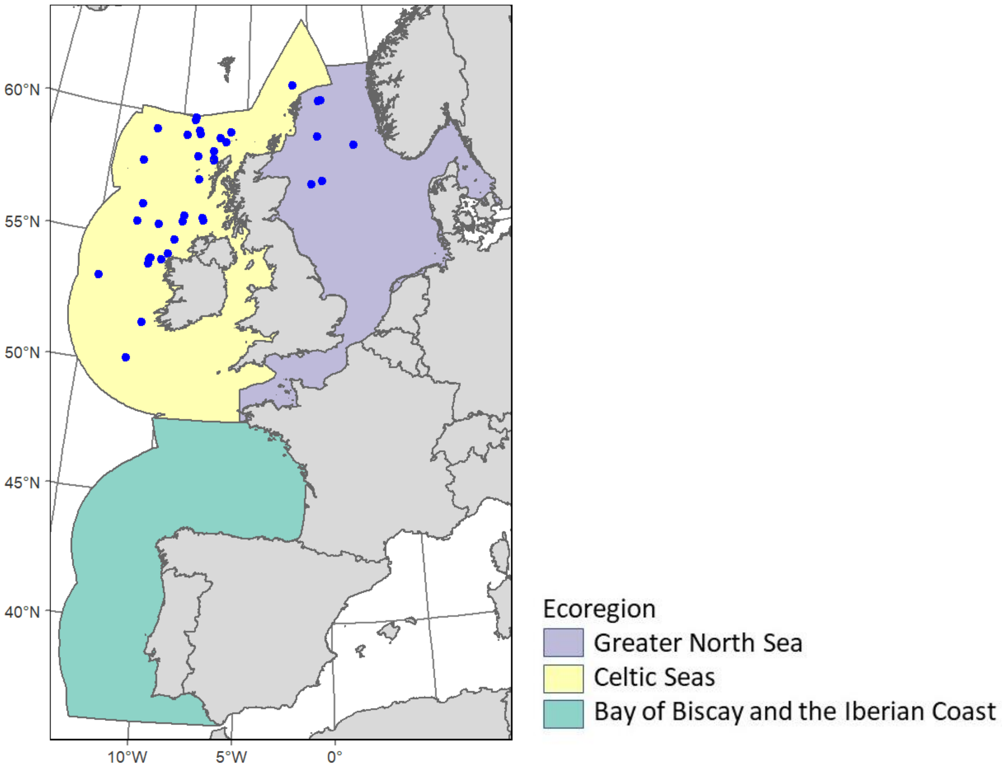

Figure 1.7-4 Locations of the combined white-sided dolphin sightings (blue dots) seen during the surveys analysed in this thesis (SCANS-II, CODA, SCANS-III and ObSERVE), showing where they were most commonly recorded in relation to the three ecoregions modelled in chapters 4 and 5.

1.7.5 Bottlenose dolphin- *Tursiops truncatus*

Bottlenose dolphins have a very wide distribution, and substantial geographical variation in morphology (Wells and Scott, 2018). In the eastern north Atlantic, the species occurs from the Faroe Islands as far south as the equator and beyond (Evans, 2020). It has been suggested that the extreme limits to bottlenose dolphin distribution are related to temperature, either directly, or indirectly through the distribution of prey (Wells and Scott, 2018). Bottlenose dolphins are often found in pelagic waters and over the continental shelf, especially along the shelf break (Reid et al., 2003; Wall et al., 2013). Mean group size from the SCANS-III survey was 4.4 animals (Hammond et al., 2021). Estimated abundance from the SCANS-III and ObSERVE surveys is 120,543 (Hammond et al., 2021; Rogan et al., 2018, see also chapter 3).

Bottlenose dolphins are known to forage both in the water column and the seabed, and were acoustically tracked dive to at least 50m in a coastal environment (Hastie et al., 2006), and using time-depth recorders were routinely carrying out night-time dives of more than 450m depth in deep water environments near Bermuda (Klatsky et al., 2007). Prey species likely vary hugely, representing the wide range of habitats used by this species. It is also likely that there are demographic differences in prey, as males and females often live in different groups, and different areas (Barros & Odell, 1990; Mead & Potter, 1990). Captive studies have estimated that adult male bottlenose dolphins would require approximately 2000 kg prey per year (Kastelein et al., 2002).

As well as oceanic bottlenose dolphins, small coastal populations of bottlenose dolphins also exist, which may be morphologically different (Louis et al., 2014; Oudejans et al., 2015). These more resident animals are better studied using other methods, such as mark recapture (e.g. Cheney et al., 2014, 2013; Arso Civil 2014) than large-scale surveys such as those analysed in this thesis. Models for this species are explored in chapter 5. Locations of sightings within the study region are shown in Figure 1.7-5

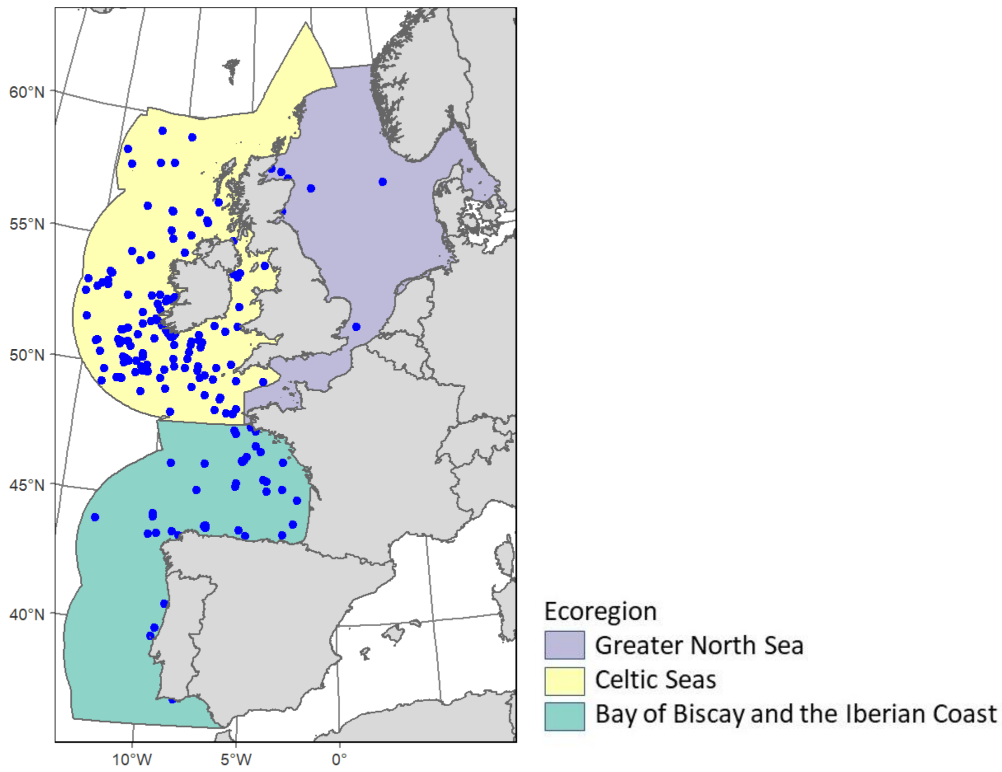

Figure 1.7-5 Locations of the combined bottlenose dolphin sightings (blue dots) seen during the surveys analysed in this thesis (SCANS-II, CODA, SCANS-III and ObSERVE), showing where they were most commonly recorded in relation to the three ecoregions modelled in chapters 4 and 5.

1.7.6 Common dolphin – *Delphinus delphis*

Common dolphins are widely distributed throughout the eastern North Atlantic, extending as far north as 65^{0}N around the west side of Norway and the Faroe Islands and well past the southern extent of the study region (Evans, 2020). Usually seen in shelf waters, common dolphins conduct considerable seasonal and inter-annual movements (e.g. Laran et al., 2017; Rogan et al., 2018).

Individuals can undertake foraging dives to at least 200m (Perrin, 2018), and they are known to feed on pelagic schooling fish (Moura et al., 2012; Pusineri et al., 2007). Spitz et al., (2012) classified common dolphins as being "energetically costly", meaning that they need to select prey with high energetic content to meet their energetic needs.

Whilst group sizes of common dolphins can number into the thousands, the mean group size from the SCANS-III survey was 7.12 animals (Hammond et al., 2021), and estimated abundance across the survey region is 487,093 543 (Hammond et al., 2021; Rogan et al., 2018, see also chapter 3). Models for this species are explored in chapter 5. Locations of sightings within the study region are shown in Figure 1.7-6.

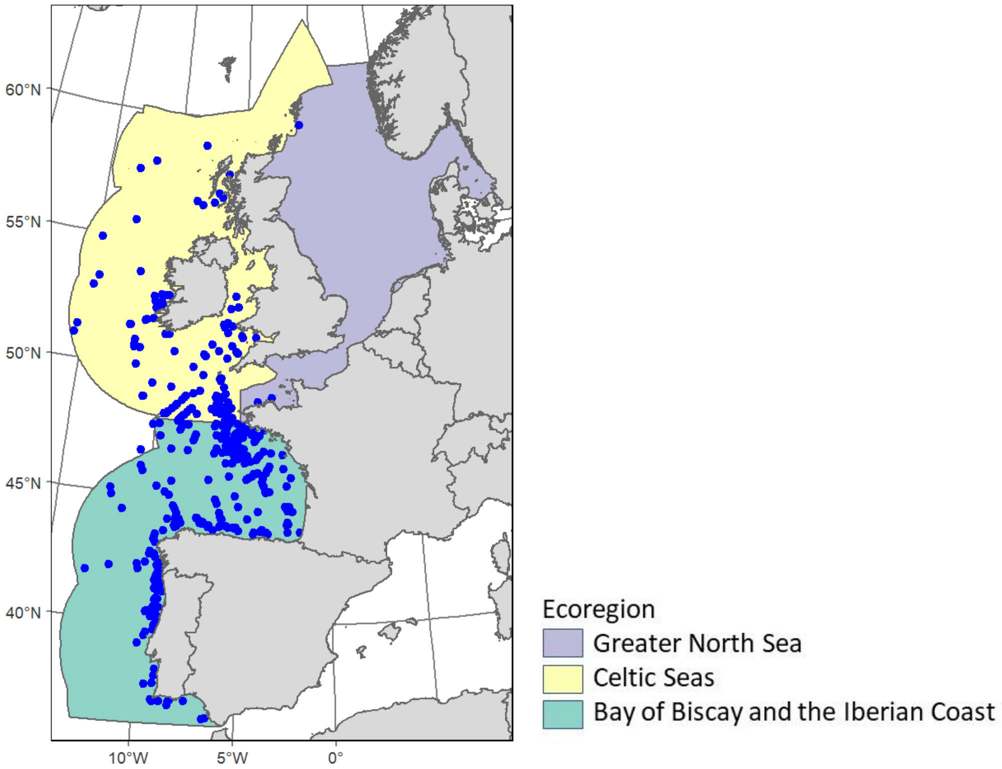

Figure 1.7-6 Locations of the combined common dolphin sightings (blue dots) seen during the surveys analysed in this thesis (SCANS-II, CODA, SCANS-III and ObSERVE), showing where they were most commonly recorded in relation to the three ecoregions modelled in chapters 4 and 5.

1.7.7 Striped dolphin – *Stenella coereualba*

Striped dolphins are found worldwide, most commonly in warm waters. An oceanic dolphin, the species is most commonly found beyond the continental shelf, in waters over the slope and beyond. Most of their records come from waters of 18^{0}C -22^{0}C The northern limit of distribution appears to be linked to the northern extent of the Gulf Stream. Striped dolphin distribution extends well past the southern extent of the study region into waters surrounding South Africa (Archer, 2018). Mean group size from the SCANS-III survey was 27.2 animals (Hammond et al., 2021), and abundance across the region was estimated as 441,455 (Hammond et al., 2021; Rogan et al., 2018, see also chapter 3).

It is thought that striped dolphins feed at depths of between 200-700m (Archer and Perrin, 1999), with the majority of feeding activity potentially taking place at night or at dusk (Ringelstein et al., 2006) when prey items may be migrating closer to the surface. Stomach content analysis of stranded animals from the Bay of Biscay has revealed a diet of fish, cephalopods and crustaceans, with lanternfish featuring prominently along with *Teuthowenia megalops* and *Histioteuthis* spp of squid (Archer and Perrin, 1999).

Striped dolphins are known to be able to utilise prey resources from a variety of different habitats, including neritic and coastal prey species as well as the more usual oceanic prey (Spitz et al., 2006). Models for this species are explored in chapter 5. Locations of sightings within the study region are shown in Figure 1.7-7.

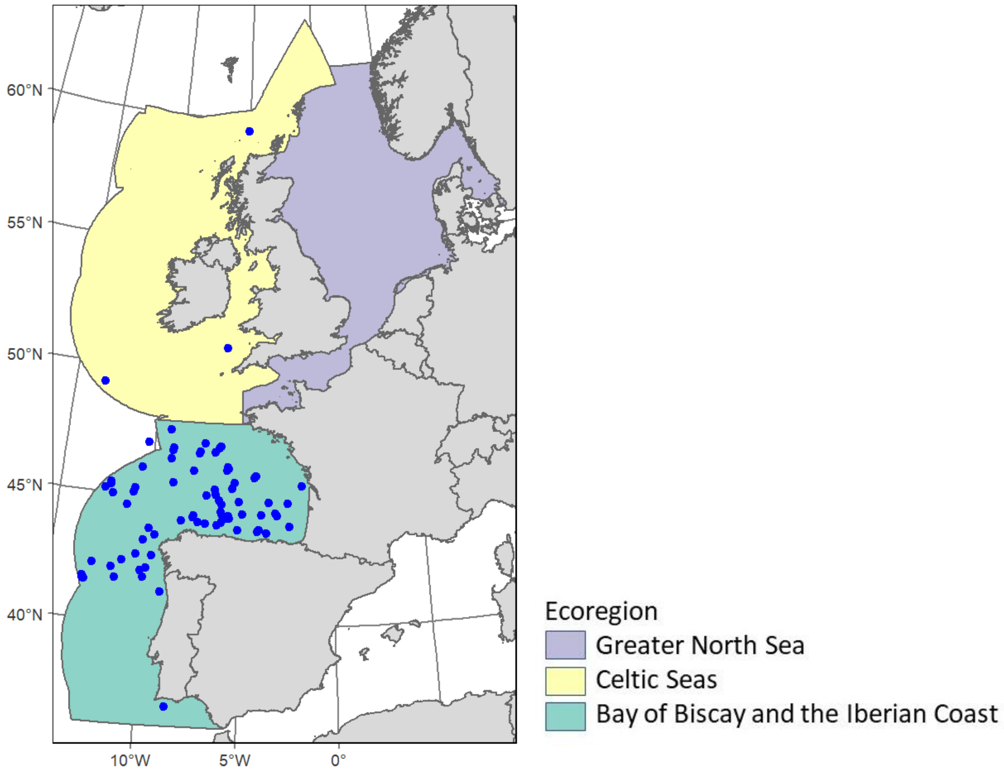

Figure 1.7-7 Locations of the combined striped dolphin sightings (blue dots) seen during the surveys analysed in this thesis (SCANS-II, CODA, SCANS-III and ObSERVE), showing where they were most commonly recorded in relation to the three ecoregions modelled in chapters 4 and 5.

1.7.8 Fin whale – *Balaenoptera physalis*

Fin whales are a cosmopolitan species and can be found from tropical to polar regions in most of the worlds large water masses (Edwards et al., 2015), with density tending to be higher beyond the continental shelf (Aguilar and García-Vernet, 2018), and most records from the study region occur in waters 400m-2000m deep (Evans, 2020). Fin whales have been associated with areas of high seabed rugosity, and areas of high zooplankton concentration (Ingram et al., 2007; Skern-Mauritzen et al., 2009). Like most baleen whale species, fin whales feed primarily in the summer and fast during the winter months. However, the geographical extent of the migration of animals in the North Atlantic is less well defined than in other areas, and it has been suggested that because of the influence of the Gulf Stream, higher latitudes are suitable as wintering grounds than would be the case elsewhere (Aguilar and García-Vernet, 2018). Alternatively, individuals may concentrate near the coast during feeding season, then move further offshore during the winter which would account for the lower number of recordings during winter months (Aguilar and García-Vernet, 2018). Certainly there are recordings from the study region year round (Reid et al., 2003; Wall et al., 2013). Mean group size from the SCANS-III survey was 1.37 animals (Hammond et al., 2021). Abundance of this species across the region was estimated as 27, 388 (Hammond et al., 2021; Rogan et al., 2018, see also chapter 3). Models for this species are explored in chapter 5. Locations of sightings within the study region are shown in Figure 1.7-8.

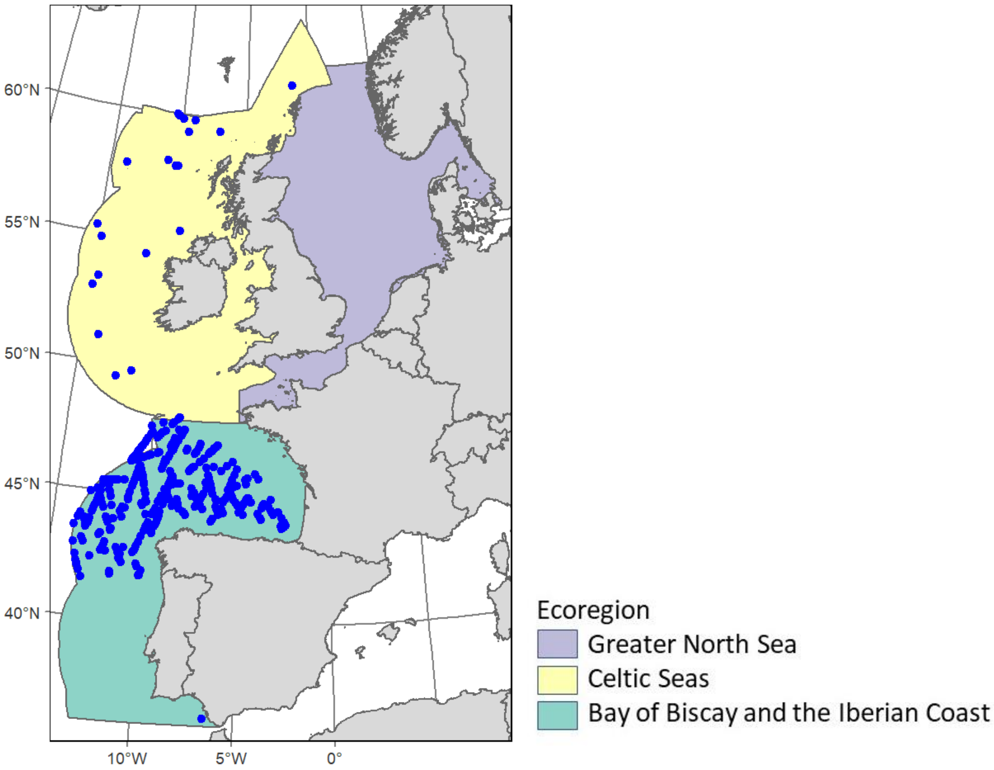

Figure 1.7-8 Locations of the combined fin whale sightings (blue dots) seen during the surveys analysed in this thesis (SCANS-II, CODA, SCANS-III and ObSERVE), showing where they were most commonly recorded in relation to the three ecoregions modelled in chapters 4 and 5.

1.8 Thesis goals and structure

This thesis is a modelling study of cetaceans in European Atlantic waters, using data collected from large scale, international surveys, namely the SCANS series of surveys (P. Hammond et al., 2021; P. S. Hammond et al., 2013, 2002), and the ObSERVE survey in Irish waters (Rogan et al., 2018).

Chapter 2 describes the field methods used for data collection across surveys, the data processing methods used to ensure modelled data were handled in a standardized fashion, the covariates used and the modelling process itself. I was cruise leader for the UK SCANS-III survey ship, which collected data for 6 weeks off in the offshore blocks to the west of Scotland and in the Bay of Biscay. The remainder of the data used in this thesis were collected by others as part of the survey projects outlined above. All the data processing and modelling was done by me.

Chapter 3 provides a snapshot overview of the study region in its entirety. This chapter is intended to give context to other three data chapters by providing the most up-to-date abundance estimates and predicted distribution maps of the cetacean species which will be examined in more detail at an ecoregion scale. The objectives of this work are to provide indications of species distribution and then explore those using initial correlative models. This overview was part of the main SCANS-III project, more details of which can be found in Lacey et al., (2022), for which I conducted all the analysis. Although sharing an origin, this chapter contains slightly different work than that the SCANS-III reports, as these models also include data from the ObSERVE surveys, which are not included in Lacey et al., (2022). The geographical area covered by this chapter is shown in Figure 1.8-1.

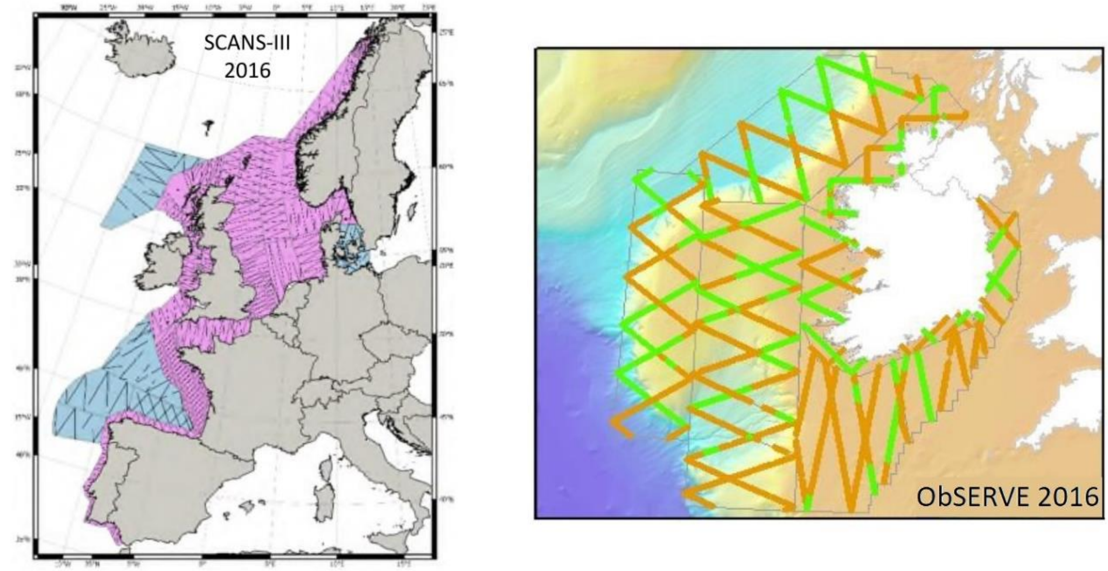

Figure 1.8-1: Completed effort for each of the main surveys for which data have been used. SCANS-II, CODA and SCANS-II data show arial survey blocks in pink, and ship survey blocks in blue. The ObSERVE map is taken from Figure 3.2 of Rogan et al., 2018. This is colour coded showing aerial effort achieved in different sea states, with seastate 1 shown in green, and seastate 2 shown in brown. All ObSERVE effort was aerial surveys.

Chapter 4 focuses on the North Sea ecoregion. It investigates the three most encountered cetacean species in the North Sea ecoregion, the harbour porpoise (*Phocoena phocoena*), minke whale (*Balaenoptera acutorostrata*), and white-beaked dolphin (*Lagenorhynchus albirostris*), using explanatory modelling including both environmental and prey data to investigate the factors driving the distribution of these three species within this ecoregion. The objectives of this work are to provide more detailed indications of species distribution within this specific ecoregion. These were then explored using initial correlative models. Combined year models aimed to identify any persistent relationships with covariates over time with the aim of these having better predictive capabilities. The geographical area covered by this chapter is shown in Figure 1.8-2

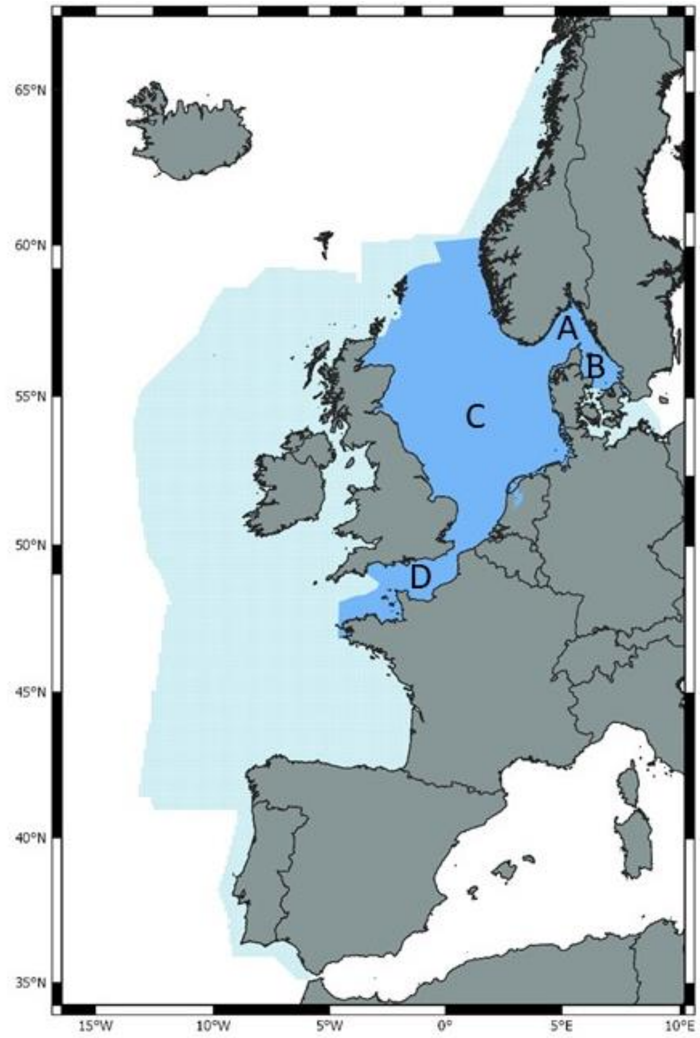

Figure 1.8-2: The Greater North Sea Ecoregion (dark blue) as defined by ICES, shown as a sub-region of the main SCANS/ObSERVE study area for which data are available. Named regions: A) Skagerrak, B), Kattegat, C) North Sea, D) English Channel.

Chapter 5 focuses on the species most encountered to the west of the UK and Ireland in the Celtic Seas, and Bay of Biscay & Iberian Coast ecoregions. Considered together because of the commonality of species across them, this chapter uses explanatory modelling to look at the environmental factors influencing the distribution of offshore bottlenose dolphin (*Tursiops truncatus*), Atlantic white-sided dolphin (*Lagenorhynchus acutus*), common dolphin (*Delphinus delphis*), striped dolphin (*Stenella coeruleoalba*), and fin whale (*Balaenoptera physalus*) in these two ecoregions. As with chapter 4, the objectives of this work are to provide more detailed indications of species distribution within this specific ecoregion. These were then explored using initial correlative models. Combined year models aimed to identify any persistent relationships with covariates over time with the aim of these having better predictive capabilities. The geographical area covered by this chapter is shown in Figure 1.8-3

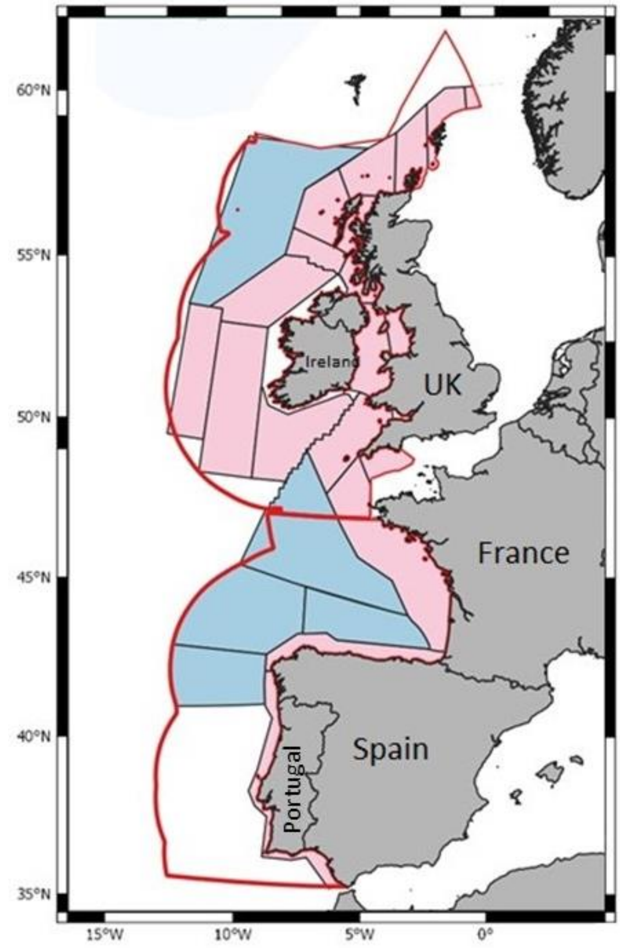

Figure 1.8-3: Location of the Celtic Sea ecoregion (top area with red boundary) and the Bay of Biscay ecoegion (lower area with red boundary) in comparison to the 2016 survey areas. Areas surveyd by ship are shown in blue, and areas survey by air are shown in pink.

Chapter 6 (general discussion) provides a final summary of the thesis results, before placing these into a wider context.

1.9 Literature Cited

Aguilar, A., García-Vernet, R., 2018. Fin Whale, in: Encyclopedia of Marine Mammals. Elsevier, pp. 368–371. https://doi.org/10.1016/B978-0-12-804327-1.00128-X

Anderwald, P., Evans, P.G.H., 2007. Minke whale populations in the North Atlantic: An overview with special reference to UK waters, in: An Integrated Approach to Non-Lethal Research on Minke Whales in European Waters, ECS Special Publication Series. San Sebastian, pp. 8–13.

Andreasen, H., Ross, S.D., Siebert, U., Andersen, N.G., Ronnenberg, K., Gilles, A., 2017. Diet composition and food consumption rate of harbor porpoises (*Phocoena phocoena*) in the western Baltic Sea. Mar. Mammal Sci. 33, 1053–1079. https://doi.org/10.1111/mms.12421

Archer, F.I., 2018. Striped Dolphin, in: Encyclopedia of Marine Mammals. Elsevier, pp. 954–956. https://doi.org/10.1016/B978-0-12-804327-1.00251-X

Archer, F.I., Perrin, W.F., 1999. *Stenella coeruleoalba*. Mamm. Species 603, 1–9.

Arso Civil, M., 2014. Population Ecology of Bottlenose Dolphins (Tursiops truncatus) off the East Coast of Scotland. University of St Andrews.

Austin, M.P., 2002. Spatial prediction of species distribution: an interface between ecological theory and statistical modelling. Ecol. Model. 157, 101–118. https://doi.org/10.1016/S0304-3800(02)00205-3

Authier, M., Commanducci, F.D., Genov, T., Holcer, D., Ridoux, V., Salivas, M., Santos, M.B., Spitz, J., 2017. Cetacean conservation in the Mediterranean and Black Seas: Fostering transboundary collaboration through the European Marine Strategy Framework Directive. Mar. Policy 82, 98–103. https://doi.org/10.1016/j.marpol.2017.05.012

Azzellino, A., Gaspari, S., Airoldi, S., Nani, B., 2008. Habitat use and preferences of cetaceans along the continental slope and the adjacent pelagic waters in the western Ligurian Sea. Deep Sea Res. Part Oceanogr. Res. Pap. 55, 296–323. https://doi.org/10.1016/j.dsr.2007.11.006

Azzellino, A., Panigada, S., Lanfredi, C., Zanardelli, M., Airoldi, S., Notarbartolo di Sciara, G., 2012. Predictive habitat models for managing marine areas: Spatial and temporal distribution of marine mammals within the Pelagos Sanctuary (Northwestern Mediterranean Sea). Ocean Coast. Manag. 67, 63–74. https://doi.org/10.1016/j.ocecoaman.2012.05.024

Baines, M., Kelly, N., Reichelt, M., Lacey, C., Pinder, S., Fielding, S., Murphy, E., Trathan, P., Biuw, M., Lindstrøm, U., Krafft, B., Jackson, J., 2021. Population abundance of recovering humpback whales (Megaptera novaeangliae) and other baleen whales in the Scotia Arc, South Atlantic. Mar. Ecol. Prog. Ser. https://doi.org/10.3354/meps13849

Barros, N.B., Odell, D.K. 1989. Food Habits of Bottlenose Dolphins in the Southeastern United States. S. Leatherwood, R.R. Reeves (Eds.), The bottlenose dolphin, Academic Press, New York, pp. 309-328

Becker, E.A., 2021. Habitat-based density estimates for cetaceans within the waters of the U.S. Exclusive Economic Zone around the Hawaiian Archipelago. https://doi.org/10.25923/X9Q9-RD73

Becker, E.A., Carretta, J.V., Forney, K.A., Barlow, J., Brodie, S., Hoopes, R., Jacox, M.G., Maxwell, S.M., Redfern, J.V., Sisson, N.B., Welch, H., Hazen, E.L., 2020. Performance evaluation of cetacean species distribution models developed using generalized additive models and boosted regression trees. Ecol. Evol. 10, 5759–5784. https://doi.org/10.1002/ece3.6316

Becker, E.A., Forney, K.A., Redfern, J.V., Barlow, J., Jacox, M.G., Roberts, J.J., Palacios, D.M., 2019. Predicting cetacean abundance and distribution in a changing climate. Divers. Distrib. 25, 626–643. https://doi.org/10.1111/ddi.12867

Begon, M., Townsend, C.R., Harper, J.L., 2006. Ecology: from individuals to ecosystems, 4th ed. ed. Blackwell Pub, Malden, MA.

Benoit-Bird, K.J., Au, W.W.L., 2003. Prey dynamics affect foraging by a pelagic predator (*stenella longirostris*) over a range of spatial and temporal scales. Behav. Ecol. Sociobiol. 53, 364–373. https://doi.org/10.1007/s00265-003-0585-4

Benoit-Bird, K.J., Battaile, B.C., Heppell, S.A., Hoover, B., Irons, D., Jones, N., Kuletz, K.J., Nordstrom, C.A., Paredes, R., Suryan, R.M., Waluk, C.M., Trites, A.W., 2013. Prey Patch Patterns Predict Habitat Use by Top Marine Predators with Diverse Foraging Strategies. PLoS ONE 8, e53348. https://doi.org/10.1371/journal.pone.0053348

Bjørge, A., Tolley, K.A., 2018. Harbor Porpoise, in: Encyclopedia of Marine Mammals. Elsevier, pp. 448–451. https://doi.org/10.1016/B978-0-12-804327-1.00144-8

Boisseau, O., Matthews, J., Gillespie, D., Lacey, C., Moscrop, A., Ouamari, N.E., 2007. A visual and acoustic survey for harbour porpoises off North-West Africa: further evidence of a discrete population. Afr. J. Mar. Sci. 29, 403–410. https://doi.org/10.2989/AJMS.2007.29.3.8.338

Booth, C., Embling, C., Gordon, J., Calderan, S., Hammond, P., 2013. Habitat preferences and distribution of the harbour porpoise *Phocoena phocoena* west of Scotland. Mar. Ecol. Prog. Ser. 478, 273–285. https://doi.org/10.3354/meps10239

Bøthun, G., Skaug, H.J., Øien, N.I., 2009. Abundance of minke whales in the Northeast Atlantic based on survey data collected over the period 2002-2007 (Report to the Sceintific Committe of the IWC No. SC/61/RMP 2).

Branch, T.A., Butterworth, D.S., 2001a. Southern Hemisphere minke whales: standardised abundance estimates from the 1978/79 to 1997/98 IDCR-SOWER surveys. J. Cetacean Res. Manag. 3, 143–174.

Branch, T.A., Butterworth, D.S., 2001b. Estimates of abundance south of 60° S for cetacean species sighted frequently on the 1978/79 to 1997/98 IWC/IDCR-SOWER sighting surveys. J. Cetacean Res. Manag. 3, 251–270.

Breen, P., Brown, S., Reid, D., Rogan, E., 2016. Modelling cetacean distribution and mapping overlap with fisheries in the northeast Atlantic. Ocean Coast. Manag. 134, 140–149. https://doi.org/10.1016/j.ocecoaman.2016.09.004

Buckland, S.T., 2001. Introduction to Distance Sampling - Estimating Abundance of Biological Populations. Oxford University Press.

Buckland, S.T., Cattanach, K.L., 1992a. Fin Whale Abundance in the North Atlantic, Estimated from Icelandic and Faroese NASS-87 and NASS-89 Data, in: Report of the International Whaling Commission, Vol 42. International Whaling Commission, Cambridge, pp. 645–651.

Buckland, S.T., Cattanach, K.L., 1992b. Fin Whale Abundance in the Eastern North Atlantic, Estimated from Spanish NASS-89 Data, in: Reports of the International Whaling Commission 42. International Whaling Commission, Cambridge, pp. 457–460.

Buckland, S.T., Rexstad, E.A., Marques, T.A., Oedekoven, C.S., 2015. Distance Sampling: Methods and Applications, Methods in Statistical Ecology. Springer International Publishing, Cham. https://doi.org/10.1007/978-3-319-19219-2

Cañadas, A., Sagarminaga, R., De Stephanis, R., Urquiola, E., Hammond, P.S., 2005. Habitat preference modelling as a conservation tool: proposals for marine protected areas for cetaceans in southern Spanish waters. Aquat. Conserv. Mar. Freshw. Ecosyst. 15, 495–521. https://doi.org/10.1002/aqc.689

Cañadas, Ana, Sagarminaga, R., García-Tiscar, S., 2002. Cetacean distribution related with depth and slope in the Mediterranean waters off southern Spain 49, 2053–2073. https://doi.org/10.1016/s0967-0637(02)00123-1

Canning, S.J., Santos, M.B., Reid, R.J., Evans, P.G.H., Sabin, R.C., Bailey, N., Pierce, G.J., 2008. Seasonal distribution of white-beaked dolphins (Lagenorhynchus *albirostris*) in UK waters with new information on diet and habitat use. J. Mar. Biol. Assoc. U. K. 88, 1159–1166. https://doi.org/10.1017/S0025315408000076

Cattanach, K.L., Sigurjónsson, J., Buckland, S.T., Gunnlaugsson, T., 1993. Sei Whale Abundance in the North Atlantic, Estimated from NASS-87 and NASS-89 Data, in: Report of the International Whaling Commission. Vol 43. International Whaling Commission, Cambridge, pp. 315–321.

Cetacean and Turtle Assessment Program (CETAP). 1982. A characterization of marine mammals and turtles in the Mid- and North-Atlantic areas of the U.S. outer continental shelf. Final report, contract AA551-CT8-48. Bureau of Land Management, Washington, DC.

Cheney, B., Corkrey, R., Durban, J.W., Grellier, K., Hammond, P.S., Islas-Villanueva, V., Janik, V.M., Lusseau, S.M., Parsons, K.M., Quick, N.J., Wilson, B., Thompson, P.M., 2014. Long-term trends in the use of a protected area by small cetaceans in relation to changes in population status. Glob. Ecol. Conserv. 2, 118–128. https://doi.org/10.1016/j.gecco.2014.08.010

Cheney, B., Thompson, P.M., Ingram, S.N., Hammond, P.S., Stevick, P.T., Durban, J.W., Culloch, R.M., Elwen, S.H., Mandleberg, L., Janik, V.M., Quick, N.J., Islas-Villanueva, V., Robinson, K.P., Costa, M., Eisfeld, S.M., Walters, A., Phillips, C., Weir, C.R., Evans, P.G.H., Anderwald, P., Reid, R.J., Reid, J.B., Wilson, B., 2013. Integrating multiple data sources to assess the distribution and abundance of bottlenose dolphins Tursiops truncatus in Scottish waters. Mammal Rev. 43, 71–88. https://doi.org/10.1111/j.1365-2907.2011.00208.x

Chivers, S.J., 2009. Cetacean Life History, in: Encyclopedia of Marine Mammals. Elsevier, pp. 215–220.

CIEEM, 2018. Guidelines for ecological impact assessment in the UK and Ireland. Terrestrial, Freshwater, Coastal and Marine. (No. Version 1.2; Updated April 2022).

Cipriano, F., 2018. Atlantic White-Sided Dolphin, in: Encyclopedia of Marine Mammals. Elsevier, pp. 42–44. https://doi.org/10.1016/B978-0-12-804327-1.00051-0

Claro, B., Pérez-Jorge, S., Frey, S., 2020. Seafloor geomorphic features as an alternative approach into modelling the distribution of cetaceans. Ecol. Inform. 58, 101092. https://doi.org/10.1016/j.ecoinf.2020.101092

Correia, A., M., Sousa-Guedes, D., Gil, Á., Valente, R., Rosso, M., Sousa-Pinto, I., Sillero, N., Pierce, G.J., 2021. Predicting Cetacean Distributions in the Eastern North Atlantic to Support Marine Management. Front. Mar. Sci. https://doi.org/10.3389/fmars.2021.643569

Craddock, J.E., Polloni, P.T., Hayward, B., Wenzel, F.W., 2009. Food habits of Atlantic white-sided dolphins (Lagenorhynchus *acutus*) off the coast of New England. Fish. Bull. 107, 384–394.

Dalpadado, P., 2000. Food and feeding conditions of Norwegian spring-spawning herring (*Clupea harengus*) through its feeding migrations. ICES J. Mar. Sci. 57, 843–857. https://doi.org/10.1006/jmsc.2000.0573

Davis, R.W., Ortega-Ortiz, J.G., Ribic, C.A., Evans, W.E., Biggs, D.C., Ressler, P.H., Cady, R.B., Leben, R.R., Mullin, K.D., Würsig, B., 2002. Cetacean habitat in the northern oceanic Gulf of Mexico. Deep Sea Res. Part Oceanogr. Res. Pap. 49, 121–142. https://doi.org/10.1016/S0967-0637(01)00035-8

Edwards, E.F., Hall, C., Moore, T.J., Sheredy, C., Redfern, J.V., 2015. Global distribution of fin whales *Balaenoptera physalus* in the post-whaling era (1980–2012). Mammal Rev. 45, 197–214. https://doi.org/10.1111/mam.12048

Elith, J., Leathwick, J.R., 2009. Species Distribution Models: Ecological Explanation and Prediction Across Space and Time. Annu. Rev. Ecol. Evol. Syst. 40, 677–697. https://doi.org/10.1146/annurev.ecolsys.110308.120159

Embling, C.B., Gillibrand, P.A., Gordon, J., Shrimpton, J., Stevick, P.T., Hammond, P.S., 2010. Using habitat models to identify suitable sites for marine protected areas for harbour porpoises (*Phocoena phocoena*). Biol. Conserv. 143, 267–279. https://doi.org/10.1016/j.biocon.2009.09.005

Evans, P.G.H., 2020. European Whales, Dolphins and Porpoises. Marine Mammal Conservation in Practice., ASCOBANS. Academic Press.

Fernandez, E., Lellouche, J.M., 2021. Product User Manual: For the Global Ocean Physical Reanalysis Product Global_Reanalysis_Phy_001_030 (No. 1.2).

Forney, K., Becker, E., Foley, D., Barlow, J., Oleson, E., 2015. Habitat-based models of cetacean density and distribution in the central North Pacific. Endanger. Species Res. 27, 1–20. https://doi.org/10.3354/esr00632

Forney, K.A., 2000. Environmental Models of Cetacean Abundance: Reducing Uncertainty in Population Trends. Conserv. Biol. 14, 1271–1286. https://doi.org/10.1046/j.1523-1739.2000.99412.x

Gilles, A., Viquerat, S., Becker, E.A., Forney, K.A., Geelhoed, S.C.V., Haelters, J., Nabe-Nielsen, J., Scheidat, M., Siebert, U., Sveegaard, S., Beest, F.M., Bemmelen, R., Aarts, G., 2016. Seasonal habitat-based density models for a marine top predator, the harbor porpoise, in a dynamic environment. Ecosphere 7. https://doi.org/10.1002/ecs2.1367

Godø, O.R., Samuelsen, A., Macaulay, G.J., Patel, R., Hjøllo, S.S., Horne, J., Kaartvedt, S., Johannessen, J.A., 2012. Mesoscale Eddies Are Oases for Higher Trophic Marine Life. PLoS ONE 7, e30161. https://doi.org/10.1371/journal.pone.0030161

Gonzalez-Pola, C., Larsen, K.M.H., Fratantoni, P., Beszczynska-Möller, A. (Eds), 2018. ICES Report on Ocean Climate 2017 (ICES Cooperative Research Report No. Special Issue #345). ICES. 119pp.

Guisan, A., Thuiller, W., 2005. Predicting species distribution: offering more than simple habitat models. Ecol. Lett. 8, 993–1009. https://doi.org/10.1111/j.1461-0248.2005.00792.x

Guisan, A., Zimmermann, N.E., 2000. Predictive habitat distribution models in ecology. Ecol. Model. 135, 147–186. https://doi.org/10.1016/S0304-3800(00)00354-9

Halpern, B.S., Frazier, M., Afflerbach, J., Lowndes, J.S., Micheli, F., O'Hara, C., Scarborough, C., Selkoe, K.A., 2019. Recent pace of change in human impact on the world's ocean. Sci. Rep. 9, 11609. https://doi.org/10.1038/s41598-019-47201-9

Halpern, B.S., Frazier, M., Potapenko, J., Casey, K.S., Koenig, K., Longo, C., Lowndes, J.S., Rockwood, R.C., Selig, E.R., Selkoe, K.A., Walbridge, S., 2015. Spatial and temporal changes in cumulative human impacts on the world's ocean. Nat. Commun. 6, 7615. https://doi.org/10.1038/ncomms8615

Hammond, P., Lacey, C., Gilles, A., Viquerat, S., Börjesson, P., Herr, H., Macleod, K., Ridoux, V., Santos, M., Teilmann, J., Vingada, J., Øien, N., 2021. Estimates of cetacean abundance in European Atlantic waters in summer 2016 from the SCANS-III aerial and shipboard surveys. Final project report. https://scans3.wp.st-andrews.ac.uk/files/2021/06/SCANS-III_design-based_estimates_final_report_revised_June_2021.pdf

Hammond, P., Macleod, K., Gillespie, D., Swift, R., Winship, A., Burt, M., Cañadas, A., Vázquez, J., Ridoux, V., Certain, G., Canneyt, O.V., Lens, S., Santos, B., Rogan, E., Uriarte, A., Hernandez, C., Castro, R., 2009. Cetacean Offshore Distribution and Abundance in the European Atlantic (CODA). Final project report. http://biology.st-andrews.ac.uk/coda/

Hammond, P.S., Berggren, P., Benke, H., Borchers, D.L., Collet, A., Heide-Jørgensen, M.P., Heimlich, S., Hiby, a. R.R., Leopold, M.F.F., Øien, N., 2002. Abundance of harbour porpoise and other cetaceans in the North Sea and adjacent waters. J. Appl. Ecol. 39, 361–376. https://doi.org/10.1046/j.1365-2664.2002.00713.x

Hammond, P. S., Berggren, P., Benke, H., Borchers, D.L., Collet, A., Jørgensen, M.P.H.-, Heimlich, S., Hiby, A.R., Leopold, M.F., Øien, N., 2002. Abundance of Harbour Porpoise and Other Cetaceans in the North Sea and Adjacent Waters. J. Appl. Ecol. 39, 361–376.

Hammond, P.S., Francis, T.B., Heinemann, D., Long, K.J., Moore, J.E., Punt, A.E., Reeves, R.R., Sepúlveda, M., Sigurðsson, G.M., Siple, M.C., Víkingsson, G., Wade, P.R., Williams, R., Zerbini, A.N., 2021. Estimating the Abundance of Marine Mammal Populations. Front. Mar. Sci. 8, 735770. https://doi.org/10.3389/fmars.2021.735770

Hammond, Philip S., Macleod, K., Berggren, P., Borchers, D.L., Burt, L., Cañadas, A., Desportes, G., Donovan, G.P., Gilles, A., Gillespie, D., Gordon, J., Hiby, L., Kuklik, I., Leaper, R., Lehnert, K., Leopold, M., Lovell, P., Øien, N., Paxton, C.G.M., Ridoux, V., Rogan, E., Samarra, F., Scheidat, M., Sequeira, M., Siebert, U., Skov, H., Swift, R., Tasker, M.L., Teilmann, J., Van Canneyt, O., Vázquez, J.A., 2013. Cetacean abundance and distribution in European Atlantic shelf waters to inform conservation and management. Biol. Conserv. 164, 107–122. https://doi.org/10.1016/j.biocon.2013.04.010

Hansen, R.G., Heide-Jørgensen, M.P., 2013. Spatial trends in abundance of long-finned pilot whales, white-beaked dolphins and harbour porpoises in West Greenland. Mar. Biol. 160, 2929–2941. https://doi.org/10.1007/s00227-013-2283-8

Hastie, G.D., Wilson, B., Thompson, P.M., 2006. Diving deep in a foraging hotspot: acoustic insights into bottlenose dolphin dive depths and feeding behaviour. Mar. Biol. 148, 1181–1188. https://doi.org/10.1007/s00227-005-0143-x

Hedley, S.L., Buckland, S.T., 2004. Spatial models for line transect sampling. J. Agric. Biol. Environ. Stat. 9, 181–199. https://doi.org/10.1198/1085711043578

Heide-Jørgensen, M.P., Iversen, M., Nielsen, N.H., Lockyer, C., Stern, H., Ribergaard, M.H., 2011. Harbour porpoises respond to climate change. Ecol. Evol. 1, 579–585. https://doi.org/10.1002/ece3.51

Heide-jørgensen, M.P., Lassen, H., Teilmann, J., Davis, R.A., 1993. An index of the Relative Abundance of Wintering Belugas, Delphinapterus leucas, and narwhals, *Monodon monoceros*, off West Greenland. Can. J. Fish. Aquat. Sci. 50, 2323–2335.

Heide-jørgensen, M.P., Reeves, R.R., 1996. Evidence of a decline in beluga, *Delphinapterus leucas*, abundance off West Greenland. ICES J. Mar. Sci. 53, 61–72. https://doi.org/10.1006/jmsc.1996.0006

Hernandez-Milian, G., Begoña Santos, M., Reid, D., Rogan, E., 2016. Insights into the diet of Atlantic white-sided dolphins (Lagenorhynchus *acutus*) in the Northeast Atlantic. Mar. Mammal Sci. 32, 735–742. https://doi.org/10.1111/mms.12272

Hooker, S., Cañadas, A., Hyrenbach, K., Corrigan, C., Polovina, J., Reeves, R., 2011. Making protected area networks effective for marine top predators. Endanger. Species Res. 13, 203–218. https://doi.org/10.3354/esr00322

ICES, 2020a. ICES Ecoregions; Uses, rational and lessons learned. (No. ICES Advice Documents). https://www.ices.dk/advice/Documents/ICES_ecoregions_use_rationale_lessons_learned.pdf

ICES, 2020b. Greater North Sea Ecoregion - Ecosystem overview. ICES Advice. https://doi.org/10.17895/ICES.ADVICE.7632

Ingram, S.N., Walshe, L., Johnston, D., Rogan, E., 2007. Habitat partitioning and the influence of benthic topography and oceanography on the distribution of fin and minke whales in the Bay of Fundy, Canada. J. Mar. Biol. Assoc. U. K. 87, 149–156. https://doi.org/10.1017/S0025315407054884

Jansen, O.E., Leopold, M.F., Meesters, E.H.W.G., Smeenk, C., 2010. Are white-beaked dolphins *Lagenorhynchus albirostris* food specialists? Their diet in the southern North Sea. J. Mar. Biol. Assoc. U. K. 90, 1501–1508. https://doi.org/10.1017/S0025315410001190

Kanwisher, J.W., Ridgway, S.H., 1983. The Physiological Ecology of Whales and Porpoises. Sci. Am. 248, 110–120. https://doi.org/10.1038/scientificamerican0683-110

Kasamatsu, F., Joyce, G.G., 1995. Current status of Odontocetes in the Antarctic. Antarct. Sci. 7, 365–379. https://doi.org/10.1017/S0954102095000514

Kaschner, K., Quick, N.J., Jewell, R., Williams, R., Harris, C.M., 2012. Global Coverage of Cetacean Line-Transect Surveys: Status Quo, Data Gaps and Future Challenges. PLoS ONE 7, e44075. https://doi.org/10.1371/journal.pone.0044075

Kastelein, R.A., Vaughan, N., Walton, S., Wiepkema, P.R., 2002. Food intake and body measurements of Atlantic bottlenose dolphins (Tursiops truncates) in captivity. Mar. Environ. Res. 53, 199–218. https://doi.org/10.1016/S0141-1136(01)00123-4

Kavanagh, A.S., Kett, G., Richardson, N., Rogan, E., Jessopp, M.J., 2018. High latitude winter sightings of common minke whale calves (*Balaenoptera acutorostrata)* in the Northeast Atlantic. Mar. Biodivers. Rec. 11, 22. https://doi.org/10.1186/s41200-018-0157-y

Khanna, D., R, Bhutiani, R., Chandra, K.S., 2009. Effect of the euphotic depth and mixing dpeth on phytoplanktonic growth mechanism. Int J Env. Res 3, 223–228.

Kingsley, M.C.S., 2000. Numbers and distribution of beluga whales, *Delphinapterus leucas*, in James Bay, eastern Hudson Bay, and Ungava Bay in Canada during the summer of 1993. Fish. Bull. 98, 736–747.

Kinze, C.C., 2018. White-beaked Dolphin, in: Encyclopedia of Marine Mammals. Elsevier, pp. 1077–1079. https://doi.org/10.1016/B978-0-12-804327-1.00274-0

Klatsky, L.J., Wells, R.S., Sweeney, J.C., 2007. Offshore Bottlenose Dolphins (*Tursiops truncatus*): Movement and Dive Behavior Near the Bermuda Pedestal. J. Mammal. 88, 59–66. https://doi.org/10.1644/05-MAMM-A-365R1.1

Kvadsheim, P.H., DeRuiter, S., Sivle, L.D., Goldbogen, J., Roland-Hansen, R., Miller, P.J.O., Lam, F.-P.A., Calambokidis, J., Friedlaender, A., Visser, F., Tyack, P.L., Kleivane, L., Southall, B., 2017. Avoidance responses of minke whales to 1–4kHz naval sonar. Mar. Pollut. Bull. 121, 60–68. https://doi.org/10.1016/j.marpolbul.2017.05.037

Lacey, C., Gilles, A., Börjesson, P., Herr, H., Macleod, K., Ridoux, V., Santos, M.B., Scheidat, M., Teilmann, J., Vingada, J., Viquerat, S., Øien, N.I., and Hammond, P.S. 2022. Modelled density surfaces of cetaceans in European Atlantic waters in summer 2016 from the SCANS-III aerial and shipboard surveys. Project report. https://scans3.wp.st-andrews.ac.uk/files/2022/08/SCANS-III_density_surface_modelling_report_final_20220815.pdf 55pp.

Lambert, C., Mannocci, L., Lehodey, P., Ridoux, V., 2014. Predicting Cetacean Habitats from Their Energetic Needs and the Distribution of Their Prey in Two Contrasted Tropical Regions. PLoS ONE 9, e105958. https://doi.org/10.1371/journal.pone.0105958

Lambert, E., MacLeod, C., Hall, K., Brereton, T., Dunn, T., Wall, D., Jepson, P., Deaville, R., Pierce, G., 2011. Quantifying likely cetacean range shifts in response to global climatic change: implications for conservation strategies in a changing world. Endanger. Species Res. 15, 205–222. https://doi.org/10.3354/esr00376

Lambert, E., Pierce, G.J., Hall, K., Brereton, T., Dunn, T.E., Wall, D., Jepson, P.D., Deaville, R., MacLeod, C.D., 2014. Cetacean range and climate in the eastern North Atlantic: future predictions and implications for conservation. Glob. Change Biol. 20, 1782–1793. https://doi.org/10.1111/gcb.12560

Laran, S., Authier, M., Blanck, A., Doremus, G., Falchetto, H., Monestiez, P., Pettex, E., Stephan, E., Van Canneyt, O., Ridoux, V., 2017. Seasonal distribution and abundance of cetaceans within French waters- Part II: The Bay of Biscay and the English Channel. Deep Sea Res. Part II Top. Stud. Oceanogr. 141, 31–40. https://doi.org/10.1016/j.dsr2.2016.12.012

Learmonth, J.A., MacLeod, C.D., Santos, M.B., Pierce, G.J., Crick, H.Q.P., Robinson, R., A., 2006. Potential effects of climate change on marine mammals, in: Oceanography and Marine Biology: An Annual Review, Volume 44, Oceanography and Marine Biology - An Annual Review. CRC Press. https://doi.org/10.1201/9781420006391

Leopold, M.F., Begeman, L., van Bleijswijk, J.D.L., IJsseldijk, L.L., Witte, H.J., Gröne, A., 2015. Exposing the grey seal as a major predator of harbour porpoises. Proc. R. Soc. B Biol. Sci. 282, 20142429. https://doi.org/10.1098/rspb.2014.2429

Lockyer, C., Pike, D. (Eds.), 2009. North Atlantic Sightings Surveys: Counting whales in the North Atlantic 1987-2001, Scientific. ed. Tromso. No.

Louis, M., Viricel, A., Lucas, T., Peltier, H., Alfonsi, E., Berrow, S., Brownlow, A., Covelo, P., Dabin, W., Deaville, R., de Stephanis, R., Gally, F., Gauffier, P., Penrose, R., Silva, M.A., Guinet, C., Simon-Bouhet, B., 2014. Habitat-driven population structure of bottlenose dolphins, *Tursiops truncatus*, in the North-East Atlantic. Mol. Ecol. 23, 857–874. https://doi.org/10.1111/mec.12653

MacLeod, C.D., Weir, C.R., Santos, M.B., Dunn, T.E., 2008. Temperature-based summer habitat partitioning between white-beaked and common dolphins around the United Kingdom and Republic of Ireland. J. Mar. Biol. Assoc. U. K. 88, 1193–1198. https://doi.org/10.1017/S002531540800074X

Maravelias, C., 1997. Trends in abundance and geographic distribution of North Sea herring in relation to environmental factors. Mar. Ecol. Prog. Ser. 159, 151–164. https://doi.org/10.3354/meps159151

McMahon, T., 1995. Some oceanographic features of North-eastern Atlantic waters west of Ireland. ICES J. Mar. Sci. 52, 221–232. https://doi.org/10.1016/1054-3139(95)80037-9

Mead, J.G., Potter, C.W. 1989. Natural History of Bottlenose Dolphins along the Central Atlantic Coast of the United States. In. The Bottlenose Dolphin. Eds Leatherwood, S., Reeves, R. Academic Press, New York (1990) 165-196,

Meier, S., Falk-Petersen, S., Aage Gade-Sørensen, L., Greenacre, M., Haug, T., Lindstrøm, U., 2016. Fatty acids in common minke whale (*Balaenoptera acutorostrata*) blubber reflect the feeding area and food selection, but also high endogenous metabolism. Mar. Biol. Res. 12, 221–238. https://doi.org/10.1080/17451000.2015.1118513

Miller, D.L., Burt, M.L., Rexstad, E.A., Thomas, L., 2013. Spatial models for distance sampling data: recent developments and future directions. Methods Ecol. Evol. 4, 1001–1010. https://doi.org/10.1111/2041-210X.12105

Moura, A.E., Sillero, N., Rodrigues, A., 2012. Common dolphin (*Delphinus delphis)* habitat preferences using data from two platforms of opportunity. Acta Oecologica 38, 24–32. https://doi.org/10.1016/j.actao.2011.08.006

Nielsen, N., Teilmann, J., Sveegaard, S., Hansen, R., Sinding, M., Dietz, R., Heide-Jørgensen, M., 2018. Oceanic movements, site fidelity and deep diving in harbour porpoises from Greenland show limited similarities to animals from the North Sea. Mar. Ecol. Prog. Ser. 597, 259–272. https://doi.org/10.3354/meps12588

NMFS, 2021. 2020 Annual Report of a Comprehensive Assessment of Marine Mammal, Marine Turtle, and Seabird Abundance and Spatial Distribution in US waters of the Western North Atlantic Ocean – AMAPPS III.

Ó Cadhla, O., Mackey, M., Aguilar de Soto, N., Rogan, E. & Connolly, N. (2004). Cetaceans and Seabirds of Ireland's Atlantic Margin. Volume II – Cetacean distribution & abundance. Report on research carried out under the Irish Infrastructure Programme (PIP): Rockall Studies Group (RSG) projects 98/6 and 00/13, Porcupine Studies Group project P00/15 and Offshore Support Group (OSG) project 99/38. 82pp.

O'Hara, C.C., Afflerbach, J.C., Scarborough, C., Kaschner, K., Halpern, B.S., 2017. Aligning marine species range data to better serve science and conservation. PLOS ONE 12, e0175739. https://doi.org/10.1371/journal.pone.0175739

Oudejans, M.G., Visser, F., Englund, A., Rogan, E., Ingram, S.N., 2015. Evidence for Distinct Coastal and Offshore Communities of Bottlenose Dolphins in the Northeast Atlantic. PLOS ONE 10, e0122668. https://doi.org/10.1371/journal.pone.0122668

Palka, D., 1995. Abundance Estimate of the Gulf of Maine Harbor Porpoise. Rep. Int. Whal. Comm. SC/44/SM24, 27–50.

Palka, D.L., Chavez-Rosales, S., Josephson, E.A., Cholewiak, D., Haas, H.L., Garrison, L., Jones, M., Sigourney, D.B., Waring, G., Jech, M., Broughton, E., Soldevilla, M.S., Davis, G., DeAngelis, A., Sasso, C.R., Winton, M.V., Smolowitz, R.J., Fay, G., LaBrecque, E., Leiness, J.B., Detloff, M., Warden, M., Murray, K., Orphanides, C., 2017. Atlantic Marine Assessment Program for Protected Species: 2010 - 2014 (No. OCS Study BOWM 2017-071.). US Dept. of the Interior, Bureau of Ocean Energy Management, Atlantic OCS Region, Wahington, DC.

Pardo, M.A., Gerrodette, T., Beier, E., Gendron, D., Forney, K.A., Chivers, S.J., Barlow, J., Palacios, D.M., 2015. Inferring Cetacean Population Densities from the Absolute Dynamic Topography of the Ocean in a Hierarchical Bayesian Framework. PLOS ONE 10, e0120727. https://doi.org/10.1371/journal.pone.0120727

Paxton, C.G.M., Scott-Hayward, L., Mackenzie, M., Rexstad, E. & Thomas, L. (2016) Revised Phase III Data Analysis of Joint Cetacean Protocol Data Resource, JNCC Report No. 517, JNCC, Peterborough, ISSN 0963-8091.

Perrin, W.F., 2018. Common Dolphin, in: Encyclopedia of Marine Mammals. Elsevier, pp. 205–209. https://doi.org/10.1016/B978-0-12-804327-1.00095-9

Perrin, W.F., Mallette, S.D., Brownell, R.L., 2018. Minke Whales, in: Encyclopedia of Marine Mammals. Elsevier, pp. 608–613. https://doi.org/10.1016/B978-0-12-804327-1.00175-8

Pierce, G.J., Santos, M.B., Reid, R.J., Patterson, I.A.P., Ross, H.M., 2004. Diet of minke whales *Balaenoptera acutorostrata* in Scottish (UK) waters with notes on strandings of this species in Scotland 1992–2002. J. Mar. Biol. Assoc. U. K. 84, 1241–1244. https://doi.org/10.1017/S0025315404010732h

Pike, D., Gunnlaugsson, T., Sigurjonsson, J., Vikingsson, G., 2020. Distribution and Abundance of Cetaceans in Icelandic Waters over 30 Years of Aerial Surveys. NAMMCO Sci. Publ. 11. https://doi.org/10.7557/3.4805

Purdon, J., Shabangu, F.W., Yemane, D., Pienaar, M., Somers, M.J., Findlay, K., 2020. Species distribution modelling of Bryde's whales, humpback whales, southern right whales, and sperm whales in the southern African region to inform their conservation in expanding economies. PeerJ 8, e9997. https://doi.org/10.7717/peerj.9997

Pusineri, C., Magnin, V., Meynier, L., Spitz, J., Hassani, S., Ridoux, V., 2007. Food and Feeding Ecology of the Common Dolphin (*Delphinus delphis*) in the Oceanic Northeast Atlantic and Comparison with Its Diet in Neritic Areas. Mar. Mammal Sci. 23, 30–47. https://doi.org/10.1111/j.1748-7692.2006.00088.x

Ransijn, J.M., Booth, C.G., Smout, S., 2019. A calorific map of harbour porpoise prey in the North Sea (No. 633), JNCC Reports. Peterborough.

Rasmussen, M.H., Akamatsu, T., Teilmann, J., Vikingsson, G., Miller, L.A., 2013. Biosonar, diving and movements of two tagged white-beaked dolphin in Icelandic waters. Deep Sea Res. Part II Top. Stud. Oceanogr. 88–89, 97–105. https://doi.org/10.1016/j.dsr2.2012.07.011

Redfern, J.V., Ferguson, M.C., Becker, E.A., Hyrenbach, K.D., Good, C., Barlow, J., Kaschner, K., Baumgartner, M.F., Forney, K.A., Ballance, L.T., Fauchald, P., Halpin, P., Hamazaki, T., Pershing, A.J., Qian, S.S., Read, A., Reilly, S.B., Torres, L., Werner, F., 2006. Techniques for cetacean-habitat modeling. Mar Ecol Prog Ser 310, 271–295.

Reid, J.B., Evans, P.G.H., Northridge, S.P., 2003. Atlas of Cetacean distribution in north-west European waters 82.

Ringelstein, J., Pusineri, C., Hassani, S., Meynier, L., Nicolas, R., Ridoux, V., 2006. Food and feeding ecology of the striped dolphin, *Stenella coeruleoalba*, in the oceanic waters of the north-east Atlantic. J. Mar. Biol. Assoc. U. K. 86, 909–918. https://doi.org/10.1017/S0025315406013865

Risch, D., Castellote, M., Clark, C.W., Davis, G.E., Dugan, P.J., Hodge, L.E., Kumar, A., Lucke, K., Mellinger, D.K., Nieukirk, S.L., Popescu, C.M., Ramp, C., Read, A.J., Rice, A.N., Silva, M.A., Siebert, U., Stafford, K.M., Verdaat, H., 2014. Seasonal migrations of North Atlantic minke whales: novel insights from large-scale passive acoustic monitoring networks 17.

Roberts, J.J., Best, B.D., Mannocci, L., Fujioka, E., Halpin, P.N., Palka, D.L., Garrison, L.P., Mullin, K.D., Cole, T.V.N., Khan, C.B., McLellan, W.A., Pabst, D.A., Lockhart, G.G., 2016. Habitat-based cetacean density models for the U.S. Atlantic and Gulf of Mexico. Sci. Rep. 6, 22615. https://doi.org/10.1038/srep22615

Rogan, E., Breen, P., Mackey, M., Cañadas, A., Scheidat, M., Geelhoed, S., Jessopp, M., 2018. Aerial Surveys of Cetaceans and Seabirds in Irish waters: Occurrence, distribution and abundance in 2015-2017 298.

Rogan, E., Cañadas, A., Macleod, K., Santos, M.B., Mikkelsen, B., Uriarte, A., Van Canneyt, O., Vázquez, J.A., Hammond, P.S., 2017. Distribution, abundance and habitat use of deep diving cetaceans in the North-East Atlantic. Deep Sea Res. Part II Top. Stud. Oceanogr. 141, 8–19. https://doi.org/10.1016/j.dsr2.2017.03.015

Roman, J., Altman, I., Dunphy-Daly, M.M., Campbell, C., Jasny, M., Read, A.J., 2013. The Marine Mammal Protection Act at 40: status, recovery, and future of U.S. marine mammals. Ann. N. Y. Acad. Sci. 1286, 29–49. https://doi.org/10.1111/nyas.12040

Ryg, M., Lydersen, C., Knutsen, L., Bjørge, A., Smith, T.G., Øritsland, N.A., 1993. Scaling of insulation in seals and whales. J. Zool. Soc. Lond. 230, 193–206.

Scales, K.L., Miller, P., L., Hawkes, L.A., Ingram, S.N., Sims, D.W., Votier, S.C., 2014. On the Front Line: frontal zones as priority at-sea conservation areas for mobile marine vertebrates. J. Appl. Ecol. 51, 1575–1583.

Skern-Mauritzen, M., Skaug, H.J., Øien, N., 2009. Line transects, environmental data and GIS: Cetacean distribution, habitat and prey selection along the Barents Sea shelf edge. NAMMCO Sci. Publ. 7, 179. https://doi.org/10.7557/3.2713

Smith, S.I., 1868. The Geographical Distribution of Animals. Am. Nat. 2, 14–23. https://doi.org/10.1086/270176

Spitz, J., Richard, E., Meynier, L., Pusineri, C., Ridoux, V., 2006. Dietary plasticity of the oceanic striped dolphin, Stenella coeruleoalba, in the neritic waters of the Bay of Biscay. J. Sea Res. 55, 309–320.

Spitz, J., Trites, A.W., Becquet, V., Brind'Amour, A., Cherel, Y., Galois, R., Ridoux, V., 2012. Cost of Living Dictates what Whales, Dolphins and Porpoises Eat: The Importance of

Prey Quality on Predator Foraging Strategies. PLoS ONE 7, e50096. https://doi.org/10.1371/journal.pone.0050096

Stephenson, F., Goetz, K., Sharp, B.R., Mouton, T.L., Beets, F.L., Roberts, J., MacDiarmid, A.B., Constantine, R., Lundquist, C.J., 2020. Modelling the spatial distribution of cetaceans in New Zealand waters. Divers. Distrib. 26, 495–516. https://doi.org/10.1111/ddi.13035

Teilmann, J., Larsen, F., Desportes, G., 2023. Time allocation and diving behaviour of harbour porpoises (*Phocoena phocoena*) in Danish and adjacent waters. J Cetacean Res Manage 9, 201–210. https://doi.org/10.47536/jcrm.v9i3.668

Thomas, L., Buckland, S.T., Rexstad, E.A., Laake, J.L., Strindberg, S., Hedley, S.L., Bishop, J.R.B., Marques, T.A., Burnham, K.P., 2010. Distance software: design and analysis of distance sampling surveys for estimating population size. J. Appl. Ecol. 47, 5–14. https://doi.org/10.1111/j.1365-2664.2009.01737.x

Tynan, C.T., Ainley, D.G., Barth, J.A., Cowles, T.J., Pierce, S.D., Spear, L.B., 2005. Cetacean distributions relative to ocean processes in the northern California Current System. Deep Sea Res. Part II Top. Stud. Oceanogr. 52, 145–167. https://doi.org/10.1016/j.dsr2.2004.09.024

Víkingsson, G.A., Elvarsson, B.Þ., Ólafsdóttir, D., Sigurjónsson, J., Chosson, V., Galan, A., 2014. Recent changes in the diet composition of common minke whales *(Balaenoptera acutorostrata)* in Icelandic waters. A consequence of climate change? Mar. Biol. Res. 10, 138–152. https://doi.org/10.1080/17451000.2013.793812

Víkingsson, G.A., Heide-Jørgensen, M.P., 2015. First indications of autumn migration routes and destination of common minke whales tracked by satellite in the North Atlantic during 2001-2011. Mar. Mammal Sci. 31, 376–385. https://doi.org/10.1111/mms.12144

Virgili, A., Authier, M., Boisseau, O., Cañadas, A., Claridge, D., Cole, T.V.N., Peter Corkeron, Dorémus, G., David, L., Di-Méglio, N., Dunn, C., Dunn, T.E., García-Barón, I., Laran, S., Lauriano, G., Lewis, M., Louzao, M., Mannocci, L., Martínez-Cedeira, J., Palka, D.L., Panigada, S., Pettex, E., Roberts, J.J., Ruiz, L., Saavedra, C., Santos, M.B., Van Canneyt, O., Bonales, J.A.V., Monestiez, P., Ridoux, V., 2019. Combining multiple visual surveys to model the habitat of deep-diving cetaceans at the basin scale. Large-scale modelling of deep-diving cetacean habitats. Glob. Ecol. Biogeogr. 28, 300–314. https://doi.org/DOI: 10.1111/geb.12850

Wade, P.R., Gerrodette, T., 1993. Estimates of Cetacean Abundance and Distribution in the Eastern Tropical Pacific, in: Donovan, G.P. (Ed.), Report of the International Whaling Commission, No. 43. International Whaling Commission, Cambridge, pp. 477–493.

Wagner, H.H., Fortin, M.-J., 2005. Spatial Analysis of Landscapes: Concepts and Statistics. Ecology 86, 1975–1987. https://doi.org/10.1890/04-0914

Wall, D., Murray, C., O'Brien, J., Kavanagh, L., Wilson, C., Ryan, C., Glanville, B., Williams, D., Enlander, I., O'Connor, I., McGrath, D., Whooley, P., Berrow, S., 2013. Atlas of the Distribution and Relative Abundance of Marine Mammals in Irish Offshore Waters: 2005 – 201 65.

Waring, G.T., Josephson, E., Maze-Foley, K., Rosel, P.E., 2013. U. S. Atlantic and Gulf of Mexico Marine Mammal Stock Assessments - 2012.

Waring, G.T., Josephson, E., Maze-foley, K., Rosel, P.E., Byrd, B., Cole, T.V.N., Engleby, L., Garrison, L.P., Hatch, J., Henry, A., Horstman, S.C., Litz, J., Mullin, K.D., Orphanides, C., Pace, R.M., Palka, D.L., Lyssikatos, M.C., Wenzel, F.W., 2015. U.S. Atlantic and Gulf of Mexico Marine Mammal Stock Assessments - 2014.

Wells, R.S., Scott, M.D., 2018. Bottlenose Dolphin, *Tursiops Truncatus*, Common Bottlenose Dolphin, in: Encyclopedia of Marine Mammals. Elsevier, pp. 118–125. https://doi.org/10.1016/B978-0-12-804327-1.00072-8

Williamson, L.D., Scott, B.E., Laxton, M., Illian, J.B., Todd, V.L.G., Miller, P.I., Brookes, K.L., 2022. Comparing distribution of harbour porpoise using generalized additive models and hierarchical Bayesian models with integrated nested laplace approximation. Ecol. Model. 470, 110011. https://doi.org/10.1016/j.ecolmodel.2022.110011

Wisniewska, D.M., Johnson, M., Teilmann, J., Rojano-Doñate, L., Shearer, J., Sveegaard, S., Miller, L.A., Siebert, U., Madsen, P.T., 2016. Ultra-High Foraging Rates of Harbor Porpoises Make Them Vulnerable to Anthropogenic Disturbance. Curr. Biol. 26, 1441–1446. https://doi.org/10.1016/j.cub.2016.03.069

Wood, S.N., 2006. Generalized Additive Models: an introduction with R 397.

Worm, B., Sandow, M., Oschlies, A., Lotze, H.K., Myers, R.A., 2005. Global Patterns of Predator Diversity in the Open Oceans. Science 309, 1365–1369. https://doi.org/10.1126/science.1113399

Worthy, G.A.J., Edwards, E.F., 1990. Morphometric and Biochemical Factors Affecting Heat Loss in a Small Temperate Cetacean (*Phocoena phocoena*) and a Small Tropical Cetacean *(Stenella attenuata*). Physiol. Zool. 63, 432–442. https://doi.org/10.1086/physzool.63.2.30158506

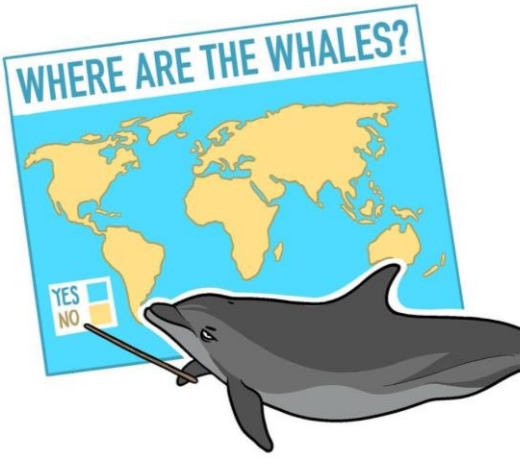

The truth is, they have no idea where the whales are.

WHALESBLOW [@WHALESBLOW] "BAD REVIEWS OF WHALE WATCHING – THE TRUTH". INSTAGRAM, JANUARY 3 2022. https://www.instagram.com/p/CYStVlzLBk

2 Methodology

This chapter outlines the data collection, data processing, and modelling methodologies used throughout this thesis. On occasions when different approaches were used, these are detailed in the relevant chapters. The environmental data used during the modelling process are also described. Results of the modelling are presented in chapters 3-5.

2.1 Data Sources

The cetacean data modelled in this thesis were all collected during the following large-scale, dedicated marine mammal surveys: the SCANS-II (Small Cetacean Abundance in the North Sea) survey, conducted during July of 2005 (Hammond et al. 2013); the CODA (Cetacean Offshore Distribution and Abundance) survey, conducted during July of 2007 (Hammond et al. 2009); the SCANS-III survey, conducted during July and the first half of August 2016 (Hammond et al. 2021) and the ObSERVE survey conducted during May, June and July of 2015 and 2016 (Rogan et al. 2018). The SCANS-II and SCANS-III surveys used a combination of ship and aerial platforms, whilst CODA used only ship-based, and ObSERVE used only aerial data collection methods. Survey design and field protocols are detailed in the literature cited above.

SCANS-II covered the North Sea and European Atlantic waters out to the edge of the continental shelf (Figure 2.1-1). The SCANS-III survey covered all the waters included in the CODA and SCANS-II surveys and extended the area north to include Norwegian coastal waters. However, Irish waters were not included in SCANS-III, instead being surveyed as part of the ObSERVE surveys. These surveys are summarised in Table 2.1-1. Completed effort achieved during each of these surveys is shown in Figure 2.1-3

Table 2.1-1 Dates and platform types of main data sources used within this thesis. NB, the ObSERVE surveys were conducted over a two-year period, in both summer and winter. Only the 2016 summer data were included for these analyses.

Survey name	Date	Platform	Figure	Primary citation
SCANS-II	June - July 2005 June - August 2005	Ship Aerial	Figure 2.1-1	Hammond et al. 2013
CODA	July 2007	Ship only	Figure 2.1-1	Hammond et al. 2009
SCANS-III	July2016 - August 2016 July2016 - August 2016	Ship Aerial	Figure 2.1-3	Hammond et al., 2021
ObSERVE	May 2016 to July 2016	Aerial only	Figure 2.1-3	Rogan et al. 2018

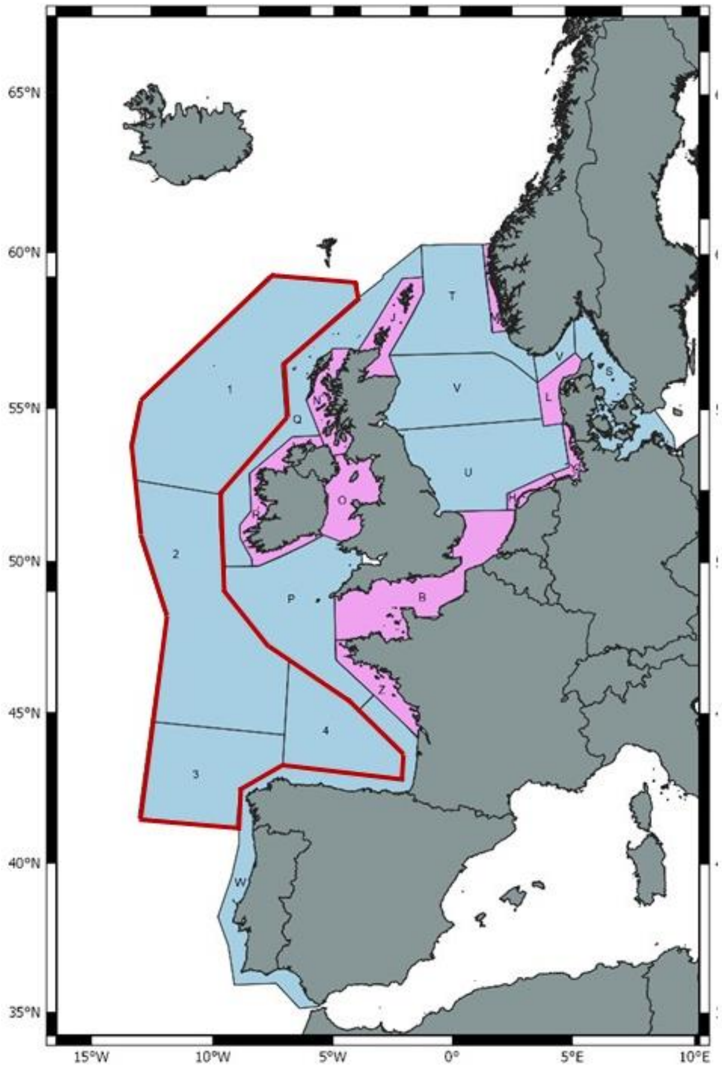

Figure 2.1-1 Survey blocks for the CODA (outlined in red, labelled 1-4) and SCANS-II (labelled with letters) surveys. Blue survey blocks were surveyed by ship. Blocks coloured pink were surveyed by aircraft.

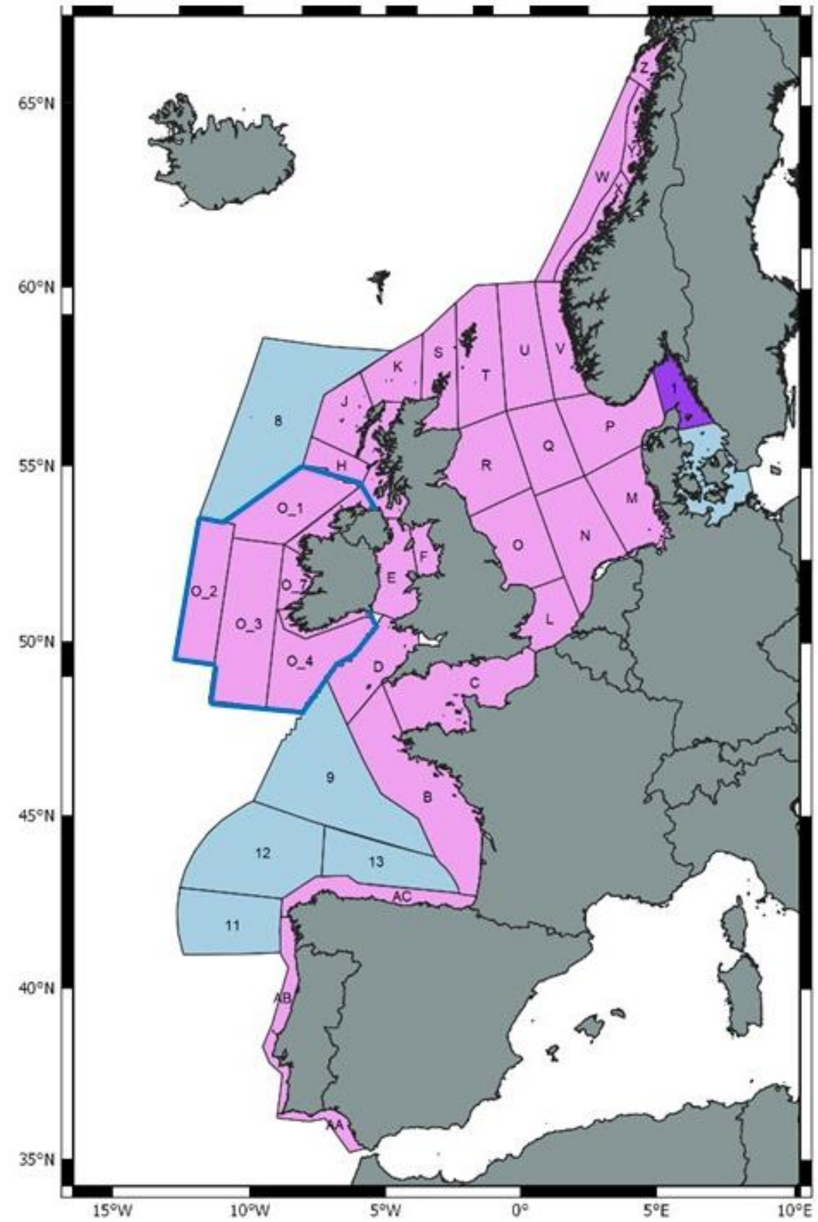

Figure 2.1-2: Survey blocks for the SCANS-III and ObSERVE (outlined in thick blue lines, labelled O_1-O_7) surveys. Blue survey blocks were surveyed by ship. Blocks coloured pink were surveyed by aircraft. SCANS-III blocks 1 was covered by both aerial and ship survey teams due to poor weather.

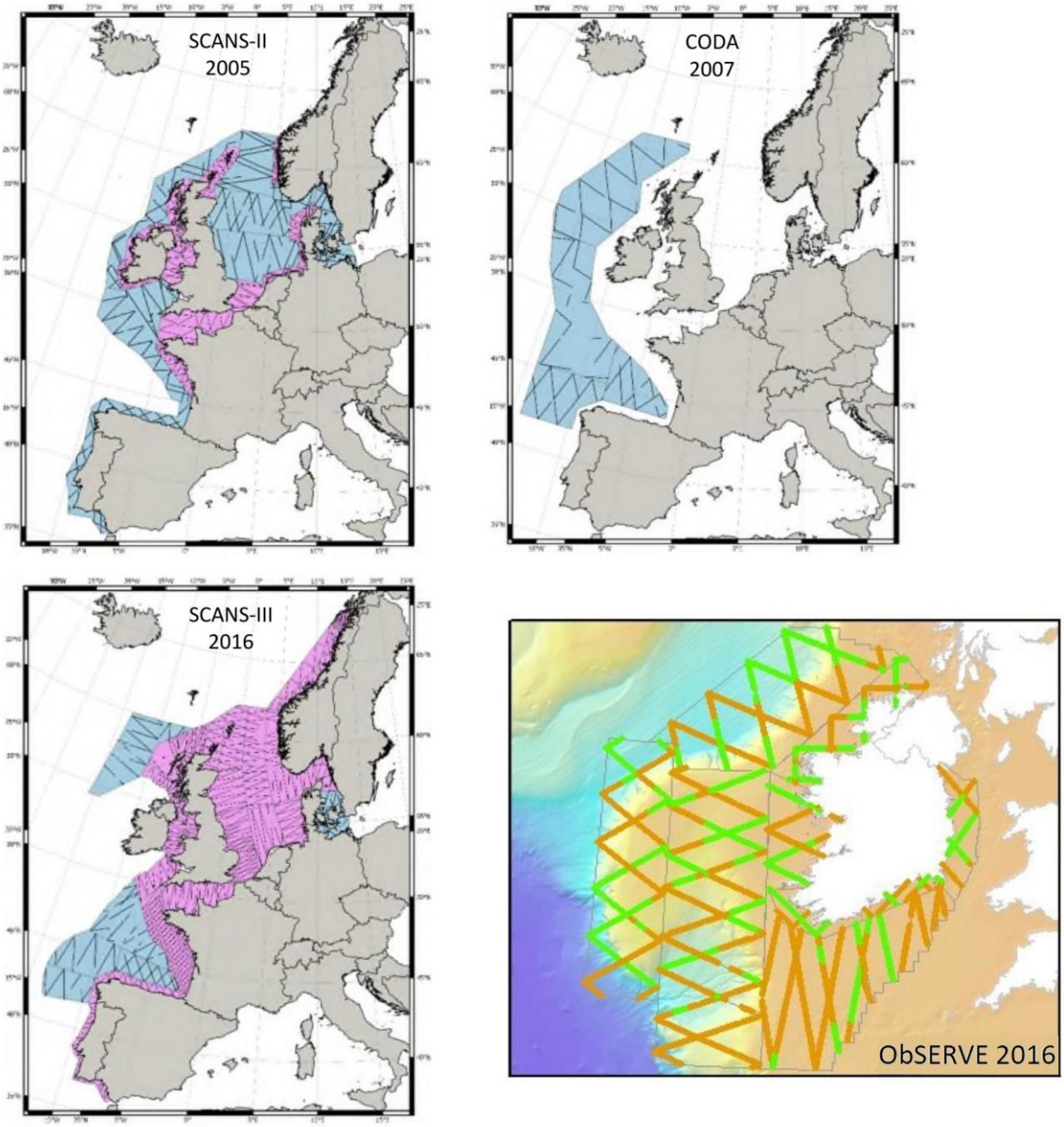

Figure 2.1-3: Completed effort for each of the main surveys for which data have been used. SCANS-II, CODA and SCANS-II data show arial survey blocks in pink, and ship survey blocks in blue. The ObSERVE map is taken from Figure 3.2 of Rogan et al., 2018. This is colour coded showing aerial effort achieved in different sea states, with seastate 1 shown in green, and seastate 2 shown in brown. All ObSERVE effort was aerial surveys.

2.1.1 Ship surveys

For SCANS-II, CODA and SCANS-III ship surveys Figure 2.1-1 & Figure 2.1-2, blue survey blocks), a double platform line transect survey was carried out in tracker configuration, in which there is one-way independence between the so-called "Tracker" and "Primary" teams on each ship (Hammond et al. 2009, 2013, 2021). The Primary team searched within 500m of the vessel using the naked eye. The Tracker team, situated higher on the vessel, searched from 500m to the horizon, using high-power (15x80) and 7x50 binoculars. This methodology generates data that allow abundance estimates to be corrected for animals missed on the transect line, g(0), and potentially for responsive movement (Laake and Borchers, 2004).

For all ships, target speed was 10 knots, although realised speed was slower when travelling into heavy swell. Observers worked in two teams of four people. The Tracker observers located animals as far ahead of the vessel as possible, then tracked the animals until they had passed abeam of the vessel. A "duplicate identifier" was assigned from the observers not currently on watch whose role was to assess whether groups of animals detected by the Tracker team were re-sighted by the Primary team. This person was located on or near (depending on ship configuration) the tracker platform, next to the data recorder, and was assessing duplicates in real time wherever possible. They were not conducting watches for animals themselves. Duplicates were defined as either "Definite" (at least 90% confident it was a duplicate), "Probable" (between 50% and 90% confident), or "Remote" (less than 50% confident). Confidence in whether a sighting was a duplicate was subjective, but informed by time of sighting, species, group size and swim direction. Trackers were also tracking these animals using binoculars for as long as possible, providing additional information to the duplicate identifier.

Effort data, including environmental conditions and sightings data, were recorded by a designated data recorder. All data were stored in a laptop computer running the LOGGER software, modified specifically for SCANS surveys (Gillespie et al. 2010). Environmental conditions data included sea conditions measured on the Beaufort scale, swell height and direction, sun glare, visibility (distance to horizon) and sightability. Sightability was a subjective measure of conditions for detecting small cetaceans comprising an assessment of all environmental conditions together. Although subjective, classifying environmental conditions in this way was done consistently by all observers. Personnel changes were recorded as they happened. Environmental data was recorded every 15 minutes or more often if conditions changed.

Distance to detected groups was measured by observers on the Primary platform using individually calibrated measuring sticks (Leaper, R. Pers. Comm).

2.1.2 Aerial surveys

Aerial data were collected according to the same protocols for each of the SCANS-II, SCANS-III and ObSERVE aerial surveys (Figure 2.1-1 & Figure 2.1-2 pink survey blocks). Aerial teams consisted of a pilot and three scientific crew members. In all cases, the target altitude was 600 feet (183 m), and the target speed was 90 knots (167 kmph). Of the three scientific crew, two acted as observers, utilising bubble windows on either side of the aircraft. The third team member was deployed as data recorder, recording both environmental conditions and sightings data; entering data into a laptop computer running bespoke dedicated data collection software package VOR, written by Phil Lovell (SCANS-II 2008 Appendix A3.2). Environmental conditions were classified based on the observers judgement about the chances of their seeing a porpoise. Conditions were classified as "good", "moderate", or "poor" based on the following definitions, which are intentionally subjective and based on the observers own judgement ((SCANS-II 2008 Appendix A3.2, p7):

Good: when the observer believes that the likelihood of seeing a porpoise should occur within the searching area is good. Normally good subjective conditions will require a sea state of two or less and a turbidity of less than 2.

Moderate: when the observer believes that the likelihood of seeing a porpoise should occur within the searching area is moderate.

Poor: when the observer believes that they are unlikely to see a porpoise should one occur within the searching area, unless for example it is showing exuberant behaviour or is very close to the trackline.

Time and angle from the observer to the sighted animal (the angle of declination) were recorded when detected cetaceans passed abeam of the aircraft. Angle of declination and altitude were used to calculate perpendicular distance. Additional detail on methods is described by Gilles *et al.* (2009).

In all surveys except ObSERVE, the circle-back or "racetrack" method (Hiby and Lovell 1998; Hiby 1999; Scheidat et al. 2008) was used to collect data from which it was possible to correct for animals missed on the transect line, g(0). When following this methodology, when a group of animals was detected, the aircraft circled back to re-survey a pre-determined section of track-line to see if animals were sighted on the second pass. GPS data, times at which animals pass abeam and measured angles of declination were used to ascertain the likelihood that pods of animals seen on the first and second pass were duplicates. “Racetrack” software, written by Lex HIby, is used to analyse the duplicates and produce estimates of g(0) (Scheidat et al. 2008).

Resulting g(0) estimates from the SCANS-III surveys were applied to data collected during ObSERVE on the basis that the same aircraft and data collection protocols were used. In SCANS-II, this method was used only for harbour porpoise. In SCANS-III, it was also implemented for dolphin species and minke whale as these were the only species with enough sightings.

2.2 Data Processing

2.2.1 Design-based estimates of Abundance

Design-based estimates of abundance were obtained for each of the species, for each of the surveys prior to completion of the modelling work described here. This includes the calculation of estimates of the total effective strip width (esw). This work does not form part of this thesis; however, the results are discussed in Chapter 3 as context to the modelling presented in that and subsequent chapters. Estimates of esw calculated in these prior studies were used in the modelling completed as part of this thesis. The esw was derived directly from the detection function, so may include multiple values depending on the conditions if the detection function incorporated multiple categorical variables. Correcting estimates for animals missed on the transect line (g(0)) was done for all species for which there were sufficient data. A summary of the models used to estimate detection probability for each species or species grouping is provided in Table 2.2-1. As data had been collected using common protocols, analysis could also be standardised across platforms and surveys. For full details of design-based abundance estimates, see Hammond *et. al.* (2013) for SCANS-II, Hammond *et al.* (2009) for CODA, Hammond *et al*. (2021) for SCANS-III and Rogan *et al.* (2018) for ObSERVE. Calculation of g(0) was not conducted as part of this thesis. Esw and g(0) estimates for the SCANS-III surveys are provided in Table 2.2-2 and Table 2.2-3.

Table 2.2-1 Summary of data and models used to estimate detection probability for each species or species grouping in the SCANS-II, CODA and SCANS-III surveys. Taken from; Hammond et al., 2009 (CODA); Hammond et al., 2013 (SCANS-II). Hammond et al., 2021 (SCANS-III). estimates for species not corrected or partially corrected are negatively biased to an unknown extent.

Survey	Ship or aerial	Species / Species grouping	Detection function covariates	G(0) corrected?
SCANS-II	Aerial	Harbour porpoise	Subjective conditions	
SCANS-II	Aerial	Minke whale	None	
SCANS-II	Aerial	White-beaked dolphin	Subjective conditions	
SCANS-II	Aerial	Common dolphin	Subjective conditions	
SCANS-II	Aerial	Bottlenose dolphin	None	
SCANS-II	Ship	Harbour porpoise	Beaufort, ship	
SCANS-II	Ship	Minke whale	None	
SCANS-II	Ship	White-beaked dolphin	None	
SCANS-II	Ship	Common dolphin	Cluster size	
SCANS-II	Ship	Bottlenose dolphin	None	
CODA	Ship	Common and striped dolphin	Beaufort, Cue	
CODA	Ship	Fin whale	Sightability, platform height	
CODA	Ship	Bottlenose dolphin	Cluster size	
CODA	Ship	Minke whale	None	
SCANS-III	Ship	Harbour porpoise	Swell, Beaufort	Yes
SCANS-III	Ship	Bottlenose dolphin	None	Yes
SCANS-III	Ship	White-sided / white-beaked dolphin	None	Yes
SCANS-III	Ship	Common and striped dolphin	Beaufort	Yes
SCANS-III	Ship	Large baleen whales (blocks 8 & 9)	Swell	
SCANS-III	Ship	Large baleen whales (blocks 11, 12, & 13)	Swell, Beaufort	
SCANS-III	Ship	Minke whale	None	
SCANS-III	Aerial	Harbour porpoise	Subjective conditions	
SCANS-III	Aerial	Dolphins (all species)	Subjective conditions	
SCANS-III	Aerial	Minke whale	None	

Table 2.2-2 Estimates of ESW (CV in parentheses) and g(0) for harbour porpoise, all dolphin species combined and minke whale, for good and moderate sighting conditions during the SCANS-III aerial survey. Note that ESW is the total effective strip width on both sides of the aircraft. Reproduced from Hammond et al., 2021.

	ESW (in meters), incorporating the effect of g(0) on detection probability		g(0)	
Conditions	Good	Moderate	Good	Moderate
Harbour porpoise	138 (0.16)	109 (0.17)	0.364	0.279
Dolphins (all species)	390 (0.13)	213 (0.14)	0.805	0.414
Minke whale	154 (0.42)		0.302	

Table 2.2-3 Estimates of ESW (CV in parentheses) and g(0) for species seen during the SCANS-III vessel survey. Note that ESW is the total effective strip width on both sides of the survey vessel. A g(0) minke whale estimate is not available for ship data. Reproduced from Hammond et al., 2021.

Species / Species group	ESW (in meters), incorporating the effect of g(0) on detection probability	g(0)
Harbour porpoise	93.9 (0.186)	0.221 (0.177)
Bottlenose dolphin	151 (0.377)	0.400 (0.358)
White-beaked and white-sided dolphin	129 (0.697)	0.455 (0.330)
Common and striped dolphin	110 (0.164)	0.421 (0.115)
Large baleen whales (blocks 8 & 9)	789 (0.061)	*Not estimated*
Large baleen whales (blocks 11, 12, 13)	933 (0.088)	0.614 (0.073)
Minke whale	208	*Not estimated*

2.2.2 Preparation of data for modelling

Data from the aerial and ship surveys were processed in the same way. For the ship surveys, only data from the primary platforms were used for modelling. Similarly, for the aerial surveys, data collected during the circle-back manoeuvres were excluded.

Short sections of searching effort were created from the raw data. Files containing effort data were linked to the GPS locations recorded every 4 seconds on the aerial survey and every 10 seconds on the ship survey. On the few occasions when the GPS data were missing for short sections, positions were interpolated linearly. This resulted in short sections of effort of approximately 200m for aerial survey and approximately 50m for the ship survey per GPS location. Multiples of these short sections were then joined to form modelling segments (see below).

To take account of environmental conditions during data collection, the short sections of effort were linked with estimates of the total effective strip width (esw), according to the environmental conditions recorded during the period when the searching took place. These estimates of esw were derived from the detection functions fitted for each species during the analysis for the design-based estimates of abundance, according to the covariates included in the detection function (section 2.2.1) (Hammond *et al.* 2009, 2013, 2021; Rogan *et al.*, 2018). Environmental conditions included the subjective assessment of conditions used on the aerial survey; and Beaufort scale, swell and overall sightability measured or assessed on the ship surveys. The effective area searched in each short section of effort was calculated as the esw multiplied by the distance travelled.

Values of depth and slope (see Section 2.2.3) were linked to each of these short sections of effort using R version 4.0.3 (R Core Team 2020), package Raster (Hijmans 2020). Particularly for depth, adding values at this stage was found to be more accurate than doing so later in the process.

Segments of effort of target 10km length (all between 1km and 15km) were created by joining consecutive short sections of effort using R function segmentate (Viquerat, pers. comm). Values of depth, slope and aspect in the short effort sections were averaged to provide values for each 10km segment.

Measurements from the centre point of each segment to the coast and to the 50m (North Sea only), 200m and 2000m isobaths at the closest point were made using the QGIS (QGIS Development Team, 2018) NNJoin plug-in. These effort segments formed the sampling unit for data analysis.

Dynamic environmental variables (see section 2.2.3 and Table 2.1) were provided as .netCDF files by either NEODAAS (https://www.neodaas.ac.uk/) or obtained from Copernicus (https://resources.marine.copernicus.eu/). These were converted to raster files, and a weighted mean value across a circle of 10km diameter originating at the mid-point of the segment was calculated and linked to the segment. For some of the shorter segments, covariate resolution was larger than length of segment.

A 10x10km spatial grid was created, and values of all environmental variables were associated with each grid cell using the same extract functions described above for the effort segments. The grid was used as a basis for predicting cetacean density spatially from the fitted models using the values of the environmental variables in each grid cell (see 2.3.7).

All data processing was undertaken in software R version 4.0.3 (R Core Team 2020).

2.2.3 Environmental Data

Table 2.2-4 shows the environmental variables that were considered as candidate covariates during modelling (see section 2.3.1). Unless otherwise stated, these were processed as described above. Two types of environmental variable were used – physiographic and dynamic. The physiographic variables included depth, slope (rate of depth change in degrees), and distance to depth and seabed features. Dynamic variables included Sea surface temperature (SST), salinity and a selection of different measurements of mesoscale activity (sea surface height, sea level anomaly, absolute dynamic topography). For dynamic variables, monthly averaged data for July (the month in which the majority of the cetacean data were collected) of the same year in which the cetacean data were collected were used. Maps of covariates are provided for the relevant geographic areas in chapters 3-5.

Table 2.2-4 Environmental variables used as candidate covariates during cetacean modelling.

Covariate	Abbreviated name	Description	Unit of measurement	Data source
X	X	Longitude converted into UTM30 coordinate system	N/A	N/A
Y	Y	Latitude converted into UTM30 coordinate system	N/A	N/A
Depth	Depth	Mean depth of the values assigned to effort making up the segment. Depth raster created using R package MARMAP (Pante and Simon-Bouhet 2013).	m	ETOPO1 database, hosted by NOAA (Amante & Eakins, 2009).
Standard deviation of depth	SDdepth	Standard deviation of depth calculated over a buffer of 5km radius. Depth raster created using R package MARMAP (Pante and Simon-Bouhet 2013). Analysis of raster conducted using R package RASTER (Hijmans, 2020)	m	ETOPO1 database, hosted by NOAA (Amante & Eakins, 2009).
Slope	Slope	Seabed gradient, extracted from a single point location using depth data extracted using R package MARMAP (Pante and Simon-Bouhet 2013). Analysis of raster conducted using R package RASTER (Hijmans, 2020)	(°)	ETOPO1 database, hosted by NOAA (Amante & Eakins, 2009).
Surface salinity	Sal	Sea water salinity	PSU	GLORYS12V1: a reanalysis of the Copernicus Marine Environment Monitoring Service (CMEMS) global ocean eddy-model, based largely on the current real-time global forecasting CMEMS system. Downloaded from https://resources.marine.copernicus.eu/ ((Fernandez and Lellouche 2021)
Mixed Layer Depth	MLD	Ocean mixed layer thickness. The depth where the density increase compared to density at 10m depth corresponds to a temperature decrease of 0.2°C in local surface conditions.	m	GLORYS12V1: a reanalysis of the Copernicus Marine Environment Monitoring Service (CMEMS) global ocean eddy-model, based largely on the current real-time global forecasting CMEMS system. Downloaded from https://resources.marine.copernicus.eu/ ((Fernandez and Lellouche 2021)

Sea surface temperature	SST		°C	This is the Optimally Interpolated (OI) merged microwave-infrared SST product from the Advanced Very High-Resolution Radiometer (AVHRR) instrument. Data provided by NEODAAS (Casey et al. 2010)
Sea Level Anomaly	SLA	Sea level anomaly is the difference between sea surface height and a mean sea surface. Sea surface height is derived from satellite altimetry, and the mean sea surface is calculated from 20 years of these data.	m	Data provided by NEODAAS
Sea surface Height	SSH	Sea surface height above the ellipsoid. SSH is the difference between the actual sea surface height at any given time and place, and that which it would have if the ocean were at rest. SSH = geoid +ADT	m	GLORYS12V1: a reanalysis of the Copernicus Marine Environment Monitoring Service (CMEMS) global ocean eddy-model, based largely on the current real-time global forecasting CMEMS system. Downloaded from https://resources.marine.copernicus.eu/ ((Fernandez and Lellouche 2021)
Absolute Dynamic Topography	ADT	ADT gives the departure of the sea surface from the geoid due to ocean dynamics. The geoid is a surface of constant geopotential with which mean sea level would coincide if the ocean were at rest. ADT is calculated from the sea level anomaly (SLA) and the mean dynamic topography (MDT): ADT = SLA +MDT	m	Data were produced by the Copernicus Marine Environment Monitoring Service (CMEMS) Sea Level-TAC multimission altimetry processing system and processed by NEODAAS
Absolute distance to the 2000 isobath	D2000_iso	Distance at shortest point. Calculated using the NNJoin package in QGIS, uses nearest neighbour analysis.	km	ETOPO1 database, hosted by NOAA (Amante & Eakins, 2009).
Absolute distance to the coast	Distance to coast	Distance at shortest point. Calculated using the NNJoin package in QGIS, uses nearest neighbour analysis.	km	
Absolute distance to the 200m isobath	D200_iso	Distance at shortest point. Calculated using the NNJoin package in QGIS, uses nearest neighbour analysis.	km	ETOPO1 database, hosted by NOAA (Amante & Eakins, 2009).
Absolute distance to the 50m isobath (North Sea only	D50_iso	Distance at shortest point. Calculated using the NNJoin package in QGIS, uses nearest neighbour analysis.	km	ETOPO1 database, hosted by NOAA (Amante & Eakins, 2009).
Distance to 200m	CS200	Distance at shortest point, but with values on	km	ETOPO1 database, hosted by NOAA (Amante & Eakins, 2009).

isobath accounting for contour		the deep side of the contour multiplied by -1 to provide a linear measure. Calculated using the NNJoin package in QGIS, uses nearest neighbour analysis.		
Distance to 50m isobath accounting for contour	CS50	Distance at shortest point, but with values on the deep side of the contour multiplied by -1 to provide a linear measure. Calculated using the NNJoin package in QGIS, uses nearest neighbour analysis.	km	ETOPO1 database, hosted by NOAA (Amante & Eakins, 2009).
Absolute distance to escarpments	Distance to escarpments	Distance at shortest point. Escarpment is the bottom of a cliff or steep slope. Calculated using the NNJoin package in QGIS, uses nearest neighbour analysis.	km	Seafloor Geomorphic Features map (Harris et al. 2014))
Absolute distance to canyons	Distance to canyons	Distance at shortest point. Canyons are deep, narrow valleys with steep sides. Calculated using the NNJoin package in QGIS, uses nearest neighbour analysis.	km	Seafloor Geomorphic Features map (Harris et al., 2014)
Absolute distance to seamounts	Distance to seamounts	Distance at shortest point. Seamounts are isolated rises in elevation of 1000m or more from the surrounding seafloor. Calculated using the NNJoin package in QGIS, uses nearest neighbour analysis.	km	Seafloor Geomorphic Features map (Harris et al., 2014)
Absolute distance to troughs	Distance to troughs	Distance at shortest point. A trough is a linear depression extending over a distance. Shallower than a canyon. Calculated using the NNJoin package in QGIS, uses nearest neighbour analysis.	km	Seafloor Geomorphic Features map (Harris et al., 2014)

2.3 Modelling Methodology

Several analyses of similar large-scale datasets have been undertaken in recent years (e.g. Becker *et al.*, 2016, 2017; Gilles *et al.*, 2016; Rogan *et al.*, 2017). The analyses undertaken here followed the same overall Generalised Additive Model (GAM) framework established in this previous work.

2.3.1 Overall GAM framework

GAMS were developed in R (v 4.0.3; (R Core Team 2020) using package "mgcv" (v 1.8.33; Wood, 2003, 2004, 2017; Marra and Wood, 2011; Wood *et al.*, 2016).

Cetacean data are often over-dispersed., meaning there is greater variability present in a dataset than would be expected. This is common due to populations being heterogeneous (non-uniform) in distribution. To combat this, Tweedie and Negative Binomial distributions were both considered as candidate error structures (Miller et al. 2013). Models for each species were tried with each error distribution, and the best fitting model was taken forward to generate predictions. Poisson distribution was not tried, due to the over-dispersion of data.

The general structure of the model, using a logarithmic link function, was:

$$n_i = exp\left[\ln(a_i) + \theta_0 + \sum f_k(z_{ik})\right]$$

where n_i is the number of individuals detected in the i^{th} effort segment, the offset a_i is the effective area searched (segment length * estimated total effective strip width) for the i^{th} segment, θ_0 is the intercept, f_k are smoothed functions of the explanatory environmental covariates, and z_{ik} is the value of the k^{th} explanatory covariate in the i^{th} segment.

Smooth functions were fitted using restricted maximum likelihood (REML) with automatic term selection (Marra and Wood 2011). Thin-plate regression splines (Wood 2003) were used for all covariates. This method was chosen because it helps avoid overfitting of the smooth functions by including a modification to slightly penalise the null space. The method can reduce the estimated degrees of freedom of a covariate term to one or less and even to zero if it does not contribute sufficiently to explaining the variability in the data.

Following initial fitting of a model including all candidate covariates, those covariates with estimated degrees of freedom of 0.1 or less were removed from the model. Selection among models was conducted based on Akaike's Information Criterion (AIC). Selecting the model with the lowest AIC can sometimes result in retention of covariates that are not significant but nevertheless contribute to explaining variability in the data. Goodness of fit of models was assessed by inspection of QQ plots and plots of model residuals.

2.3.2 Correlated environmental covariates.

Prior to conducting any modelling, correlation matrices were calculated using the `corrplot` R package, version 0.92 (Wei and Simko 2021). This was used investigate the level of correlation which existed between similar covariates. A cut off of 0.6 / -0.6 was used. Cut-off points of 0.7 is commonly considered to be a "strong correlation", so 0.6 was chosen to be on the precautionary side (Schober et al. 2018) Covariates on distance to coast or isobaths were found to be correlated in many cases, although the levels of correlation depended on the exact dataset modelled (see Chapters 3-5). To select which of the correlated covariates should be included in the model in each instance, they were first modelled independently, and the covariate resulting in the lowest AIC score was taken forward for use in subsequent modelling.

2.3.3 Model application

The following steps were followed to apply the models. Firstly, for covariates that were considered to be of the same "type", for example SD depth and slope, or SLA, SSH and ADT, individual models were run with each of these variables individually (Table 2.3-1). These models were then compared by AIC, and the best of these models was taken forward to the next stage. This process was done for both the negative binomial and Tweedie distributions separately.

Table 2.3-1 Example table showing the potential number of models that would arise from a stepwise forward selection model building process, if that had been used here. Some of the covariates are in sets of the same type, of which only one would go into a model -so for example both SD and slope would never end up in the same model.

Covariate "type"	Number of options	Candidates
Depth	1	1 – depth
Salinity	1	1 - salinity
Sea surface temperature	1	1 – sea surface temperature
Seabed rugosity	2	-Slope -SD depth
Mixed Layer depth	2	-MLD -Log MLD
Mesoscale activity	3	- SSH - ADT - SLA
Distance to feature	10	- CS50 - Dist_50_iso - CS200 - Dist_20_iso - Distance to coast - Dist_2000_iso - Distance to escarpments - Distance to canyons - Distance to troughs - Distance to seamounts

Matrices were then built to check for correlation between covariates that have been selected for the model. The same covariates were often selected by the negative binomial and Tweedie model-sets, but not exclusively. In cases where different covariates went through each time, a correlation matrix was prepared for each error distribution.

“Full” models were then built which modelled the cetacean data as either individuals or groups (section 2.3.3) against one covariate of each type (Depth+salinity+SST+1 of “seabed slope” + 1 of “mesoscale activity”+1 of “distance to”) all included in the same model. In instances where there was a correlation score higher than 0.6 or lower than -0.6. two separate models were run, one for each covariate, alongside all of the other candidate covariates.

Results of this “full” model were examined, and any covariate found to retain fewer than 0.1 estimated degrees of freedom (edf) was removed, and the model run again. This approach was pioneered by Mara and Wood (2011) to help avoid overfitting, and also aids in efficient evaluation of candidate covariates. Building a model by adding one covariate at a time could have resulted in up to 2349 candidate models for each species, repeated for each error distribution to evaluate all of the potential options (Table 2.3-2). The use of REML with automatic term selection allows a much more efficient examination of large numbers of candidate covariates.

Table 2.3-2 Example table showing the potential number of models that would arise from a stepwise forward selection model building process, if that had been used here. Some of the covariates are in sets of the same type, of which only one would go into a model -so for example both SD and slope would never end up in the same model.

Number of potential individual covariate models	18
Possible number of two covariate models	171
Possible number of three covariate models	1200
Possible number of four covariate models	720
Possible number of five covariate models	160
Possible number of six covariate models	80
Total number of models for each error distribution	2349

The threshold of 0.1 edf was chosen as the cut-off as per Canadas et al (2021, pers comm). This represents a covariate with a flat slope, in which the covariate is causing little or no partial effect.

2.3.4 Individuals or groups?

All species were first modelled using the number of individuals detected in a segment as the response variable. For some species, these models did not fit well, and so the data were re-modelled using the number of groups detected in a segment instead of individuals. Species for which individual models did not fit well were typically those with large groups sizes (e.g., common dolphins). The larger group sizes cause more severe over-dispersion in the distribution of counts of individuals. Following the methodology outlined by Becker *et al.*, (2016), if the number of groups was modelled, models of group size were also developed to establish if group size varied across the study area. However, in all such models of group size, an intercept only model was the most supported. Therefore, in all these cases, estimated densities of groups from the selected models were multiplied by observed mean group size to generate estimates of the density of individuals (see section 2.3.7).

2.3.5 Inclusion of XY variables

Latitude and longitude (often modelled as X,Y) are often included in models as a catch-all proxy for specific or unknown habitat features (Forney 2000). These covariates are included as an isotropic smooth, along with other environmental covariates selected during the model selection process described above. Since space is often the best descriptor of a species' distribution, with the XY covariates accounting for a lot of the unknown variability, the inclusion of these covariates usually results in excellent "predictive" models, best describing the current distribution of animals based on the field data collected. However, these models can be difficult to interpret ecologically, as it is not always clear what processes the XY variables are acting as a proxy for (Guisan et al. 2002; Redfern et al. 2006).

Explanatory models are run using only the environmental covariates, with no XY smooth. These models may not be as good a descriptor of where the animals were seen, but they are better suited to describe the environmental features that might explain the ecological processes that define spatial distribution (Becker et al. 2019). Whether or not to include Latitude and Longitude really depends what question you are hoping the model will answer (Shmueli 2010). Predictive models are used in Chapter 3 to best describe the current state of knowledge on study species using the most recent available data. Explanatory models are used in Chapters 4 and 5 with an aim of explaining what could be causing the observed distributions.

2.3.6 Modelling process

The same steps were followed to complete the modelling in all subsequent chapters unless otherwise described. Prior to starting, the data for the specific region to be modelled were subset from the overall master dataset, which had been prepared as described above.

In some cases, effort segments contained missing values for specific covariates. This usually occurred when segments were very short. All effort segments which contained missing covariate values were removed to ensure the same dataset was used when comparing models by AIC.

The correlation coefficients for the environmental covariates to be considered for the model were calculated. Covariates with a correlation coefficient greater than 0.6 or less than -0.6 were modelled individually. Of these individually modelled, correlated covariates, the covariate with the lowest AIC score from the individual models was selected to take forward into the full model.

Using the covariates selected this way, a full model containing the best of any correlated covariates along with all other candidate covariates, was run using number of individuals as the response variable. Model results were examined, and all covariates resulting in an edf of <0.1 were removed, and the model re-run. This process was repeated until no covariates with edf <0.1 remained.

Depending on the species and overall model fit, it was sometimes necessary to repeat this process again, using the number of groups instead of number of individuals as the response variable.

Model diagnostics for the final Tweedie and Negative Binomial models were examined and the best model selected and used for prediction. A step-by-step version of this process is provided in Appendix 1.

2.3.7 Model Prediction

Model prediction grids consisting of 10 x 10km grid cells (as described in section 2.2.2) were prepared for the area being modelled. Covariate values for the effort segments were compared with those of the prepared prediction grid, and any grid squares containing values of covariates which were outside the range covered by the covariates in the effort segments were removed from the prediction grid. This was done to avoid predicting in areas where covariate values were outside the range of the modelled data.

Best models, as determined using the process described above, were predicted onto this grid using the `mgcv` predict.gam function to predict density and standard error. The predicted density was plotted to create maps of density for each species. Map figures were created in R using the `tmap` package (Tennekes 2018), coordinate reference system EPSG:4326.

For species modelled as number of groups instead of number of individuals, the density of groups was predicted and multiplied by mean group size, to generate estimates of density of individuals. Maps were created using this estimated density (from the `mgcv` predict.gam function, as described above) of individuals to ensure maximum comparability between species.

2.3.8 Calculating prediction Coefficient of Variation

The coefficient of variation (CV) of predicted density in each grid cell was estimated using methods described by Schleimer et al. (2019), which are based on simulation of posterior distributions of the model results. Function `mvrnorm` from the MASS library in R (Venables and Ripley 2002) was used to simulate 1,000 vectors of the model coefficients. From these, 1,000 predictions of density in each grid cell were created and the standard deviation and hence CV of density was calculated from these.

The estimated CV includes variability in encounter rate (how the count varies along the transect line) but does not include uncertainty in ESW and will therefore be underestimated, the extent of which will depend on the precision of estimates of ESW.

Maps of CV were included alongside the maps of model predictions to provide an indication of confidence in the predictions, particularly at higher densities, which is indicated by CV. Maps of standard error (SE) of density have also been provided.

2.4 Literature cited.

Becker, E., Forney, K., Fiedler, P., Barlow, J., Chivers, S., Edwards, C., Moore, A., and Redfern, J. 2016. Moving Towards Dynamic Ocean Management: How Well Do Modelled Ocean Products Predict Species Distributions? Remote Sens. 8(2): 149. doi:10.3390/rs8020149.

Becker, E.A., Forney, K.A., Redfern, J.V., Barlow, J., Jacox, M.G., Roberts, J.J., and Palacios, D.M. 2019. Predicting cetacean abundance and distribution in a changing climate. Divers. Distrib. 25(4): 626–643. doi:10.1111/ddi.12867.

Becker, E.A., Forney, K.A., Thayre, B.J., Debich, A.J., Campbell, G.S., Whitaker, K., Douglas, A.B., Gilles, A., Hoopes, R., and Hildebrand, J.A. 2017. Habitat-Based Density Models for Three Cetacean Species Off Southern California Illustrate Pronounced Seasonal Differences. Front. Mar. Sci. 4: 121. doi:10.3389/fmars.2017.00121.

Caadas, Ana. 2021. Model review workshop, 24-25 June 2021. Marine Mammal Density models for the US Nay 6th Fleet Study Area. Pers. Comm.

Casey, K.S., Brandon, T.B., Cornillon, P., and Evans, R. 2010. The Past, Present and Future of the AVHRR Pathfinder SST Program. *In* Oceanography from Space. Springer.

Fernandez, E., and Lellouche, J.M. 2021. Product User Manual: For the Global Ocean Physical Reanalysis Product Global_Reanalysis_Phy_001_030. Information provided with the covariates from NEODASS.

Forney, K.A. 2000. Environmental Models of Cetacean Abundance: Reducing Uncertainty in Population Trends. Conserv. Biol. 14(5): 1271–1286. doi:10.1046/j.1523-1739.2000.99412. x.

Gilles, A., Scheidat, M., and Siebert, U. 2009. Seasonal distribution of harbour porpoises and possible interference of offshore wind farms in the German North Sea. Mar. Ecol. Prog. Ser. 383: 295–307. doi:10.3354/meps08020.

Gilles, A., Viquerat, S., Becker, E.A., Forney, K.A., Geelhoed, S.C.V., Haelters, J., Nabe-Nielsen, J., Scheidat, M., Siebert, U., Sveegaard, S., Beest, F.M., Bemmelen, R., and Aarts, G. 2016. Seasonal habitat-based density models for a marine top predator, the harbor porpoise, in a dynamic environment. Ecosphere 7(6). doi:10.1002/ecs2.1367.

Gillespie, D., Leaper, R., Gordon, J., and Macleod, K. 2010. An integrated data collection system for line transect surveys. J. Cetacean Res. Manag. 11(3): 217–227.

Guisan, A., Edwards, T.C., and Hastie, T. 2002. Generalized linear and generalized additive models in studies of species distributions: setting the scene. Ecol. Model. 157(2–3): 89–100. doi:10.1016/S0304-3800(02)00204-1.

Hammond, P., Lacey, C., Gilles, A., Viquerat, S., Börjesson, P., Herr, H., Macleod, K., Ridoux, V., Santos, M., Teilmann, J., Vingada, J., and Øien, N. 2021. Estimates of cetacean abundance in European Atlantic waters in summer 2016 from the SCANS-III aerial and shipboard surveys. Final project report. https://scans3.wp.st-andrews.ac.uk/files/2021/06/SCANS-III_design-based_estimates_final_report_revised_June_2021.pdf

Hammond, P., Macleod, K., Gillespie, D., Swift, R., Winship, A., Burt, M., Cañadas, A., Vázquez, J., Ridoux, V., Certain, G., Canneyt, O.V., Lens, S., Santos, B., Rogan, E., Uriarte, A., Hernandez, C., Castro, R., 2009. Cetacean Offshore Distribution and Abundance in the European Atlantic (CODA). Final project report. http://biology.st-andrews.ac.uk/coda/

Hammond, P.S., Macleod, K., Berggren, P., Borchers, D.L., Burt, L., Cañadas, A., Desportes, G., Donovan, G.P., Gilles, A., Gillespie, D., Gordon, J., Hiby, L., Kuklik, I., Leaper, R., Lehnert, K., Leopold, M., Lovell, P., Øien, N., Paxton, C.G.M., Ridoux, V., Rogan, E., Samarra, F., Scheidat, M., Sequeira, M., Siebert, U., Skov, H., Swift, R., Tasker, M.L., Teilmann, J., Van Canneyt, O., and Vázquez, J.A. 2013. Cetacean abundance and distribution in European Atlantic shelf waters to inform conservation and management. Biol. Conserv. 164: 107–122. doi:10.1016/j.biocon.2013.04.010.

Harris, P.T., Macmillan-Lawler, M., Rupp, J., and Baker, E.K. 2014. Geomorphology of the oceans. Mar. Geol. 352: 4–24. doi:10.1016/j.margeo.2014.01.011.

Hiby, L. 1999. The objective identification of duplicate sightings in aerial survey for porpoise. *In* Marine Mammal Survey and Assessment Methods. CRC Press, Amsterdam. pp. 179–189.

Hiby, L., and Lovell, P. 1998. Using Aircraft in Tandem Formation to Estimate Abundance of Harbour Porpoise. Biometrics 54: 1280–1289.

Hijmans, R.J. 2020. raster: Geographic data analysis and modelling. manual. Available from https://CRAN.R-project.org/package=raster.

Laake, J.L. and D. L. Borchers. 2004. Methods for incomplete detection at distance zero. *In* Advanced Distance Sampling. Oxford University Press.434pp.

Marra, G., and Wood, S.N. 2011. Practical variable selection for generalized additive models. Comput. Stat. Data Anal. 55(7): 2372–2387. doi:10.1016/j.csda.2011.02.004.

Miller, D.L., Burt, M.L., Rexstad, E.A., and Thomas, L. 2013. Spatial models for distance sampling data: recent developments and future directions. Methods Ecol. Evol. 4(11): 1001–1010. doi:10.1111/2041-210X.12105.

Pante, E., and Simon-Bouhet, B. 2013. marmap: A package for importing, plotting and analyzing bathymetric and topographic data in r. PLoS ONE 8(9): e73051.

QGIS Development Team,. 2018. QGIS Geographic Information System. Open Source Geospatial Foundation Project. k. Available from http://qgis.osgeo.org.

R Core Team. 2020. R: A language and environment for statistical computing. manual, Vienna, Austria. Available from https://www.R-project.org/.

Redfern, J.V., Ferguson, M.C., Becker, E.A., Hyrenbach, K.D., Good, C., Barlow, J., Kaschner, K., Baumgartner, M.F., Forney, K.A., Ballance, L.T., Fauchald, P., Halpin, P., Hamazaki, T., Pershing, A.J., Qian, S.S., Read, A., Reilly, S.B., Torres, L., and Werner, F. 2006. Techniques for cetacean-habitat modeling. Mar Ecol Prog Ser 310: 271–295.

Rogan, E., Breen, P., Mackey, M., Cañadas, A., Scheidat, M., Geelhoed, S., and Jessopp, M. 2018. Aerial Surveys of Cetaceans and Seabirds in Irish waters: Occurrence, distribution and abundance in 2015-2017. : 298.

Rogan, E., Cañadas, A., Macleod, K., Santos, M.B., Mikkelsen, B., Uriarte, A., Van Canneyt, O., Vázquez, J.A., and Hammond, P.S. 2017. Distribution, abundance and habitat use of deep diving cetaceans in the North-East Atlantic. Deep Sea Res. Part II Top. Stud. Oceanogr. 141: 8–19. doi:10.1016/j.dsr2.2017.03.015.

SCANS-II. 2008. Small Cetaceans in the European Atlantic and North Sea (SCANS-II). Final Report. University of St Andrews, UK. . Available from http://biology.st-andrews.ac.uk/scans2/.

Scheidat, M., Gilles, A., Kock, K., and Siebert, U. 2008. Harbour porpoise Phocoena phocoena abundance in the southwestern Baltic Sea. Endanger. Species Res. 5: 215–223. doi:10.3354/esr00161.

Schleimer, A., Ramp, C., Plourde, S., Lehoux, C., Sears, R., and Hammond, P. 2019. Spatio-temporal patterns in fin whale Balaenoptera physalus habitat use in the northern Gulf of St. Lawrence. Mar. Ecol. Prog. Ser. 623: 221–234. doi:10.3354/meps13020.

Schober, P., Boer, C., and Schwarte, L.A. 2018. Correlation Coefficients: Appropriate Use and Interpretation. Anesth. Analg. 126(5): 1763. doi:10.1213/ANE.0000000000002864.

Shmueli, G. 2010. To Explain or to Predict? Stat. Sci. 25(3). doi:10.1214/10-STS330.

Tennekes, M. 2018. tmap: Thematic Maps in R. J. Stat. Softw. 84(6): 1–39. doi:https://doi.org/10.18637/jss.v084.i06.

Venables, W.N., and Ripley, B.D. 2002. Modern Applied Statistics with S-Plus. Fourth Edition. Springer, New York.562pp.

Wei, T., and Simko, V. 2021. R package “corrplot”: Visualization of a correlation matrix. manual. Available from https://github.com/taiyun/corrplot.

Wood, S.N. 2003. Thin-plate regression splines. J. R. Stat. Soc. B 65(1): 95–114.

Wood, S.N. 2004. Stable and efficient multiple smoothing parameter estimation for generalized additive models. J. Am. Stat. Assoc. 99(467): 673–686.

Wood, S.N. 2017. Generalized additive models: An introduction with r. *In* 2nd edition. Chapman and Hall/CRC.497pp

Wood, S.N., N., Pya, and Safken, B. 2016. Smoothing parameter and model selection for general smooth models (with discussion). J. Am. Stat. Assoc. 111: 1548–1575.

3 The Big Picture

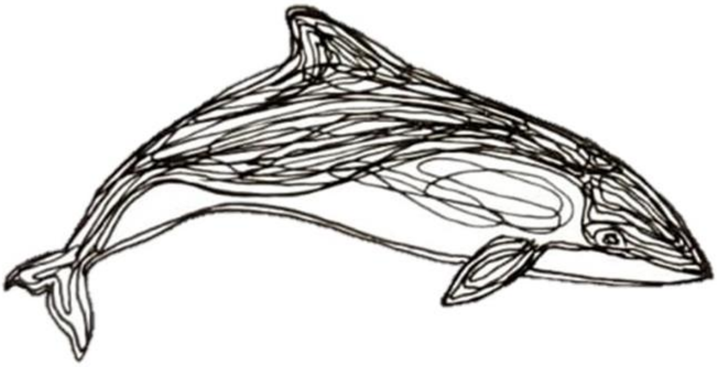

Harbour porpoise doodle, courtesy of Anni Sharpe

The current status – distribution and abundance – of eight species of cetacean in the European Atlantic using the best available data, from the SCANS-III and ObSERVE surveys (2016).

3.1 Introduction

Large-scale surveys of cetaceans are designed to obtain design-based abundance estimates over a large geographical area and are often designed as multi-species surveys. They typically take place from large ships and may also incorporate the collection of data on other taxa, often seabirds, as well as oceanographic parameters. These types of surveys have been conducted in a wide range of locations, including (but not limited to) the Hawaiian Exclusive Economic zone (EEZ) (Bradford et al. 2017); the Eastern Tropical Pacific (ETP) (Wade 1993), the South Atlantic (Baines et al. 2021), the western North Atlantic (Palka et al. 2017)(CETAP 1982), the U.S Atlantic Outer Continental Shelf (Palka et al. 2017), and the Central and Eastern North Atlantic (Hammond et al. 2002, Lockyer and Pike, 2009). Depending on the location of the study area, aerial surveys may also be used, for example in northern Canada (Kingsley 2000), and the North Sea (Scheidat et al. 2012).

These types of survey routinely generate abundance estimates within their survey region. These regions may be split into smaller sub-regions, or strata; and depending on the data collected, estimates may be available for species for these smaller sub-regions (Hammond et al. 2013). The availability of the estimates for smaller regions is determined by the survey design and the data collected and it may not always be possible to calculate estimates for regions of interest, if the regions were not taken into account during the original survey design.

As discussed in section 1.4, modelling analyses can use data collected on these large-scale surveys and conduct further analysis. They can be used to combine data from multiple surveys, to investigate patterns and possible causes of patters, predict future distribution, and generate spatially explicit model-based abundance estimates, which may be of smaller sub-regions than the original survey. The wide range of applications makes these very popular, and there have been a considerable number of previous studies (Becker et al. 2012; Forney et al. 2012; Roberts et al. 2016; Breen et al. 2016; Mannocci et al. 2017; Becker 2021).

3.1.1 Study area

This chapter uses approximately 60,000 km of survey effort (Table 3.2-1) collected via shipboard and aerial surveys during the SCANS-III and ObSERVE cetacean surveys (Rogan et al. 2018; Hammond et al. 2021). These data were all collected during the summer of 2016. Further information on the surveys is provided in section 2. The area covered by the surveys is shown in Figure 2.1-2.

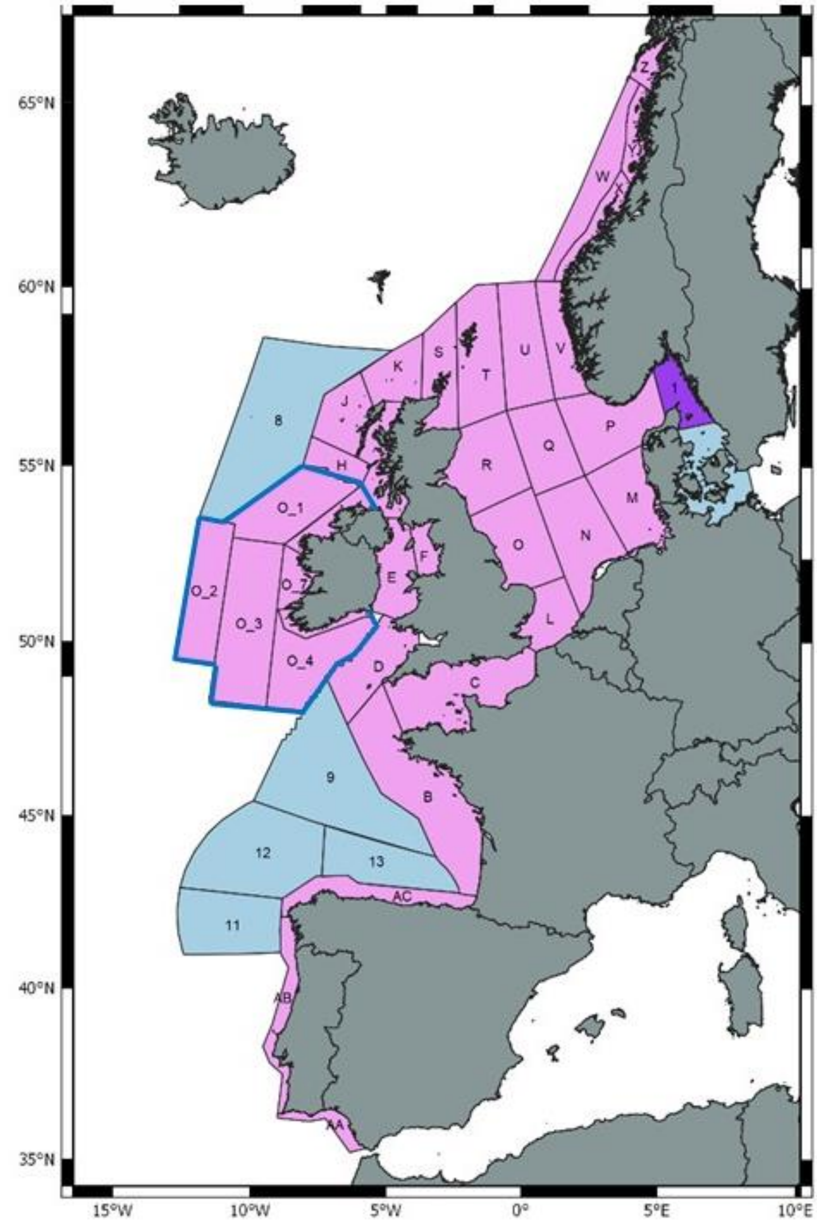

Figure 3.1-1: Survey blocks for the SCANS-III and ObSERVE (outlined in thick blue lines, labelled O_1-O_7) surveys. Blue survey blocks were surveyed by ship. Blocks coloured pink were surveyed by aircraft. SCANS-III block 1 was covered by both aerial and ship survey teams due to poor weather.

3.1.2 Cetaceans within the study area

At least 28 species of cetacean are known to have occurred within the area covered by the SCANS-III and ObSERVE surveys (hereafter, the study area) (Reid et al. 2003; Wall et al. 2006, 2013). The number of species which are regularly present in the study area vary between 13 (Evans and Hammond 2004) and 15 (Weir et al. 2001), with the remainder being classed as either vagrant (eight species) or occasional visitors. Of the 13 or so regularly present species, the SCANS-III survey was able to calculate design-based estimates of abundance – derived using distance analysis as per

Buckland (2001) – for ten of these (Hammond et al., 2021). The ObSERVE survey was able to estimate design-based abundance for 11 species (Rogan et al., 2018). This demonstrates the applicability and value of these large-scale surveys in providing baseline and snapshot data. Furthermore, models of these data have been independently produced on a survey-by-survey basis (Rogan et al., 2019, Lacey et al., 2022). In contrast to the two independent modelling studies, the models presented in this chapter are fitted to the two datasets combined. This analysis provides a much more complete snapshot of the summer 2016 distribution than looking at the two areas in isolation, as animals are highly mobile and could easily be moving between the two areas. Models are presented for harbour porpoise, five species of delphinid, minke whale and fin whale. As context for the following work, Table 3.1-1 provides the design-based abundance estimates for the eight species which are further explored in this thesis.

Table 3.1-1 Design based abundance estimates and confidence intervals for 8 cetacean species within the SCANS-III and ObSERVE survey areas. SCANS-III estimates are taken from Hammond et al., 2021l; ObSERVE estimates are taken from Rogan et al., 2018. NA values are provided if an abundance estimate was not calculated from a survey.

Species	SCANS-III estimate	SCANS-III Lower 95% CI	SCANS-III Upper 95% CI	ObSERVE estimate (season 3 – Summer 2016)	ObSERVE Lower 95% CI	ObSERVE Upper 95% CI	Total
Harbour porpoise	466,569	345,306	630,417	38,260	30,972	47,265	504,829
Minke whale	14,759	8,016	27,173	6,579	3,576	12,104	21,338
White-beaked dolphin	36,287	20,790	63,334	NA	NA	NA	36,287
White-sided dolphin	15,510	4,389	54,807	2,906	120	1,030	18,416
Bottlenose dolphin	33,123	20,305	54,033	87,330	58,029	131,426	120,453
Common dolphin	473,461	286,094	783,539	13,633	5,214	35,646	487,093
Striped dolphin	441,455	245,974	792290	NA	NA	NA	4
Fin whale	27,293	13,187	56,487	95	26	342	27,388

3.1.3 Chapter objective

The aim of this chapter is to use the combined SCANS-III and ObSERVE dataset (see Rogan et al., 2018 for ObSERVE; Hammond et al., 2021 for SCANS-III) to produce predictive models (including an isotropic X, Y smooth) to best describe the distribution of eight different species of cetacean across the study region. These selected species include the two baleen whale species for which there are sufficient data, the delphinid species for which there are sufficient data, and the harbour porpoise.

3.2 Methods

Predictive GAMS, including an isotropic smooth of latitude and longitude (converted into UTM30 coordinate system, represented as X & Y) as well as environmental covariates (Section 2.3.1) were fitted to data for 10 cetacean species, the species that were most frequently encountered across the two surveys. Both negative binomial and Tweedie error distributions were tried for each species, and the distribution found to allow the best fit of the model to the data is presented below. For species for which models of individual animals did not fit well, (common dolphins, striped dolphins and pilot whales) the number of groups was modelled as the response variable as described in Section 2.3.3. Separate models were run for environmental data incorporating a time lag (section 2.3.5) and a model using just the July data. The best of these are presented below.

3.2.1 Description of data

3.2.1.1 Cetacean data

The data modelled in this chapter all come from the SCANS-III survey (Hammond et al. 2021) and the ObSERVE survey (Rogan et al. 2018). Data are all from the summer of 2016. More specific details of the surveys are outlined in section 2.1. The area covered by the survey is shown in Figure 2.1-2.

Table 3.2-1 summarises the effort and sightings available for modelling the whole of the SCANS-III and ObSERVE (hereafter S3/ObSERVE) survey region. Only data collected in sea conditions less than Beaufort 3 were used for harbour porpoise modelling (less than Beaufort 5 for other species). Maps showing achieved survey effort and the locations of the sightings included in the modelling are included alongside the relevant predictions below.

The survey area is large, and as a consequence there are a large number of segments with no sightings. For the harbour porpoise, the most commonly sighted species, there were sightings in 0.15% of the effort segments. For the other species, only 0.002-0.04% of the segments contained sightings.

Table 3.2-1 Number of effort segments and number of groups and individuals sighted of each species used in analysis of data from the combined SCANS-III and ObSERVE dataset, collected during summer 2016.

Species	Total no. of effort segments	Total effort (km)	No. of effort segments with groups	Number of groups	Number of Individuals	Mean group size
Minke whale	6961	62,375	96 (0.01%)	114	118	1.04
White-beaked dolphin	6961	62,375	68 (0.01%)	111	435	3.92
Harbour porpoise	6448	57,150	945 (0.15%)	1584	2146	1.35
White-sided dolphin	6961	62,375	15 (0.002%)	20	87	4.35
Bottlenose dolphin	6961	62,375	138 (0.02%)	222	1346	6.06
Common dolphin	6961	62,375	224 (0.03%)	557	4779	8.58
Striped dolphin	6961	62,375	54 (0.008%)	74	1974	26.7
Fin whale	6961	62,375	261 (0.04%)	567	797	1.4

3.2.2 Covariate data – static covariates

Covariates for models of the S3/ ObSERVE dataset were selected using the methods outlined in Chapter 2. The values of each covariate assigned to the modelled effort segments, are summarised in

Table 3.2-2Table 3.2-2 and Figure 3.2-1 to Figure 3.2-3. In this area, water depth ranges from the coast to more than 5,000m (0-5,364m) with most segments having depths shallower than 500m (Figure 3.2-1 to Figure 3.2-3). The slope is generally shallow across the region, with most of the segments having less than 1^0 of gradient, although some are very steeply sloped, with the maximum being 19^0.

Most effort segments are within 200km of the coast and 250km of the 200m depth isobath – with the majority of the segments being in waters less than 200m deep. Similarly, most segments are within 250km of escarpments and troughs, whilst distances to seamount and trough features are typically further Figure 3.2-1 to Figure 3.2-3. Maps of covariates are provided in Figure 3.2-4 to Figure 3.2-8.

Table 3.2-2: Summary of static covariate values assigned to effort segments used to model the cetacean data across the full SCANS-III and ObSERVE area.

Variable	Min	Max
Depth (m)	0	-5364
Standard deviation of depth (SDdepth)	0	806
Slope (^{0})	0	19.4
Distance to coast (km) (Dcoast)	0	503
Distance to 200m isobath (km) (D200_iso)	0	820
Distance to 2000m isobath (km) (D2000_iso)	0	1255
Distance to 200m isobath, scaled to take account of whether segments are deeper (negative numbers) or shallower (positive numbers) than 200m (CS200) (km)	-479	820
Distance to escarpments (km)	0	1234
Distance to canyons (km)	0	1115
Distance to seamounts (km)	13	1815
Distance to troughs (km)	0	182

3.2.3 Covariate data – dynamic covariates

Monthly mean values for dynamic covariates for the effort segments within the study region are provided in Table 3.2-3 below. Mean sea surface temperature (SST) varied from 11.7^0 to 23.9^0 across the region, with warmer areas to the south. Mean depth of mixed layer depth (MLD) ranged from 6.9m to 25m. Salinity varied from a low of 20 PSU up to 36 PSU. Maps of covariates are provided in Figure 3.2-4 to Figure 3.2-8.

Table 3.2-3: Summary of dynamic covariate values assigned to effort segments used to model the cetacean data across the full S3/ ObSERVE region.

Variable	Min	Max
Sea surface temperature (SST) (°C)	11.7	23.9
Sea Level Anomaly (SLA) (m)	-0.1	0.2
Sea Surface Height (SSH) (m)	-0.58	0.14
Absolute Dynamic Topography (ADT) (m)	-0.3	0.3
Mixed Layer Depth (MLD) (m)	6.9	25.2
Salinity (SAL) (PSU)	20.1	36.3

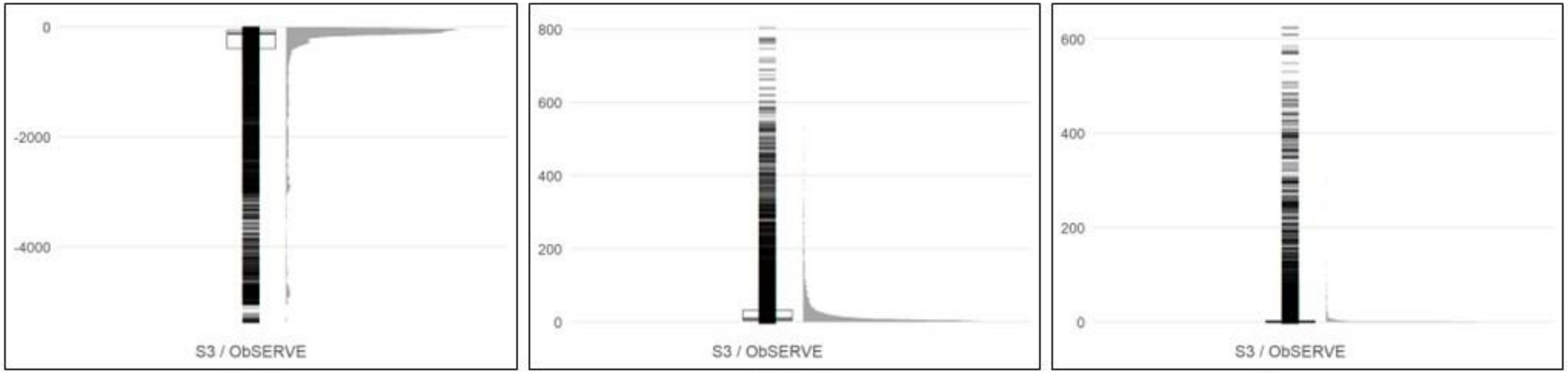

Depth **SD depth** **Slope**

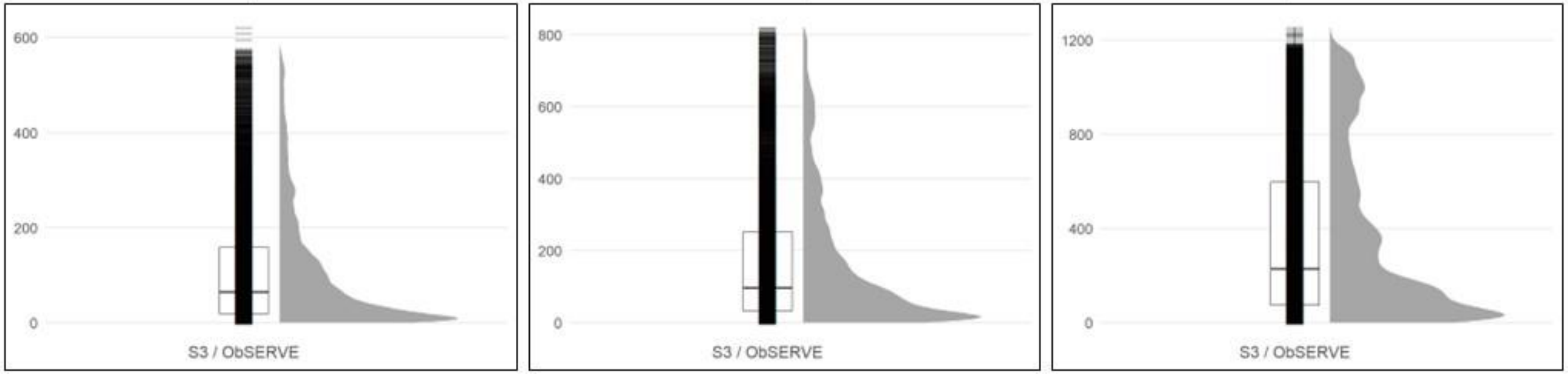

Dist 50m isobath **Dist 200m isobath** **Dist 2000m isobath**

Figure 3.2-1: Raincloud plots showing the distribution of covariate data for depth, SD depth, slope, distance to the 50m isobath, distance to the 200m isobath and distance to the 2000m isobath associated with the effort segments used to model the S3/ObSERVE cetacean data

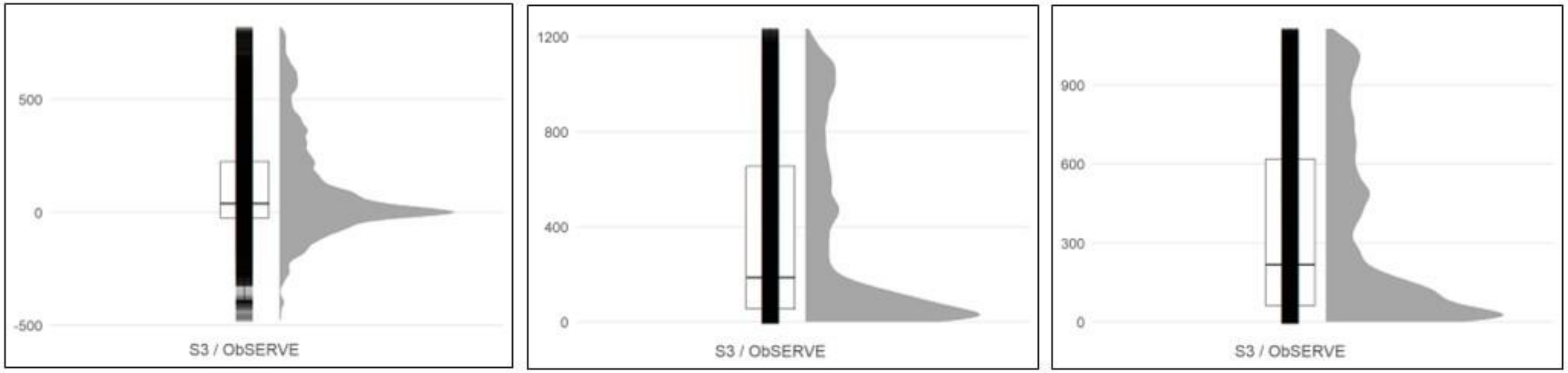

CS 200 **Escarpments** **Canyons**

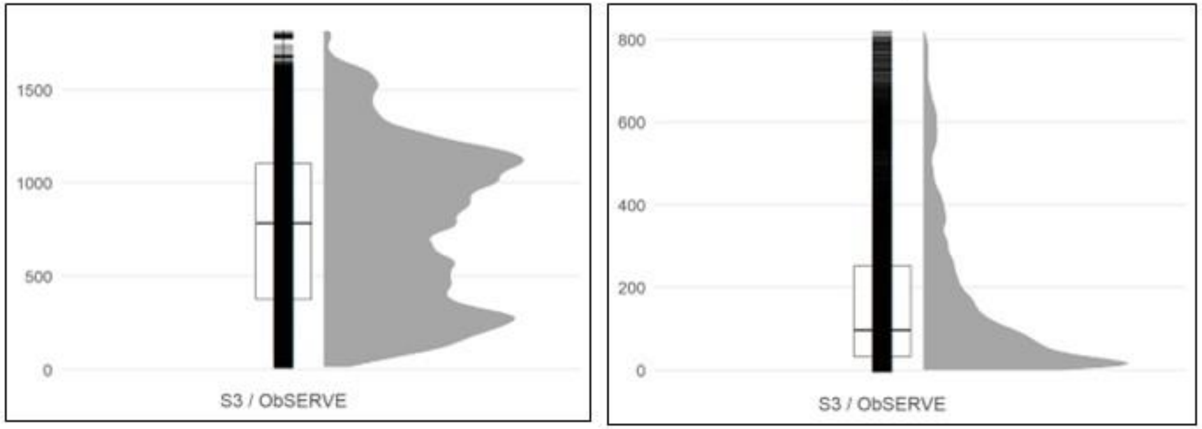

Seamounts **Troughs**

Figure 3.2-2: Raincloud plots showing the distribution of covariate data for contour-side scaled distance to 200m isobath, distance to escarpments, distance to canyons, distance to seamounts and distance to trough covariates associated with the effort segments used to model the S3/ObSERVE cetacean data

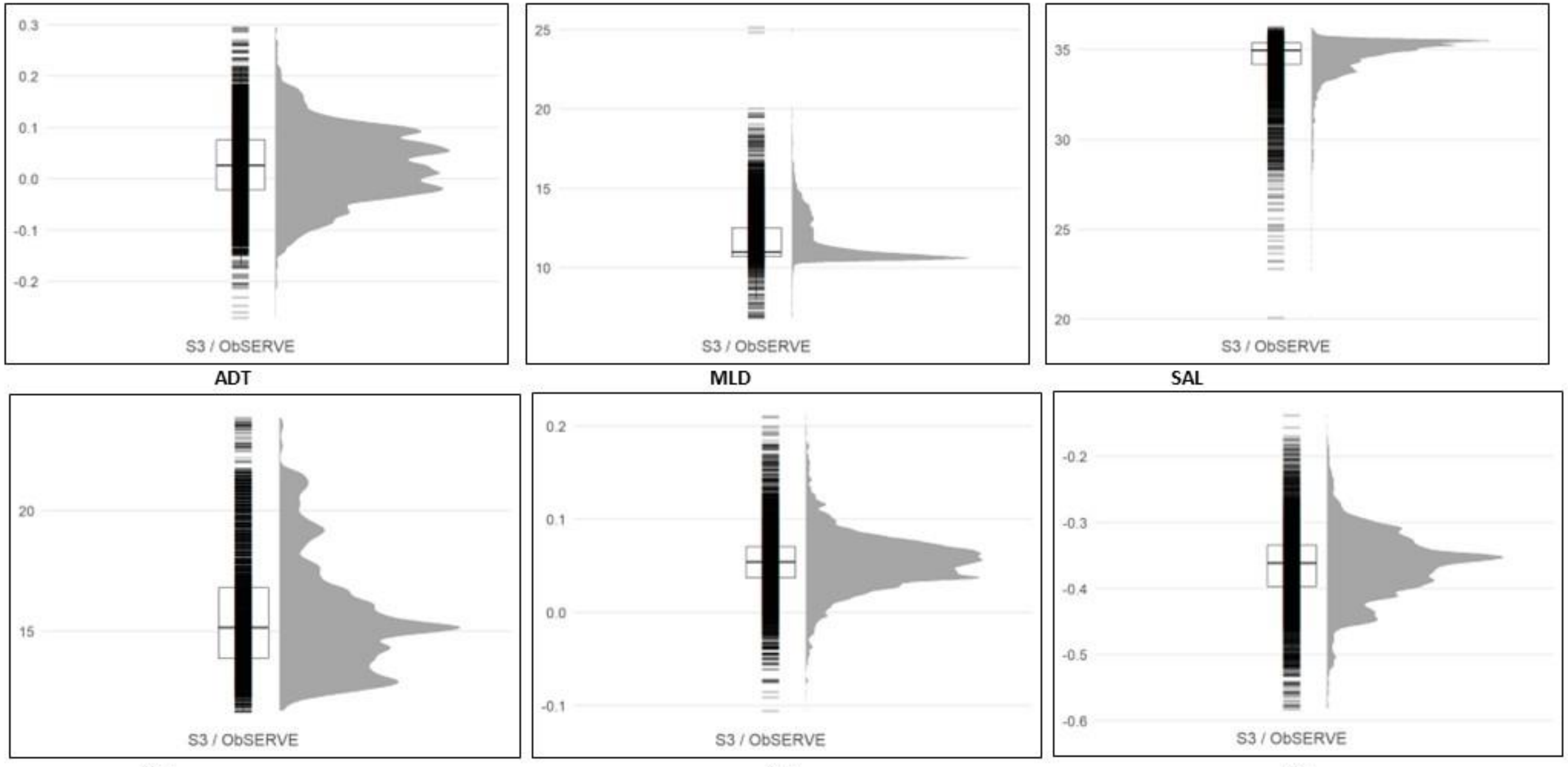

Figure 3.2-3: Raincloud plots showing the distribution of covariate data for absolute dynamic topography (ADT), mixed layer depth (MLD), salinity (SAL), sea surface temperature (SST), sea level anomaly (SLA) and sea surface height (SSH covariates associated with the effort segments used to model the S3/ObSERVE cetacean data.

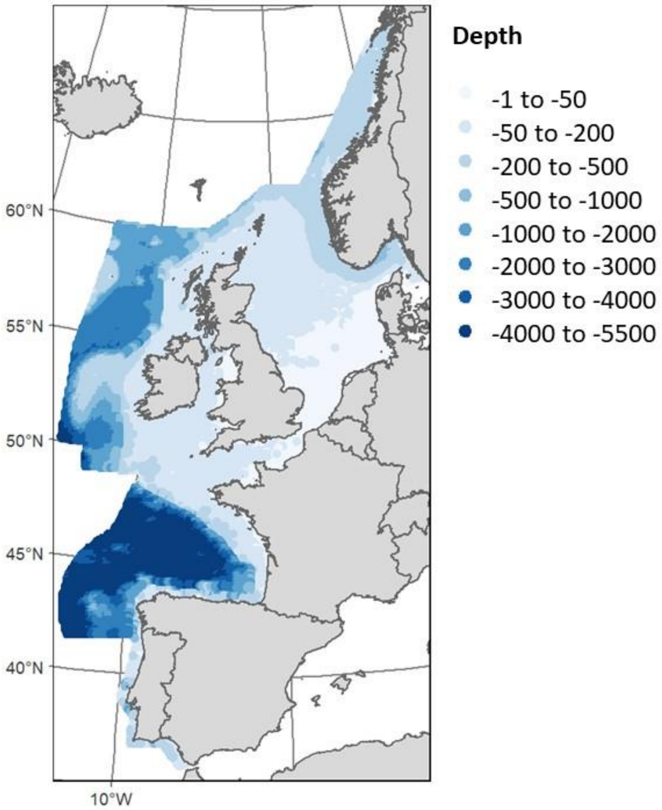

Figure 3.2-4 Map of the depth(m) covariate data associated used to model the S3 / ObSERVE cetacean data.

Figure 3.2-5 Map of the standard deviation of depth(m) covariate (LEFT) and the slope covariate (degrees) (RIGHT) data associated used to model the S3 / ObSERVE cetacean data

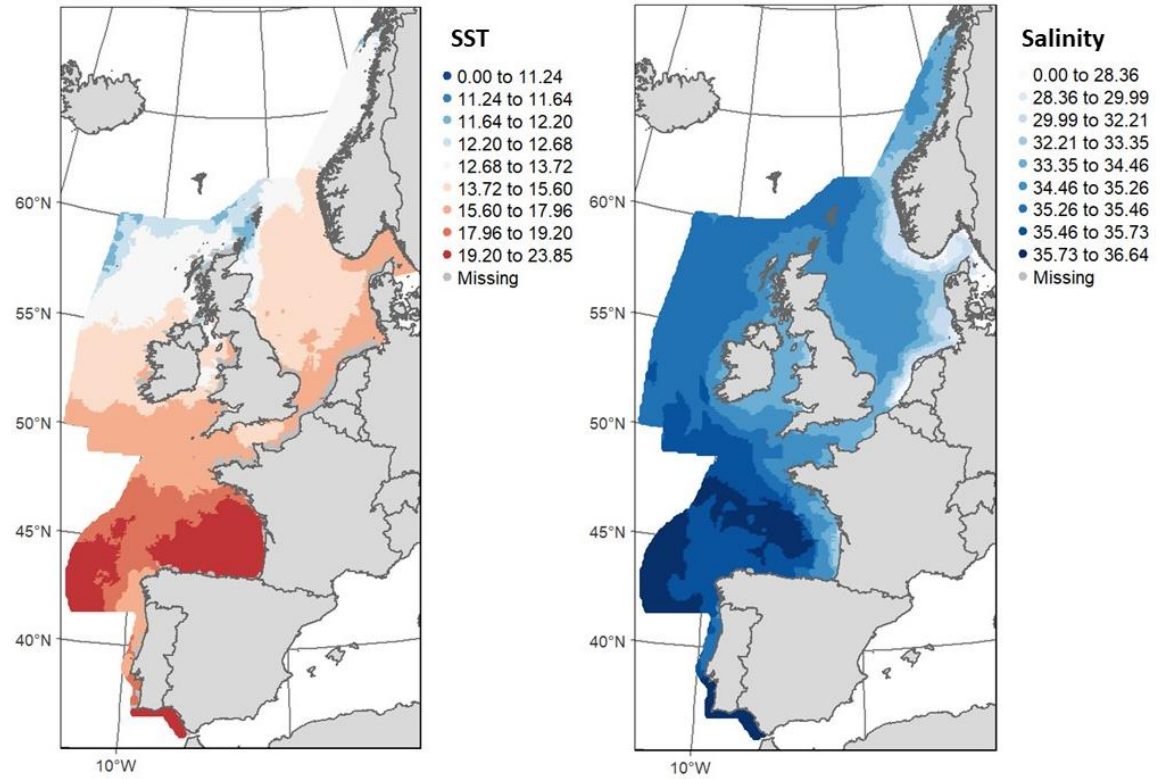

Figure 3.2-6: Map of the sea surface temperature (°C) covariate (LEFT) and the salinity covariate (PSU) (RIGHT) data associated used to model the S3 / ObSERVE cetacean data

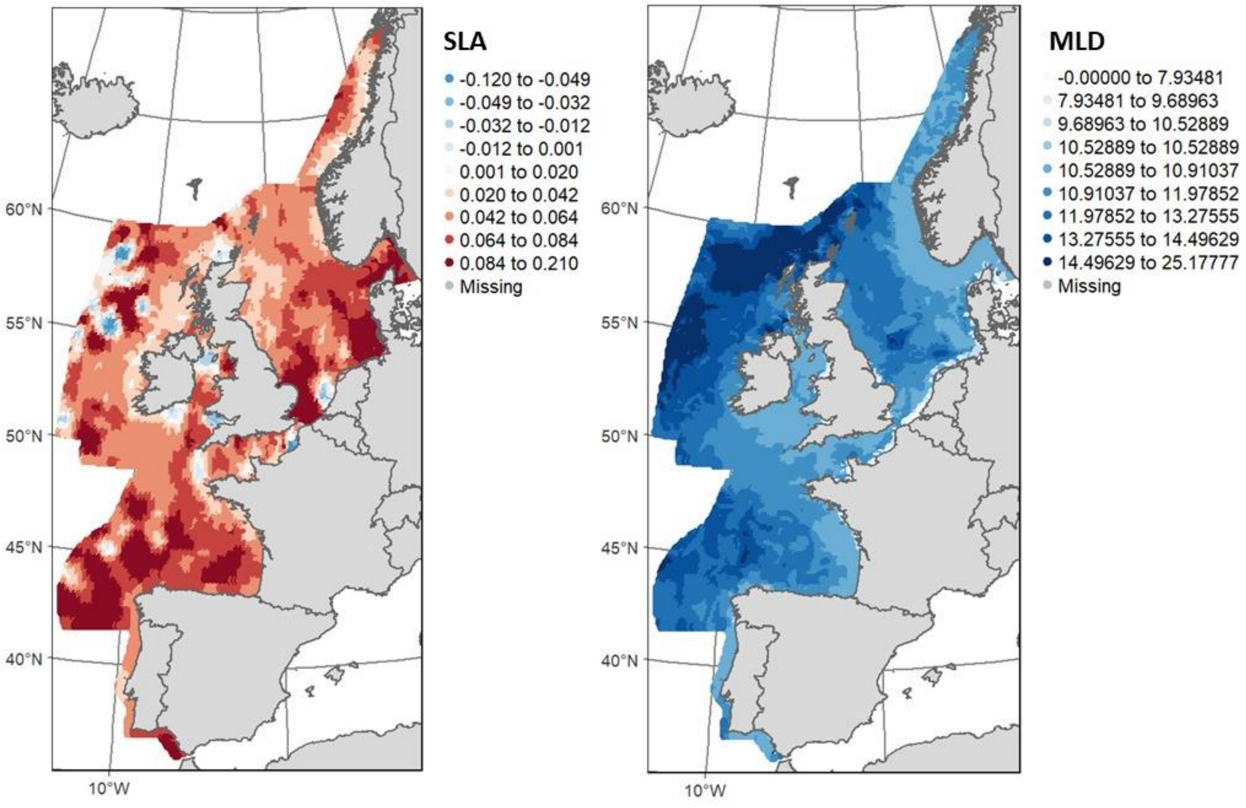

Figure 3.2-7 Map of the sea level anomaly (m) covariate (LEFT) and the mixed layer depth covariate (m) (RIGHT) data associated used to model the S3 / ObSERVE cetacean data

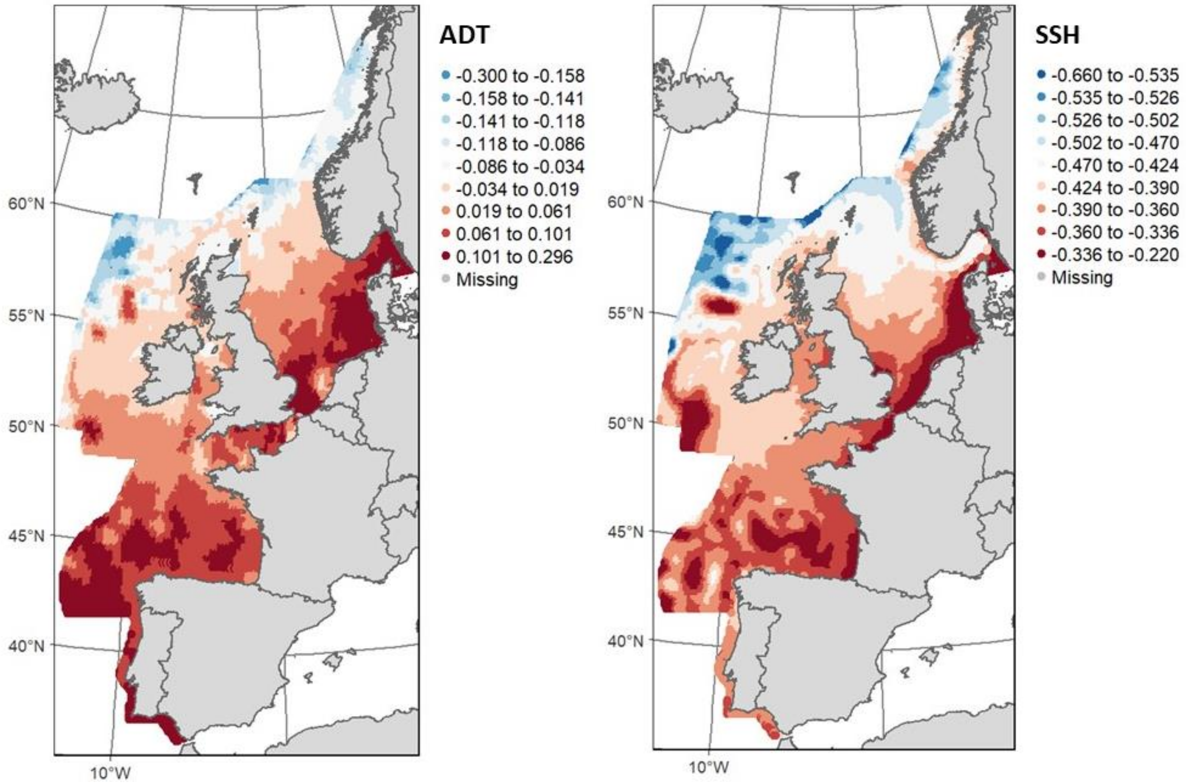

Figure 3.2-8: Map of the absolute dynamic topography (m) covariate (LEFT) and the sea surface height covariate (m) (RIGHT) data associated used to model the S3 / ObSERVE cetacean data

3.3 Results

3.3.1 Harbour porpoise

Summary results of the final model selected for harbour porpoises across the full survey area are provided in Table 3.3-1. Model diagnostics indicated a satisfactory fit to the data, with the proportion of null deviance explained by the model being 42.1%. The QQ plot and the residuals vs linear are provided in (Appendix 2); partial effects plots of the fitted smooth functions in Figure 3.3-2. The negative binomial error distribution best described the data. The fitted smooth functions showed relatively low levels of "wiggliness", with all environmental covariates (excluding the isotropic XY smooth) requiring less than 1 estimated degree of freedom (edf) except for ADT_July.

Harbour porpoise predicted density ranged from 0 to 1.7 animals per km^2(Figure 3.3-3). There were higher estimated densities of harbour porpoises at areas of flat seabed (low SDdepth), and shallow depths, with density decreasing linearly with increase in depth and increased levels of variation in seabed topography.

There were also positive effects for increased distance from the 200m isobath, with a clear preference for the shallower side of the contour (CS200). The July data for two dynamic covariates were retained in the final model, with a positive linear effect for slightly higher salinity. The absolute dynamic topography (ADT) covariate is the only one not to show a clear, non-linear signal, with the highest densities of harbour porpoises being predicted at values of zero ADT, decreasing as ADT values both increased and decreased. This suggests there was no strong association to current mesoscale activity. The highest densities of harbour porpoises were predicted in the North Sea, particularly the south-western part of the North Sea (Figure 3.3-3 b), which is a good match with the observed sightings data (Figure 3.3-3 a). The plot of predicted CV shows reasonable levels of confidence in the model except in the Bay of Biscay region (Figure 3.3-4c). Prediction standard errors (SE) are provided in Figure 3.3-4 d.

Table 3.3-1 Model outputs for harbour porpoise predictive GAM

Error distribution	**Model covariates**	**Estimated degrees of freedom**	**P value**	**% Deviance explained**	**Model degrees of freedom**
Negative binomial	X, Y	21.65	2e-16	42.1	29.0
	SDdepth	0.60	0.12		
	Depth	0.97	4.2e-6		
	ADT	3.35	4.2e-6		
	Salinity	0.92	4.7e-4		
	CS200	0.55	0.07		

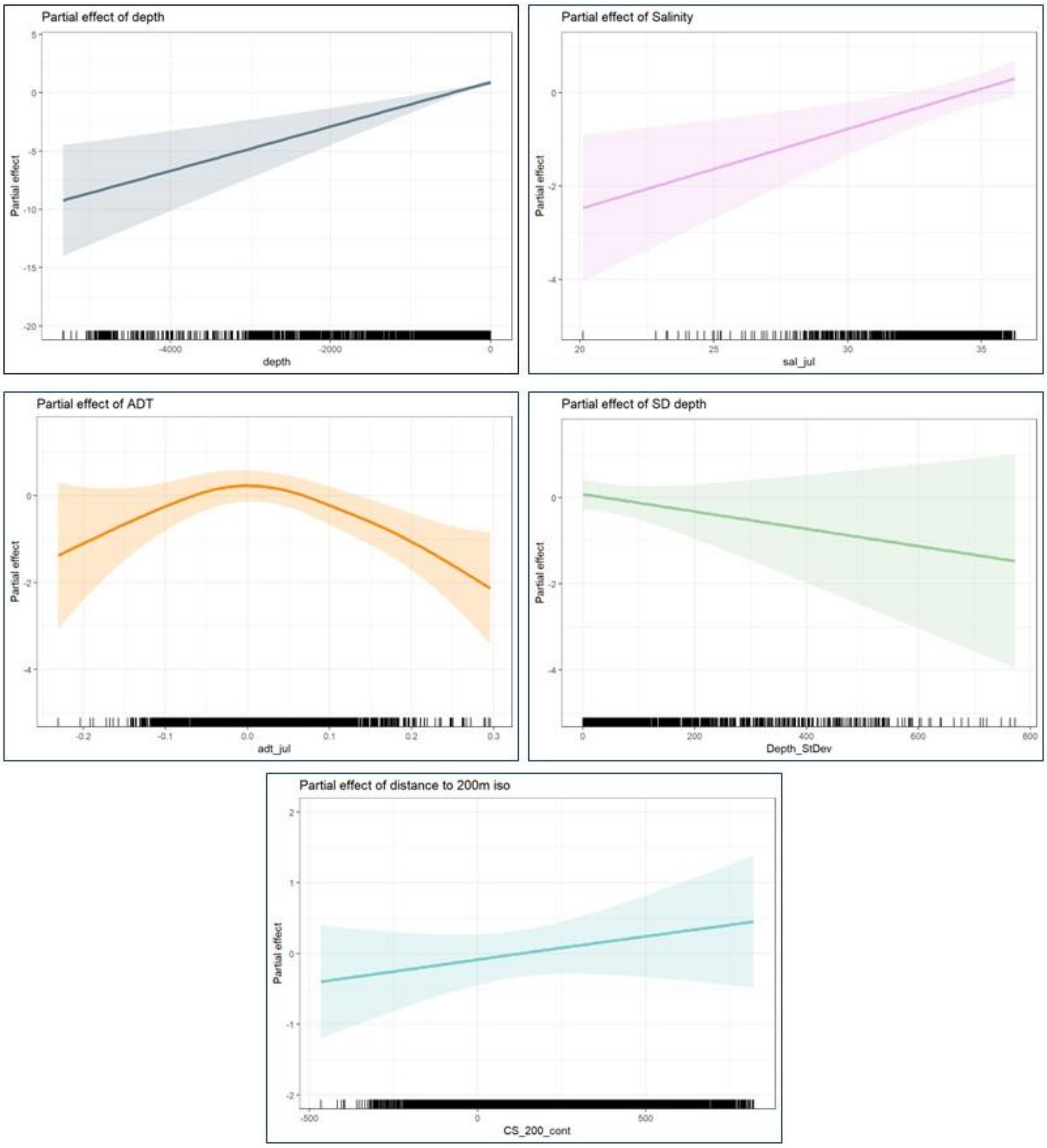

Figure 3.3-1. Plots of the fitted smooth functions for the harbour porpoise predictive GAM. “Rug” marks on the x-axis of the fitted smooth plots show the distribution of the data. Shaded areas represent the 95% confidence intervals.

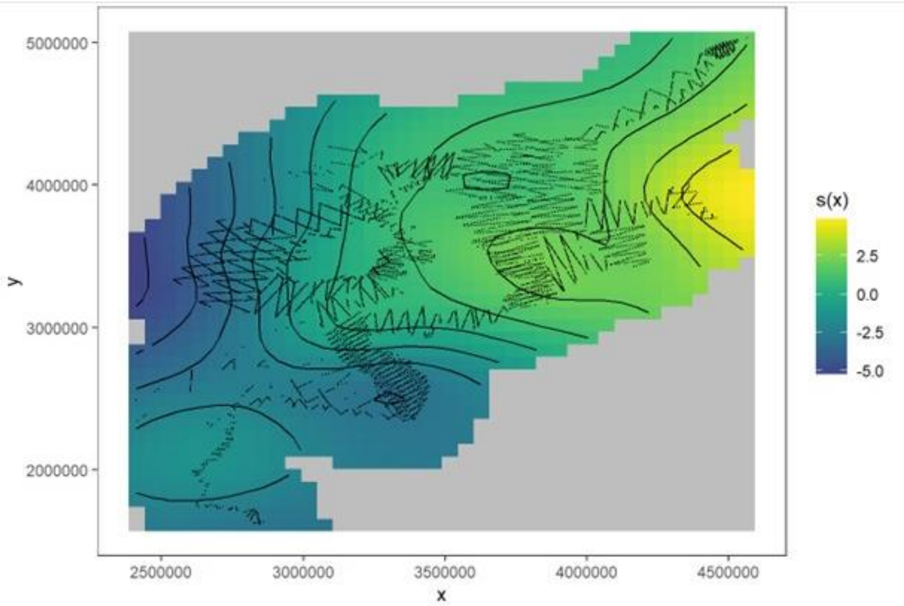

Figure 3.3-2. X, Y spline plot for the harbour porpoise predictive GAM, also showing survey effort

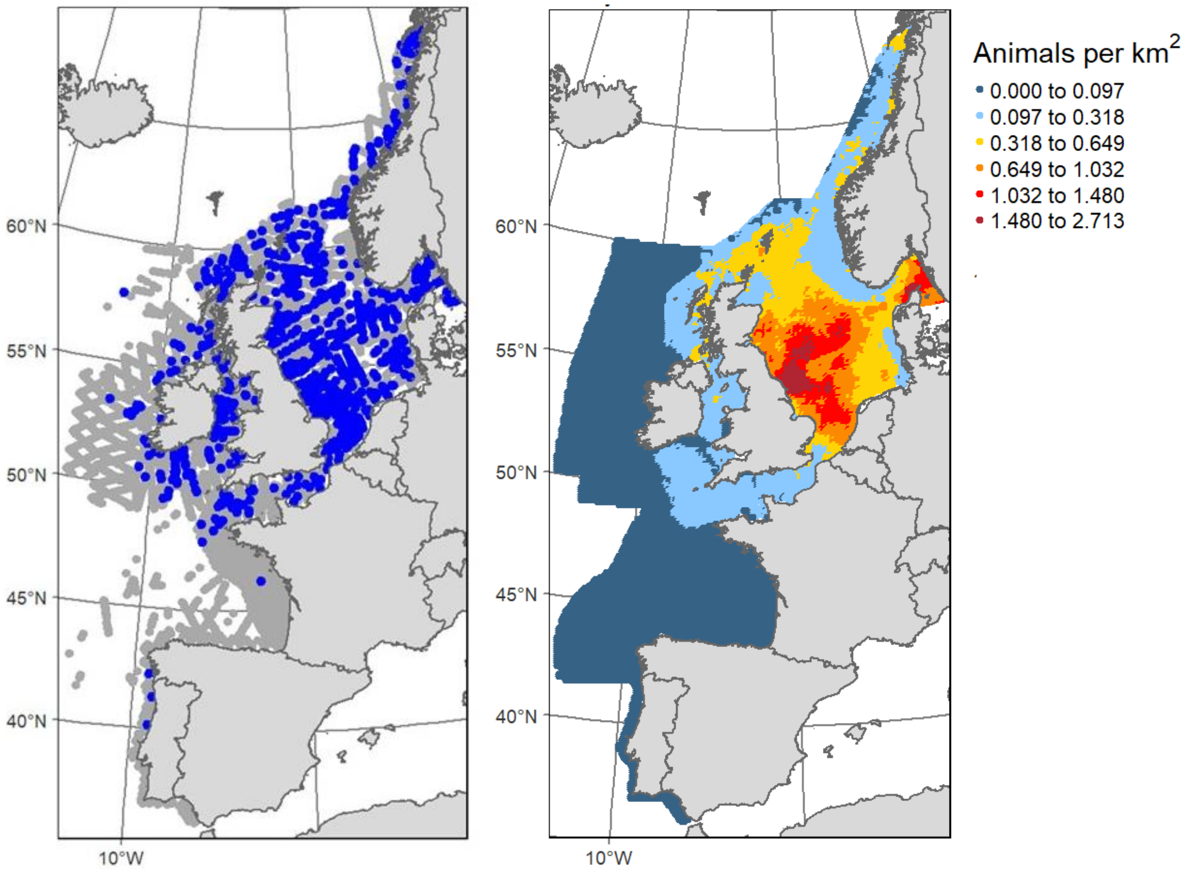

Figure 3.3-3: Location of effort and sightings (LEFT) and predicted density surface (RIGHT) for the harbour porpoise S3/ObSERVE model. models. White areas are outside of predictive space. In some cases, prediction grid cells had covariate values which were outside the range encompassed by the modelled effort segments. In these instances, grid-cells were excluded from the prediction.

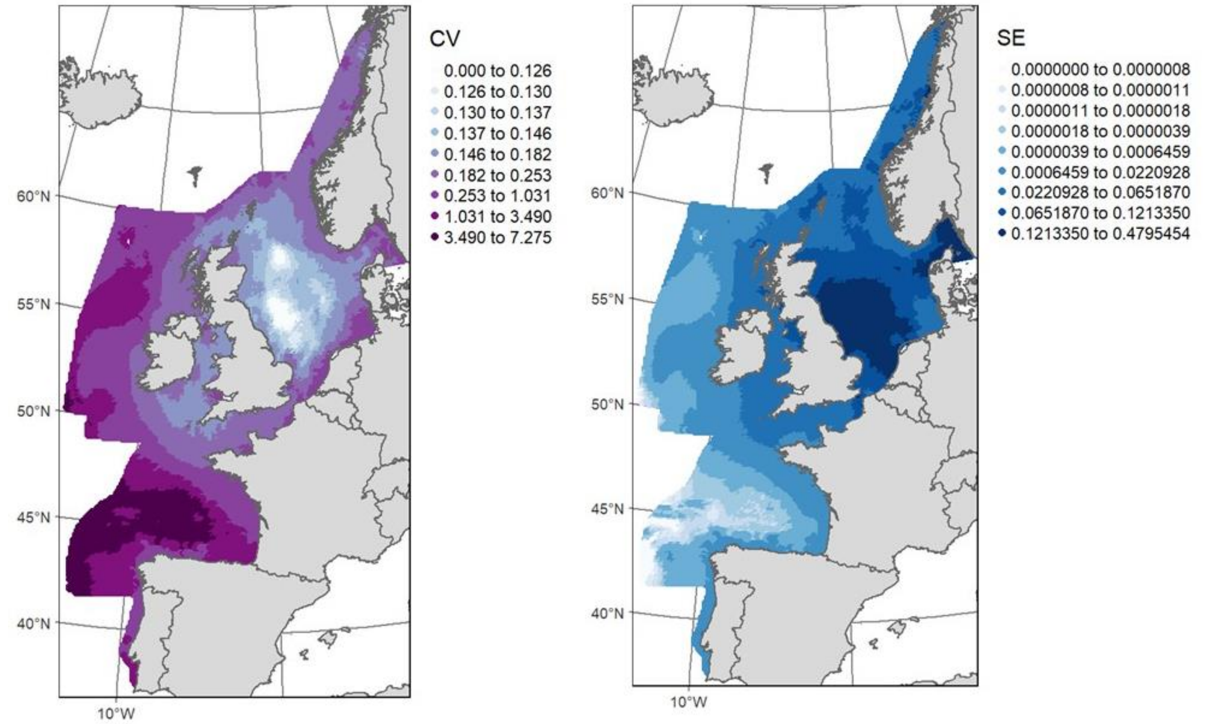

Figure 3.3-4: Coefficient of variation CV of density (CV) (LEFT) and standard error (SE) (RIGHT) for S3/ObSERVE survey data. Range of values represented by colours in the maps show the 1%, 2%, 5%, 10%, 25%, 50%, 75%, 90% and 100% quantiles. White areas are outside of predictive space. In some cases, prediction grid cells had covariate values which were outside the range encompassed by the modelled effort segments. In these instances, grid-cells were excluded from the prediction.

3.3.2 White-beaked dolphin

Summary results of the final model selected for white-beaked dolphins across the full survey area are provided in Table 3.3-2. Although model diagnostics (Appendix 2) indicated a good fit to the data, the amount of null deviance explained by the model was high at 60.4%, which could be indicative of a high signal to noise ratio, likely in particular due to the restricted spatial distribution of this species in comparison with the full study region (Figure 3.3-5).

The negative binomial error distribution best described the data. The fitted smooth functions are linear, with both remaining environmental covariates (excluding the isotropic XY smooth) requiring fewer than 1 estimated degrees of freedom. The density of white-beaked dolphins was predicted to decrease as depth increased, whilst the highest estimated densities were also predicted to increase with increasing salinity (Figure 3.3-5). There is a broad, north-south pattern visible in the XY spline (Figure 3.3-6) with the highest densities predicted in the north of the study region.

Predicted density of white-beaked dolphins is between 0 and 0.27 across the region, with the highest densities of white-beaked dolphins were predicted in the coastal waters around the north of Scotland (Figure 3.3-8). This is a good match with the sightings and reflects their overall distribution. The plot of predicted CV shows reasonable levels of confidence in the model outside the Bay of Biscay region (Figure 3.3-8).

Table 3.3-2. Model outputs for white-beaked dolphin predictive GAM

Error distribution	Model covariates	Estimated degrees of freedom	P value	% Deviance explained	Model degrees of freedom
Negative binomial	X, Y	10.55	2e-16	58.1%	13.3
	Depth	0.89	0.006		
	Salinity	0.84	0.008		

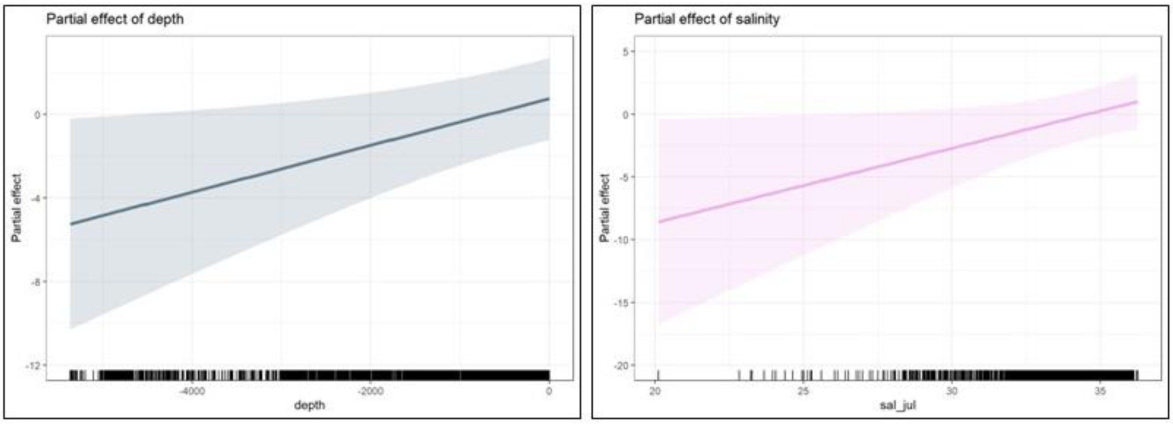

Figure 3.3-5. Plots of the fitted smooth functions for the white-beaked dolphin predictive GAM. "Rug" marks on the x-axis of the fitted smooth plots show the distribution of the data. Shaded areas represent the 95% confidence intervals.

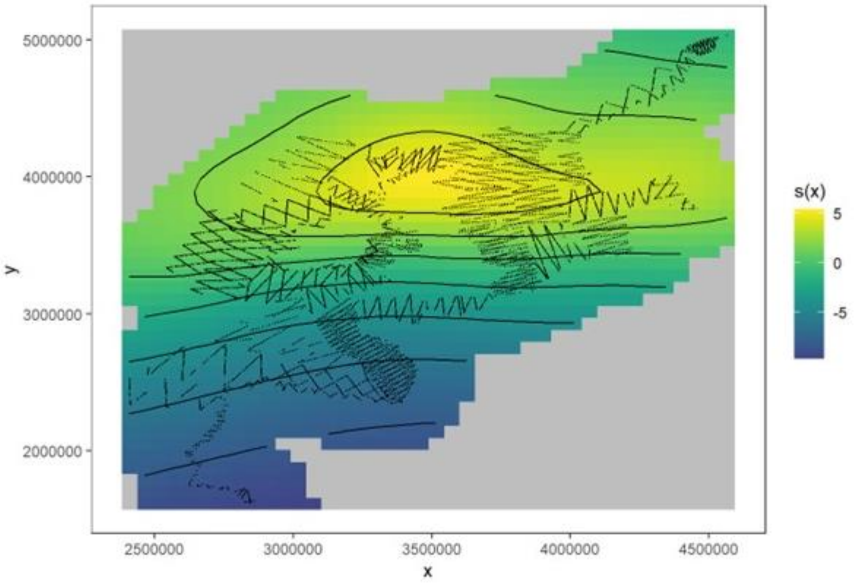

Figure 3.3-6. X, Y spline plot for the white-beaked dolphin predictive GAM, also showing survey effort

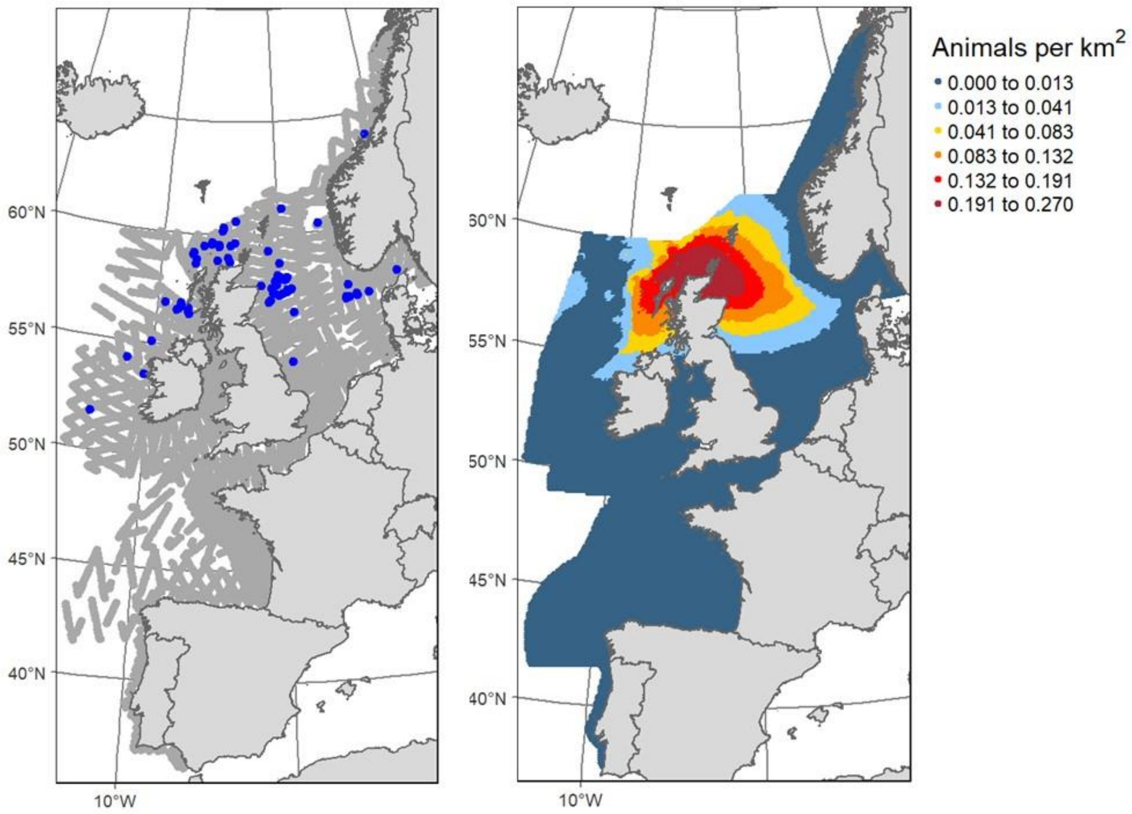

Figure 3.3-7: Location of effort and sightings (LEFT) and predicted density surface (RIGHT) for the white-beaked dolphin S3/ObSERVE model. models. White areas are outside of predictive space. In some cases, prediction grid cells had covariate values which were outside the range encompassed by the modelled effort segments. In these instances, grid-cells were excluded from the prediction.

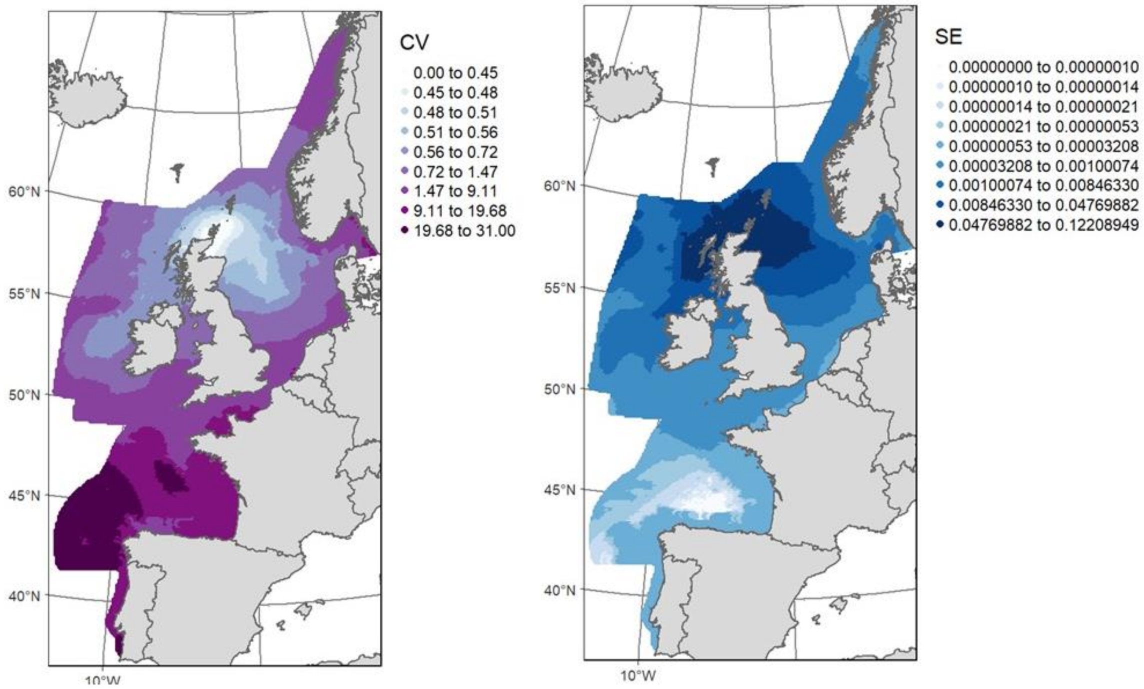

Figure 3.3-8: Coefficient of variation CV of density (CV) (LEFT) and standard error (SE) (RIGHT) for S3/ObSERVE survey data. Range of values represented by colours in the maps show the 1%, 2%, 5%, 10%, 25%, 50%, 75%, 90% and 100% quantiles. White areas are outside of predictive space. In some cases, prediction grid cells had covariate values which were outside the range encompassed by the modelled effort segments. In these instances, grid-cells were excluded from the prediction.

.

3.3.3 White sided dolphin

Summary results of the final model selected for white-sided dolphins across the full survey area are provided in Table 3.3-3. Model diagnostics indicated a reasonable fit to the data, and the amount of null deviance explained by the model was 35.8%. The QQ plot and the residuals vs linear plot are provided in Appendix 2. Partial effects plots are provided in Figure 3.3-9.

For white-sided dolphins, the Tweedie error distribution best described the data. The fitted smooth functions showed relatively low levels of “wiggliness”, with all environmental covariates requiring fewer than 1 estimated degrees of freedom. This is likely due to low numbers of sightings for this species The X, Y smooth was not retained in the model.

Maximum predicted density across the region was 0.11. This was associated with increased water depths, density decreased linearly as depth decreased.

In addition to water depth, white-sided dolphin density was associated with areas with low SDdepth, with density decreasing with increasing variability in the seabed gradient (increasing levels of SDdepth). The confidence limits around this fitted relationship were wide, especially towards the most extreme (variable) end of the scale. White-sided dolphin density was also predicted to be highest in areas of highest salinity, with a linear decrease in predicted density as salinity decreased. The confidence levels were very wide towards lower salinity (and density), where there was a reduced number of data points. Finally, highest dolphin densities were predicted in the areas of coolest sea surface temperatures, with predicted density declining as temperatures increased.

The highest densities of white-sided dolphins were predicted in the waters to the far northwest of the study area (Figure 3.3-10). Whilst this is a good match to most of the detections of this species (**Figure 3.3-7** a), there were a few sightings in the northern North Sea which were not reflected in the density surface. The plot of predicted CV showed reasonable levels of confidence in the model in most areas, with the main areas of higher CV being close to the coast of Norway (Figure 3.3-11).

Table 3.3-3. Model outputs for white-sided dolphin predictive GAM

Error distribution	Model covariates	Estimated degrees of freedom	P value	% Deviance explained	Model degrees of freedom
Tweedie	SDdepth	0.81	0.63	35.8	4.5
	Depth	0.87	0.005		
	Salinity	0.85	0.02		
	SST	1.01	7.3e-6		

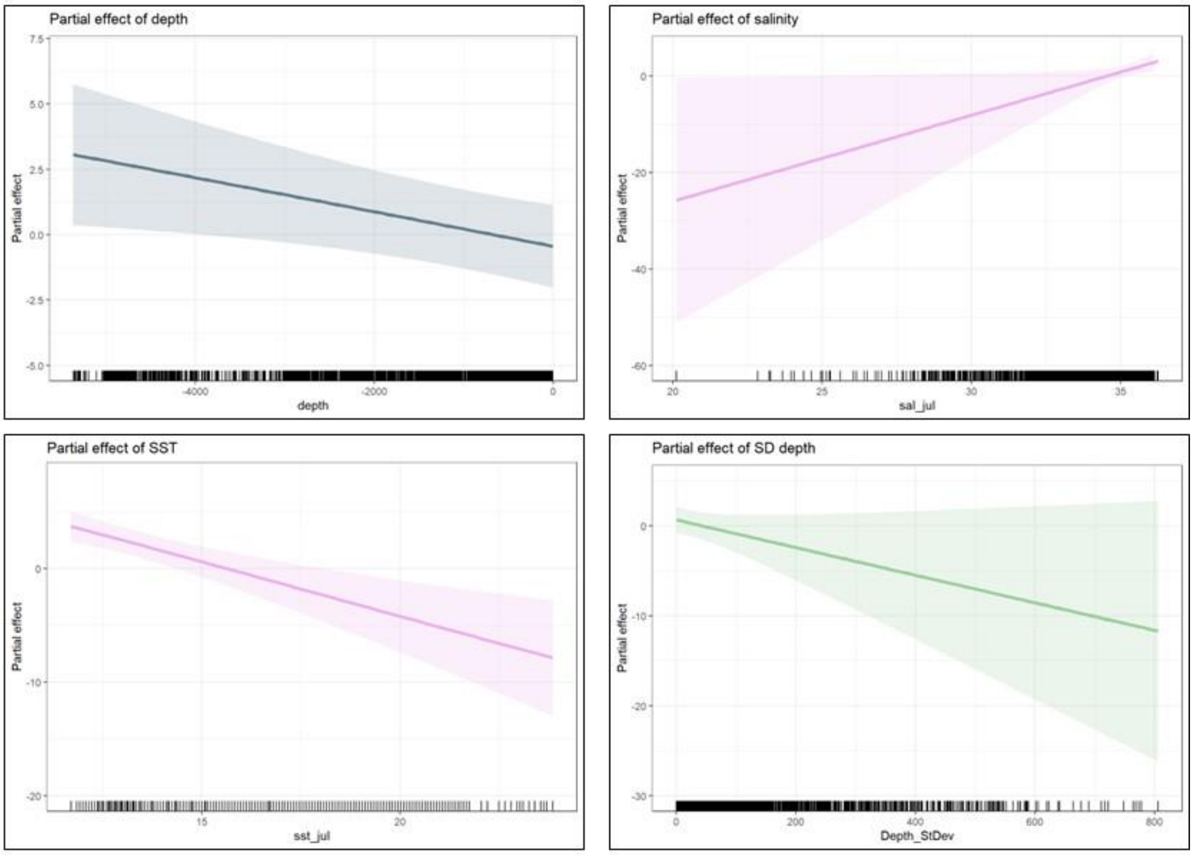

Figure 3.3-9 Plots of the fitted smooth functions for the white-sided dolphin predictive GAM. "Rug" marks on the x-axis of the fitted smooth plots show the distribution of the data. Shaded areas represent the 95% confidence intervals.

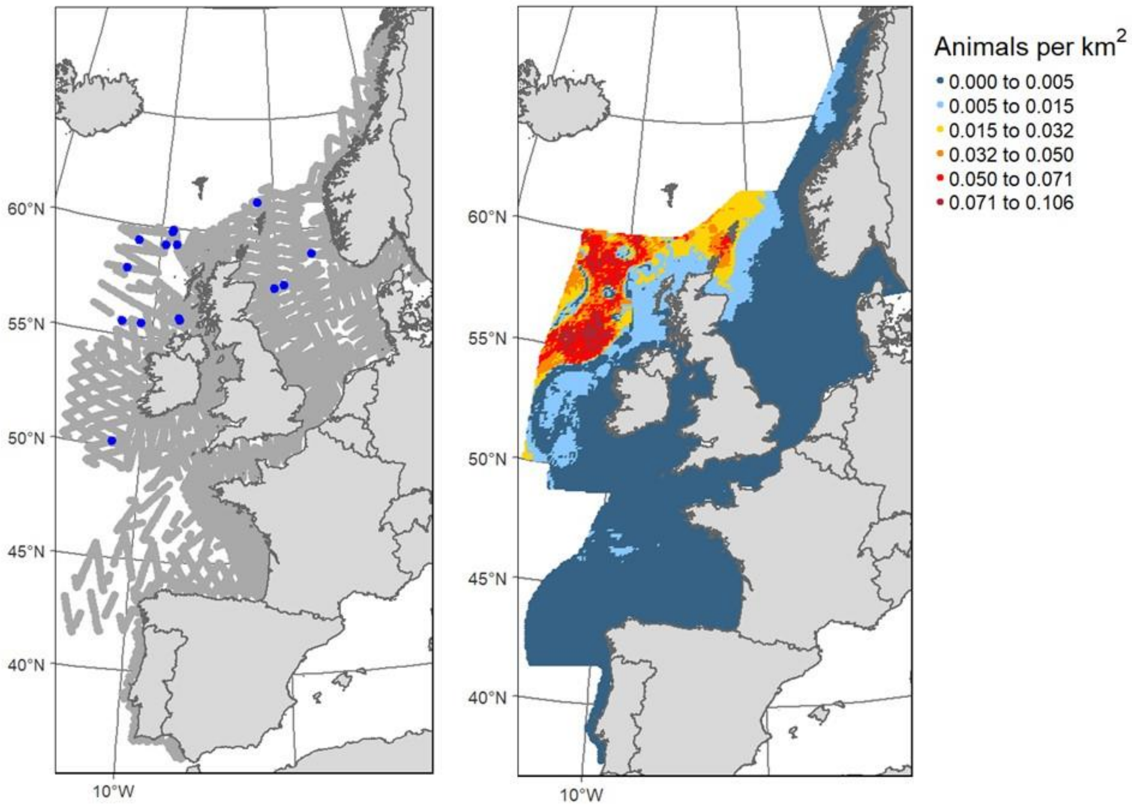

Figure 3.3-10: Location of effort and sightings (LEFT) and predicted density surface (RIGHT) for the white-sided dolphin S3/ObSERVE model. models. White areas are outside of predictive space. In some cases, prediction grid cells had covariate values which were outside the range encompassed by the modelled effort segments. In these instances, grid-cells were excluded from the prediction.

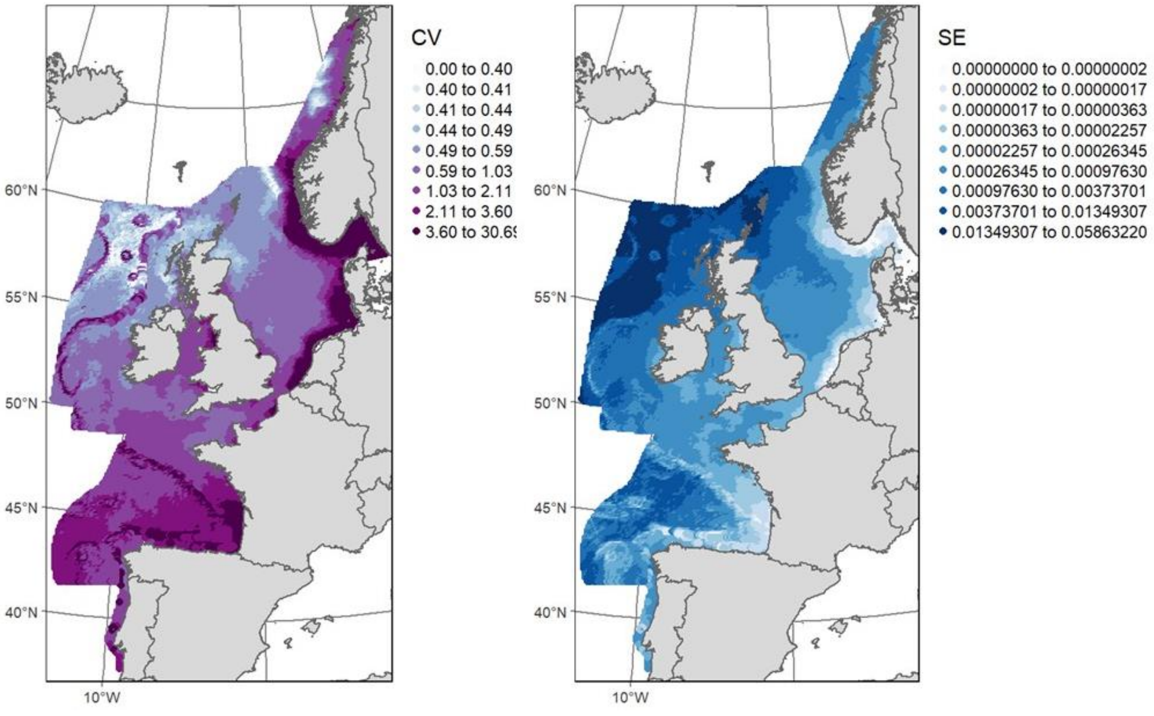

Figure 3.3-11: Coefficient of variation CV of density (CV) (LEFT) and standard error (SE) (RIGHT) for S3/ObSERVE survey data. Range of values represented by colours in the maps show the 1%, 2%, 5%, 10%, 25%, 50%, 75%, 90% and 100% quantiles. White areas are outside of predictive space. In some cases, prediction grid cells had covariate values which were outside the range encompassed by the modelled effort segments. In these instances, grid-cells were excluded from the prediction.

3.3.4 Bottlenose dolphin

The bottlenose dolphin results summary is provided in Table 3.3-4. Model diagnostics indicated an adequate fit to the data, which explained 38% of the null variance. The QQ plot and the residuals vs linear plot are provided in Appendix 2. Plots of the fitted smooth functions are provided in Figure 3.3-12. The Tweedie error distribution best described the data. The fitted smooth functions showed relatively low levels of “wiggliness”, with all environmental covariates (excluding the isotropic XY smooth) requiring fewer than 1 estimated degrees of freedom.

High density of bottlenose dolphins was predicted in areas of shallow water depth, with density declining as depth increased, although this effect was small.

Bottlenose dolphin density was associated with lower sea surface height, with density showing a linear decrease as sea surface height increased, which was towards the south of the region. Distance to coast was retained as a covariate in the model, with dolphin density being highest closer to the coast, and decreasing linearly with distance from coast. The XY spline showed a general increase from east to west, with the highest densities being predicted in the west of the study region (Figure 3.3-13).

The highest densities of bottlenose dolphins, 1.15 animals per km^2, were predicted to the south-west of Ireland (Figure 3.3-14 -RIGHT). Whilst this is a good match to the detections of this species (Figure 3.3-14 -LEFT. The plot of predicted CV showed reasonable levels of confidence in the model outside of the Bay of Biscay region Figure 3.3-15).

Table 3.3-4. Results of the best predictive model for bottlenose dolphin.

Error distribution	Model covariates	Estimated degrees of freedom	P value	% Deviance explained	Model degrees of freedom
Tweedie	X, Y	14.4	2e-16	38.3	17.8
	Depth	0.7	0.05		
	SSH	0.8	0.02		
	Distance to coast	0.8	0.008		

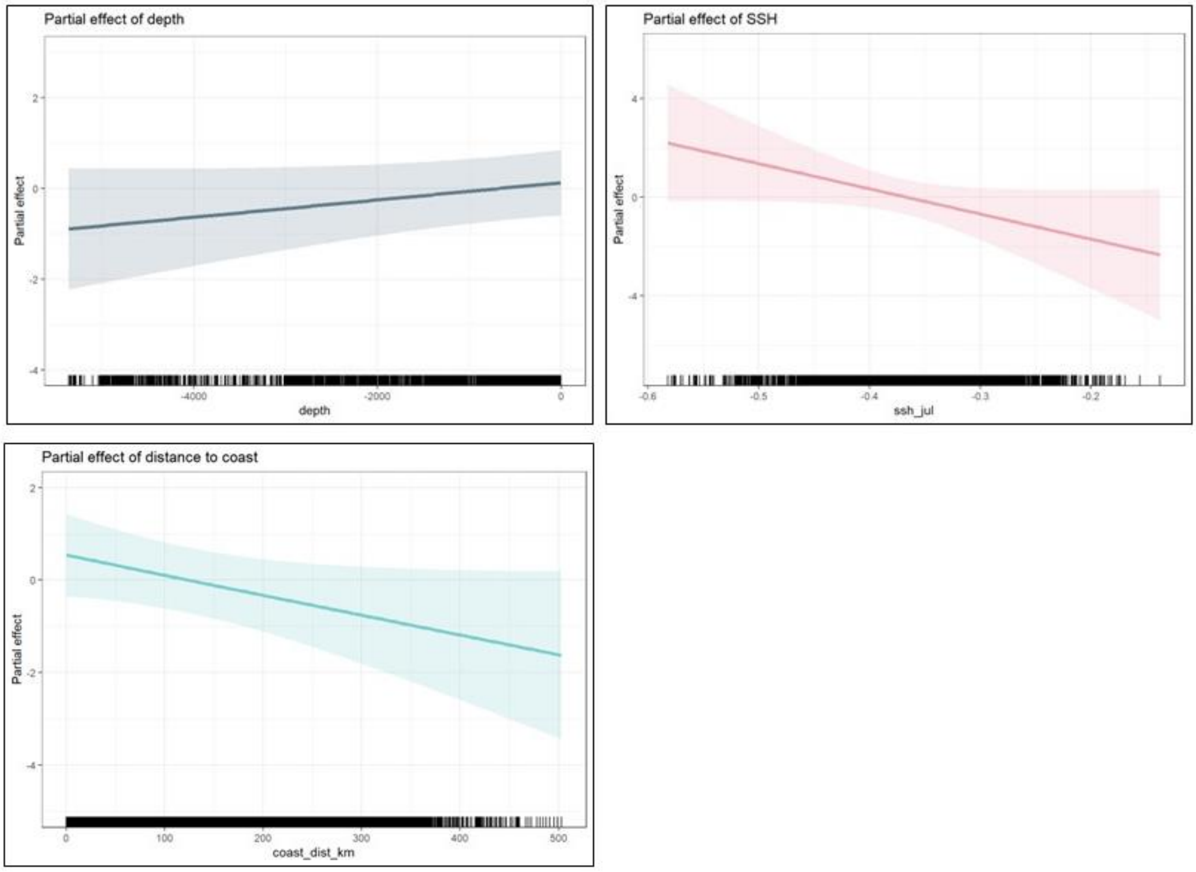

Figure 3.3-12. Plots of the fitted smooth functions for the bottlenose dolphin predictive GAM. "Rug" marks on the x-axis of the fitted smooth plots show the distribution of the data. Shaded areas represent the 95% confidence intervals.

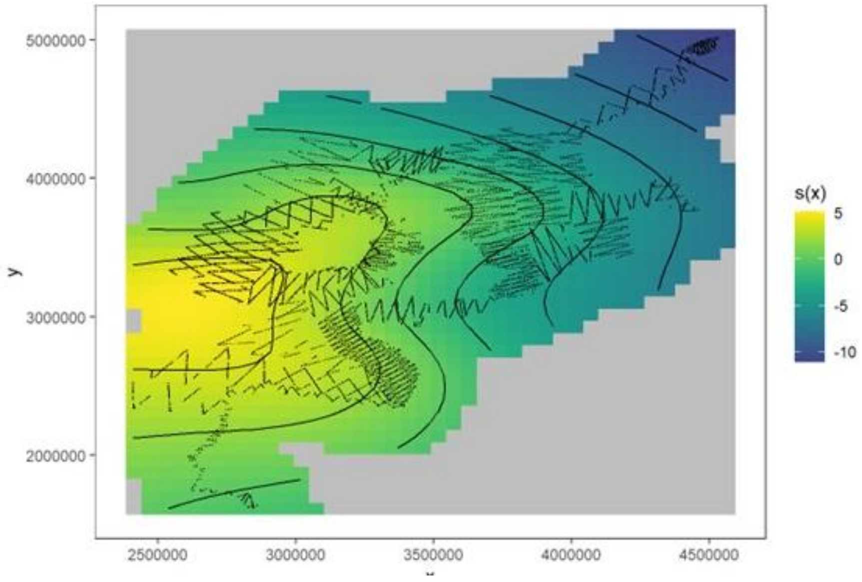

Figure 3.3-13. X, Y spline plot for the bottlenose dolphin predictive GAM, also showing survey effort

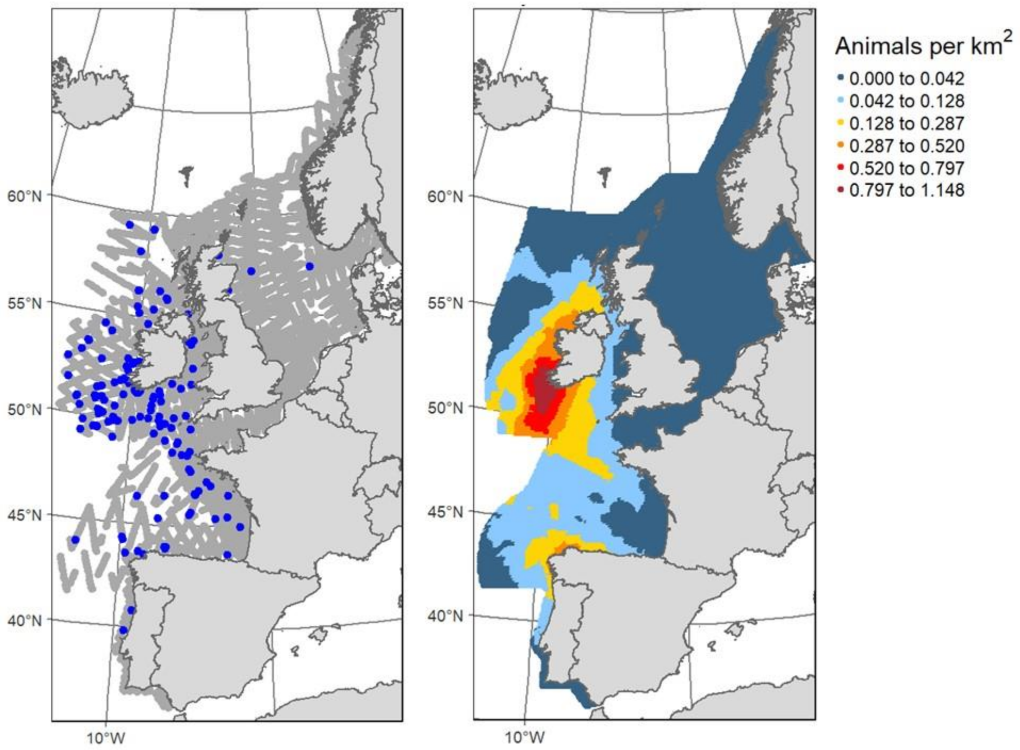

Figure 3.3-14: Location of effort and sightings (LEFT) and predicted density surface (RIGHT) for the bottlenose dolphin S3/ObSERVE model. models. White areas are outside of predictive space. In some cases, prediction grid cells had covariate values which were outside the range encompassed by the modelled effort segments. In these instances, grid-cells were excluded from the prediction.

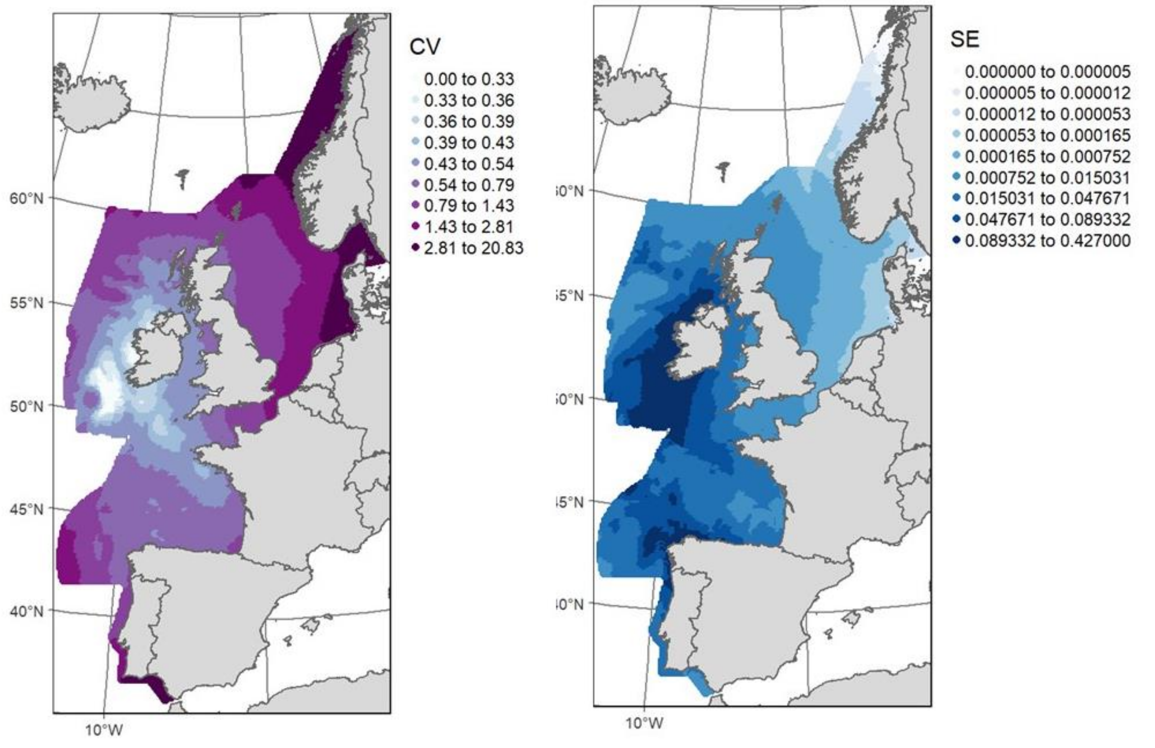

Figure 3.3-15: Coefficient of variation CV of density (CV) (LEFT) and standard error (SE) (RIGHT) for S3/ObSERVE survey data. Range of values represented by colours in the maps show the 1%, 2%, 5%, 10%, 25%, 50%, 75%, 90% and 100% quantiles. White areas are outside of predictive space. In some cases, prediction grid cells had covariate values which were outside the range encompassed by the modelled effort segments. In these instances, grid-cells were excluded from the prediction.

3.3.5 Common dolphins

Summary results of the final model selected for common dolphins across the full survey area are provided in Table 3.3-5. The model diagnostics indicated an adequate fit to the data, but the amount of null deviance explained by the model was high at 63.4%, indicating that the model could have over-fitted. The QQ plot and the residuals vs linear plot are provided in Appendix 2. The residuals show a little deviation outside of the confidence interval at the higher end of the QQ plot. Partial effects plots are shown in Figure 3.3-16.

Common dolphins were modelled as groups, rather than as individuals. The negative binomial error distribution best described the data. The fitted smooth functions showed higher levels of “wiggliness” compared to the species presented so far, with only depth having a linear relationship and fewer than 1 estimated degrees of freedom. It is possible this due to higher numbers of sightings for this species than for the majority of the others (Table 3.2-1).

Predicted density of common dolphins was highest at shallow depths and decreased linearly with increasing depth. Density of common dolphins was highest in areas with moderate levels of seabed variation, peaking at around SDdepth = 200m, suggesting that shallow slope habitats are preferred. The highest density of common dolphins was predicted at sea surface temperatures around 18^0. The slope for D200 iso was a curious shape, showing a dip in predicted density at around 200m from the 200m depth isobath, with higher densities both closer and further away from this feature.

The XY spline shows a general east-west tendency, with higher densities of animals predicted in the west of the region Figure 3.3-17. The highest densities of common dolphins (2.8 animals per km^2) were predicted in coastal waters around Portugal, and further offshore in the northern part of the Bay of Biscay (Figure 3.3-18 RIGHT). The prediction is a good match to the sightings (Figure 3.3-18 LEFT) The plot of prediction CV showed reasonable levels of confidence in the model outside the North Sea and Norwegian waters. Standard errors are highest around areas of high predicted density (Figure 3.3-19).

Table 3.3-5. Results of the best predictive model for common dolphin.

Error distribution		Model covariates	Estimated degrees of freedom	P value	% Deviance explained	Model degrees of freedom
NB		X, Y	15.01	2e-16	63.4	24.7
		Depth	0.93	4.5e-4		
		SDdepth	2.15	0.003		
		SST	1.89	0.086		
		D200 iso	3.68	2e-16		

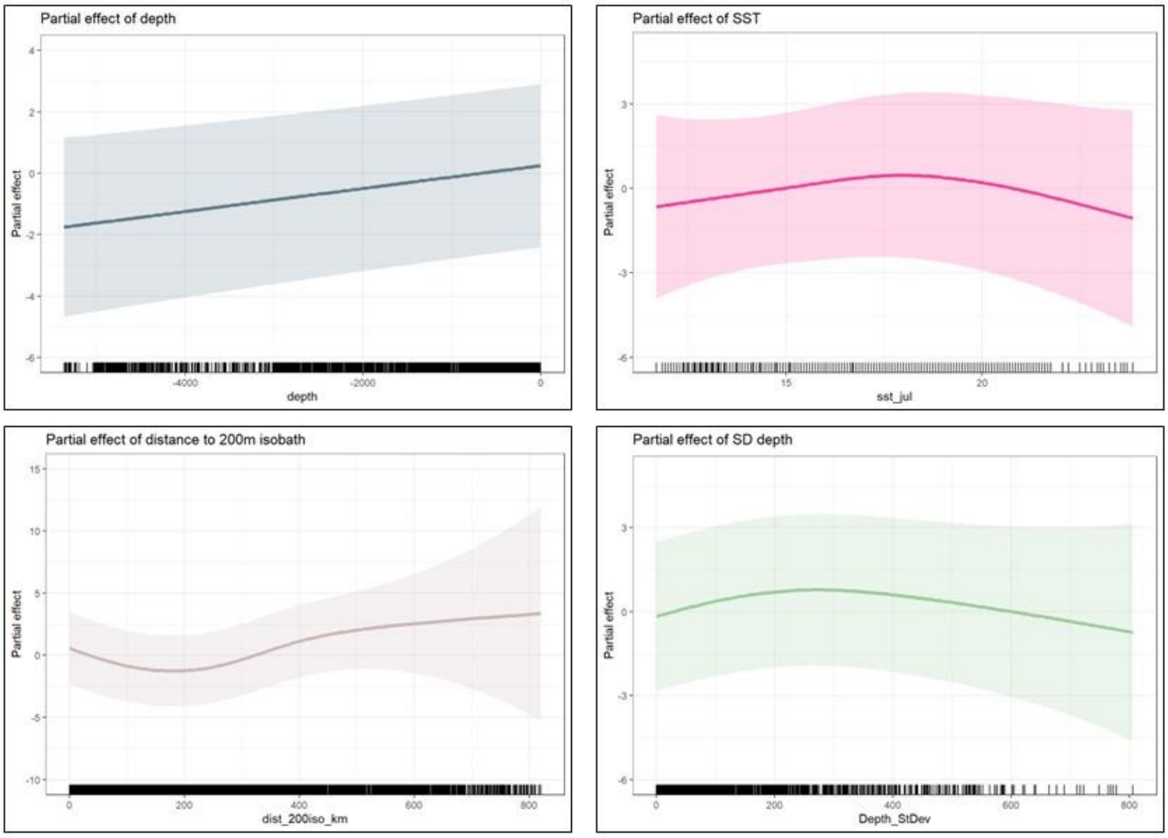

Figure 3.3-16. Plots of the fitted smooth functions for the common dolphin predictive GAM. “Rug” marks on the x-axis of the fitted smooth plots show the distribution of the data. Shaded areas represent the 95% confidence intervals.

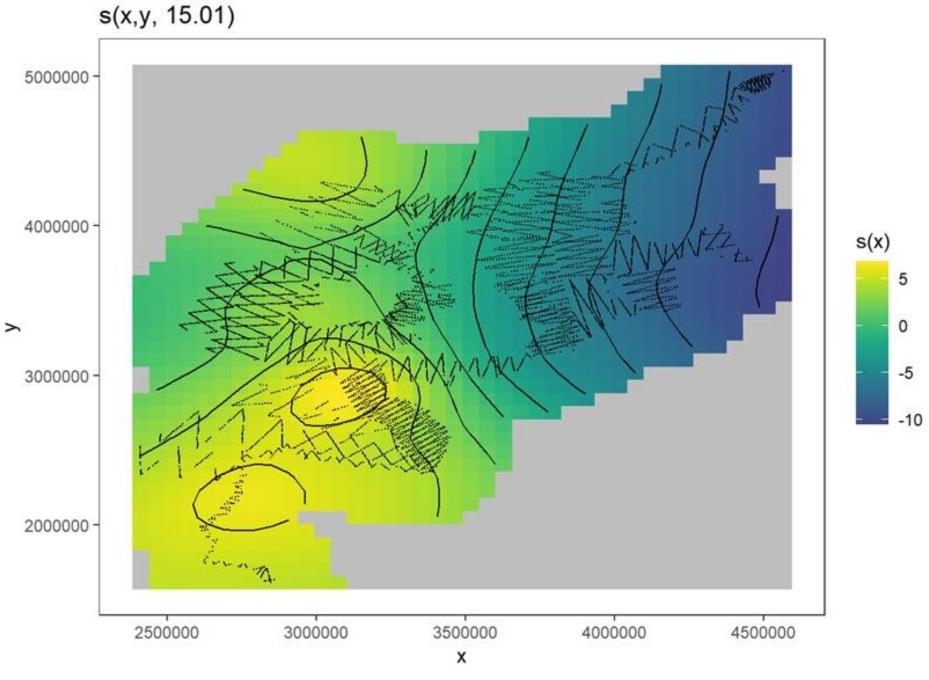

Figure 3.3-17. X, Y spline plot for the common dolphin predictive GAM, also showing survey effort

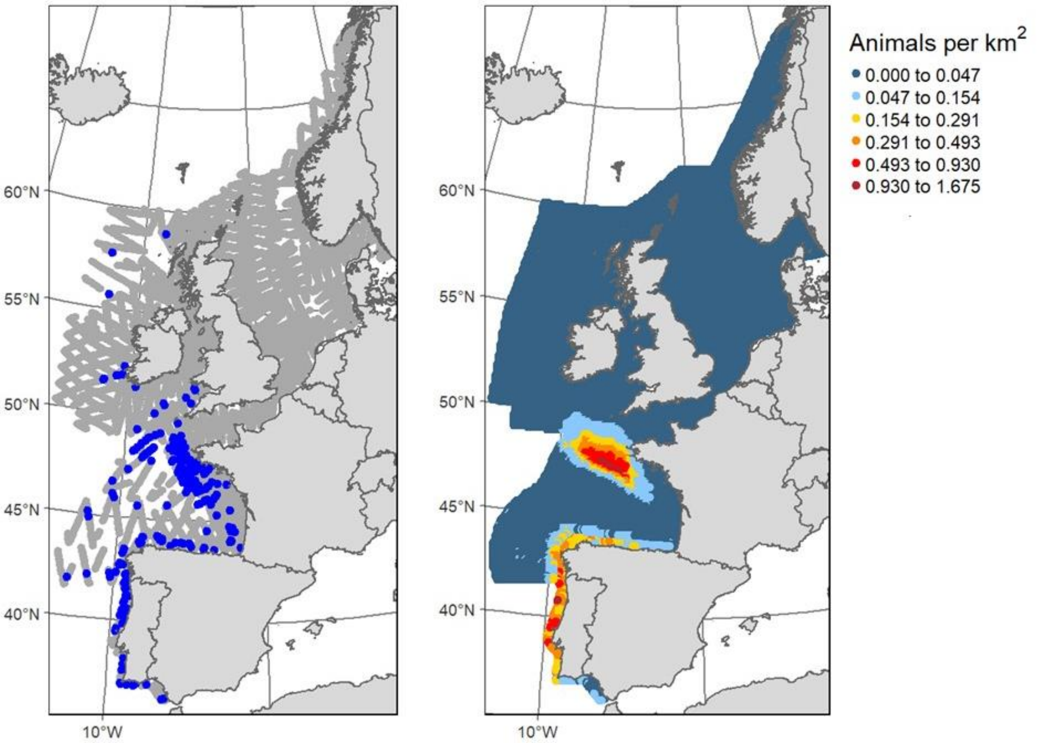

Figure 3.3-18: Location of effort and sightings (LEFT) and predicted density surface (RIGHT) for the common dolphin S3/ObSERVE model. models. White areas are outside of predictive space. In some cases, prediction grid cells had covariate values which were outside the range encompassed by the modelled effort segments. In these instances, grid-cells were excluded from the prediction.

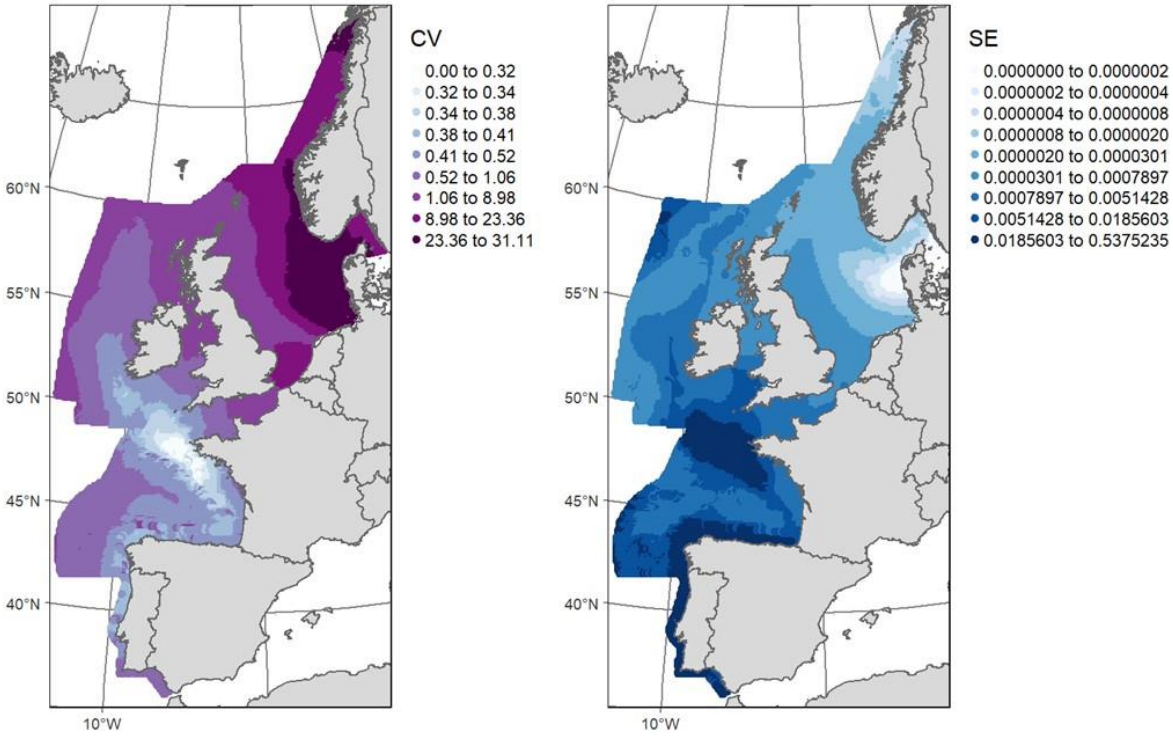

Figure 3.3-19: Coefficient of variation CV of density (CV) (LEFT) and standard error (SE) (RIGHT) for S3/ObSERVE survey data. Range of values represented by colours in the maps show the 1%, 2%, 5%, 10%, 25%, 50%, 75%, 90% and 100% quantiles. White areas are outside of predictive space. In some cases, prediction grid cells had covariate values which were outside the range encompassed by the modelled effort segments. In these instances, grid-cells were excluded from the prediction.

3.3.6 Striped dolphin

Summary results of the final model for striped dolphins are provided in Table 3.3-6. Model diagnostics (Appendix 2) indicated a sufficient fit to the data, although the residuals deviate from the optimised line, they fall within the confidence interval of the QQ plot. The amount of null deviance explained by the model was 55.2%. This is comparatively high and may be indicative of the model potentially over-fitting. Plots of the fitted smooth functions are provided in Figure 3.3-20. Striped dolphins were modelled as groups.

The negative binomial error distribution best described the data. Highest striped dolphin density was predicted by deeper water, with predicted density decreasing linearly with decreasing depth. Predicted density also increased with increasing SD depth, suggesting a preference for habitats of steep slope. Higher salinity values were also found to predict higher dolphin densities, with a linear decrease in predicted density with decreasing salinity. The confidence levels were very wide towards the lower salinity (and density) areas, where there was a reduced number of data points. The XY spline shows a high effect in the south-west part of the study area Figure 3.3-21..

The highest densities of striped dolphins (0.28 animals per km^2) were predicted in the offshore waters of the Bay of Biscay (Figure 3.3-22 LEFT), which was a good match to the observed detections (Figure 3.3-22 RIGHT). The plot of prediction CV shows good levels of confidence across the majority of the area (Figure 3.3-23 c).

Table 3.3-6. Results of the best predictive model for striped dolphin.

Error distribution	Model covariates	Estimated degrees of freedom	P value	% Deviance explained	Model degrees of freedom
Negative binomial	X, Y	5.3	2.e-6	56.2	11.4
	Depth	0.9	6e-4		
	SLA	2.6	0.005		
	SD depth	0.9	0.0005		
	Salinity	0.7	0.07		

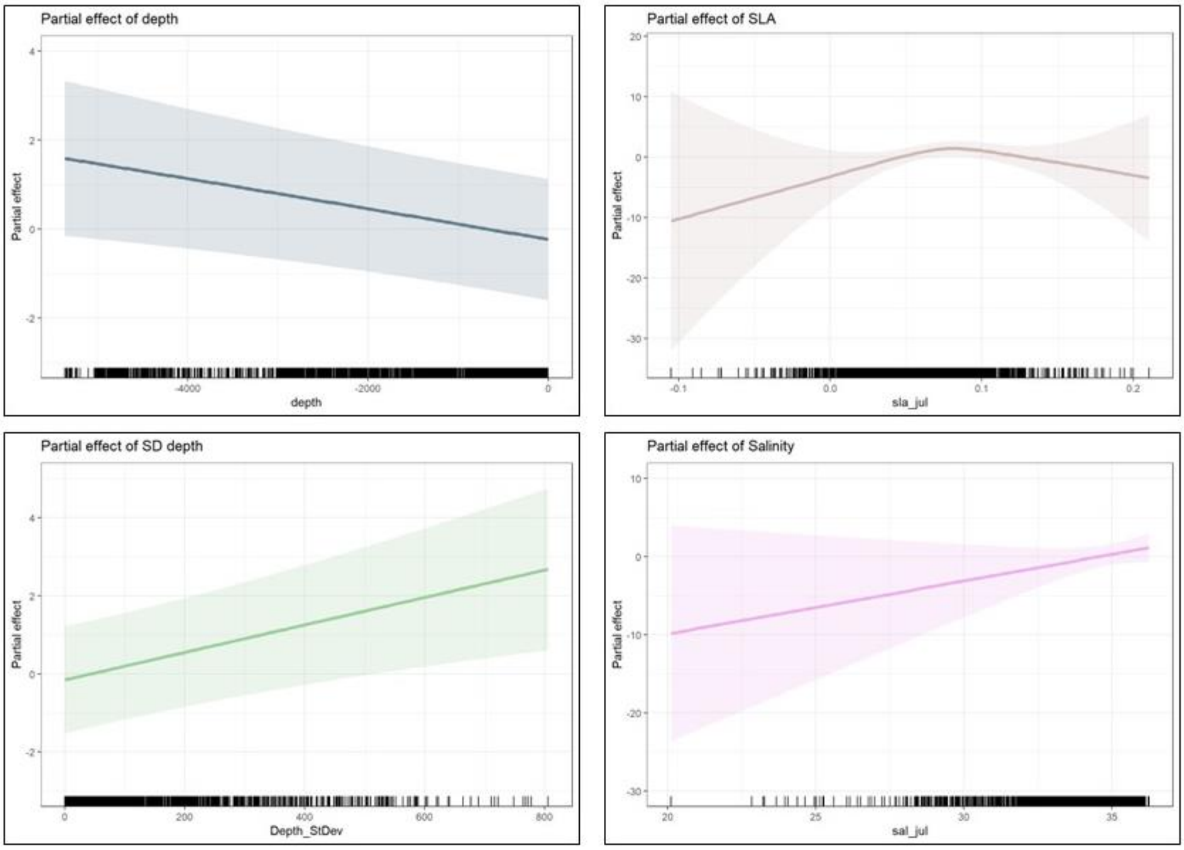

Figure 3.3-20. Plots of the fitted smooth functions for the striped dolphin predictive GAM. "Rug" marks on the x-axis of the fitted smooth plots show the distribution of the data. Shaded areas represent the 95% confidence intervals.

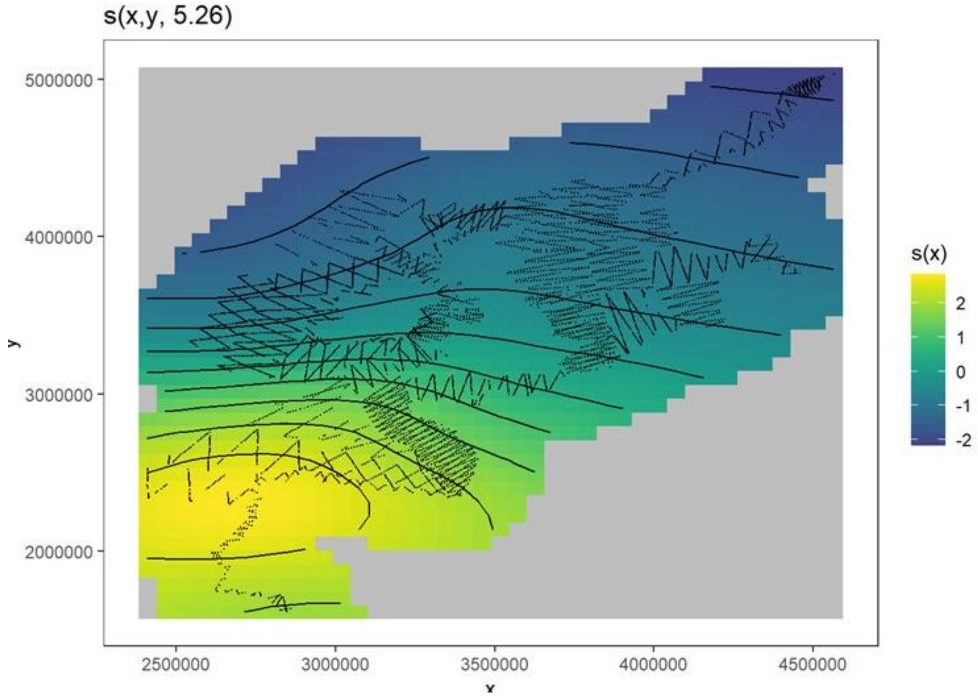

Figure 3.3-21. X, Y spline plot for the striped dolphin predictive GAM, also showing survey effort

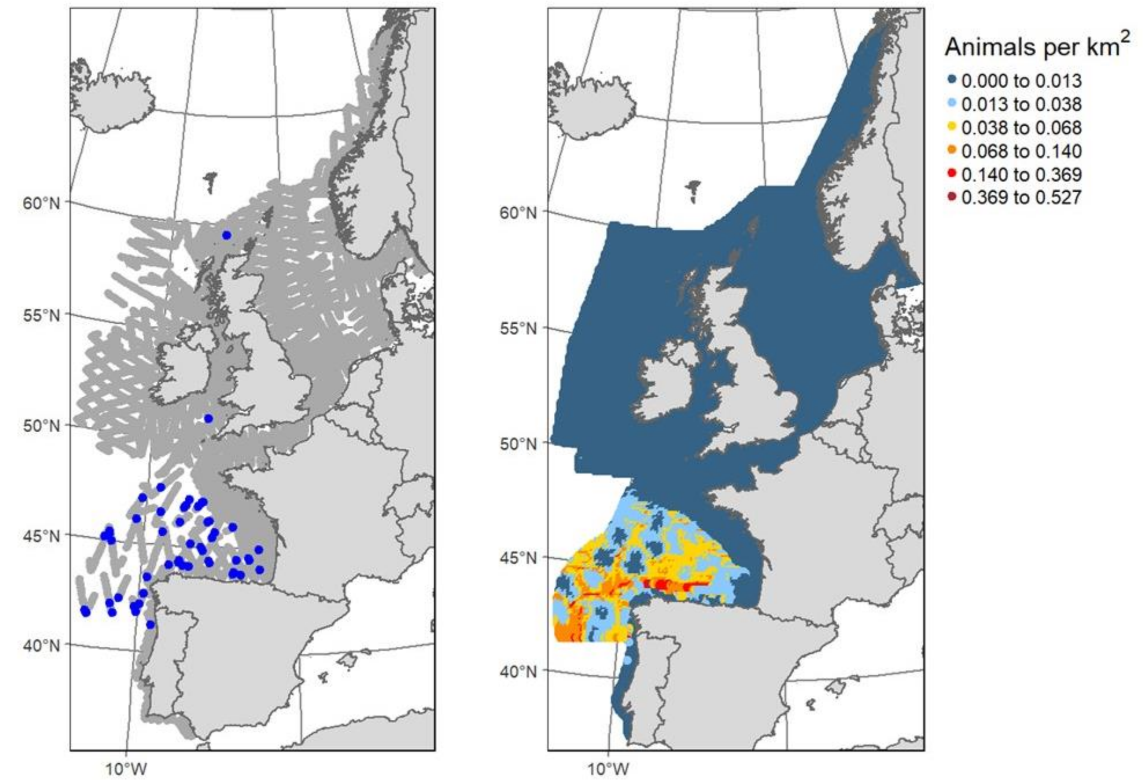

Figure 3.3-22: Location of effort and sightings (LEFT) and predicted density surface (RIGHT) for the striped dolphin S3/ObSERVE model. models. White areas are outside of predictive space. In some cases, prediction grid cells had covariate values which were outside the range encompassed by the modelled effort segments. In these instances, grid-cells were excluded from the prediction.

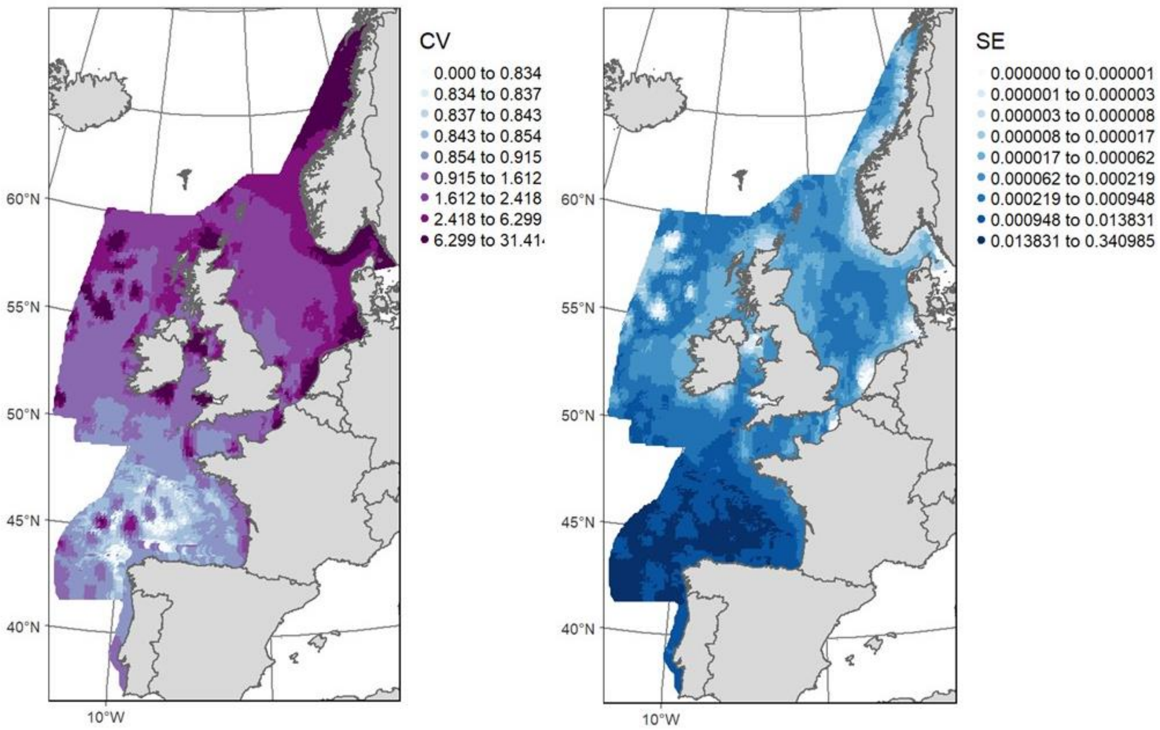

Figure 3.3-23: Coefficient of variation CV of density (CV) (LEFT) and standard error (SE) (RIGHT) for S3/ObSERVE survey data. Range of values represented by colours in the maps show the 1%, 2%, 5%, 10%, 25%, 50%, 75%, 90% and 100% quantiles. White areas are outside of predictive space. In some cases, prediction grid cells had covariate values which were outside the range encompassed by the modelled effort segments. In these instances, grid-cells were excluded from the prediction.

.

3.3.7 Minke whale

A summary of the results of the final model selected for minke whales across the full survey area is provided in Table 3.3-7. The QQ plot and the residuals vs linear are provided in Appendix 2. The model explained 28.2% of null deviance, and partial effects plots are provided in Figure 3.3-24. The negative binomial error distribution best described the data. The fitted smooth functions showed relatively low levels of "wiggliness", with all environmental covariates (excluding the isotropic XY smooth) requiring one or fewer edf.

There were positive effects (higher estimated density of minke whales) in shallow depths, decreasing linearly as waters became deeper. It should be noted, however, that the confidence intervals increased with depth, particularly once depth exceeded 1,000m. Estimated density of minke whales also decreased linearly with increased depth of the mixed layer. Confidence intervals around this fitted smooth function were much wider at the extremes of the data, providing less confidence in the relationship where there were fewer data points, particularly in the places where the mixed layer exceeded 20m depth. A similar pattern can be seen in the modelled relationship between the predicted density of minke whales and sea surface height, with higher densities of minke whales being predicted in areas of lower SSH, and density declining as SSH increased, which was generally towards the southern part of the region. The XY spline shows highest effects around the coastal waters of the UK(Figure 3.3-25).

The highest densities of minke whales (0.2 animals per km^2) were predicted to the west of Ireland and in the Hebridean Sea, to the west of Scotland, with medium density areas being predicted in the North Sea (Figure 3.3-26 LEFT), which is a reasonable match with the observed sightings data (Figure 3.3-26 RIGHT). The plot of prediction CV shows relatively high levels of confidence for the majority of the shelf seas, although this is much reduced to the west of the Bay of Biscay region (Figure 3.3-27 c).

Table 3.3-7. Results of the best predictive model for minke whale.

Error distribution	Model covariates	Estimated degrees of freedom	P value	% Deviance explained	Model degrees of freedom
Negative binomial	XY	12.46	2e-16	28.2	16.3
	Depth	0.92	0.001		
	MLD	0.87	0.004		
	SSH	1.04	4e-65		

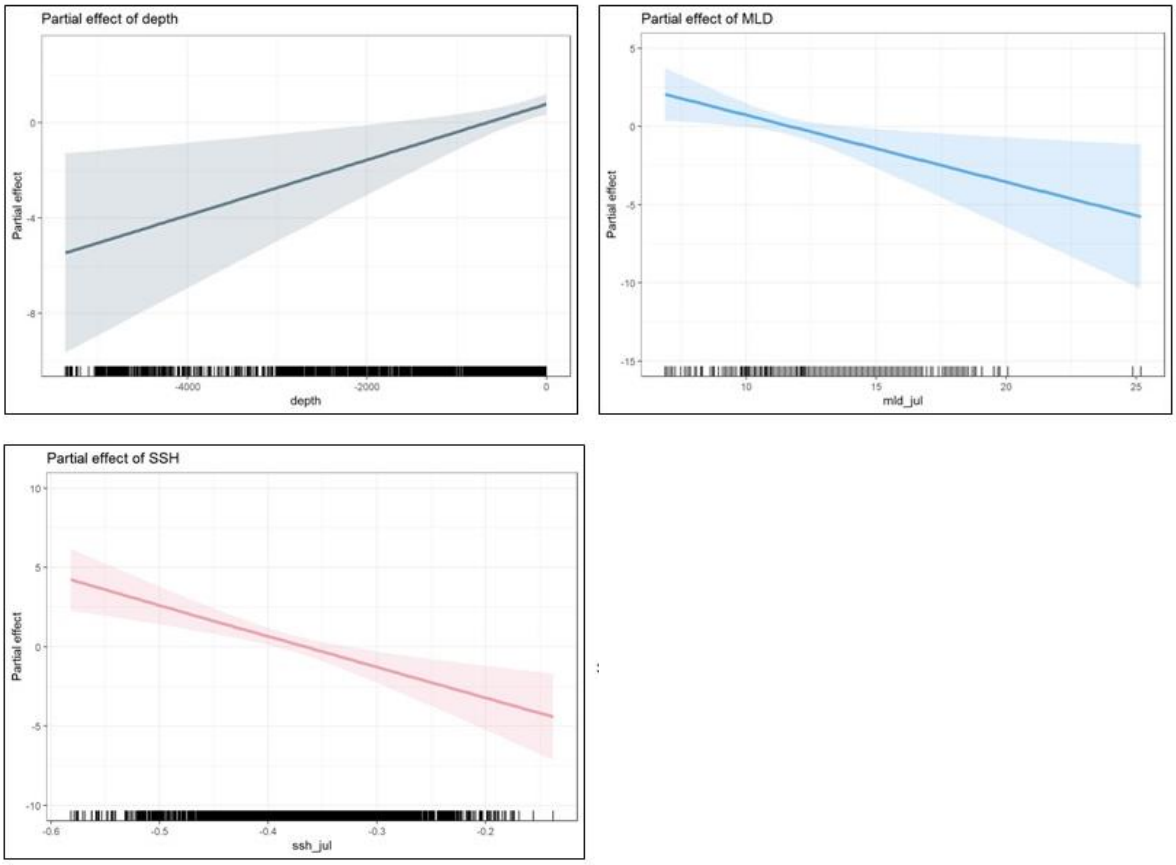

Figure 3.3-24. Plots of the fitted smooth functions for the minke whale predictive GAM. "Rug" marks on the x-axis of the fitted smooth plots show the distribution of the data. Shaded areas represent the 95% confidence intervals.

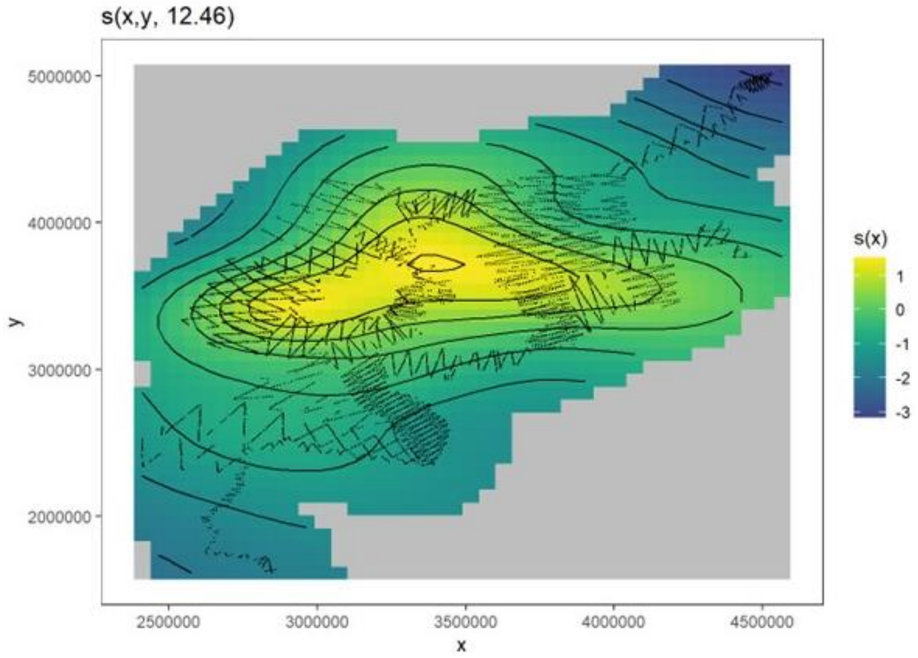

Figure 3.3-25. X, Y spline plot for the minke whale predictive GAM, also showing survey effort

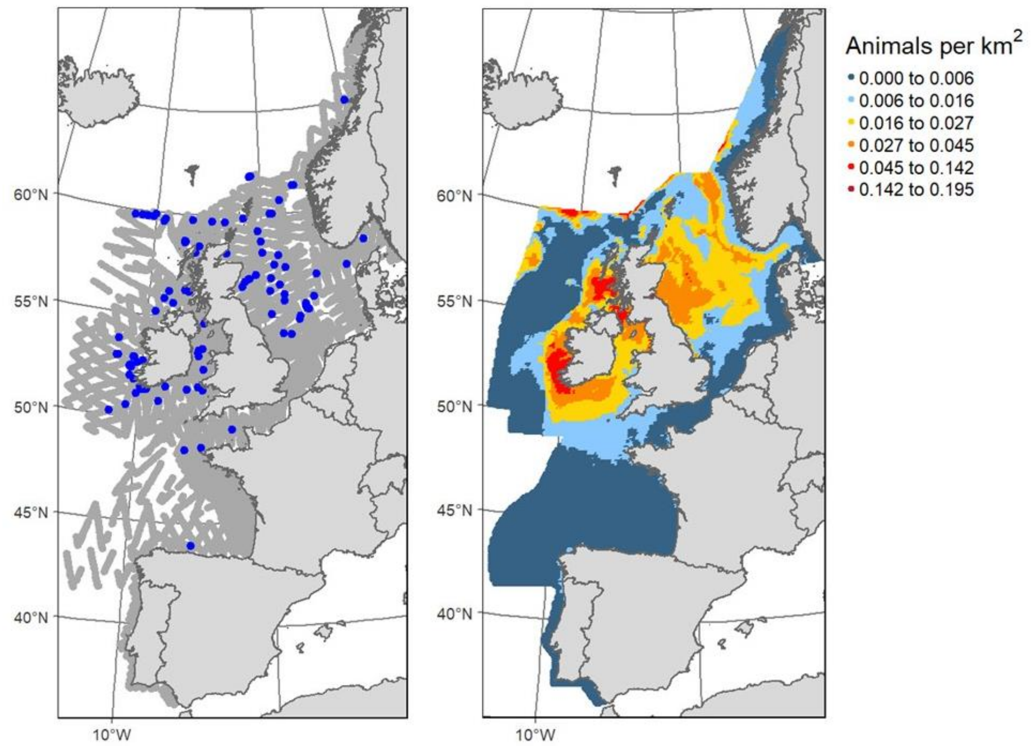

Figure 3.3-26: Location of effort and sightings (LEFT) and predicted density surface (RIGHT) for the minke whale S3/ObSERVE model. models. White areas are outside of predictive space. In some cases, prediction grid cells had covariate values which were outside the range encompassed by the modelled effort segments. In these instances, grid-cells were excluded from the prediction.

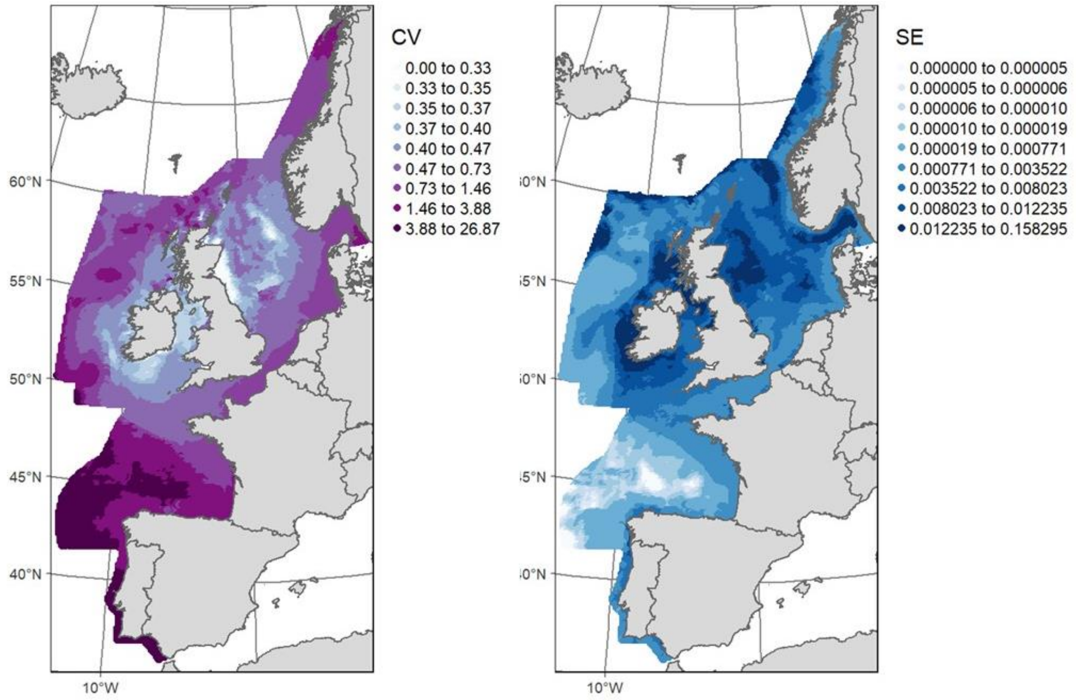

Figure 3.3-27: Coefficient of variation CV of density (CV) (LEFT) and standard error (SE) (RIGHT) for S3/ObSERVE survey data. Range of values represented by colours in the maps show the 1%, 2%, 5%, 10%, 25%, 50%, 75%, 90% and 100% quantiles. White areas are outside of predictive space. In some cases, prediction grid cells had covariate values which were outside the range encompassed by the modelled effort segments. In these instances, grid-cells were excluded from the prediction.

3.3.8 Fin whale

Summary results of the final model selected for fin whales across the full survey area are provided in Table 3.3-8. The model diagnostics indicated a good fit to the data and the amount of null deviance explained by the model was 73%. The QQ plot and the residuals vs linear plot are provided along with plots of the fitted smooth functions in Figure 3.3-28.

The negative binomial error distribution best described the data. Only one covariate, CS200, was retained in addition to the isotropic XY smooth. This showed a positive effect (highest density of fin whales) in waters close to, and deeper than the 200m isobath, with a rapid decline in density at increasing distances from the isobath on the shallower side. The confidence interval also increased to be extremely wide here. The XY spline shows the highest effects in the areas around the Bay of Biscay (Figure 3.3-29).

The highest densities of fin whales (0.02 animals per km^2) were predicted in the offshore waters of the Bay of Biscay Figure 3.3-30 LEFT). Whilst this was a good match to the large majority of the detections of this species (Figure 3.3-30 RIGHT), there were a few sightings in the far north of the survey area, which are not reflected in the density surface. The plot of predicted CV reflected the confidence interval around the smooth function for CS200; in deeper waters the prediction is precise but is less so in waters shallower than 200m (Figure 3.3-31 c).

Table 3.3-8 . Results of the best predictive model for fin whales.

Error distribution	Model covariates	Estimated degrees of freedom	P value	% Deviance explained	Model degrees of freedom
Negative binomial	XY	12.03	2e-16	73.1	16.9
	CS200	3.91	2e-16		

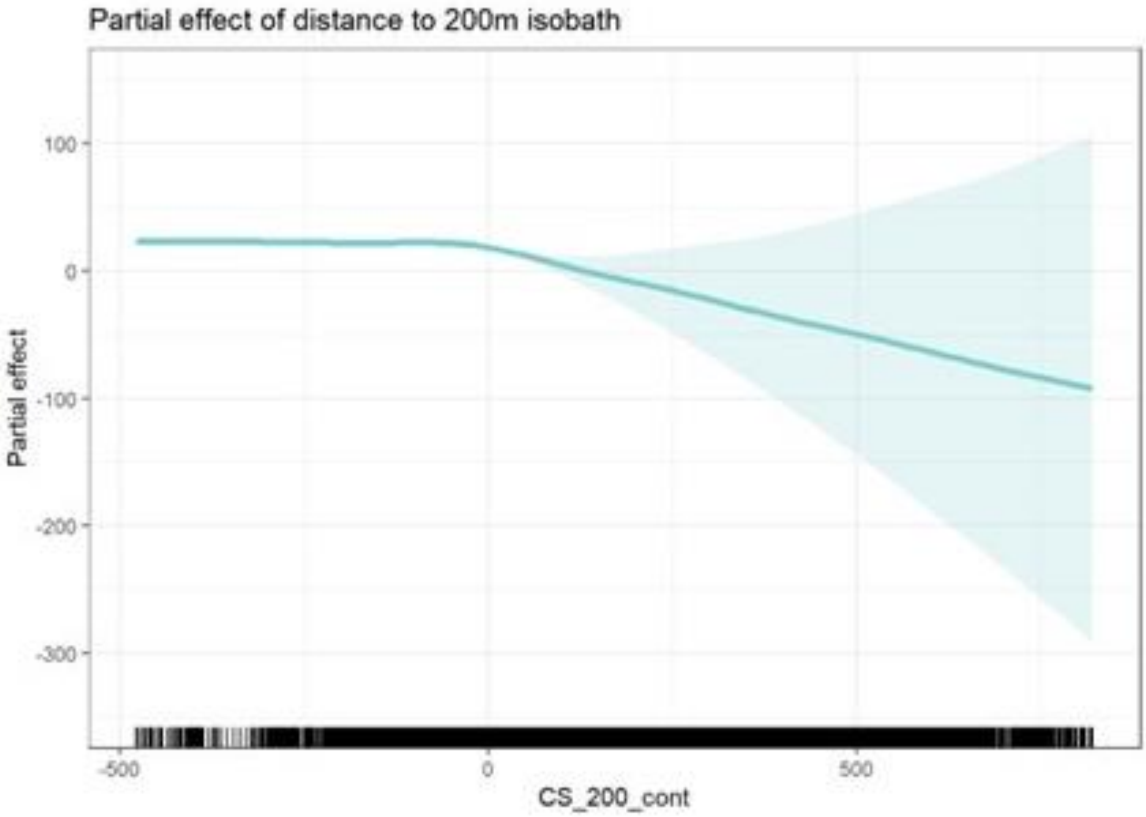

Figure 3.3-28. Plots of the fitted smooth function for the fin whale predictive GAM. “Rug” marks on the x-axis of the fitted smooth plots show the distribution of the data. Shaded areas represent the 95% confidence intervals.

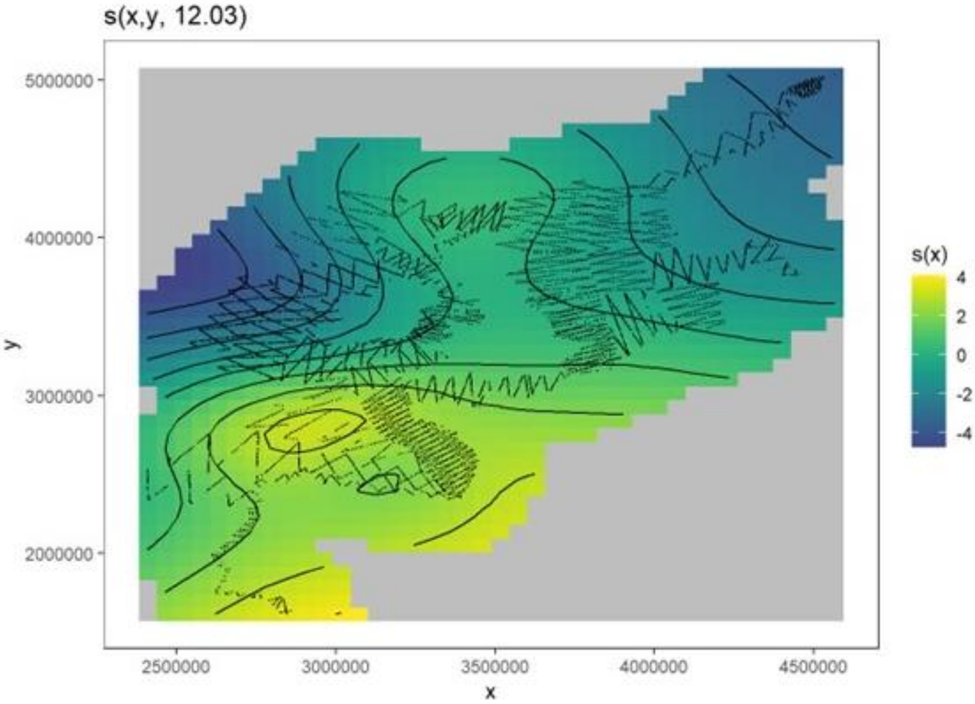

Figure 3.3-29. X, Y spline plot for the fin whale predictive GAM, also showing survey effort

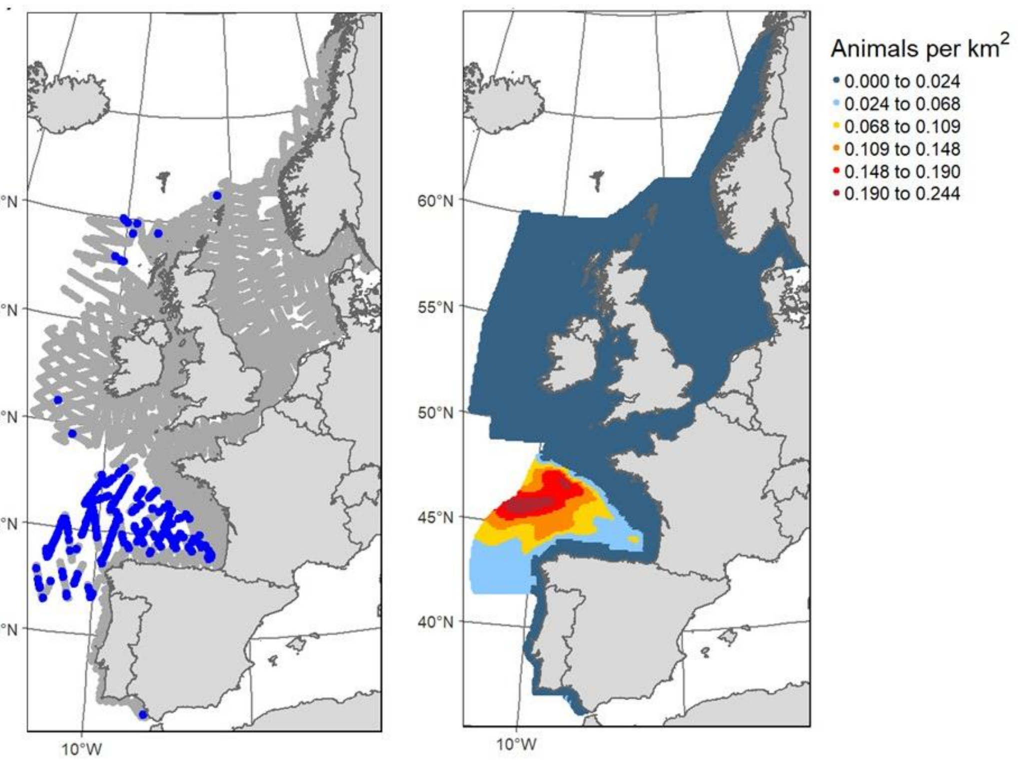

Figure 3.3-30: Location of effort and sightings (LEFT) and predicted density surface (RIGHT) for the minke whale S3/ObSERVE model. models. White areas are outside of predictive space. In some cases, prediction grid cells had covariate values which were outside the range encompassed by the modelled effort segments. In these instances, grid-cells were excluded from the prediction.

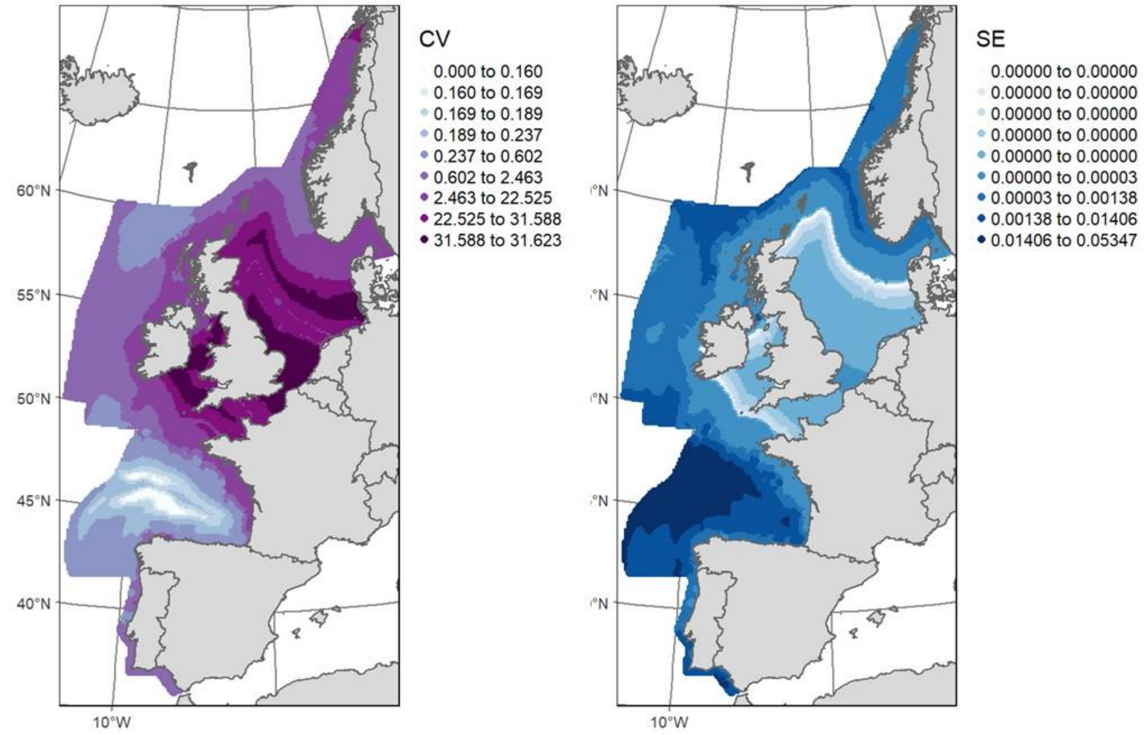

Figure 3.3-31: Coefficient of variation CV of density (CV) (LEFT) and standard error (SE) (RIGHT) for S3/ObSERVE survey data. Range of values represented by colours in the maps show the 1%, 2%, 5%, 10%, 25%, 50%, 75%, 90% and 100% quantiles. White areas are outside of predictive space. In some cases, prediction grid cells had covariate values which were outside the range encompassed by the modelled effort segments. In these instances, grid-cells were excluded from the prediction.

3.4 Discussion

This chapter provides predictive models for eight species of cetacean using combined data from the SCANS-III and ObSERVE surveys, which were conducted during the summer of 2016, with the majority of the data being collected during July. Models were created using a selection of static environmental covariates, including X, Y; depth, slope and standard deviation of depth, as well as remote-sensed, monthly averaged dynamic environmental covariates, for which July 2016 data was used.

These types of studies are subject to error during both data collection and analysis stages (Barry and Elith 2006). As the data sources and analysis framework used was the same for this chapter and chapters 4 and 5, sources of error are reviewed and discussed for these three chapters together in section 6.1.2.

3.4.1 Harbour porpoise

One of the notable results of the 2005 SCANS-II survey, was the shift in distribution of harbour porpoises to the south in the North Sea when compared with the results of the original SCANS survey in 1994 (Hammond et al., 2013). The model of the SCANS-III and ObSERVE data shows a similar predicted distribution to that presented for 2005, indicating that whatever had led to that shift (likely changes in prey availability, Hammond et al., 2013) persisted through 2016 (Figure 3.4-1).

A range of covariates was retained in the final harbour porpoise model, including SDdepth, depth, ADT, Sal and CS200, as well as an X, Y smooth. The model of the ObSERVE only part of the data also included a relationship with the 200m depth isobath (the side of the contour was not modelled) (Rogan et al., 2018), as did the model for the SCANS-III only part of the data, which also similarly retained ADT and depth (Lacey et al., 2022).

This modelling framework allowed only one “distance to” parameter to be included, which for the harbour porpoise model was CS200. Several other studies have found distance to coast to be an important predictor (Marubini et al. 2009; Gilles et al. 2011; Booth et al. 2013). The large spatial scale of the model presented here seems to have accounted for this relationship as distance from the 200m contour, on the shallower side, with highest densities being in water depths shallower than 200m, at large distances from the contour, that is, in shallower water.

Depth has also been found to be an important predictor of harbour porpoise density (e.g. Marubini et al. 2009; Gilles et al. 2011; Booth et al. 2013), as it was in earlier, separate models of the SCANS-III and ObSERVE data. This is not the case throughout the range. In the Iberian peninsula, Goetz et al.

(2015) found no relationship between water depth and harbour porpoise distribution, although animals were found primarily on the continental shelf.

The modelled relationship with ADT, an indicator of mesoscale activity, does not indicate a preference of harbour porpoise for more productive waters. In contrast, other studies have demonstrated that harbour porpoises have a preference for waters such as headland wakes, which may aggregate prey species spatially (Johnston et al. 2005), as well as tidal current (Embling et al. 2010), and residual current (Gilles et al. 2011). The process of prey aggregation may therefore be occurring at a finer scale than that represented by the ADT covariate when modelled over the scale of the whole study region.

More detailed explanatory modelling of harbour porpoises at a smaller ecoregion area will be presented in Chapter 4.

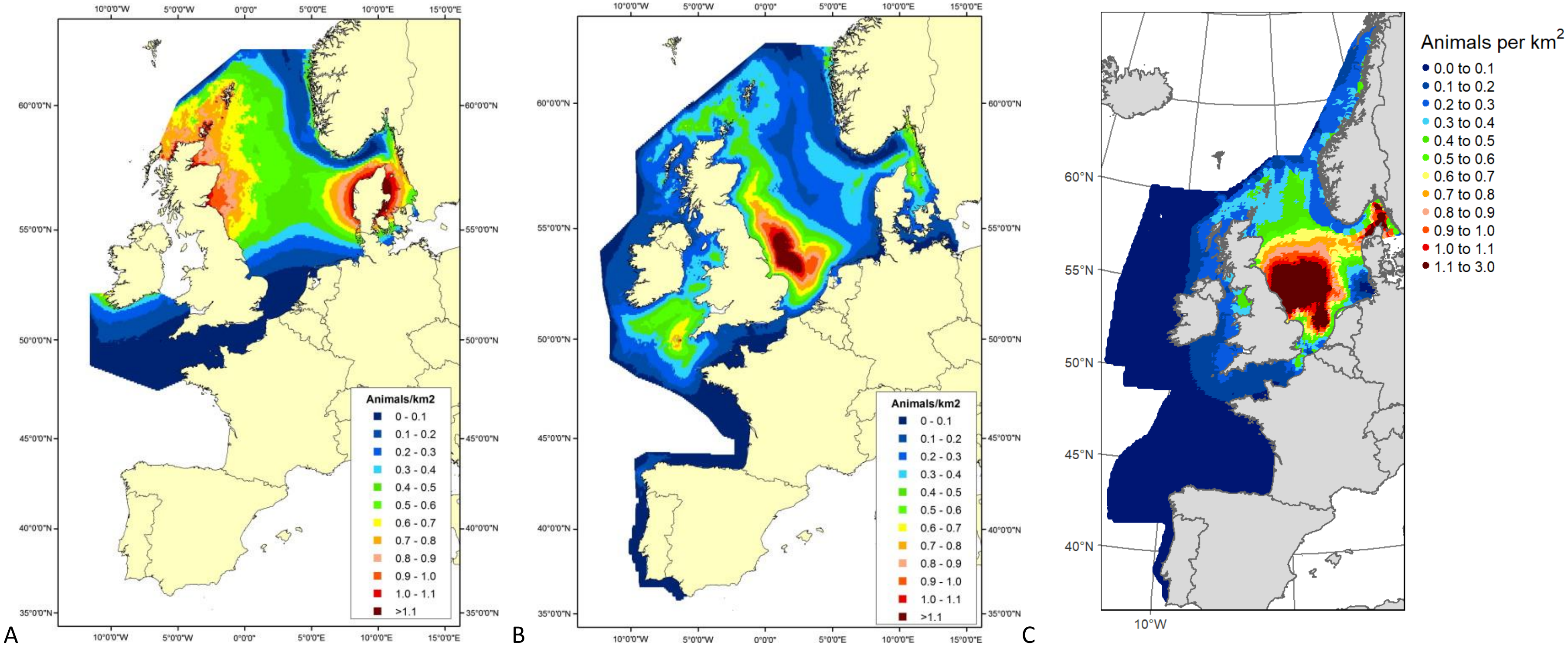

Figure 3.4-1: Maps of predicted harbour porpoise distribution from surveys undertaken in 1994 (A), 2005 (B) and 2016 (C). Maps A & B are taken from Figures 7 & 8 of Hammond et al., (2013). Map C is the same as that presented in Figure 3.3.3 but recoloured to match the scale of these maps from the earlier surveys. Please note that the survey area is different for all three of these surveys, expanding s each time.

3.4.2 White-beaked dolphin.

The final white-beaked dolphin model retained depth and salinity as well as an X, Y smooth. White-beaked dolphins weren't modelled as part of the ObSERVE survey (Rogan et al., 2018), but the SCANS-III only model retained SST and distance to the 200m contour as covariates, both of which have been found to be significant predictors of white-beaked dolphin distribution in previous studies (Evans et al. 2003; MacLeod et al. 2008). The retention of the depth predictor in the final model also corroborates the well-documented preference of this species for shelf waters (Macleod 2013). Slope has been suggested as an important predictor of this species from previous studies (MacLeod et al. 2007; Weir et al. 2009), but those were undertaken on the west coast of Scotland, an area where there is slope close to the coast. A large number of the sightings in this study came from the North Sea, which has very little seabed gradient at all, consequently it is not surprising that slope was not selected as an important covariate in this area.

There was a positive effect of salinity on predicted density of white-beaked dolphins. It is unlikely that the salinity is having a physiological effect on the dolphins themselves, but instead influencing the availability of prey organisms through its effect on the oceanography of the region (Fiedler 2018). Breen et al. (2016) have also found salinity to be a driver of white-beaked dolphin density.

More detailed explanatory modelling of white-beaked dolphins at a smaller ecoregion, with a more detailed focus on prey modelling area will be presented in Chapter 4.

3.4.3 White-sided dolphin.

The final white-sided dolphin model retained SDdepth, depth, sea surface temperature and salinity. As with white-beaked dolphins, there is no ObSERVE only model for this species (Rogan et al., 2018), and it was also not modelled individually for SCANS-III (Lacey et al., 2022). It is a less well studied species than many of the others, but the predicted offshore distribution and predicted density increasing with depth is consistent with that found by (MacLeod et al. 2007). Similarly to white-beaked dolphins, there is a positive effect of salinity on the predicted density, which is likely influencing the distribution of prey organisms indirectly. Doksæter et al. (2008) found a positive link between areas of steeper slope and white-sided dolphin density. That is the opposite of what was found in this model. Whilst it did not retain the slope covariate, it did retain SDdepth. This is a measure of variability in the seabed – and white-sided dolphin density is predicted by levels of high consistency – the areas are all at similar depths – so not areas of slope. In the northeastern United States, white-sided dolphins have been associated with cool sea surface temperatures and less saline waters (Selzer and Payne 1988), which is the opposite relationship with salinity to the one shown here, but the same relationship with sea surface temperature. Differing relationships with seabed relief and salinity may indicate different prey preferences than those from other areas.

More detailed explanatory modelling of white-sided dolphins at a smaller ecoregion will be presented in chapter 5.

3.4.4 Bottlenose dolphin.

This species retained a comparatively high number of covariates from a range of different months. With the exception of XY, none of these are the same as were retained for the SCANS-III only model and only depth is the same as for the ObSERVE model (Rogan et al., 2018). The lack of consistency in retained predictors and the variety of months of covariate retained for this species suggest that none of the retained covariates have a particularly strong link with predicted density of this species. Bottlenose dolphins are known to exist in both coastal and offshore ecotypes; the number of retained covariates may be indicative of the two ecotypes being modelled together (Bearzi et al. 2009). More detailed explanatory modelling of bottlenose dolphins at a smaller ecoregion will be presented in chapter 5.

3.4.5 Common dolphin.

The common dolphin model also retained a comparatively high number of covariates. Due to insufficient sightings, the ObSERVE survey did not produce a comparable model for common dolphins, whilst the SCANS-III only model retained depth, slope and aspect as well as X, Y. Depth was retained in the final model here too, as was SDdepth, which although not the same as slope, does also provide an indication of levels of variability in the seabed.

This model, like many others, has found a positive link between predicted common dolphin and sea surface temperatures (e.g. MacLeod et al. 2008; Weir et al. 2009; Svendsen et al. 2015; Correia et al. 2019), with the link also being associated not just with daily distribution patterns, but also with genomic variation (Amaral et al. 2012; Barceló et al. 2022).

Measures of seabed uniformity (either slope or SDdepth) were retained both in this model and in the SCANS-III only model (Lacey et al., 2022). This species is very closely associated with preying on locally abundant pelagic fish, and so any predictors which might suggest regions where these fish aggregate are likely to be good indicators for high densities of common dolphins (Cañadas and Hammond 2008; Moura et al. 2012; Castro et al. 2020) More detailed explanatory modelling of common dolphins at a smaller ecoregion will be presented in chapter 5.

3.4.6 Striped dolphin.

The striped dolphin model retained depth, SDdepth, SLA and salinity as predictors as well as XY. Due to insufficient sightings, the ObSERVE survey did not produce a comparable model for striped dolphins, and the SCANS-III only model retained depth, SDdepth and aspect as well as XY.

Striped dolphins are generally considered to be an offshore species (Carlucci et al. 2016), associated with deeper waters, and this association is borne out by the model here as well as that for the SCANS-III only data (Lacey et al., 2022). SD depth is also common to both models, likely implying that higher variability of seabed gradient is associated with striped dolphin predicted density, as has also been shown in other studies (Ballance et al. 2006; Azzolin et al. 2020).

Salinity (June data) is a good predictor of striped dolphin density in this model. Whether salinity itself is contributing to distribution, or whether the areas of higher salinity (Appendix 1) simply reflect the offshore areas in which striped dolphins live is not clear.

More detailed explanatory modelling of striped dolphins at a smaller ecoregion will be presented in Chapter 5.

3.4.7 Minke whale

The final minke whale model retained depth, MLD and SSH as well as an X,Y smooth. The model of the ObSERVE-only part of the data included only a relationship with the coast along with latitude and longitude (Rogan et al., 2018), whereas the model for the SCANS-III only part of the data retained X,Y, depth, ADT and distance to coast (Lacey et al. 2022). The different suite of predictors that were retained by each of the models may indicate that different processes are driving distribution in different parts of the minke whales' range, or that there are no strong relationships between these predictors and minke whale distribution.

Previous modelling studies have found substrate to be a significant predictor of minke whale presence, particularly substrate which is good habitat for sandeels (Naud et al. 2003; Macleod et al. 2004; de Boer 2010). Unfortunately, substrate data were not available for the full region so were not included in this model.

MLD has previously been linked to the presence of herring (Maravelias 1997), in which deeper mixed layers were associated with higher probabilities of encountering herring (*Clupea harengus*), but that herring were also present in well-mixed waters. These models predict the density of minke whales to decrease with increasing MLD, which would suggest that either high probability of encountering herring is not the primary driver of distribution in this area, or that MLD is not a good predictor of herring in this instance.

The modelled relationship with SSH, an indicator of mesoscale activity, indicates a preference of minke whale for slightly cooler, more productive waters, which may be aggregating minke whale prey species such as mackerel (*Scomber scombrus*), which are known to feed on euphausiids and copepods in this region.

The field data on which these models are built were collected during the summer season, during which time minke whales are feeding. Consequently, it is intuitive that minke whale summer distribution would be largely predicted based on prey resources. Like harbour porpoises, there are now density surfaces available for minke whales over a 30-year time span (Figure 3.4-2). Overall distribution is not hugely different to 2005 (B), but densities across the area are lower across the region, except for around the west coast of Scotland. This may reflect changes in the distribution of prey species across the region.

More detailed explanatory modelling of minke whale at a smaller ecoregion, with a more detailed focus on prey modelling will be presented in Chapter 4.

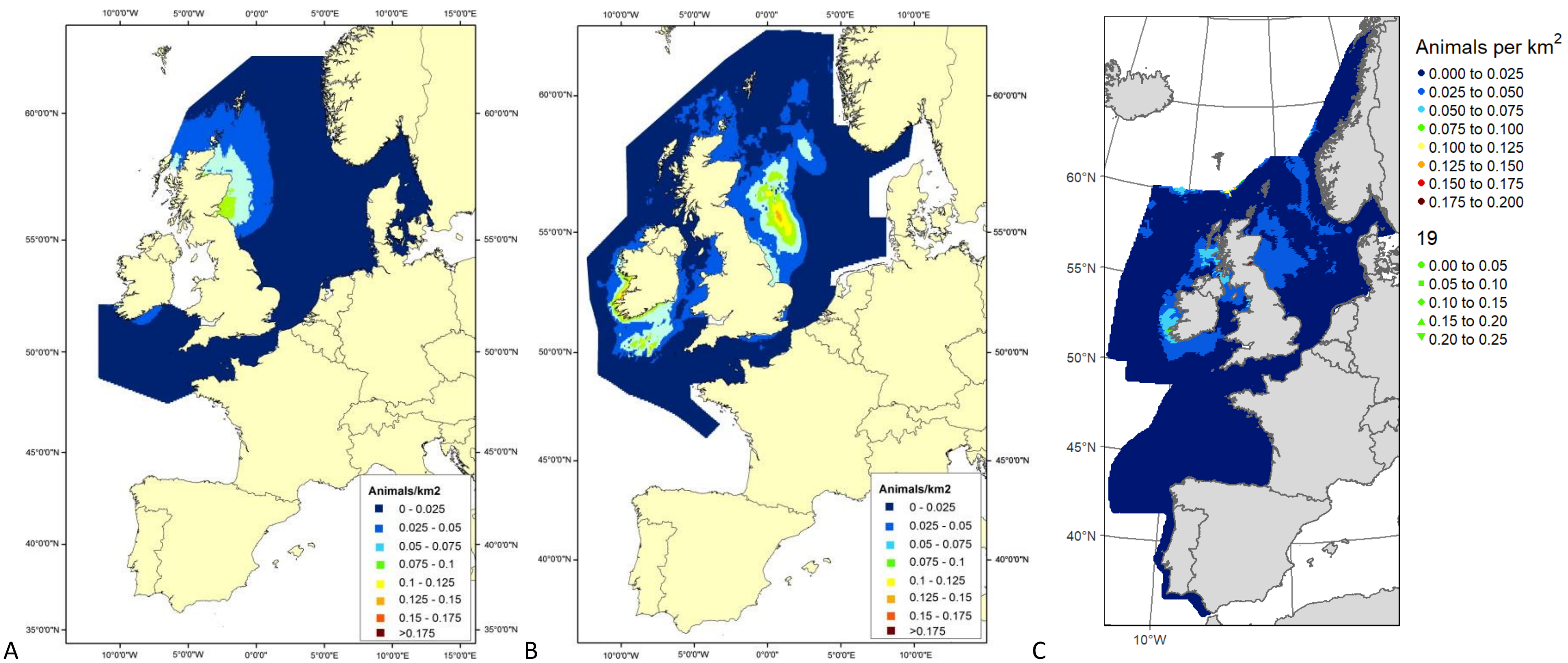

Figure 3.4-2: Maps of predicted minke whale distribution from surveys undertaken in 1994 (A), 2005 (B) and 2016 (C). Maps A & B are taken from Figures 9 & 10 of Hammond et al., (2013). Map C is the same as that presented in Figure 3.3.26 but recoloured to match the scale of these maps from the earlier surveys. Please note that the survey area is different for all three of these surveys, expanding s each time

3.4.8 Fin whale

The fin whale model retained only one covariate alongside XY, which was distance to the 200m isobath. It was not modelled for ObSERVE, and whilst the covariate is different (CS200 in this model, SDdepth in Lacey et al., 2022), a single covariate was retained for the SCANS-III only model also.

This model is in accord with previous work which notes that fin whales are likely to be found in waters outside the continental shelf (Aguilar and García-Vernet 2018).

The model of the full area presented above is a good match to the field data. More detailed explanatory modelling of fin whales at a smaller ecoregion will be presented in Chapter 5.

3.4.9 Conclusion

These models represent the most up-to-date knowledge on the 2016 distribution of these species that is available for this region, representing the field observations well. Some of the models have found similar patterns with those of earlier studies, whilst others have not. This is a large modelling region compared to many of the previous studies and may reflect different patterns due to variation across the geographical scale. Modelling of smaller geographical regions is presented in the following two chapters.

3.5 Literature Cited

Aguilar, A., and García-Vernet, R. 2018. Fin Whale. *In* Encyclopedia of Marine Mammals. Elsevier. pp. 368–371. doi:10.1016/B978-0-12-804327-1.00128-X.

Amaral, A.R., Beheregaray, L.B., Bilgmann, K., Boutov, D., Freitas, L., Robertson, K.M., Sequeira, M., Stockin, K.A., Coelho, M.M., and Möller, L.M. 2012. Seascape Genetics of a Globally Distributed, Highly Mobile Marine Mammal: The Short-Beaked Common Dolphin (Genus *Delphinus*). PLoS ONE 7(2): e31482. doi: 10.1371/journal.pone.0031482.

Azzolin, M., Arcangeli, A., Cipriano, G., Crosti, R., Maglietta, R., Pietroluongo, G., Saintingan, S., Zampollo, A., Fanizza, C., and Carlucci, R. 2020. Spatial distribution modelling of striped dolphin *(Stenella coeruleoalba)* at different geographical scales within the EU Adriatic and Ionian Sea Region, central-eastern Mediterranean Sea. Aquat. Conserv. Mar. Freshw. Ecosyst. 30(6): 1194–1207. doi:10.1002/aqc.3314.

Baines, M., Kelly, N., Reichelt, M., Lacey, C., Pinder, S., Fielding, S., Murphy, E., Trathan, P., Biuw, M., Lindstrøm, U., Krafft, B., and Jackson, J. 2021. Population abundance of recovering humpback whales (*Megaptera novaeangliae*) and other baleen whales in the Scotia Arc, South Atlantic. Mar. Ecol. Prog. Ser. doi:10.3354/meps13849.

Ballance, L.T., Pitman, R.L., and Fiedler, P.C. 2006. Oceanographic influences on seabirds and cetaceans of the eastern tropical pacific: a review. Prog. Oceanogr. 69(2–4): 360–390. doi: 10.1016/j.pocean.2006.03.013.

Barceló, A., Sandoval-Castillo, J., Brauer, C.J., Bilgmann, K., Parra, G.J., Beheregaray, L.B., and Möller, L.M. 2022. Seascape genomics of common dolphins (*Delphinus delphis*) reveals adaptive diversity linked to regional and local oceanography. BMC Ecol. Evol. 22(1): 88. doi:10.1186/s12862-022-02038-1.

Barry, S., and Elith, J. 2006. Error and uncertainty in habitat models. J. Appl. Ecol. 43(3): 413–423. doi:10.1111/j.1365-2664.2006.01136. x.

Bearzi, M., Saylan, C.A., and Hwang, A. 2009. Ecology and comparison of coastal and offshore bottlenose dolphins (*Tursiops truncatus*) in California. Mar. Freshw. Res. 60(6): 584–593. CSIRO PUBLISHING. doi:10.1071/MF08279.

Becker, E., Foley, D., Forney, K., Barlow, J., Redfern, J., and Gentemann, C. 2012. Forecasting cetacean abundance patterns to enhance management decisions. Endanger. Species Res. 16(2): 97–112. doi:10.3354/esr00390.

Becker, E.A. 2021. Habitat-based density estimates for cetaceans within the waters of the U.S. Exclusive Economic Zone around the Hawaiian Archipelago. Pacific Islands Fisheries Science Center. doi:10.25923/X9Q9-RD73.

de Boer, M. 2010. Spring distribution and density of minke whale *Balaenoptera acutorostrata* along an offshore bank in the central North Sea. Mar. Ecol. Prog. Ser. 408: 265–274. doi:10.3354/meps08598.

Booth, C., Embling, C., Gordon, J., Calderan, S., and Hammond, P. 2013. Habitat preferences and distribution of the harbour porpoise *Phocoena phocoena* west of Scotland. Mar. Ecol. Prog. Ser. 478: 273–285. doi:10.3354/meps10239.

Bradford, A.L., Forney, K.A., Oleson, E.M., and Barlow, J. 2017. Abundance estimates of cetaceans from a line-transect survey within the U.S. Hawaiian Islands exclusive economic zone. Fish. Bull. 115(2): 129–142. doi:10.7755/FB.115.2.1.

Breen, P., Brown, S., Reid, D., and Rogan, E. 2016. Modelling cetacean distribution and mapping overlap with fisheries in the northeast Atlantic. Ocean Coast. Manag. 134: 140–149. doi: 10.1016/j.ocecoaman.2016.09.004.

Cañadas, A., and Hammond, P. 2008. Abundance and habitat preferences of the short-beaked common dolphin *Delphinus delphis* in the southwestern Mediterranean: implications for conservation. Endanger. Species Res. 4: 309–331. doi:10.3354/esr00073.

Carlucci, R., Fanizza, C., Cipriano, G., Paoli, C., Russo, T., and Vassallo, P. 2016. Modeling the spatial distribution of the striped dolphin (*Stenella coeruleoalba*) and common bottlenose dolphin (*Tursiops truncatus*) in the Gulf of Taranto (Northern Ionian Sea, Central-eastern Mediterranean Sea). Ecol. Indic. 69: 707–721. doi: 10.1016/j.ecolind.2016.05.035.

Castro, J., Couto, A., Borges, F.O., Cid, A., Laborde, M.I., Pearson, H.C., and Rosa, R. 2020. Oceanographic Determinants of the Abundance of Common Dolphins (*Delphinus delphis)* in the South of Portugal. Oceans 1(3): 165–173. doi:10.3390/oceans1030012.

Correia, A., Gil, A., Valente, R., Rosso, M., Pierce, G., and Sousa Pinto, I. 2019. Distribution and habitat modelling of common dolphins (*Delphinus delphis*) in the eastern North Atlantic. J. Mar. Biol. Assoc. UK 99: 1443–1457. doi:10.1017/S0025315419000249.

Doksæter, L., Olsen, E., Nøttestad, L., and Fernö, A. 2008. Distribution and feeding ecology of dolphins along the Mid-Atlantic Ridge between Iceland and the Azores. Deep Sea Res. Part II Top. Stud. Oceanogr. 55(1–2): 243–253. doi: 10.1016/j.dsr2.2007.09.009.

Embling, C.B., Gillibrand, P.A., Gordon, J., Shrimpton, J., Stevick, P.T., and Hammond, P.S. 2010. Using habitat models to identify suitable sites for marine protected areas for harbour porpoises (*Phocoena phocoena*). Biol. Conserv. 143(2): 267–279. doi: 10.1016/j.biocon.2009.09.005.

Evans, P.G.H., Anderwald, P., and Baines, M.E. 2003. UK Cetacean Status Review. Seawatch Foundation. Report to English Nature & Countryside Council for Wales. Oxford. 162pp.

Evans, P.G.H., and Hammond, P.S. 2004. Monitoring cetaceans in European waters. Mammal Rev. 34(1–2): 131–156. doi:10.1046/j.0305-1838.2003.00027. x.

Fiedler, P.C. 2018. Ocean Environments. *In* Encyclopedia of Marine Mammals, 3rd edition. Elsevier. pp. 649–653.

Forney, K., Ferguson, M., Becker, E., Fiedler, P., Redfern, J., Barlow, J., Vilchis, I., and Ballance, L. 2012. Habitat-based spatial models of cetacean density in the eastern Pacific Ocean. Endanger. Species Res. 16(2): 113–133. doi:10.3354/esr00393.

Gilles, A., Adler, S., Kaschner, K., Scheidat, M., and Siebert, U. 2011. Modelling harbour porpoise seasonal density as a function of the German Bight environment: implications for management. Endanger. Species Res. 14(2): 157–169. doi:10.3354/esr00344.

Goetz, S., Read, F.L., Ferreira, M., Portela, J.M., Santos, M.B., Vingada, J., Siebert, U., Marçalo, A., Santos, J., Araújo, H., Monteiro, S., Caldas, M., Riera, M., and Pierce, G.J. 2015. Cetacean occurrence, habitat preferences and potential for cetacean–fishery interactions in Iberian Atlantic waters: results from cooperative research involving local stakeholders. Aquat. Conserv. Mar. Freshw. Ecosyst. 25(1): 138–154. doi:10.1002/aqc.2481.

Hammond, P., Lacey, C., Gilles, A., Viquerat, S., Börjesson, P., Herr, H., Macleod, K., Ridoux, V., Santos, M., Teilmann, J., Vingada, J., and Øien, N. 2021. Estimates of cetacean abundance in European Atlantic waters in summer 2016 from the SCANS-III aerial and shipboard surveys. Final project report. https://scans3.wp.st-andrews.ac.uk/files/2021/06/SCANS-III_design-based_estimates_final_report_revised_June_2021.pdf

Hammond, P.S., Macleod, K., Berggren, P., Borchers, D.L., Burt, L., Cañadas, A., Desportes, G., Donovan, G.P., Gilles, A., Gillespie, D., Gordon, J., Hiby, L., Kuklik, I., Leaper, R., Lehnert, K., Leopold, M., Lovell, P., Øien, N., Paxton, C.G.M., Ridoux, V., Rogan, E., Samarra, F., Scheidat, M., Sequeira, M., Siebert, U., Skov, H., Swift, R., Tasker, M.L., Teilmann, J., Van Canneyt, O., and Vázquez, J.A. 2013. Cetacean abundance and distribution in European Atlantic shelf waters to inform conservation and management. Biol. Conserv. 164: 107–122. doi: 10.1016/j.biocon.2013.04.010.

Kingsley, M.C.S. 2000. Numbers and distribution of beluga whales, *Delphinapterus leucas*, in James Bay, eastern Hudson Bay, and Ungava Bay in Canada during the summer of 1993. Fish. Bull. 98(4): 736–736. National Marine Fisheries Service.

Lacey, C., Gilles, A., Börjesson, P., Herr, H., Macleod, K., Ridoux, V., Santos, M.B., Scheidat, M., Teilmann, J., Vingada, J., Viquerat, S., Øien, N.I., and Hammond, P.S. 2022. Modelled density surfaces of cetaceans in European Atlantic waters in summer 2016 from the SCANS-III aerial and shipboard surveys. Project report. https://scans3.wp.st-andrews.ac.uk/files/2022/08/SCANS-III_density_surface_modelling_report_final_20220815.pdf 55pp.

MacLeod, C.D., Weir, C.R., Pierpoint, C., and Harland, E.J. 2007. The habitat preferences of marine mammals west of Scotland (UK). J. Mar. Biol. Assoc. U. K. 87(1): 157–164. doi:10.1017/S0025315407055270.

MacLeod, C.D., Weir, C.R., Santos, M.B., and Dunn, T.E. 2008. Temperature-based summer habitat partitioning between white-beaked and common dolphins around the United Kingdom and Republic of Ireland. J. Mar. Biol. Assoc. U. K. 88(6): 1193–1198. doi:10.1017/S002531540800074X.

Macleod, K., Fairbairns, R., Gill, A., Fairbairns, B., Gordon, J., Blair-Myers, C., and Parsons, E. 2004. Seasonal distribution of minke whales *Balaenoptera acutorostrata* in relation to physiography and prey off the Isle of Mull, Scotland. Mar. Ecol. Prog. Ser. 277: 263–274. doi:10.3354/meps277263.

Mannocci, L., Roberts, J.J., Miller, D.L., and Halpin, P.N. 2017. Extrapolating cetacean densities to quantitatively assess human impacts on populations in the high seas: Cetacean Densities in the High Seas. Conserv. Biol. 31(3): 601–614. doi:10.1111/cobi.12856.

Maravelias, C. 1997. Trends in abundance and geographic distribution of North Sea herring in relation to environmental factors. Mar. Ecol. Prog. Ser. 159: 151–164. doi:10.3354/meps159151.

Marubini, F., Gimona, A., Evans, P., Wright, P., and Pierce, G. 2009. Habitat preferences and interannual variability in occurrence of the harbour porpoise *Phocoena phocoena* off northwest Scotland. Mar. Ecol. Prog. Ser. 381: 297–310. doi:10.3354/meps07893.

Moura, A.E., Sillero, N., and Rodrigues, A. 2012. Common dolphin *(Delphinus delphis)* habitat preferences using data from two platforms of opportunity. Acta Oecologica 38: 24–32. doi: 10.1016/j.actao.2011.08.006.

Naud, M.-J., Long, B., Brethes, J.-C., and Sears, R. 2003. Influences of underwater bottom topography and geomorphology on minke whale (*Balaenoptera acutorostrata*) distribution in the Mingan Islands (Canada). J. Mar. Biol. Assoc. U. K. 83: 889–896.

Palka, D.L., Chavez-Rosales, S., Josephson, E.A., Cholewiak, D., Haas, H.L., Garrison, L., Jones, M., Sigourney, D.B., Waring, G., Jech, M., Broughton, E., Soldevilla, M.S., Davis, G., DeAngelis, A., Sasso, C.R., Winton, M.V., Smolowitz, R.J., Fay, G., LaBrecque, E., Leiness, J.B., Detloff, M., Warden, M., Murray, K., and Orphanides, C. 2017. Atlantic Marine Assessment Program for Protected Species: 2010 - 2014. US Dept. of the Interior, Bureau of Ocean Energy Management, Atlantic OCS Region, Wahington, DC. Available from https://espis.boem.gov/final%20reports/5638.pdf.

Reid, J.B., Evans, P.G.H., and Northridge, S.P. 2003. Atlas of Cetacean distribution in north-west European waters.: 82.

Roberts, J.J., Best, B.D., Mannocci, L., Fujioka, E., Halpin, P.N., Palka, D.L., Garrison, L.P., Mullin, K.D., Cole, T.V.N., Khan, C.B., McLellan, W.A., Pabst, D.A., and Lockhart, G.G. 2016. Habitat-based cetacean density models for the U.S. Atlantic and Gulf of Mexico. Sci. Rep. 6(1): 22615. doi:10.1038/srep22615.

Rogan, E., Breen, P., Mackey, M., Cañadas, A., Scheidat, M., Geelhoed, S., and Jessopp, M. 2018. Aerial Surveys of Cetaceans and Seabirds in Irish waters: Occurrence, distribution and abundance in 2015-2017.: 298.

Scheidat, M., Verdaat, H., and Aarts, G. 2012. Using aerial surveys to estimate density and distribution of harbour porpoises in Dutch waters. J. Sea Res. 69: 1–7. doi: 10.1016/j.seares.2011.12.004.

Selzer, L.A., and Payne, P.M. 1988. The Distribution of White-Sided (*Lagenorhynchus acutus*) and Common Dolphins (*Delphinus delphis)* Vs. Environmental Features of the Continental Shelf of the Northeastern United States. Mar. Mammal Sci. 4(2): 141–153. doi:10.1111/j.1748-7692. 1988.tb00194.x.

Svendsen, G.M., Romero, M.A., Williams, G.N., Gagliardini, D.A., Crespo, E.A., Dans, S.L., and González, R.A. 2015. Environmental Niche Overlap between Common and Dusky Dolphins in North Patagonia, Argentina. PLOS ONE 10(6): e0126182. doi: 10.1371/journal.pone.0126182.

Wade, P.R. 1993. Estimates of Cetacean Abundance and Distribution in the Eastern Tropical Pacific.

Wall, D., Murray, C., O'Brien, J., Kavanagh, L., Wilson, C., Ryan, C., Glanville, B., Williams, D., Enlander, I., O'Connor, I., McGrath, D., Whooley, P., and Berrow, S. 2013. Atlas of the Distribution and Relative Abundance of Marine Mammals in Irish Offshore Waters: 2005 – 201.: 65.

Wall, D., O'Brien, J., Meade, J., and Allen, B.M. 2006. Summer Distribution and Relative Abundance of Cetaceans off the West Coast of Ireland. Biol. Environ. Proc. R. Ir. Acad. 106(2): 135–142. doi:10.3318/BIOE.2006.106.2.135.

Weir, C.R., Macleod, C.D., and Calderan, S.V. 2009. Fine-scale habitat selection by white-beaked and common dolphins in the Minch (Scotland, UK): evidence for interspecific competition or coexistence? J. Mar. Biol. Assoc. U. K. 89(5): 951–960. doi:10.1017/S0025315408003287.

Weir, C.R., Pollock, C., Cronin, C., and Taylor, S. 2001. Cetaceans of the Atlantic Frontier, north and west of Scotland. Cont. Shelf Res. 21(8–10): 1047–1071. doi:10.1016/S0278-4343(00)00124-2.

4 Cetaceans in the Greater North Sea Ecoregion

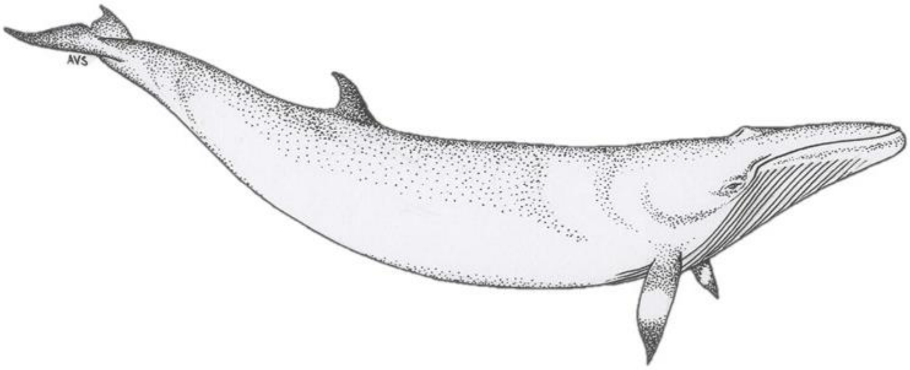

Minke whale sketch, courtesy of Anni Sharpe

A focus on the three most common species of cetaceans in the Greater North Sea Ecoregion; do the factors affecting their distribution differ in this distinct body of water, as compared to the wider area? Have these factors changed between 2005 and 2016?

4.1 Introduction

Ecology "plays out" at various different scales, both temporally and spatially and, as Wiens (1989) noted, "to understand the drama, we must view it on the appropriate scale". The distribution of a species can span a very large geographical area; for example the common minke whale (*Balaenoptera acutorostrata*) is found in waters at all latitudes from almost 70^0S to 80^0N (Cooke 2018). When a species has such a wide geographic range, a wide variety of different habitats and different environmental processes will be encountered. Individuals in different locations will interact with their environment in different ways, with processes acting at different geographical scales. Individuals of a species may also be highly mobile, and different parts of the range of individual animals may be used for different purposes, such as feeding and breeding (Risch *et al*. 2014). It therefore is not surprising that studies on marine top predators have shown that the relative importance of different habitat variables can depend upon the spatial scale of the study (Pribil and Picman 1997; Hastie *et al*. 2003).

The work presented in the previous chapter covered a large geographical area and a range of habitats. The aim of this chapter is to investigate the environmental features that influence the distribution of cetaceans in a smaller section of the overall study area, the North Sea ecoregion, as defined by ICES (ICES 2020). Ecoregions are areas with relative homogeneity of environment and ecosystems and as such are often used as units of analysis for environmental assessment (Loveland and Merchant 2004). This chapter compares models using abiotic variables (often proxies) with those using more direct measures of prey for the three most common cetacean species within this ecoregion, the common minke whale (hereafter minke whale), the white-beaked dolphin (*Lagenorynchus albirostris*) and the harbour porpoise (*Phocoena phocoeana*).

4.1.1 Regional description

The North Sea, an approximately rectangular-shaped basin, is situated in the northeast Atlantic between Britain, France, Belgium, the Netherlands, Germany, Denmark, and Norway. For the purposes of this chapter, the term "North Sea" refers to the entire Greater North Sea ecoregion, as defined by (ICES 2020), which also includes the English Channel and the Skagerrak and Kattegat Figure 1.8-2).

This is a shallow shelf-sea area. The water depth averages 70m (Huthnance 1991), although there is a general depth gradient from shallower waters in the south to deeper waters in the north, with a much deeper channel to the northeast along the Norwegian coast in which depths exceed 650m (Figure 4.1-1). Most of the water mass within the North Sea flows in from the Atlantic in the north (Turrell *et al*. 1992). This means the northern parts of the region are strongly influenced by oceanic mixing, and the area is well stratified during the summer (Clark and Frid 2001; ICES,2020, Figure 4.2-6) including the months during which the cetacean data used in these analysis were collected. A pronounced thermocline is usually present by June and remains in place usually until November (Clark and Frid, 2001).

A second large influx of water enters through the Straits of Dover via the English Channel (Salomon and Breton 1993), which leads to the waters of the south and east of the region being almost permanently thermally mixed (ICES 2020). To the east, the waters of the Skagerrak and Kattegat join the Baltic Sea and are both less tidal and less saline than the rest of the ecoregion. The waters of the Skagerrak and Kattegat are usually well mixed (ICES, 2020).The primary direction of water mass circulation is in an anticlockwise gyre (Laane 1996).

The North Sea has been the subject of a long-running, marine monitoring programme with the community of subsurface plankton studied via Continuous Plankton Recorders since 1931 (Laane 1996; Edwards 2001; Reid *et al*. 2003b; Alvarez-Fernandez *et al*. 2012). During this period there have been multiple regime changes which can be defined as “apparent shifts in oceanic and climatic conditions and marine community structure” (Alvarez-Fernandez *et al*. 2012). These are documented to have taken place around 1977, 1988 and 1998, although the 1998 shift is less pronounced (Weijerman *et al*. 2005) . Following the 1977 “cold” shift, the spring bloom was less pronounced, biomass peaked later in the year, and there was a rise in the numbers of cold water copepods (Reid and Edwards 2001; Edwards *et al*. 2002). The post-1988 phase saw waters warming, a return to a warm-type plankton system, and overall higher phytoplankton biomass (Alvarez-Fernandez *et al*. 2012). The 1998 shift saw a decline in the total number of copepods, particularly in neritic species. The North Sea is thus a highly dynamic ecosystem.

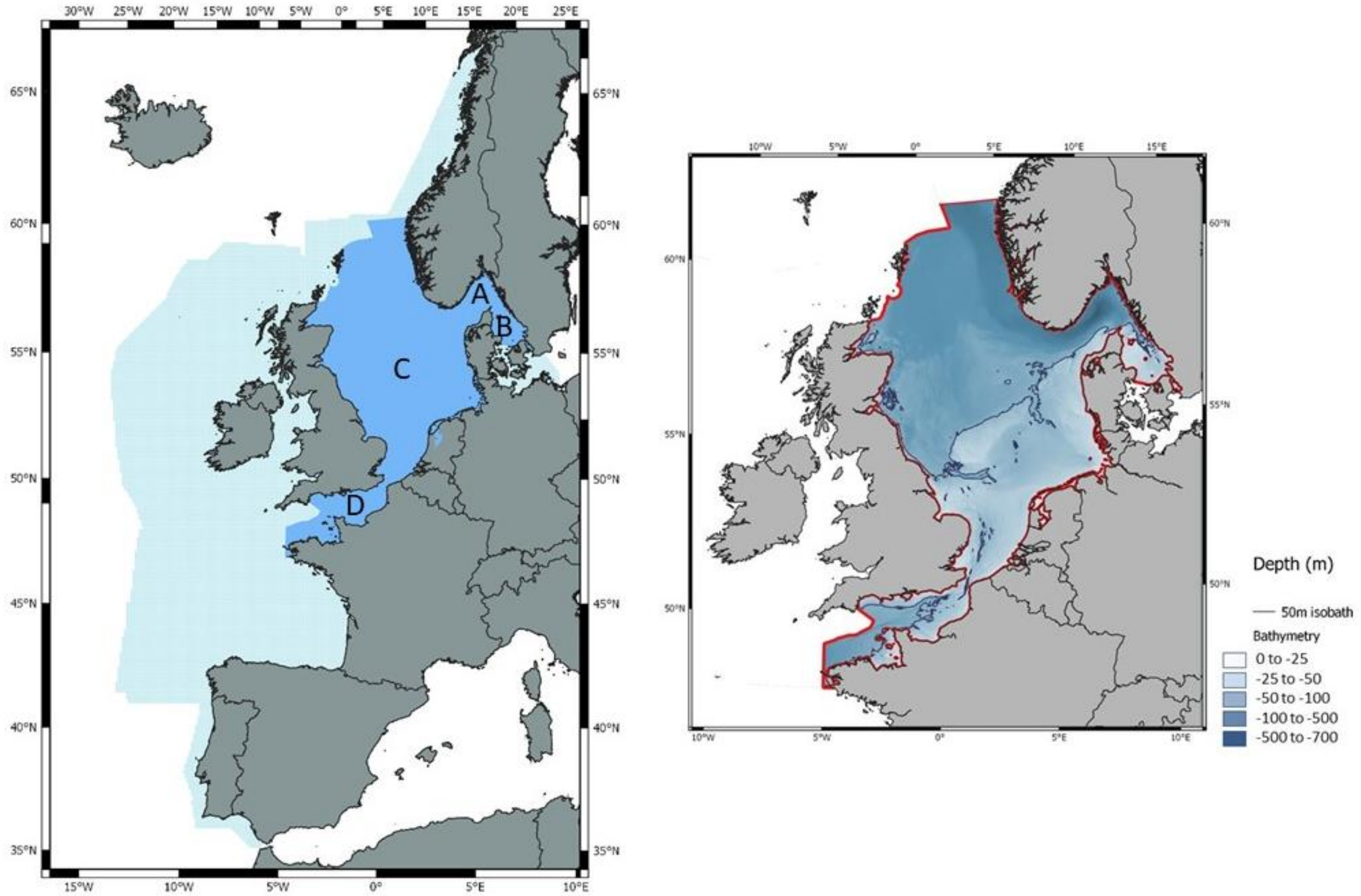

Figure 4.1-1: Left panel: The Greater North Sea Ecoregion (dark blue) as defined by ICES, shown as a sub-region of the main SCANS/ObSERVE study area for which data are available. Named regions: A) Skagerrak, B), Kattegat, C) North Sea, D) English Channel. Right panel: Bathymetry of the Greater North Sea ecoregion. The 50m depth contour, used as a modelling covariate, is shown in grey.

4.1.2 Cetaceans within the North Sea

At least 21 different species of cetacean have been recorded in the North Sea, either as sightings of live individuals (Reid *et al*. 2003) or as strandings records (Kinze *et al*. 2021).

Some of these species, including the blue whale (*Balaenoptera musculus*) are occasional visitors only and make up a very small portion of the record; only a single blue whale stranding was reported from the German portion of the North Sea in the period between 1818 and 2017 (Kinze *et al*., 2021), and no sightings are reported by Reid *et al*., in the period up to 2003.

Some other species, particularly deep diving species, including the sperm whale (*Physeter macrocephalus*), visit comparatively regularly (Reid *et al*., 2003), but these visits often end with the animals stranding (IJsseldijk *et al*. 2018). Sperm whales are known to use the deeper Norwegian trench at the northern end of the North Sea, and it is theorised that animals enter the North Sea from there. Due to the particularly shallow southern region, and the coastline acting like something of a dead-end, the North Sea has been recognised as one of the global hotspots for sperm whale strandings, despite it not representing core habitat for the species (Smeenk 1997; IJsseldijk *et al*. 2018).

Of the more frequently recorded species, four have been extensively documented and studied in the region: the bottlenose dolphin (*Tursiops truncatus*) (Wilson *et al*. 1997; Janik 2000; Cheney *et al*. 2013; Arso Civil *et al*. 2019), harbour porpoise (*Phocoena phocoena*) (Hammond *et al*. 2002, 2013 ; Santos and Pierce 2003; Peschko *et al*. 2016; Gilles *et al*. 2016) and to a lesser extent, the white-beaked dolphin (*Lagenorhynchus albirostris*) (Weir *et al*. 2007; Canning *et al*. 2008; Jansen *et al*. 2010) and minke whale (*Balaenoptera acutorostrata*) (Olsen and Holst 2001 ; Andersen *et al*. 2003 ; Macleod *et al*. 2004 ; de Boer 2010).

During the SCANS-III aerial surveys in 2016 (Chapter 2), six cetacean species were recorded within the ecoregion; harbour porpoise, bottlenose dolphin, Risso's dolphin (*Grampus griseus*), white-beaked dolphin, white-sided dolphin (*Lagenorhynchus acutus*) and minke whale (Hammond *et al*. 2021). Of these, two species – Risso's dolphin and white-sided dolphin were seen only once each in this area, whilst bottlenose dolphins were seen only three times. The small number of sightings of these species within the ecoregion means that they will not be considered further in this chapter. This chapter focuses on the three species – minke whale, harbour porpoise and white-beaked dolphin - that were seen in sufficient numbers for meaningful analysis to be conducted. Estimates of the abundance of these species within the ecoregion from the SCANS-III survey are shown in Table 4.1-1. Error around these summed estimates from multiple blocks was derived by taking the sum of the variances of the estimates, then taking the square root to derive the SE of the sum. This was then used to derive a CV for the pooled estimate log-normal confidence interval.

Table 4.1-1: Estimates of abundance of minke whale, white-beaked dolphin and harbour porpoise from the SCANS-III surveys (Hammond *et al.* 2021). Estimates for survey blocks P1, P, V, U, T, R, Q, O, N, M, L, C (Figure 3.1-1) have been summed to provide an estimate for the Greater North Sea Ecoregion.

	Abundance	Lower 95% CL	Higher 95% CL
Minke whale	9,040	5,161	15,834
White-beaked dolphin	20,711	10,211	42,008
Harbour porpoise	347,399	289,687	416,609

4.1.2.1 Minke whales in the Greater North Sea Ecoregion

Minke whales have been recorded throughout the Greater North Sea ecoregion, although this species is less frequently sighted in the south of this area (Reid *et al*., 2003; Hammond *et al*., 2013; Hammond *et al*., 2021). Minke whales are seen predominantly in the summer months (Reid *et al*. 2003a; Weir *et al*. 2007), with a peak in reporting from July to September (Evans *et al*. 2003; MacLeod, Colin D. *et al*. 2007; Weir *et al*. 2007). Their winter distribution is not well understood, although eastern Atlantic wintering grounds extend at least to the Straits of Gibraltar (Perrin *et al*. 2018). It is not known whether North Sea animals undertake southerly migrations like those undertaken by minke whales in more northern latitudes, or whether they simply move further from the coast and thus are seen less often during the winter months, potentially due to poorer conditions and lower search effort during these months. Seasonal variation in body condition has been reported for whales in the northeast Atlantic, implying some type of cessation of feeding, during the winter months, consistent with that seen in other baleen whales (Niæss *et al*. 1998). Telemetry studies of Icelandic minke whales have shown them heading south along the mid-Atlantic ridge, with signals received from one animal until it had passed the Azores (3,700 km and 100 days) (Víkingsson and Heide-Jørgensen 2015).

Minke whales consume a wide variety of different prey species. Although they show some degree of specialisation within season and area (Anderwald and Evans 2007), they have not been found to exhibit strong preferences for any particular species when multiple options are available (Skaug *et al*. 1997). Diet studies on northeast Atlantic minke whales from whales lethally sampled in Norwegian and Icelandic waters show the diet to comprise various species and sizes of fish and crustaceans, and to vary both spatially and temporally (Windsland *et al*. 2007). Of 210 whales sampled in different areas of the north-eastern Atlantic between 2000-04, krill dominated in the Barents Sea and capelin dominated in northern Norway, but this changed over time, with herring and haddock making up a larger part of the diet in later years. The diet of whales in the Norwegian Sea consisted mainly of mature herring. In the North Sea prey samples were dominated by sand eels and mackerel (Windsland *et al*. 2007). Similar spatial differentiation was confirmed by fatty acid composition analysis using blubber of 56 minke whales caught during whaling operations between 2009-2011 at four different feeding grounds including the North Sea (Meier *et al*. 2016). This study also found sandeel and mackerel to be the dominant prey for North Sea whales and reported no indication of differences between male and female whales, or whales of smaller sizes indicating there is no segregation of feeding. Other studies of Norwegian and Icelandic waters have reported similar findings, with species predated upon being reported as krill, capelin, herring, mackerel, whiting and haddock (Lindstrøm *et al*. 1997; Olsen and Holst 2001; Lindstrøm 2002; Víkingsson *et al*. 2014). Studies of stomach contents from stranded animals from Scottish waters showed a majority of herring, sprat, mackerel and sandeels (Pierce *et al*. 2004) in the diet of the sampled individuals.

4.1.2.2 White-beaked dolphins in the Greater North Sea Ecoregion

White-beaked dolphins are found throughout the Greater North Sea ecoregion, although, similarly to minke whales, this species is less frequently sighted in the south of the area of interest (Reid *et al*., 2003; Hammond *et al*., 2013; Hammond *et al*., 2021). Their seasonal movements are not well known, although they seem to be more frequent within the ecoregion during summer (Reid *et al*., 2003. Evans *et al*., 2003, Weir *et al*., 2007). In this region, white-beaked dolphins are found mainly in waters ranging from 50-100m depth, and almost exclusively within waters less than 200m depth (Evans *et al*., 2003).

White-beaked dolphin diet has been shown to vary geographically. Analysis of stomach contents from stranded animals from the east coast of Scotland found haddock and whiting to be the primary prey species in the diet, with cod, herring and mackerel also being represented (Canning *et al*. 2008). Outside the North Sea, interactions with the Dutch mid-water trawl fishery west of Ireland have been reported, leading to the supposition that white-beaked dolphins in this area are targeting mackerel in spring (Couperus 1997). Cod, hake, octopus and sandeel have also been reported in stomach contents of stranded animals from elsewhere around the UK (MacLeod 2013). Stomach contents of Dutch stranded animals were dominated by whiting and cod (Jansen *et al*. 2010).

Elsewhere in their range, the species is anecdotally linked with capelin (in the Barents Sea) (Fall and Skern-Mauritzen 2013).

4.1.2.3 Harbour porpoise in the Greater North Sea Ecoregion

The harbour porpoise is the most abundant cetacean in the ecoregion and is found throughout the Greater North Sea (Reid *et al*., 2003; Hammond *et al*., 2013; Hammond *et al*, 2021). In the north-east Atlantic, the species is primarily restricted to the continental shelf, in waters less than 200m deep (Evans *et al*., 2003), although this is not the case throughout its range (Nielsen *et al*. 2018).

The diet of the harbour porpoise comprises small fish of a wide variety of species (Read 1999). They generally forage near the sea bed in waters less than 200m deep, but they do also forage in the water column, particularly at night time (Schaffeld *et al*. 2016) Sandeels have been shown to be important prey items in Scottish waters, particularly early in the year (Santos *et al*. 2004). Strandings along the entire British coastline from 1989-1994 found the most important prey items to be gadoids, including whiting, haddock and pollock. Norway pout was eaten in Shetland, but not found in stomachs from anywhere else. Danish porpoises were found to eat much higher proportions of gobies than elsewhere (Santos and Pierce 2003).

4.1.3 Chapter aims.

This chapter aims to explore the relationships between three different species of cetacean and different aspects of their environment. To do this, I have used explanatory (Guisan *et al*. 2002) generalised additive models (GAMs) to statistically explore the strength of the relationship between animal density and a variety of environmental – *explanatory* – variables, including sea surface temperature, depth, distance to the 50m isobath, salinity and seabed rugosity (modelled via slope and standard deviation of depth within a grid cell), hereafter termed “environmental models”. These variables are frequently selected when modelling marine mammals as proxies for prey data as data on prey species themselves can be very hard to obtain. Whilst it is noted that distribution of cetaceans may also be influenced by predators, competitors and conspecifics as well as by availability of prey, it is not possible in this instance to model these other factors which may influence distribution.

GAMs exploring the strength of the relationship between animal density and some candidate prey species have also been implemented. These models use as covariates the estimated amount of energy which would be available from different prey species in the form of modelled surfaces created by Ransijn *et al*. (2019), and provide information for a portion of the Greater North Sea ecoregion. This second set of explanatory models was created to investigate any potential relationships between the density of the three cetacean species of interest and the modelled amount of available prey energy. They are termed “prey models”. Both environmental and prey models were run separately for data from 2005 (Hammond *et al*., 2013) and 2016 (Hammond *et al*., 2021). They were also run for the two time periods combined to investigate whether relationships persisted between years. Information on the time periods and surveys can be found in Table 2.1-1.

4.2 Methods

4.2.1 Description of data

4.2.1.1 Cetacean data

Table 4.2-1 summarises the effort and sightings available for modelling the whole of the Greater North Sea Ecoregion in both 2016 and 2005. Only data collected in sea conditions less than Beaufort 3 were used for harbour porpoise modelling (less than Beaufort 5 for other species). Maps showing the locations of the sightings included in the modelling are shown in Figure 4.2-1, Figure 4.2-2 and Figure 4.2-3.

Table 4.2-1 Number of effort segments and number of groups and individuals sighted of each species used in analysis of data from the Greater North Sea ecoregion in 2016 and 2005.

Year	Species	Total no. of effort segments	No. of effort segments with groups	Number of groups	Number of Individuals	Mean group size
2016	Minke whale	2208	36 (1.6%)	36	41	1.1
	White-beaked dolphin	2208	35 (1.6%)	64	221	3.5
	Harbour porpoise	2239	664 (29%)	1313	1662	1.3
2005	Minke whale	1259	24 (1.9%)	35	36	1.0
	White-beaked dolphin	1259	21 (1.7%)	23	109	4.7
	Harbour porpoise	1021	250 (25%)	505	749	1.5

For the harbour porpoise, there were sightings in 25% or more of the effort segments. For the other species, only 1.5-2% of the segments contained sightings. There are slightly more harbour porpoise effort segments than for the other two species. This was due to additional ship survey effort in the Kattegat and Skaggerak regions which was included in the datasets for harbour porpoise, but not for minke whales or white-beaked dolphins No sightings of white-beaked dolphins or minke whales were made on this effort.

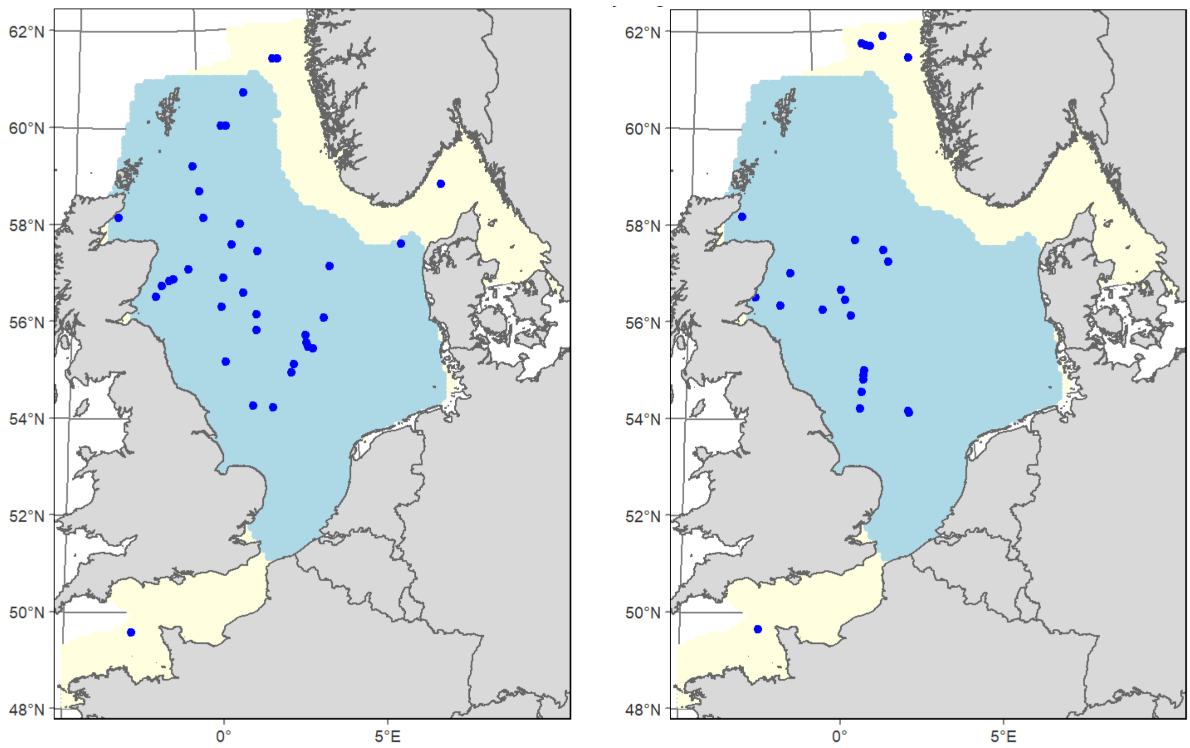

Figure 4.2-1: 2016 (left) and 2005 (right) minke whale sightings used in modelling the relationships between minke whale density and a range of environmental covariates. The full ecoregion is indicated by the blue and yellow regions combined. The area (and sightings) included in the prey models are represented just by the blue area.

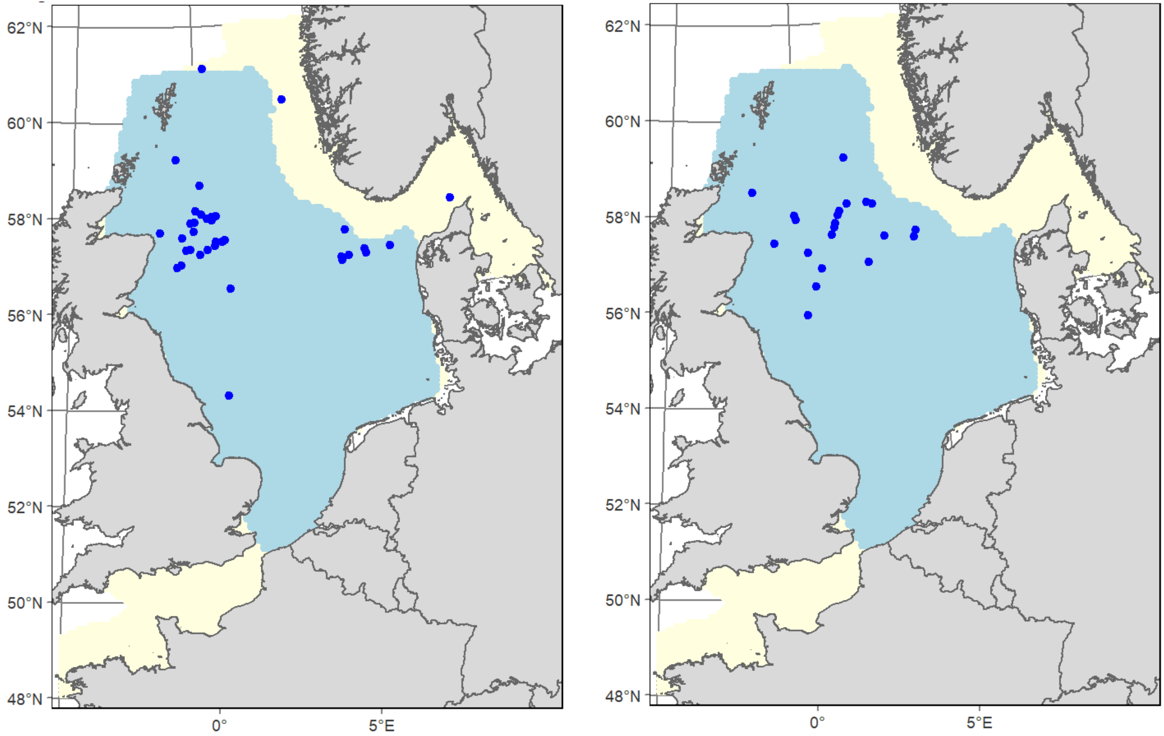

Figure 4.2-2: 2016 (left) and 2005 (right) white-beaked dolphin sightings used in modelling the relationships between density and a range of environmental covariates. The full ecoregion is indicated by the blue and yellow regions combined. The area (and sightings) included in the prey models are represented just by the blue area.

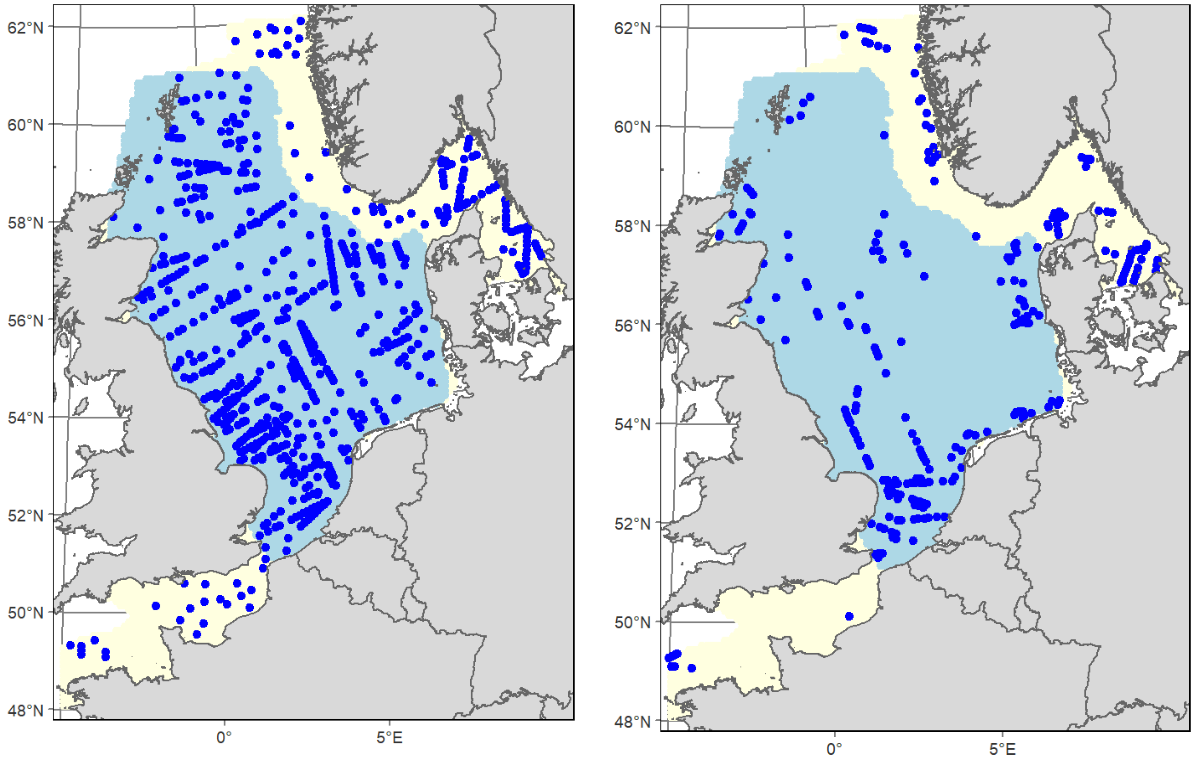

Figure 4.2-3: 2016 (left) and 2005 (right) harbour porpoise sightings used in modelling the relationships between porpoise density and a range of environmental covariates. The full ecoregion is indicated by the blue and yellow regions combined. The area (and sightings) included in the prey models are represented just by the blue area.

4.2.1.2 Covariate data

Covariates for models of the full ecoregion were selected using the method outlined in Chapter 2, and covariate values assigned to the effort segments, are summarised in Table 4.2-2,

Table 4.2-3 and Figure 4.2-4 to Figure 4.2-6. The full range of water depths within the ecoregion was represented (0—657m) with most of the segments having depths shallower than 200m (Figure 4.2-4). The slope was generally shallow across the region, which is to be expected considering the relatively flat bathymetry across most of the ecoregion, with most of the segments having less than 1^0 of gradient.

Due to the shape of the North Sea basin, only distance to 50m isobath was considered as a “distance to” covariate. By including either distance to coast or distance to 200m isobath, the covariates mimicked the effect of including latitude and longitude in the model and so these were not considered. The maximum distance from the 50m isobath to any effort segment was 319km. No seabed covariates (escarpments, canyons, troughs or seamounts) were included in these models, because the seabed features to which the distances are measured are located outside the ecoregion.

In addition to the static covariates, monthly mean values for sea surface temperature (SST), mixed layer depth (MLD), salinity (SAL), absolute dynamic topography (ADT), sea surface height (SSH) and Sea Level Anomaly (SLA) were also used in the models. The mean value for the month of July was used in each instance as this was the month in which the majority of the cetacean survey data were collected.

Table 4.2-2: Summary of static covariate values assigned to effort segments used to model the cetacean data from 2005 and 2016. These are presented for both data collection periods due to differences in geographical coverage between the two surveys.

Year	Covariate	Min	Max	Mean
2005	Depth (m)	-1	-640	-87
2005	Standard deviation of depth (SDdepth)	0	136	7
2005	Slope (^{0})	0	3.3	0.1
2005	Distance to 50m isobath (km) (D50_iso)	0	319	70
2016	Depth (m)	-3	-658	-84
2016	Standard deviation of depth (SDdepth)	0	160	6
2016	Slope (^{0})	0	1.6	0.2
2016	Distance to 50m isobath (km) (D50_iso)	0	330	75

Table 4.2-3: Summary of dynamic covariate values assigned to effort segments used to model the cetacean data from 2005 and 2016. These are monthly averages for July of the year of the survey.

Year	Covariate	Min	Max	Mean
2005	Sea surface temperature (SST) (^{0}C)	10	21	15.8
2005	Sea level anomaly (SLA) (m)	-0.11	0.14	0.02
2005	Sea surface height (SSH) (m)	-0.51	-0.17	-0.4
2005	Absolute dynamic topography (ADT) (m)	-0.17	0.3	0.02
2005	Mixed layer depth (MLD) (m)	7	17	11
2005	Salinity (SAL) (PSU)	11	35	33
2016	Sea surface temperature (SST) (^{0}C)	12	18	15
2016	Sea level anomaly (SLA) (m)	-0.06	0	0.07
2016	Sea surface height (SSH) (m)	-0.5	-0.1	-0.36
2016	Absolute dynamic topography (ADT) (m)	-0.12	0.2	0.06
2016	Mixed layer depth (MLD) (m)	7	16	11
2016	Salinity (SAL) (PSU)	20	35	33.8

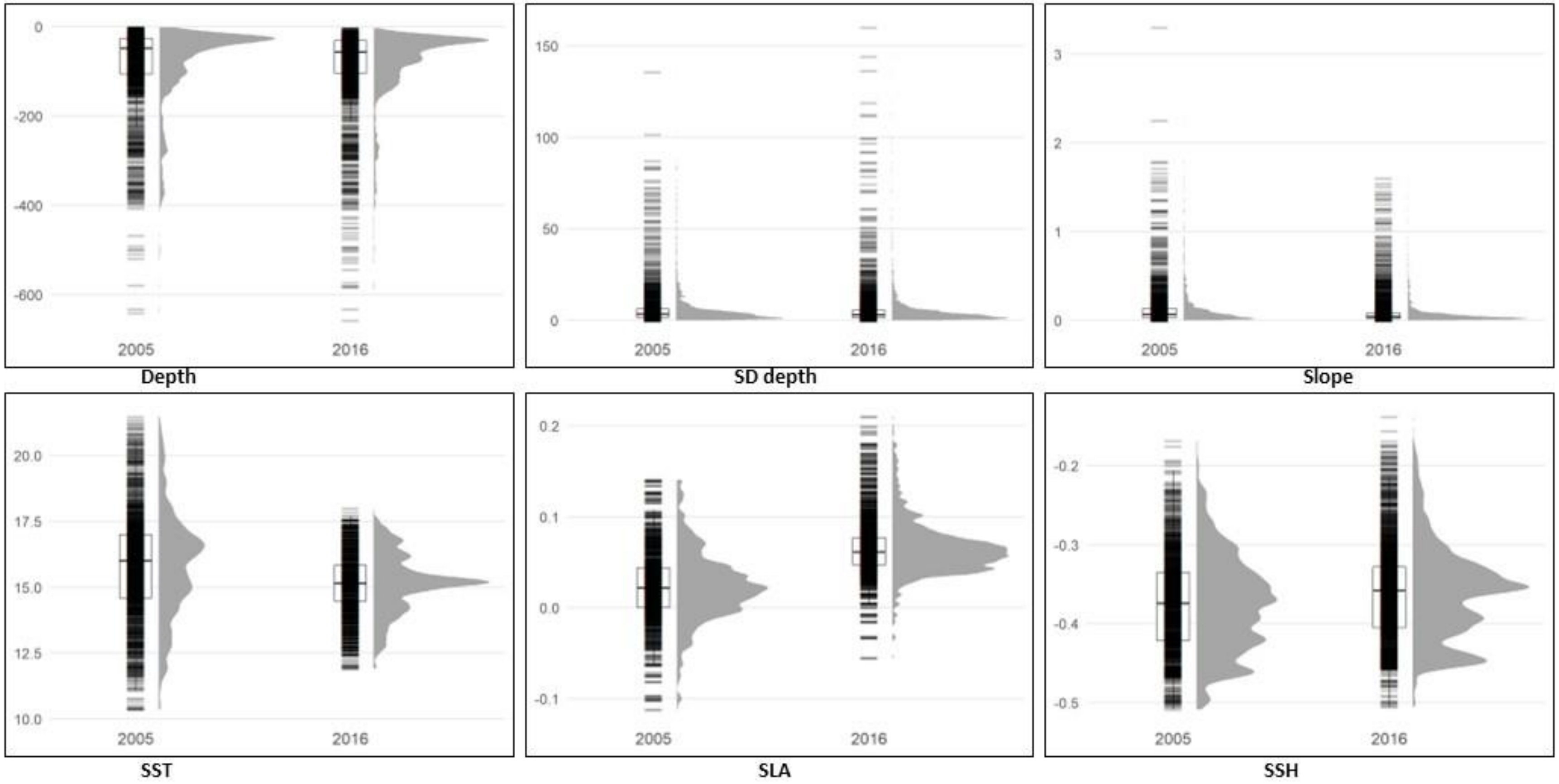

Figure 4.2-4: Raincloud plots showing the distribution of covariate data associated with the effort segments used to model the 2005 and 2016 cetacean data.

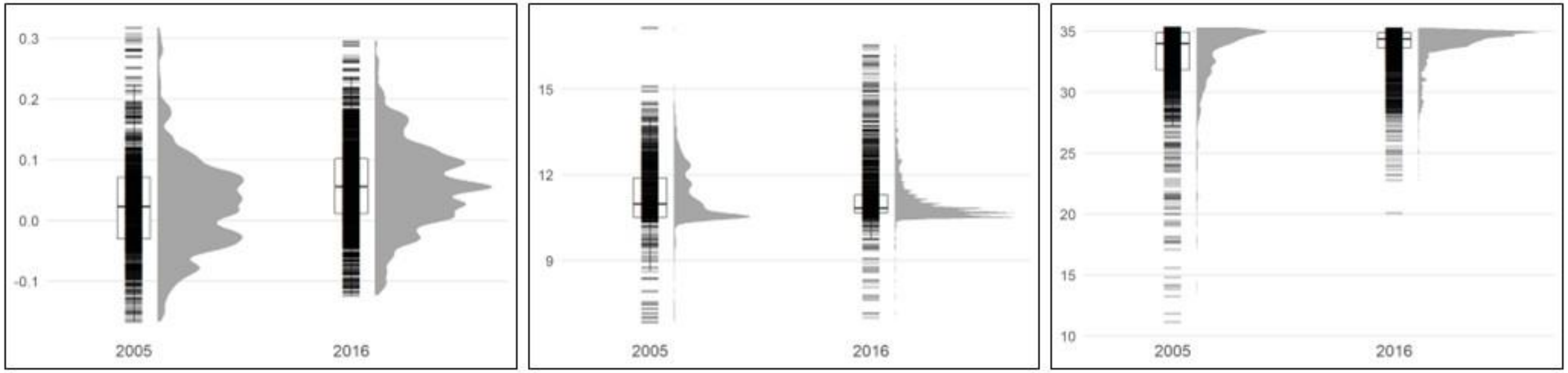

ADT **MLD** **SAL**

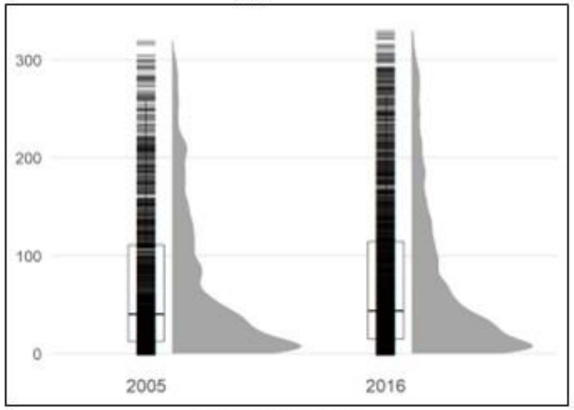

Dist 50m isobath

Figure 4.2-5: Raincloud plots showing the distribution of covariate data associated with the effort segments used to model the 2005 and 2016 cetacean data.

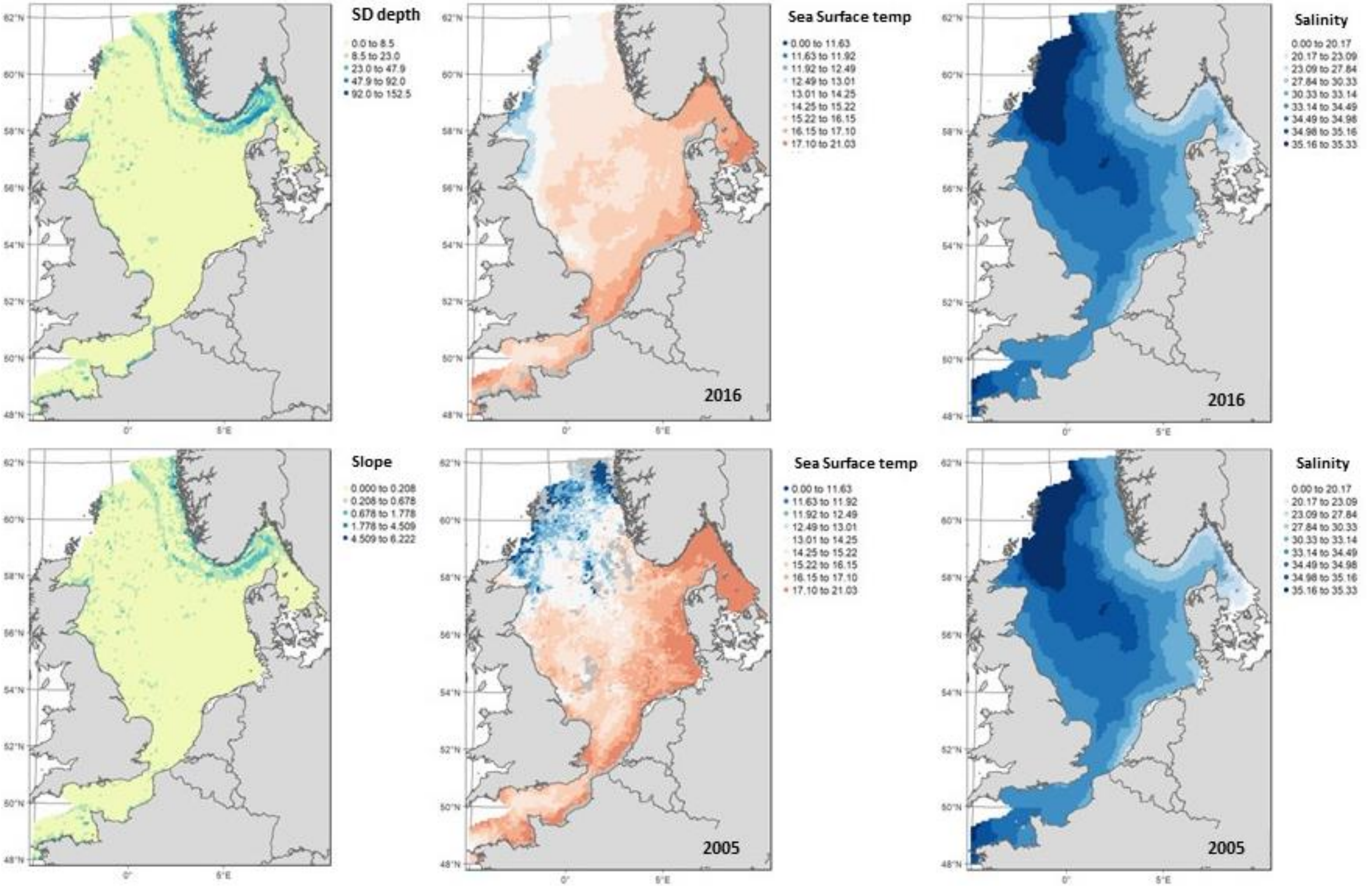

Figure 4.2-6a: Maps of the covariate data associated with the effort segments used to model the 2005 and 2016 cetacean data.

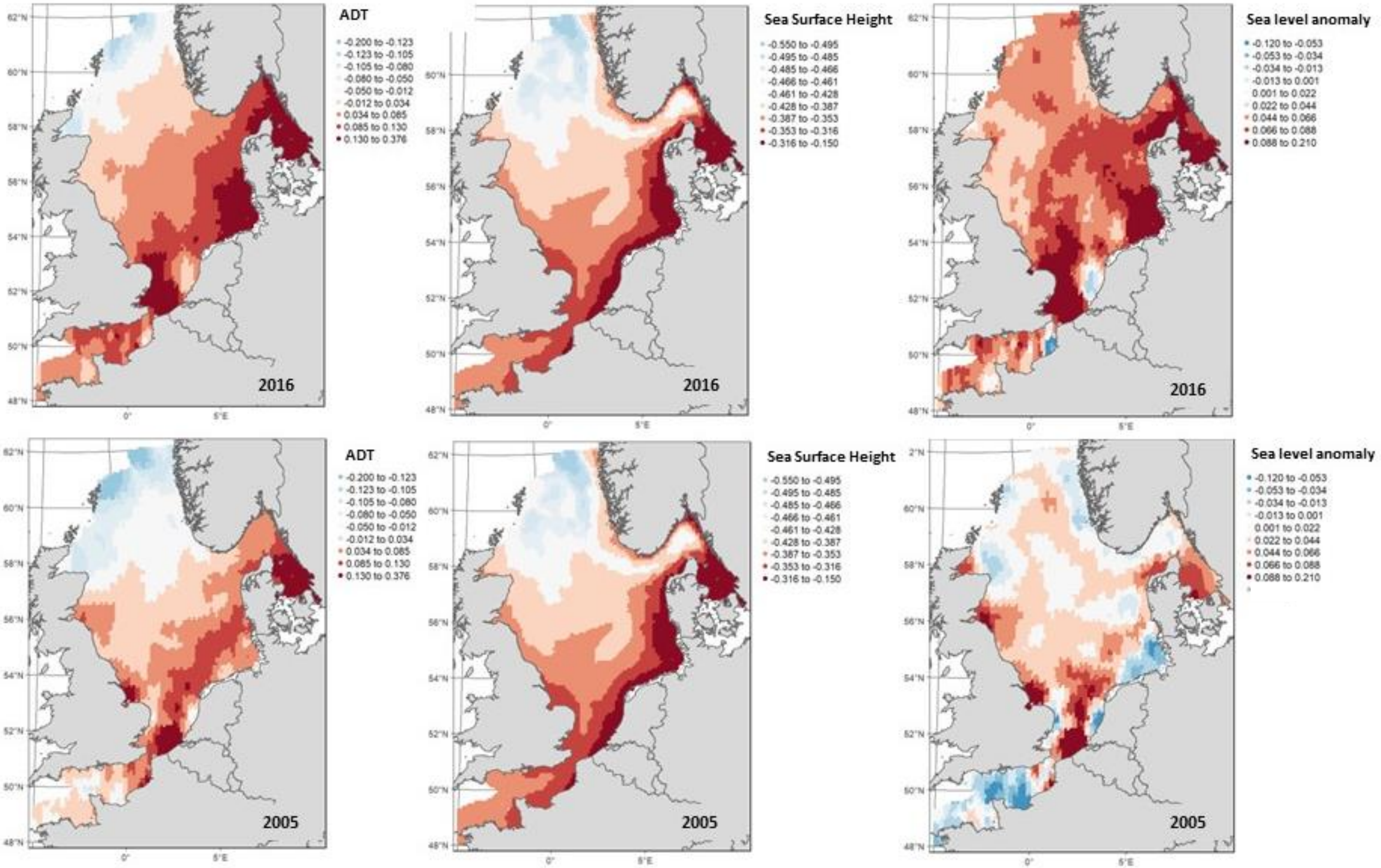

Figure 4.2-6b: Maps of the covariate data associated with the effort segments used to model the 2005 and 2016 cetacean data.

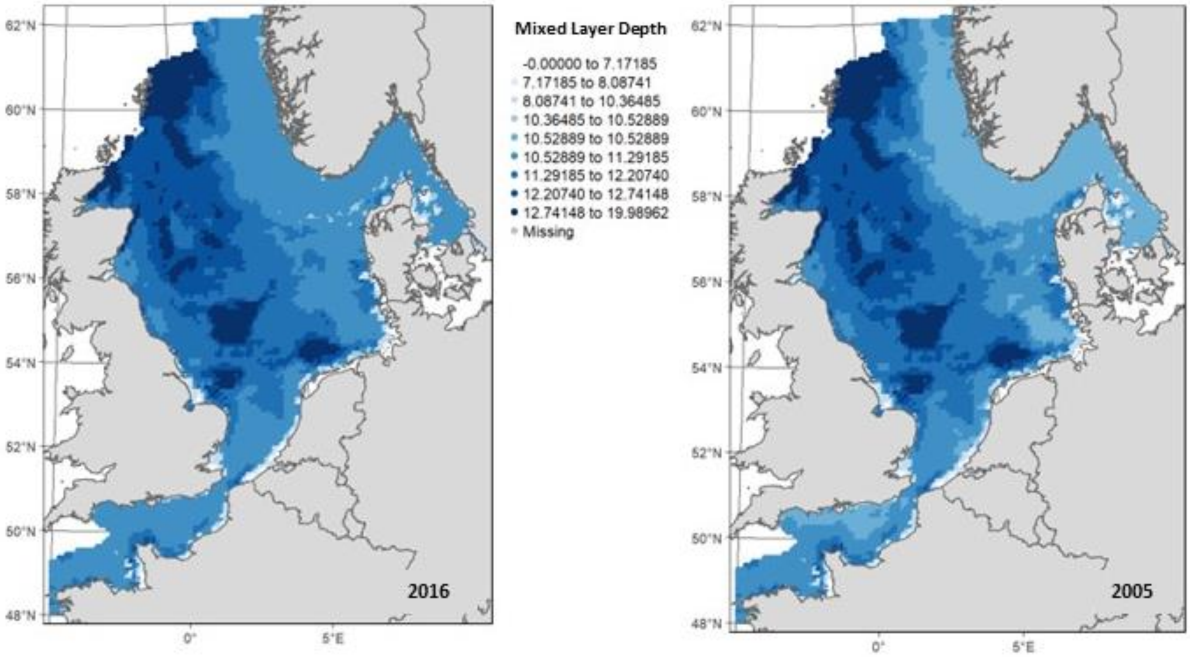

Figure 4.2-6c: Maps pf the covariate data associated with the effort segments used to model the 2005 and 2016 cetacean data.

4.2.2 Modelling methodology

4.2.2.1 Environmental models

Explanatory GAMS (not including latitude and longitude as covariates) were used to model minke whale, white-beaked dolphin, and harbour porpoise density as a function of environmental covariates. In these environmental models all data collected within the full Greater North Sea ecoregion were used, for both 2016 and 2005. Separate models were fitted for each species and each year. A third model combining the years for each species was also fitted.

4.2.2.2 Modelling cetacean prey more directly

It is typically assumed that prey is the main driver of cetacean species distribution, but proxy covariates usually need to be used because prey data are not available. However, for a large part of the Greater North Sea Ecoregion, data on the energetic availability of four key prey species were available in the form of summer (Jun-Aug) energy surfaces (Ransijn *et al*. 2019). The fish energy surfaces were produced by running GAMS to generate density surface models using data collected from International Bottom Trawl survey data for the selected prey species. Biomass of fish was converted to energetic content using values from the literature. Only fish smaller than 40cm were included in the models as this work was designed with harbour porpoise prey in mind. Efforts were made by the authors to correct for catchability, time of year, gear type and size of fish. Density These were predicted on to a 1km x 1km grid.

These energy surfaces can be used to model the density of the three cetacean species of interest. These models are termed “prey models”. The prey species for which energy data were available were cod, whiting, herring, and sprat (Figure 4.2-7). Ransijn *et al* (2019) did also produce a model of sandeel energy distribution, however, due to the highly localised nature of sandeel density, distance to sandeel ground (km) (Jensen *et al*. 2011) was modelled instead of energy, similar to the approach taken by Gilles *et al*. (2016) (Figure 4.2-8). Summaries of the fish energy data are provided in Figure 4.2-9.

In addition to the fish energy covariates, the same environmental covariates initially considered for the full ecoregion environmental models were considered for the prey models. However, several were excluded for various reasons. Depth (and consequently derivative covariates such as SDdepth) were excluded from the modelling because they were included in the models that generated the fish energy maps, and their inclusion here would have led to multicollinearity in the models. As the sandeel models used distance to grounds, and not the sandeel energy layer, these models were able to retain both depth and standard deviation of depth covariates without risk of collinearity.

Several physical covariates (sea surface temperature, sea level height anomaly, sea surface height, sea surface temperature, salinity and absolute dynamic topography) were also excluded because the mechanism by which they are thought likely to act on cetacean distribution is through distribution of prey, which was described by the fish energy covariates.

The spatial extent of the modelled prey energy data is slightly smaller than that of the full ecoregion. For the prey models, only cetacean data collected within the area covered by the prey models was included in these “prey models”.

4.2.2.3 Prey modelling methods – covariate selection

Therefore, in addition to fish energy, four candidate covariates were available for inclusion in the prey models: slope, aspect, distance to 50m isobath (D50_iso), and CS_50_cont. Because D50_iso and CS_50_cont are colinear, these were both modelled separately, and the best covariate (selected by AIC) was taken forward into subsequent modelling. This process was carried out for each fish species individually. In addition to the individual fish species energy layers, Ransijn *et al* (2019) also calculated a layer containing energy for all fish species combined (“All prey”). Therefore, for each cetacean species, a total of seven prey models were fitted: one for each species energy layer (cod, herring, whiting, sprat), one for distance to sandeel grounds, one for the “All prey” layer, and one combining the energy layer for all individual species together into the same model. The best prey model for each cetacean species, as selected by AIC, was then predicted. Maps showing the uncertainty surrounding these modelled prey energy surfaces, taken from Ransijn *et al*. (2020) are provided in Appendix 3. These figures show that the uncertainty around the predicted energy levels is generally higher where prey energy is predicted to be higher, as would be expected (Ransijn *et al*. 2020).

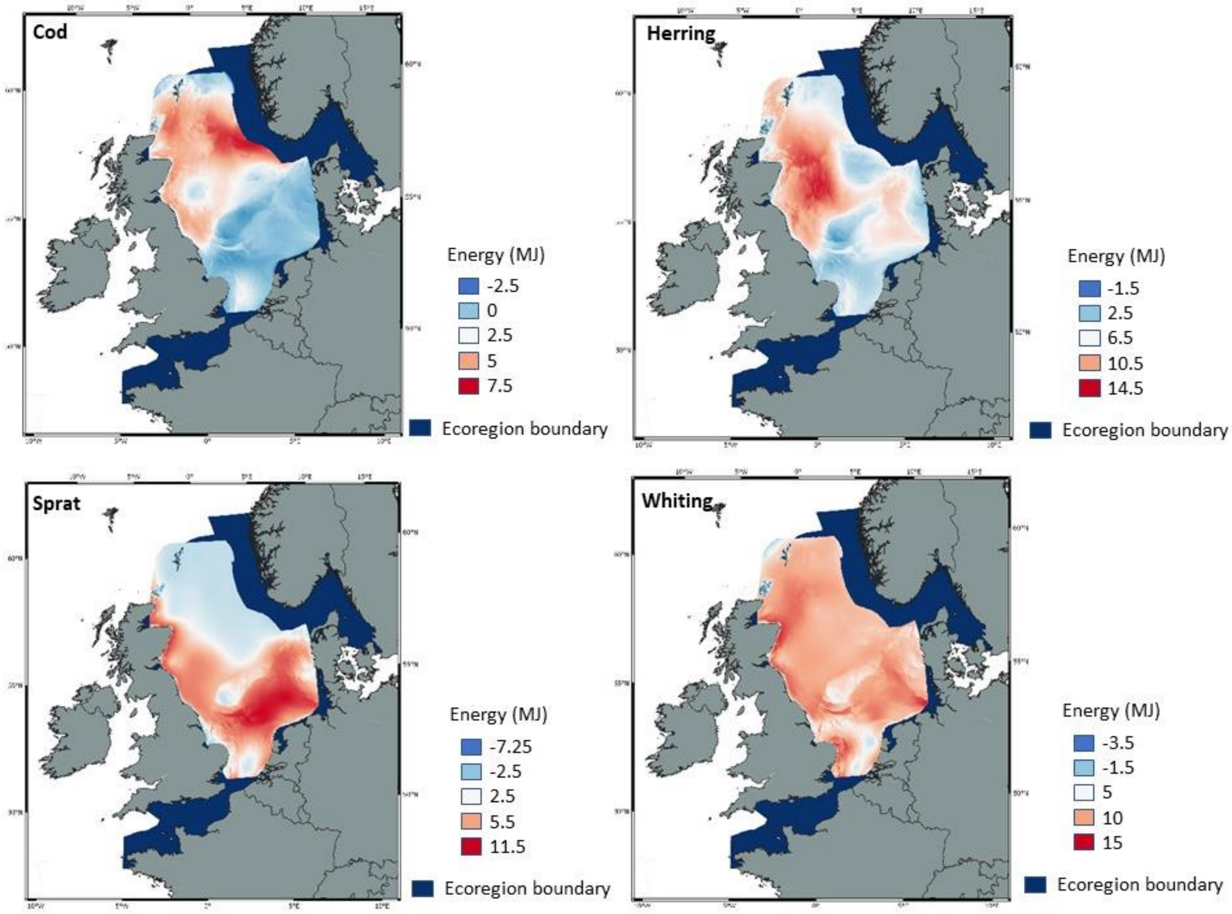

Figure 4.2-7: Distribution of energy (MJ) per Km^2 of four different fish prey species throughout the North Sea. The dark blue area shows the extent of the full ecoregion. Fish energy data (from Ransijn *et al*, 2019) are only available for a subset of this.

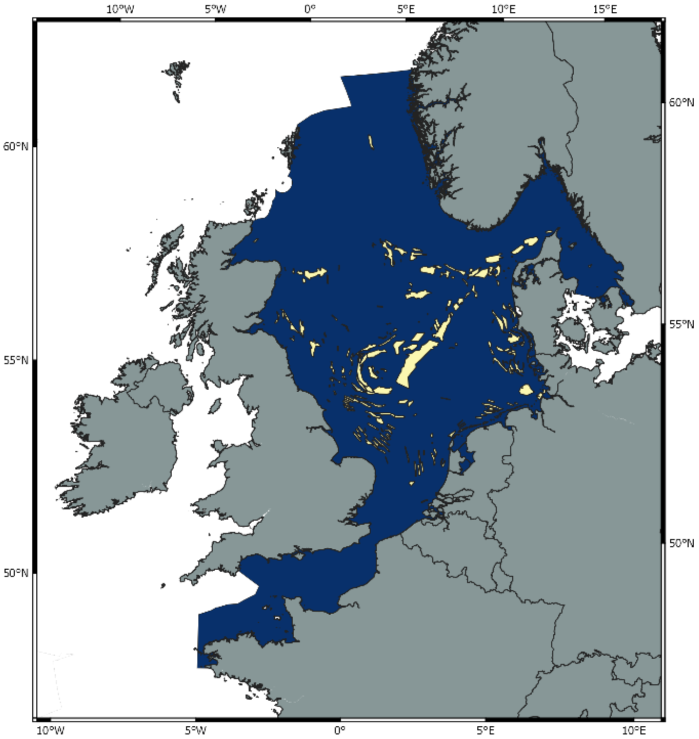

Figure 4.2-8: Location of sandeel grounds (yellow) from Jensen *et al.*, 2011.

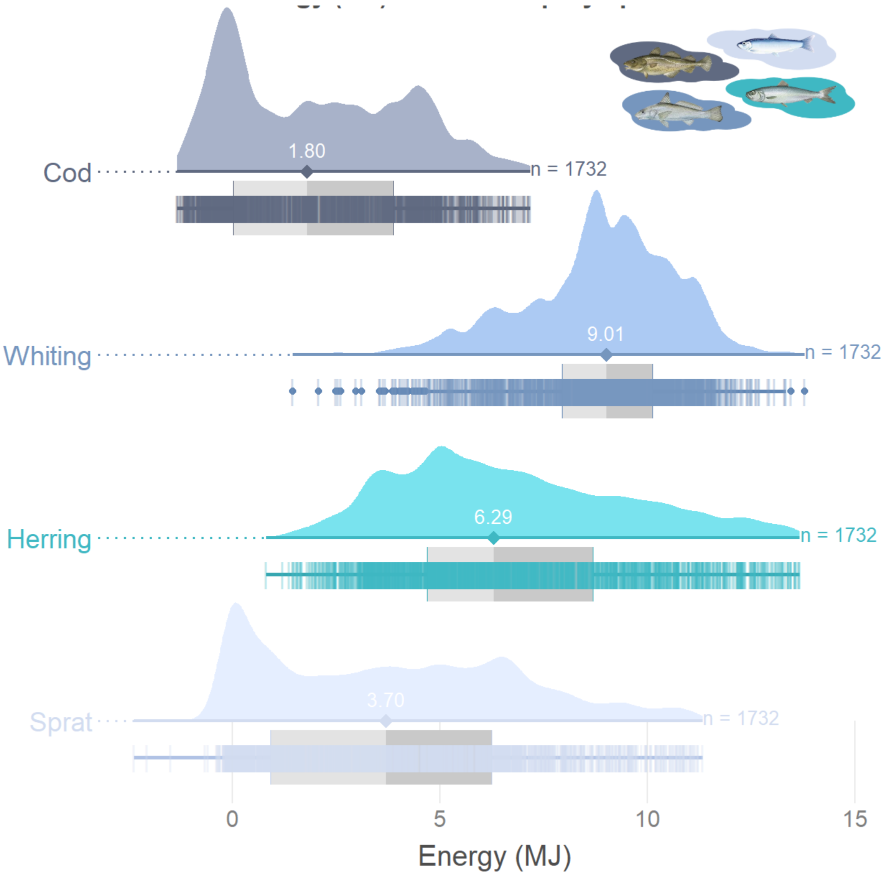

Figure 4.2-9: Summary statistics for the fish energy data, in MJ, as calculated by Ransijn *et al.*, (2019).

4.1. Results of full ecoregion environmental models

4.1.1. Minke whale

Summary results of the final full ecoregion environmental models selected for minke whales are provided in Table 4.1-1. Model diagnostics (Appendix 3) indicate a satisfactory fit to the data, with the proportion of null deviance explained by the 2016 model being 18.2%., and for the 2005 model being 30.7%. The 2016 data were best described using the negative binomial distribution, whilst the Tweedie error distribution best described the data for the 2005 data. An additional model combining the data from the two years and adding year as a categorical variable was also run. This explained 29% of the null deviance (Table 4.1-2).

The fitted smooth functions (Figure 4.1-1) show relatively low levels of “wiggliness” – with only SSH, when modelled for 2016 and in the combined model, requiring more than 1 estimated degrees of freedom. This is possibly due to low numbers of data points. The satisfactory fit of the models as indicated by the residual and QQ plots (Appendix 3) indicates that the resulting predictions should be an appropriate representation of the relationships between minke whale density and the model covariates.

For the 2016 data, there were positive effects (higher estimated density of minke whales) in areas of flatter seabed (lower SD depth values) although the confidence interval here is wide at higher SD depth, reflecting the lower number of modelled segments with higher values. This covariate was not retained in either the 2005 model or the combined model. Depth was retained in both, showing a similar relationship in both models in which predicted density of minke whales decreased as depth decreased. The confidence interval increases in width towards the higher depths, likely driven again by the very low number of modelled segments with these deep-water values.

A similar relationship with the log mixed layer depth data was found across all three minke whale models, in which predicted density increased with increasing mixed layer depth. Sea surface height was also retained in all three models. Here the relationship was very similar for 2016 and the combined model, where it was largely flat across most of the range of covariates, but predicted density decreased as SSH became larger than around -0.35. In the 2005 model the estimated density of whales increased as SSH increased from -0.5 to -0.2, but the effect was not very strong. It is possible that in this model the effect of SSH is acting as a proxy for an unknown, unmodelled covariate.

Both the 2005 model and the combined model also retained salinity, although 2016 did not. The relationship was similar in both models, showing a decrease in predicted density as salinity decreased. The confidence intervals at low salinities y end of the graphs are wide, particularly for the

2005 model. The number of effort segments with low salinity values was quite small and the confidence intervals around the two slopes reflected that.

The highest densities of minke whales were predicted in the central and northern parts of the North Sea for 2016 (Figure 4.1-1b), which reflects the location of the sightings (Figure 4.1-1a). The plot of predicted CV shows that we can be confident in these predictions, except for in the very far north of the region (Figure 4.1-1c), which is reflected in the map of standard error of the predictions (Figure 4.1-1d).

The 2005 prediction was a less good reflection of the observations (Figure 4.1-1a, b). The model has been overly influenced by datapoints at the edge of the predicted region, causing levels of over prediction in this area and reflected by the higher CV across the area (Figure 4.1-1c). The standard errors are highest in the northern part of the region.

A similar pattern is also visible in the combined 2016 and 2005 model. Areas of high predicted density matched the sightings fairly well giving confidence in the predictions (Figure 4.1-1-a, b).

Table 4.1-1: Model outputs for minke whale GAMs for 2016 and 2005 data.

Model	Error distribution	Model covariates	Estimated degrees of freedom	% Deviance explained	Model degrees of freedom	P value
2016	Negative binomial	SD Depth	0.7	18.2	5.9	0.09
		Sea surface height	3.5			0.002
		Ln Mixed Layer depth	0.7			0.05
2005	Tweedie	Depth	1.0	30.7	4.5	4.25e-6
		Salinity	0.9			0.0003
		Sea surface height	0.8			0.04
		Ln Mixed Layer depth	0.8			0.02

Table 4.1-2: Model outputs for combined 2005 and 2016 minke whale GAM

Model	Factor levels	Estimate	Std. Error	Z value	PR(>z)	
Combined 2016 & 2005 model	Intercept (2005)	-137.7	67.0	-2.05	0.04	
	Year = 2016	0.07	0.03	1.96	0.05	
	Error distribution	**Model covariates**	**Estimated degrees of freedom**	**% Deviance explained**	**Model degrees of freedom**	**P value**
Combined 2016 & 2005 model	Negative binomial	Depth	0.8	29.2	8.6	0.02
		Salinity	0.9			0.002
		Sea surface height	3.9			0.0002
		Ln Mixed Layer depth	0.9			0.003

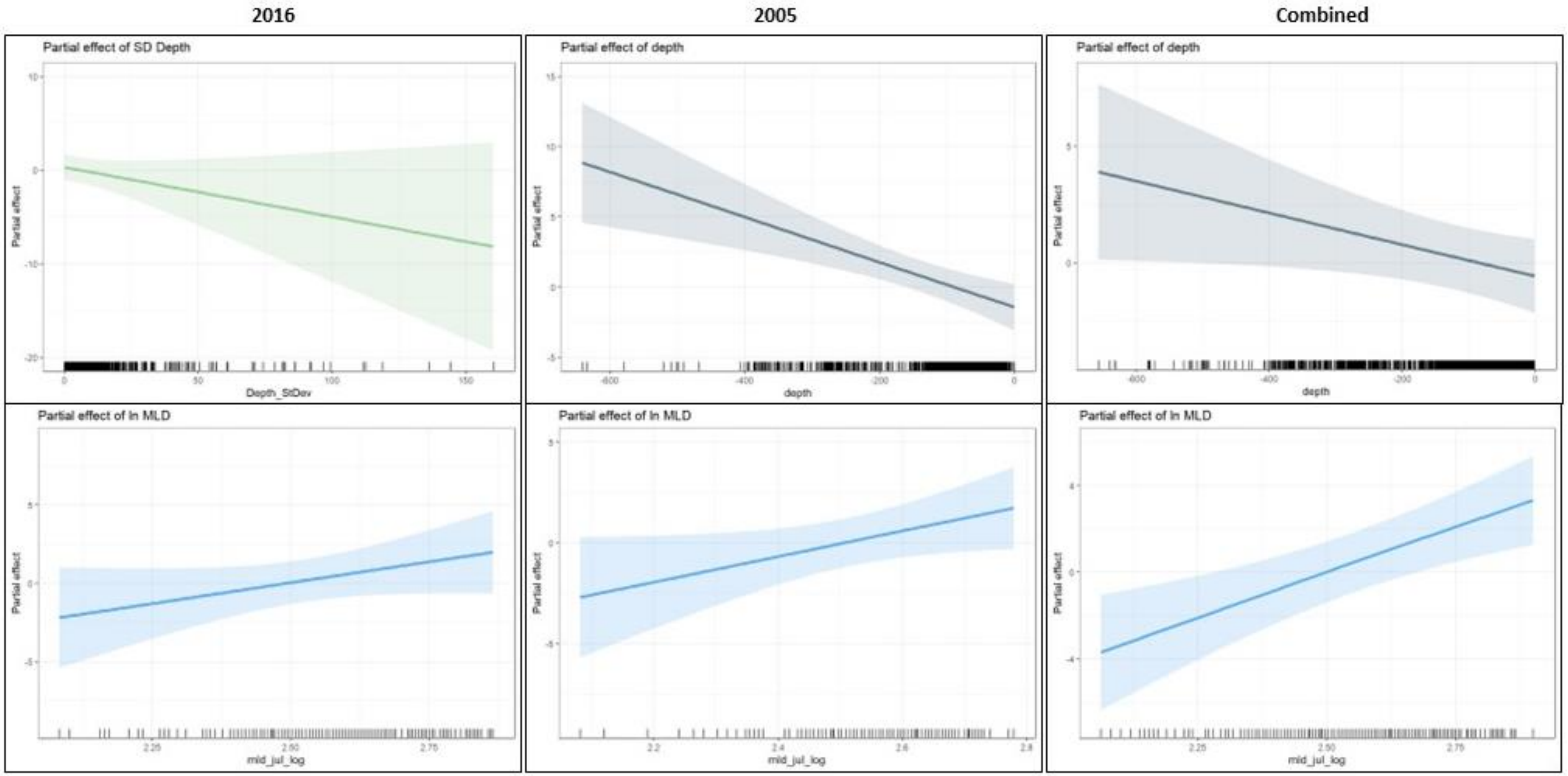

Figure 4.1-1: Plots of the fitted smooth functions for minke whale GAMS for 2016, 2005 and the combined model. "Rug" marks on the x-axis of the fitted smooth plots show the distribution of the data. Shaded areas represent the 95% confidence intervals. Where the same covariate is retained in multiple models, the smooths are shown on the same row. Effect sizes are variable, so axis scales are also variable in order to preserve necessary detail.

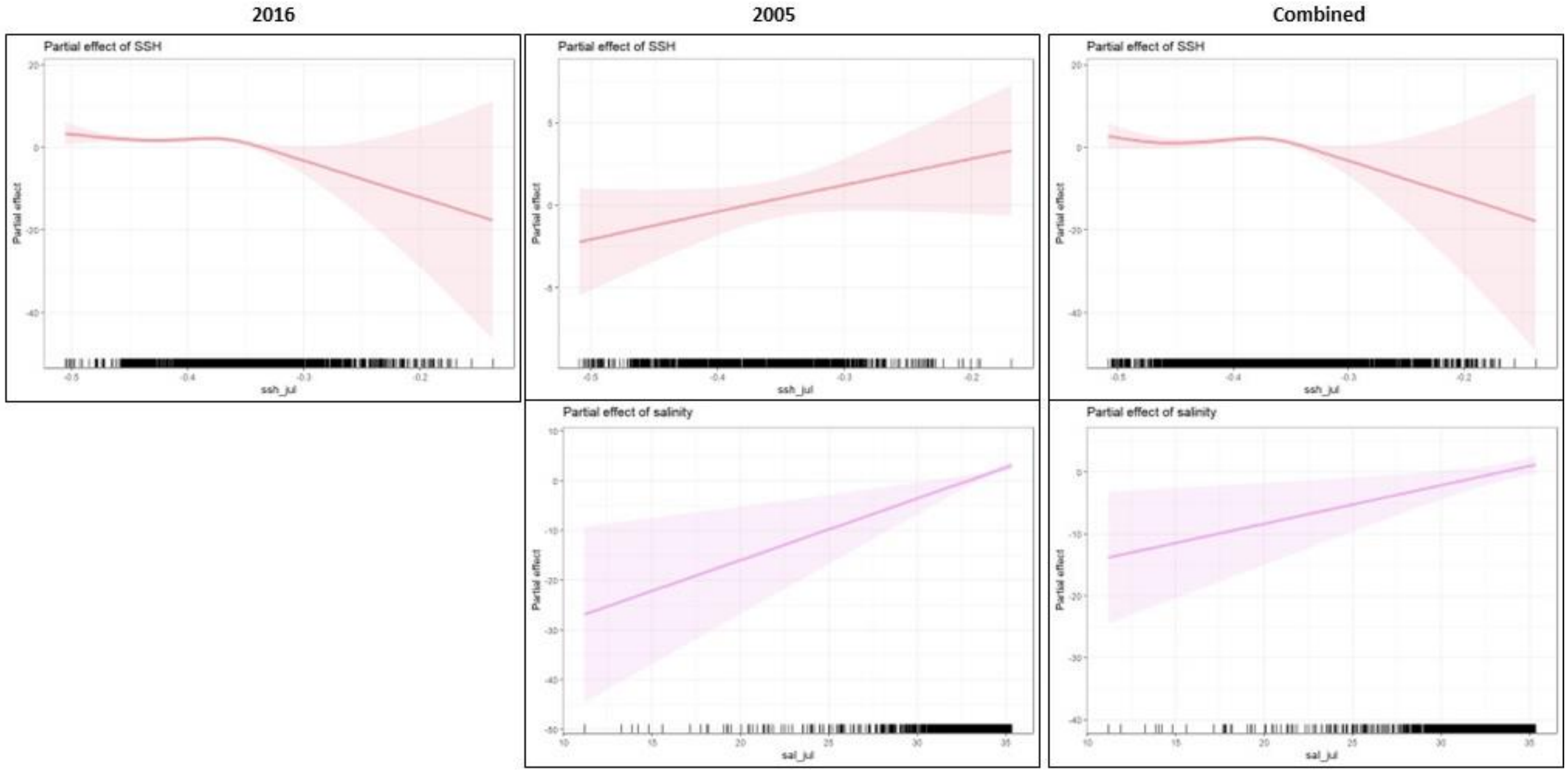

Figure 4.1.1 ctd: Plots of the fitted smooth functions for minke whale GAMS for 2016, 2005 and the combined model. "Rug" marks on the x-axis of the fitted smooth plots show the distribution of the data. Shaded areas represent the 95% confidence intervals. Where the same covariate is retained in multiple models, the smooths are shown on the same row. Effect sizes are variable, so axis scales are also variable in order to preserve necessary detail.

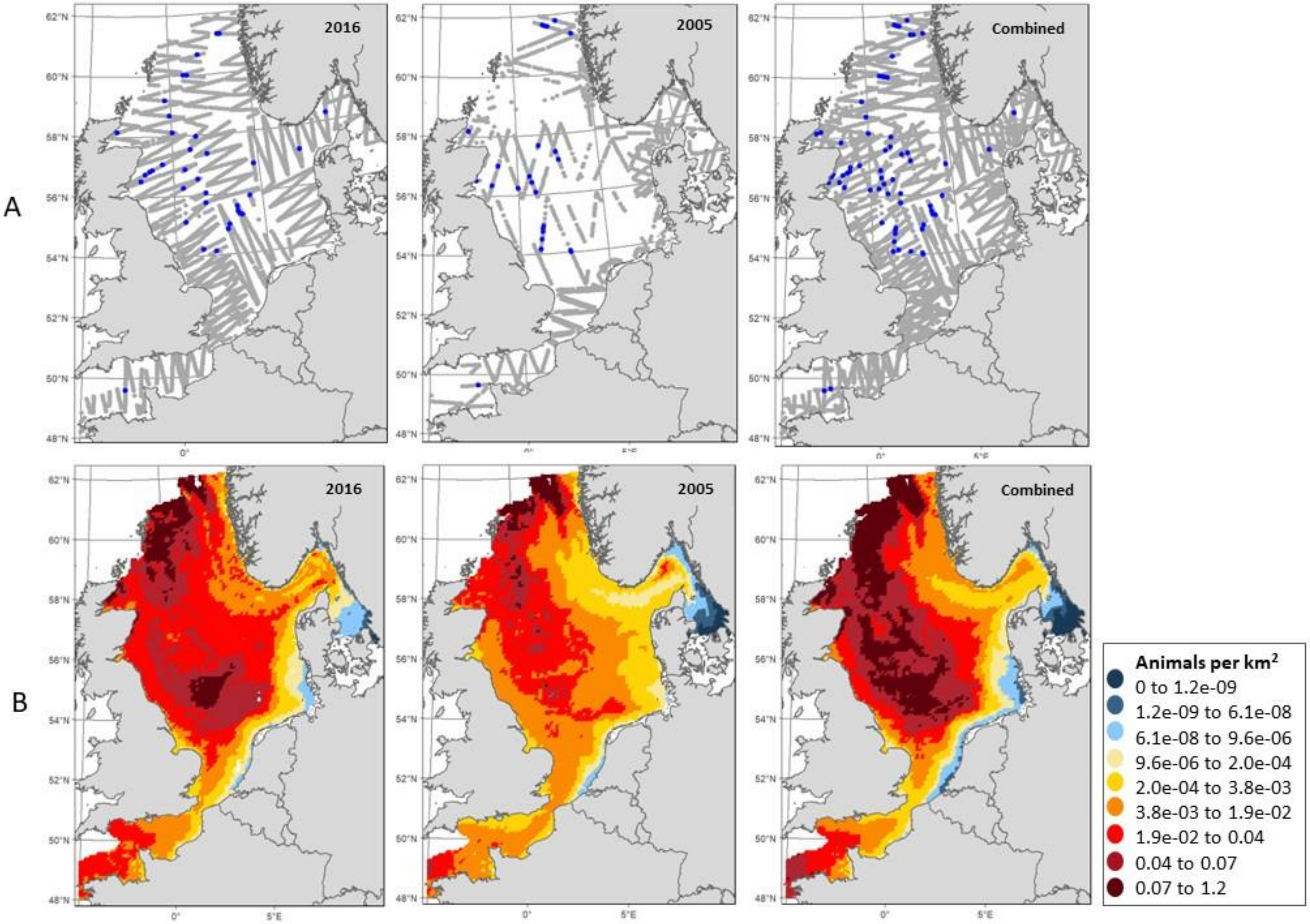
A
B
2016
2005
Combined
2016
2005
Combined
62°N
60°N
58°N
56°N
54°N
52°N
50°N
48°N
0°
5°E
Animals per km^2
0 to 1.2e-09
1.2e-09 to 6.1e-08
6.1e-08 to 9.6e-06
9.6e-06 to 2.0e-04
2.0e-04 to 3.8e-03
3.8e-03 to 1.9e-02
1.9e-02 to 0.04
0.04 to 0.07
0.07 to 1.2

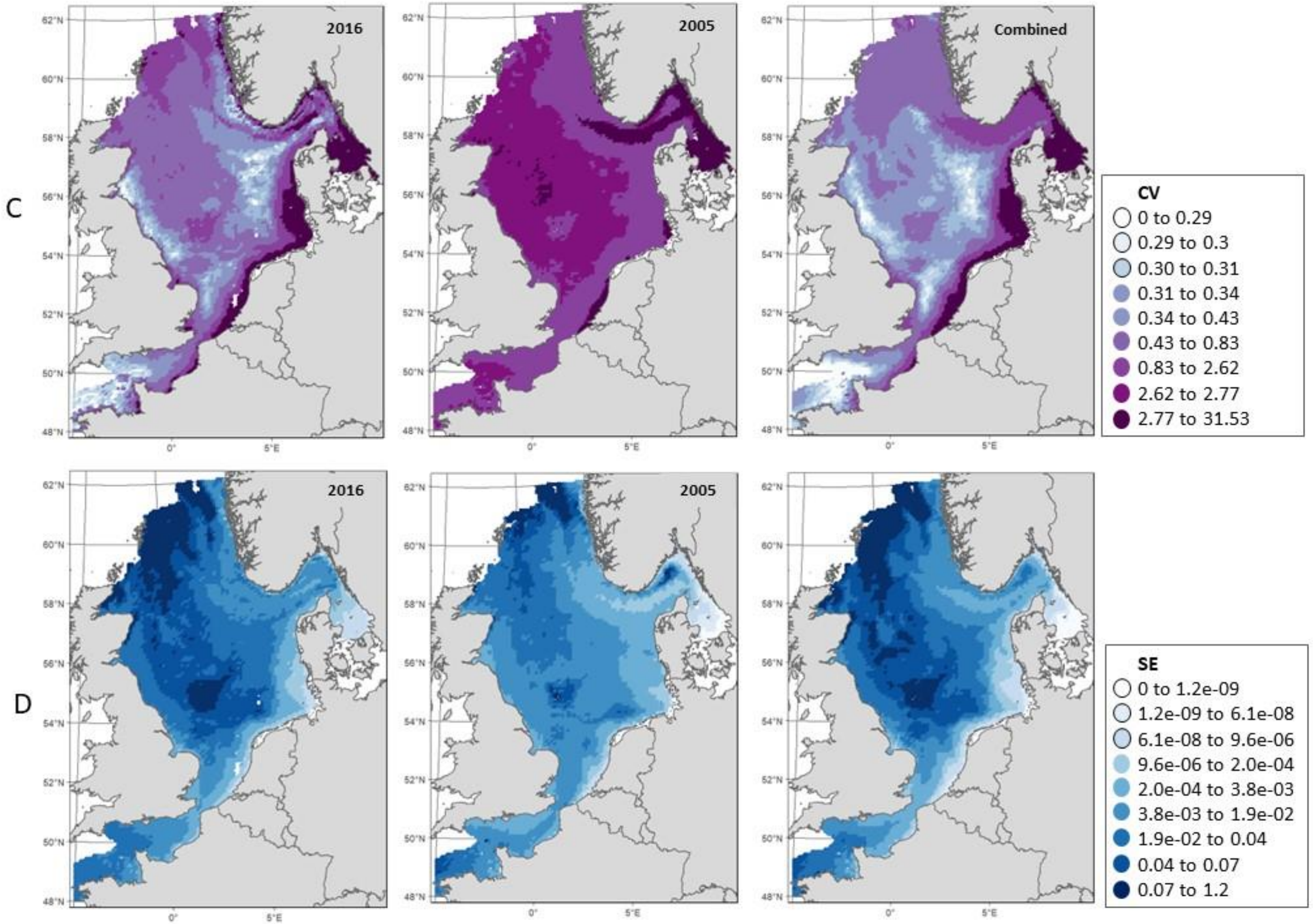

Figure 4.1-2: Location of effort and sightings (A), predicted density surface (B) coefficient of variation CV of density (CV) (C) and standard error (SE) (D) for 2016, 2005 and combined year minke whale models. Range of values represented by colours in the maps show the 1%, 2%, 5%, 10%, 25%, 50%, 75%, 90% and 100% quantiles. White areas are outside of predictive space. In some cases, prediction grid cells had covariate values which were outside the range encompassed by the modelled effort segments. In these instances, grid-cells were excluded from the prediction. Combined year data are predicted using 2016 covariates.

4.1.2. White-beaked dolphin

Summary results of the final full ecoregion environmental models selected for white-beaked dolphin are provided in Table 4.1-3. Model diagnostics indicate a satisfactory fit to the data (Appendix 3), with the proportion of null deviance explained by the model being 34.1% for the 2016 model, 49.4% for the 2005 model and 38.1% for the combined years model. The residual and QQ plots for these models are provided in Appendix 3. Plots of the fitted smooth functions are provided in Figure 4.1-3: Plots of the fitted smooth functions for white-beaked dolphin GAMS for 2016, 2005 and the combined model. “Rug” marks on the x-axis of the fitted smooth plots show the distribution of the data. Shaded areas represent the 95% confidence intervals. Where the same covariate is retained in multiple models, the smooths are shown on the same row. Effect sizes are variable, so axis scales are also variable in order to preserve necessary detail. The negative binomial error distribution best described the 2016 and combined years model; the Tweedie error distribution best described the data for 2005. The effect of year, modelled as a categorical variable, was not retained in the best combined year model.

The 2016 model showed a positive linear effect on estimated density of white-beaked dolphins of increasing distance from the 50m depth contour, on the deep-water side of the contour. This covariate was only retained in the 2016 model.

All three models retained one of the measures of mesoscale activity. For the 2016 model, this was sea level anomaly. The partial effects plot for this covariate shows a linear relationship, with higher predicted dolphin density being found at low SLA. The confidence intervals are wider at either end of the smooth where there are fewer datapoints.

Dolphin density was predicted to decrease with decreasing salinity. This relationship was found in both the 2016 and 2005 data. There were only a very few effort segments with low salinity values leading to a comparatively wide confidence interval, although overall the effect is small in 2016.

The highest densities of white-beaked dolphins were predicted in the northern part of the North Sea (Figure 4.1-4) as well as in the south of the study region, in the waters of the English Channel, where there are no sightings of this species in the modelled data. This prediction is thus not a good reflection of all the sightings.

The 2005 model retained three covariates: mixed layer depth, salinity and sea surface height. The relationship with mixed layer depth was linear; the highest densities of white-beaked dolphins were predicted at shallow mixed layer depths, and the predicted density decreased as MLD increased. The confidence intervals were uniform across the range of the data.

The shape of the salinity smooth for the 2005 data is very similar, albeit with a larger effect, to that from the 2016 model showing an increase in predicted dolphin density with increasing salinity. Predicted dolphin density peaked at a sea surface height of -0.45m, with decreases at both higher and lower values. The confidence intervals around this become very wide as SSH increases, however.

The highest densities of white-beaked dolphins were predicted in the central part of the North Sea (Figure 4.1-4 b), which is a good reflection of the observed sightings (Figure 4.1-4 a). The plot of prediction CV shows low levels of confidence in waters close to the eastern coastline to the south of the North Sea (Figure 4.1-4 c).

The combined 2005-2016 model retained depth, mixed layer depth, sea surface height and slope. The shape of the mixed layer depth smooth was very similar to that of the 2005 model but the effect was smaller.

Whereas the 2005 model showed a peak predicted density of dolphins at -0.45m SSH, the combined model showed a linear decline with increasing values of SSH. Slope and depth covariates were both retained in the combined model, despite not being retained in either of the individual year models. Predicted densities of dolphins were highest in areas of flatter seabed (lower slope), and shallower waters. For both covariates the confidence intervals are wide at the extremes of the covariate range with the fewest data points.

Table 4.1-3: Model outputs for white-beaked dolphin GAMs for 2016, 2005 and combined 2016 & 2005 data.

Model	**Error distribution**	**Model covariates**	**Estimated degrees of freedom**	**% Deviance explained**	**Model degrees of freedom**	**P value**
2016	Negative binomial	CS_50_cont	1.1	34.1	3.65	2e-16
		Sea Level Anomaly	0.9			0.002
		Salinity	0.7			0.12
2005	Tweedie	Salinity	0.9	49.4	5.6	0.002
		Sea surface height	2.8			0.001
		Mixed Layer depth	0.9			0.003
2016 and 2005 combined	Negative binomial	Depth	1.0	38.1	4.1	1.1e-4
		Ln Mixed Layer depth	0.3			0.30
		Sea surface height	1.2			2e-16
		Slope	0.7			0.06

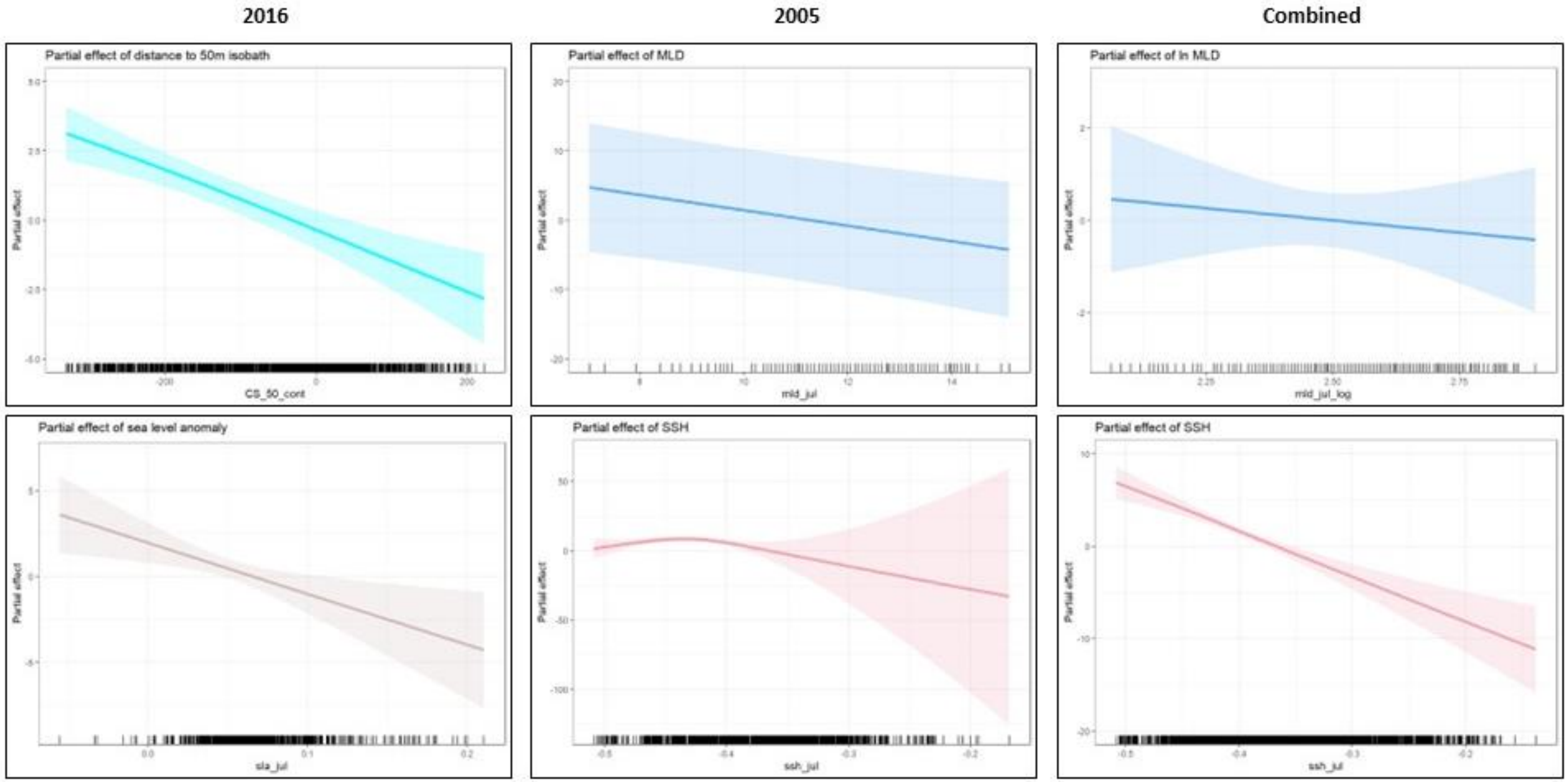

Figure 4.1-3: Plots of the fitted smooth functions for white-beaked dolphin GAMS for 2016, 2005 and the combined model. "Rug" marks on the x-axis of the fitted smooth plots show the distribution of the data. Shaded areas represent the 95% confidence intervals. Where the same covariate is retained in multiple models, the smooths are shown on the same row. Effect sizes are variable, so axis scales are also variable in order to preserve necessary detail.

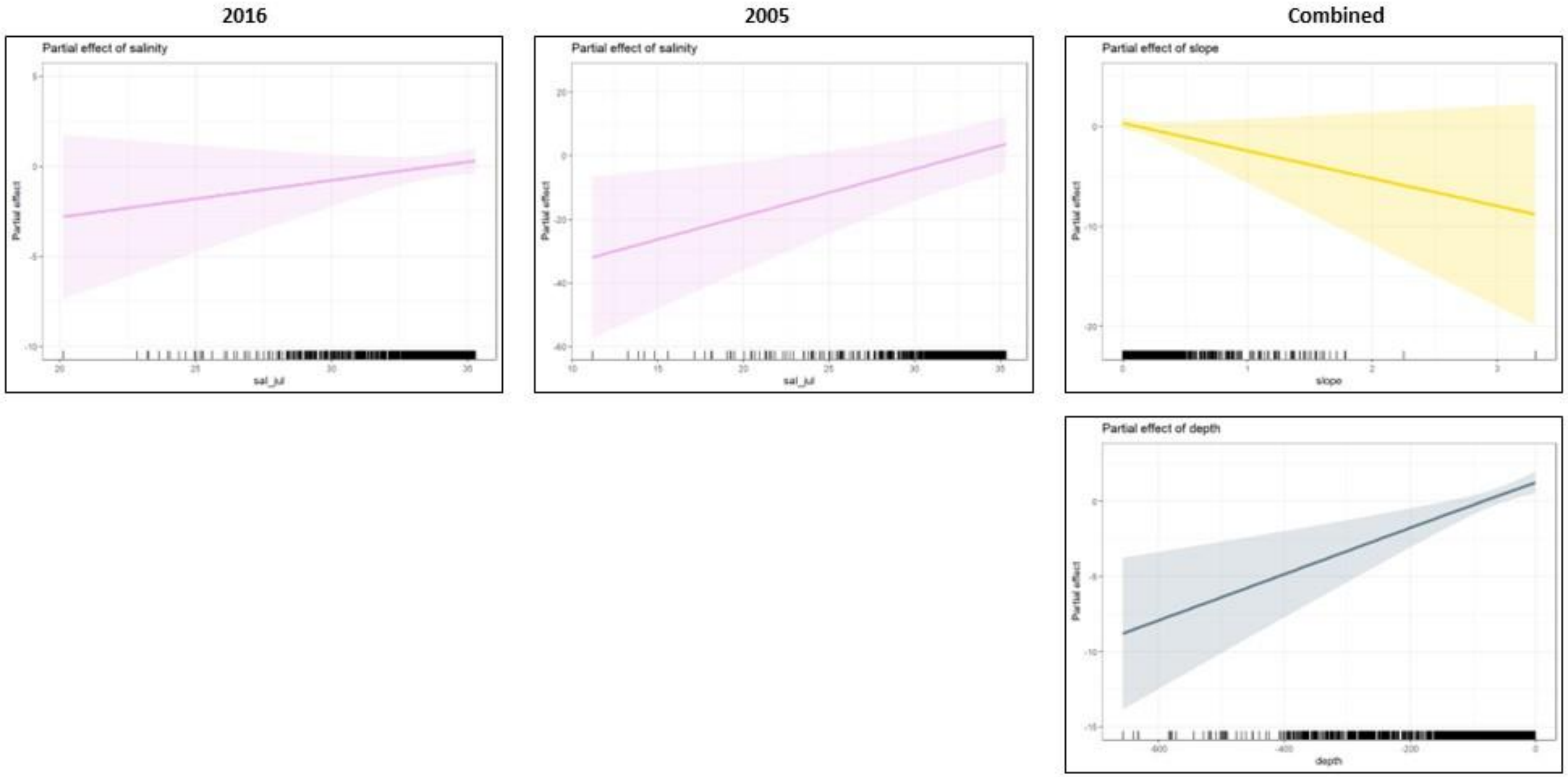

Figure 4.3-3 ctd. Plots of the fitted smooth functions for white-beaked dolphin GAMS for 2016, 2005 and the combined model. "Rug" marks on the x-axis of the fitted smooth plots show the distribution of the data. Shaded areas represent the 95% confidence intervals. Where the same covariate is retained in multiple models, the smooths are shown on the same row. Effect sizes are variable, so axis scales are also variable in order to preserve necessary detail.

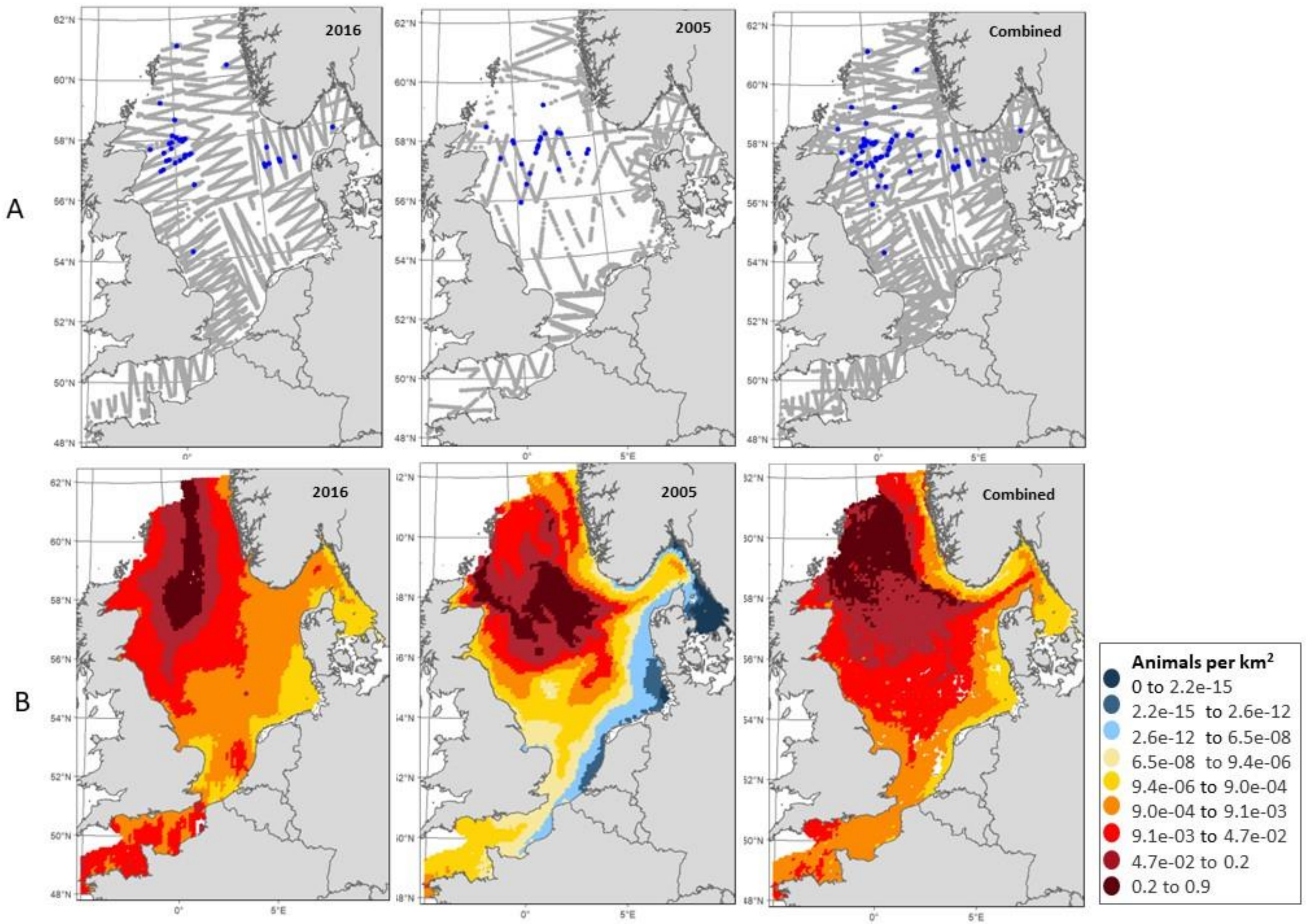

Figure 4.1-4: Location of effort and sightings (A), predicted density surface (B) for 2016, 2005 and combined year white-beaked dolphin models. Range of values represented by colours in the maps show the 1%, 2%, 5%, 10%, 25%, 50%, 75%, 90% and 100% quantiles. White areas are outside of predictive space. In some cases, prediction grid cells had covariate values which were outside the range encompassed by the modelled effort segments. In these instances, grid-cells were excluded from the prediction. Combined year data are predicted using 2016 covariates.

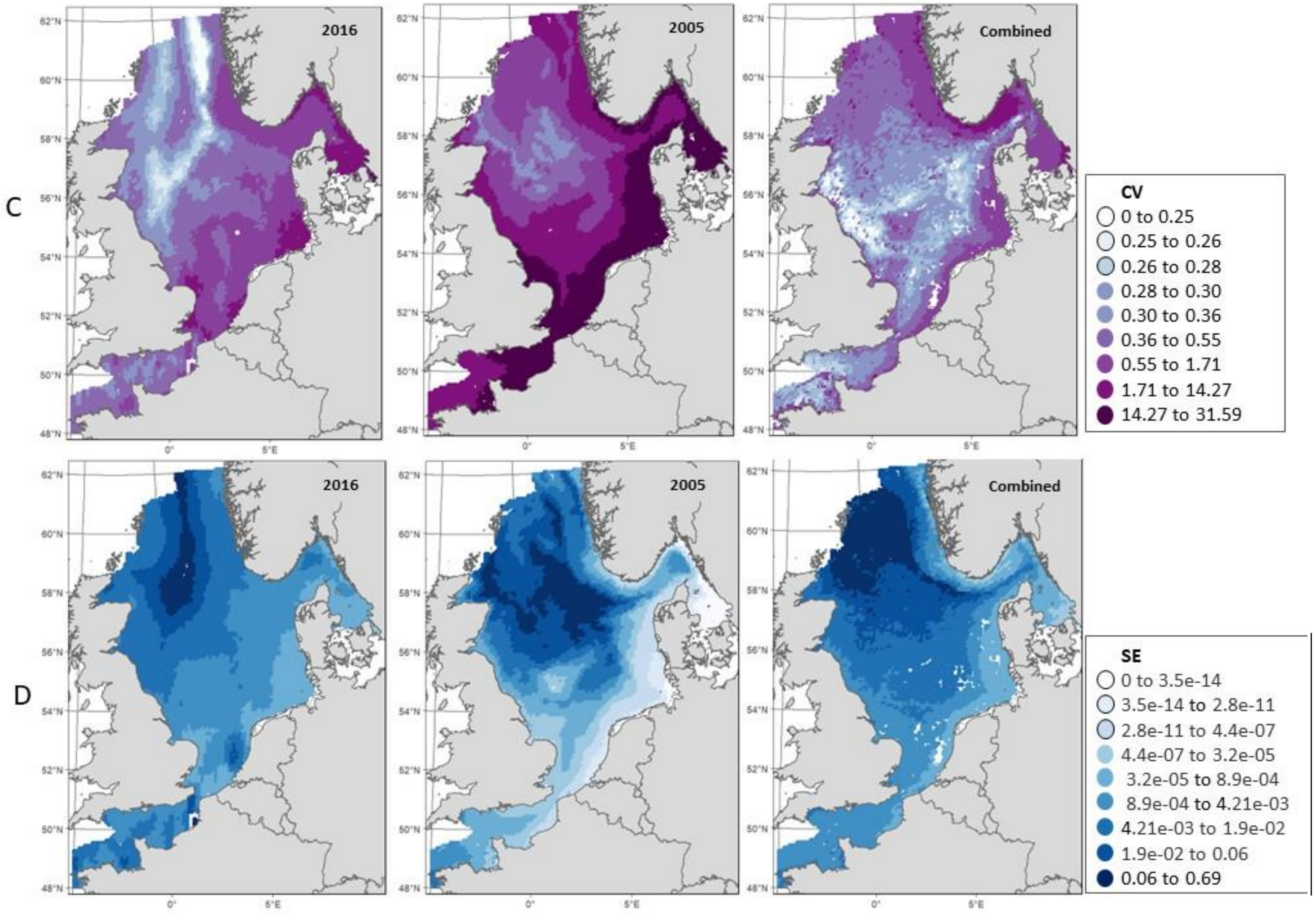

Figure 4.3-4 ctd. Maps of predicted coefficient of variation CV of density (CV) (C) and standard error (SE) (D) for 2016, 2005 and combined year white-beaked dolphin models. Range of values represented by colours in the maps show the 1%, 2%, 5%, 10%, 25%, 50%, 75%, 90% and 100% quantiles. White areas are outside of predictive space. In some cases, prediction grid cells had covariate values which were outside the range encompassed by the modelled effort segments. In these instances, grid-cells were excluded from the prediction.

4.1.3. Harbour porpoise

Summary results of the final full ecoregion environmental models selected for harbour porpoise are provided in Table 4.1-4. Model diagnostics indicated a good fit to the data in both cases (Appendix 3), and the proportion of null deviance explained by the model was 9.3% for the 2016 model, 12.8% for the 2005 model and 7.5% for the combined model. The partial effects plots are included in Figure 4.1-5. The negative binomial error distribution best described the data for all three models.

The partial effects plot for depth shows comparatively high amounts of wiggliness for 2016. Estimated density declined sharply with increasing depth to approximately 250m depth. In waters deeper than 250m density was then predicted to increase linearly. The confidence interval was very narrow at shallower depths but increased in deeper waters where there were fewer data points, suggesting less confidence in this part of the relationship, although the effect was quite small. The broad shape of the plot was replicated in the combined 2005/2016 model which showed a similar dip in predicted density at around 300m depth. The 2005 slope relationship was linear, with predicted density peaking at deeper depths. Although the effect was small, the confidence intervals were wider at this end of the plot indicating that this relationship should be interpreted with caution.

The partial effects plots for mixed layer depth for 2016 and for the combined years model show that highest densities of porpoises were predicted in waters with a mixed layer depth of around 10.5m or deeper; the relationship was then relatively flat at deeper depths. The confidence intervals were comparatively narrow, particularly around the inflection point. They widened where there were fewer data points, namely at very shallow mixed layer depths. For 2005 the relationship was linear with lower predicted densities at shallower MLD and higher densities at deeper MLD.

The 2016 model predicted porpoise density decreasing with increasing salinity. The shape of this relationship appears to be driven by a few datapoints at the lower end of the salinity range where the confidence intervals are also widest. This covariate was not retained in the other models. The relationship was not strong, with a low partial effect.

The 2005 model retained CS_50_cont. This predicted a peak in predicted density of porpoises in waters close to but deeper than the 50m contour, and a decline on either side. Again, confidence intervals at either end of the range where there were fewer datapoints were wider. This covariate was not retained in the other models.

The combined years model retained SST, with density of porpoises predicted to increase linearly with temperature. Confidence intervals were narrower where there were more data in the centre of the range. This covariate was not retained by the other models.

All three models retained a covariate measuring mesoscale activity. For 2016 and 2005 it was ADT, for the combined model it was SLA. The relationships for ADT are very wiggly, with 5.8 edf in 2016 and 4.7 edf in 2005. The confidence intervals were narrow for the central part of the relationship, which may be a result of the larger number of sightings of this species over the range of the covariate when compared with other species. The two years showed broadly opposite relationships. Coupled with this covariate not being retained in the combined years model, this suggests that this covariate may be acting as a proxy for an unknown process. The SLA covariate in the combined years model predicted a peak in porpoise density in areas with a 0.1m SLA, decreasing on either side.

The 2016 and combined years models show positive effects higher estimated density of harbour porpoises) at areas of flatter seabed (lower values of slope), which decreased linearly but not strongly as the slope angle increased. The confidence interval became much wider at the steeper slope angles reflecting fewer data points here. The 2005 model retained SD depth instead of slope, but the shape of the relationship is the same as for slope, with higher densities of porpoises being predicted at lower seabed rugosity.

The combined model with year as a categorical variable was found to be better (lower AIC) than the one which did not contain year. However, the effect was weak and not significant ($p = 0.55$) (Table 4.1-5).

The highest densities of harbour porpoises for 2016 were predicted throughout the central and southern North Sea (Figure 4.1-6b), and in areas of the Skagerrak and Kattegat around Denmark, Norway and Sweden. This is a good match with many of the observed sightings; however, animals were also seen to the south in the English Channel and in northern areas (Figure 4.1-6 a). Low CV was predicted throughout most of the area (Figure 4.1-6 c).

The highest densities of harbour porpoises in 2005 were predicted in the southern part of the North Sea and in the Kattegat/Belt Seas region, which reflects many of the observed sightings (Figure 4.1-6 a). The plot of predicted CV showed adequate levels of confidence in the predictions except in deep waters to the south of Norway and in the central northern North Sea (Figure 4.1-6 c).

As would be expected from the 2016 and 2005 predictions, density predicted from the model of the combined data is also a good reflection of the combined sightings data.

Table 4.1-4: Model outputs for harbour porpoise GAMs for 2016 and 2005 model.

Model	Error distribution	Model covariates	Estimated degrees of freedom	% Deviance explained	Model degrees of freedom	P value
2016 data	Negative binomial	Depth	6.6	9.3	19.3	2e-16
		MLD	4.1			0.001
		ADT	5.8			2e-16
		Slope	0.9			0.0024
		Salinity	1.0			8.53e-7
2005 data	Negative binomial	Depth	0.7	12.8	10.4	0.093
		CS_50_cont	2.3			0.017
		ADT	4.7			2e-16
		SD depth	0.9			0.011
		MLD	0.9			0.0049

Table 4.1-5: Model outputs for combined 2005 and 2016 harbour porpoise GAM

Model	Factor levels	Estimate	Std. Error	Z value	PR(>z)	
Combined 2016 & 2005 model	Intercept (2005)	-13.07	20.7	-0.6	0.53	
	Year = 2016	0.006	0.01	0.6	0.55	
	Error distribution	**Model covariates**	**Estimated degrees of freedom**	**% Deviance explained**	**Model degrees of freedom**	**P value**
Combined 2016 & 2005 model	Negative binomial	Depth	3.5	7.5	15.3	2.27e-6
		MLD	3.4			0.0009
		SST	0.8			0.0303
		Slope	0.9			0.0009
		SLA	4.9			2e-16

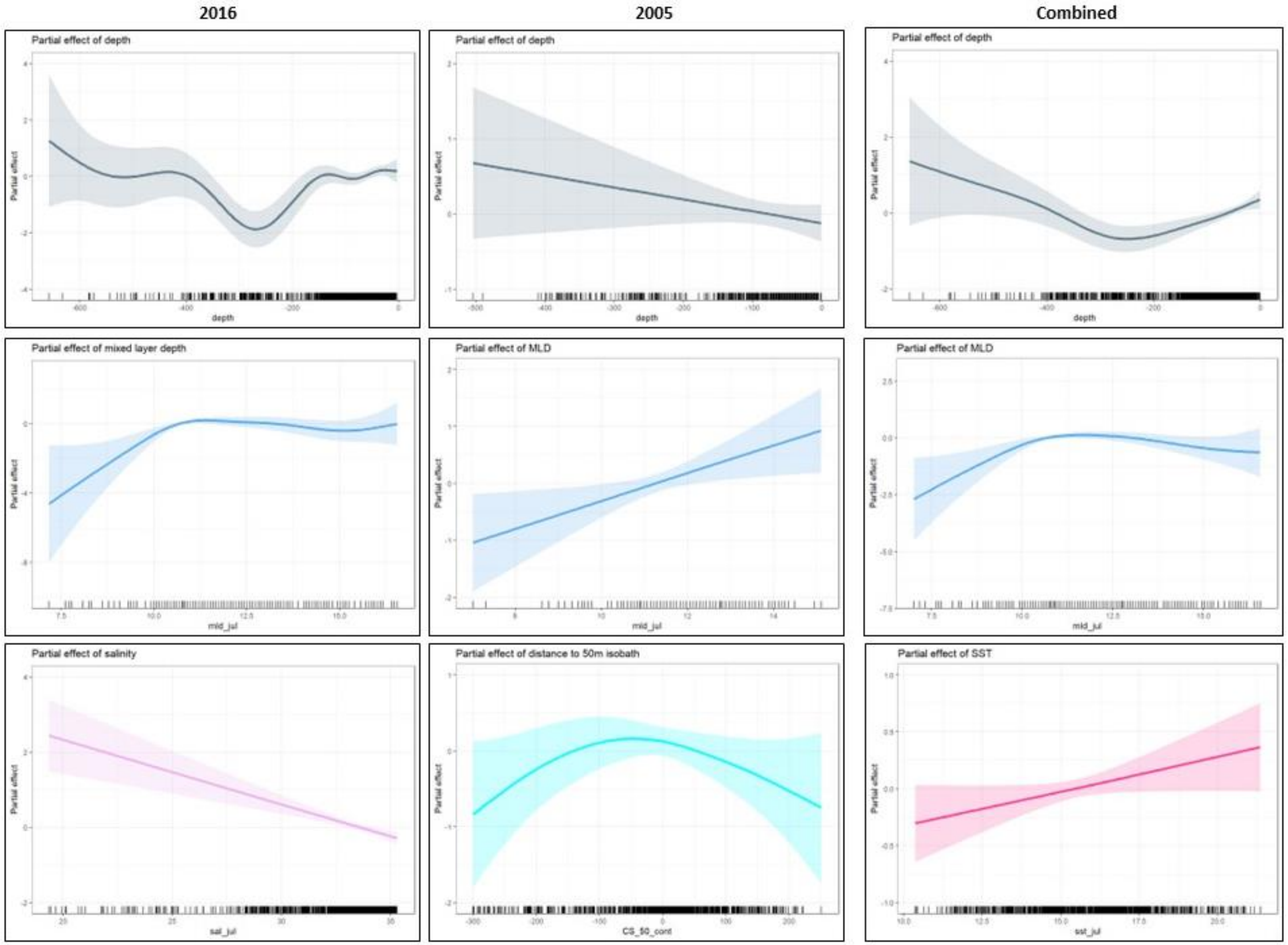

Figure 4.1-5: Plots of the fitted smooth functions for harbour porpoise GAMS for 2016, 2005 and the combined model. “Rug” marks on the x-axis of the fitted smooth plots show the distribution of the data. Shaded areas represent the 95% confidence intervals. Where the same covariate is retained in multiple models, the smooths are shown on the same row. Effect sizes are variable, so axis scales are also variable in order to preserve necessary detail.

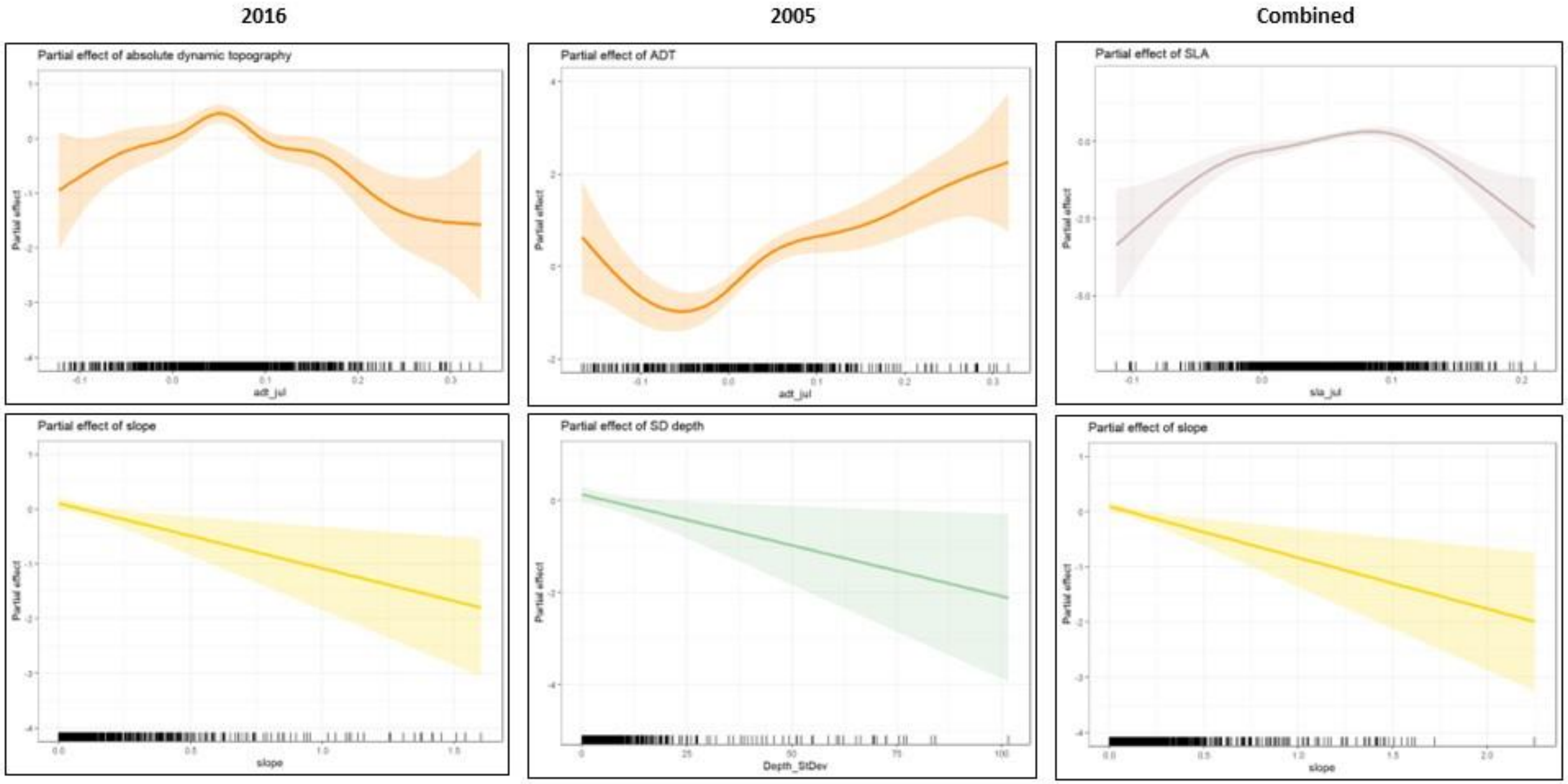

Figure 4.3-5 ctd: Plots of the fitted smooth functions for harbour porpoise GAMS for 2016, 2005 and the combined model. “Rug” marks on the x-axis of the fitted smooth plots show the distribution of the data. Shaded areas represent the 95% confidence intervals. Where the same covariate is retained in multiple models, the smooths are shown on the same row. Effect sizes are variable, so axis scales are also variable in order to preserve necessary detail.

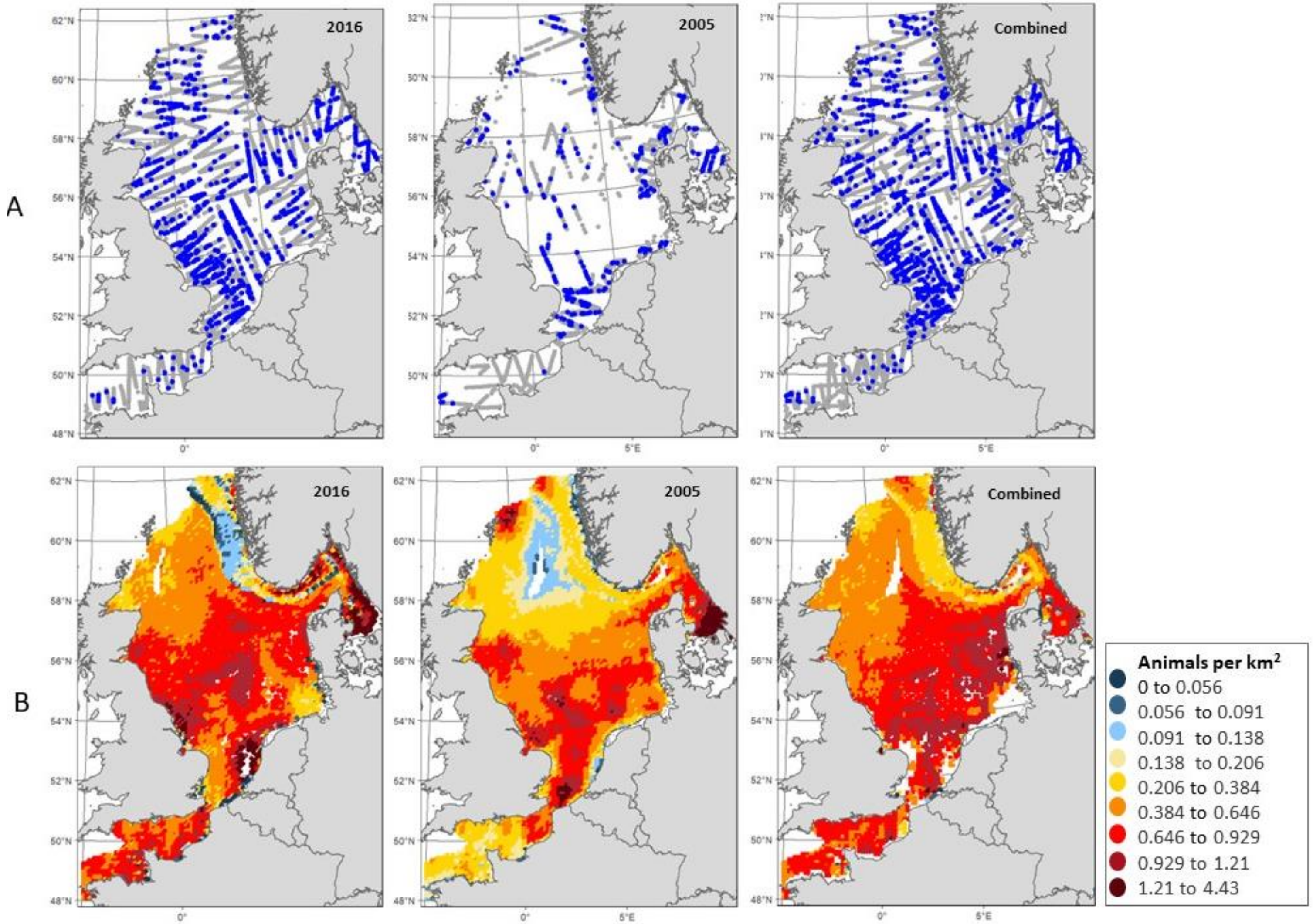

Figure 4.1-6: Location of effort and sightings (A), predicted density surface (B) for 2016, 2005 and combined year harbour porpoise models. Range of values represented by colours in the maps show the 1%, 2%, 5%, 10%, 25%, 50%, 75%, 90% and 100% quantiles. White areas are outside of predictive space. In some cases, prediction grid cells had covariate values which were outside the range encompassed by the modelled effort segments. In these instances, grid-cells were excluded from the prediction. Combined year data are predicted using 2016 covariates.

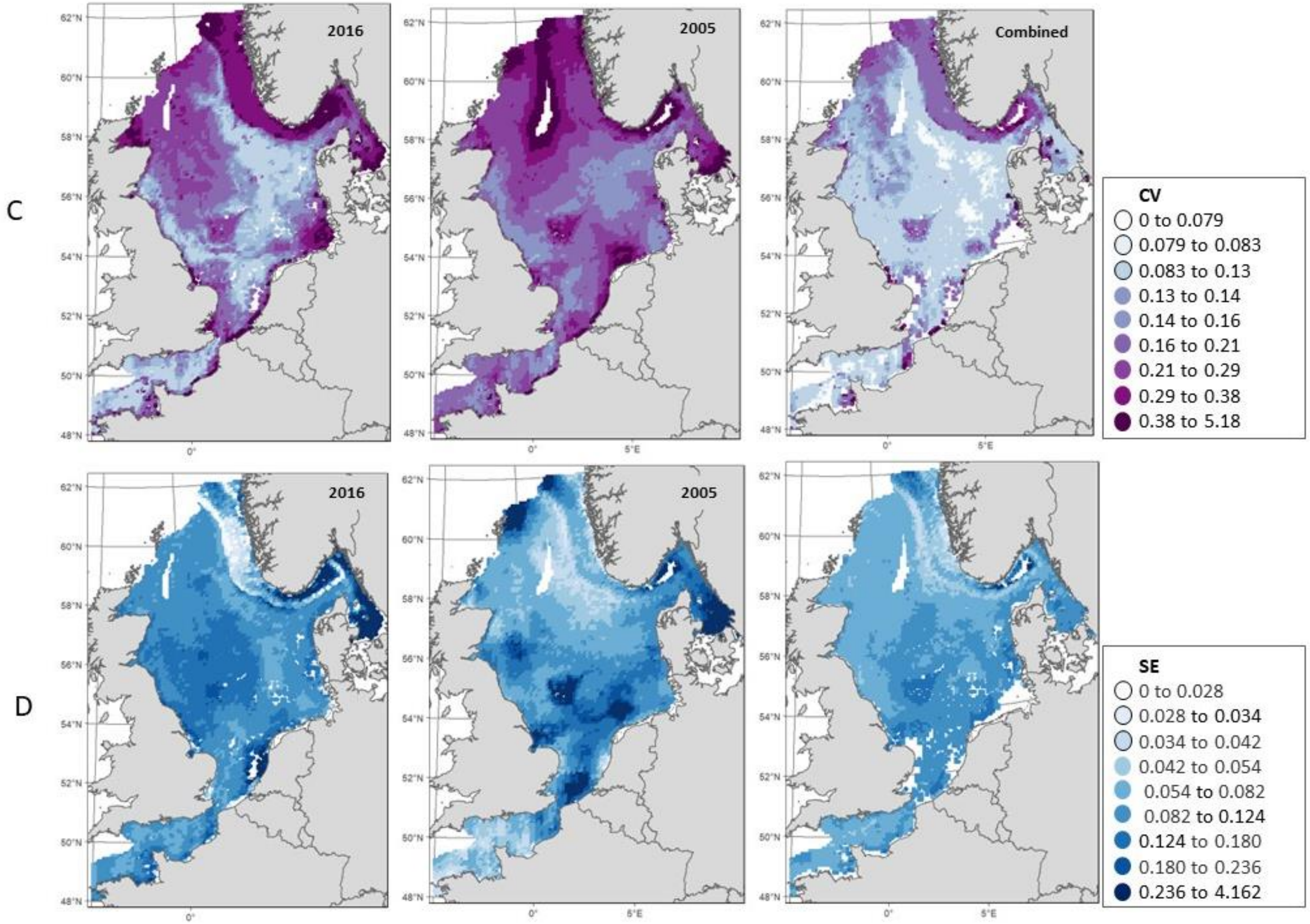

Figure 4.3-6 ctd: Maps of predicted coefficient of variation CV of density (CV) © and standard error (SE) (D) for 2016, 2005 and combined year harbour porpoise models. Range of values represented by colours in the maps show the 1%, 2%, 5%, 10%, 25%, 50%, 75%, 90% and 100% quantiles. White areas are outside of predictive space. In some cases, prediction grid cells had covariate values which were outside the range encompassed by the modelled effort segments. In these instances, grid-cells were excluded from the prediction.

4.2.Results of prey models

The area for which prey data were available was smaller than the full ecoregion. As a result, there were fewer modelling segments used for each model. The number of segments for both the 2016 and 2005 data are shown in Table 4.2-1. In 2016, all but three minke whale and white-beaked dolphin sightings occurred within the North Sea section of the ecoregion for which prey data were available.

Table 4.2-1 Number of effort segments and number of groups and individuals sighted of each species used in prey data for the North Sea.

Year	Species	Total no. of effort segments	No. of effort segments with groups	Number of groups	Number of Individuals	Mean group size
2016	Minke whale	1667	33 (1.9%)	36	38	1.1
	White-beaked dolphin	1667	32 (1.9%)	61	212	3.5
	Harbour porpoise	1604	533 (33%)	1002	1323	1.3
2005	Minke whale	726	18 (2.4%)	27	28	1.0
	White-beaked dolphin	726	21 (2.9%)	23	109	4.8
	Harbour porpoise	576	164 (28%)	327	479	1.5

4.2.3

4.2.1. Minke whales prey models

The results of the best model for each of the individual prey species are shown in Table 4.2-2: Model output for minke whale prey models, 2016 data. The best models for cod, herring and sprat retained no environmental covariates. The whiting covariate was not retained in the whiting model, meaning that an intercept only model was the best model (results not presented). The “All fish species separately” in one model retained only herring.

The cod model, with no additional environmental covariates was selected as the best model. The partial effects plots are shown in Figure 4.2-1. The model prediction with associated SE and CV is shown in Figure 4.2-3. The smooth relationship for slope used 3.7 edf and showed a peak in predicted density of minke whales in areas where there was approximately 4 MJ of cod energy. There was a second peak in areas with no cod present, with lowest predicted densities of porpoises at either low, or high (higher than 4MJ) cod energy levels. The confidence intervals are very wide when there were few cod data.

Table 4.2-2: Model output for minke whale prey models, 2016 data.

Model ID	Error distribution	Model covariates	Estimated degrees of freedom	% Deviance explained	Model degrees of freedom	Model AIC
Cod	Negative binomial	Cod – Summer 2016	3.7	10.3	4.7	348.8
Herring	Negative binomial	Herring – Summer 2016	0.8	3.4	1.8	354.5
Sprat	Negative binomial	Sprat – summer 2016	2.0	4.1	3.0	356.4
Sandeel	Negative binomial	Depth	0.9	6.4	2.8	358.2
		Dist_sandeels	0.8			
All prey combined	Negative binomial	All prey combined – summer 2016	0.7	2.2	1.8	356.6
All fish species separately	Negative binomial	Herring – Summer 2016	0.8	3.4	1.8	354.4

For the 2005 data, the “All prey combined” model, Table 4.1-4 was selected as the best model, with no additional environmental covariates. The partial effects plot is shown in Figure 4.2-1. The relationship was linear, with highest predicted minke whale density being associated with highest prey energy. The confidence interval was wider at the extremes of the covariate data where there were fewer data points. The model prediction with associated SE and CV is shown in Figure 4.2-3 c, d.

Table 4.2-3: Model output for minke whale prey models, 2005 data. Neither herring nor sprat was retained in the final model for minke whales, so were not taken further.

Model ID	Error distribution	Model covariates	Estimated degrees of freedom	% Deviance explained	Model degrees of freedom	Model AIC
Cod	Negative binomial	Cod – Summer 2016	3.1	25.6	6.2	200.6
		Slope	2.1			
Whiting	Negative binomial	Whiting – summer 2016	3.1	21.0	4.1	199.3
Sandeel	Negative binomial	Depth	0.9	15.3	3.3	201.7
		Slope	0.5			
		Dist_sandeels	0.9			
All prey combined	Negative binomial	All prey combined – summer 2016	1.0	15.2	2.0	198.8
All fish species separately	Negative binomial	Slope	0.7	15.9	4.1	203.8
		Herring – Summer 2016	0.9			
		Cod – Summer 2016	0.7			
		Dist_sandeels	0.8			

For the combined 2016 and 2005 model, individual covariates for whiting, herring and cod were retained, as was distance to sandeel grounds and slope (Table 4.2-5). Partial effects plots are provided in Figure 4.2-2. The smooths for whiting and cod energy follow the same shape, with peaks of predicted minke whale density being associated with whiting energy of around 10 MJ and cod energy of around 4 MJ. This is a similar shape to that of cod in the 2016 model. For both cod and whiting in the combined model, there was a second peak in areas with no prey energy present, with lowest predicted densities of porpoises at either low or highest fish energy levels. Year was not retained as a covariate in the combined model.

The relationship for herring energy was linear, with predicted minke whale density increasing as herring energy increased. Minke whale predicted density was also highest in areas with close proximity to sandeel grounds, with predicted density decreasing as distance increased. Slope was also retained in this final minke whale model, with predicted density of minke whales increasing slightly as slope increased. This relationship has very wide confidence intervals, however, and so should be interpreted with caution.

The prey models produced very different predictions from the environmental-only models for the corresponding years (Figure 4.2-3 b), with predicted minke whale densities from the prey models being much higher and extending much further south into the central North Sea, into areas where there were no sightings of this species. The prey models showed very high levels of over-prediction, which is likely driving this change in predicted density. Maps of CV and SE (Figure 4.2-3 c, d) show these values to be correspondingly high.

Table 4.2-4: Model output for best minke whale combined year prey model.

Model ID	Error distribution	Model covariates	Estimated degrees of freedom	P value	% Deviance explained	Model degrees of freedom	Model AIC
All fish species separately	Negative binomial	Slope	0.8	0.021	18.7	11.2	594.3
		Cod energy	3.9	0.003			
		Whiting energy	3.7	0.021			
		Dist_sandeels	0.8	0.025			

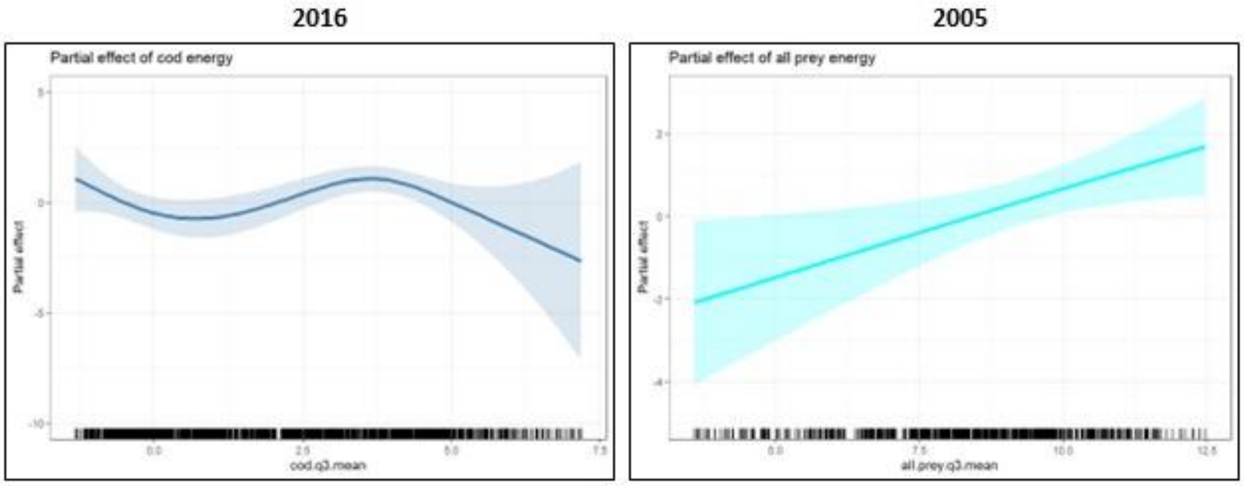

Figure 4.2-1: Plots of the fitted smooth function for the 2016 and 2005 best prey models for minke whale. The 2016 model retained only the cod covariate, the 2005 model retained only the "all prey" covariate.

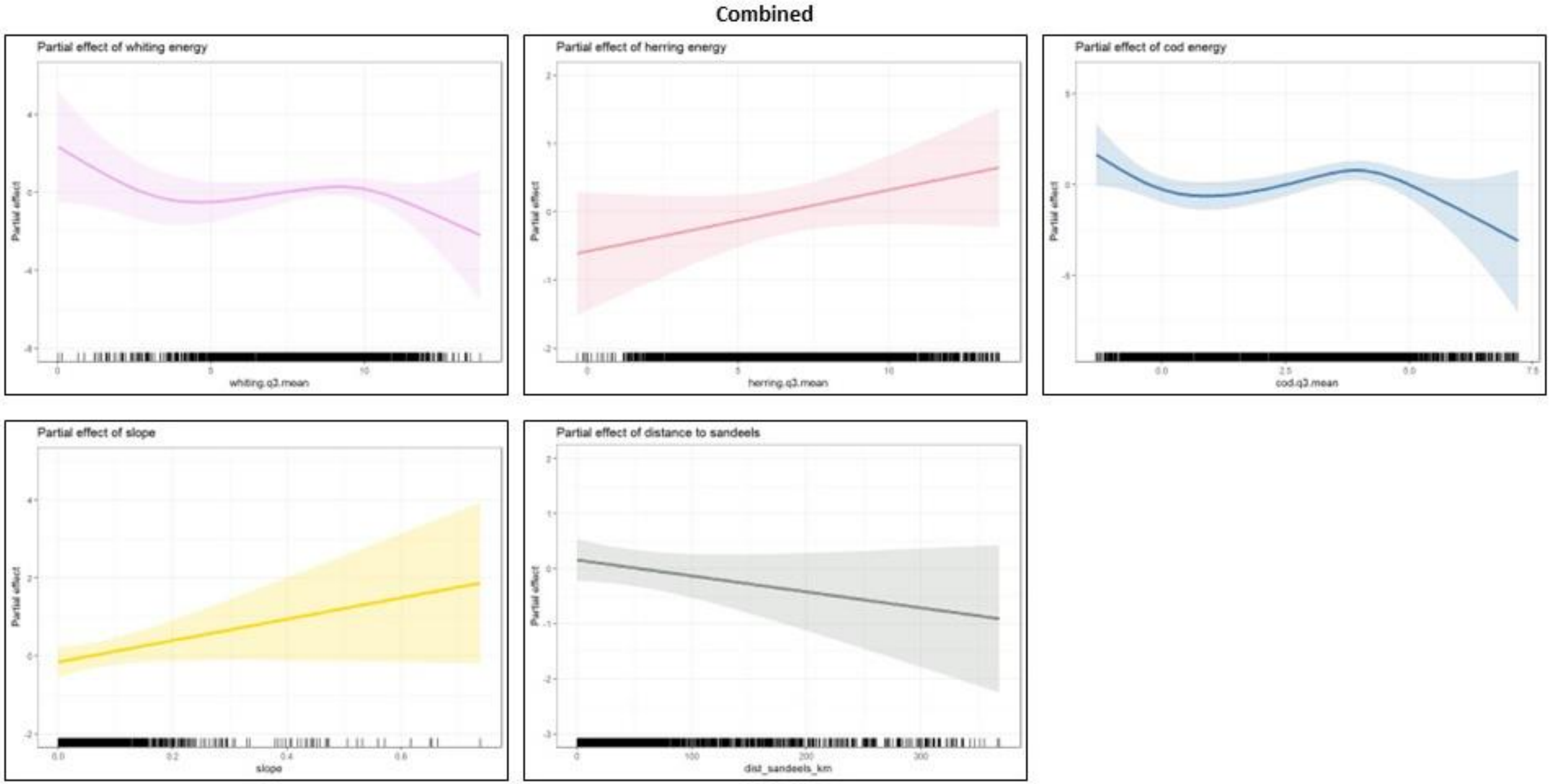

Figure 4.2-2: Plots of the fitted smooth functions for the combined 2016 and 2005 prey model for minke whale.

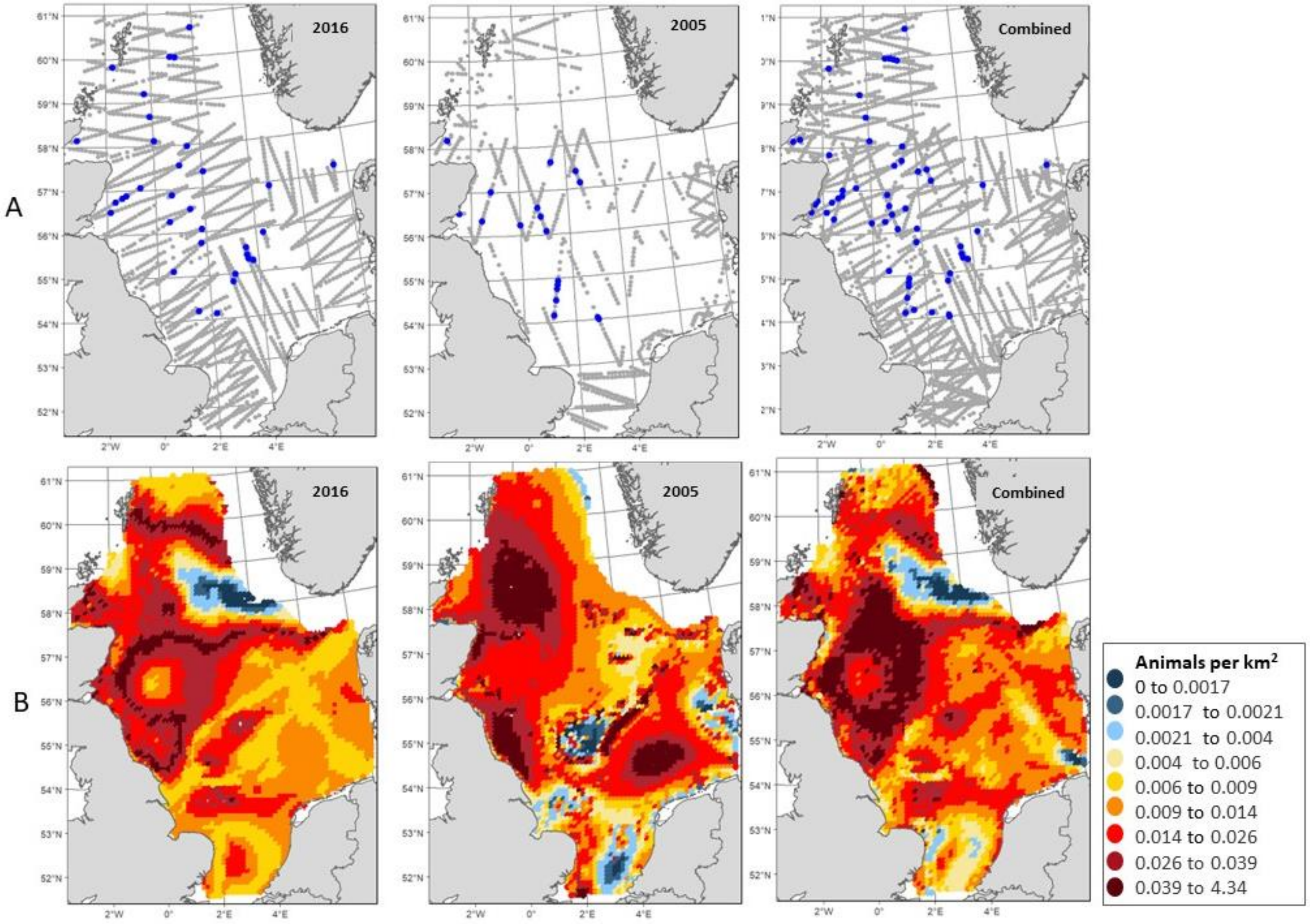

Figure 4.2-3: Location of effort and sightings (A), predicted density surface (B) for 2016, 2005 and combined year minke whale prey models. Range of values represented by colours in the maps show the 1%, 2%, 5%, 10%, 25%, 50%, 75%, 90% and 100% quantiles. White areas are outside of predictive space. In some cases, prediction grid cells had covariate values which were outside the range encompassed by the modelled effort segments. In these instances, grid-cells were excluded from the prediction. Combined year data are predicted using 2016 covariates.

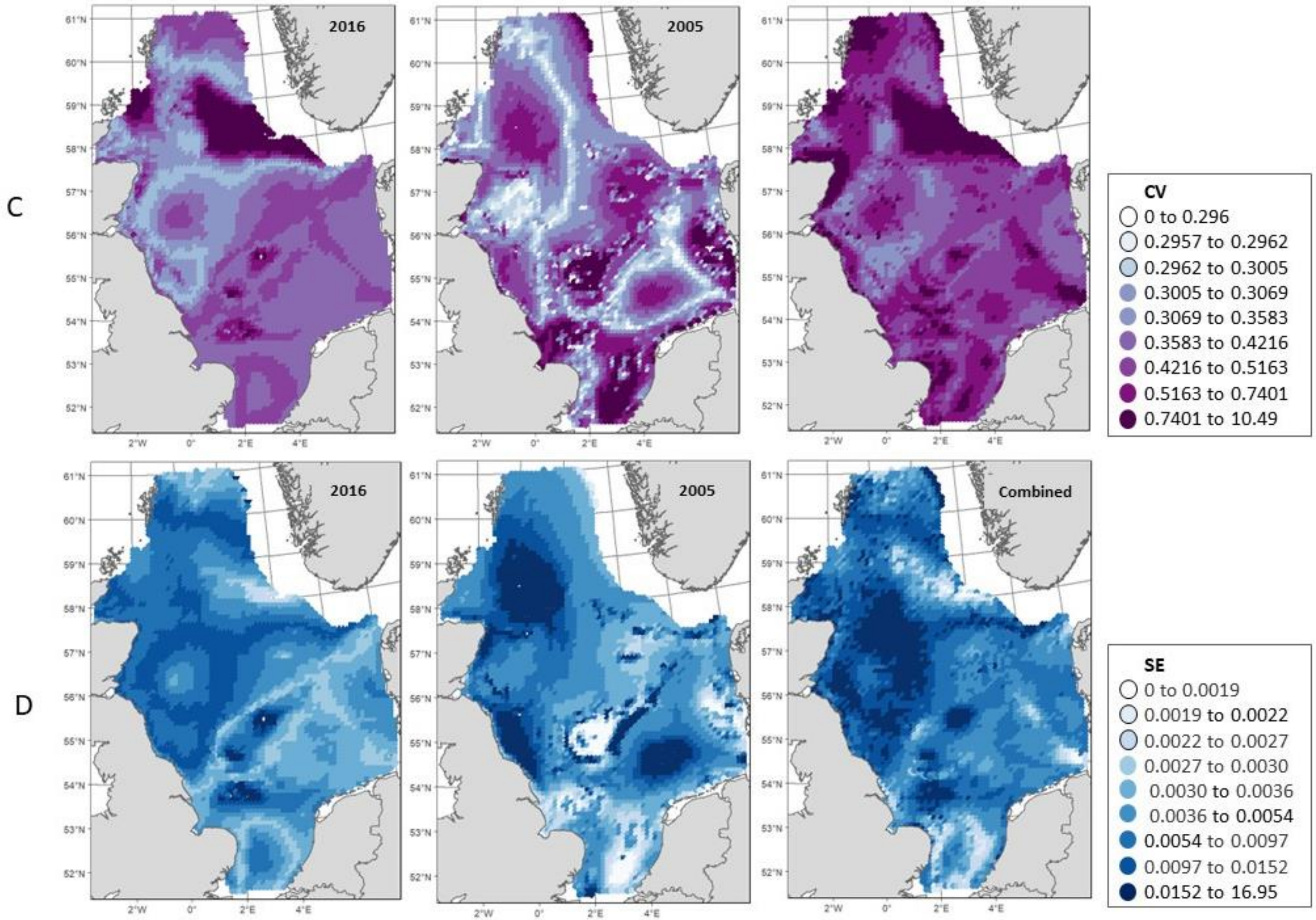

Figure 4.3-3 ctd: Maps of predicted coefficient of variation CV of density (CV) (C) and standard error (SE) (D) for 2016, 2005 and combined year minke whale prey models. Range of values represented by colours in the maps show the 1%, 2%, 5%, 10%, 25%, 50%, 75%, 90% and 100% quantiles. White areas are outside of predictive space. In some cases, prediction grid cells had covariate values which were outside the range encompassed by the modelled effort segments. In these instances, grid-cells were excluded from the prediction.

4.2.2. White-beaked dolphins

The results of the best white-beaked dolphin model for each of the individual prey species are shown in Table 4.2-5. The best models for most prey species retained no environmental covariates, although the herring model retained slope and the sandeel model retained depth in addition to the prey covariate.

The best model, with a lot more support from the data than any other model, and used for prediction, was the "All fish species separately" model. Partial effects plots and predictions of this model, along with SE and CV are shown in Figure 4.2-4 and Figure 4.2-5. This retained all fish species, as well as slope and CS_50_cont. All relationships were linear, with higher levels of white-beaked dolphin density being associated with low slope values, larger distances to the 50m contour on the shallower side of the contour, low levels of cod energy, low levels of sprat energy, but high levels of herring and whiting energy, and proximity to sandeel grounds. The confidence intervals of slope and cod energy were wide, particularly for slope.

Table 4.2-5: Model output for white-beaked dolphin prey models, 2016 data.

Model ID	Error distribution	Model covariates	Estimated degrees of freedom	% Deviance explained	Model degrees of freedom	Model AIC
Cod	Negative binomial	Cod – Summer 2016	3.3	40.4	4.3	465.0
Herring	Negative binomial	Slope	0.6	49.2	5.8	455.3
		Herring – Summer 2016	4.2			
Whiting	Negative binomial	Whiting – summer 2016	0.8	3.3	1.8	499.6
Sprat	Negative binomial	Sprat – summer 2016	2.4	35.5	3.4	472.0
Sandeel	Negative binomial	Depth	2.8	57	5.3	501.2
		Dist_sandeels	1.1			
All prey combined	Negative binomial	All prey combined – summer 2016	1.6	26.8	2.6	476.8
All fish species separately	Negative binomial	Slope	0.7	61.3%	7.1	429.5
		CS_50_cont	0.8			
		Cod – Summer 2016	0.4			
		Herring – Summer 2016	1.1			
		Whiting – summer 2016	0.9			
		Sprat – summer 2016	1.1			
		Dist_sandeels	1.0			

Some of the white-beaked dolphin prey models, including the best model, had unrealistically high levels of deviance explained given the relatively small sample size. The best model used for prediction – the "All fish species separately" model also showed evidence of over-predicting abundance, resulting in approximately 29,000 animals in the North Sea area, compared to the design-based estimate for the full ecoregion of 20,525 animals (Hammond *et al*. 2021). However, whilst the densities were high, the actual pattern of the prediction did reflect the observed locations of animals.

For the 2005 data, the best prey model, and used for prediction, was the "All fish species separately" model. Outputs, diagnostics and predictions of this model , along with CVs and SEs, are shown in Table 4.2-6, Figure 4.2-4 and Figure 4.2-5. The relationships for herring, sprat and distance to sandeel grounds were linear, with higher levels of white-beaked dolphin density being predicted at higher levels of herring energy, closer distances to sandeel grounds and lower levels of sprat energy. The cod relationship had a peak predicted density of dolphins at around 5MJ of energy.

Table 4.2-6: Model output for white-beaked dolphin prey models, 2005 data.

Model ID	Error distribution	Model covariates	Estimated degrees of freedom	% Deviance explained	Model degrees of freedom	Model AIC
Cod	Negative binomial	Cod – Summer 2005	2.8	43.2	3.8	292.0
Herring	Negative binomial	Herring – Summer 2005	0.9	11.2	1.9	312.0
Whiting	Negative binomial	Whiting – summer 2005	1.0	14.2	2.0	310.2
Sprat	Negative binomial	Sprat – summer 2005	1.0	27.2	2.0	300.9
Sandeel	Negative binomial	Depth	3.0	55.1	4.9	281.3
		Dist_sandeels	0.9			
All prey combined	Negative binomial	All prey combined – summer 2005	0.8	5.7	1.8	315.2
All fish species separately	Negative binomial	Herring – Summer 2005	0.9	58.6	6.3	279.5
		Cod – summer 2005	2.6			
		Sprat – summer 2005	0.9			
		Dist_sandeels	0.9			

For the combined 2016 and 2005 model, individual covariates for whiting, herring, sprat and distance to sandeel grounds were retained, but no environmental covariates (Table 4.2-7). Year was retained as a covariate in the combined model and was significant ($p < 0.05$). Partial effects plots are provided in Figure 4.2-4.

The partial effect for herring energy was linear in this combined year model with predicted white-beaked dolphin density increasing as herring energy increased. This was also the case with the 2005 data and 2016 data when modelled separately. The plot for whiting shows the same shape, although this covariate was not retained in the 2005 model.

White-beaked dolphin predicted density was highest in areas in close proximity to sandeel grounds, with predicted density decreasing as distance increased; again, this effect was seen in all three models.

The relationship for sprat was linear and in the opposite direction to the other fish species. This predicted the lowest dolphin density at highest sprat energy values. This pattern is seen in all three models.

Table 4.2-7: Model outputs for combined 2005 and 2016 white-beaked dolphin prey model

Name	Factor levels	Estimate	Std. Error	Z value	PR(>z)	
Combined 2016 & 2005 model	Intercept (2005)	175.6	83.5	-2.1	0.034	
	Year = 2016	-0.09	0.04	-2.2	0.030	
Model	**Error distribution**	**Model covariates**	**Estimated degrees of freedom**	**% Deviance explained**	**Model degrees of freedom**	**P value**
Combined 2016 & 2005 model	Negative binomial	Herring energy	1.15	52.8	6.2	2e-16
		Whiting energy	0.9			0.012
		Sprat energy	1.1			2e-16
		Distance to sandeels	1.02			2e-16

Some of the white-beaked dolphin prey models, including the best model, had unrealistically high levels of deviance explained given the relatively small sample size. These models also showed strong evidence of over-predicting abundance, the 2016 model resulting in approximately 70,725 animals in the North Sea area, compared to the design-based estimate for the full ecoregion of 9,588 animals (Hammond et al. 2021). However, whilst the densities are very high, the actual pattern of the prediction is an adequate reflection of the observed locations of animals.

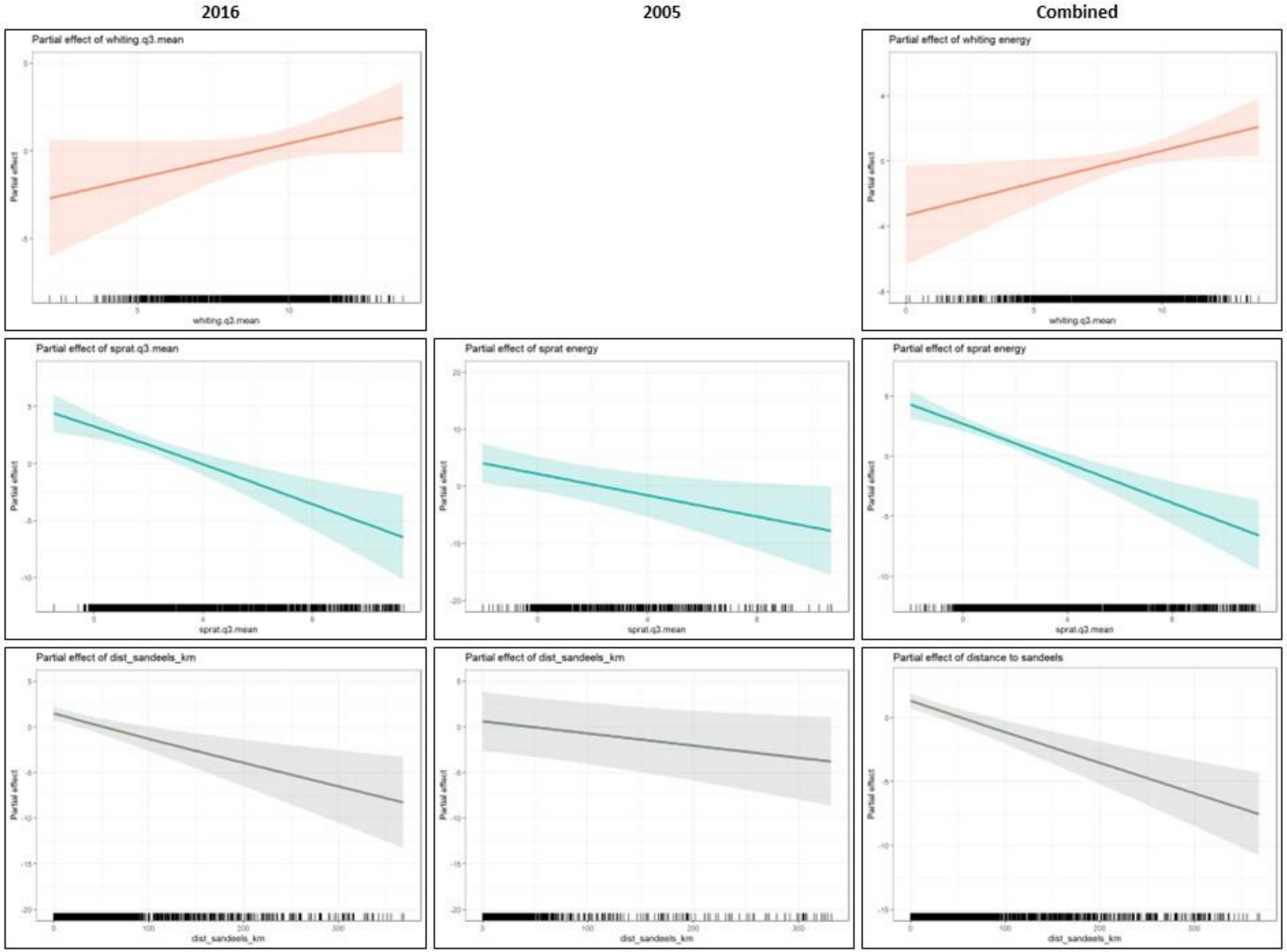

Figure 4.2-4: Plots of the fitted smooth functions for the 2016, 2005 and the combined 2016 and 2005 prey model for white beaked dolphin prey models.

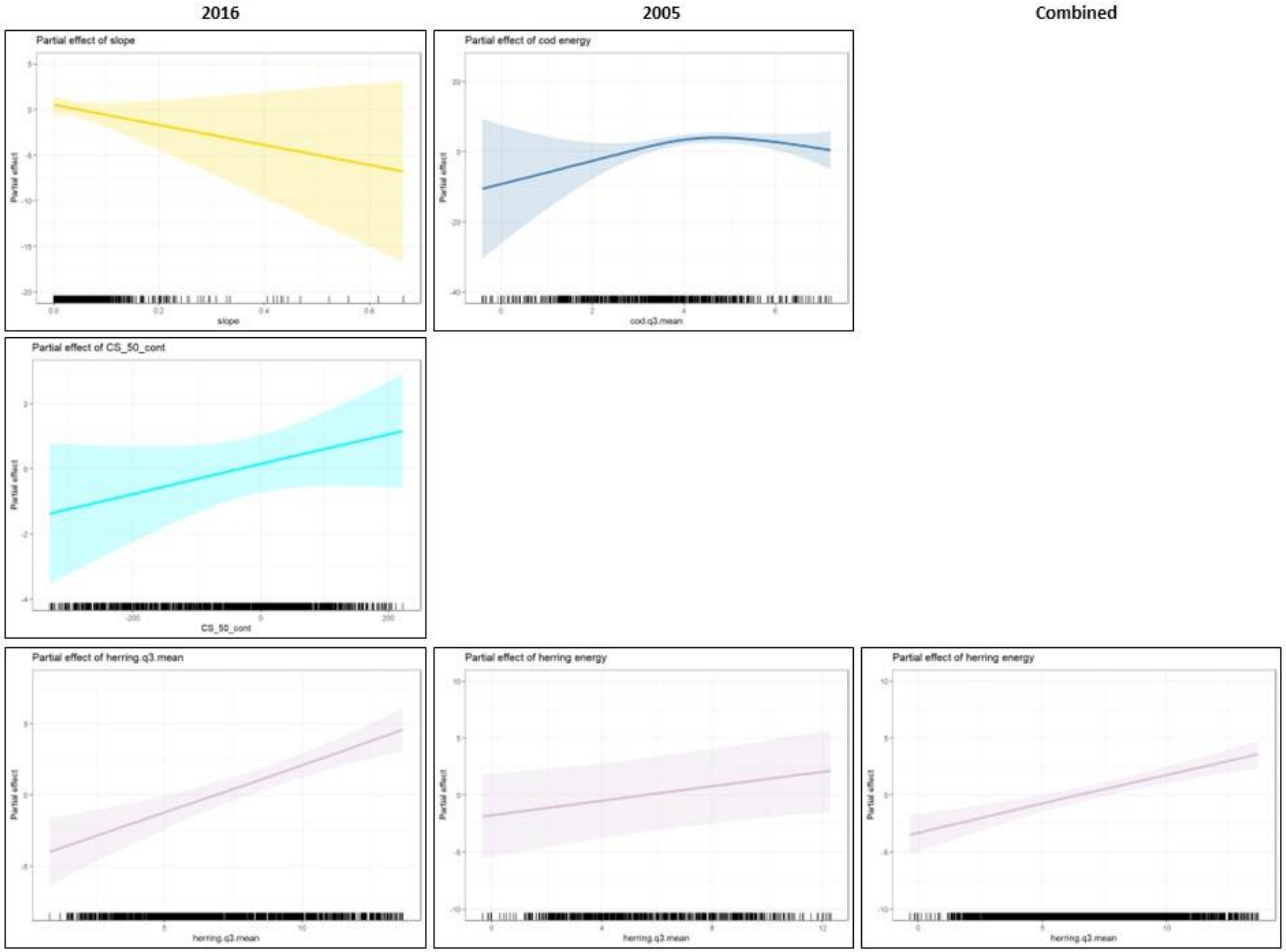

Plots of the fitted smooth functions for the 2016, 2005 and the combined 2016 and 2005 prey model for white beaked dolphin prey models.

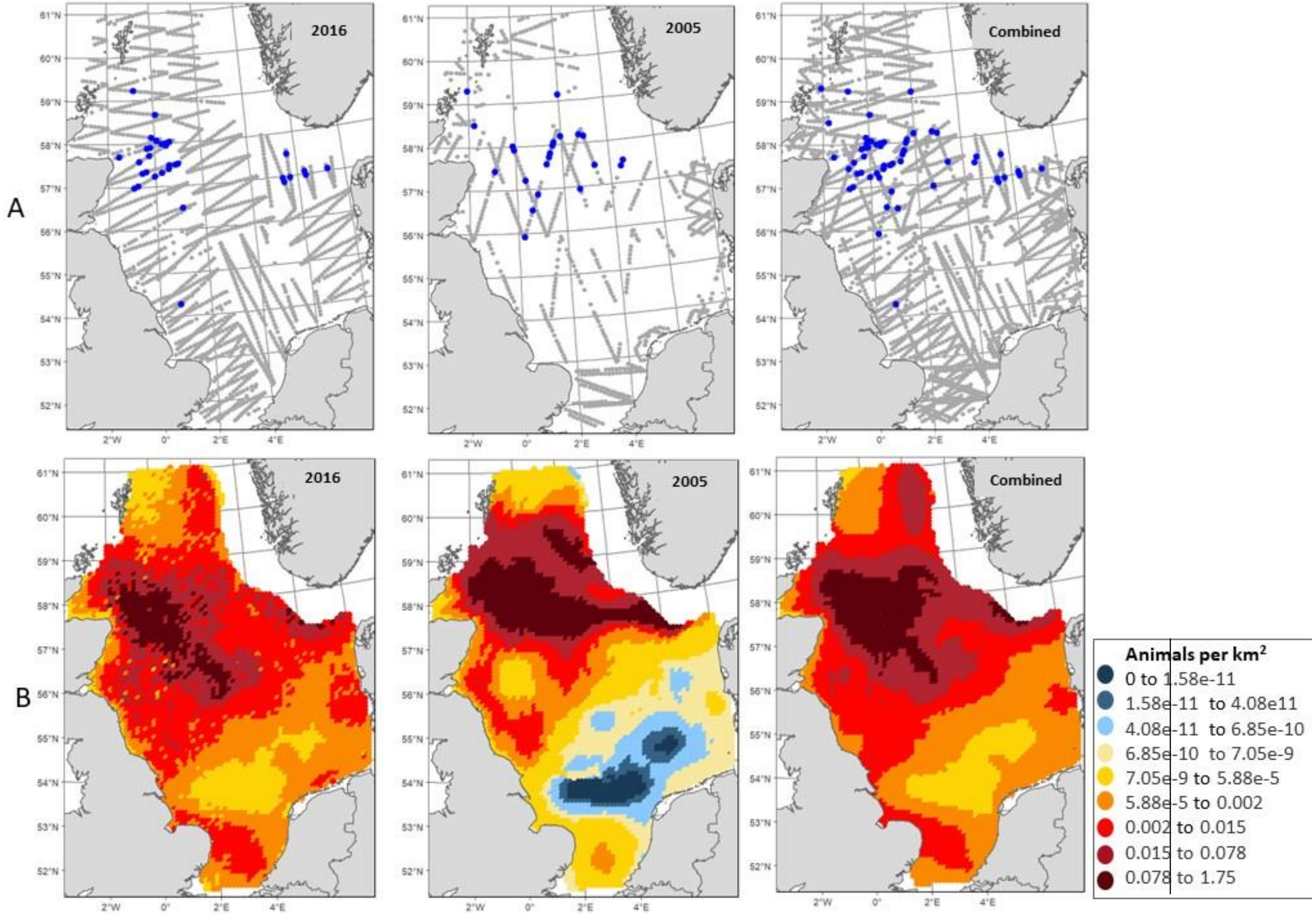

Figure 4.2-5: Location of effort and sightings (A), predicted density surface (B) for 2016, 2005 and combined year white-beaked dolphin models. Range of values represented by colours in the maps show the 1%, 2%, 5%, 10%, 25%, 50%, 75%, 90% and 100% quantiles. White areas are outside of predictive space. In some cases, prediction grid cells had covariate values which were outside the range encompassed by the modelled effort segments. In these instances, grid-cells were excluded from the prediction. Combined year data are predicted using 2016 covariates.

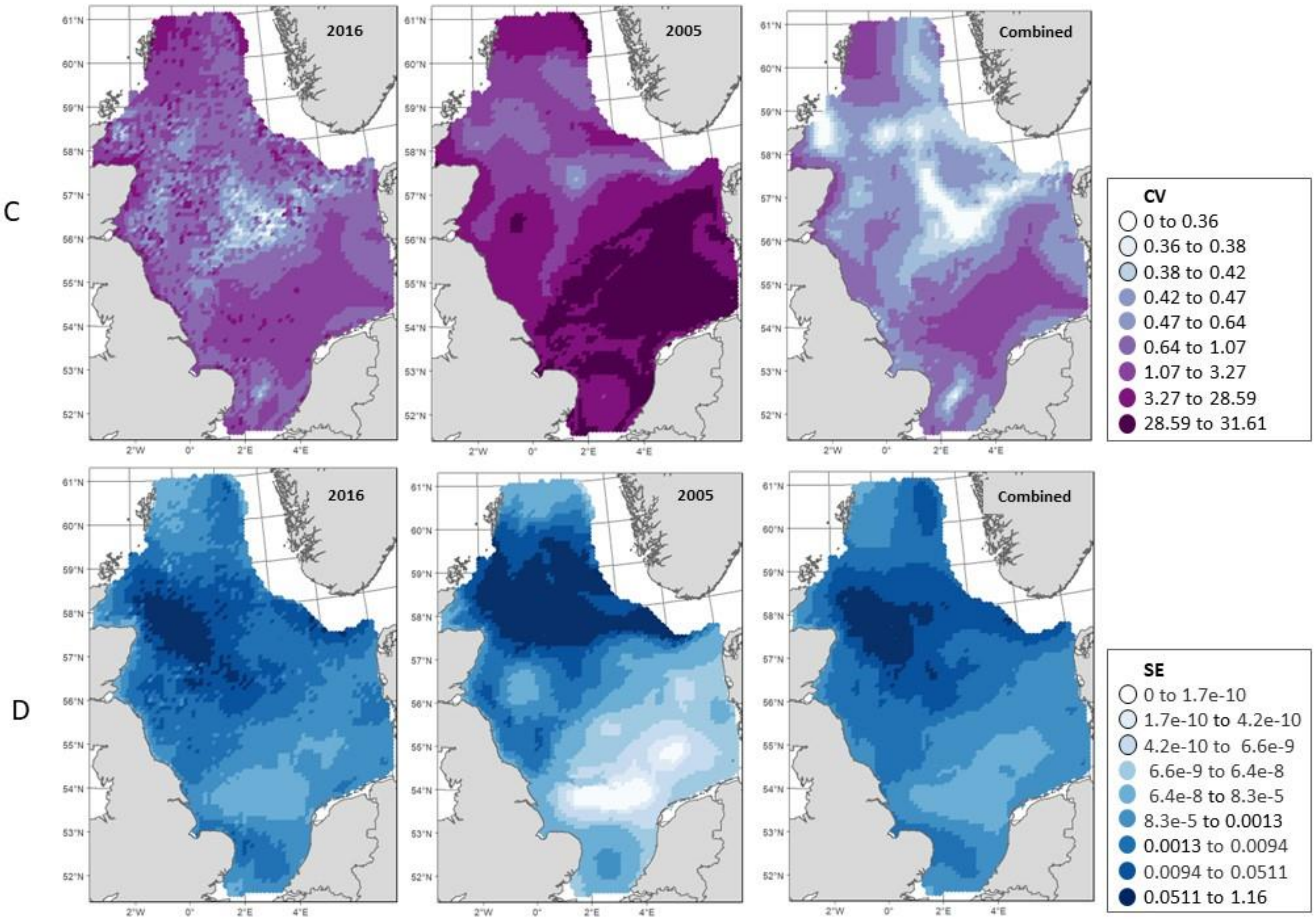

Figure 4.4-5 ctd: Maps of predicted coefficient of variation CV of density (CV) (C) and standard error (SE) (D) for 2016, 2005 and combined year white-beaked dolphin models. Range of values represented by colours in the maps show the 1%, 2%, 5%, 10%, 25%, 50%, 75%, 90% and 100% quantiles. White areas are outside of predictive space. In some cases, prediction grid cells had covariate values which were outside the range encompassed by the modelled effort segments. In these instances, grid-cells were excluded from the prediction.

4.2.3. Harbour porpoise

The results of the best prey models for each of the individual prey species for harbour porpoise are shown in Table 4.2-8. The “All fish species separately” model was selected as the best harbour porpoise prey model. Partial effects plots are provided in Figure 4.2-6, diagnostics in Appendix 3 and predictions of this model, along with SE and CV, are shown in Figure 4.2-7 . Three covariates were retained. Slope was also retained in the 2005 model and the combined years model with a similar relationship in each. In all three cases this predicted the highest densities of harbour porpoise in areas of flat seabed (low slope).

The relationship for sprat energy had a peak predicted porpoise density at around 5MJ sprat energy, following which porpoise density was predicted to decrease rapidly, in particular at higher energy levels. The same relationship could be seen in the combined years model.

Porpoise density was associated with close proximity to sandeel grounds, although the decline was not linear and there was a very small secondary peak at around 200km distance. The confidence interval at larger distances was wide. This relationship was also replicated in the combined years model, although the effects in the model were larger.

Table 4.2-8: Model output for harbour porpoise prey models, 2016 data. Slope was retained in all models along with the prey covariate(s).

Model ID	Error distribution	Model covariates	Estimated degrees of freedom	% Deviance explained	Model degrees of freedom	Model AIC
Cod	Negative binomial	Slope	0.9	4.4	8.0	3764.9
		Cod – Summer 2016	6.1			
Herring	Negative binomial	Slope	0.9	1.8	2.8	3784.8
		Herring – Summer 2016	0.9			
Whiting	Negative binomial	Slope	0.9	1.8	2.8	3789.2
		Whiting – summer 2016	0.9			
Sprat	Negative binomial	Slope	0.9	3.0	4.8	3775.6
		Sprat – summer 2016	2.9			
Sandeel	Negative binomial	Slope	0.6	3.9	5.1	3766.6
		Dist_sandeels	3.5			
All prey combined	Negative binomial	Slope	0.9	1.2	2.5	3791.6
		All prey combined – summer 2016	0.6			
All fish species separately	Negative binomial	Slope	0.86	5.5	7.14	3759.2
		Sprat – summer 2016	2.33			
		Dist_sandeels	2.94			

For 2005, the results of the best harbour porpoise prey model for each of the individual prey species are shown in Table 4.2-9. The "All fish species separately" model was selected as the best model. Partial effects plots are provided in Figure 4.2-6, diagnostics in Appendix 3 and predictions of this model, along with SE and CV, are shown in Figure 4.2-7.

Both of the retained covariates had linear relationships predicting porpoise density. Porpoise predicted density was highest at shallow slopes, as described for the 2016 model, and declined linearly as slope steepness increased. There were fewer data points at steeper slopes, however, and the confidence intervals here were very wide. Predicted porpoise density was highest in areas of low whiting energy and decreased linearly as whiting energy increased.

Table 4.2-9: Model output for harbour porpoise prey model, 2005 data. The "All fish species separately" model had each fish species as a separate covariate, along with environmental covariates. AllPrey was not retained in the final model for that fish species, so this was not taken further.

Model ID	Error distribution	Model covariates	Estimated degrees of freedom	% Deviance explained	Model degrees of freedom	Model AIC
Cod	Negative binomial	Slope	0.7	1.8	2.4	1301.0
		Cod – Summer 2016	0.7			
Herring	Negative binomial	Herring – Summer 2016	0.9	2.6	1.9	1296.4
Whiting	Negative binomial	Whiting – summer 2016	1.0	4.2	2.0	1290.4
Sprat	Negative binomial	Slope	0.8	1.3	2.3	1302.2
		Sprat – summer 2016	0.3			
Sandeel	Negative binomial	Depth	0.9	2.3	2.3	1298.5
		Dist_sandeels	0.4			
All prey combined	Negative binomial	Slope	0.8	1.1	1.8	1301.8
All fish species separately	Negative binomial	Slope	0.4	5.1	3.1	1290.0
		Whiting – summer 2016	1.0			
		Sprat – summer 2016	0.7			

The combined years model retained four covariates (Table 4.2-10), all of which appeared in at least one of the single year models. Partial effects plots are provided in Figure 4.2-6, diagnostics in Appendix 3 and predictions of this model, along with SE and CV, are shown in Figure 4.2-7.

The only major difference in the shape of the relationship between harbour porpoise predicted density and any of the covariates in this combined model, compared with the individual year models, was in the whiting energy plot. The 2005 relationship was linear whereas in this combined model it was slightly curved, with the lowest porpoise densities being predicted at around 8 MJ of whiting energy. It is possible that this increased edf may be a result of the larger number of data points available for modelling in the combined year model.

Table 4.2-10: Model output for best harbour porpoise combined year prey model.

Model ID	Error distribution	Model covariates	Estimated degrees of freedom	P value	% Deviance explained	Model degrees of freedom	Model AIC
All fish species separately	Negative binomial	Slope	0.9	0.0006	5.4	10.2	5399.3
		Whiting energy	1.78	0.0324			
		Sprat energy	2.5	0.0040			
		Dist_sandeels	4.0	8.88e-6			

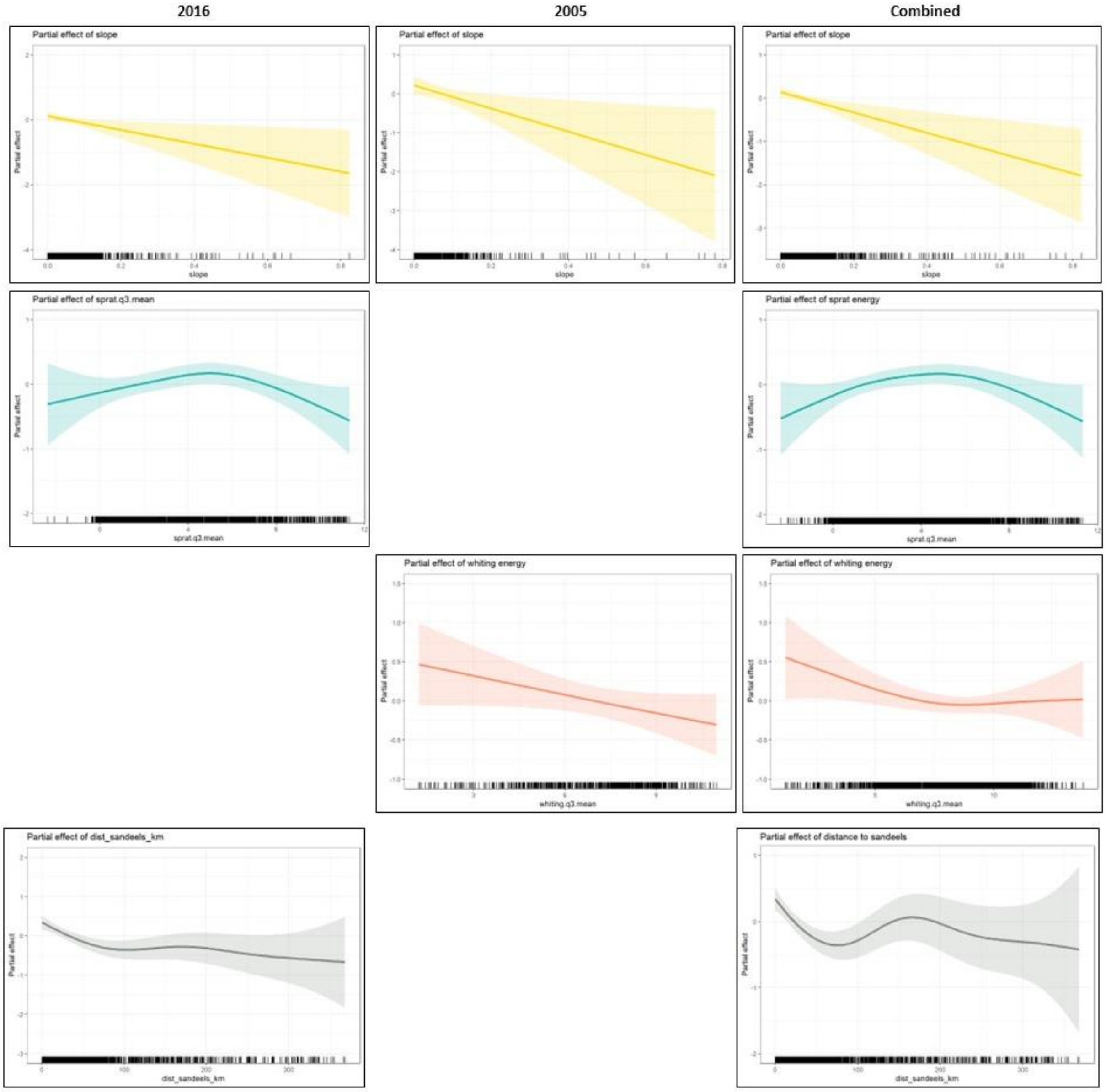

Figure 4.2-6: Plots of the fitted smooth functions for the 2016, 2005 and the combined 2016 and 2005 prey model for harbour porpoise prey models.

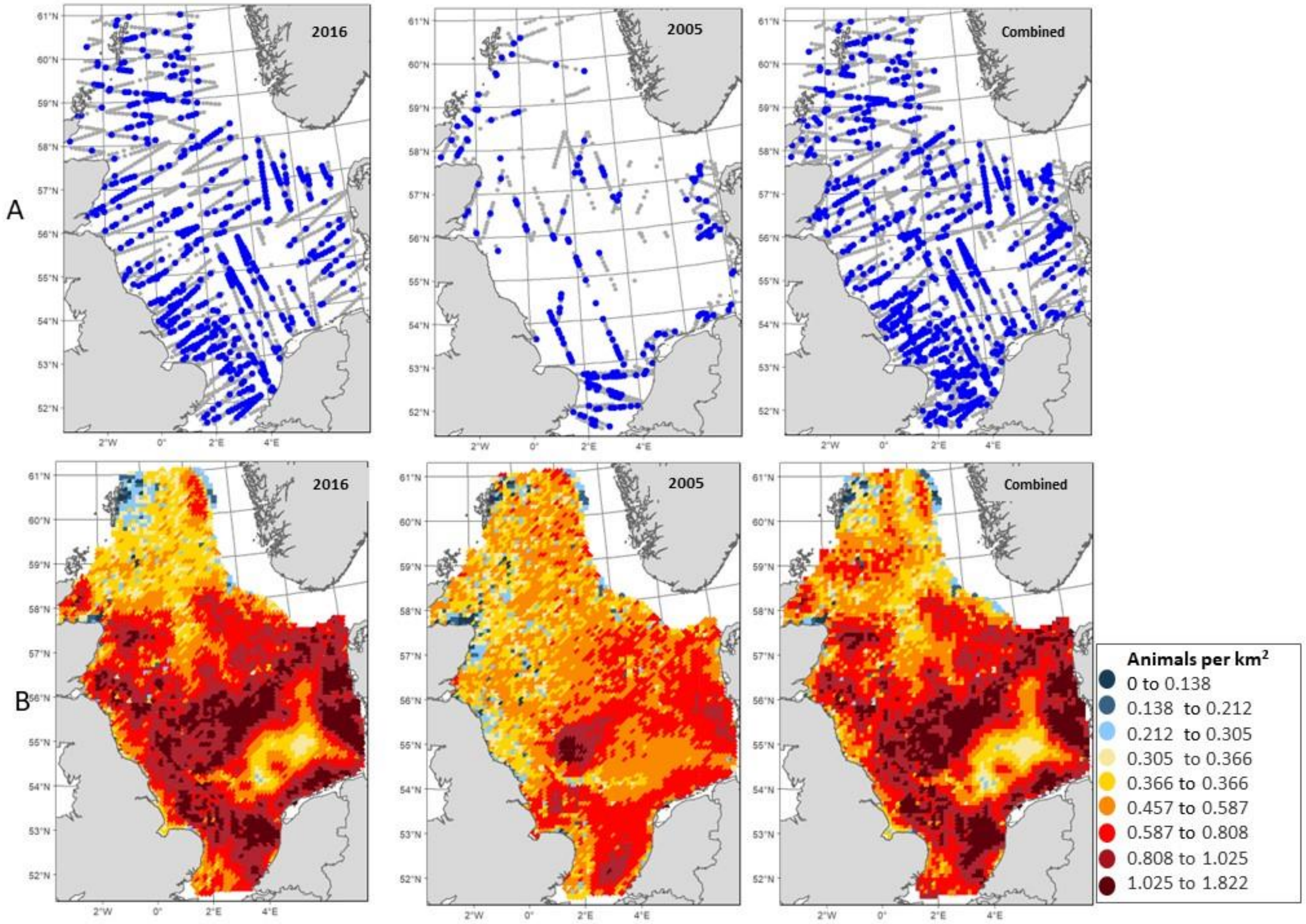

Figure 4.2-7: Location of effort and sightings (A), predicted density surface (B) for 2016, 2005 and combined year harbour porpoise models. Range of values represented by colours in the maps show the 1%, 2%, 5%, 10%, 25%, 50%, 75%, 90% and 100% quantiles. White areas are outside of predictive space. In some cases, prediction grid cells had covariate values which were outside the range encompassed by the modelled effort segments. In these instances, grid-cells were excluded from the prediction. Combined year data are predicted using 2016 covariates.

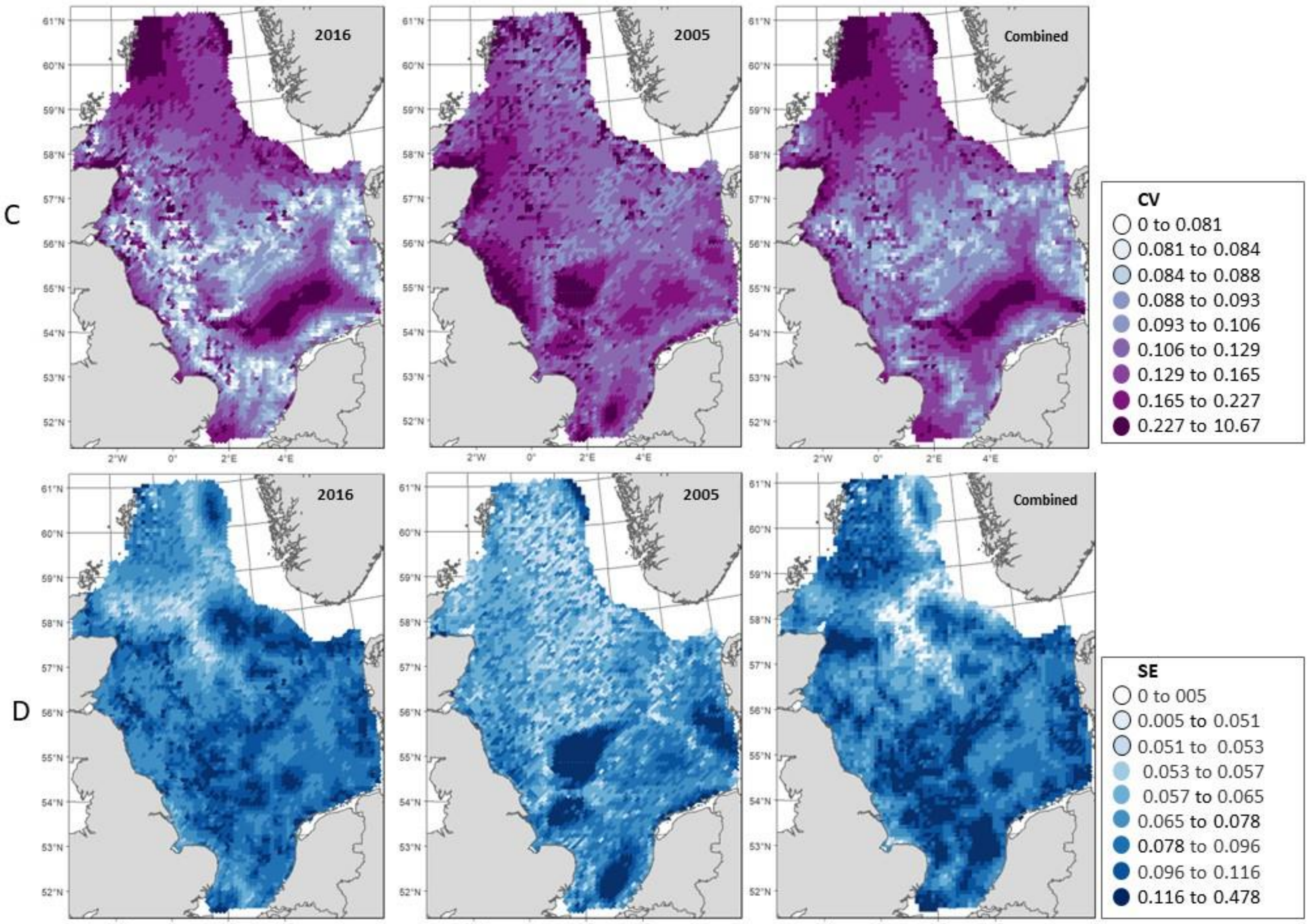

Maps of predicted coefficient of variation CV of density (CV) (C) and standard error (SE) (D) for 2016, 2005 and combined year harbour porpoise models. Range of values represented by colours in the maps show the 1%, 2%, 5%, 10%, 25%, 50%, 75%, 90% and 100% quantiles. White areas are outside of predictive space. In some cases, prediction grid cells had covariate values which were outside the range encompassed by the modelled effort segments. In these instances, grid-cells were excluded from the prediction.

4.3. Discussion:

This chapter presents the results of explanatory density surface models for the three species of cetacean most commonly found in the North Sea ecoregion, modelled firstly using environmental covariates and secondly using prey energy covariates.

To the best of my knowledge, the models presented in this chapter represent the first attempt to create an ecoregion-wide predicted density surface for two of these three species. Whilst previous studies have been conducted in this region, they are generally focussed on either a much smaller study region or a much larger one. This means they are likely to capture much finer scale movements than would show up at this scale, or incorporate multiple different environmental regions, which may conflate relationships. They may use data collected over a longer timescale, for example Tetley *et al*. (2008) and de Boer (2010) for minke whales and Canning *et al*. (2008) for white-beaked dolphin. Paxton *et al*. (2016) used the Joint Cetacean Protocol data to produce density surfaces over a wide area from multiple combined sources, covering a 17-year period. This and other larger-scale projects (e.g., SCANS, ObSERVE) covered a wide geographic region, which may span multiple biogeographic regions. Cetaceans can inhabit a wide range of environments and exploit multiple niches; the aim of the work presented in this chapter was to investigate the relationship between species and their environment across a single complete ecoregion, an area with shared biogeographic characteristics.

4.3.1. Sources of error

These types of studies are subject to error during both data collection and analysis stages (Barry and Elith 2006). As the data sources and analysis framework used was the same for this chapter and Chapters 3 and 5, sources of error are reviewed and discussed for these three chapters together in section 6.1.2.

The fish energy surfaces which were included in the “prey” models also have their own sources of unquantified error, which may come from catchability of the fish species, energy content and spatiotemporal model predictions (Ransijn et al. 2019). There are elements of uncertainty acknowledged by the authors which are not included in these prey energy surfaces, to which they estimate catchability uncertainty would be the largest source of error. This unquantified uncertainty would, of course, propagate forward into the models presented here as well.

4.3.2. Minke whale

The distributions of minke whales predicted by the selected full ecoregion, environmental models show the highest density to the north of the ecoregion. For 2016, this area of high density also has an area of high density in the central North Sea. The high-density area for 2005 is limited to the central northern area. The combined years model shows very high densities in the north of the region, which extend southwards through the central North Sea. There is a secondary area of high density to the western end of the English Channel (Figure 4.1-2).

A limited number of explanatory covariates were retained in the full ecoregion minke whale models. The 2016 model for minke whales retained SD depth, SSH and mixed layer depth with minke whale density being associated with lower SSH and increasing MLD. The MLD shows an approximate east-west gradient, with higher values being towards the western half of the North Sea (Figure 4.2-6c). These waters are also shallower, avoiding the trench around the Norwegian coastline.

Most baleen whale species segregate their breeding and feeding activities both temporally and spatially. As a consequence, during the summer their distribution in an area *should* be a reflection of the availability of their prey or of preferred feeding areas (Anderwald *et al*. 2012). Minke whales feed on a wide variety of prey species, which vary seasonally and geographically (Anderwald and Evans 2007), with little preference when many options are available (Skaug *et al*. 1997). In the North Sea, prey samples are dominated by sand eels and mackerel (Windsland *et al*. 2007), so it could be expected that covariates explaining the distribution of these prey species may be important.

During summer months, Atlantic mackerel use the north-east Atlantic, including the North Sea, to spawn and feed. Mackerel spawning distribution has shifted northwards between 1992 and 2013 but studies have been unable to link this to a direct set of oceanographic variables, including MLD and SST (Bruge *et al*. 2016). Stomach samples of mackerel from the North Sea have found their prey to be dominated by copepods, euphausiids and fish (Mehl and Westgard 1983). Minke whales may be targeting areas of cooler SST as these may be more likely to have increased availability of mackerel, but SST was not retained in any of the minke whale models. It is possible the temperature range is not wide enough to fully show this effect.

The covariates retained for 2005 were different; MLD and SSH as with 2016, but also depth and salinity addition. Low salinities are primarily found in shallower waters closest to the coast, and the relationships for both depth and salinity show minke whale predicted density increasing with increasing depth and salinity. The few data points at low salinity (and associated poor precision) may be driving the strength of this relationship. The combined year model retained all the covariates which had been used in the separate year models. The relationships were all broadly similar, and the selection of the model containing the year covariate showed that there may be a difference in the individual relationships depending on the year.

Whereas it is often necessary to rely on proxy covariates such as SSH, here, in the absence of in-situ prey information, I was able to include the energy represented by a range of prey species in separate prey models. Of the species tested, cod energy was found to explain most variation in the minke whale data in 2016, and “All prey combined” in 2005. The selected model itself was not a particularly good fit to the data, and the predicted density surface was not a good match to the sightings for this species. The 2005 “all prey” energy surface shows an increase in predicted density of minke whales as combined prey energy increases. In both instances, the prey models produced a very different spatial density prediction from the environmental models for the corresponding years, with predicted minke whale densities extending much further south into the central North Sea into areas where there were no sightings of this species. The prey models showed very high levels of over-prediction leading to the conclusion that, at least in this instance, the prey covariates modelled here are not good predictors of minke whale density. If mackerel is still the dominant prey species for minke whales in the North Sea, this is perhaps not surprising because energy layers were not available for mackerel, so it was not possible to include this species in the prey model.

Various modelling studies have previously attempted to link minke whale distribution to a range of explanatory variables. The linked variables vary both spatially and temporally. Studies around Scotland (some outside the ecoregion modelled in this chapter, but geographically close) have positively linked minke whale presence with areas with a high probability of sandeel occurrence (month of June only) (Anderwald *et al*. 2012); seabed topography (Macleod *et al*. 2004; Robinson *et al*. 2009); and depth or a particular depth contour (Tetley 2004; Gutiérrez-Muñoz *et al*. 2021). In addition, sea surface temperature (SST) was found to be significant in June and August/September but not during July (Anderwald *et al*. 2012). Seabed type has also been found to influence minke whale presence (Macleod *et al*. 2004). Different age classes have been reported to have different preferences, with juvenile minke whales reportedly preferring shallow inshore waters with sandy-gravel sediments and adults preferring deeper offshore waters with a steeper slope (Robinson *et al*. 2021). This wide variety of different selected predictors perhaps highlights how difficult it is to find meaningful relationships. That the ones in this study persist across time periods perhaps suggests that they are more likely to represent significant predictors.

Further afield, minke whale distribution has been positively associated with heterogenous seabed topography (Doniol-Valcroze *et al*. 2007), continental shelf structures and their slopes (Solvang *et al*. 2015) and the presence of underwater sand dunes (Naud *et al*. 2003).

Studies of minke whales in this ecoregion, albeit earlier in the year than the data in this study were collected, show a link with the slopes of Dogger Bank in the south-east of the ecoregion as well as the 50m depth contour (de Boer 2010).

4.3.3. White beaked dolphin

Environmental covariate models predicted white-beaked dolphins to be primarily in the northern part of the ecoregion. This pattern holds true for both time periods modelled and is a good fit with the observed locations of animals from sightings data.

Whilst previous studies have found white-beaked dolphin distribution to be linked to certain temperature ranges (Macleod *et al*. 2008), that was not the case with these models, and no sea surface temperature covariates were retained. It should be noted, however, that the Macleod *et al*., (2008) study was conducted in areas in which there is overlap between common dolphins (*Delphinus delphis*) and white-beaked dolphins. In the absence of common dolphins (which are not found routinely throughout the North Sea ecoregion), such partitioning may be irrelevant. It should also be noted that the sea surface temperatures within the ecoregion during the time of the study, which ranged from 10^0C to 21^0C in 2005 and 12^0C to 18^0C in 2016 (

Table 4.2-3) are, except for the very high temperatures of 2005, within the preferred habitat range for this species, which has been reported as 13^0C -18^0C (Macleod, 2013), which may also explain why this covariate was not retained.

In the combined years model white-beaked dolphin distribution is predicted to linearly decrease with increasing depth. Described by Kinze (2018) as a species that is present where prey items concentrate, this strong association with depth is not unexpected. Species which are known prey items of white-beaked dolphins, North Sea haddock and whiting, are found in waters less than 200m depth (ICES 2014a, 2014b) .

The only covariate retained by both 2016 and 2005 models was salinity, and this was not retained in the combined year model. As the lowest salinities within the region are to be found in areas very close to the coast, it is possible that the relationship here is not with the water salinity *per se*, but that this is working as a proxy variable for a more general set of conditions found nearer the coast, or in shallow waters.

Areas with lower SSH are associated with areas of colder water, which may be more productive; thus, this could be considered a proxy for areas of higher prey aggregations. However, the wide confidence intervals of the 2005 model preclude making strong assumptions about habitat preferences based on SSH alone.

Slope was retained in the combined year model, with higher dolphin densities being associated with shallower slopes. The majority of the North Sea area is very flat, so this is not particularly informative within the study area covered by this model. Canning *et al*. (2008) also reported an effect of slope, although they found this to be linked with aspect, which was not used as a covariate in these models. Canning *et al* (2008) found that steep north-facing slopes resulted in lower dolphin densities, and east-facing shallow slopes were associated with higher dolphin densities.

Compared to other species, there have been very few investigations of habitat use in white-beaked dolphins. Studies of this species to the west of Scotland (outside the North Sea ecoregion) have noted that white-beaked dolphins are predominantly found in waters less than 13^{0}C (MacLeod *et al*. 2008), and that in waters over 18^{0}C they are almost entirely absent, with a preference between 5^{0}C - 15^{0}C (Kinze 2018). This pattern appears to be supported by the strandings record, with fewer white-beaked dolphin strandings being found toward the south of the region where waters are warmer (IJsseldijk *et al*. 2018a). Other studies in the same area have linked white-beaked dolphins with a depth range of 106-135m and a distance from shore of 22-32km (Weir *et al*. 2009). On the east coast of Scotland, slope and aspect have been related to dolphin presence, as well as variation in temperature which reportedly explained almost 45% of the variation in observed group size; higher sea surface temperatures were linked with smaller group sizes (Canning *et al*. 2008). This species has been reported to be present where prey items congregate, in areas such as fronts, or where there is upwelling (Kinze 2018). Further afield, white-beaked dolphins in Greenland have been shown to prefer habitats with deep water over steep slopes (Hansen and Heide-Jørgensen 2013), implying that their distribution is prey-driven and not due to limits of the species physiology.

The prey model predictions were an acceptable reflection of the sightings data but were subject to a large amount of over-prediction. That the “best fish model”, which includes all fish combined into one model was the best for white-beaked dolphins is perhaps expected because this species preys on a variety of different species (Canning *et al*. 2008; Jansen *et al*. 2010; MacLeod 2013). However, there is also some regional specialisation. South-eastern North Sea white-beaked dolphins show a very strong preference for cod and whiting as prey (Jansen 2013). A model that can in some way approximate this is likely to do better at predicting density. In the 2016 model, higher numbers of dolphins were predicted by shallower slopes, being on the shallower side of and not too close to, the 50m isobath, low sprat energy, high herring energy, high whiting energy and proximity to sandeel grounds. It is possible that herring, whiting and sandeels may have been important prey species during July 2016. This corresponds to the preference for shallower waters shown from the environmental only model. The relationships with herring, sprat and sandeel covariates persist across all three models.

The 2005 model did not retain whiting but did retain cod. Cod energy of 4MJ resulted in the highest prediction of dolphins. No environmental covariates were retained, which is also true for the combined year model, suggesting that these are perhaps not important over long time periods, or at least explain less variability than the fish species.

4.3.4. Harbour porpoise

Harbour porpoises are found throughout the North Sea, particularly in the central and southern parts and this pattern is reflected in the predicted distributions provided by these models. In previous studies, covariates in harbour porpoise habitat models which have been found to explain variation in the data include proxies for primary productivity (Gilles *et al*., 2011), distance to coast (Marubini *et al*. 2009; Gilles *et al*. 2011; Booth *et al*. 2013), water depth (Marubini *et al*. 2009; Gilles *et al*. 2011; Booth *et al*. 2013), slope (Isojunno *et al*. 2012; Booth *et al*. 2013; Stalder *et al*. 2020), residual current (Gilles *et al*. 2011), maximum tidal current (Embling *et al*. 2010), distribution of herring (Sveegaard *et al*. 2012) and salinity (Van Beest et al. 2018). Residual current and tidal current data were not available for the full area, so these were not included as candidate covariates in this thesis. There are some shared predictors in the best-supported models here with previous studies, however. The 2016 model retained five covariates, including depth and slope in common with those earlier studies but also MLD, ADT and salinity. The 2005 model retained SDdepth, depth, distance to 50m isobath, ADT and MLD. Depth, slope and MLD were also retained in the combined year model, suggesting that these may be useful predictors over time.

Despite the number of retained covariates, the amount of deviance explained was low: only 9.3% for 2016 and 12.8% for 2005. There were considerably more sightings for harbour porpoise than there were for either of the other two species, and this might explain why so many more edf were used in the modelled relationships for the harbour porpoise models than for the other species, and possibly also why there were so many more covariates retained. Seabed topography (slope for 2016, SDDepth for 2005) maintained a linear relationship for both models. Despite the low levels of deviance explained, predicted density surfaces for both years reflected the sightings data well.

The use of prey covariates did not improve the predictions for harbour porpoises. The 2016 model retained slope, sprat and distance to sandeel grounds. As with the environmental model, these relationships used more edf than for other species, with only slope showing a linear relationship.

Highest levels of harbour porpoise predicted density was associated with shallow slope, mid-levels of sprat energy and proximity to sandeel grounds.

The 2005 model also retained slope as well as whiting. In this model, relationships were linear, and peak porpoise density was predicted by shallow slope and low levels of whiting energy.

The combined year model was a combination of the previous two, retaining the covariates from each model, namely slope, sprat, whiting and distance to sandeels.

That the prey models did not perform better is somewhat surprising, considering harbour porpoises have been shown to be susceptible to rapid loss of body condition during periods of fasting and are thought likely to have a requirement to consume prey on a daily basis, with Wisniewska *et al*. (2018) reporting almost continual foraging to fulfil their energy needs. Studies have found large proportions of sandeels in the diet of North Sea harbour porpoises (Santos *et al*. 2004; Jansen 2013), and a recent modelling framework suggests that harbour porpoises demonstrate a preference for sandeels as prey, even when other species are available (Ransijn *et al*. 2021). Sandeels were retained in two of the three models, but even so the predictions are no better than the environmental model. For several of the fish covariates, there was a negative relationship, with porpoise density being higher at lower energies of some prey species. This may be due to selection of specific size classes of prey by porpoises, which cannot be shown in the model energy surface. It is possible that the scale at which these models are run is too large to capture the detail for fine-scale prey-related interactions.

Marine ecosystems, particularly the North Sea, are constantly changing, and cetacean species – which can be very wide ranging and are highly mobile –are able to respond to this variability by changing their distribution patterns (Forney 2000), which can make representing the processes driving this distribution and establishing what processes are the most critical very challenging.

A number of harbour porpoise spatial modelling studies have been conducted with findings suggesting a range of different parameters may all be significant at explaining harbour porpoise occurrence, depending on the area and the time of year. Covariates which have been found to be important predictors in harbour porpoise habitat models include proxies for primary productivity (Gilles *et al*., 2011), distance to coast (Marubini *et al*. 2009; Gilles *et al*. 2011; Booth *et al*. 2013), water depth (Marubini *et al*. 2009; Gilles *et al*. 2011; Booth *et al*. 2013), slope (Isojunno *et al*. 2012; Booth *et al*. 2013; Stalder *et al*. 2020), residual current (Gilles *et al*. 2011), maximum tidal current (Embling *et al*. 2010), distribution of herring (Sveegaard *et al*. 2012) , distribution of sandeel grounds

(Giles *et al*., 2016) and relatively low salinity (Stalder *et al*. 2020); whilst movement models also indicated the presence of foraging in shallower and more saline waters (van Beest *et al*. 2018).

A large scale modelling study by Gilles et al. (2016) produced seasonal models of a very similar area to that covered by this investigation. The SCANS-III design-based abundance estimate for this region is 347,399 (95% CI = 289-687 – 416,609) (Table 4.1-1), and Gilles et al. (2016) produced a model based estimate of summer distribution which is comparable, 361,146 animals (95% CI = 159,264 – 329,022), although it should be noted that the Gilles et al. (2016) study was completed prior to the collection of data on the SCANS-III survey, so these time periods do not overlap. Their best model retained depth, distance to coast and distance to sandeel ground as well as day length, SST-SD Time (SST for 8- d period ending on each survey day) and SST- SD- Space20 (SST variability in 41 × 41 km box), which were not included in models run as part of this thesis. The most comparable time period included in this modelling is the 2005 model. The predicted density surfaces from the environmental model and the prey model are shown in Figure 4.3-1 alongside the predicted density surface for summer from Gilles et al. (2016) for comparison. There are some important things to note when comparing these, namely that the Gilles et al. (2016) model contains an XY smooth, which is not included in the models generated in this chapter. The only shared parameter between the environmental model from the prey model and the Gilles et al. (2016) model is depth, and with the prey model, the distance to sandeel grounds was the only shared covariate. The predictions generated by the models are quite different, but since the Gilles et al. (2016) model was run on a much larger dataset, containing data from much finer-scale surveys, and also included different covariates, as well as a XY smooth, this is perhaps unsurprising.

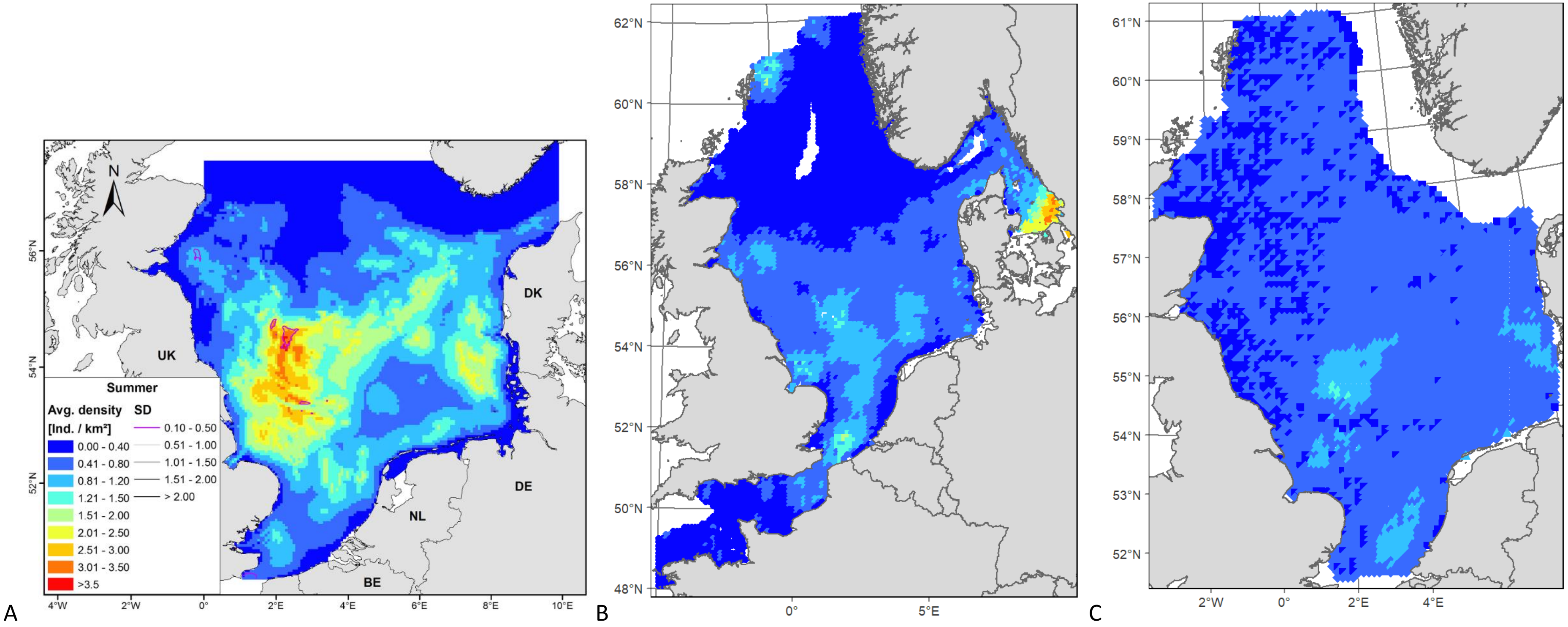

Figure 4.3-1 : Maps of predicted harbour porpoise distribution in the North Sea generated for data collected up to and including SCANS-II by Gilles et al (2016) (A) and the environmental (B) and prey(C) models for 2005 generated in this study. Maps B & C are the same as that presented in Figure 4.1-6 and Figure 4.2-7 but recoloured to match the scale of the map from Gilles et al. (2016). Please note the slight differences in study regions.

4.3.5. Conclusions

The environmental models produced in this chapter provide reasonable fits to the data. Despite small numbers of datapoints in the case of minke whales and white-beaked dolphins, the model diagnostics are acceptable, and the predictions generally fit the observed data. Overall, the 2005 data fit less well than the 2016 data, which may be due to less good survey coverage across the area. Some of the covariates persisted in multi-year models, which may indicate that these are covariates linked to distribution of these species.

Whilst comparing models with and without XY smooths directly is difficult, due to the amount of variability explained by the XY covariates, mixed layer depth and sea surface height have been retained in all minke whale models using environmental covariates. White beaked dolphin models show less persistent covariates, with none of them present in all models run so far. For harbour porpoises, for which there is by far the largest amount of data, MLD, depth persisted across all North Sea environmental models, and depth was also retained in the full survey model from Chapter 3, again possibly indicating the value of this covariate in predicting distribution.

The prey models overall performed much less well than the environmental models. There are multiple reasons for this. The prey species energy layers were prepared using only small fish (<40cm, (Ransijn et al. 2019), as they were produced with harbour porpoises in mind. It is possible that they are not representative of the size classes of prey being targeted. Only a select number of species were available as prey energy surfaces, which may not reflect the preferred prey of all three of these cetacean species, which are all known to take a wide variety of prey species.

It is also worth noting that the prey surfaces represent an average of prey energy over a grid cell. The prediction grid used for these density surfaces is at a finer scale than that at which the cetacean data are modelled (1km x 1km for the prey grid vs 10km x 10km for the cetacean grid), but that cetacean species are likely selecting prey at a finer scale than can be represented by these models.

For these three species, it seems that going forward the best focus for building a predictive model would not be to focus on prey, but instead to refine the environmental model further. Aside from the XY smooth, future work could investigate the use of further interaction terms with environmental covariates with clear geographical variation, for example a SST: latitude interaction term (as per (Becker et al. 2019)). It has been suggested that models incorporating static and dynamic predictors, as well as more complicated interaction terms may be more appropriate for predicting changes in distribution with changing conditions, so this is certainly an area that would merit future investigations (Araujo and New 2007; Gritti et al. 2013).

4.4. Literature Cited.

Alvarez-Fernandez, S., Lindeboom, H., and Meesters, E. 2012. Temporal changes in plankton of the North Sea: community shifts and environmental drivers. Mar. Ecol. Prog. Ser. 462: 21–38. doi:10.3354/meps09817.

Andersen, L., Born, E., Dietz, R., Haug, T., Øien, N., and Bendixen, C. 2003. Genetic population structure of minke whales *Balaenoptera acutorostrata* from Greenland, the North East Atlantic and the North Sea probably reflects different ecological regions. Mar. Ecol. Prog. Ser. 247: 263–280. doi:10.3354/meps247263.

Anderwald, P., Evans, P., Dyer, R., Dale, A., Wright, P., and Hoelzel, A. 2012. Spatial scale and environmental determinants in minke whale habitat use and foraging. Mar. Ecol. Prog. Ser. 450: 259–274. doi:10.3354/meps09573.

Anderwald, P., and Evans, P.G.H. 2007. Minke whale populations in the North Atlantic: An overview with special reference to UK waters. *In* An integrated approach to non-lethal research on minke whales in European waters. San Sebastian. pp. 8–13.

Araujo, M., and New, M. 2007. Ensemble forecasting of species distributions. Trends Ecol. Evol. 22(1): 42–47. doi:10.1016/j.tree.2006.09.010.

Arso Civil, M., Quick, N.J., Cheney, B., Pirotta, E., Thompson, P.M., and Hammond, P.S. 2019. Changing distribution of the east coast of Scotland bottlenose dolphin population and the challenges of area-based management. Aquat. Conserv. Mar. Freshw. Ecosyst. 29(S1): 178–196. doi:10.1002/aqc.3102.

Barry, S., and Elith, J. 2006. Error and uncertainty in habitat models. J. Appl. Ecol. 43(3): 413–423. doi:10.1111/j.1365-2664.2006.01136.x.

Becker, E.A., Forney, K.A., Redfern, J.V., Barlow, J., Jacox, M.G., Roberts, J.J., and Palacios, D.M. 2019. Predicting cetacean abundance and distribution in a changing climate. Divers. Distrib. 25(4): 626–643. doi:10.1111/ddi.12867.

van Beest, F.M., Teilmann, J., Dietz, R., Galatius, A., Mikkelsen, L., Stalder, D., Sveegaard, S., and Nabe-Nielsen, J. 2018. Environmental drivers of harbour porpoise fine-scale movements. Mar. Biol. 165(5): 95. doi:10.1007/s00227-018-3346-7.

de Boer, M. 2010. Spring distribution and density of minke whale *Balaenoptera acutorostrata* along an offshore bank in the central North Sea. Mar. Ecol. Prog. Ser. 408: 265–274. doi:10.3354/meps08598.

Booth, C., Embling, C., Gordon, J., Calderan, S., and Hammond, P. 2013. Habitat preferences and distribution of the harbour porpoise *Phocoena phocoena* west of Scotland. Mar. Ecol. Prog. Ser. 478: 273–285. doi:10.3354/meps10239.

Bruge, A., Alvarez, P., Fontán, A., Cotano, U., and Chust, G. 2016. Thermal Niche Tracking and Future Distribution of Atlantic Mackerel Spawning in Response to Ocean Warming. Front. Mar. Sci. 3. Available from https://www.frontiersin.org/articles/10.3389/fmars.2016.00086 [accessed 7 August 2022].

Canning, S.J., Santos, M.B., Reid, R.J., Evans, P.G.H., Sabin, R.C., Bailey, N., and Pierce, G.J. 2008. Seasonal distribution of white-beaked dolphins (*Lagenorhynchus albirostris*) in UK waters with new information on diet and habitat use. J. Mar. Biol. Assoc. U. K. 88(6): 1159–1166. doi:10.1017/S0025315408000076.

Cheney, B., Thompson, P.M., Ingram, S.N., Hammond, P.S., Stevick, P.T., Durban, J.W., Culloch, R.M., Elwen, S.H., Mandleberg, L., Janik, V.M., Quick, N.J., ISLAS-Villanueva, V., Robinson, K.P., Costa, M., Eisfeld, S.M., Walters, A., Phillips, C., Weir, C.R., Evans, P.G.H., Anderwald, P., Reid, R.J., Reid, J.B., and Wilson, B. 2013. Integrating multiple data sources to assess the distribution and abundance of bottlenose dolphins *Tursiops truncatus* in Scottish waters: Abundance of bottlenose dolphins around Scotland. Mammal Rev. 43(1): 71–88. doi:10.1111/j.1365-2907.2011.00208.x.

Clark, R.A., and Frid, C.L. 2001. Long-term changes in the North Sea ecosystem. Environ. Rev. 9(3): 131–187. doi:10.1139/a01-005.

Cooke, J.G. 2018. *Balaenoptera acutorostrata*: The IUCN Red List of Threatened Species. International Union for Conservation of Nature. doi:10.2305/IUCN.UK.2018-2.RLTS.T2474A50348265.en.

Couperus, A.S. 1997. Interactions Between Dutch Midwater Trawl and Atlantic White-sided Dolphins(*Lagenorhynchus acutus*) Southwest of Ireland. J. Northwest Atl. Fish. Sci. 22: 209–218. doi:10.2960/J.v22.a16.

Doniol-Valcroze, T., Berteaux, D., Larouche, P., and Sears, R. 2007. Influence of thermal fronts on habitat selection by four rorqual whale species in the Gulf of St. Lawrence. Mar. Ecol. Prog. Ser. 335: 207–216. doi:10.3354/meps335207.

Edwards, M. 2001. Long-term and regional variability of phytoplankton biomass in the Northeast Atlantic (1960–1995). ICES J. Mar. Sci. 58(1): 39–49. doi:10.1006/jmsc.2000.0987.

Edwards, M., Beaugrand, G., Reid, P., Rowden, A., and Jones, M. 2002. Ocean climate anomalies and the ecology of the North Sea. Mar. Ecol. Prog. Ser. 239: 1–10. doi:10.3354/meps239001.

Embling, C.B., Gillibrand, P.A., Gordon, J., Shrimpton, J., Stevick, P.T., and Hammond, P.S. 2010. Using habitat models to identify suitable sites for marine protected areas for harbour porpoises (*Phocoena phocoena*). Biol. Conserv. 143(2): 267–279. doi:10.1016/j.biocon.2009.09.005.

Evans, P.G.H., Anderwald, P., and Baines, M.E. 2003. UK Cetacean Status Review. Seawatch Foundation.

Fall, J., and Skern-Mauritzen, M. 2013. White-beaked dolphin distributions and prey associations in the Barents Sea. *In* Towards a conservation strategy for white-beaked dolphins in the Northeast Atlantic. pp. 91–98.

Forney, K.A. 2000. Environmental Models of Cetacean Abundance: Reducing Uncertainty in Population Trends. Conserv. Biol. 14(5): 1271–1286. doi:10.1046/j.1523-1739.2000.99412.x.

Gilles, A., Adler, S., Kaschner, K., Scheidat, M., and Siebert, U. 2011. Modelling harbour porpoise seasonal density as a function of the German Bight environment: implications for management. Endanger. Species Res. 14(2): 157–169. doi:10.3354/esr00344.

Gilles, A., Viquerat, S., Becker, E.A., Forney, K.A., Geelhoed, S.C.V., Haelters, J., Nabe-Nielsen, J., Scheidat, M., Siebert, U., Sveegaard, S., Beest, F.M., Bemmelen, R., and Aarts, G. 2016. Seasonal habitat-based density models for a marine top predator, the harbor porpoise, in a dynamic environment. Ecosphere 7(6). doi:10.1002/ecs2.1367.

Gritti, E.S., Gaucherel, C., Crespo-Perez, M.-V., and Chuine, I. 2013. How Can Model Comparison Help Improving Species Distribution Models? PLoS ONE 8(7): e68823. doi:10.1371/journal.pone.0068823.

Guisan, A., Edwards, T.C., and Hastie, T. 2002. Generalized linear and generalized additive models in studies of species distributions: setting the scene. Ecol. Model. 157(2–3): 89–100. doi:10.1016/S0304-3800(02)00204-1.

Gutiérrez-Muñoz, P., Walters, A.E.M., Dolman, S.J., and Pierce, G.J. 2021. Patterns and Trends in Cetacean Occurrence Revealed by Shorewatch, a Land-Based Citizen Science Program in Scotland (United Kingdom). Front. Mar. Sci. 8: 642386. doi:10.3389/fmars.2021.642386.

Hammond, P., Lacey, C., Gilles, A., Viquerat, S., Börjesson, P., Herr, H., Macleod, K., Ridoux, V., Santos, M., Teilmann, J., Vingada, J., and Øien, N. 2021. Estimates of cetacean abundance in European Atlantic waters in summer 2016 from the SCANS-III aerial and shipboard surveys. Final project report. https://scans3.wp.st-andrews.ac.uk/files/2021/06/SCANS-III_design-based_estimates_final_report_revised_June_2021.pdf

Hammond, P.S., Berggren, P., Benke, H., Borchers, D.L., Collet, A., Jørgensen, M.P.H.-, Heimlich, S., Hiby, A.R., Leopold, M.F., and Øien, N. 2002. Abundance of Harbour Porpoise and Other Cetaceans in the North Sea and Adjacent Waters. J. Appl. Ecol. 39(2): 361–376.

Hammond, P.S., Macleod, K., Berggren, P., Borchers, D.L., Burt, L., Cañadas, A., Desportes, G., Donovan, G.P., Gilles, A., Gillespie, D., Gordon, J., Hiby, L., Kuklik, I., Leaper, R., Lehnert, K., Leopold, M., Lovell, P., Øien, N., Paxton, C.G.M., Ridoux, V., Rogan, E., Samarra, F., Scheidat, M., Sequeira, M., Siebert, U., Skov, H., Swift, R., Tasker, M.L., Teilmann, J., Van Canneyt, O., and Vázquez, J.A. 2013. Cetacean abundance and distribution in European Atlantic shelf waters to inform conservation and management. Biol. Conserv. 164: 107–122. doi:10.1016/j.biocon.2013.04.010.

Hansen, R.G., and Heide-Jørgensen, M.P. 2013. Spatial trends in abundance of long-finned pilot whales, white-beaked dolphins and harbour porpoises in West Greenland. Mar. Biol. 160(11): 2929–2941. doi:10.1007/s00227-013-2283-8.

Hastie, G.D., Wilson, B., and Thompson, P.M. 2003. Fine-scale habitat selection by coastal bottlenose dolphins: application of a new land-based video-montage technique. Can. J. Zool. 81(3): 469–478. doi:10.1139/z03-028.

Huthnance, J.M. 1991. Physical Oceanography of the North Sea. Ocean Shorel. Manag. 16: 199–231.

ICES. 2014a. ICES FishMap Species factsheet- Whiting. ICES. Available from https://www.ices.dk/about-ICES/projects/EU-RFP/EU%20Repository/ICES%20FIshMap/ICES%20FishMap%20species%20factsheet-whiting.pdf.

ICES. 2014b. ICES FishMap Species factsheet - Haddock. Available from https://www.ices.dk/about-ICES/projects/EU-RFP/EU%20Repository/ICES%20FIshMap/ICES%20FishMap%20species%20factsheet-haddock.pdf.

ICES. 2020. Greater North Sea Ecoregion - Ecosystem overview. ICES. doi:10.17895/ICES.ADVICE.7632.

IJsseldijk, L.L., Brownlow, A., Davison, N.J., Deaville, R., Keijl, G., and Siebert, U. 2018a. Spatiotemporal trends in white-beaked dolphin strandings along the North Sea coast from 1991–2017. : 11.

IJsseldijk, L.L., van Neer, A., Deaville, R., Begeman, L., van de Bildt, M., van den Brand, J.M.A., Brownlow, A., Czeck, R., Dabin, W., ten Doeschate, M., Herder, V., Herr, H., IJzer, J., Jauniaux, T., Jensen, L.F., Jepson, P.D., Jo, W.K., Lakemeyer, J., Lehnert, K., Leopold, M.F., Osterhaus, A., Perkins, M.W., Piatkowski, U., Prenger-Berninghoff, E., Pund, R., Wohlsein, P., Gröne, A., and Siebert, U. 2018b. Beached bachelors: An extensive study on the largest recorded sperm whale Physeter macrocephalus mortality event in the North Sea. PLOS ONE 13(8): e0201221. doi:10.1371/journal.pone.0201221.

Isojunno, S., Matthiopoulos, J., and Evans, P. 2012. Harbour porpoise habitat preferences: robust spatio-temporal inferences from opportunistic data. Mar. Ecol. Prog. Ser. 448: 155–170. doi:10.3354/meps09415.

Janik, V.M. 2000. Source levels and the estimated active space of bottlenose dolphin (Tursiops truncatus) whistles in the Moray Firth, Scotland. J. Comp. Physiol. A 186(7–8): 673–680. doi:10.1007/s003590000120.

Jansen, O.E. 2013. Fishing for Food: feeding ecology of harbour porpoises Phocoena phocoena and white-beaked dolphins *Lagenorhynchus albirostris* in Dutch waters. PhD, Wageningen University. Available from https://edepot.wur.nl/249934.

Jansen, O.E., Leopold, M.F., Meesters, E.H.W.G., and Smeenk, C. 2010. Are white-beaked dolphins *Lagenorhynchus albirostris* food specialists? Their diet in the southern North Sea. J. Mar. Biol. Assoc. U. K. 90(8): 1501–1508. doi:10.1017/S0025315410001190.

Jensen, H., Rindorf, A., Wright, P.J., and Mosegaard, H. 2011. Inferring the location and scale of mixing between habitat areas of lesser sandeel through information from the fishery. ICES J. Mar. Sci. 68(1): 43–51. doi:10.1093/icesjms/fsq154.

Kinze, C.C. 2018. White-beaked Dolphin. *In* Encyclopedia of Marine Mammals. Elsevier. pp. 1077–1079. doi:10.1016/B978-0-12-804327-1.00274-0.

Kinze, C.C., Czeck, R., Herr, H., and Siebert, U. 2021. Cetacean strandings along the German North Sea coastline 1604–2017. J. Mar. Biol. Assoc. U. K. 101(3): 483–502. doi:10.1017/S0025315421000503.

Laane, R. 1996. Changes and causes of variability in salinity and dissolved inorganic phosphate in the Irish Sea, English Channel, and Dutch coastal zone. ICES J. Mar. Sci. 53(6): 933–944. doi:10.1006/jmsc.1996.0115.

Lindstrøm, U. 2002. Predation on herring, *Clupea harengus*, by minke whales, Balaenoptera acutorostrata, in the Barents Sea. ICES J. Mar. Sci. 59(1): 58–70. doi:10.1006/jmsc.2001.1135.

Lindstrøm, U., Haug, T., and Nilssen, K.T. 1997. Diet studies based on contents from two separate stomach compartments of northeast Atlantic minke whales *Balaenoptera acutorostrata*. Sarsia 82(1): 63–68. doi:10.1080/00364827.1997.10413638.

Loveland, T.R., and Merchant, J.M. 2004. Ecoregions and Ecoregionalization: Geographical and Ecological Perspectives. Environ. Manage. 34(1): S1–S13. doi:10.1007/s00267-003-5181-x.

MacLeod, C.D. 2013. White-beaked Dolphins in the Northeast Atlantic: A brief review of their ecology and potential threats to conservation status. *In* Towards a Conservation Strategy for White-beaked Dolphins in the Northeast Atlantic. pp. 26–36.

MacLeod, C.D., Bannon, S.M., Brereton, T., and Wall, D. 2007. Using passenger ferries to study seasonal patterns of minke whale occurrence in NW Europe. *In* An integrated approach to non-lethal research on minke whales in European Waters. San Sebastian. pp. 32–37.

MacLeod, C.D., Weir, C.R., Santos, M.B., and Dunn, T.E. 2008. Temperature-based summer habitat partitioning between white-beaked and common dolphins around the United Kingdom and Republic of Ireland. J. Mar. Biol. Assoc. U. K. 88(6): 1193–1198. doi:10.1017/S002531540800074X.

Macleod, K., Fairbairns, R., Gill, A., Fairbairns, B., Gordon, J., Blair-Myers, C., and Parsons, E. 2004. Seasonal distribution of minke whales *Balaenoptera acutorostrata* in relation to physiography and prey off the Isle of Mull, Scotland. Mar. Ecol. Prog. Ser. 277: 263–274. doi:10.3354/meps277263.

Marubini, F., Gimona, A., Evans, P., Wright, P., and Pierce, G. 2009. Habitat preferences and interannual variability in occurrence of the harbour porpoise *Phocoena phocoena* off northwest Scotland. Mar. Ecol. Prog. Ser. 381: 297–310. doi:10.3354/meps07893.

Mehl, S., and Westgard, T. 1983. The diet and consumption of mackerel in the North Sea (A preliminary report). ICES.

Meier, S., Falk-Petersen, S., Aage Gade-Sørensen, L., Greenacre, M., Haug, T., and Lindstrøm, U. 2016. Fatty acids in common minke whale (*Balaenoptera acutorostrata*) blubber reflect the feeding area and food selection, but also high endogenous metabolism. Mar. Biol. Res. 12(3): 221–238. doi:10.1080/17451000.2015.1118513.

Naud, M.-J., Long, B., Brethes, J.-C., and Sears, R. 2003. Influences of underwater bottom topography and geomorphology on minke whale (*Balaenoptera acutorostrata*) distribution in the Mingan Islands (Canada). J. Mar. Biol. Assoc. U. K. 83: 889–896.

Niæss, A., Haug, T., and Nilssen, E.M. 1998. Seasonal variation in body condition and muscular lipid contents in northeast Atlantic minke whale, *Balaenoptera acutorostrata*. Sarsia 83(3): 211–218. doi:10.1080/00364827.1998.10413682.

Nielsen, N., Teilmann, J., Sveegaard, S., Hansen, R., Sinding, M., Dietz, R., and Heide-Jørgensen, M. 2018. Oceanic movements, site fidelity and deep diving in harbour porpoises from Greenland show limited similarities to animals from the North Sea. Mar. Ecol. Prog. Ser. 597: 259–272. doi:10.3354/meps12588.

Olsen, E., and Holst, J.C. 2001. A note on common minke whale (*Balaenoptera acutorostrata*) diets in the Norwegian Sea and the North Sea. J. Cetacean Res. Manag. 3(2): 179–183.

Perrin, W.F., Mallette, S.D., and Brownell, R.L. 2018. Minke Whales. *In* Encyclopedia of Marine Mammals. Elsevier. pp. 608–613. doi:10.1016/B978-0-12-804327-1.00175-8.

Peschko, V., Ronnenberg, K., Siebert, U., and Gilles, A. 2016. Trends of harbour porpoise (*Phocoena phocoena*) density in the southern North Sea. Ecol. Indic. 60: 174–183. doi:10.1016/j.ecolind.2015.06.030.

Pierce, G.J., Santos, M.B., Reid, R.J., Patterson, I.A.P., and Ross, H.M. 2004. Diet of minke whales *Balaenoptera acutorostrata* in Scottish (UK) waters with notes on strandings of this species in Scotland 1992–2002. J. Mar. Biol. Assoc. U. K. 84(6): 1241–1244. doi:10.1017/S0025315404010732h.

Pribil, S., and Picman, J. 1997. The importance of using the proper methodology and spatial scale in the study of habitat selection by birds. Can. J. Zool. 75(11): 1835–1844. doi:10.1139/z97-813.

Ransijn, J., Lacey, C., Smout, S., Hammond, P.S., and Booth, C.G. 2020. Understanding changes in harbour porpoise density in the context of prey in the North Sea. JNCC Report.

Ransijn, J.M., Booth, C. & Smout, S.C. 2019. A calorific map of harbour porpoise prey in the North
Sea. JNCC Report No. 633. JNCC, Peterborough, ISSN 0963 8091.

Ransijn, J.M., Hammond, P.S., Leopold, M.F., Sveegaard, S., and Smout, S.C. 2021. Integrating disparate datasets to model the functional response of a marine predator: A case study of harbour porpoises in the southern North Sea. Ecol. Evol. 11(23): 17458–17470. doi:10.1002/ece3.8380.

Reid, J.B., Evans, P.G.H., and Northridge, S.P. 2003a. Atlas of Cetacean distribution in north-west European waters. : 82.

Reid, P.C., and Edwards, M. 2001. Long-term changes in the pelagos, benthos and fisheries of the North Sea. Senckenberg. Maritima 31(2): 107–115. doi:10.1007/BF03043021.

Reid, P.C., Edwards, M., Beaugrand, G., Skogen, M., and Stevens, D. 2003b. Periodic changes in the zooplankton of the North Sea during the twentieth century linked to oceanic inflow: *Calanus* and oceanic inflow to the North Sea. Fish. Oceanogr. 12(4–5): 260–269. doi:10.1046/j.1365-2419.2003.00252.x.

Risch, D., Castellote, M., Clark, C.W., Davis, G.E., Dugan, P.J., Hodge, L.E., Kumar, A., Lucke, K., Mellinger, D.K., Nieukirk, S.L., Popescu, C.M., Ramp, C., Read, A.J., Rice, A.N., Silva, M.A., Siebert, U., Stafford, K.M., and Verdaat, H. 2014. Seasonal migrations of North Atlantic minke whales: novel insights from large-scale passive acoustic monitoring networks. : 17.

Robinson, K.P., Bamford, C.C.G., Brown, W.J., Culloch, R.M., Dolan, C.J., Hall, R., Russell, G., Sidiropoulos, T., Spinou, E., Sim, T.M.C., Stroud, E., Williams, G., and Haskins, G.N. 2021. Ecological habitat partitioning and feeding specialisations of coastal minke whales (*Balaenoptera acutorostrata*) using a designated MPA in northeast Scotland. preprint, Ecology. doi:10.1101/2021.01.25.428066.

Robinson, K.P., Tetley, M.J., and Mitchelson-Jacob, E.G. 2009. The distribution and habitat preference of coastally occurring minke whales (*Balaenoptera acutorostrata*) in the outer southern Moray Firth, northeast Scotland. J. Coast. Conserv. 13(1): 39–48. doi:10.1007/s11852-009-0050-2.

Salomon, J.-C., and Breton, M. 1993. An atlas of long-term currents in the Channel. Oceanol. Acta 16(5): 439–448.

Santos, M.B., and Pierce, G.J. 2003. The diet of harbour porpoise (*Phocoena phocoena)* in the northeast Atlantic. Oceanogr. Mar. Biol. Annu. Rev. 41: 355–390.

Santos, M.B., Pierce, G.J., Learmonth, J.A., Reid, R.J., Ross, H.M., Patterson, I.A.P., Reid, D.G., and Beare, D. 2004. Variability in the diet of harbour porpoises (*Phocoena phocoena*) in Scottish waters 1992-2003. Mar. Mammal Sci. 20(1): 1–27. doi:10.1111/j.1748-7692.2004.tb01138.x.

Schaffeld, T., Bräger, S., Gallus, A., Dähne, M., Krügel, K., Herrmann, A., Jabbusch, M., Ruf, T., Verfuß, U., Benke, H., and Koblitz, J. 2016. Diel and seasonal patterns in acoustic presence and foraging behaviour of free-ranging harbour porpoises. Mar. Ecol. Prog. Ser. 547: 257–272. doi:10.3354/meps11627.

Skaug, H.J., Gjosæter, H., Haug, T., Nilssen, K.T., and Lindstrøm, U. 1997. Do Minke Whales (*Balaenoptera acutorostrata*) Exhibit Particular Prey Preferences? J. Northwest Atl. Fish. Sci. 22: 91–104. doi:10.2960/J.v22.a8.

Smeenk, C. 1997. Strandings of sperm whales *Physeter macrocephalus* in the North Sea: history and patterns. Bull. Inst. R. Sci. Nat. Belg. 67: 15–28.

Solvang, H.K., Skaug, H.J., and Øien, N.I. 2015. Abundance estimates of common minke whales in the Northeast Atlantic based on survey data collected over the period 2008-2013. Paper submitted to the IWC Scientific Committee 66a, San Diego.

Stalder, D., van Beest, F., Sveegaard, S., Dietz, R., Teilmann, J., and Nabe-Nielsen, J. 2020. Influence of environmental variability on harbour porpoise movement. Mar. Ecol. Prog. Ser. 648: 207–219. doi:10.3354/meps13412.

Sveegaard, S., Nabe-Nielsen, J., Stæhr, K., Jensen, T., Mouritsen, K., and Teilmann, J. 2012. Spatial interactions between marine predators and their prey: herring abundance as a driver for the distributions of mackerel and harbour porpoise. Mar. Ecol. Prog. Ser. 468: 245–253. doi:10.3354/meps09959.

Tetley, M.J. 2004. The distribution and habitat preference of the North Atlantic minke whale (*Balaenoptera acutorostrata acutorostrata*) in the Southern Outer Moray Firth, NE Scotland. Master of Science, University of Wales, Bangor, Bangor.

Tetley, M.J., Mitchelson-Jacob, E.G., and Robinson, K.P. 2008. The summer distribution of coastal minke whales (*Balaenoptera acutorostrata*) in the southern outer Moray Firth, NE Scotland, in relation to co-occurring mesoscale oceanographic features. Remote Sens. Environ. 112(8): 3449–3454. doi:10.1016/j.rse.2007.10.015.

Turrell, W.R., Henderson, E.W., Slesser, G., Payne, R., and Adams, R.D. 1992. Seasonal changes in the circulation of the northern North Sea. Cont. Shelf Res. 12(2–3): 257–286. doi:10.1016/0278-4343(92)90032-F.

Víkingsson, G.A., Elvarsson, B.Þ., Ólafsdóttir, D., Sigurjónsson, J., Chosson, V., and Galan, A. 2014. Recent changes in the diet composition of common minke whales *(Balaenoptera acutorostrata)* in Icelandic waters. A consequence of climate change? Mar. Biol. Res. 10(2): 138–152. doi:10.1080/17451000.2013.793812.

Víkingsson, G.A., and Heide-Jørgensen, M.P. 2015. First indications of autumn migration routes and destination of common minke whales tracked by satellite in the North Atlantic during 2001-2011. Mar. Mammal Sci. 31(1): 376–385. doi:10.1111/mms.12144.

Weijerman, M., Lindeboom, H., and Zuur, A. 2005. Regime shifts in marine ecosystems of the North Sea and Wadden Sea. Mar. Ecol. Prog. Ser. 298: 21–39. doi:10.3354/meps298021.

Weir, C.R., Macleod, C.D., and Calderan, S.V. 2009. Fine-scale habitat selection by white-beaked and common dolphins in the Minch (Scotland, UK): evidence for interspecific competition or coexistence? J. Mar. Biol. Assoc. U. K. 89(5): 951–960. doi:10.1017/S0025315408003287.

Weir, C.R., Stockin, K.A., and Pierce, G.J. 2007. Spatial and temporal trends in the distribution of harbour porpoises, white-beaked dolphins and minke whales off Aberdeenshire (UK), north-western North Sea. J. Mar. Biol. Assoc. U. K. 87(1): 327–338. doi:10.1017/S0025315407052721.

Wiens, J.A. 1989. Spatial Scaling in Ecology. Funct. Ecol. 3(4): 385–397. [British Ecological Society, Wiley]. doi:10.2307/2389612.

Wilson, B., Thompson, P.M., and Hammond, P.S. 1997. Habitat Use by Bottlenose Dolphins: Seasonal Distribution and Stratified Movement Patterns in the Moray Firth, Scotland. J. Appl. Ecol. 34(6): 1365. doi:10.2307/2405254.

Windsland, K., Lindstrøm, U., Nilssen, K.T., and Haug, T. 2007. Relative abundance and size composition of prey in the common minke whale diet in selected areas of the northeastern Atlantic during 2000-04. J. Cetacean Res. Manag. 9(3): 167–178.

Wisniewska, D.M., Johnson, M., Teilmann, J., Siebert, U., Galatius, A., Dietz, R., and Madsen, P.T. 2018. High rates of vessel noise disrupt foraging in wild harbour porpoises. Proc. R. Soc. B Biol. Sci. 285: 10. doi:http://dx.doi.org/10.1098/rspb.2017.2314.

5. Cetaceans of the Celtic Sea and Bay of Biscay & Iberian Peninsula ecoregions

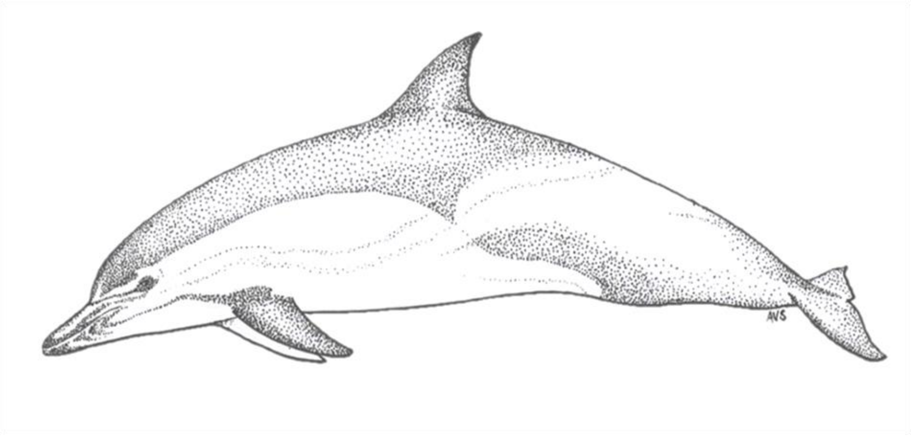

Common dolphin sketch, courtesy of Anni Sharpe

A focus on five of the species found in the Celtic Sea and Bay of Biscay Ecoregions; do the factors affecting their distribution differ, as compared to the wider area? Do they differ between these two ecoregions? Have they changed between 2005 and 2016?

5.1 Introduction

Following on from the investigations of the Greater North Sea ecoregion in chapter 4, this chapter continues the ecoregion scale investigations to look at cetacean distribution towards the western edge of the survey region. This chapter compares models using abiotic for five species of cetacean, common within these ecoregions. These are the Atlantic white-sided dolphin (*Lagenorynchus acutus*), common bottlenose dolphin (*Tursiops truncatus*), common dolphin (*Delphinus delphis*), striped dolphin (*Stenella coerualba*) and fin whale (*Balaenoptera physalus*).

5.1.1 Physical regional description

The work in this chapter is linked to two different ecoregions – the Celtic Seas ecoregion, and the Bay of Biscay & Iberian Peninsula ecoregion (hereafter Bay of Biscay) (**Figure 5.1-1**).

The Celtic Seas ecoregion extends from Shetland to Brittany and contains both coastal seas and deeper Atlantic Ocean regions (ICES, 2020a). It has an extensive continental self-area (OSPAR Commission, 2000), with a steep drop off. The ecoregion has several notable bathymetric features; the western part of the shelf edge contains the Porcupine Sea bight, north of which is Porcupine Bank, an area of relatively shallow water (200m depth), approximately 120 miles west of Ireland. To the North of Porcupine Bank is the Rockall Trough, a deep water feature running approximately southwest to northeast (Mason et al., 2006)(**Figure 5.1-2**).

The Bay of Biscay ecoregion is characterised by a wide shelf in most of the region, in which upwelling events are known to occur during the summer. There are also some low salinity regions associated with river outflows. There is marked seasonal mixing and stratification, as is typical for temperate seas, although the over-shelf upwelling is wind driven. In conjunction with the tidal processes of the region, this results in increased productivity, but also a large variation, as the offshore habitats are instead shaped by the Atlantic Ocean (ICES, 2020b).

The temperature across both regions varies between 7 and 15^{0}c, and the salinity sits at a mean of 35 PSU or higher throughout the water column (EEA 2017). Primary productivity increases from approximately 45g carbon/m^2 in the south of the region to 90g carbon/m^2 over the summer season in the north of the region. The main large-scale current is the North Atlantic Current, which becomes the North Atlantic Drift Current (Mason et al., 2006).

The two ecoregions are quite different, but many of the cetaceans that inhabit these two regions have ranges that span both, making it more appropriate to assess the two together than to separate them.

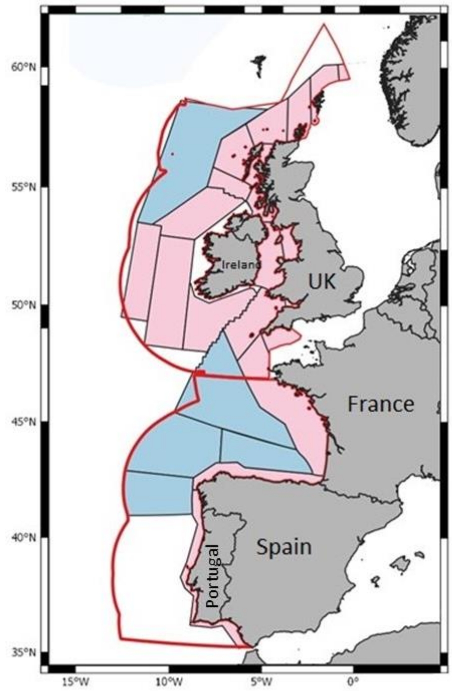

Figure 5.1-1: Location of the Celtic Sea ecoregion (top area with red boundary) and the Bay of Biscay ecoegion (lower area with red boundary) in comparison to the 2016 survey areas. Areas surveyd by ship are shown in blue, and areas survey by air are shown in pink. CRS: EPSG 32630.

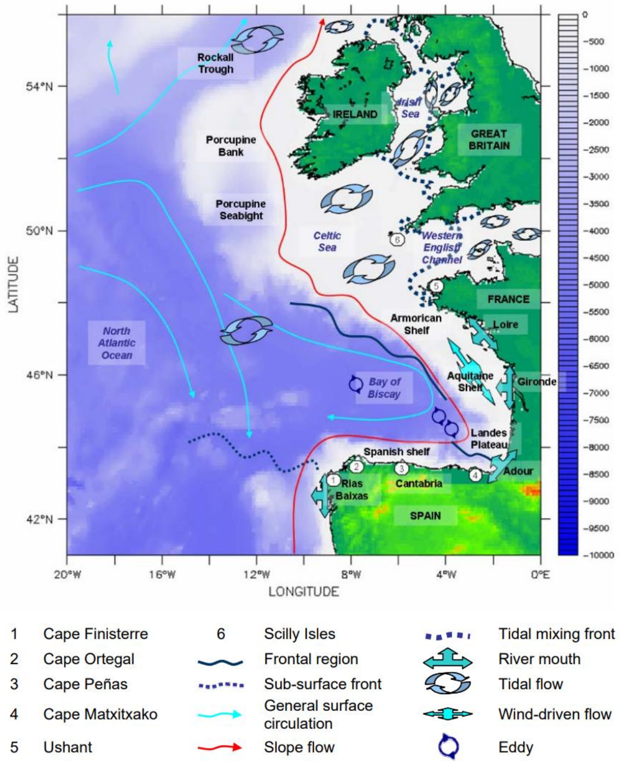

Figure 5.1-2 General diagram showing the main features of the Celtic Sea and Bay of Biscay. Taken from Mason et al., 2006, page 17.

5.1.2 Cetaceans in the study region

At least 25 different species have been recorded in these waters (Hammond et al., 2009, 2013; Reid et al., 2003; Rogan et al., 2018; Wall et al., 2013) and, of these, at least 15 are considered to be resident (Reid et al., 2003; Wall et al., 2013). Three of the shelf species have already been considered in chapter 3, and this chapter will focus on five of the species which are more commonly recorded in the deeper, more offshore western regions of the European Atlantic study area. Whilst other species were recorded during the surveys of these areas, these are the species which dominated the sightings record, and for which there are sufficient data to complete analyses. As with all species investigated in this thesis, the study area, although large, covers only a small section of the full range for these species.

5.1.2.1 Atlantic white-sided dolphin – Lagenorhynchus acutus

Atlantic white-sided dolphins (hereafter white-sided dolphins) are regularly sighted on surveys of this region, most commonly over the edge of continental shelf and slope, extending into the deeper, more oceanic areas (Hammond et al., 2009; MacLeod et al., 2007; Macleod, 2004; Wall et al., 2006; Weir et al., 2001).

Diet studies have concluded that white-sided dolphins show a preference for an oceanic and continental slope diet, which varies in composition depending on whether the samples come from adults or juveniles, with juvenile dolphins diet containing mainly mesopelagic prey and blue whiting, whilst mackerel dominated the adult diet (Hernandez-Milian et al., 2016). Capelin, lanternfish and *Gonatus* squid species have also been positively correlated with white-sided dolphin presence (Doksæter et al., 2008).

5.1.2.2 Bottlenose dolphin – Tursiops truncatus

Bottlenose dolphins have been described as belonging to either a coastal or an offshore ecotype in many areas worldwide (Perrin et al., 2011; Rosel et al., 2009; Tezanos-Pinto et al., 2009), including in the study area (Louis et al., 2014; Oudejans et al., 2015).

Characterisation of the two ecotypes can be morphological (e.g. Perrin et al., 2011) and genetic (e.g. Oudejans et al., 2015; Tezanos-Pintos et al., 2009); although field identification can be difficult (Simões-Lopes et al., 2019). Ecotypes often result from niche specialization (Louis et al., 2014). In bottlenose dolphins, the coastal ecotype is characterized by relatively high site fidelity, whereas oceanic ecotype dolphins tend towards low-site fidelity and more extensive movement patterns (Oudejans et al., 2015). It would be expected that the factors driving the distribution of the coastal and offshore ecotypes of bottlenose dolphins would differ.

Coastal bottlenose dolphins in the region have been studied in several key locations where they demonstrate high levels of site fidelity. These locations include Cardigan Bay, Wales (e.g. Bristow and Rees, 2001; Simon et al., 2010), the Sound of Barra, Scotland (Grellier and Wilson, 2003), the Shannon Estuary, Ireland (e.g. Berrow, 2012; Ingram and Rogan, 2002) and the Sado Estuary, Portugal (e.g. Gaspar, 2003; Harzen, 1998). Large scale surveys of the sort analysed in this thesis are not designed to capture the detail of small patchy populations (Hammond et al., 2014), such as coastal bottlenose dolphins. However, due to the difficulties in telling which ecotype an animal belongs to in the field, both coastal and offshore ecotypes may be represented in the data collected. Due to the locations of the majority of the sightings Figure 5.3-5 a & d), it is likely that these primarily represent offshore bottlenose dolphins.

5.1.2.3 Common dolphin – *Delphinus delphis*

The common dolphin is one of the most frequently sighted cetacean species throughout the Celtic Sea and Bay of Biscay ecoregions (Hammond et al., 2021, 2009; Laran et al., 2017; Rogan et al., 2018), although distribution can be patchy and is known to change year on year (Moura et al., 2012).

Common dolphin distribution around the Iberian Peninsula has been found to be best predicted by chlorophyll concentration. Not because the chlorophyll itself was important but, it was suggested, due to it acting as a proxy for pelagic schooling fish, a known prey type of common dolphins in this area (Moura et al., 2012; Pusineri et al., 2007). Chlorophyll has also been linked to common dolphin abundance in the Alboran Sea (Cañadas and Hammond, 2008). Moura et al (2012) suggest that common dolphins may be an “ecological specialist” with diet being restricted to small pelagic schooling fish. These prey species are filter feeders and tend to occur in nutrient-rich waters (Amaral et al., 2012)

5.1.2.4 Striped dolphin – *Stenella coerualba*

Striped dolphins are typically found off the continental shelf, in the southern part of the study area (Hammond et al., 2021, 2009; Kiszka et al., 2007; Laran et al., 2017; Rogan et al., 2018)).

Stomach content analysis of stranded animals from the Bay of Biscay has revealed a diet of fish, cephalopods and crustaceans, with lanternfish featuring prominently along with *Teuthowenia megalops* and *Histioteuthis* spp of squid. Striped dolphins may be feeding at depths of between 200-700m (Archer and Perrin, 1999). The majority of feeding activity potentially takes place at night or at dusk (Ringelstein et al., 2006) when prey items may be migrating closer to the surface. Striped dolphins are known to be able to utilise prey resources from a variety of different habitats, including neritic and coastal prey species as well as the more usual oceanic prey (Spitz et al., 2006)

5.1.2.5 Fin whale – Balaenoptera physalus

The Bay of Biscay represents an important area for fin whales during the summer months (Hammond et al., 2021, 2009; Rogan et al., 2018). Unlike the other species discussed so far, this species is characterized by large seasonal migrations. As such, their habitat preferences are likely to change spatio-temporally. The analysis presented here is relevant only to their summer distribution. There is evidence that some animals remain in the area year-round, however (Clark and Charif, 1998). In the northern part of the Celtic Sea ecoregion, animals are most often seen in waters more than 1000m deep (Weir et al., 2001).

5.1.3 Chapter aims

This chapter aims to explore the relationships between five different species of cetacean and different aspects of their environment. To do this, I have used explanatory (Guisan *et al*. 2002) generalised additive models (GAMs) to statistically explore the strength of the relationship between animal density and a variety of environmental – *explanatory* – variables, including sea surface temperature, depth, distance to the a variety of bathymetric features (Section 5.2.1.1) , salinity and seabed rugosity (modelled via slope and standard deviation of depth within a grid cell), hereafter termed “environmental models”. As noted in previous chapters, these variables are frequently selected when modelling marine mammals as proxies for prey data because data on prey species themselves can be very hard to obtain. It is also acknowledged that these may not be the only drivers of cetacean distribution. As with chapter 4, an ecoregion approach has been used to define the area of investigation. The distribution of the majority of the species described in this chapter spans two ecoregions within the study area (the Celtic Sea ecoregion and the Bay of Biscay ecoregion), so these are both considered here. The modelling attempts to take account of this by including ecoregion as a categorical variable; retention of this variable in the model implies that there is a difference in importance of different covariates to a species between the two ecoregions.

Data are available from two time periods – 2005/2007 (from the SCANS-II and CODA surveys, modelled as a single dataset), and 2016. Environmental models were run separately for data from 2005/7 (Hammond et al., 2009, 2013) and 2016 (Hammond *et al*., 2021). They were also run for the two time periods combined to investigate whether relationships persisted between years. Information on the time periods and surveys can be found in Table 2.1-1.

5.2 Methods

5.2.1 Variations to standard methodology

The modelling methodology is largely the same as described in Chapter 2, but with the addition of a categorical covariate to the models with two levels – one for each of the two ecoregions included in this chapter. The modelling process was followed in the same way as described previously, but the "full model" – that which contains the best of each set of correlated covariates – was run both with and without the inclusion of the categorical variable for ecoregion. The best of these two was selected by AIC and is presented in the results section below.

None of the surveys for which data have been analysed in this thesis cover the entire region of interest and in this chapter, surveys have been combined to provide the best coverage. Surveys SCANS-II and CODA represent summer of 2005 and 2007 (S2 / CODA in figure legends) and surveys SCANS-III and ObSERVE have been combined to represent summer of 2016 (S3 / ObSERVE in figure legends).

5.2.2 Description of data

5.2.2.1 Cetacean data

This chapter uses data from the SCANS-II (SCANS-II 2008; Hammond et al. 2013), CODA (CODA 2009), SCANS-III (Hammond et al. 2021) and ObSERVE (Rogan et al. 2018) visual surveys, which have been described in Chapter 2.

The species modelled in the chapter are Atlantic white-sided dolphin, offshore bottlenose dolphin (hereafter bottlenose dolphin), common dolphin, striped dolphin, and fin whale. A summary of the data used is provided in **Table 5.2-1**.

Table 5.2-1 Number of effort segments and number of groups and individuals sighted for each species used in analysis of data from the Celtic Sea and Bay of Biscay ecoregions in 2016 and 2005/7.

Year	Species	Total no. of effort segments	No. of effort segments with groups	Number of groups	Number of Individuals	Mean group size
2016	White-sided dolphin	4400	12 (0.3%)	17	79	4.6
	Bottlenose dolphin	4400	134 (3.0%)	216	1322	6.1
	Common dolphin	4400	224 (5.1%)	557	4779	8.6
	Striped dolphin	4400	53 (1.2%)	74	1975	26.7
	Fin whale	4400	261 (5.9%)	467	798	1.7
2005/7	White-sided dolphin	2057	17 (0.8%)	20	234	11.7
	Bottlenose dolphin	2057	34 (1.7%)	39	348	8.9
	Common dolphin	2057	131 (6.4%)	243	3,397	14.0
	Striped dolphin	2057	24 (1.2%)	30	525	17.5
	Fin whale	2057	98 (4.7%)	149	232	1.6

There is a wide disparity in the number of segments with sightings between species. White-sided dolphins for 2016 had sightings in only 0.3% of the effort segments, whereas there were fin whale sightings in 5.9% of the effort segments. A similar pattern was evident in the 2005/7 data, with white-sided dolphin sightings occurring in only 0.8% of the effort segments, and common dolphin sightings occurring in 6.4%. Within species, the percentages are broadly similar between the two survey periods, with the exception of bottlenose dolphins for which there are approximately 50% fewer segments with sightings in 2005/7 compared with 2016. The number of white-sided dolphin sightings is small in both surveys.

5.2.2.2 Covariate data

Covariates for models of both ecoregions combined were selected using the method outlined in Chapter 2, and covariate values assigned to the effort segments are summarised in **Table 5.2-2**, and Figure 4.2-4.to **Figure 5.2-7**. Water depths range from -4.9 to -5364m Slope varied across the two regions, which both include areas of steep slope and relatively flat seabed. Distance to a variety of different bathymetric features has also been included.

In addition to the static covariates, monthly mean values for sea surface temperature (SST), mixed layer depth (MLD), salinity (SAL), absolute dynamic topography (ADT), sea surface height (SSH) and Sea Level Anomaly (SLA) were also used in the models. The mean value for the month of July was used in each instance as this was the month in which the majority of the cetacean survey data were collected. These values shown in raincloud plots below (Figure 5.2-1-3), which are provided to demonstrate the spread of values within the dataset. From these it is apparent that there are both between region and between time-period differences in the July data.

Table 5.2-2: Summary of static covariate values assigned to effort segments used to model the cetacean data from in the two ecoregions.

	Celtic Sea Ecoregion			**Biscay Ecoregion**		
	Min	**Max**	**Mean**	**Min**	**Max**	**Mean**
Depth (m)	-4.9	-4417	-696	-7.3	-5364	-1676
Standard deviation of depth (SD depth)	0.6	773	60.4	1.4	805	70
Slope (^{0})	0	9	0.7	0	19	2
Distance to coast (km) (Dcoast)	0	406	130	0.2	503	127
Distance to 200m isobath (km) (D200_iso)	0	458	112	0	478	81
Distance to 200m isobath (km) – taking side into account (CS200)	-322	458	34	161	-477	-41
Distance to 2000m isobath (km) (D2000_iso)	0	778	200	0	266	78
Distance to escarpments (km) (Descarp)	0	726	195	0	203	51
Distance to seamounts (km) (Dseam)	86	1232	684	13	452	215
Distance to canyons (km) (Dcanyon)	0	727	210	0	280	280
Distance to troughs (km) (Dtrough)	0	1023	414	526	1149	892

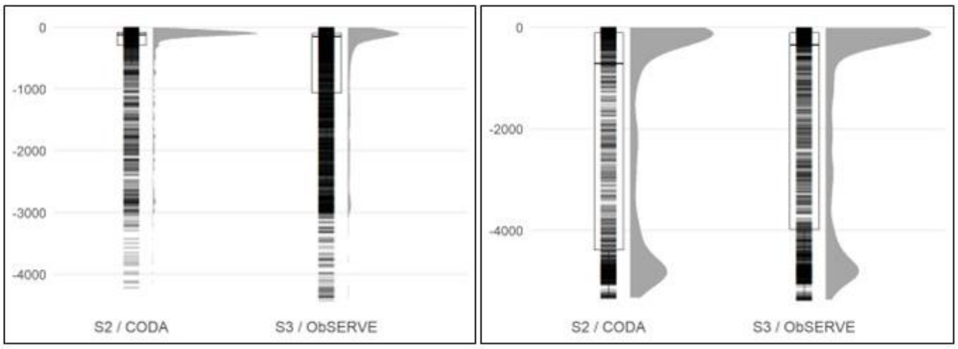

Celtic Sea **Depth** Bay of Biscay

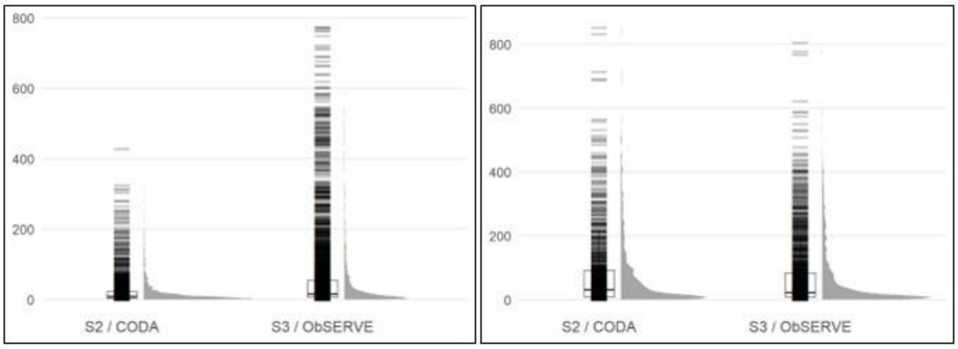

Celtic Sea **SD Depth** Bay of Biscay

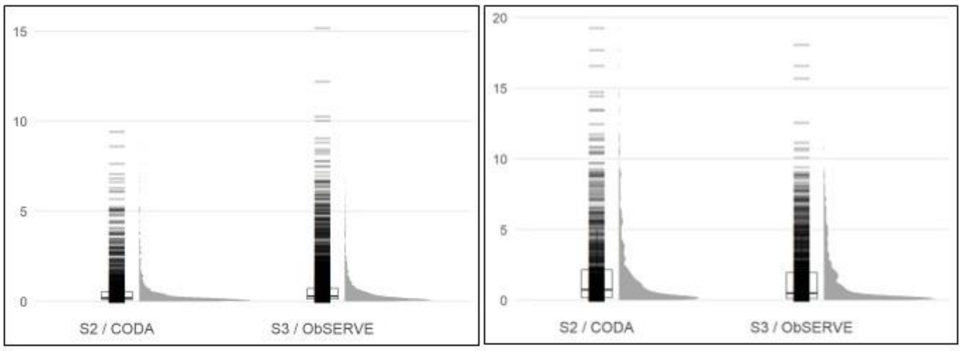

Celtic Sea **Slope** Bay of Biscay

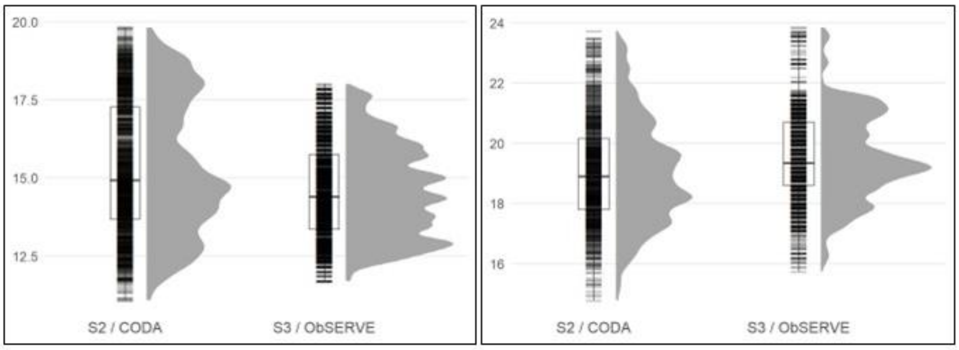

Celtic Sea **SST** Bay of Biscay

Figure 5.2-1: Raincloud plots showing the distribution of covariate data associated with the effort segments used to model the cetacean survey data in both ecoregions.

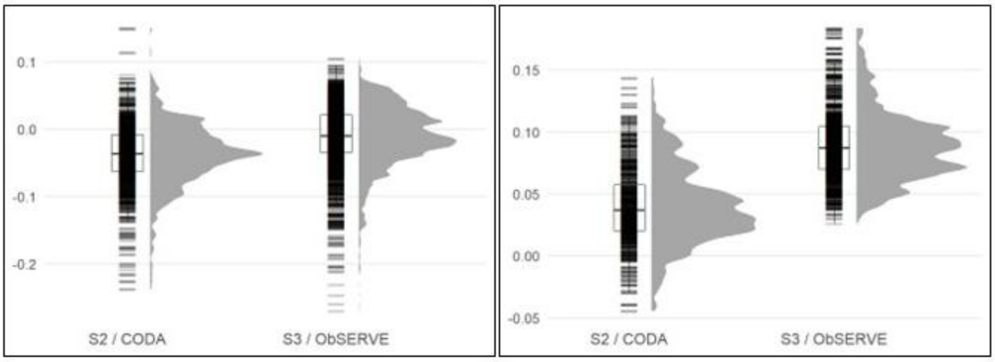

Celtic Sea **ADT** Bay of Biscay

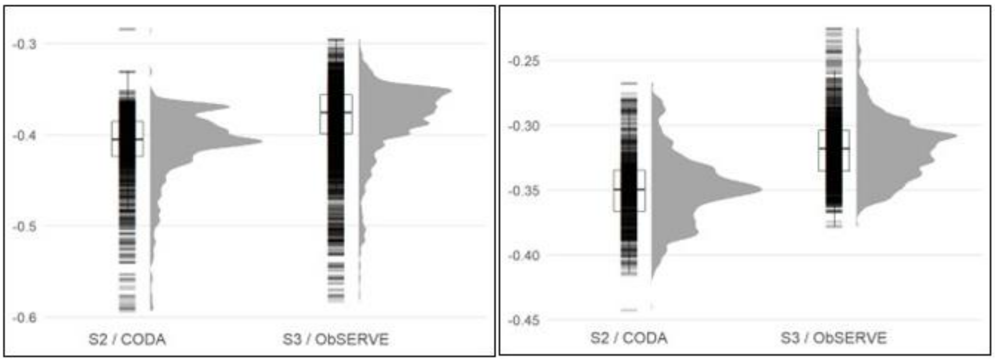

Celtic Sea **SSH** Bay of Biscay

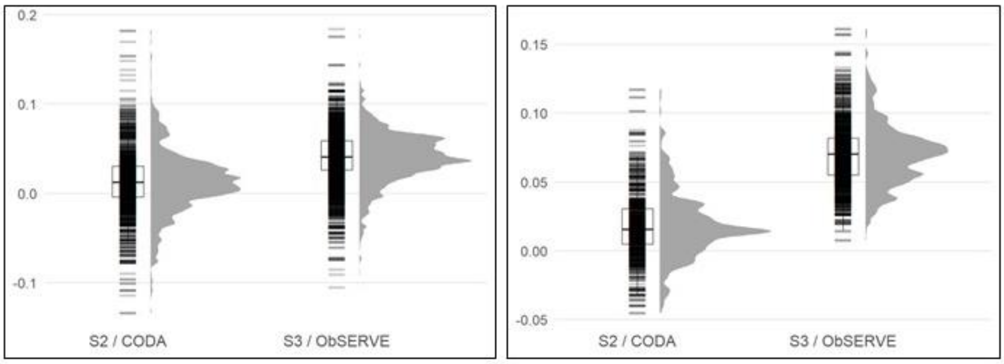

Celtic Sea **SLA** Bay of Biscay

Figure 5.2-2: Raincloud plots showing the distribution of covariate data associated with the effort segments used to model the cetacean survey data in both ecoregions.

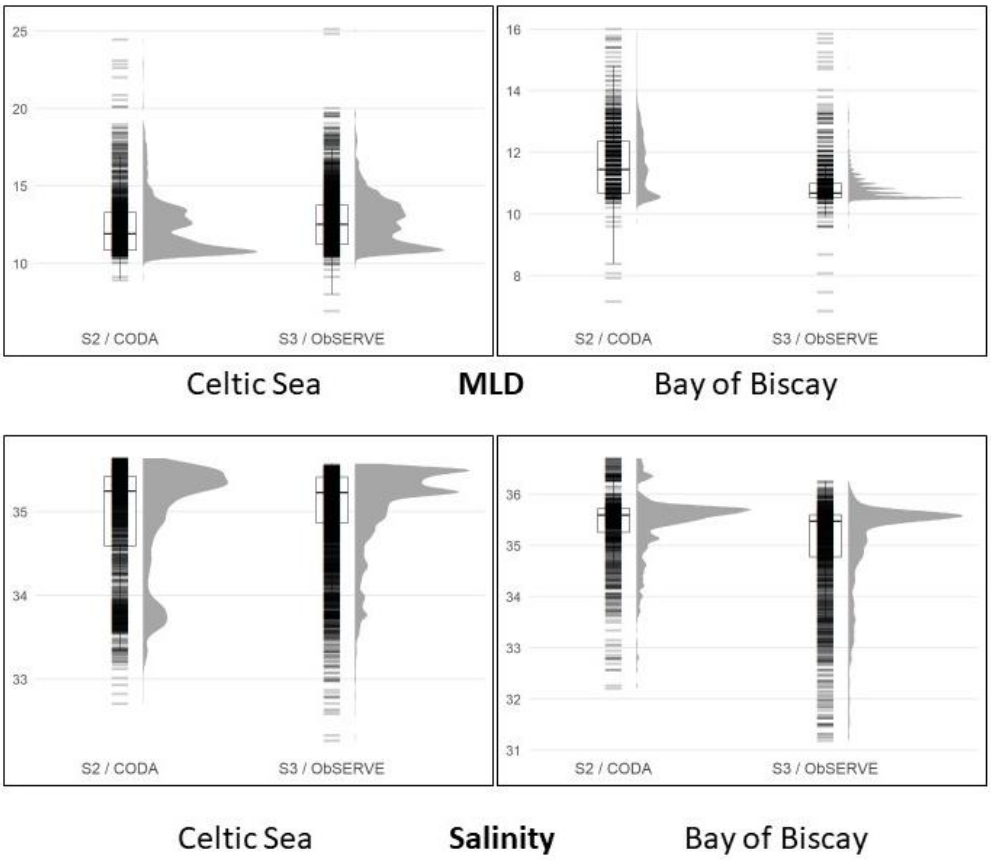

Figure 5.2-3: Raincloud plots showing the distribution of covariate data associated with the effort segments used to model the cetacean survey data in both ecoregions.

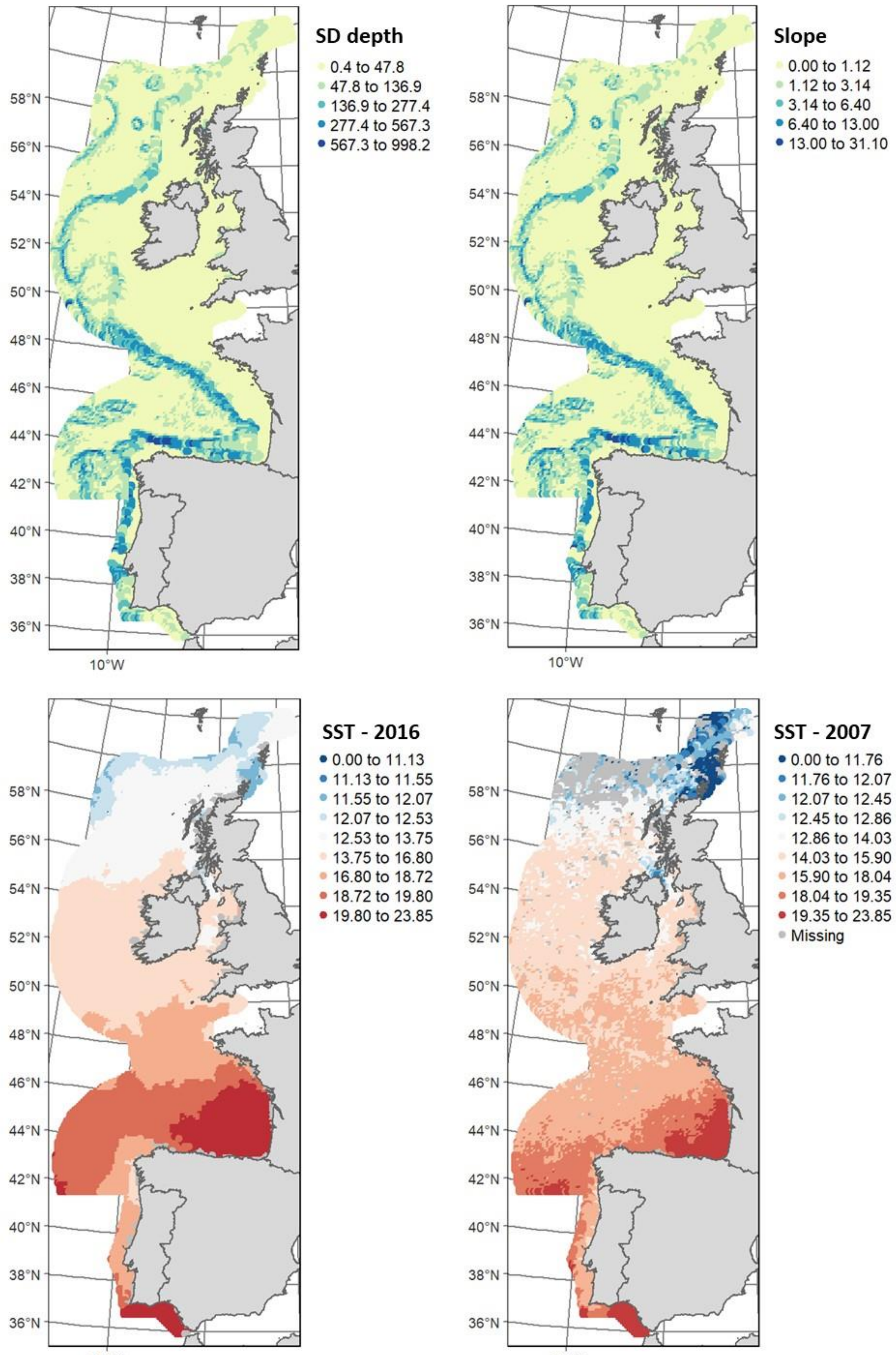

Figure 5.2-4: Maps showing the distribution of covariate data associated with the effort segments used to model the cetacean survey data in both ecoregions.

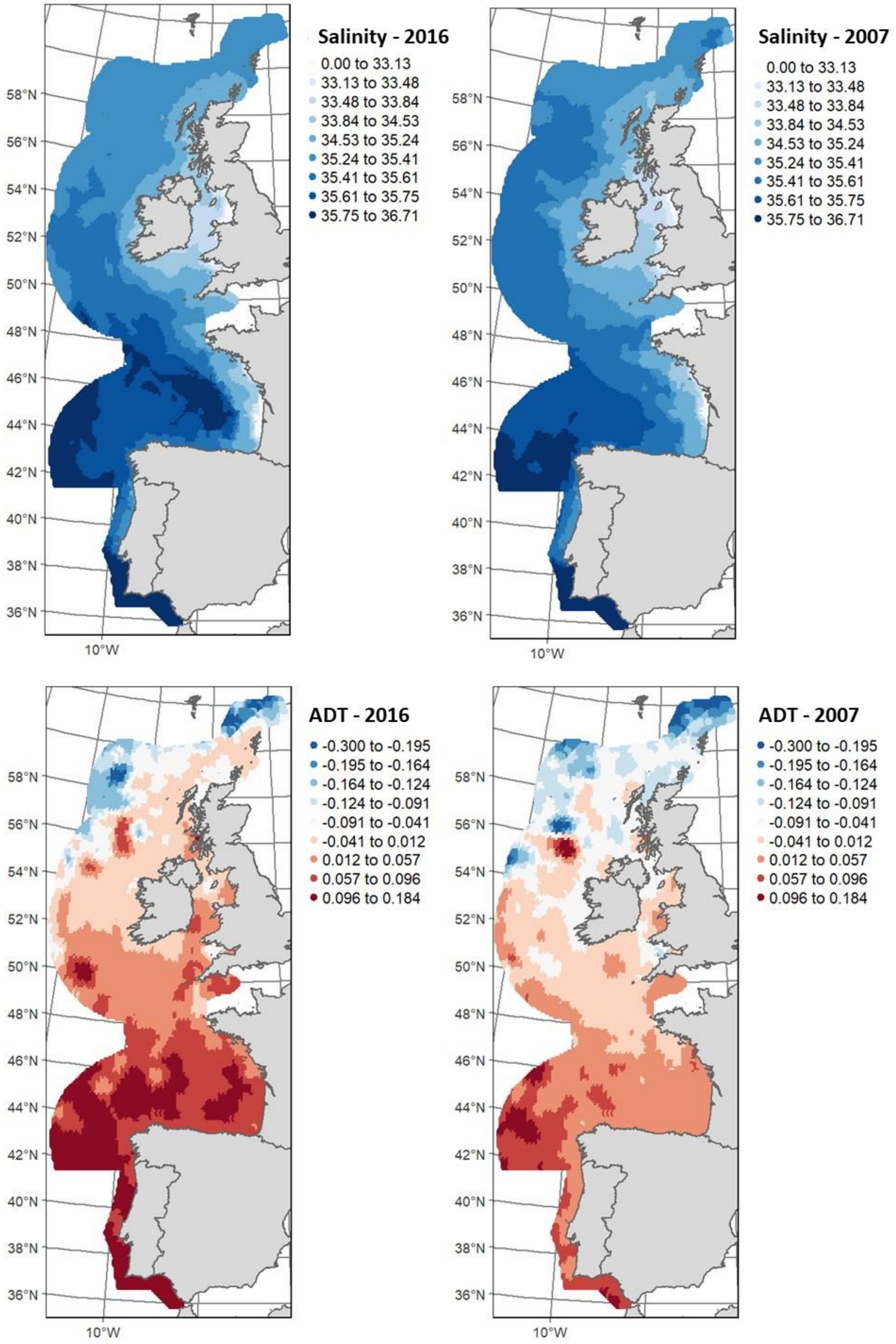

Figure 5.2-5: Maps showing the distribution of covariate data associated with the effort segments used to model the cetacean survey data in both ecoregions.

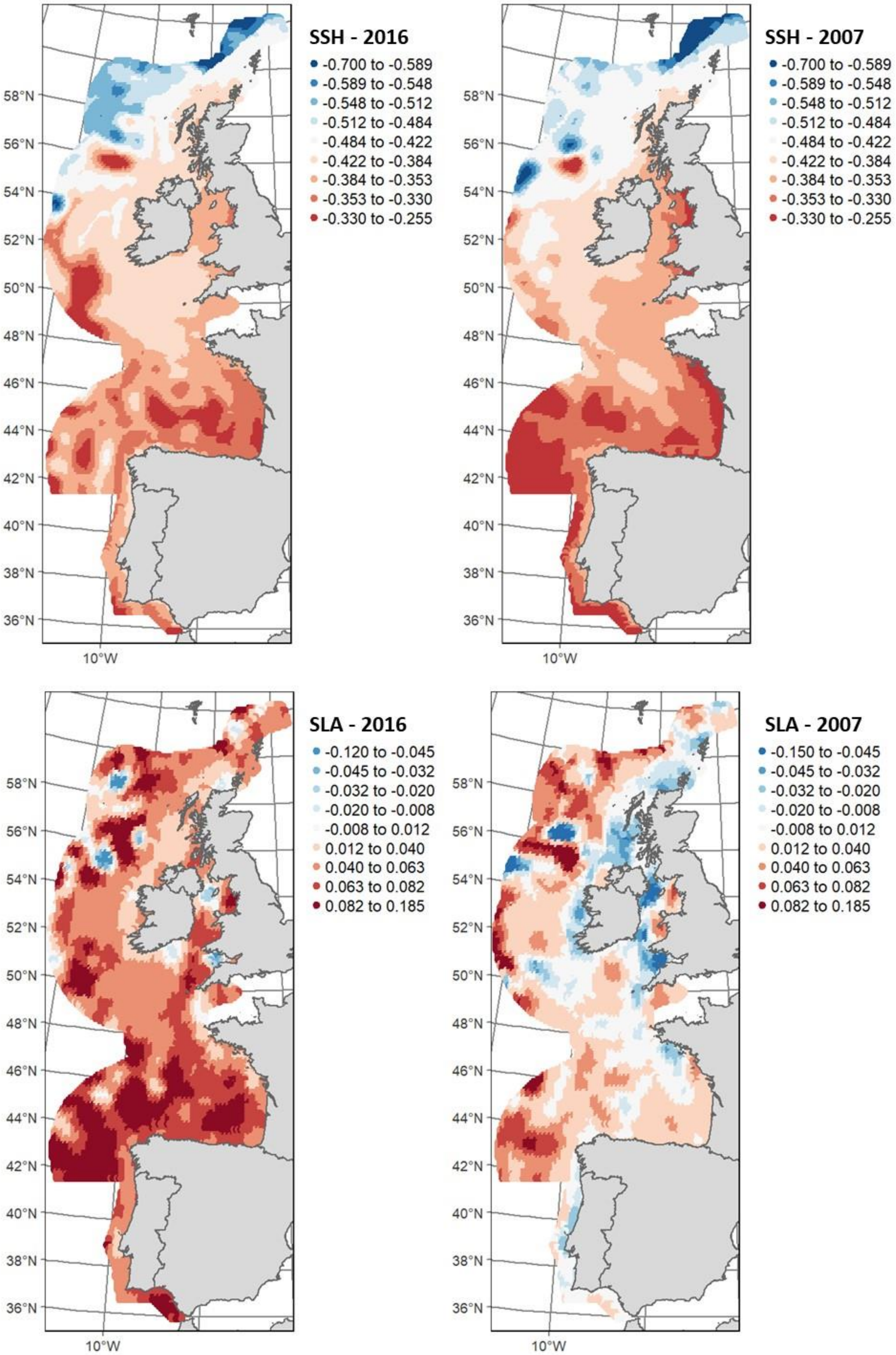

Figure 5.2-6: Maps showing the distribution of covariate data associated with the effort segments used to model the cetacean survey data in both ecoregions.

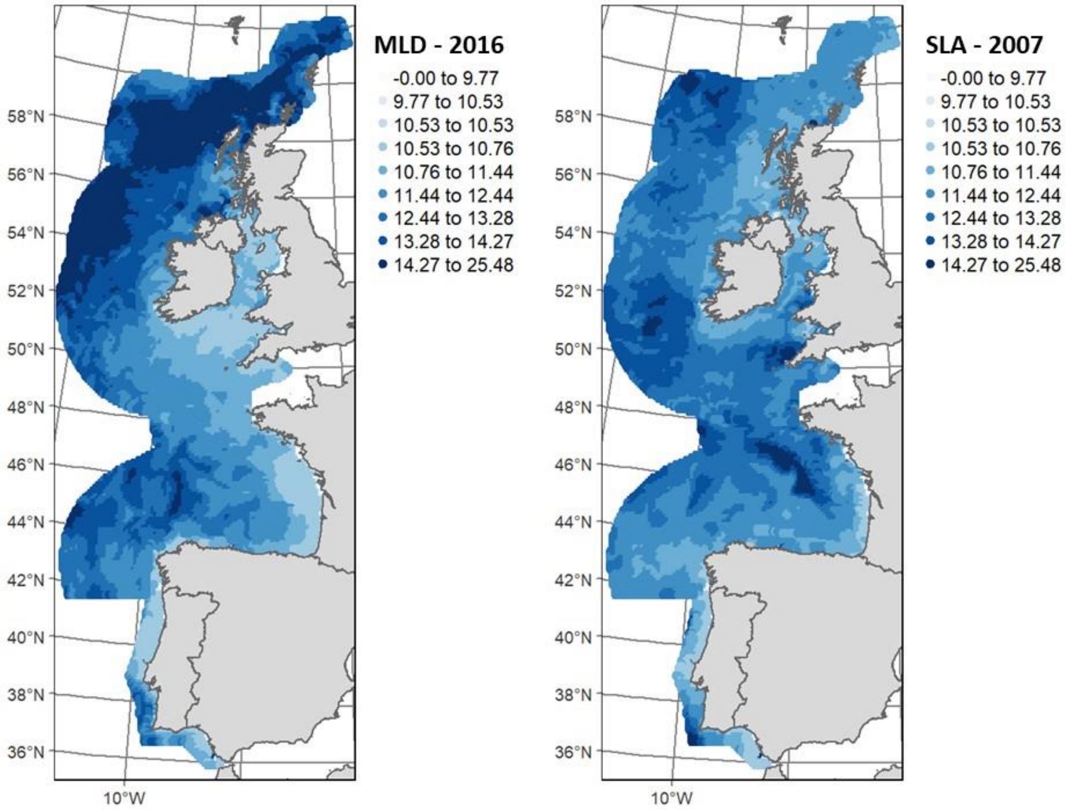

Figure 5.2-7: Maps showing the distribution of covariate data associated with the effort segments used to model the cetacean survey data in both ecoregions.

5.3 Results of combined ecoregion environmental models

5.3.1 White-sided dolphin

Summary results of the final environmental models for both ecoregions combined selected for white-sided dolphins are provided in **Table 5.3-1**. Model diagnostics indicated a satisfactory fit to the data, with the proportion of null deviance explained by the S3/ObSERVE model being 37.1%., and for the S2 / CODA model being 22.7%. A model containing the data from both combined surveys modelled together is also presented in **Table 5.3-2**. This model included year as a categorical variable. Deviance explained by this model was 35.8%.

The QQ plots and the residuals vs linear plots for all three models are provided in Appendix 4. The adequate fit of the models indicates that the resulting predictions should be an appropriate representation of the relationships between predicted white-sided dolphin density and the model covariates, despite the low number of sightings. Partial effects plots are shown in **Figure 5.3-1**

The data in all cases were best described using the Tweedie distribution. Due to both the low number of sightings and the fact that white-sided dolphins were only seen in the Celtic Sea region, a factor covariate for ecoregion was not included in these models.

For the S3/ObSERVE model, there were higher estimated densities of dolphins in areas of flatter seabed (low SD depth) with estimated densities decreasing as slope became steeper, with a very wide confidence interval around the steepest slopes. This pattern was also seen in the combined survey model. White-sided dolphin density was predicted to decrease as depth increased, although this relationship was only found in the S3/ObSERVE model.

In addition, higher levels of predicted density were associated with cooler SST – a relationship that held through all three models. Higher dolphin densities were also predicted at higher levels of salinity. Confidence intervals were very wide at the lowest salinity values, where there were few data points. All the relationships were linear, likely reflecting the low number of sightings.

For the S2/CODA model, only SST and salinity were retained, both showing the same relationship as described above for S3/ObSERVE. The combined survey model retained the same three covariates as the S3/ObSERVE model, two of which were also retained for the S2/CODA model. The year factor was found to be significant (P = 0.0001).

The highest densities of white-sided dolphins were predicted throughout the northern part of the Celtic Seas ecoregion in 2016, with very few animals predicted south of 54^0N (Figure 5.3-2b); this is a reasonable reflection of the sightings data (Figure 5.3-2-a). The plot of predicted CV shows we can be reasonably confident in this model for most of the ecoregion, although there is an area of lower precision running along the shelf-edge (Figure 5.3-4-c).

The 2005 prediction is also an acceptable reflection of the observations in terms of patterns of density in the northern part of the study region but shows much higher densities than would be expected (over-predicting). In the southern part of the region, the model predicted high densities of animals further to the south and west, where there were no comparable field sightings. The combined survey prediction reflects the combined sightings well to the north of 52^0N, but less so to the south of that.

Table 5.3-1: Model outputs for white-sided dolphin GAMs for S3/ObSERVE and S2/CODA data.

Model	Error distribution	Model covariates	Estimated degrees of freedom	P-value	% Deviance explained	Model degrees of freedom
S3/ObSERVE	Tweedie	SD depth	0.8	0.79	37.1	4.4
		Depth	0.9	0.009		
		SST	1.0	3.8e-5		
		Salinity	0.7	0.102		
S2/CODA	Tweedie	SST	0.9	0.013	22.7	2.9
		Salinity	1.0	4.1e-6		

Table 5.3-2: Model outputs for combined S2/CODA and S3/ObSERVE white-sided dolphin GAM.

Name	Factor levels	Estimate	Std. Error	Z value	PR(>z)	
Combined S2/CODA and S3/ObSERVE model	Intercept (2007)	343.8	90.6	3.8	0.0002	
	Year = 2016	-0.17	0.05	-3.8	0.0001	
Model	**Error distribution**	**Model covariates**	**Estimated degrees of freedom**	**% Deviance explained**	**Model degrees of freedom**	**P value**
Combined 2016 & 2005 model	Tweedie	SD depth	0.9	35.8	5.0	0.02
		SST	1.2			2e-16
		Salinity	1.0			0.0003

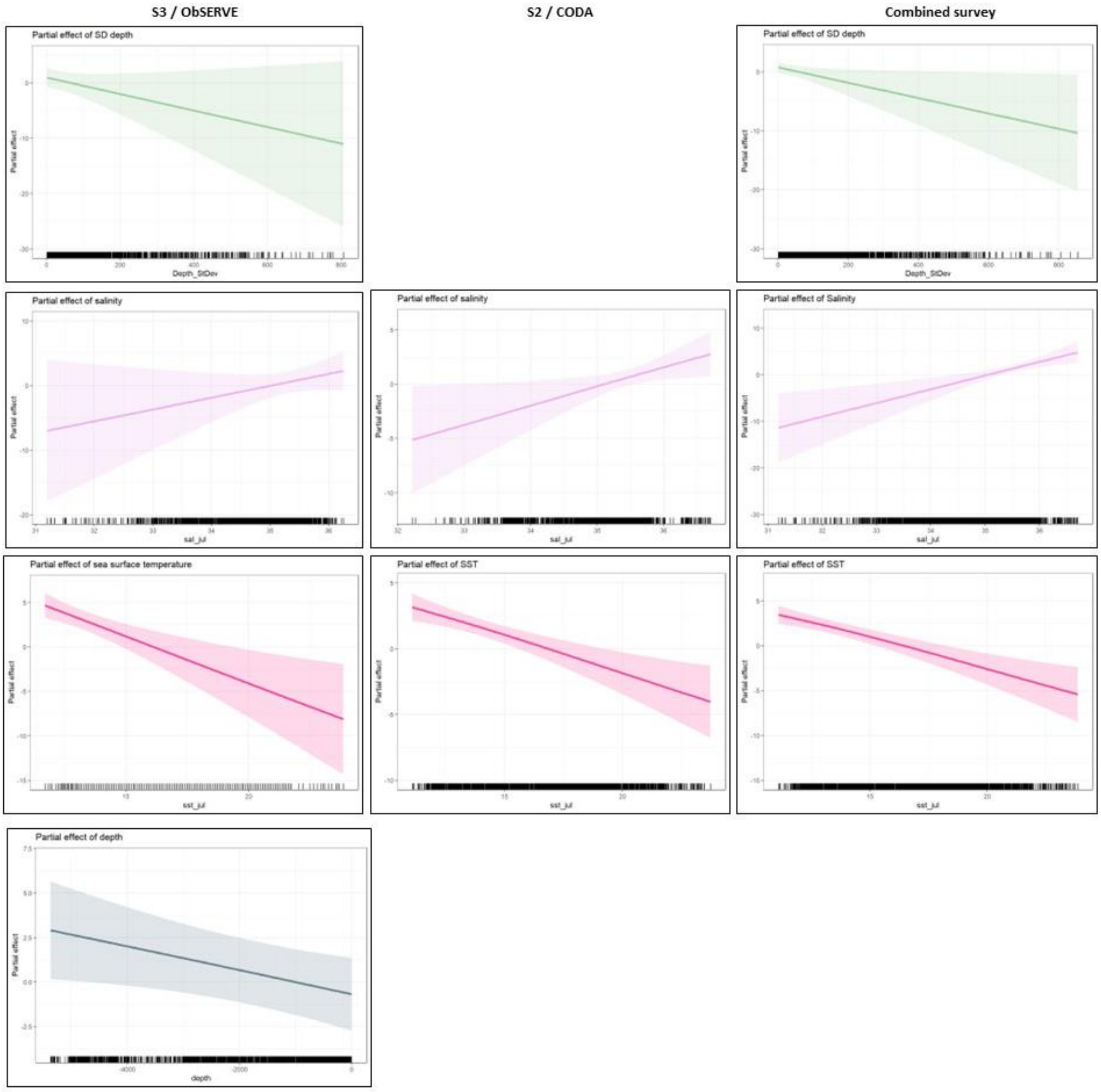

Figure 5.3-1: Plots of the fitted smooth functions for white-sided dolphin GAMS for S3/ObSERVE, S2/CODA and the combined survey model. “Rug” marks on the x-axis of the fitted smooth plots show the distribution of the data. Shaded areas represent the 95% confidence intervals. Where the same covariate is retained in multiple models, the smooths are shown on the same row. Effect sizes are variable, so axis scales are also variable in order to preserve necessary detail.

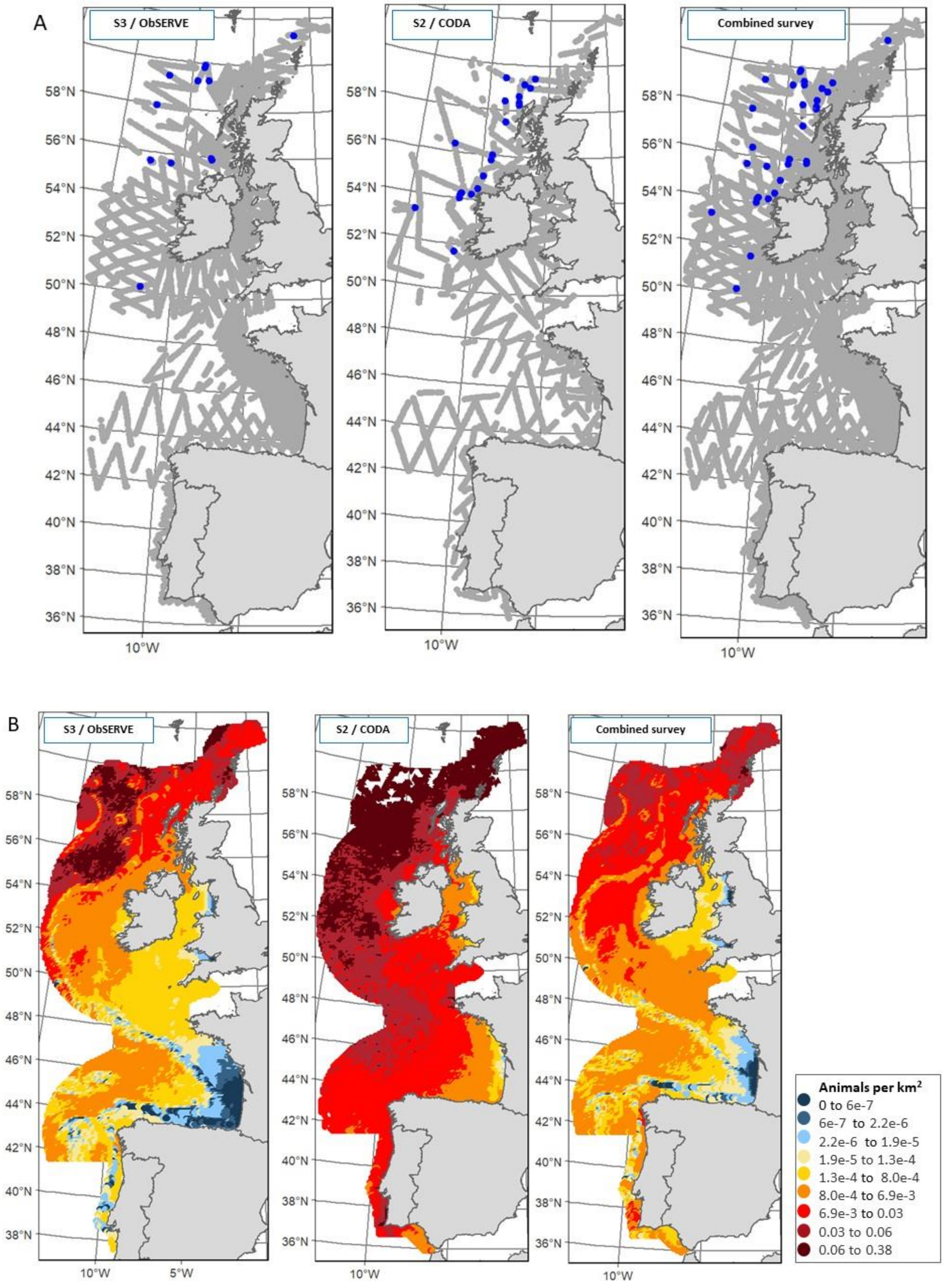

Figure 5.3-2: Location of effort and sightings (a), predicted density surface (b) for S2 / CODA , S3 / ObSERVE and combined survey white-sided dolphin models. Range of values represented by colours in the maps show the 1%, 2%, 5%, 10%, 25%, 50%, 75%, 90% and 100% quantiles. White areas are outside of predictive space. In some cases, prediction grid cells had covariate values which were outside the range encompassed by the modelled effort segments. In these instances, grid-cells were excluded from the prediction. Combined survey data are predicted using 2016 covariates.

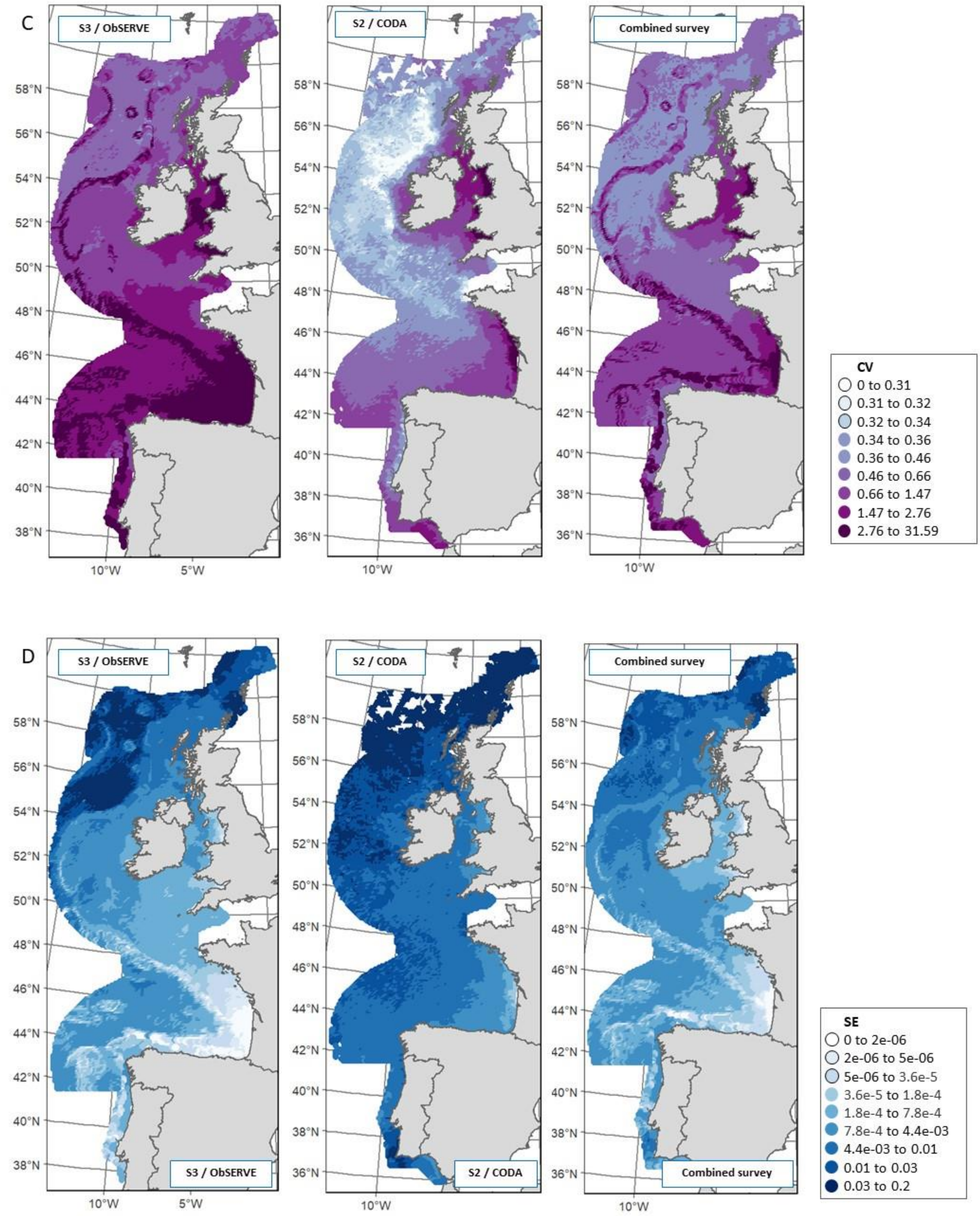

Figure 5.3-3: Coefficient of variation (CV) of density (C) and standard error (SE) of density (D) for S2 / CODA , S3 / ObSERVE and combined survey white-sided dolphin models. Range of values represented by colours in the maps show the 1%, 2%, 5%, 10%, 25%, 50%, 75%, 90% and 100% quantiles. White areas are outside of predictive space. In some cases, prediction grid cells had covariate values which were outside the range encompassed by the modelled effort segments. In these instances, grid-cells were excluded from the prediction. Combined survey data are predicted using 2016 covariates.

5.3.2 Offshore bottlenose dolphin

Summary results of the final environmental models for both ecoregions combined selected for bottlenose dolphins are provided in **Table 5.3-3**. Model diagnostics indicated a satisfactory fit to the data, although the proportion of null deviance explained by the S3/ObSERVE model was very low, just 4.2%. This was considerably higher for the S2/CODA model at 20.9%. The model containing the combined survey data explained 15% of the null deviance (Table 5.3-4). This model included both survey year and ecoregion as categorical variables.

The QQ and residual plots for all three models are provided in appendix 4. The adequate fit of the models indicates that the resulting predictions should be an appropriate representation of the relationships between predicted bottlenose dolphin density and the model covariates overall. Partial effects plots are shown in **Figure 5.3-4**. The data in call cases were best described using the negative binomial distribution.

All three models retained depth, showing the same relationship in each instance in which predicted density of dolphins is highest in shallower waters and decreases linearly as depth increases.

Two of the models retained salinity. For the S3/ObSERVE model, there were higher estimated densities of dolphins at higher salinity. This was a pattern echoed in the combined survey model, although the partial effect was smaller in the combined model. In both cases the confidence interval was wider towards the areas of lower salinity for which fewer data were available.

All three models retained a covariate representing mesoscale activity, but a different covariate was selected for each model. In S3/ObSERVE, the covariate selected was SLA, and predicted density of dolphins was highest in areas of low SLA values. The S2/CODA model retained ADT, but the partial effect plot shows a very similar relationship as was observed in the previously described model with SLA. The combined model used the SSH covariate. The predicted density of dolphins was again highest in areas of low SSH, decreasing as SSH increased.

No further covariates were retained in the S3/ObSERVE model. Of these, MLD was also retained in the combined survey model. In both cases the highest density of dolphins was predicted at shallower mixed layer depths, with dolphin density predicted to decrease as MLD increased. The partial effect for the combined survey is smaller than for the S2/CODA survey only.

Both S2/CODA and the combined survey model also retained a distance to feature covariate. For S2/CODA it was canyons and for the combined survey model it was seamounts. For both of these the predicted density of dolphins was highest closest to the selected feature and declined with distance.

The final covariate which was retained only in the combined survey model was SD depth. This showed only a very small partial effect but predicted highest dolphin densities at high seabed rugosity (high SD depth). Confidence intervals were comparatively wide at highest SD depth values. All the slopes were linear, likely reflecting the low number of sightings.

High densities of bottlenose dolphins were predicted throughout the Celtic Seas ecoregion in 2016, with lower densities throughout most of the Bay of Biscay ecoregion (Figure 5.3-5-b); this is a reasonable reflection of the sightings data (Figure 5.3-5a). The plot of predicted CV shows we can be reasonably confident in this model, except in the very far south of the region (Figure 5.3-6-c).

The 2005 prediction was not such a good reflection of the observations, indicating a level of over prediction at the highest densities (Figure 5.3-6 e, d). The model predicted high densities of animals in the north of the region, where there were no comparable sightings.

The combined years model predicted adequately well in the centre of the region, but at the far north of the area showed some considerable over prediction of very high densities in locations where there were no sightings. This is reflected in the CV plots, the combined survey plot having by far the large CVs throughout the region. The flagged areas of over prediction also show very high Standard Errors Figure 5.3-6e, d).

Table 5.3-3: Model outputs for bottlenose dolphin GAMs for S3/ObSERVE and S2/CODA data.

Model	Error distribution	Model covariates	Estimated degrees of freedom	P-value	% Deviance explained	Model degrees of freedom
S3/ObSERVE	Negative binomial	Depth	0.7	0.067	4.2	3.5
		SLA	0.9	0.003		
		Salinity	0.9	0.002		
S2/CODA	Tweedie	Depth	0.9	0.002	20.9	4.6
		MLD	0.7	0.06		
		ADT	0.7	0.005		
		Distance to canyons	1.0	0.0001		

Table 5.3-4: Model outputs for combined S2/CODA and S3/ObSERVE bottlenose dolphin GAM.

Name	Factor levels	Estimate	Std. Error	Z value	PR(>z)	
Combined S2/CODA and S3/ObSERVE model	Intercept	-4.2	0.4	-11.2	2e-16	
	Year (2007)	0.5	0.6	0.9	0.4	
	Year (2016	2.2	0.4	6.0	3e-9	
	Ecoregion Bay of Biscay	-1.4	0.5	-3.0	0.003	
Model	**Error distribution**	**Model covariates**	**Estimated degrees of freedom**	**% Deviance explained**	**Model degrees of freedom**	**P value**
Combined S2/CODA and S3/ObSERVE model	Tweedie	SD depth	0.3	15	8.4	0.23
		Depth	0.9			0.01
		MLD	0.8			0.02
		SSH	1.0			3e-4
		Salinity	0.3			0.36
		Distance to seamounts	1.1			5e-7

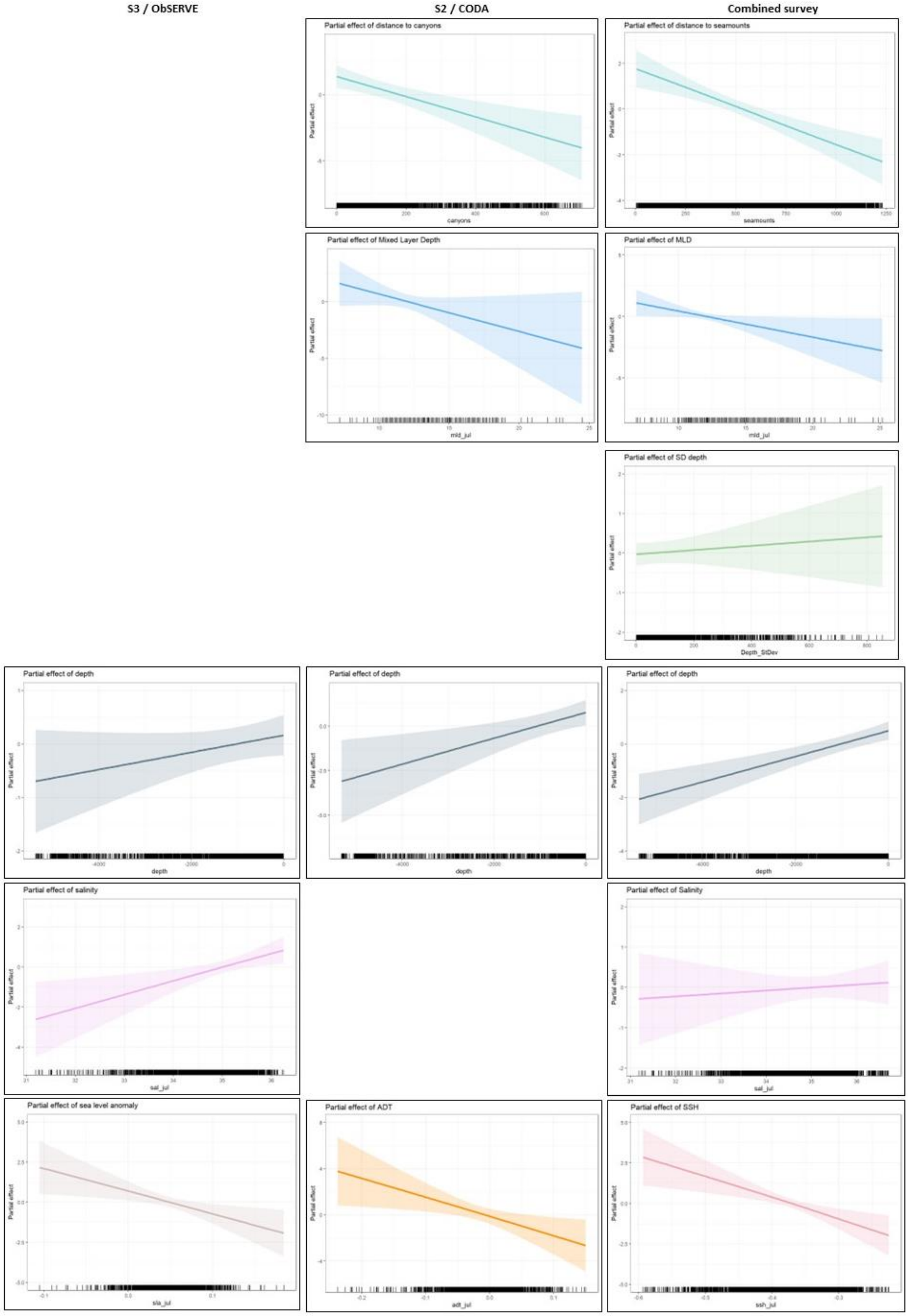

Figure 5.3-4: Plots of the fitted smooth functions for bottlenose dolphin GAMS for S3/ObSERVE, S2/CODA and the combined survey model. "Rug" marks on the x-axis of the fitted smooth plots show the distribution of the data. Shaded areas represent the 95% confidence intervals. Where the same covariate is retained in multiple models, the smooths are shown on the same row. Effect sizes are variable, so axis scales are also variable in order to preserve necessary detail.

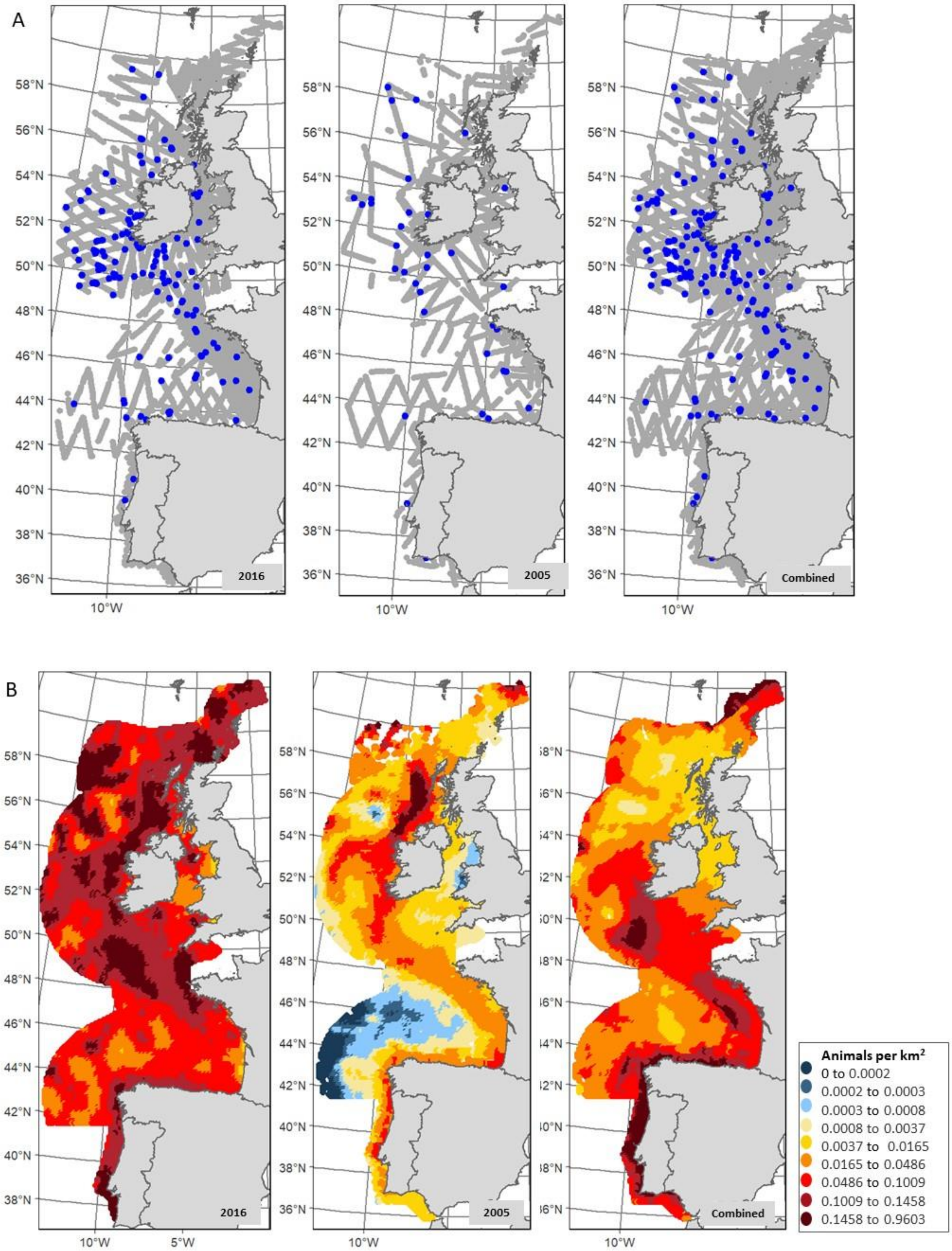

Figure 5.3-5: Location of effort and sightings (a), predicted density surface (b) for S2 / CODA, S3 / ObSERVE and combined survey bottlenose dolphin models. Range of values represented by colours in the maps show the 1%, 2%, 5%, 10%, 25%, 50%, 75%, 90% and 100% quantiles. White areas are outside of predictive space. In some cases, prediction grid cells had covariate values which were outside the range encompassed by the modelled effort segments. In these instances, grid-cells were excluded from the prediction. Combined survey data are predicted using 2016 covariates.

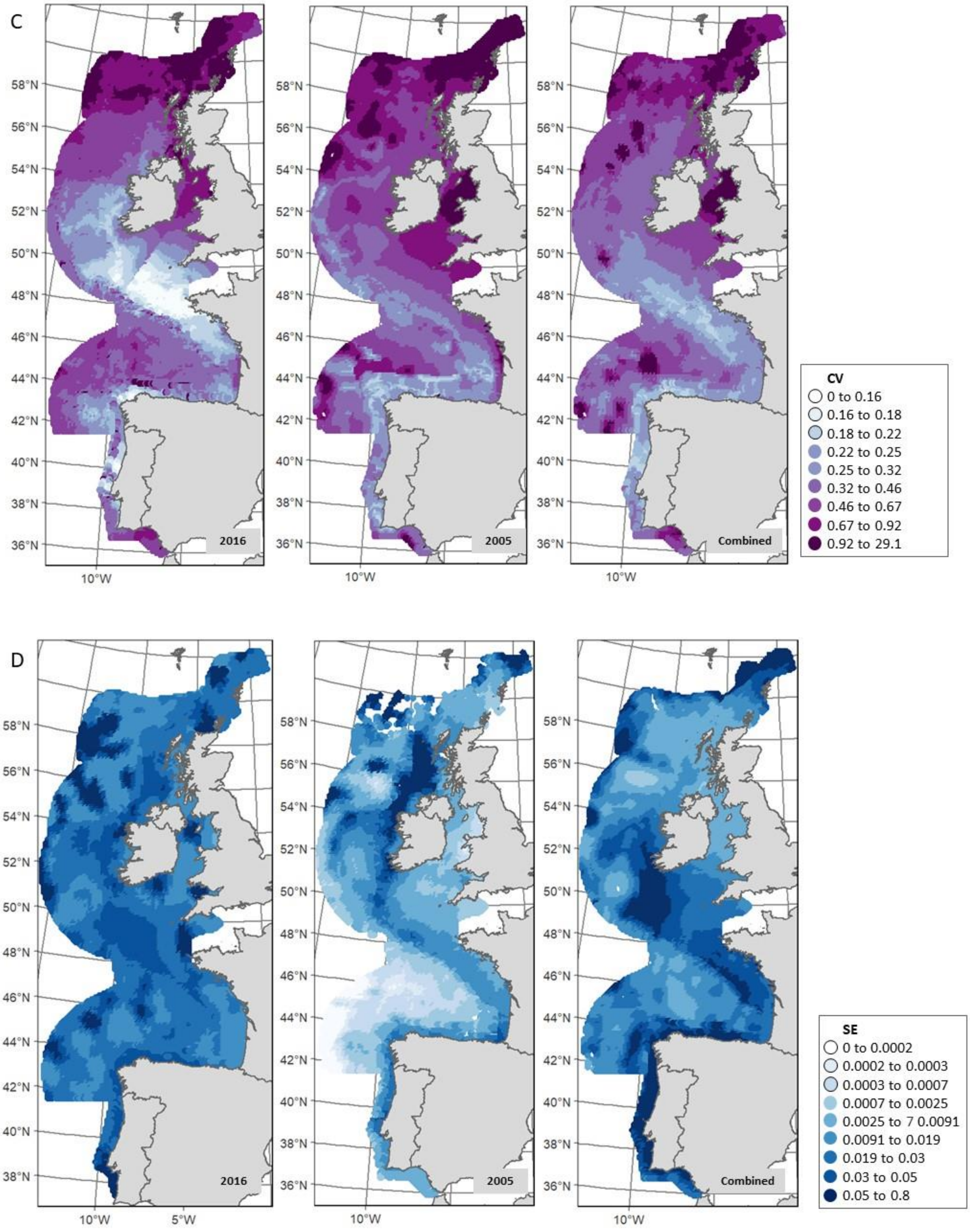

Figure 5.3-6: Coefficient of variation (CV) of density (C) and standard error (SE) of density (D) for S2 / CODA, S3 / ObSERVE and combined survey bottlenose dolphin models. Range of values represented by colours in the maps show the 1%, 2%, 5%, 10%, 25%, 50%, 75%, 90% and 100% quantiles. White areas are outside of predictive space. In some cases, prediction grid cells had covariate values which were outside the range encompassed by the modelled effort segments. In these instances, grid-cells were excluded from the prediction. Combined survey data are predicted using 2016 covariates.

5.3.3 Fin whale

Summary results of the final environmental models for both ecoregions combined selected for fin whales are provided in Table 5.3-5. Model diagnostics indicated a good fit to the data, with the proportion of null deviance explained by the 2016 model being 66.3%., and for the 2005 model being 60.1%. The combined survey model showed 63.9% deviance explained. The QQ and residual plots are provided in Appendix 4. Partial effects plots are given in **Figure 5.3-7**. The good fit of the models indicates that the resulting predictions should be a good representation of the relationships between predicted fin whale density and the model covariates.

All three data combinations were best described using the negative binomial distribution. The best fin whale model for S2/CODA (**Table 5.3-6**) was the model retaining a factor for ecoregion (p=2.3e-5). The combined survey model also retained categorical covariates, with both ecoregion and year being significant (8.4e-4, 8.4e-4, 3.6e-16 for 2007, 2016 and ecoregion Bay of Biscay, respectively). The best fin whale model for S2/CODA and S3/ObSERVE combined is shown in **Table 5.3-7**.

All three models retained at least four covariates. Depth was retained in all three models and maintained a broadly similar shaped relationship in all models. In all cases, predicted fin whale density was lowest in very shallow waters, increasing to around 1000m depth, then broadly plateauing until around 5000m depth, when the predicted density started to decrease again.

Sea surface temperature was retained in the models for S3/ObSERVE and S2/CODA. The relationship was wigglier in the S3/ObSERVE model, but the general trend was for predicted density to increase as temperature increases, although not linearly. In the S2/CODA model, the relationship was less wiggly and went in the opposite direction, with predicted density decreasing as temperature increases. As the two relationships are opposite and the covariate is not retained in the combined survey model, which spans a much wider time frame, it can be inferred that this covariate is not representing any useful biological relationships here, but rather picking up on an unknown source of variability.

For the 2016 data, there were positive effects (higher estimated density of fin whales) at water depths of at least 1000m, at low MLD (which decreased linearly as MLD increased), and an increase in SST, with a general increase in density as SST increased. Highest fin whale density was also associated with areas at least 100km from the 200m isobath.

SD depth was retained in S2/CODA and the combined surveys model with a very similar, linear relationship in both instances, with predicted density of whales decreasing as SD depth increases. Salinity was also retained in the same two models, also with a very similar relationship across the two models, with predicted density increasing as salinity increases.

The only “distance to” covariate was retained in the S3/ObSERVE model, which retained distance to the 200m isobath. This plot shows predicted whale density increasing until around 100km from the 200m isobath, at which point it broadly levels off, with small fluctuations. This would support the relationship proposed by the depth plot, which showed higher predicted densities in deeper waters.

Mixed layer depth was retained in all three models. In the S3/ObSERVE and S2/CODA surveys the relationship was linear, with highest predicted densities at lowest mixed layer depths and density decreasing as mixed layer depth increased. In the combined survey model, the relationship was slightly different with the peak predicted density at a mixed layer depth of around 10m and decreases in density at higher and lower MLD.

The predicted high densities of fin whales were strongly concentrated in the Bay of Biscay in 2016 which reflected the sightings well (**Figure 5.3-8**-a). The plot of predicted CV shows we can be reasonably confident in this model, particularly in the Bay of Biscay region (Figure 5.3-9c). That the ecoregion categorical variable was retained in the combined model and the S2/CODA model shows that the relationship between whale density and covariates varies by region.

The 2005 prediction was not such a good reflection of the observations (**Figure 5.3-8**-e, d). Whilst the sightings were again concentrated in the Bay of Biscay, this model predicted high densities of animals in the north of the region, where there were very few comparable sightings. This is reflected in the map of standard error of density. The combined survey model does a good job overall, and also shows comparatively low CVs.

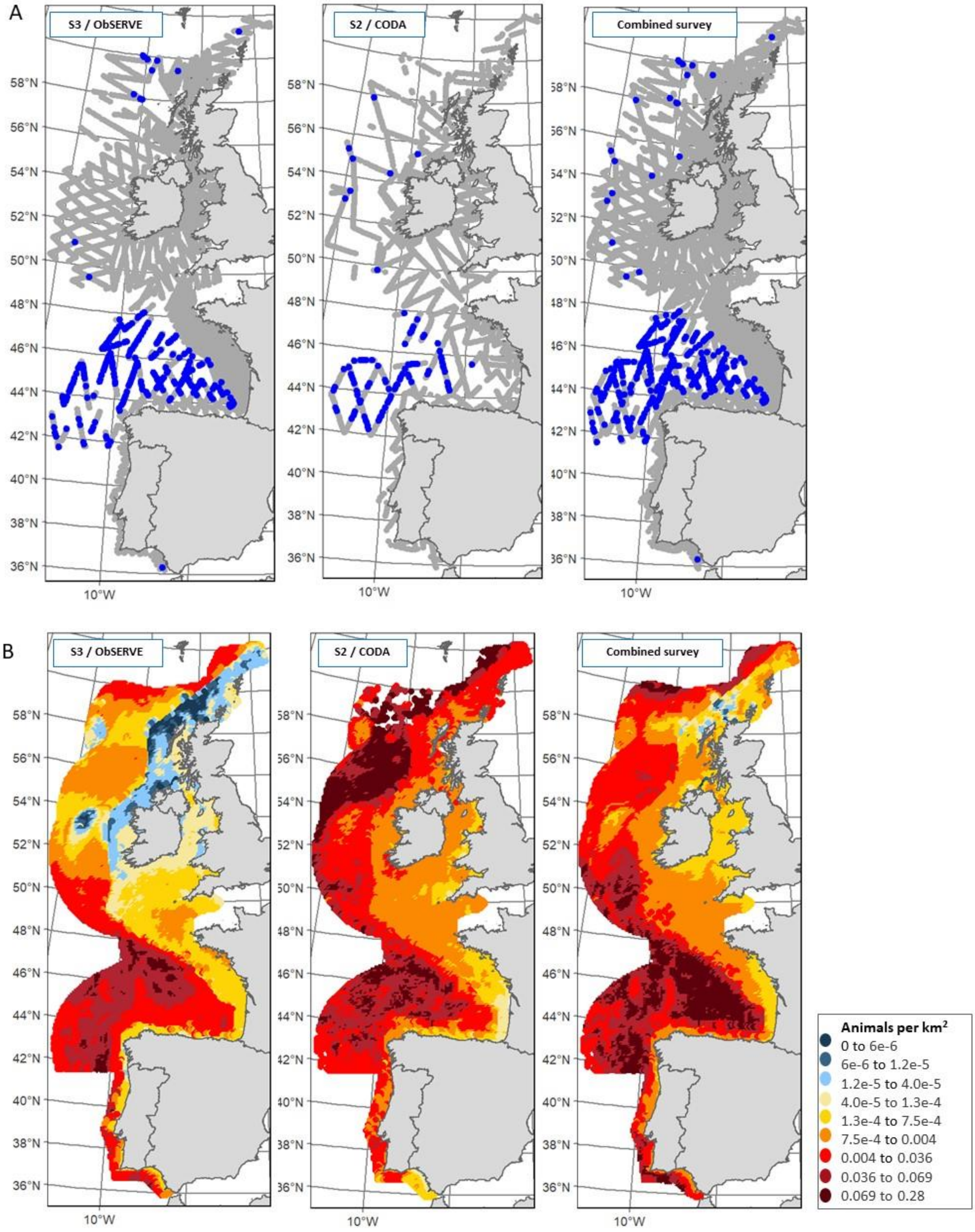
A
S3 / ObSERVE
S2 / CODA
Combined survey
58°N
56°N
54°N
52°N
50°N
48°N
46°N
44°N
42°N
40°N
38°N
36°N
10°W
B
S3 / ObSERVE
S2 / CODA
Combined survey
Animals per km^2
0 to 6e-6
6e-6 to 1.2e-5
1.2e-5 to 4.0e-5
4.0e-5 to 1.3e-4
1.3e-4 to 7.5e-4
7.5e-4 to 0.004
0.004 to 0.036
0.036 to 0.069
0.069 to 0.28

Table 5.3-5: Model outputs for fin whale GAMs for S3/ObSERVE data.

Model	Error distribution	Model covariates	Estimated degrees of freedom	P-value	% Deviance explained	Model degrees of freedom
S3/ObSERVE	Negative binomial	Depth	7.3	2e-16	66.3	18.9
		MLD	0.9	7.5e-5		
		SST	5.5	2e-16		
		Distance to 200m isobath (km)	4.2	7.1e-5		

Table 5.3-6: Model outputs for combined S2/CODA fin whale GAM

Name	Factor levels	Estimate	Std. Error	Z value	PR(>z)	
Combined S2/CODA and S3/ObSERVE model	Intercept (Ecoregion Celtic seas)	-8.99	0.54	-16.5	2e-16	
	Ecoregion Bay of Biscay	2.90	0.61	4.7	2.3e-5	
Model	**Error distribution**	**Model covariates**	**Estimated degrees of freedom**	**% Deviance explained**	**Model degrees of freedom**	**P value**
Combined S2/CODA and S3/ObSERVE model	Negative Binomial	SD depth	0.91	60.1	10.8	0.002
		Depth	4.96			2e-16
		MLD	0.92			6e-4
		SST	2.51			3e-4
		Salinity	0.62			0.15

Table 5.3-7: Model outputs for combined S2/CODA and S3/ObSERVE fin whale GAM.

Name	Factor levels	Estimate	Std. Error	Z value	PR(>z)	
Combined S2/CODA and S3/ObSERVE model	Intercept	-12.07	1.09	-11.09	2e-15	
	Year (2007)	3.46	1.04	3.34	8.4e-4	
	Year (2016	4.12	1.04	3.97	8.4e-4	
	Ecoregion Bay of Biscay	2.24	0.28	7.86	3.6e-16	
Model	**Error distribution**	**Model covariates**	**Estimated degrees of freedom**	**% Deviance explained**	**Model degrees of freedom**	**P value**
Combined S2/CODA and S3/ObSERVE model	Negative binomial	SD depth	0.96	63.9	15.6	2.1e-5
		Depth	7.24			2e-16
		MLD	2.65			8.4e-4
		Salinity	0.75			7.1e-5

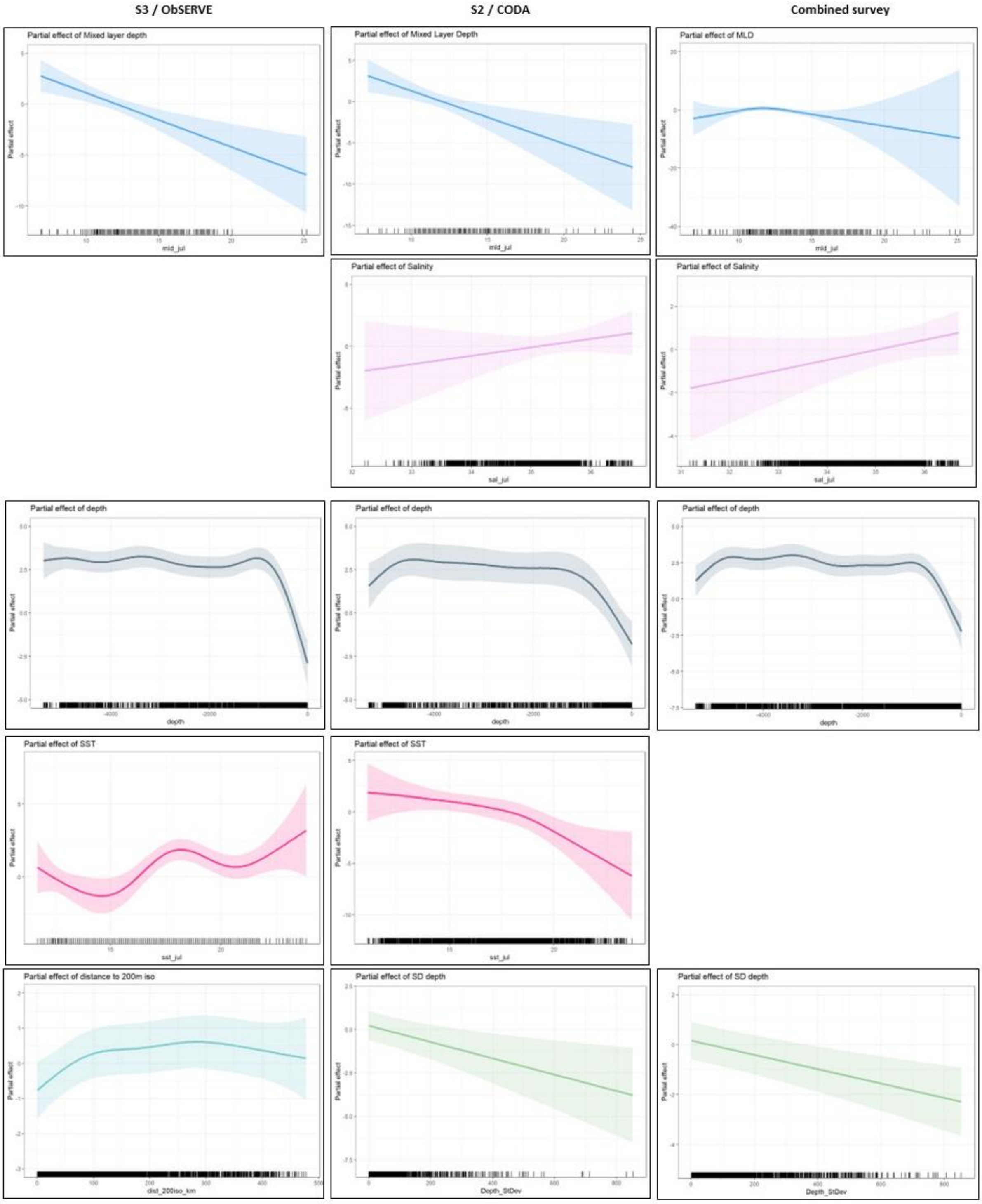

Figure 5.3-7: Plots of the fitted smooth functions for fin whale GAMS for S3/ObSERVE, S2/CODA and the combined survey model. "Rug" marks on the x-axis of the fitted smooth plots show the distribution of the data. Shaded areas represent the 95% confidence intervals. Where the same covariate is retained in multiple models, the smooths are shown on the same row. Effect sizes are variable, so axis scales are also variable in order to preserve necessary detail.

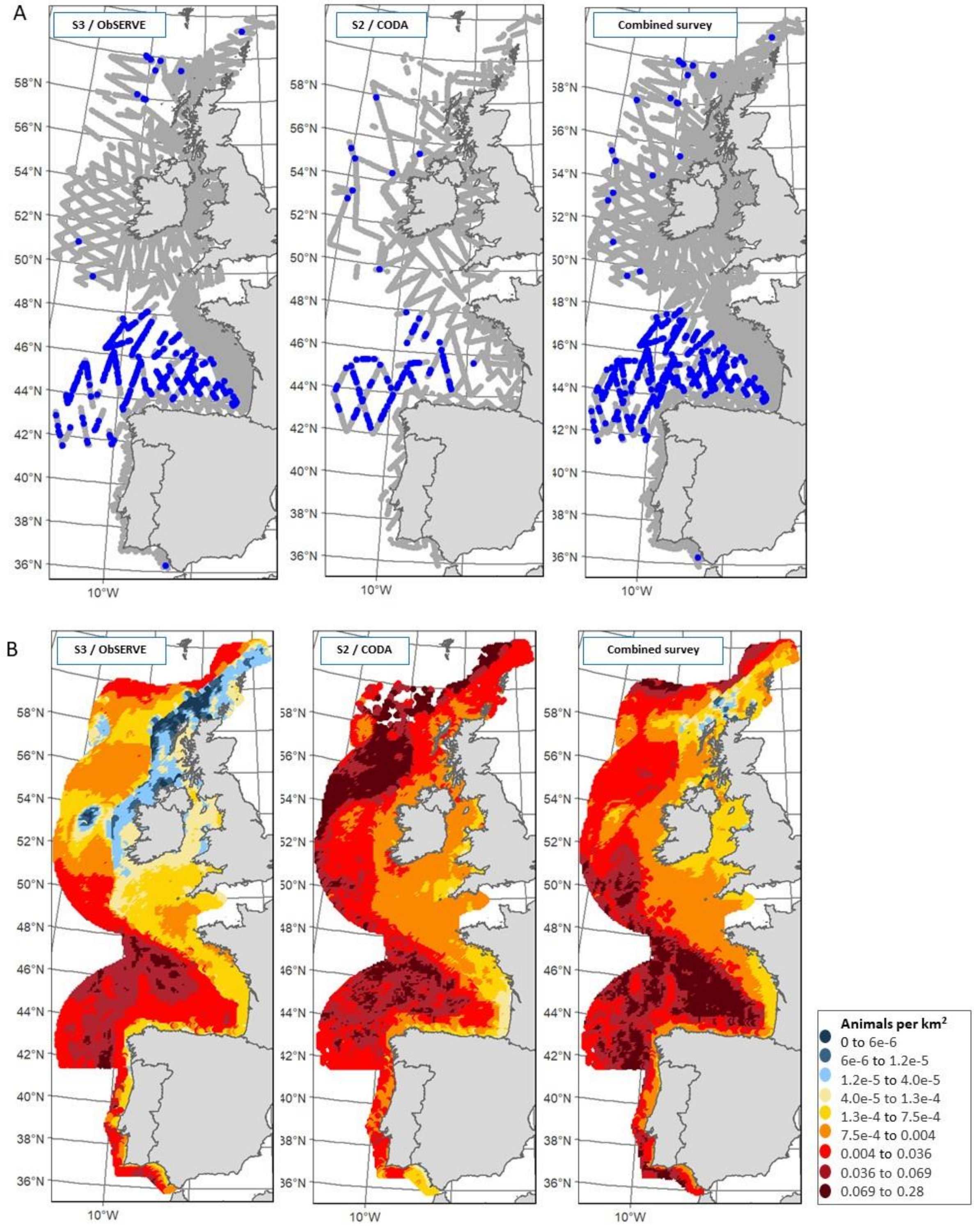

Figure 5.3-8: Location of effort and sightings (a), predicted density surface (b) for S2/CODA, S3/ObSERVE and combined survey fin whale models. Range of values represented by colours in the maps show the 1%, 2%, 5%, 10%, 25%, 50%, 75%, 90% and 100% quantiles. White areas are outside of predictive space. In some cases, prediction grid cells had covariate values which were outside the range encompassed by the modelled effort segments. In these instances, grid-cells were excluded from the prediction. Combined survey data are predicted using 2016 covariates.

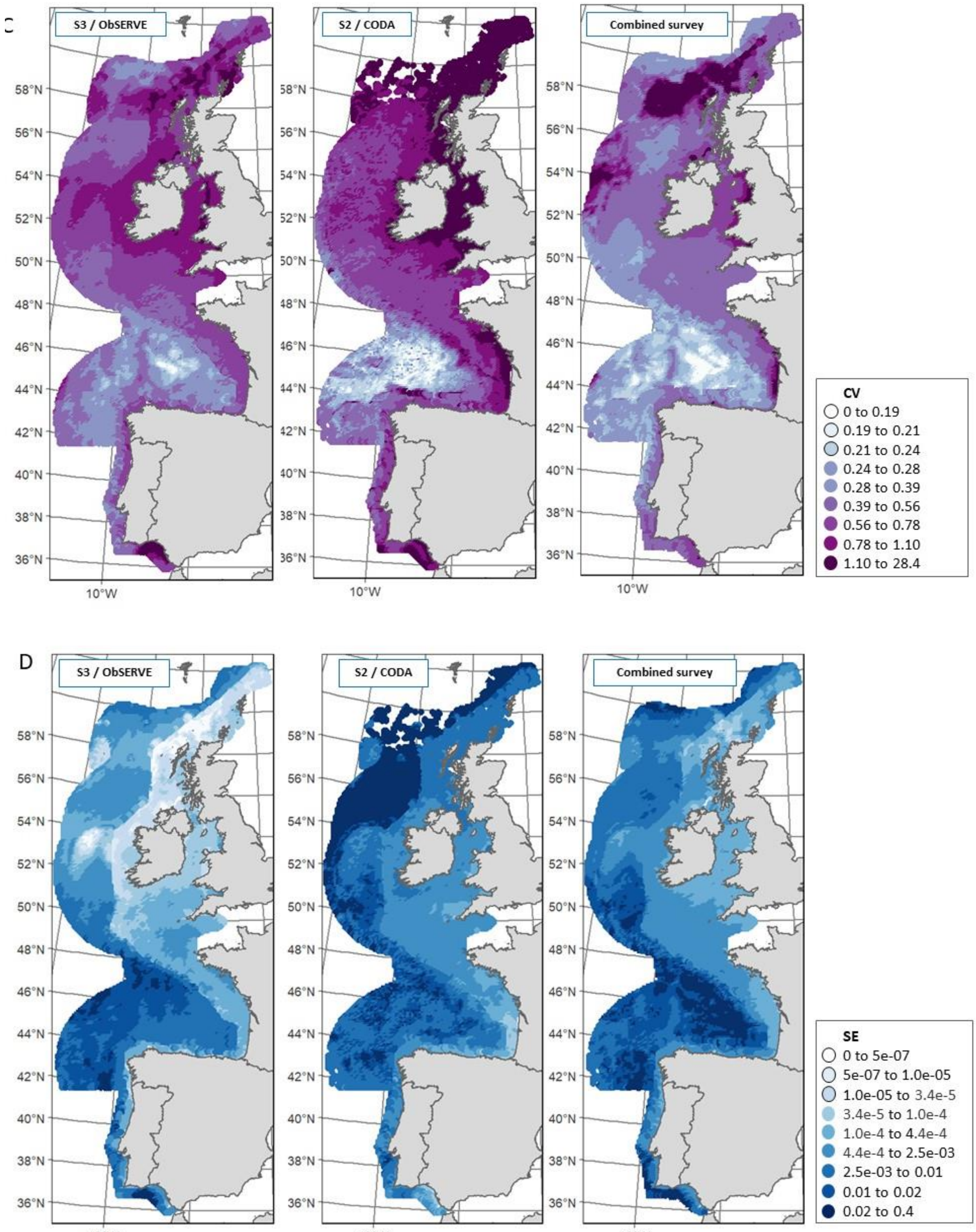

Figure 5.3-9: Coefficient of variation (CV) of density (C) and standard error (SE) of density (D) for S2/CODA, S3/ObSERVE and combined survey fin whale models. Range of values represented by colours in the maps show the 1%, 2%, 5%, 10%, 25%, 50%, 75%, 90% and 100% quantiles. White areas are outside of predictive space. In some cases, prediction grid cells had covariate values which were outside the range encompassed by the modelled effort segments. In these instances, grid-cells were excluded from the prediction. Combined survey data are predicted using 2016 covariates.

5.3.4 Common dolphins

Summary results of the final environmental models for both ecoregions combined selected for common dolphins are provided in **Table 5.3-8** to **Table 5.3-10**. Model diagnostics indicated a satisfactory fit to the data, with the proportion of null deviance explained by the S3/ObSERVE model being 49.4%., the S2/CODA model being 26.7% and the combined survey model being 46.4%. The QQ and residual plots are provided in Appendix 4 along with plots of the partial effects plots in **Figure 5.3-10**. The adequate fit of the models indicates that the resulting predictions should be an appropriate representation of the relationships between predicted common dolphin density and the model covariates.

Common dolphins were modelled as groups. All three of the survey datasets were best described using the negative binomial distribution. The S2/CODA model retained ecoregion as a categorical variable (P=5.3e-6), whilst the combined survey model retained ecoregion and year (P= 5.6e-4, 0.3 and 2e-16 for ecoregion Bay of Biscay, 2007 and 2016, respectively).

All three models retained a high number of covariates compared to models of other species. MLD was the only covariate to be retained in all three models. In each case, highest predicted density of dolphins was predicted at the shallowest MLDs and decreased as MLD increased. In the S3/ObSERVE model and the combined survey model, this decrease in predicted density was linear. In the S2/CODA model, density remained high until MLD was approximately 14m, then started to decline. In all cases the deepest MLD has fewest data points, leading to wider confidence intervals in these regions.

All three models retained a “distance to” covariate, although for S3/ObSERVE it was distance to the 2000m isobath, and for the other two models it was distance to escarpment features. In reality, these are very similar covariates, because escarpment features are the areas located at the bottom of steep slopes. In the S3/ObSERVE model, highest predicted densities of dolphins were found close to the 2000m isobath, and then to decline with increasing distance. The two escarpment relationships both showed higher levels of wiggliness and the same overall shape, although the combined survey model had a decreasing trend overall which the S2/CODA model did not have.

Common dolphin density was predicted to decrease linearly with depth in both the S3/ObSERVE and combined survey models. The same two models also retained SST and salinity. The relationship with salinity revealed a peak in predicted density at around 17PSU, and a decrease in density at values both higher and lower than this. The relationship with salinity was linear for both the S3/ObSERVE model and the combined model, although the effect was less in the combined model. In both cases the predicted density increased with increasing salinity.

The SST with the highest predicted density was around 17^{0}C, with a sharp decrease in density as temperature became either cooler than 15^{0}C or warmer than 20^{0}C. As previously, the confidence interval was wider at the extremes of the range of the covariate where there were fewest data points. Proximity to the 2000m isobath resulted in higher predicted density in this model, with a steep linear decline as distance from this feature increased. High predicted density was associated with high levels of salinity.

High densities of common dolphins were predicted throughout the more southerly shelf waters of the Celtic Seas and along the Portuguese coast of the Bay of Biscay ecoregion in 2016, with lower densities throughout most offshore waters (Figure 5.3-11-b); this is a reasonable reflection of the sightings data (Figure 5.3-11-a). The plot of predicted CV shows we can be reasonably confident in this model, except for in the very far north of the region (Figure 5.3-12c).

The 2005/7 prediction was also a reasonable reflection of the sightings (Figure 5.3-11-e, d) although the CV was very throughout most of the region (Figure 5.3-12).

Table 5.3-8: Model outputs for common dolphin GAMs for S3/ObSERVE data.

Model	Error distribution	Model covariates	Estimated degrees of freedom	P Value	% Deviance explained	Model degrees of freedom
2016	Negative binomial	Slope	2.2	0.0005	49.4	11.5
		Depth	1.0	2e-16		
		MLD	1.0	2e-16		
		SST	4.3	2e-16		
		SAL	1.0	2e-16		
		Distance to 2000m isobath	1.0	3e-5		

Table 5.3-9: Model outputs for combined S2/CODA common dolphin GAM

Name	Factor levels	Estimate	Std. Error	Z value	PR(>z)	
Combined S2/CODA and S3/ObSERVE model	Intercept (Ecoregion Celtic seas)	-6.6	0.2	-29.3	2e-16	
	Ecoregion Bay of Biscay	1.9	0.41	4.6	5.3e-6	
Model	**Error distribution**	**Model covariates**	**Estimated degrees of freedom**	**% Deviance explained**	**Model degrees of freedom**	**P value**
Combined S2/CODA and S3/ObSERVE model	Negative Binomial	MLD	2.1	26.7	12.9	0.004
		SSH	3.2			2.8e-4
		Distance to escarpments	6.7			2e-16

Table 5.3-10: Model outputs for combined S2/CODA common dolphin GAM

Name	Factor levels	Estimate	Std. Error	Z value	PR(>z)	
Combined S2/CODA and S3/ObSERVE model	Intercept	-6.7	0.2	-32.0	2e-16	
	Ecoregion Bay of Biscay	0.9	0.3	3.5	5.6e-4	
	Year (2007)	0.3	0.3	1.03	0.3	
	Year (2016)	1.8	0.2	7.8	2e-16	
Model	**Error distribution**	**Model covariates**	**Estimated degrees of freedom**	**% Deviance explained**	**Model degrees of freedom**	**P value**
Combined S2/CODA and S3/ObSERVE model	Negative binomial	Depth	1.0	46.6	26.2	2e-16
		SLA	6.5			2e-16
		MLD	0.9			0.0001
		Salinity	0.5			0.18
		SST	6.3			2e-16
		Distance to escarpments	6.9			2e-16

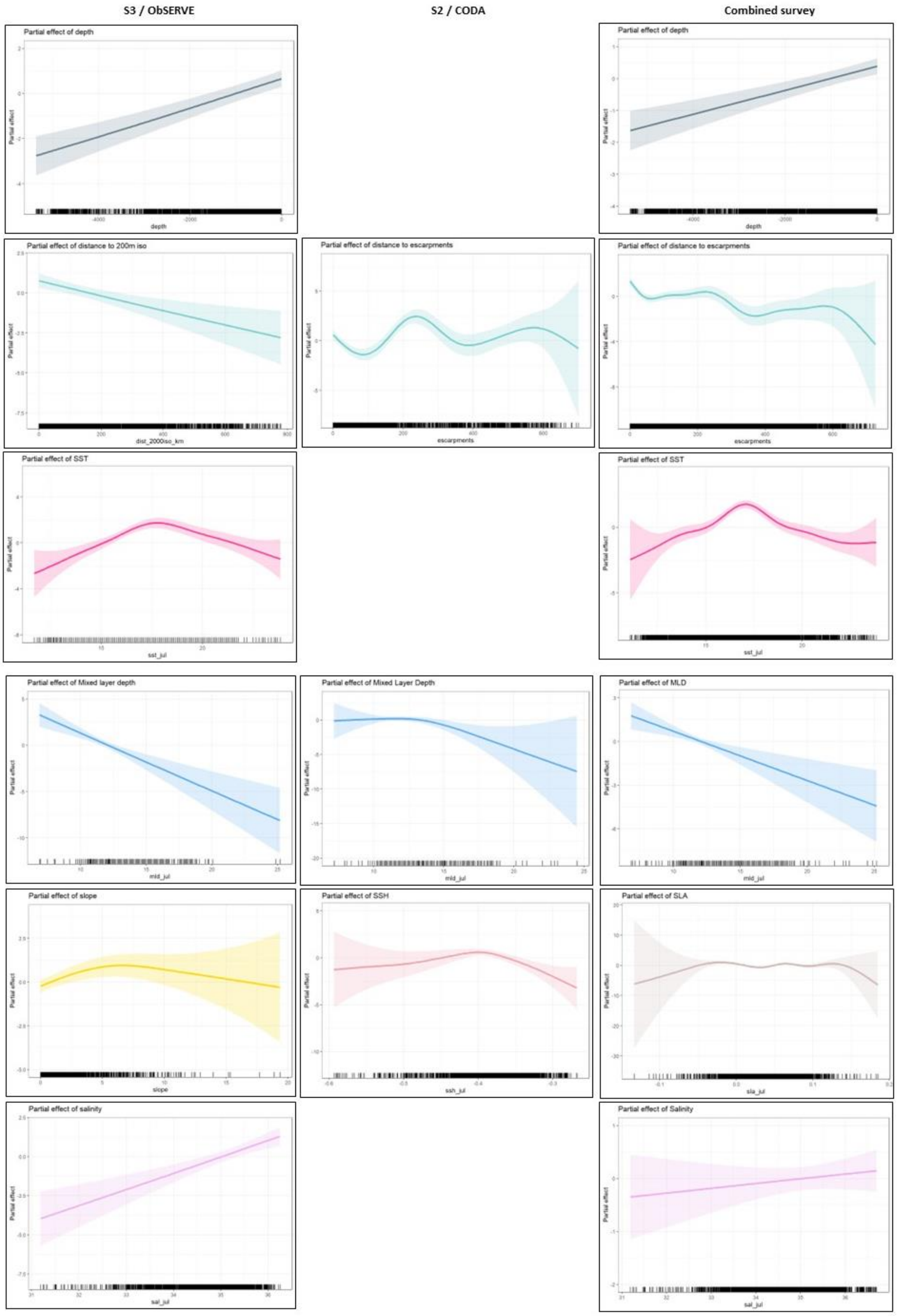

Figure 5.3-10: Plots of the fitted smooth functions for common dolphin group GAMS for S3/ObSERVE, S2/CODA and the combined survey model. "Rug" marks on the x-axis of the fitted smooth plots show the distribution of the data. Shaded areas represent the 95% confidence intervals. Where the same covariate is retained in multiple models, the smooths are shown on the same row. Effect sizes are variable, so axis scales are also variable in order to preserve necessary detail.

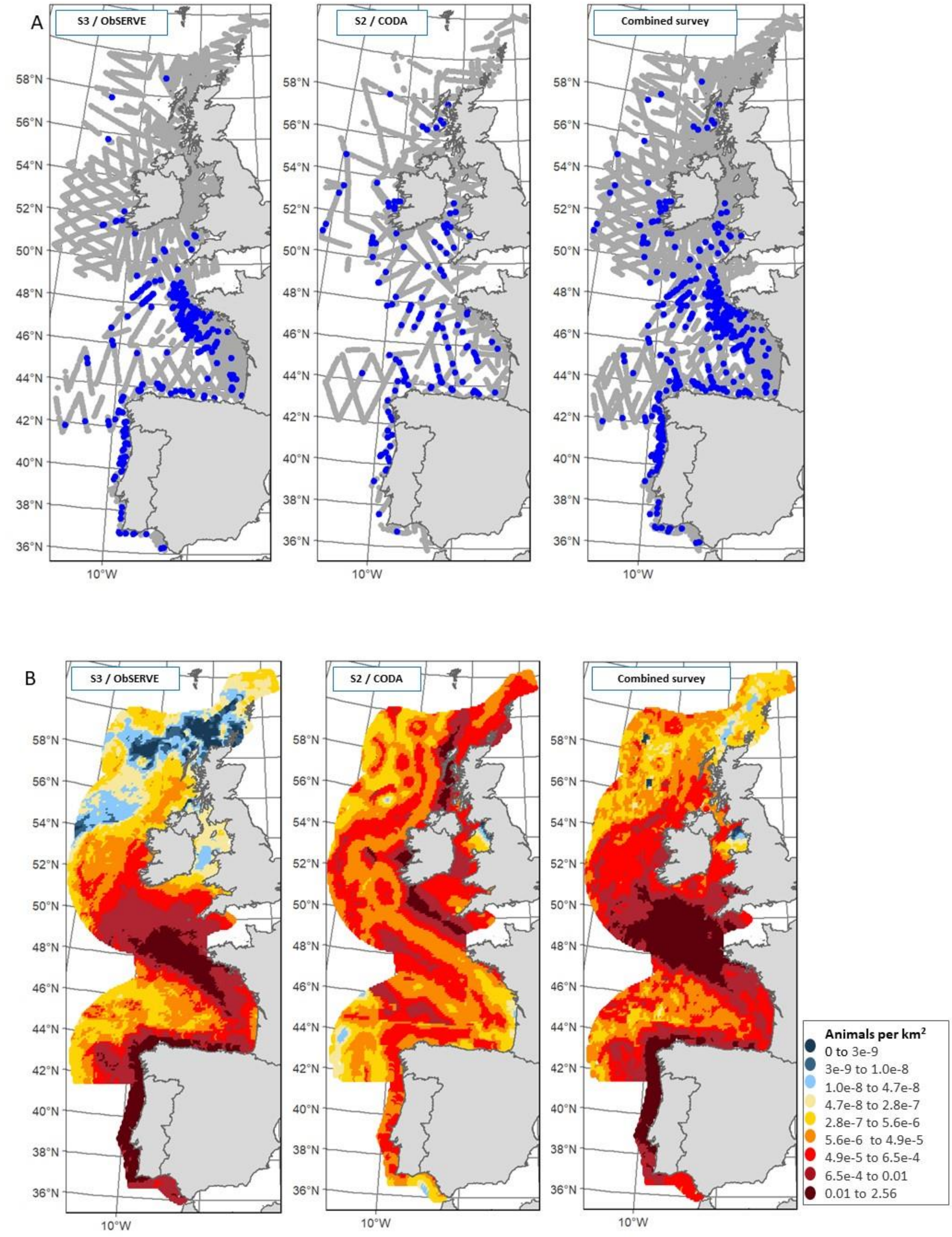

Figure 5.3-11: Location of effort and sightings (a), predicted density surface (b) for S2/CODA, S3/ObSERVE and combined survey fin whale models. Range of values represented by colours in the maps show the 1%, 2%, 5%, 10%, 25%, 50%, 75%, 90% and 100% quantiles. White areas are outside of predictive space. In some cases, prediction grid cells had covariate values which were outside the range encompassed by the modelled effort segments. In these instances, grid-cells were excluded from the prediction. Combined survey data are predicted using 2016 covariates.

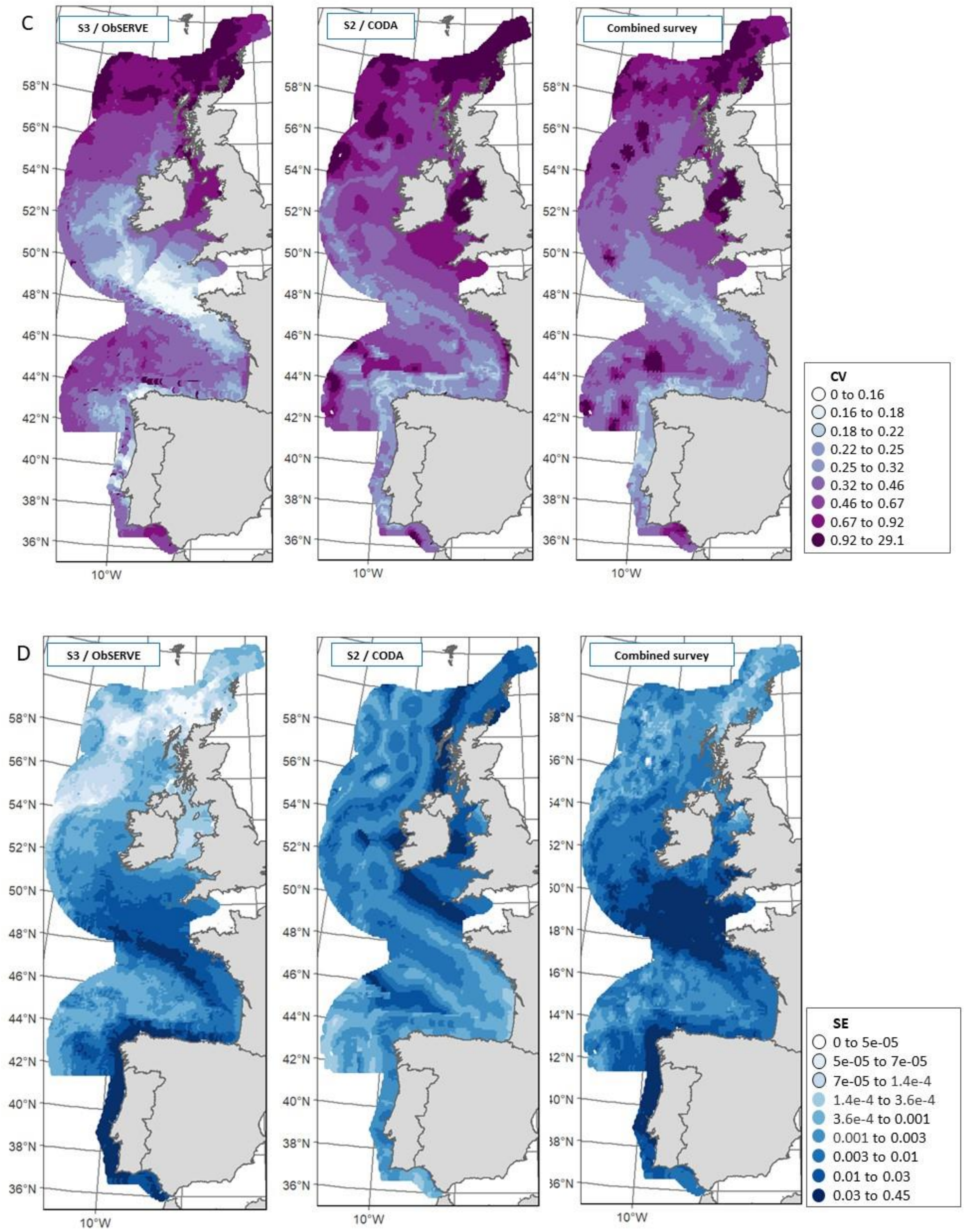

Figure 5.3-12: Coefficient of variation (CV) of density (C) and standard error (SE) of density (D) for S2 / CODA , S3 / ObSERVE and combined survey common dolphin group models. Range of values represented by colours in the maps show the 1%, 2%, 5%, 10%, 25%, 50%, 75%, 90% and 100% quantiles. White areas are outside of predictive space. In some cases, prediction grid cells had covariate values which were outside the range encompassed by the modelled effort segments. In these instances, grid-cells were excluded from the prediction. Combined survey data are predicted using 2016 covariates.

5.3.5 Striped dolphins

Summary results of the final environmental models for both ecoregions combined selected for striped dolphins are provided in **Table 5.3-11**. Model diagnostics indicated a satisfactory fit to the data, with the proportion of null deviance explained by the S3/ObSERVE model being 45.8%., and for the S2/CODA model being 34.2%. The combined survey plot explained 51.9% of the null deviance. The QQ plots and the residuals vs linear plots are provided in Appendix 4. Partial effects plots of the fitted smooth functions are shown in **Figure 5.3-13**. The satisfactory fit of the models indicates that the resulting predictions should be an appropriate representation of the relationships between predicted striped dolphin density and the model covariates.

All three models were best described using the negative binomial distribution. For both S3/ObSERVE and S2/CODA models, the model without a factor covariate for ecoregion was best. In the combined survey models, the model containing factor covariates for ecoregion and year was best (**Table 5.3-12**).

None of the covariates were retained in all three models. However, slope was retained in both S2/CODA and the combined survey model, and SD depth was retained in the S3/ObSERVE model. All three show the same relationship, with predicted dolphin density increasing linearly with increasing measure of seabed rugosity. In the two slope plots, the confidence intervals became wide towards the high end of the scale.

Depth was retained in both S2/CODA and the combined survey model. In S2/CODA, the relationship was linear, with predicted dolphin density being highest in deep water. This was refined somewhat in the combined survey model, with a slight shoulder to the shape of the relationship with peak predicted densities at around 3000-4000m depth.

The S3/ObSERVE model retained ADT, which showed an increase in predicted density with increasing ADT until 0.1m, at which point it started to decline gradually. The S2/CODA model retained SST, which showed a linear relationship between predicted density and temperature, with predicted density increasing with temperature.

Both S3/ObSERVE and the combined survey model retained salinity. The same relationship is evident in both plots, with predicted density increasing linearly with increasing salinity.

The S3/ObSERVE model also retained the distance to coast covariate. The effect of this was not very pronounced, however it did show an increase in predicted density further from the coast.

The highest densities of striped dolphins were predicted throughout the offshore part of the Bay of Biscay ecoregion in the S3/ObSERVE model, with very few animals predicted in the Celtic Seas ecoregion (Figure 5.3-14-b); this is a good reflection of the sightings data (Figure 5.3-14-a). The plot of predicted CV shows high CVs in areas of low predicted density (Figure 5.3-15c).

The S2/CODA prediction is a reasonable reflection of field sightings across most of the range except for predicting high densities of animals along the Portuguese coast in shelf waters where there are no observations (Figure 5.3-14-e, d). The combined model shows some evidence of over prediction, with large densities of dolphin groups being predicted along the shelf edge into waters much further north than those which contained any sightings.

Table 5.3-11: Model outputs for striped dolphin GAMs for 2016 and 2005 data.

Model	Error distribution	Model covariates	Estimated degrees of freedom	P value	% Deviance explained	Model degrees of freedom
2016	Negative binomial	SDdepth	0.9	0.0006	45.8	6.2
		ADT	3.2	2e-16		
		Salinity	0.9	0.001		
		Distance to coastline	0.7	0.082		
2005	Negative binomial	Depth	1.0	2e-16	34.2	3.7
		SST	1.0	0.0003		
		Slope	0.7	0.1		

Table 5.3-12: Model outputs for combined S2/CODA striped dolphin GAM

<table>
<tr><th>Name</th><th>Factor levels</th><th>Estimate</th><th>Std. Error</th><th>Z value</th><th colspan="2">PR(>z)</th></tr>
<tr><td rowspan="4">Combined S2/CODA and S3/ObSERVE model</td><td>Intercept</td><td>-11.2</td><td>0.78</td><td>-14.4</td><td colspan="2">2e-16</td></tr>
<tr><td>Ecoregion Bay of Biscay</td><td>3.7</td><td>0.62</td><td>6.1</td><td colspan="2">1.3e-9</td></tr>
<tr><td>Year (2007)</td><td>-0.3</td><td>0.62</td><td>-0.5</td><td colspan="2">0.6</td></tr>
<tr><td>Year (2016)</td><td>2.5</td><td>0.57</td><td>4.4</td><td colspan="2">9.1e-5</td></tr>
<tr><td>Model</td><td>Error distribution</td><td>Model covariates</td><td>Estimated degrees of freedom</td><td>% Deviance explained</td><td>Model degrees of freedom</td><td>P value</td></tr>
<tr><td rowspan="3">Combined S2/CODA and S3/ObSERVE model</td><td rowspan="3">Negative binomial</td><td>Slope</td><td>0.6</td><td rowspan="3">51.9</td><td rowspan="3">7.9</td><td>0.1</td></tr>
<tr><td>Depth</td><td>2.5</td><td>3.7e-7</td></tr>
<tr><td>Salinity</td><td>0.7</td><td>0.06</td></tr>
</table>

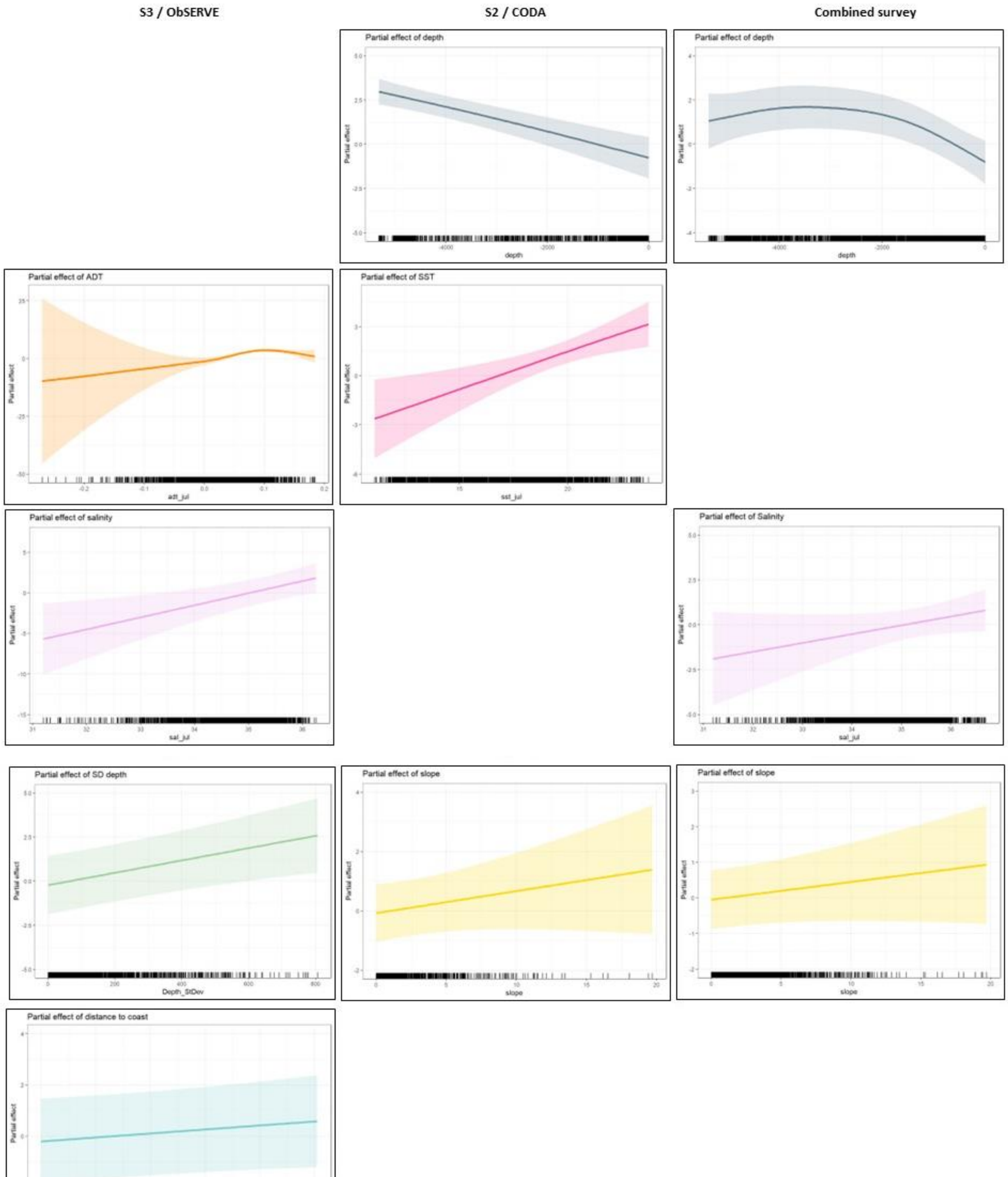

Figure 5.3-13: Plots of the fitted smooth functions for striped dolphin group GAMS for S3/ObSERVE, S2/CODA and the combined survey model. "Rug" marks on the x-axis of the fitted smooth plots show the distribution of the data. Shaded areas represent the 95% confidence intervals. Where the same covariate is retained in multiple models, the smooths are shown on the same row. Effect sizes are variable, so axis scales are also variable in order to preserve necessary detail.

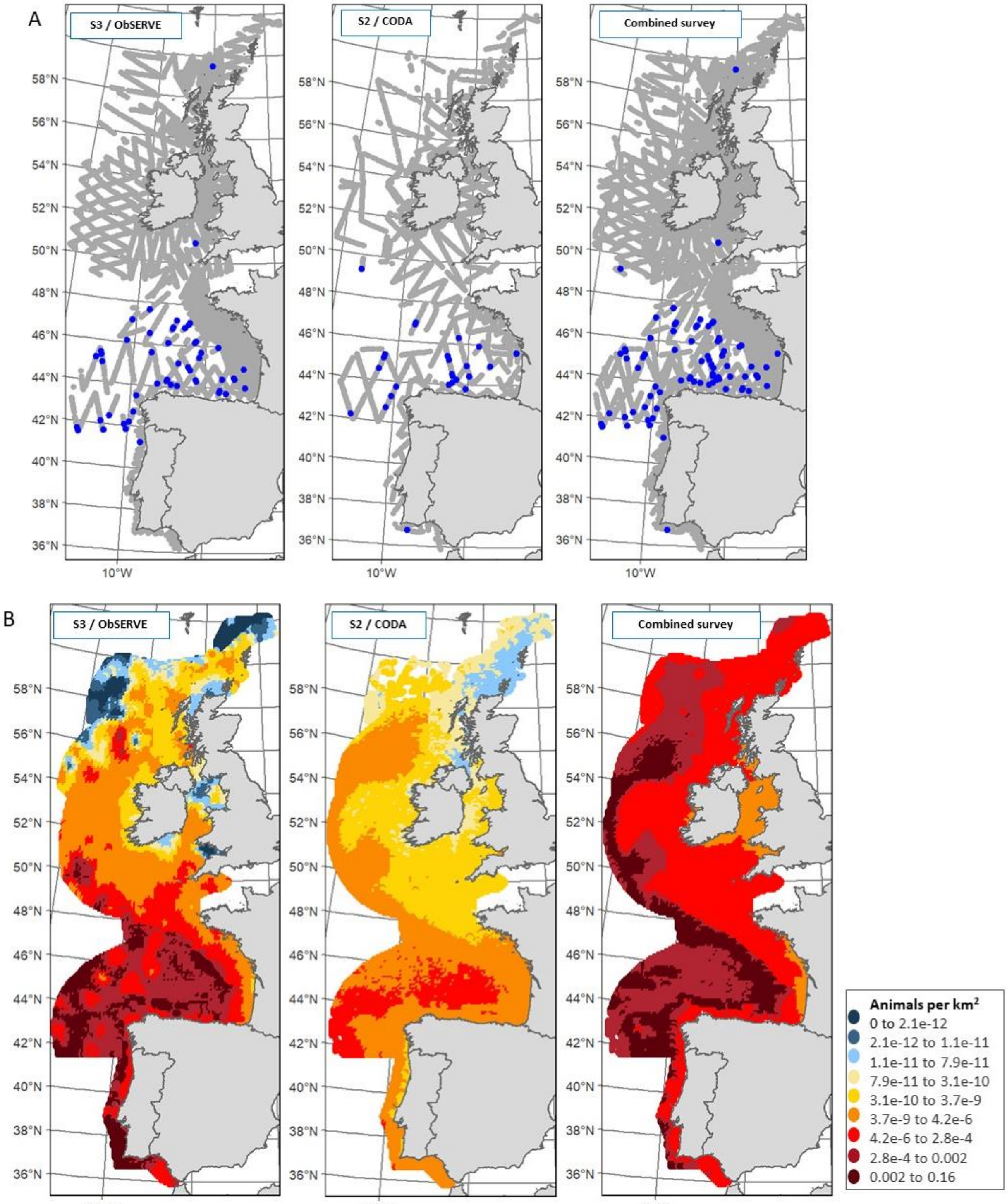

Figure 5.3-14: Location of effort and sightings (a), predicted density surface (b) for S2/CODA, S3/ObSERVE and combined survey striped dolphin models. Range of values represented by colours in the maps show the 1%, 2%, 5%, 10%, 25%, 50%, 75%, 90% and 100% quantiles. White areas are outside of predictive space. In some cases, prediction grid cells had covariate values which were outside the range encompassed by the modelled effort segments. In these instances, grid-cells were excluded from the prediction. Combined survey data are predicted using 2016 covariates.

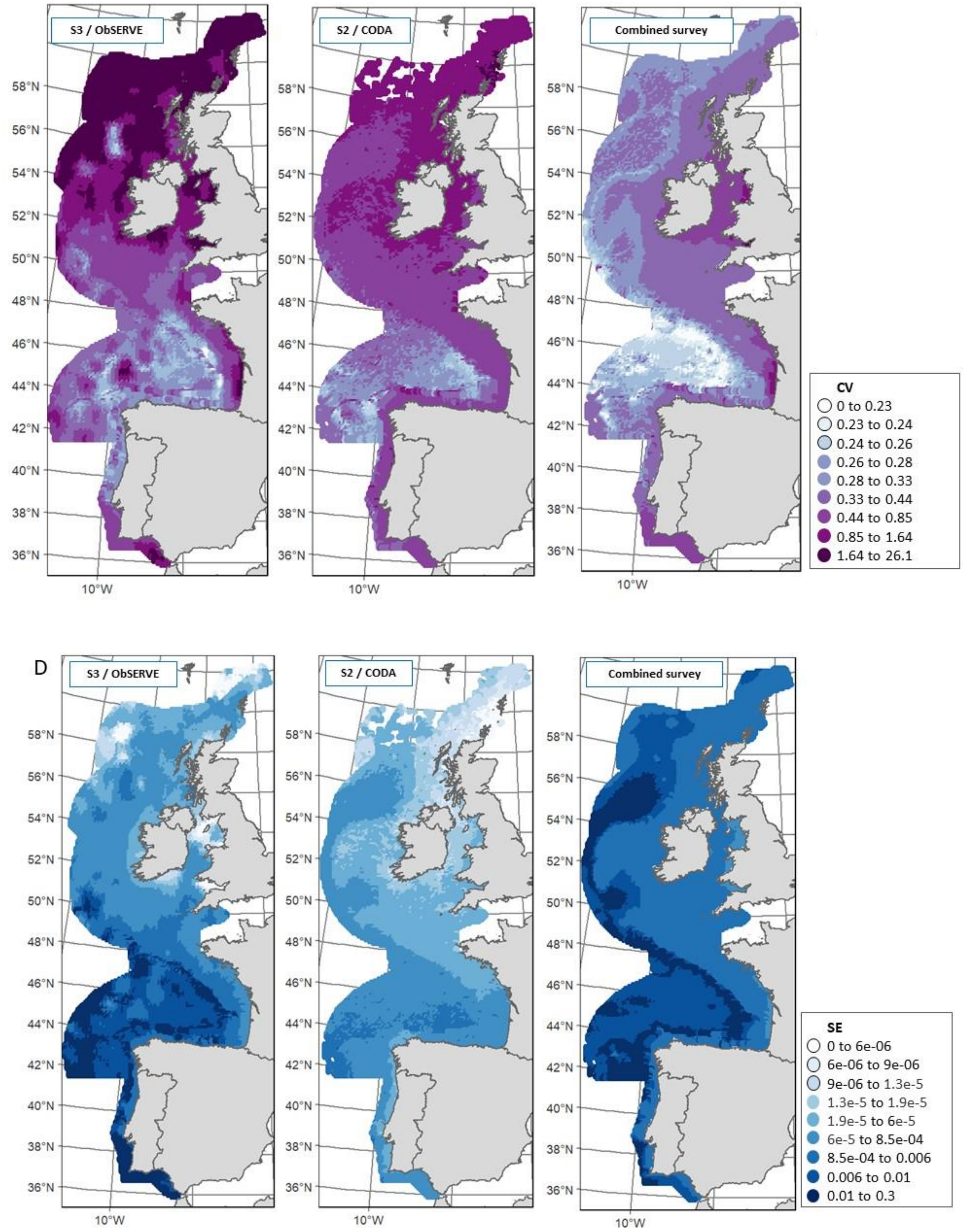

Figure 5.3-15: Coefficient of variation (CV) of density (C) and standard error (SE) of density (D) for S2/CODA, S3/ObSERVE and combined survey striped dolphin group models. Range of values represented by colours in the maps show the 1%, 2%, 5%, 10%, 25%, 50%, 75%, 90% and 100% quantiles. White areas are outside of predictive space. In some cases, prediction grid cells had covariate values which were outside the range encompassed by the modelled effort segments. In these instances, grid-cells were excluded from the prediction. Combined survey data are predicted using 2016 covariates.

5.4 Discussion

The highest predicted densities of white-sided dolphins are in the very north of the Celtic Seas ecoregion (S3/ObSERVE), and mid to north Celtic Seas ecoregion (S2/CODA). From the field data alone, it does appear that there was a more northerly distribution in 2016, and this is reflected in the model predictions. Compared to the other species included in this chapter, it should be noted that there were relatively few data upon which these models are based.

The final model for both time periods, as well as for the combined year period, retained SST and salinity, whilst the S3/ObSERVE model also retained depth and SD depth, and the combined year model retained SD depth. The relationships for covariates which occur in multiple models show the same, or very similar shapes. The preference for waters of a higher salinity may be an artefact of animals preferring deeper or more offshore waters rather than a preference for the salinity itself.

Possibly due to their more offshore distribution, this species has been the subject of fewer habitat modelling studies than many of the other species in the chapter. Some studies have been conducted however, and have reported a strong preference for the 200m isobath (particularly associated with the Rockall Bank) (Breen et al., 2016), and distance to coast (MacLeod et al., 2007). Despite being considered as a cooler water species, white-sided dolphins prefer waters that are not too cold, being associated with waters warmer than 12.2^{0}C (MacLeod et al., 2007). The July mean values of SST for 2016 was 14.6^{0}C and for 2007 was 15.3^{0}C. With there being minimal data for waters below 12^{0}C, that may explain why SST was not retained in these models.

Areas of steeper slopes have also been linked to dolphin occurrence (Doksæter et al., 2008). This was not found to be the case with these models, which predicted highest density in areas of low SD depth, which are areas with minimal change of depth, so therefore low or no slope. Doksæter et al., (2008) reported white-sided dolphins to be associated primarily with water with a salinity of 35.02 PSU, which is comparable to that in areas where sightings occurred.

5.4.1 Offshore bottlenose dolphins

Sightings of this species were widely distributed throughout the central part of both ecoregions. There are considerably more sightings data from 2016 than from 2005/7, but the overall distribution of sightings is broadly similar.

A variety of covariates were retained across the three models, but the only one to persist in all three was depth, which predicted highest densities of dolphins in shallower waters, with a linear decrease in density as depth increased. The shape of this relationship was consistent across the models. The wide variety of variables and the differences between years is perhaps indicative of two things.

Firstly, the bottlenose dolphin is a highly opportunistic species, with a variable worldwide distribution, and a wide range of known prey species. Secondly, this species is known to contain different ecotypes, which inhabit different ecological niches (Perrin et al., 2011; Rosel et al., 2009; Tezanos-Pinto et al., 2009), including in the study area (Louis et al., 2014; Oudejans et al., 2015). It is likely that the survey in both years sampled animals from both offshore and coastal ecotypes in different parts of their range. The ecological drivers of distribution for each ecotype may not be the same, and this may be reflected here in the range of different variables which are linked with high predicted density.

5.4.2 Fin whales

The 2016 field sightings of fin whales are largely in the Bay of Biscay, with a few to the far north of Scotland, and two to the south-west of Ireland. These are reasonably well reflected in the predicted density surface, where the majority of the prediction is centred on the Bay of Biscay.

The 2005/7 field sightings are also largely centred in the Bay of Biscay, with a few to the north of the area – this time to the northwest of Ireland. The predicted density map however is a poorer reflection of the observations for this time period, with the highest densities being predicted off of the west of Ireland where there only a handful of field detections. This model is the only one for which the model containing a factor for ecoregion was the best.

Two of the same covariates were maintained across all three models – MLD and depth.

In both of the two single year models, depth of the mixed layer predicted density of fin whales to linearly decrease as the mixed layer became deeper. For the combined year model, there was a peak density of whales predicted for a mixed layer depth of around 12m. Data for very shallow and very deep mixed layer depths are sparce, however, and the confidence intervals are correspondingly wide at the extremities.

Depth was also retained in the 2016 model and predicted densities were more or less constant in waters deeper than 1000m. Tagging studies of fin whales have shown that prey consumption can increase by as much as 4x during deep dives compared with shallow foraging, so whales may be targeting deeper areas to maximise feeding efficiency (Friedlaender et al., 2020). This is an areas in which fin whales are known to feed during the summer months (Spitz et al., 2018).

5.4.3 Common dolphin

Whilst there are field sightings and model predictions of common dolphins in both ecoregions, the majority are predicted in the Bay of Biscay region, in the shelf waters. They are also predicted into the Irish Sea in the S2/ObSERVE model and further offshore into the Bay of Biscay, to the north of Spain. There are a large number, comparatively, of sightings of common dolphins, and this allowed for more covariates to be retained in both final models. Common dolphins conduct considerable seasonal and inter-annual movements (e.g. Laran et al., 2017; Rogan et al., 2018). and that may be reflected in the different distribution of sightings seen in the data between the two survey periods.

Previous studies have linked their presence strongly with temperature variables, with presence around the UK and Ireland predicted to be more likely in temperatures warmer than 12^0C (MacLeod et al., 2008, 2007). In contrast, in the Alboran Sea in the Mediterranean Sea, where maximum SST can be higher, there is a preference for temperatures below 20^0C (Cañadas and Hammond, 2008). A preference for depth in the range 100-400m has been predicted from surveys in the Alboran Sea (Cañadas et al., 2005), but an association with deeper waters and shelf-edge features at depths of 400-1000m have been found in areas of the offshore North Atlantic (Cañadas et al., 2009).

In this study, the only covariate to persist in all three models in MLD. It shows a broadly similar shape in all three models, with declining density of dolphins predicted as MLD increases. The S2/CODA model is flat to around 14m before decreasing, the other two years show a simple linear decrease.

Previous studies have found that common dolphin distribution is best predicted by chlorophyll concentration, as a proxy for pelagic schooling fish (Moura et al., 2012; Cañadas and Hammond, 2008, Pusineri et al., 2007). Chlorophyll was not included in any of these models, however in the case of this species, it is possible that the dynamic covariates retained in the modelling process are not sufficient to capture the variability of distribution of this wide-ranging species. It has been hypothesized that they follow small pelagic schooling fish, and inter-annual distribution can vary widely, so further studies of common dolphins may be best targeted towards modelling predictors specific to their preferred prey items (Moura et al, 2012). It should be noted, however, that this is not straightforward, as was shown by the inclusion of prey covariates in the previous chapter, which were less successful than the environmental only models. It has been suggested that overall relationships between environmental variables and distribution or even population structure in common dolphins may be caused by prey behaviour. This, Amaral et al., (2012) suggests is believed to determine their movement patterns as well as their associations with environmental characteristics.

5.4.4 Striped dolphins

Striped dolphins field sightings were primarily located in the Bay of Biscay ecoregion. The predicted density surfaces for all models were both relatively good reflections of the sightings, however the maps of CVs show high levels of uncertainty in the predictions. From looking at the field sightings and comparing the distribution of the two species, there appears to be broad separation of common and striped dolphins around the 200m depth contour, with striped dolphins found primarily in deeper waters, and common dolphins primarily in shallower waters. This is particularly marked in the S3/ObSERVE data. (Reilly, 1990) also reported a summer separation in the distribution of these two species from large scale surveys of the Eastern Tropical Pacific.

Much of the previous work on striped dolphin distribution has been conducted on animals in the Mediterranean Sea. Here, bathymetric variables have been found to be the most useful predictors, although a relationship with the temperature range 21-24^{0}C has also been described (Panigada et al., 2008). Distance from coast, depth and distance from industrial areas and slope have also been found to be useful predictors (Azzolin et al., 2020; Carlucci et al., 2016).

None of the same covariates were retained across the three models. The highest densities of animals in S3/ObSERVE models were predicted by high levels of seabed rugosity, areas of higher ADT (associated with warmer water), areas of high salinity, and increasing distance from coast.

The highest densities of animals in the S2/CODA model were predicted in areas of steep slope, increasing depth, and increasing SST. The combined year model retained slope, depth and salinity.

The association with sea surface temperature is in broad agreement with findings from studies in the Mediterranean by Panigada et al (2008), and the relationships with depth and distance to coast are in broad agreement with the findings of Azzolin et al., (2020) and Carlucci et al., (2016). The lack of shared covariates between years, and the high CV in the predicted densities suggests however that the distribution of this species cannot be well predicted by the environmental covariates used in these models. Dietary studies of striped dolphins have found them to be able to feed on prey items of more than 30 distinct taxa, including individuals representing oceanic, neritic and coastal prey types, indicating high levels of prey plasticity (Spitz et al., 2006), with prey composition and size range differing slightly with sex and age / size of the dolphins themselves (Ringelstein et al., 2006; Saavedra et al., 2022). This level of adaptability likely compromises our ability to describe environmental drivers of distribution.

5.4.5 Conclusions

The environmental models produced in this chapter provide reasonable fits to the data. Despite small numbers of datapoints in the case of white-sided dolphins in particular, the model diagnostics are generally acceptable, and the predictions fit the observed data. Overall, the S2/CODA data fit less well than the S3/ObSERVE data, which may be due to less good survey coverage across the area. In an attempt to investigate this, multi-year models were also produced. In some cases, some of the covariates persisted in multi-year models, for example MLD and depth in fin whales, which may indicate that these are covariates represent genuine ecological relationships. In other instances, such as striped dolphins, there were no covariates which were retained in all three models.

This chapter was focused on species with a more offshore distribution, which are known to conduct seasonal movements and migrations (Aguilar and García-Vernet, 2018; Couperus, 1997; Laran et al., 2017; Rogan et al., 2018). The study region, large as it is, represents only a small proportion of their potential habitat, as such we are able to capture only a small proportion of their summer distribution, and only able to model a small fraction of what processes may be acting on this species.

5.5 Literature Cited

Aguilar, A., García-Vernet, R., 2018. Fin Whale, in: Encyclopedia of Marine Mammals. Elsevier, pp. 368–371. https://doi.org/10.1016/B978-0-12-804327-1.00128-X

Amaral, A.R., Beheregaray, L.B., Bilgmann, K., Boutov, D., Freitas, L., Robertson, K.M., Sequeira, M., Stockin, K.A., Coelho, M.M., Möller, L.M., 2012. Seascape Genetics of a Globally Distributed, Highly Mobile Marine Mammal: The Short-Beaked Common Dolphin (Genus *Delphinus*). PLoS ONE 7, e31482. https://doi.org/10.1371/journal.pone.0031482

Archer, F.I., Perrin, W.F., 1999. *Stenella coeruleoalba*. Mamm. Species 603, 1–9.

Azzolin, M., Arcangeli, A., Cipriano, G., Crosti, R., Maglietta, R., Pietroluongo, G., Saintingan, S., Zampollo, A., Fanizza, C., Carlucci, R., 2020. Spatial distribution modelling of striped dolphin (Stenella coeruleoalba) at different geographical scales within the EU Adriatic and Ionian Sea Region, central-eastern Mediterranean Sea. Aquat. Conserv. Mar. Freshw. Ecosyst. 30, 1194–1207. https://doi.org/10.1002/aqc.3314

Berrow, S., 2012. Abundance Estimate of Bottlenose Dolphins (*Tursiops truncatus*) in the Lower River Shannon candidate Special Area of Conservation, Ireland. Aquat. Mamm. 38, 136–144. https://doi.org/10.1578/AM.38.2.2012.136

Breen, P., Brown, S., Reid, D., Rogan, E., 2016. Modelling cetacean distribution and mapping overlap with fisheries in the northeast Atlantic. Ocean Coast. Manag. 134, 140–149. https://doi.org/10.1016/j.ocecoaman.2016.09.004

Bristow, T., Rees, E.I.S., 2001. Site fidelity and behaviour of bottlenose dolphins (*Tursiops truncatus*) in Cardigan Bay, Wales. Aquat. Mamm. 27, 1–10.

Cañadas, A., Donovan, G.P., Desportes, G., Borchers, D.L., 2009. A short review of the distribution of short-beaked common dolphins (*Delphinus delphis*) in the central and eastern North Atlantic with an abundance estimate for part of this area. NAMMCO Sci. Publ. 7, 201. https://doi.org/10.7557/3.2714

Cañadas, A., Hammond, P., 2008. Abundance and habitat preferences of the short-beaked common dolphin *Delphinus delphis* in the southwestern Mediterranean: implications for conservation. Endanger. Species Res. 4, 309–331. https://doi.org/10.3354/esr00073

Cañadas, A., Sagarminaga, R., De Stephanis, R., Urquiola, E., Hammond, P.S., 2005. Habitat preference modelling as a conservation tool: proposals for marine protected areas for cetaceans in southern Spanish waters. Aquat. Conserv. Mar. Freshw. Ecosyst. 15, 495–521. https://doi.org/10.1002/aqc.689

Carlucci, R., Fanizza, C., Cipriano, G., Paoli, C., Russo, T., Vassallo, P., 2016. Modeling the spatial distribution of the striped dolphin (*Stenella coeruleoalba*) and common bottlenose dolphin (*Tursiops truncatus*) in the Gulf of Taranto (Northern Ionian Sea, Central-eastern Mediterranean Sea). Ecol. Indic. 69, 707–721. https://doi.org/10.1016/j.ecolind.2016.05.035

Couperus, A.S., 1997. Interactions Between Dutch Midwater Trawl and Atlantic White-sided Dolphins (*Lagenorhynchus acutus*) Southwest of Ireland. J. Northwest Atl. Fish. Sci. 22, 209–218. https://doi.org/10.2960/J.v22.a16

Doksæter, L., Olsen, E., Nøttestad, L., Fernö, A., 2008. Distribution and feeding ecology of dolphins along the Mid-Atlantic Ridge between Iceland and the Azores. Deep Sea Res. Part II Top. Stud. Oceanogr. 55, 243–253. https://doi.org/10.1016/j.dsr2.2007.09.009

Friedlaender, A.S., Bowers, M.T., Cade, D., Hazen, E.L., Stimpert, A.K., Allen, A.N., Calambokidis, J., Fahlbusch, J., Segre, P., Visser, F., Southall, B.L., Goldbogen, J.A., 2020. The advantages of diving deep: Fin whales quadruple their energy intake when targeting deep krill patches. Funct. Ecol. 34, 497–506. https://doi.org/10.1111/1365-2435.13471

Gaspar, R., 2003. Status of the resident bottlenose dolphin population in the Sado estuary: past, present and future (Thesis). University of St Andrews.

Grellier, K., Wilson, B., 2003. Bottlenose dolphins using the Sound of Barra, Scotland. Aquat. Mamm. 29, 378–382. https://doi.org/10.1578/01675420360736550

Guisan, A., Edwards, T.C., Hastie, T., 2002. Generalized linear and generalized additive models in studies of species distributions: setting the scene. Ecol. Model. 157, 89–100. https://doi.org/10.1016/S0304-3800(02)00204-1

Hammond, P., Lacey, C., Gilles, A., Viquerat, S., Börjesson, P., Herr, H., Macleod, K., Ridoux, V., Santos, M., Teilmann, J., Vingada, J., and Øien, N. 2021. Estimates of cetacean abundance in European Atlantic waters in summer 2016 from the SCANS-III aerial and shipboard surveys. Final project report. https://scans3.wp.st-andrews.ac.uk/files/2021/06/SCANS-III_design-based_estimates_final_report_revised_June_2021.pdf

Hammond, P., Macleod, K., Gillespie, D., Swift, R., Winship, A., Burt, M., Cañadas, A., Vázquez, J., Ridoux, V., Certain, G., Canneyt, O.V., Lens, S., Santos, B., Rogan, E., Uriarte, A., Hernandez, C., Castro, R., 2009. Cetacean Offshore Distribution and Abundance in the European Atlantic (CODA). Final project report. http://biology.st-andrews.ac.uk/coda/

Hammond, P.S., Gillespie, D., Lovell, P., Samarra, F., Swift, R., Macleod, K., Tasker, M.L., Berggren, P., Borchers, D.L., Burt, L., Paxton, C.G.M., Cañadas, A., Desportes, G., Donovan, G.P., Gilles, A., Lehnert, K., Siebert, U., Gordon, J., Leaper, R., Leopold, M., Scheidat, M., Øien, N., Ridoux, V., Rogan, E., Skov, H., Teilmann, J., Van Canneyt, O., Vázquez, J.A., 2014. Large scale surveys for cetaceans: Line transect assumptions, reliability of abundance estimates and improving survey efficiency – A response to MacLeod. Biol. Conserv. 170, 338–339. https://doi.org/10.1016/j.biocon.2014.01.016

Harzen, S., 1998. Habitat use by the bottlenose dolphin (Tursiops truncatus) in the Sado Estuary, Portugal. Aquat. Mamm. 24.

Hernandez-Milian, G., Begoña Santos, M., Reid, D., Rogan, E., 2016. Insights into the diet of Atlantic white-sided dolphins (*Lagenorhynchus acutus*) in the Northeast Atlantic. Mar. Mammal Sci. 32, 735–742. https://doi.org/10.1111/mms.12272

ICES, 2020a. Celtic Seas Ecoregion: Ecosystem overview. https://doi.org/10.17895/ICES.ADVICE.7631

ICES, 2020b. Bay of Biscay and the Iberian Coast Ecoregion. Ecosystem overview. https://ices-library.figshare.com/articles/report/Bay_of_Biscay_and_the_Iberian_Coast_ecoregion_Ecosystem_Overview/21731579

Ingram, S., Rogan, E., 2002. Identifying critical areas and habitat preferences of bottlenose dolphins Tursiops truncatus. Mar. Ecol. Prog. Ser. 244, 247–255. https://doi.org/10.3354/meps244247

Kiszka, J., Macleod, K., Van Canneyt, O., Walker, D., Ridoux, V., 2007. Distribution, encounter rates, and habitat characteristics of toothed cetaceans in the Bay of Biscay and adjacent waters from platform-of-opportunity data. ICES J. Mar. Sci. 64, 1033–1043. https://doi.org/10.1093/icesjms/fsm067

Laran, S., Authier, M., Blanck, A., Doremus, G., Falchetto, H., Monestiez, P., Pettex, E., Stephan, E., Van Canneyt, O., Ridoux, V., 2017. Seasonal distribution and abundance of cetaceans within French waters- Part II: The Bay of Biscay and the English Channel. Deep Sea Res. Part II Top. Stud. Oceanogr. 141, 31–40. https://doi.org/10.1016/j.dsr2.2016.12.012

Louis, M., Viricel, A., Lucas, T., Peltier, H., Alfonsi, E., Berrow, S., Brownlow, A., Covelo, P., Dabin, W., Deaville, R., de Stephanis, R., Gally, F., Gauffier, P., Penrose, R., Silva, M.A., Guinet, C., Simon-Bouhet, B., 2014. Habitat-driven population structure of bottlenose dolphins, *Tursiops truncatus*, in the North-East Atlantic. Mol. Ecol. 23, 857–874. https://doi.org/10.1111/mec.12653

MacLeod, C.D., Weir, C.R., Pierpoint, C., Harland, E.J., 2007. The habitat preferences of marine mammals west of Scotland (UK). J. Mar. Biol. Assoc. U. K. 87, 157–164. https://doi.org/10.1017/S0025315407055270

MacLeod, C.D., Weir, C.R., Santos, M.B., Dunn, T.E., 2008. Temperature-based summer habitat partitioning between white-beaked and common dolphins around the United Kingdom and Republic of Ireland. J. Mar. Biol. Assoc. U. K. 88, 1193–1198. https://doi.org/10.1017/S002531540800074X

Macleod, K., 2004. Abundance of Atlantic white-sided dolphin (*Lagenorhynchus acutus*) during summer off northwest Scotland 9.

Mason, E., Coombs, S., Oliveira, P.B., 2006. An overview of the literature concerning the oceanography of the Eastern North Atlantic region (No. 33), Relatorios cientificose e Tecnicos.

Moura, A.E., Sillero, N., Rodrigues, A., 2012. Common dolphin (Delphinus delphis) habitat preferences using data from two platforms of opportunity. Acta Oecologica 38, 24–32. https://doi.org/10.1016/j.actao.2011.08.006

OSPAR Commission (Ed.), 2000. Quality status report 2000. London.

Oudejans, M.G., Visser, F., Englund, A., Rogan, E., Ingram, S.N., 2015. Evidence for Distinct Coastal and Offshore Communities of Bottlenose Dolphins in the Northeast Atlantic. PLOS ONE 10, e0122668. https://doi.org/10.1371/journal.pone.0122668

Panigada, S., Zanardelli, M., MacKenzie, M., Donovan, C., Mélin, F., Hammond, P.S., 2008. Modelling habitat preferences for fin whales and striped dolphins in the Pelagos Sanctuary (Western Mediterranean Sea) with physiographic and remote sensing variables. Remote Sens. Environ. 112, 3400–3412. https://doi.org/10.1016/j.rse.2007.11.017

Perrin, W.F., Thieleking, J.L., Walker, W.A., Archer, F.I., Robertson, K.M., 2011. Common bottlenose dolphins (Tursiops truncatus) in California waters: Cranial differentiation of coastal and offshore ecotypes. Mar. Mammal Sci. 27, 769–792. https://doi.org/10.1111/j.1748-7692.2010.00442.x

Pusineri, C., Magnin, V., Meynier, L., Spitz, J., Hassani, S., Ridoux, V., 2007. Food and Feeding Ecology of the Common Dolphin (*Delphinus delphis*) in the Oceanic Northeast Atlantic and Comparison with Its Diet in Neritic Areas. Mar. Mammal Sci. 23, 30–47. https://doi.org/10.1111/j.1748-7692.2006.00088.x

Reid, J.B., Evans, P.G.H., Northridge, S.P., 2003. Atlas of Cetacean distribution in north-west European waters 82.

Reilly, S.B., 1990. Seasonal changes in distribution and habitat differences among dolphins in the eastern tropical pacific. Mar. Ecol. Prog. Ser. 66, 1–11. https://doi.org/10.3354/meps066001

Ringelstein, J., Pusineri, C., Hassani, S., Meynier, L., Nicolas, R., Ridoux, V., 2006. Food and feeding ecology of the striped dolphin, *Stenella coeruleoalba*, in the oceanic waters of the north-east Atlantic. J. Mar. Biol. Assoc. U. K. 86, 909–918. https://doi.org/10.1017/S0025315406013865

Rogan, E., Breen, P., Mackey, M., Cañadas, A., Scheidat, M., Geelhoed, S., Jessopp, M., 2018. Aerial Surveys of Cetaceans and Seabirds in Irish waters: Occurrence, distribution and abundance in 2015-2017 298.

Rosel, P.E., Hansen, L., Hohn, A.A., 2009. Restricted dispersal in a continuously distributed marine species: common bottlenose dolphins *Tursiops truncatus* in coastal waters of the western North Atlantic. Mol. Ecol. 18, 5030–5045. https://doi.org/10.1111/j.1365-294X.2009.04413.x

Saavedra, C., García-Polo, M., Giménez, J., Mons, J.L., Castillo, J.J., Fernández-Maldonado, C., de Stephanis, R., Pierce, G.J., Santos, M.B., 2022. Diet of striped dolphins (*Stenella coeruleoalba*) in southern Spanish waters. Mar. Mammal Sci. mms.12945. https://doi.org/10.1111/mms.12945

Simões-Lopes, P., Daura-Jorge, F., Lodi, L., Bezamat, C., Costa, A., Wedekin, L., 2019. Bottlenose dolphin ecotypes of the western South Atlantic: the puzzle of habitats, coloration patterns and dorsal fin shapes. Aquat. Biol. 28, 101–111. https://doi.org/10.3354/ab00712

Simon, M., Nuuttila, H., Reyes-Zamudio, M.M., Ugarte, F., Verfub, U., Evans, P.G.H., 2010. Passive acoustic monitoring of bottlenose dolphin and harbour porpoise, in Cardigan Bay, Wales, with implications for habitat use and partitioning. J. Mar. Biol. Assoc. U. K. 90, 1539–1545. https://doi.org/10.1017/S0025315409991226

Spitz, J., Richard, E., Meynier, L., Pusineri, C., Ridoux, V., 2006. Dietary plasticity of the oceanic striped dolphin, *Stenella coeruleoalba*, in the neritic waters of the Bay of Biscay. J. Sea Res. 55, 309–320.

Spitz, J., Ridoux, V., Trites, A.W., Laran, S., Authier, M., 2018. Prey consumption by cetaceans reveals the importance of energy-rich food webs in the Bay of Biscay. Prog. Oceanogr. 166, 148–158. https://doi.org/10.1016/j.pocean.2017.09.013

Tezanos-Pinto, G., Baker, C.S., Russell, K., Martien, K., Baird, R.W., Hutt, A., Stone, G., Mignucci-Giannoni, A.A., Caballero, S., Endo, T., Lavery, S., Oremus, M., Olavarría, C., Garrigue, C., 2009. A Worldwide Perspective on the Population Structure and Genetic Diversity of Bottlenose Dolphins (*Tursiops truncatus*) in New Zealand. J. Hered. 100, 11–24. https://doi.org/10.1093/jhered/esn039

Wall, D., Murray, C., O'Brien, J., Kavanagh, L., Wilson, C., Ryan, C., Glanville, B., Williams, D., Enlander, I., O'Connor, I., McGrath, D., Whooley, P., Berrow, S., 2013. Atlas of the Distribution and Relative Abundance of Marine Mammals in Irish Offshore Waters: 2005 – 201 65.

Wall, D., O'Brien, J., Meade, J., Allen, B.M., 2006. Summer Distribution and Relative Abundance of Cetaceans off the West Coast of Ireland. Biol. Environ. Proc. R. Ir. Acad. 106, 135–142. https://doi.org/10.3318/BIOE.2006.106.2.135

Weir, C.R., Pollock, C., Cronin, C., Taylor, S., 2001. Cetaceans of the Atlantic Frontier, north and west of Scotland. Cont. Shelf Res. 21, 1047–1071. https://doi.org/10.1016/S0278-4343(00)00124-2

6. Discussion

This thesis has examined the use of density surfaces to model the distribution of cetaceans. It has presented models using XY covariates to best explain the current distribution (Chapter 3) of animals, providing the best available snapshot of summer 2016 distribution currently available for this region. In addition, models intended to examine ecological relationships have been conducted at smaller spatial scales. This was an attempt to model a more homogeneous study area, in the hopes this would provide clearer indications of relationships within this environment. For one of these regions, the North Sea (Chapter 4) models including prey covariates were also attempted. The use of prey covariates did not improve the models, however the use of the smaller, North Sea ecoregion was successful. The larger ecoregions modelled in Chapter 5 provided fewer clear relationships.

6.1 Evaluation of methodology

6.1.1 Use of GAMs

GAMs are widely used in ecology due to their ability to model potentially complex and non-linear relationships, particularly when there are a large number of candidate explanatory covariates to be considered (Chambers and Dinsmore, 2014). One of the disadvantages of this technique, however, is the propensity of GAMs to overfit. For species models with very low numbers of sightings this can be a major issue. In this thesis, in many of the models fitted to data that had a low percentage of effort segments with observations, few covariates were retained, and those that were had very low estimated degrees of freedom (edf), with relationships often reduced to linear. Whilst this is not intrinsically problematic, in this case it is likely this was due to insufficient data to fully describe relationships, and further investigations of these relationships may benefit from limiting the initial number of starting covariates to see if more complex relationships were retained.

Ecological systems are complex by their nature, and trying to summarise this complexity with a set of predictor variables inevitably introduces error (Barry and Elith, 2006). This can be exacerbated if there is error during data collection which may cause masking of genuine ecological relationships. Because the data for this study were collected by multiple platforms across multiple years, it is possible that data collection errors were introduced. Effort was taken to standardize the data however, both during collection – which was done using common protocols and consideration given to having survey areas which were adjacent but not overlapping - and during the pre-modelling data assimilation phase in which the disparate datasets were merged. If collection errors persisted in the data, it would be impossible to remove these.

Whenever maps of predictions are presented in this thesis, I have provided a map of uncertainty associated with the prediction to try to make the reader as aware of the modelling uncertainty surrounding each model as possible (Barry and Elith, 2006; Miller et al., 2021). The data collection error remains unquantified. These unquantified errors are discussed below.

Cetacean data used in this these were collected using line transect methodology. This relies on the assumption that all objects on the transect line are detected with certainty (g(0) = 1). In reality, for cetacean surveys, this is known not to be the case. There are two reasons why animals may be missed.

1) They may be under water, and thus unavailable for detection (availability bias)
2) They may be available for detection, but they may be missed by the observers (perception bias) ((Buckland, 2001)

Increasing Beaufort sea state has been shown to have a deleterious impact on the ability of observers to detect animals at the surface (Palka, 2000), and so field efforts were only conducted during conditions of Beaufort 4 or less, 2 or less for harbour porpoises, in order to minimize perception bias from this source. This does not, of course, ensure that no animals were missed.

Survey specific estimates of g(0) were calculated for as many species as had sufficient amounts of data. This work was not undertaken as part of this thesis, but the results are outlined in Chapter 2. These detection probabilities are incorporated into the density surface models via an offset, by modelling effective area searched. The offset is the length of the modelling segment, multiplied by the effective strip width (ESW). This ESW incorporates the estimate of detection probability, meaning that the modelling segment is able to expand and contract with different environmental conditions, as they were collected in the field (Cañadas et al., 2018).

The use of these two combined stages aims to take account of changes in detectability of the animals but they are not the only sources of uncertainty. Others include the smooths within the spatial model (the GAM) itself, since these are estimated; variability in environmental covariates, movement of animal into or out of the study area during the study period and availability of the animals for detection (Miller et al., 2022). These remain unquantified in this study, however the mechanism proposed by Miller et al. (2022) for quantifying these would be a good candidate for further investigation.

6.1.2 Error from environmental covariates

Variability in environmental covariates used in the models also comes from a variety of different sources. The dynamic model covariates used in this study are monthly averages. They do not take into account any short-term ephemeral features, such as upwelling events, that may have taken place, and may influence cetacean distribution in the short term.

The resolution of the covariates is also fairly course. Whilst every effort has been made to match these with the resolution of the cetacean prediction grid, they are still smoothed, averaged surfaces, often derived from remote sensed data. Data were provided from NEODASS as “Level 3 data” which means they are satellite derived data, that have been geocorrected for position and view angle, before being projected into a mapped image. Data were requested at a resolution of 9km, to ensure that there was at least one measurement per prediction grid square (resolution of prediction grid is 10km x 10km) (NEODASS 2017). Some ground-truthing with in-situ measurements would be a valuable addition. There have been studies comparing the use of remotely sensed data with those collected *in situ* for the process of habitat modelling, which found that the two performed comparably. However, it should be noted that the scale of the remote sensed data, as well as the time period over which averages were taken, was at a much finer scale than those used in this study (Becker et al., 2010).

6.1.3 Explanatory vs predictive models

There is a difference between explanatory and predictive modelling (Shmueli, 2010). Models including XY covariates (explanatory models) often do best at describing the current distribution of a species, but perform less well at predicting patterns in distributions over time, due to the amount of variability usually explained by the XY covariates (Lambert et al., 2014). As the primary aim of this work was to highlight the association between particular species and their environment, the majority of the work conducted was explanatory modelling (with no XY smooth), although predictive modelling was conducted in chapter 3 in order to provide a snapshot of the current status of cetacean distribution across the full study region. Predictive models explained between 28% (minke whales) and 73% (fin whales) null deviance, with the majority of models explaining at least 30%. These values are comparable with other cetacean modelling studies (e.g. Becker et al., 2017; Gilles et al., 2016; Virgili et al., 2019).

Explanatory models conducted in chapters 4-5 generally explained less of the deviance, with values ranging from 7.5% (harbour porpoise, chapter 4) to 64% (fin whale model, chapter 5). This was not unexpected, as using X,Y in predictive models tends to account for variability that can’t be explained by the limited number of covariates in the explanatory models Whilst deviance explained itself is not a direct indication of how well a model is performing, since an over-fitting model can provide a very high deviance explained, if the other model diagnostics indicate an appropriate model, it can provide a useful indicator of model performance.

6.1.4 Model fit.

Two different error distributions were considered in order to try to produce the most appropriate model for the data. The Negative Binomial distribution is a generalisation of a Poisson regression, which loosens the assumption that variance is equal to the mean. This is often used to model counts, particularly for count data which is over dispersed – that is, contains greater variability than would be expected (Jain and Consul, 1971) Tweedie is a family of exponential type distributions, are tolerant to large numbers of zero observations (Candy, 2004). In most, but not all cases, the negative binomial distribution was found to better fit the data.

In general models using number of individuals as the response variable had better fit than models using groups of animals as the response variable. The group models often had worse diagnostics, deviance explained and diagnostic plots. The worse a model fits, the less well you would expect it to predict. This is due to the relationship between expected (fitted) and observed (actual data) is less good. The worse the fit, the less variability is generally explained, and the greater deviation there is between expected values and observed, as seen in the residual plots.

The chapter 5 models have the least good diagnostic plots, and the common dolphin models from chapter 5 have the worst diagnostic plots of all. These models are characterized by retention of lots of covariates, few of which persist between years. The predicted surfaces show levels of over prediction. In general, the chapter 5 models are characterized by low numbers of segments with data, which may help explain their less good fit.

6.1.5 Spatial scale

The study area covered in this study is very large –2,447,300 km^2 for the modelling conducted in chapter 3 - and is simultaneously both too large and too small to be an accurate unit for assessing cetacean distribution. Despite its large scale, it represents only a fraction of the North Atlantic distribution for many of the species included in the thesis, which for some may include the entire North Atlantic (chapter 1). When representing a small proportion of the habitat of highly mobile organisms, associations between density and environmental variables should be considered with due caution. As this is a multi-year study, it is worth noting that for a survey region that does not include the entire range of a population, a variable proportion of the population is likely to have been available for sampling on each of the sampling occasions, which may have an influence on the resulting modelling (Forney 2000).

The study region is also large enough to be made up of multiple diverse habitats, comprising three ICES ecoregions in entirety, as well as small sections of four additional ones. It is reasonable to assume that the processes driving distribution of a species will vary depending on the conditions within the habitat, and the modelling conducted in chapters 4-6 was an attempt to investigate the extent to which this is true. One piece of further additional work which could be conducted would be to use the models derived for each ecoregion and predict those across the full study area covered in chapter 3 to quantify how transferable the relationships with environmental covariates are.

As stated, the surveys from which the data are derived are large-scale, designed to provide a snapshot overview over a wide area. As such, the scale at which they can be modelled is also broad. The unit of prediction used throughout this thesis was a 10km x 10km grid cell. Whilst this is sufficient to gather broad scale distribution patterns across the large area of the study area, it is not sufficiently detailed to draw any conclusions on fine-scale habitat usage by the cetacean species modelled in this study. Typically, this would involve modelling the data on a finer scale prediction grid, such as the 4km x 4km grid used by Booth et al. (2013)

It is not possible to directly compare whether the large-scale models conducted in chapter 3 are better or worse at capturing relationships between cetaceans and their environment than the ecoregion models presented in chapters 4-6, because the chapter 3 models were predictive and included a geographical XY predictor. At this stage, therefore, it is not possible to quantify whether the ecoregion model approach was a success, but this is an avenue that should be explored further. It should be noted that species–habitat relationships are scale-dependent, however (Balance et al.,2006) and the outcome of species–habitat modelling will thus also be scale dependent.

6.1.6 Direct vs indirect predictors

Oceanic environments are inherently variable, however there are some aspects which are predictable. Physical geomorphological features such as seamounts, canyons and escarpments are associated with predictable patterns of higher primary productivity and prey aggregation (Genin, 2004), and other persistent features such as oceanic fronts or water mass boundaries are often also predictable areas of prey aggregation. It would be expected that high-level predators, such as the cetacean species included in this thesis, would target persistent features in order to reduce time spent searching for prey. This has been shown for cetaceans in the Pacific (Ballance et al., 2006), and telemetry studies of oceanic predators in the Southern Ocean and southern Indian Ocean have found penguin and seal species to also use this strategy (e.g. Baylis et al., 2012; Bost et al., 1997, 2009).

Indirect predictors, such as geomorphological features, are used throughout this thesis. This is primarily because these data are much easier to obtain for use in models. Due to the timespan and spatial area covered by this project, data for some covariates were not available. For example, the British Geographical Society provided an excellent substrate dataset, but this covered only UK territorial waters; it did not cover the whole of any ecoregion in its entirety.

Some direct predictors were available for the North Sea ecoregion to use in models for minke whale, white-beaked dolphin and harbour porpoise (Chapter 4). Models that used direct predictors generally explained less deviance than the models using indirect predictors. Whilst all species modelled in this thesis are known to be feeding in the area, distribution of animals is also determined by other factors, including access to areas used for resting and breeding, avoidance of predators, and anthropogenic activity (Davis et al., 2002). In this area, for these species, we do not have detailed knowledge on all of these other components to distribution, so modelling direct predictors like prey was worth investigating. Based on the results, however, it seems that the modelling was either not conducted on the right scale or using the right prey covariates for this to be successful.

Across all chapters, depth was the covariate retained most often by a considerable margin (22/28 times). From a management perspective, this is perhaps useful as indirect predictors are generally more available and more transferable between areas and may make for more robust models when predicting distribution. All three of the species which were modelled using direct predictors can exploit a wide range of different prey resources, which also vary spatially. It is possible that the direct predictors available did not sufficiently encompass the full range of prey species which are exploited in this region.

The use of GAMS is successful, and these models have been shown to work well. For occasions when data may be available at a more detailed resolution, Bayesian methods could be worth exploring to better understand more fine-scale movements and associations (Williamson et al., 2022).

6.1.7 Anthropogenic impacts

Anthropogenic pressures can strongly affect habitat quality, and it stands to reason that this may obscure any relationships between cetaceans and environmental data. As well as climate change (Lambert et al., 2014; MacLeod et al., 2005), the three main ICES ecoregions modelled chapters 4-6 have between them no less than 13 different anthropogenic activities highlighted as pressures to the region. These include fishing, aquaculture, dredging, offshore structures, agriculture (causing nutrient and organic enrichment), pollution from urban and industry run-off, coastal construction, shipping transport, tourism, telecommunications, aggregate extraction, military activities and renewable energy (ICES, 2020a, 2020b, 2020c). Whilst these will not all act directly on cetacean populations, their effects may range from impacting the seabed, to degrading the water column, to depleting prey species to causing direct injury to cetacean species. These changes to habitat may, directly or indirectly, cause cetaceans to change their relationship with their environment – either temporarily (Thompson et al., 2013) or more longer term (MacLeod et al., 2005).

6.2 Final conclusions

Cetacean distribution is driven by lots of different factors. Relationships may not be with a specific feature, but may be with combinations of variables, all of which operate on a gradient. These relationships change with both time and space, and many of these are dynamic in themselves (Ballance et al., 2006).

Some predictors performed better than others. The most frequently retained covariate in these analyses was depth. The success of this could be due to a number of factors. Not only is this a static covariate which persists through time without change, but it is a good indicator or limiter of niche. For example, species that feed on bottom dwelling prey and are limited by their own dive capacity will be closely associated with a particular depth profile – there is little requirement for them to be associated with predictors outside of this habitat. For some species more dynamic covariates were also useful, however care must be taken when selecting these to ensure that the chosen predictors are representative of genuine habitat parameters.

For species for which at-sea detection is difficult, the approaches covered in this thesis provide useful additional information which would not be possible without pooling datasets. Initiatives which are able to expand on this, potentially via the use of community science initiatives, would be increasingly valuable.

The ecoregion approach was attempted to investigate whether modelling across regions of comparatively homogenous habitat would make ecologically meaningful relationships more apparent. This worked well for the environmental models of the North Sea (Chapter 4) but was less successful in the more offshore Celtic Sea and Bay of Biscay ecoregions (chapter 4). This is perhaps due to the larger movements undertaken by the species modelled in this chapter. In all cases, relationships may be obscured by un-modelled factors. Within the study region, these are most likely to be anthropogenic in origin. It may be possible to incorporate some of these into future models (for example the presence of structures) but many of these may be ephemeral, and also cumulative, making their quantification very difficult.

6.3 Literature Cited

Ballance, L.T., Pitman, R.L., Fiedler, P.C., 2006. Oceanographic influences on seabirds and cetaceans of the eastern tropical pacific: a review. Prog. Oceanogr. 69, 360–390. https://doi.org/10.1016/j.pocean.2006.03.013

Barry, S., Elith, J., 2006. Error and uncertainty in habitat models. J. Appl. Ecol. 43, 413–423. https://doi.org/10.1111/j.1365-2664.2006.01136.x

Baylis, A.M.M., Page, B., McKenzie, J., Goldsworthy, S.D., 2012. Individual foraging site fidelity in lactating New Zealand fur seals: Continental shelf vs. oceanic habitats. Mar. Mammal Sci. 28, 276–294. https://doi.org/10.1111/j.1748-7692.2011.00487.x

Becker, E., Forney, K., Ferguson, M., Foley, D., Smith, R., Barlow, J., Redfern, J., 2010. Comparing California Current cetacean–habitat models developed using in situ and remotely sensed sea surface temperature data. Mar. Ecol. Prog. Ser. 413, 163–183. https://doi.org/10.3354/meps08696

Becker, E.A., Forney, K.A., Thayre, B.J., Debich, A.J., Campbell, G.S., Whitaker, K., Douglas, A.B., Gilles, A., Hoopes, R., Hildebrand, J.A., 2017. Habitat-Based Density Models for Three Cetacean Species Off Southern California Illustrate Pronounced Seasonal Differences. Front. Mar. Sci. 4, 121. https://doi.org/10.3389/fmars.2017.00121

Booth, C., Embling, C., Gordon, J., Calderan, S., Hammond, P., 2013. Habitat preferences and distribution of the harbour porpoise Phocoena phocoena west of Scotland. Mar. Ecol. Prog. Ser. 478, 273–285. https://doi.org/10.3354/meps10239

Bost, C., Georges, J., Guinet, C., Cherel, Y., Pütz, K., Charrassin, J., Handrich, Y., Zorn, T., Lage, J., Le Maho, Y., 1997. Foraging habitat and food intake of satellite-tracked king penguins during the austral summer at Crozet Archipelago. Mar. Ecol. Prog. Ser. 150, 21–33. https://doi.org/10.3354/meps150021

Bost, C.A., Cotté, C., Bailleul, F., Cherel, Y., Charrassin, J.B., Guinet, C., Ainley, D.G., Weimerskirch, H., 2009. The importance of oceanographic fronts to marine birds and mammals of the southern oceans. J. Mar. Syst., Special Issue on Observational Studies of Oceanic Fronts 78, 363–376. https://doi.org/10.1016/j.jmarsys.2008.11.022

Buckland, S.T., 2001. Introduction to Distance Sampling - Estimating Abundance of Biological Populations. Oxford University Press.

Cañadas, A., Aguilar de Soto, N., Aissi, M., Arcangeli, A., Azzolin, M., B-Nagy, A., Bearzi, G., Campana, I., Chicote, C., Cotte, C., Crosti, R., David, L., Di Natale, A., Fortuna, C., Frantzis, A., Garcia, P., Gazo, M., Gutierrez-Xarxa, R., Holcer, D., Laran, S., Lauriano, G., Lewis, T., Moulins, A., Mussi, B., Notarbartolo di Sciara, G., Panigada, S., Pastor, X., Politi, E., Pulcini, M., Raga, J.A., Rendell, L., Rosso, M., Tepsich, P., Tomás, J., Tringali, M., Roger, Th., 2018. The challenge of habitat modelling for threatened low density species using heterogeneous data: The case of Cuvier's beaked whales in the Mediterranean. Ecol. Indic. 85, 128–136. https://doi.org/10.1016/j.ecolind.2017.10.021

Candy, S.G., 2004. Modeling catch and effort data using Generalised Linear Models, the Tweedie Distriution, Random Vessel Effects and Random Stratum-by-Year effects. CCAMLR Sci. 11, 59–80.

Chambers, M., Dinsmore, T.W., 2014. Advanced Analytics Methodologies: Driving Business Value with Analytics.

Davis, R.W., Ortega-Ortiz, J.G., Ribic, C.A., Evans, W.E., Biggs, D.C., Ressler, P.H., Cady, R.B., Leben, R.R., Mullin, K.D., Würsig, B., 2002. Cetacean habitat in the northern oceanic Gulf of Mexico. Deep Sea Res. Part Oceanogr. Res. Pap. 49, 121–142. https://doi.org/10.1016/S0967-0637(01)00035-8

Genin, A., 2004. Bio-physical coupling in the formation of zooplankton and fish aggregations over abrupt topographies. J. Mar. Syst. 50, 3–20. https://doi.org/10.1016/j.jmarsys.2003.10.008

Gilles, A., Viquerat, S., Becker, E.A., Forney, K.A., Geelhoed, S.C.V., Haelters, J., Nabe-Nielsen, J., Scheidat, M., Siebert, U., Sveegaard, S., Beest, F.M., Bemmelen, R., Aarts, G., 2016. Seasonal habitat-based density models for a marine top predator, the harbor porpoise, in a dynamic environment. Ecosphere 7. https://doi.org/10.1002/ecs2.1367

ICES, 2020a. Bay of Biscay and the Iberian Coast Ecoregion. Ecosystem overview. https://ices-library.figshare.com/articles/report/Bay_of_Biscay_and_the_Iberian_Coast_ecoregion_Ecosystem_Overview/21731579

ICES, 2020b. Celtic Seas Ecoregion: Ecosystem overview. https://doi.org/10.17895/ICES.ADVICE.7631

ICES, 2020c. Greater North Sea Ecoregion - Ecosystem overview. ICES Advice. https://doi.org/10.17895/ICES.ADVICE.7632

Jain, G.C., Consul, P.C., 1971. A Generalized Negative Binomial Distribution. SIAM J. Appl. Math. 21, 501–513. https://doi.org/10.1137/0121056

Lambert, E., Pierce, G.J., Hall, K., Brereton, T., Dunn, T.E., Wall, D., Jepson, P.D., Deaville, R., MacLeod, C.D., 2014. Cetacean range and climate in the eastern North Atlantic: future predictions and implications for conservation. Glob. Change Biol. 20, 1782–1793. https://doi.org/10.1111/gcb.12560

MacLeod, C.D., Bannon, S.M., Pierce, G.J., Schweder, C., Learmonth, J.A., Herman, J.S., Reid, R.J., 2005. Climate change and the cetacean community of north-west Scotland. Biol. Conserv. 124, 477–483. https://doi.org/10.1016/j.biocon.2005.02.004

Miller, D.L., Becker, E.A., Forney, K.A., Roberts, J.J., Cañadas, A., Schick, R.S., 2022. Estimating uncertainty in density surface models. PeerJ 10, e13950. https://doi.org/10.7717/peerj.13950

Miller, D.L., Fifield, D., Wakefield, E., Sigourney, D.B., 2021. Extending density surface models to include multiple and double-observer survey data. PeerJ 9, e12113. https://doi.org/10.7717/peerj.12113

NOEDASS 2017. Delivery report – Readme file provided with the data. Unpublished.

Palka, D.L. 2000. Abundance of the Gulf of Maine/Bay of Fundy harbor porpoise based on shipboard and aerial surveys during 1999. Northeast Fisheries Science Center reference document; 00-07. Northeast Fisheries Science Center (U.S.). https://repository.library.noaa.gov/view/noaa/3290

Shmueli, G., 2010. To Explain or to Predict? Stat. Sci. 25. https://doi.org/10.1214/10-STS330

Thompson, P.M., Brookes, K.L., Graham, I.M., Barton, T.R., Needham, K., Bradbury, G., Merchant, N.D., 2013. Short-term disturbance by a commercial two-dimensional seismic survey does not lead to long-term displacement of harbour porpoises. Proc. R. Soc. B Biol. Sci. 280, 20132001. https://doi.org/10.1098/rspb.2013.2001

Virgili, A., Authier, M., Boisseau, O., Cañadas, A., Claridge, D., Cole, T.V.N., Peter Corkeron, Dorémus, G., David, L., Di-Méglio, N., Dunn, C., Dunn, T.E., García-Barón, I., Laran, S., Lauriano, G., Lewis, M., Louzao, M., Mannocci, L., Martínez-Cedeira, J., Palka, D.L., Panigada, S., Pettex, E., Roberts, J.J., Ruiz, L., Saavedra, C., Santos, M.B., Van Canneyt, O., Bonales, J.A.V., Monestiez, P., Ridoux, V., 2019. Combining multiple visual surveys to model the habitat of deep-diving cetaceans at the basin scale. Large-scale modelling of deep-diving cetacean habitats. Glob. Ecol. Biogeogr. 28, 300–314. https://doi.org/DOI: 10.1111/geb.12850

Williamson, L.D., Scott, B.E., Laxton, M., Illian, J.B., Todd, V.L.G., Miller, P.I., Brookes, K.L., 2022. Comparing distribution of harbour porpoise using generalized additive models and hierarchical Bayesian models with integrated nested laplace approximation. Ecol. Model. 470, 110011. https://doi.org/10.1016/j.ecolmodel.2022.110011

Appendix 1 – Appendix for Chapter 2

Illustration of the model building process, using the minke whale models for 2016, chapter 4 as a worked example.

Modelling process – illustrated using the minke whale models from chapter 3.

Step 1: Choose best of each covariate “type.”

Model structure: *GAM= SumIndivids~Covariate +offset*

a) Select best mesoscale activity type. Models are selected by AIC, and selected models are highlighted in red.

ModelID	dev	devexp	n	REML	AIC	deltaAIC	AICweight
gam1.nb.ssh_best	153.6054	14.832492	1659	168.2299	330.6509	0.00000	0.9648702
gam1.nb.adt_best	152.4775	10.513914	1659	169.9863	337.4966	6.84572	0.0314731
gam1.nb.sla_best	154.3563	7.595971	1659	171.7197	341.8018	11.15085	0.0036567

b) Select best MLD type.

ModelID	dev	devexp	n	REML	AIC	deltaAIC	AICweight
gam1.nb.mld_log_best	153.8442	0.1575239	1659	173.4053	349.5962	0.0000000	0.5213901
gam1.nb.mld_best	153.8504	0.4721391	1659	173.3815	349.7674	0.1712252	0.47

c) Select best seabed rugosity type.

ModelID	dev	devexp	n	REML	AIC	deltaAIC	AICweight
gam1.nb.d_sd	153.8997	8.23e-05	1659	173.408	349.3259	0.0000000	0.5000246
gam1.nb.slope	153.8999	6.00e-07	1659	173.408	349.3261	0.0001967	0.4999754

d) Select best distance to covariate

ModelID	dev	devexp	n	REML	AIC	deltaAIC	AICweight
gam1.nb.CS_50	153.6826	2.5652027	1659	172.516	347.2352	0.000000	0.7398682
gam1.nb.dist_50	153.8998	0.0000214	1659	173.408	349.3258	2.090568	0.2601318

Please note, this example contains only 2 “distance to” covariates, as it is taken from the modelling of the North Sea ecoregion where only these two were considered. For full details please see chapter 4.

Step 2: Build a correlation matrix using the best models selected in step 1, plus depth, sea surface temperature and salinity. Correlations over 0.6 / -0.6, indicating they are not to go in the same full model, are highlighted with red borders.

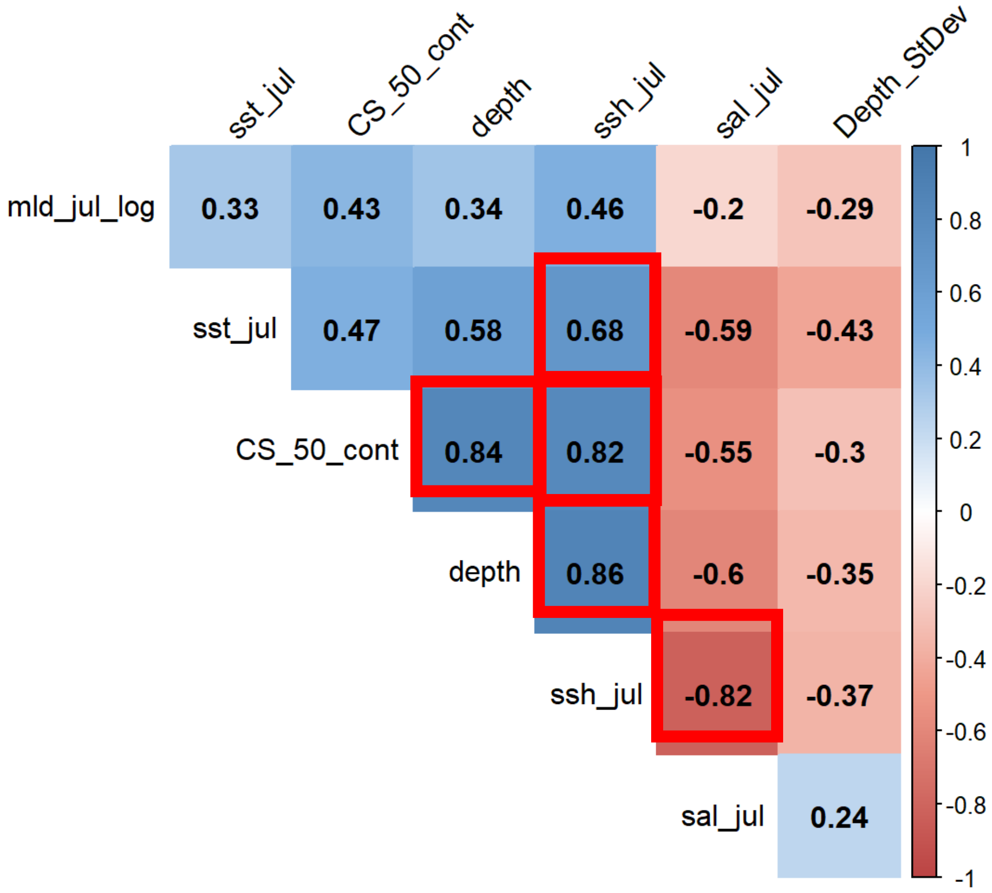

	sst_jul	CS_50_cont	depth	ssh_jul	sal_jul	Depth_StDev
mld_jul_log	0.33	0.43	0.34	0.46	-0.2	-0.29
sst_jul		0.47	0.58	0.68	-0.59	-0.43
CS_50_cont			0.84	0.82	-0.55	-0.3
depth				0.86	-0.6	-0.35
ssh_jul					-0.82	-0.37
sal_jul						0.24

Step 3: Build a series of "full" models for each combination of covariates to ensure no correlated ones (as indicated in step 2) are in the same model. In this case three distinct models are required to encompass all combinations.

Model structure: *GAM= SumIndivids~Covariate +Covariate+Covariate+offset*

a) Full model 1

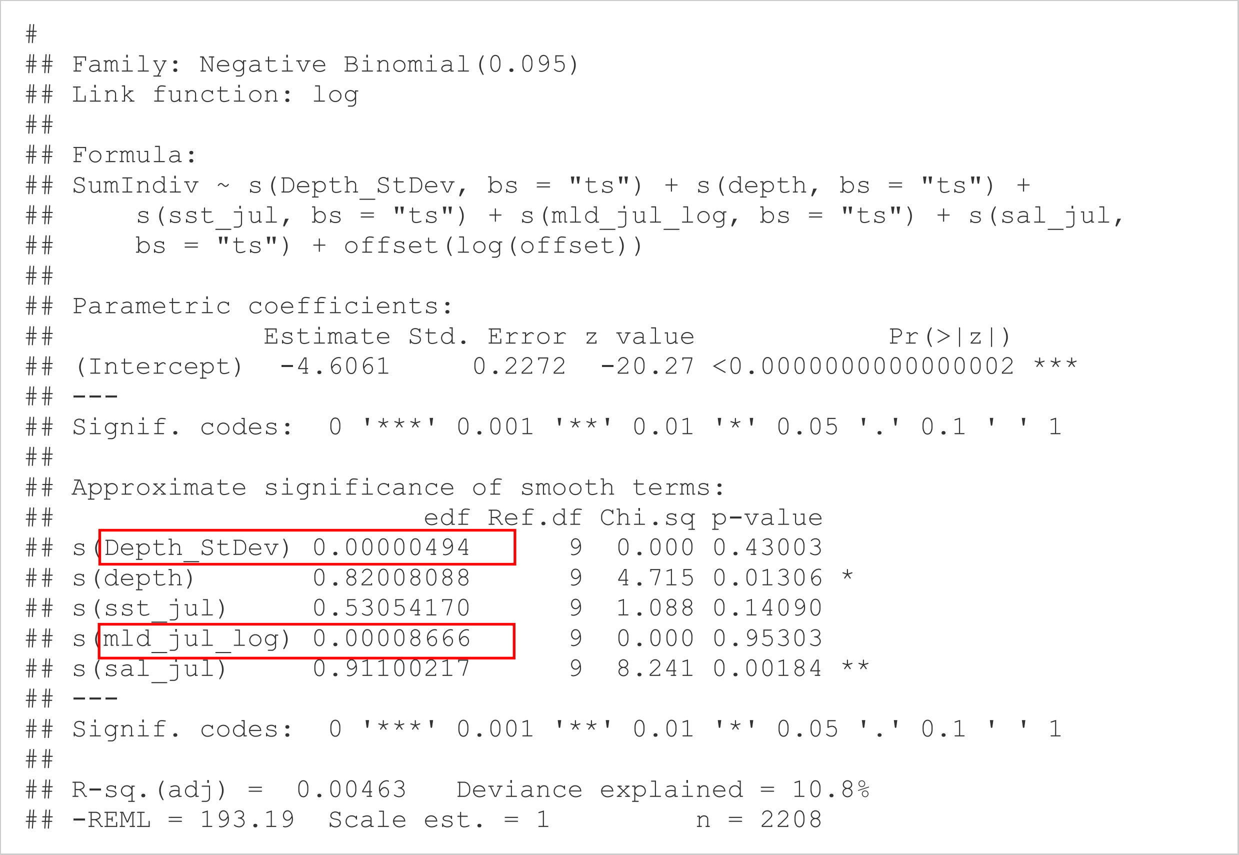

```
#
## Family: Negative Binomial(0.095)
## Link function: log
##
## Formula:
## SumIndiv ~ s(Depth_StDev, bs = "ts") + s(depth, bs = "ts") +
##     s(sst_jul, bs = "ts") + s(mld_jul_log, bs = "ts") + s(sal_jul,
##     bs = "ts") + offset(log(offset))
##
## Parametric coefficients:
##             Estimate Std. Error z value            Pr(>|z|)
## (Intercept)  -4.6061     0.2272  -20.27 <0.0000000000000002 ***
## ---
## Signif. codes:  0 '***' 0.001 '**' 0.01 '*' 0.05 '.' 0.1 ' ' 1
##
## Approximate significance of smooth terms:
##                     edf Ref.df Chi.sq p-value
## s(Depth_StDev) 0.00000494      9  0.000 0.43003
## s(depth)       0.82008088      9  4.715 0.01306 *
## s(sst_jul)     0.53054170      9  1.088 0.14090
## s(mld_jul_log) 0.00008666      9  0.000 0.95303
## s(sal_jul)     0.91100217      9  8.241 0.00184 **
## ---
## Signif. codes:  0 '***' 0.001 '**' 0.01 '*' 0.05 '.' 0.1 ' ' 1
##
## R-sq.(adj) =  0.00463   Deviance explained = 10.8%
## -REML = 193.19  Scale est. = 1         n = 2208
```

Full model, remove any covariates with edf <0.1 (outlined red above).

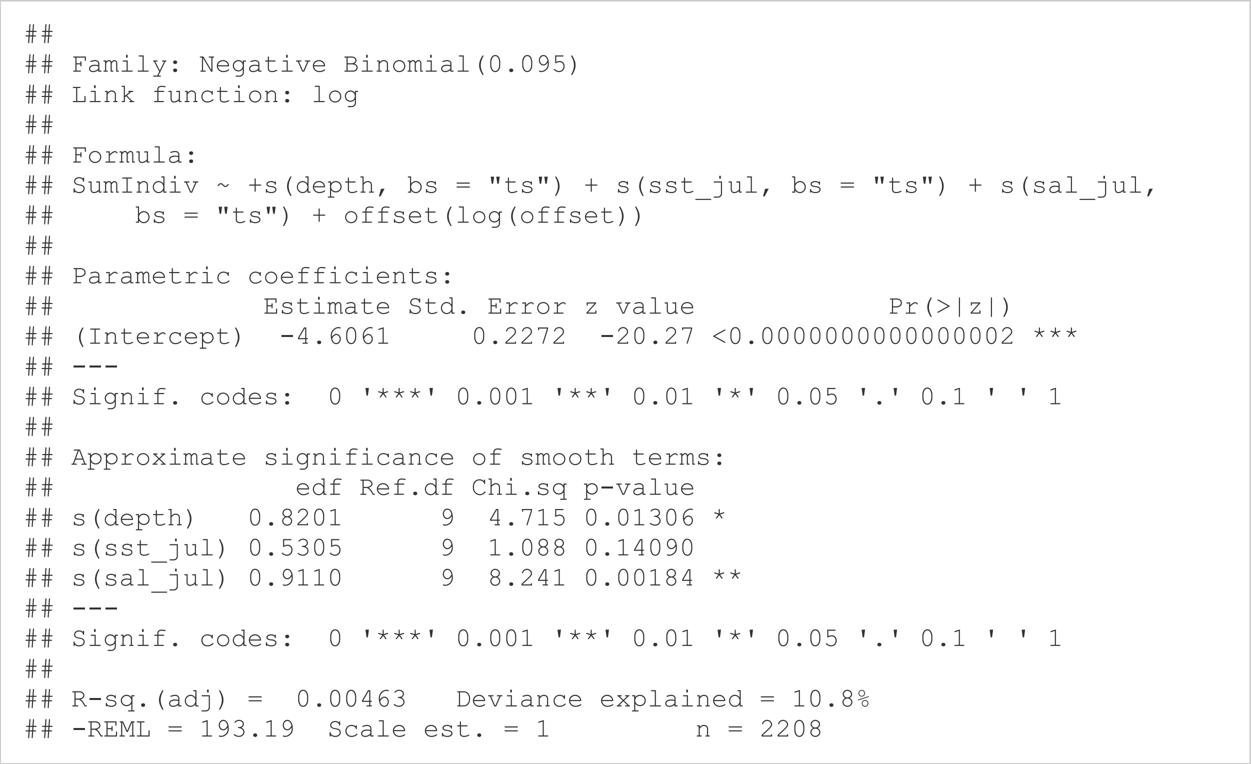

```
##
## Family: Negative Binomial(0.095)
## Link function: log
##
## Formula:
## SumIndiv ~ +s(depth, bs = "ts") + s(sst_jul, bs = "ts") + s(sal_jul,
##     bs = "ts") + offset(log(offset))
##
## Parametric coefficients:
##             Estimate Std. Error z value            Pr(>|z|)
## (Intercept)  -4.6061     0.2272  -20.27 <0.0000000000000002 ***
## ---
## Signif. codes:  0 '***' 0.001 '**' 0.01 '*' 0.05 '.' 0.1 ' ' 1
##
## Approximate significance of smooth terms:
##               edf Ref.df Chi.sq p-value
## s(depth)   0.8201      9  4.715 0.01306 *
## s(sst_jul) 0.5305      9  1.088 0.14090
## s(sal_jul) 0.9110      9  8.241 0.00184 **
## ---
## Signif. codes:  0 '***' 0.001 '**' 0.01 '*' 0.05 '.' 0.1 ' ' 1
##
## R-sq.(adj) =  0.00463   Deviance explained = 10.8%
## -REML = 193.19  Scale est. = 1         n = 2208
```

b) Full model 2

```
##
## Family: Negative Binomial(0.097)
## Link function: log
##
## Formula:
## SumIndiv ~ s(Depth_StDev, bs = "ts") + s(CS_50_cont, bs = "ts") +
##     s(sst_jul, bs = "ts") + s(mld_jul_log, bs = "ts") + s(sal_jul,
##     bs = "ts") + offset(log(offset))
##
## Parametric coefficients:
##             Estimate Std. Error z value             Pr(>|z|)
## (Intercept)  -4.5408     0.2185  -20.78 <0.0000000000000002 ***
## ---
## Signif. codes:  0 '***' 0.001 '**' 0.01 '*' 0.05 '.' 0.1 ' ' 1
##
## Approximate significance of smooth terms:
##                       edf Ref.df Chi.sq p-value
## s(Depth_StDev) 0.00010035      9  0.000  0.5750
## s(CS_50_cont)  0.00020251      9  0.000  0.3683
## s(sst_jul)     0.82674166      9  4.215  0.0217 *
## s(mld_jul_log) 0.00005638      9  0.000  0.7907
## s(sal_jul)     0.84248902      9  4.349  0.0216 *
## ---
## Signif. codes:  0 '***' 0.001 '**' 0.01 '*' 0.05 '.' 0.1 ' ' 1
##
## R-sq.(adj) =  0.00629   Deviance explained =  8.6%
## -REML = 194.28  Scale est. = 1         n = 2208
```

Full model, remove any covariates with edf <0.1 (outlined red above).##

```
## Family: Negative Binomial(0.097)
## Link function: log
##
## Formula:
## SumIndiv ~ +s(sst_jul, bs = "ts") + s(sal_jul, bs = "ts") +
offset(log(offset))
##
## Parametric coefficients:
##             Estimate Std. Error z value             Pr(>|z|)
## (Intercept)  -4.5408     0.2185  -20.78 <0.0000000000000002 ***
## ---
## Signif. codes:  0 '***' 0.001 '**' 0.01 '*' 0.05 '.' 0.1 ' ' 1
##
## Approximate significance of smooth terms:
##               edf Ref.df Chi.sq p-value
## s(sst_jul) 0.8267      9  4.215  0.0217 *
## s(sal_jul) 0.8425      9  4.349  0.0216 *
## ---
## Signif. codes:  0 '***' 0.001 '**' 0.01 '*' 0.05 '.' 0.1 ' ' 1
##
## R-sq.(adj) =  0.00629   Deviance explained =  8.6%
## -REML = 194.28  Scale est. = 1         n = 2208
```

c) Full model 3

```
##
## Family: Negative Binomial(0.13)
## Link function: log
##
## Formula:
## SumIndiv ~ s(Depth_StDev, bs = "ts") + s(ssh_jul, bs = "ts") +
##     s(mld_jul_log, bs = "ts") + offset(log(offset))
##
## Parametric coefficients:
##             Estimate Std. Error z value             Pr(>|z|)
## (Intercept)  -5.6356     0.6974  -8.081 0.000000000000000644 ***
## ---
## Signif. codes:  0 '***' 0.001 '**' 0.01 '*' 0.05 '.' 0.1 ' ' 1
##
## Approximate significance of smooth terms:
##                  edf Ref.df Chi.sq p-value
## s(Depth_StDev) 0.7420      9  2.172 0.08598 .
## s(ssh_jul)     3.4648      9 13.817 0.00232 **
## s(mld_jul_log) 0.7072      9  2.557 0.05421 .
## ---
## Signif. codes:  0 '***' 0.001 '**' 0.01 '*' 0.05 '.' 0.1 ' ' 1
##
## R-sq.(adj) =  0.0145   Deviance explained = 18.2%
## -REML = 191.77  Scale est. = 1         n = 2208
```

No covariates to remove from this model

Step 4: Compare AIC of the three models with edf<0.1 removed. Select lowest AIC as best model.

ModelID	dev	devexp	n	REML	AIC	deltaAIC	AICweight
gam1.nb.xy.v3	177.8759	18.215181	2208	191.7671	376.5276	0.00000	0.9932707
gam1.nb.xy.v1	178.2555	10.816397	2208	193.1942	386.9468	10.41915	0.0054272
gam1.nb.xy.v2	183.8772	8.595936	2208	194.2823	389.8017	13.27410	0.0013021

Step 5: Check diagnostic plots of chosen model to assess model fit.

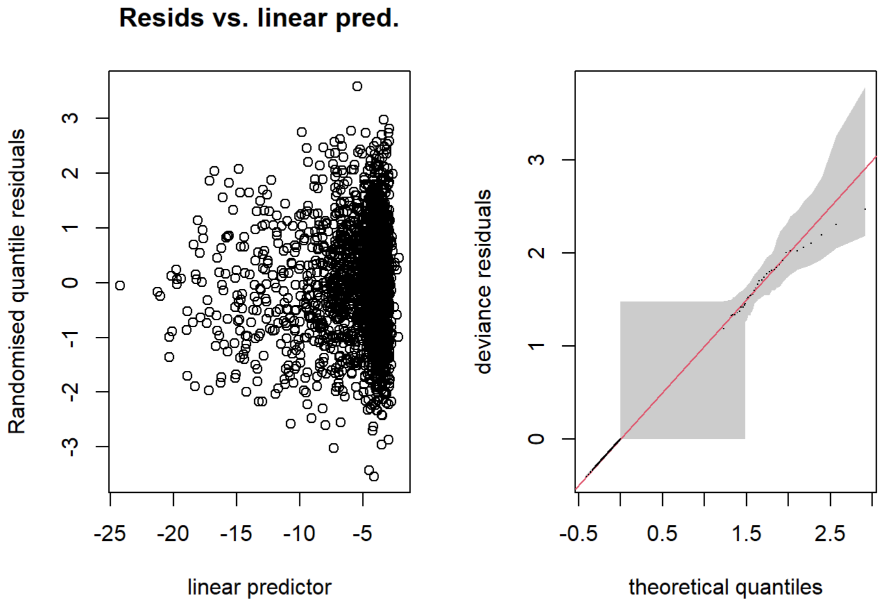

Step 6: Repeat steps 1-4 using Tweedie error distribution instead of negative biniomial error distribution (not shown).

Step 7: Compare diagnostic plots, primarily QQ plot and residuals vs linear plots of the chosen model of the two error distributions. Based on these diagnostics, chose the error distribution that best represents the data, use this model going forward for predictions.

Appendix 2 – Appendix for Chapter 3

Residual and QQ plots for models presented in Chapter 3.

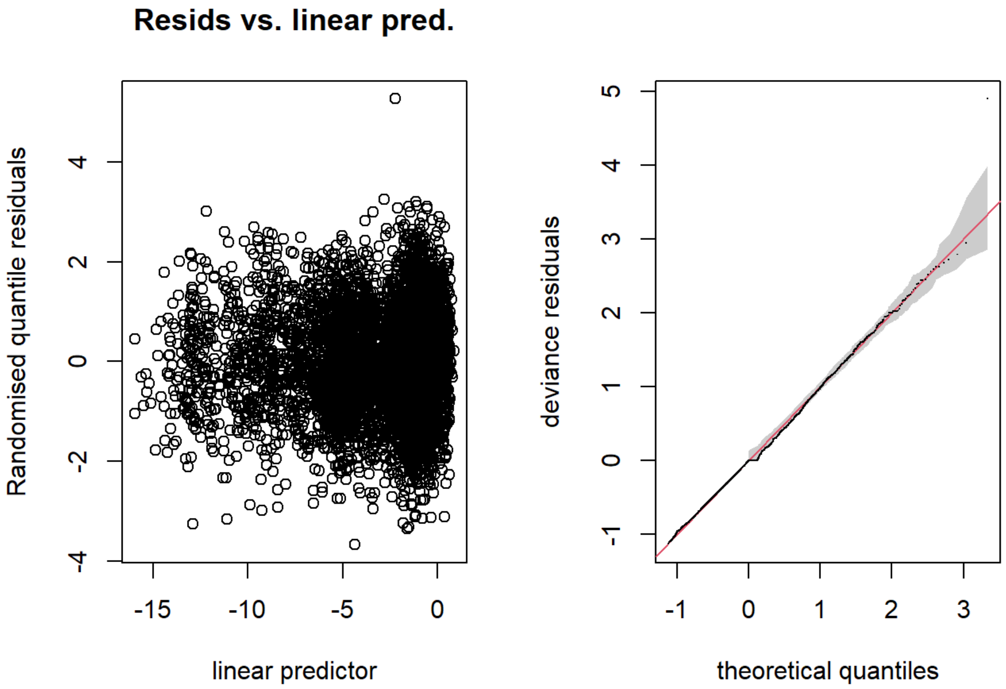

A2.1 Residual and QQ plots from the harbour porpoise explanatory model for the S3/ObSERVE data.

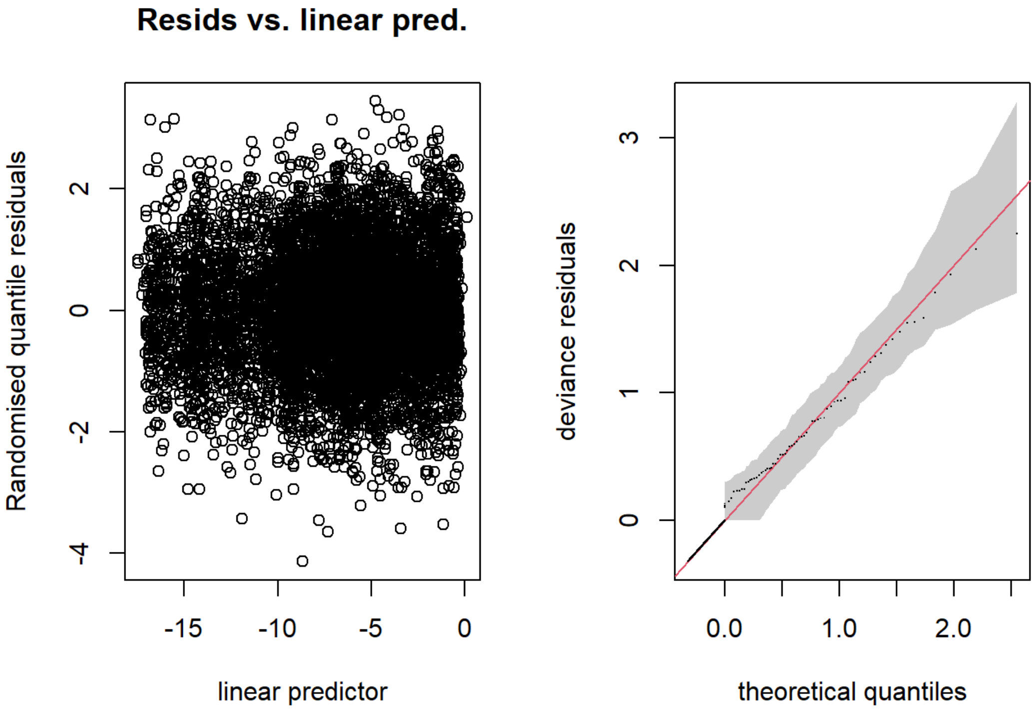

A2.2 Residual and QQ plots from the white-beaked dolphin explanatory model for the S3/ObSERVE data.

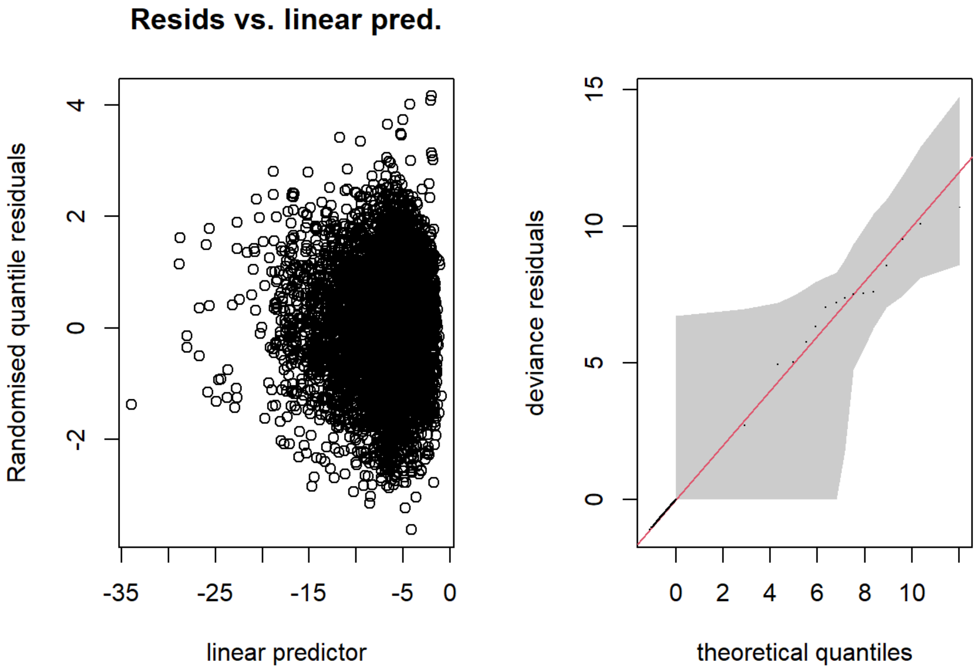

A2.3 Residual and QQ plots from the Atlantic white-sided dolphin explanatory model for the S3/ObSERVE data.

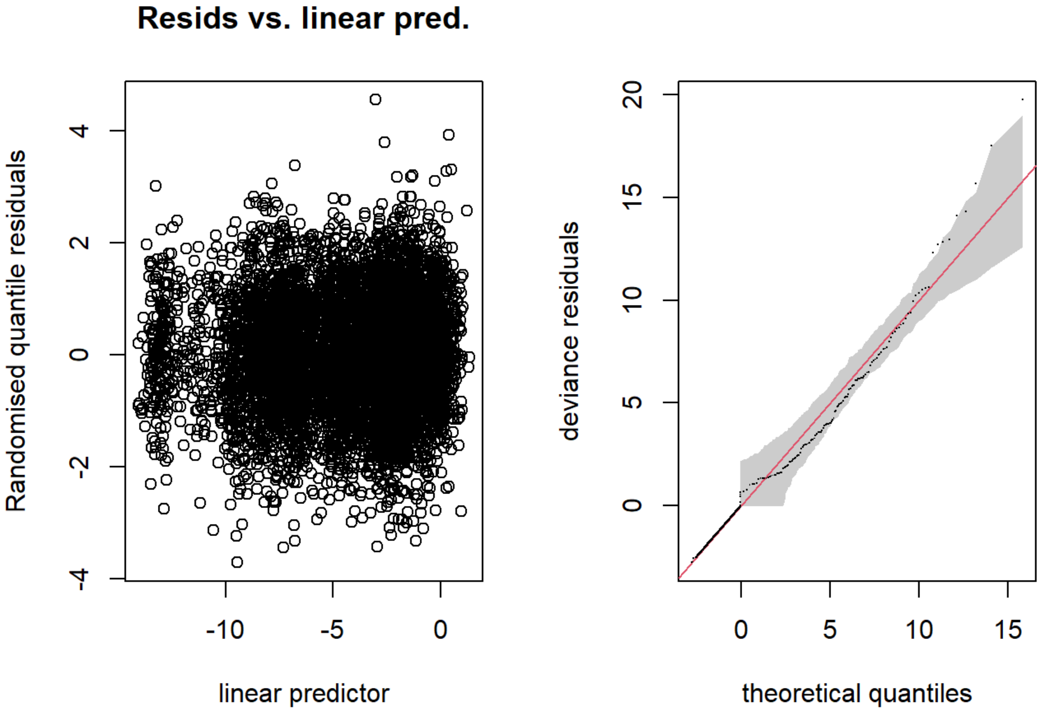

A2.4 Residual and QQ plots from the bottlenose dolphin explanatory model for the S3/ObSERVE data.

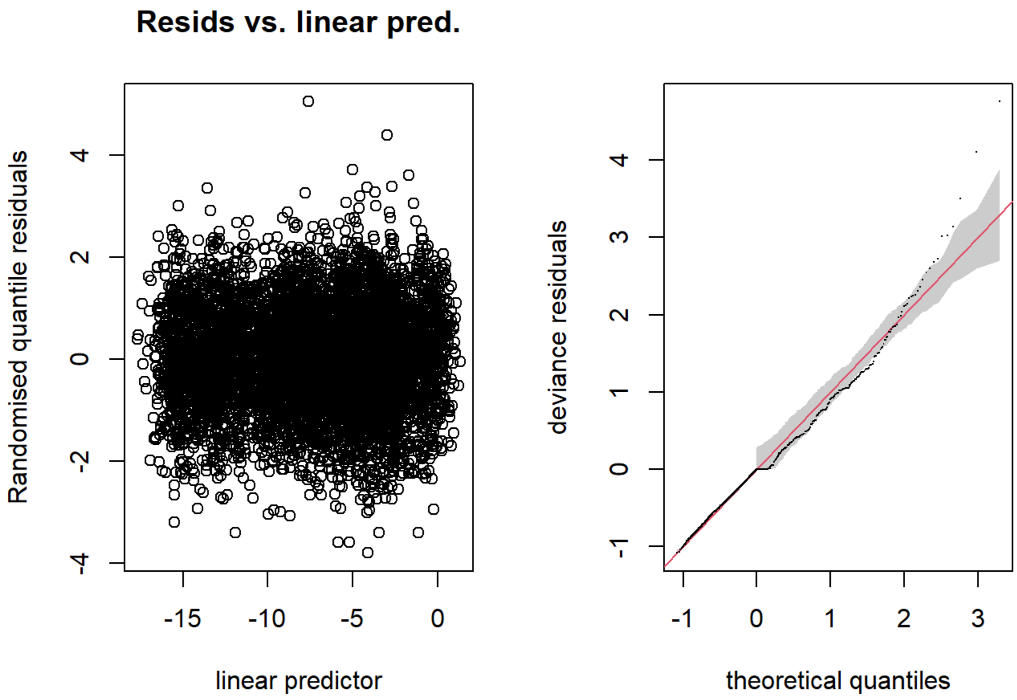

A2.5 Residual and QQ plots from the common dolphin explanatory model for the S3/ObSERVE data.

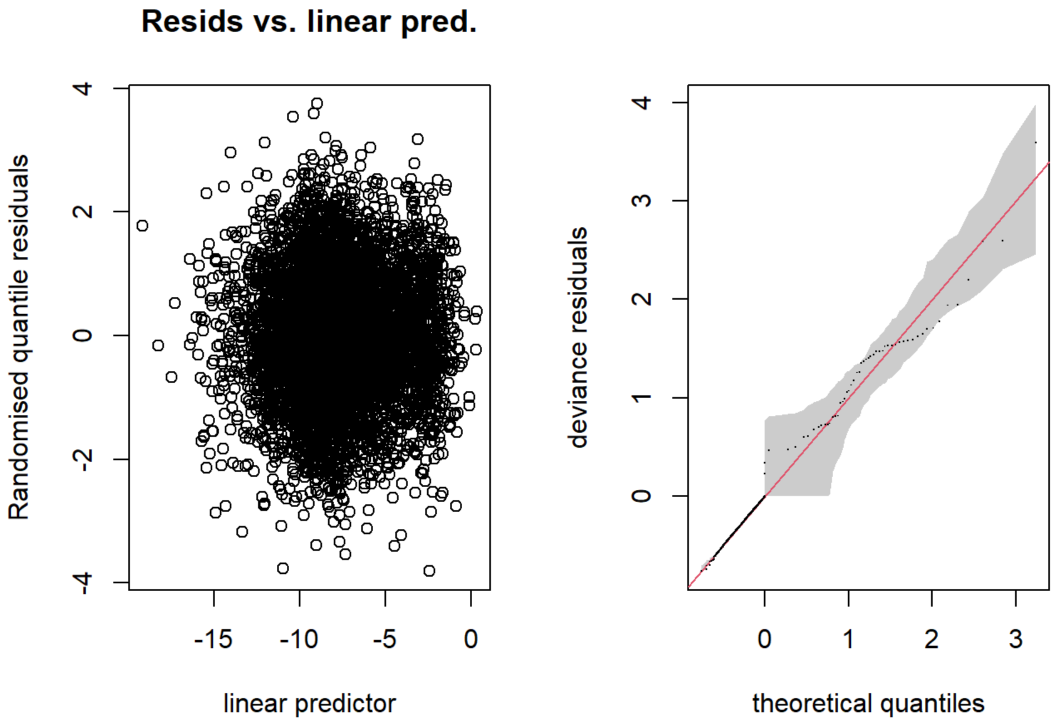

A2.6 Residual and QQ plots from the striped dolphin explanatory model for the S3/ObSERVE data.

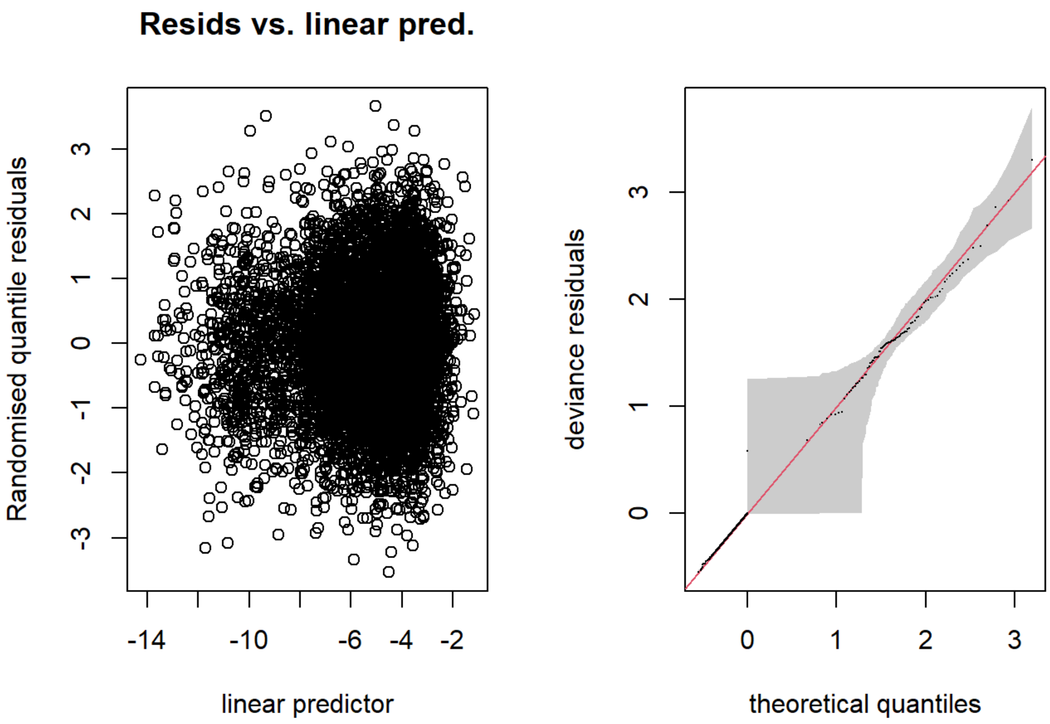

A2.7 Residual and QQ plots from the minke whale explanatory model for the S3/ObSERVE data.

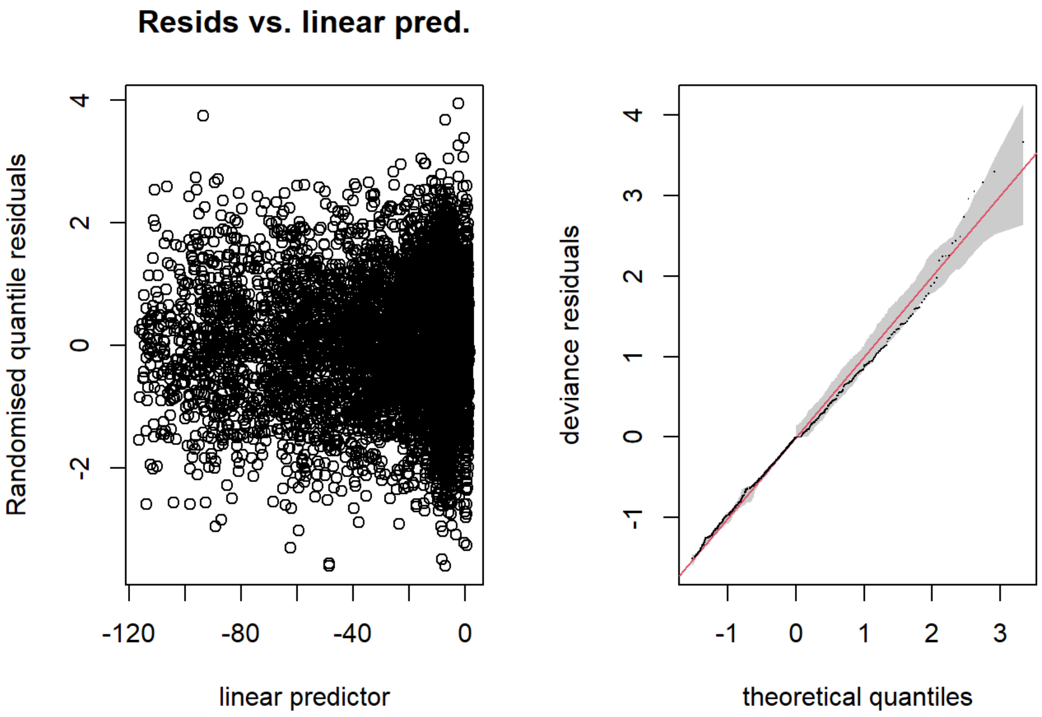

A2.8 Residual and QQ plots from the fin whale explanatory model for the S3/ObSERVE data.

Appendix 3 –Appendix for Chapter 4

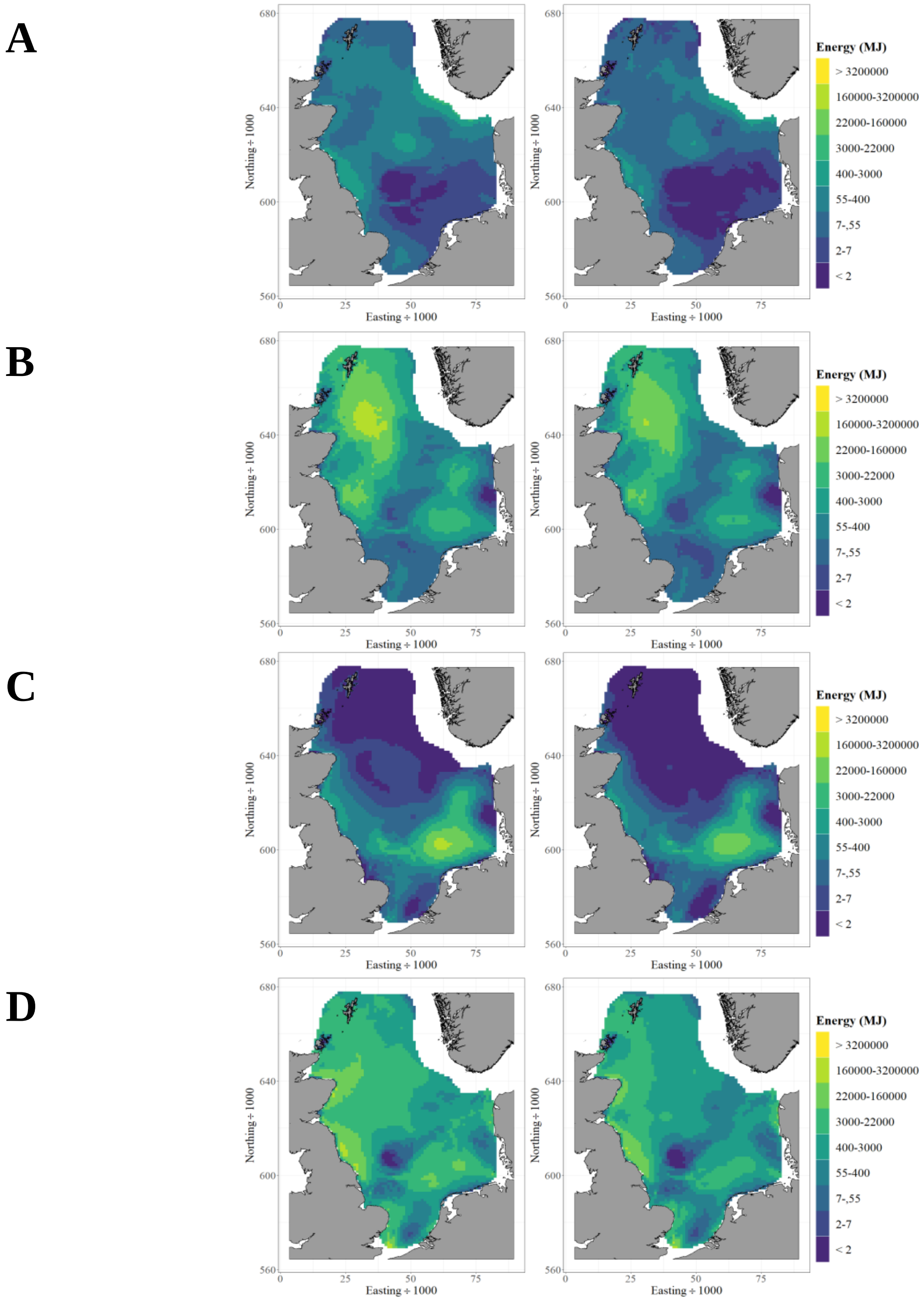

A3.1 Spatiotemporal summer (July-September), 2005 distribution and uncertainty estimate of porpoise prey species energy density in (MJ) per 10 x 10 km for the North Sea. Plots indicate (A) cod, (B) herring, (C) sprat, (D) whiting. Left panel illustrates original model predictions, and right panel shows standard deviation. The colour scale relates to maps of both model prediction and standard deviation. The standard deviation is a measure of absolute uncertainty in

predicted energy in the same units as the mean; it is not a relative measure of the confidence in the model prediction. Taken from Ransijin et al., 2020.

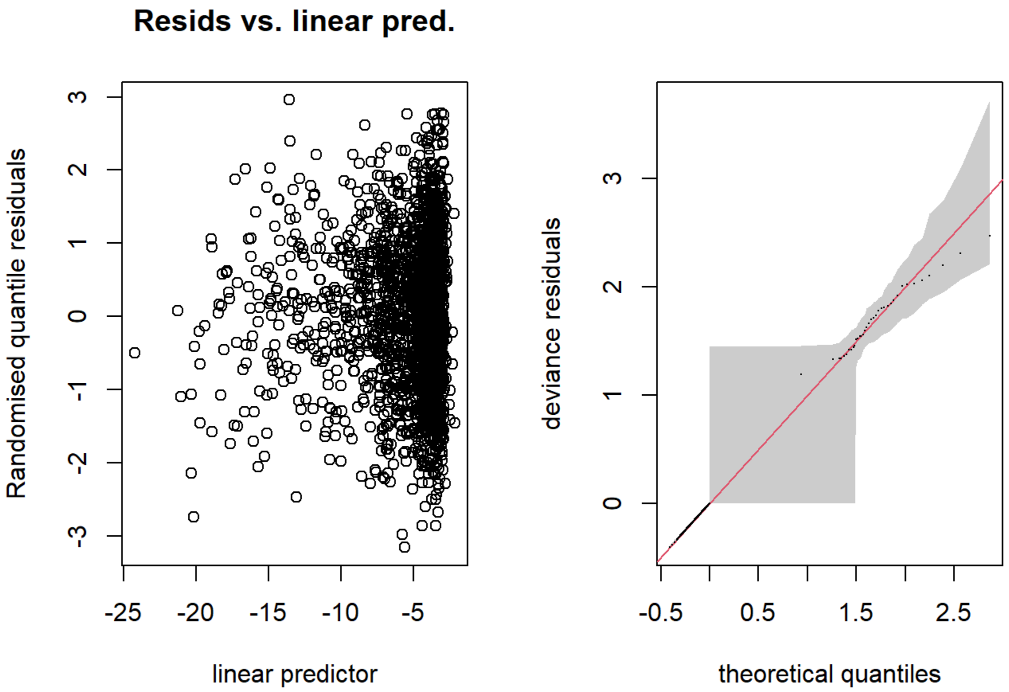

A3.2 Residual and QQ plots from the minke whale environmental model for the 2016 data

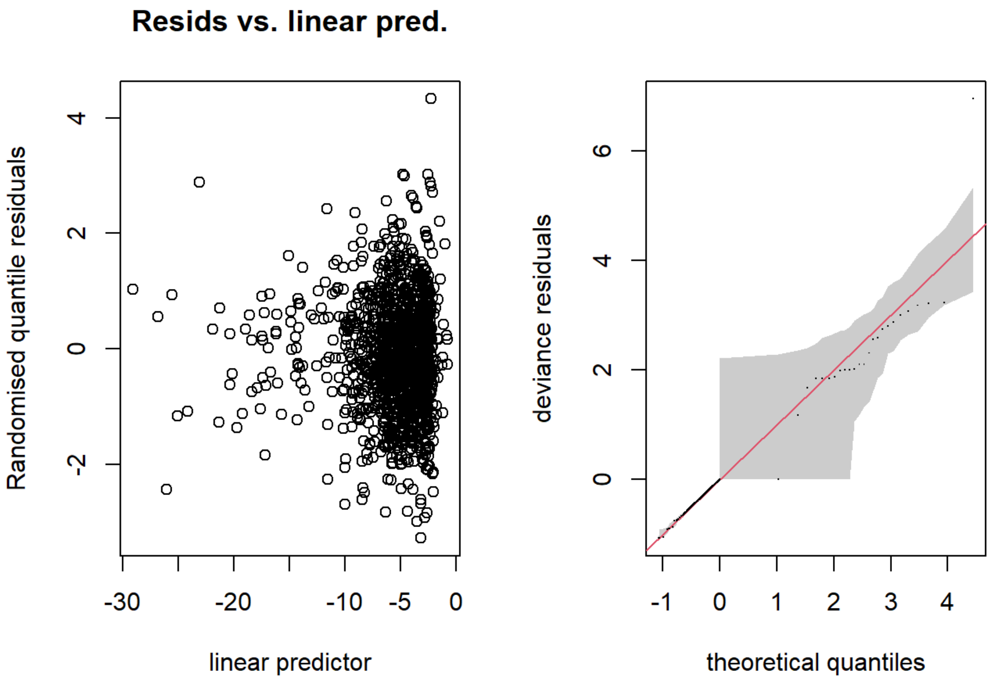

A3.3 Residual and QQ plots from the minke whale environmental model for the 2005 data

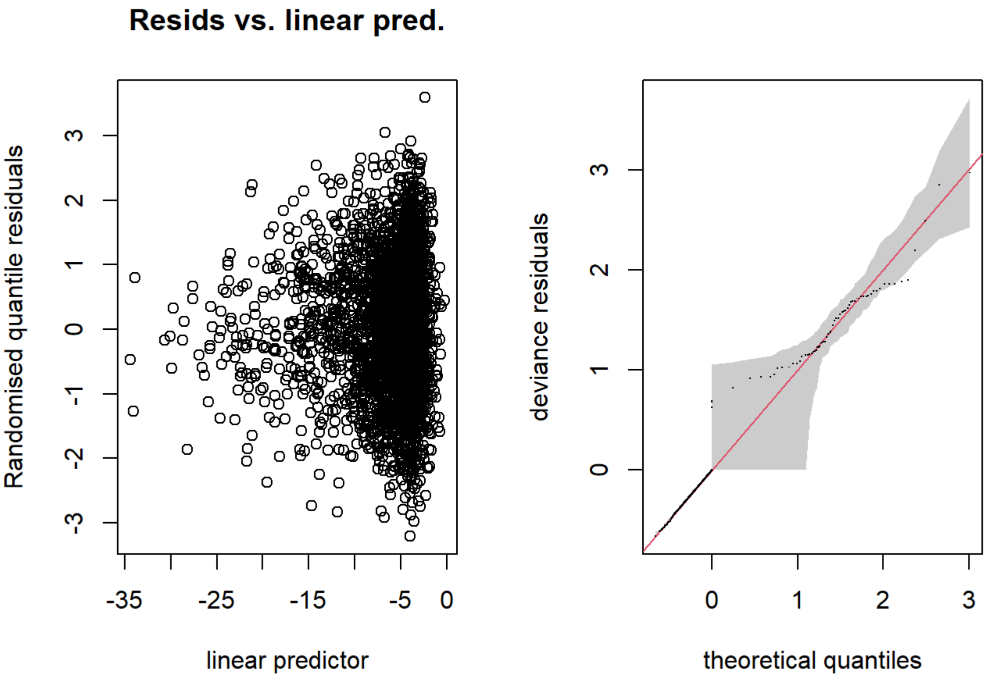

A3.4 Residual and QQ plots from the minke whale environmental model for the combined 2005 / 2016 data

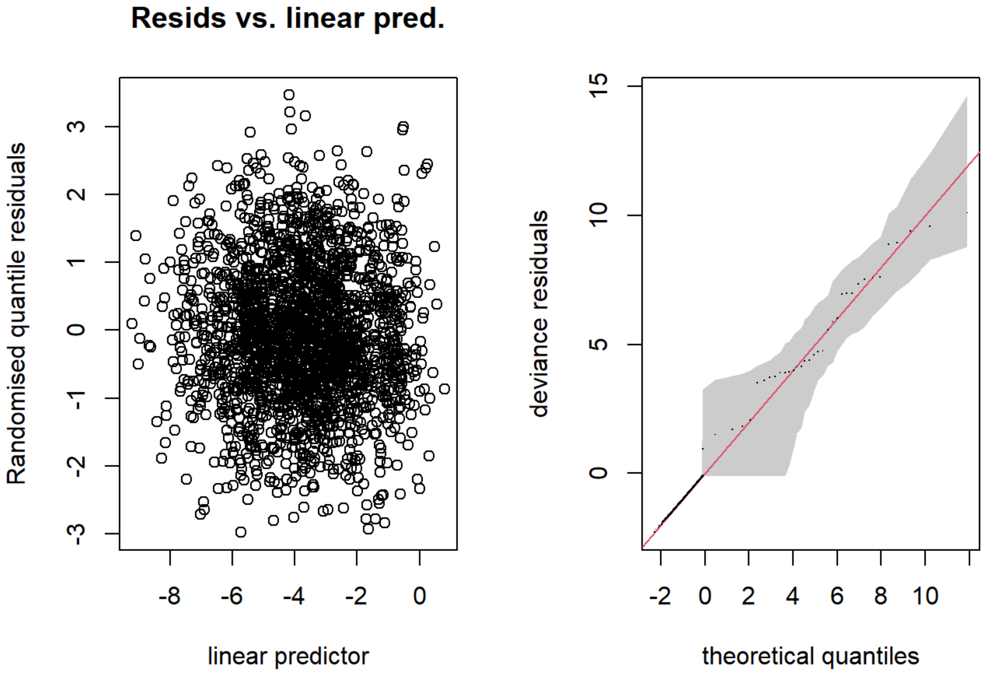

A3.5 Residual and QQ plots from the white-beaked dolphin environmental model for the 2016 data

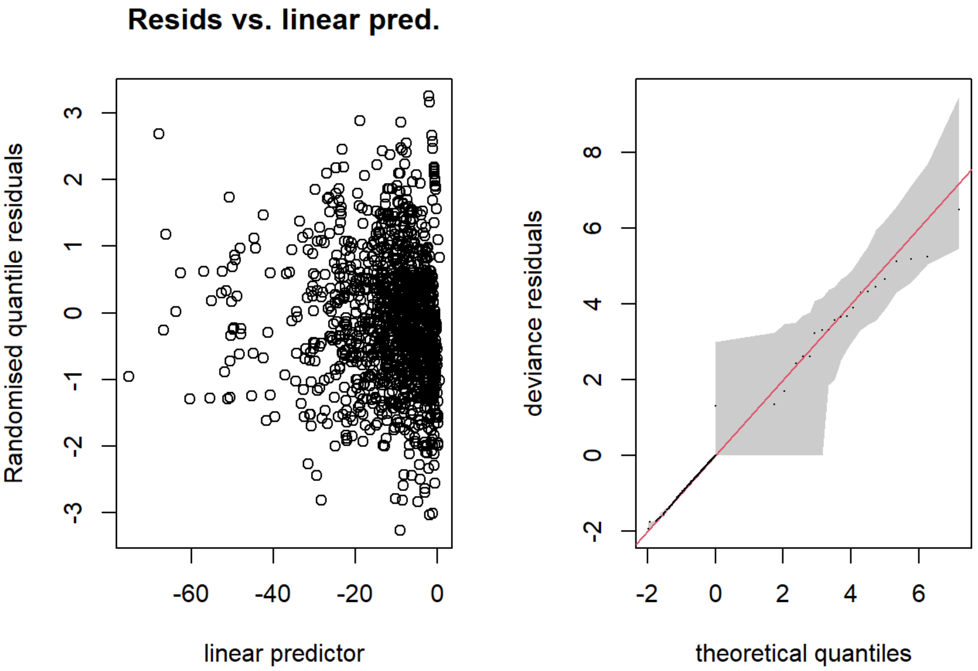

A3.6 Residual and QQ plots from the white-beaked dolphin environmental model for the combined 2005 data

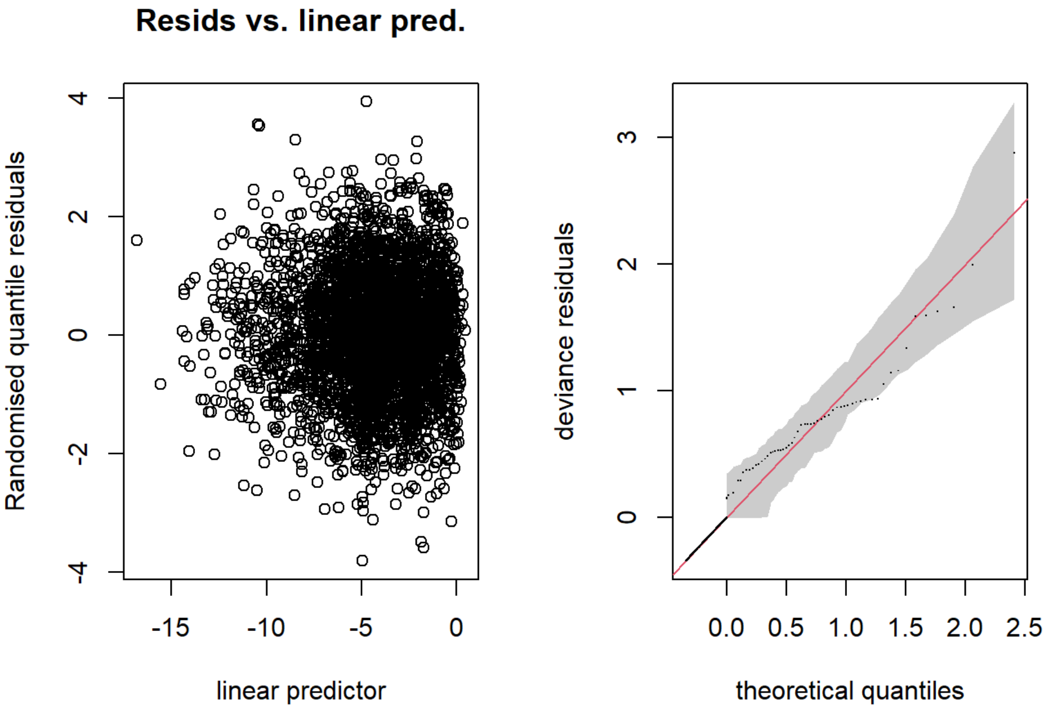

A3.7 Residual and QQ plots from the white-beaked dolphin environmental model for the 2005 data

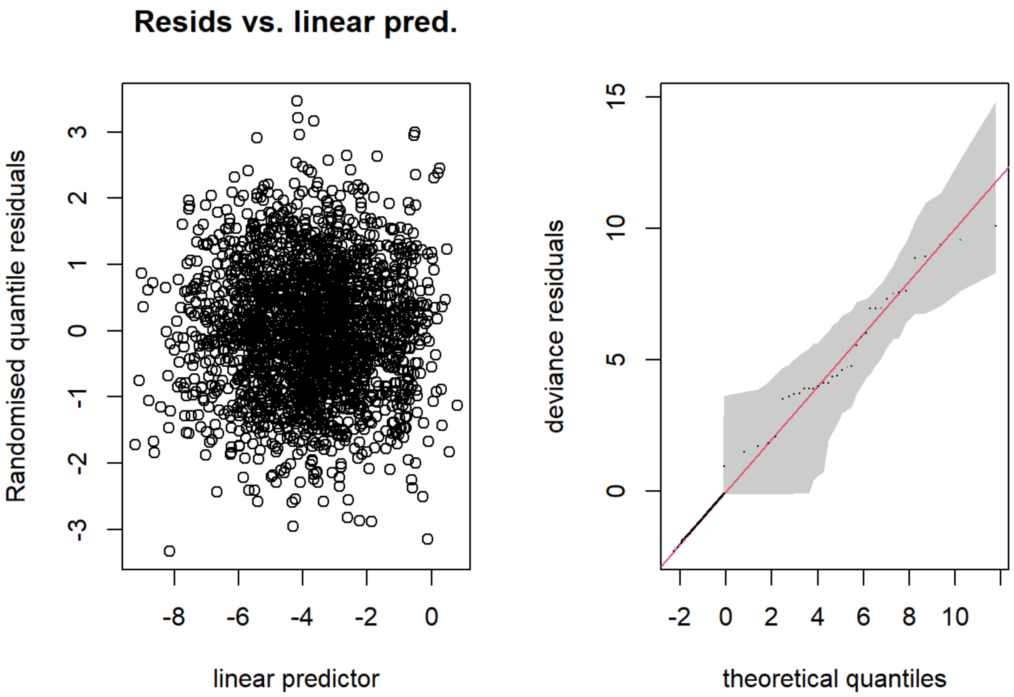

A3.8 Residual and QQ plots from the white-beaked dolphin environmental model for the combined 2005 / 2016 data

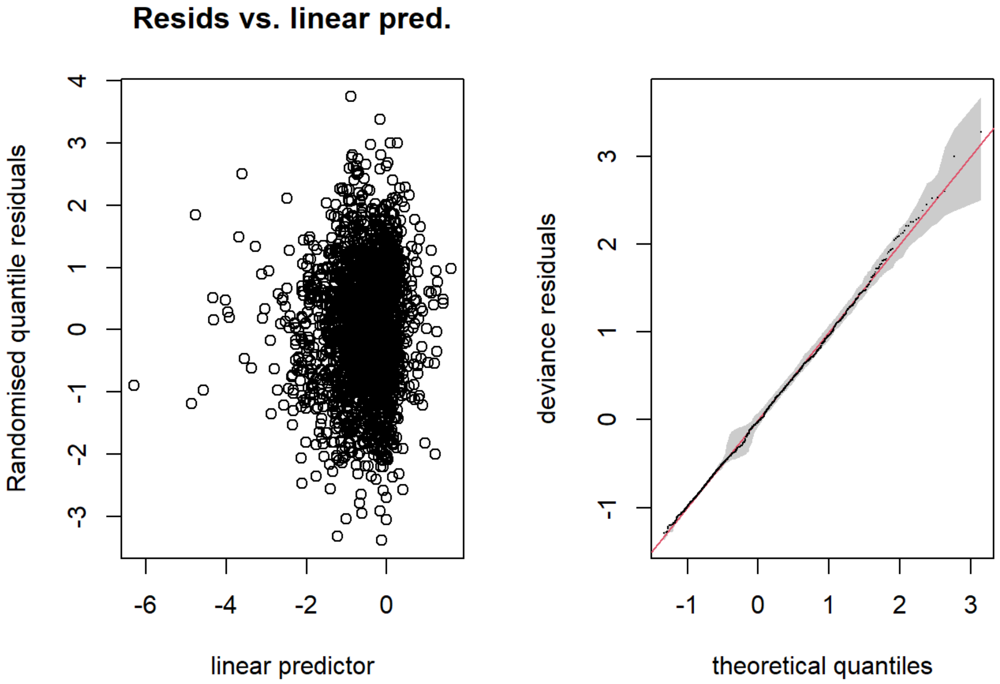

A3.9 Residual and QQ plots from the harbour porpoise environmental model for the 2016 data

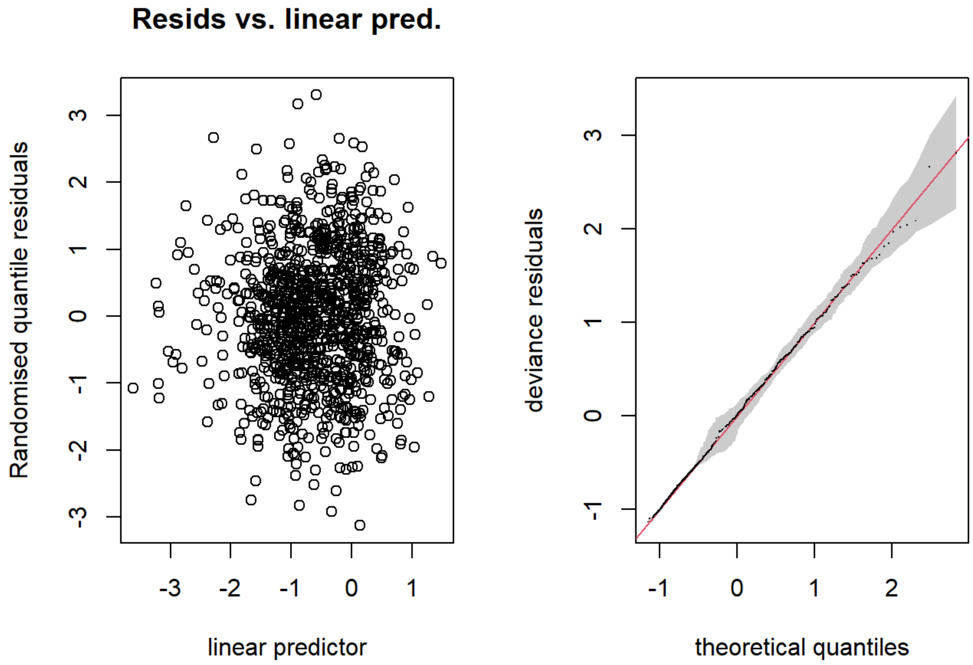

A3.10 Residual and QQ plots from the harbour porpoise environmental model for the 2005 data

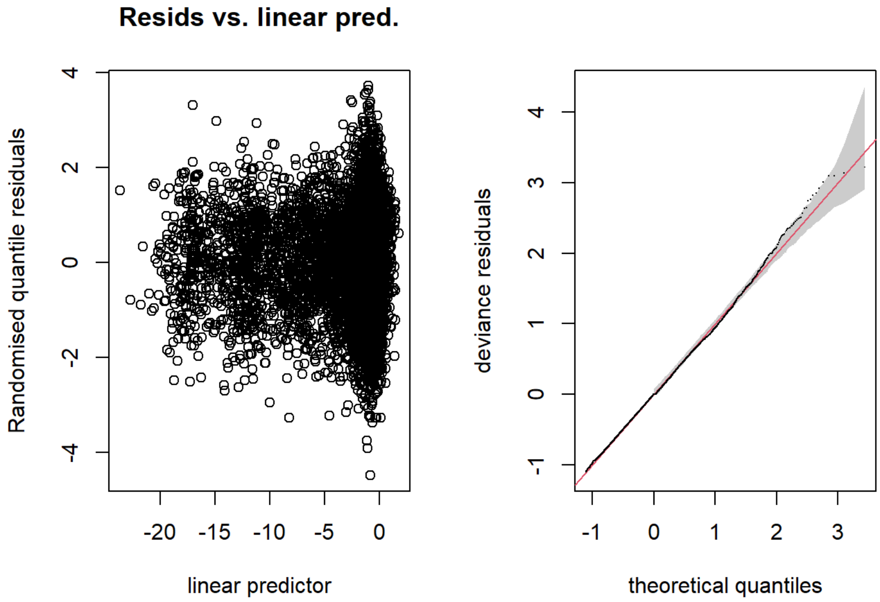

A3.11 Residual and QQ plots from the harbour porpoise environmental model for the combined 2005 / 2016 data

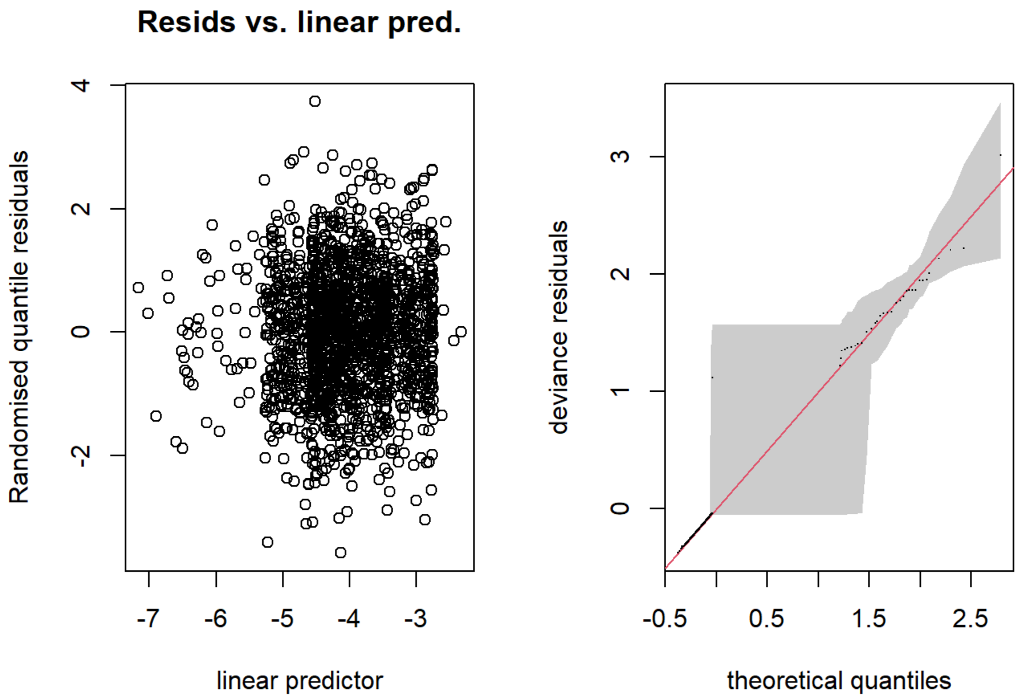

A3.12 Residual and QQ plots from the minke whale prey model for the 2016 data

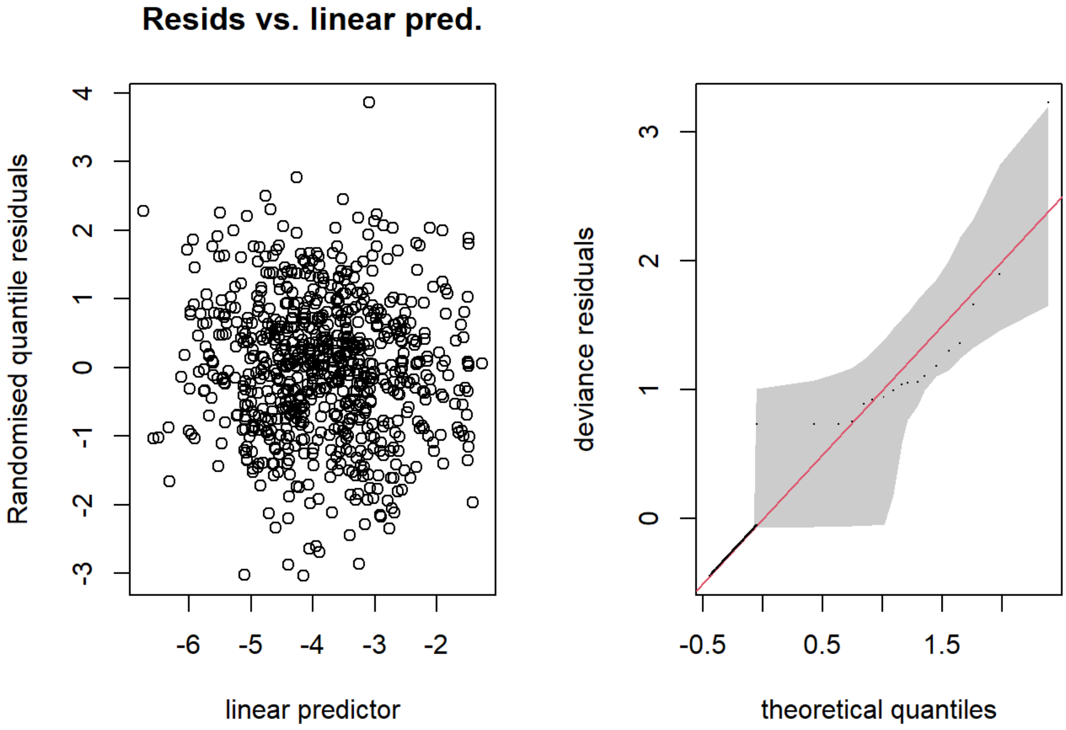

A3.13 Residual and QQ plots from the minke whale prey model for the 2005 data

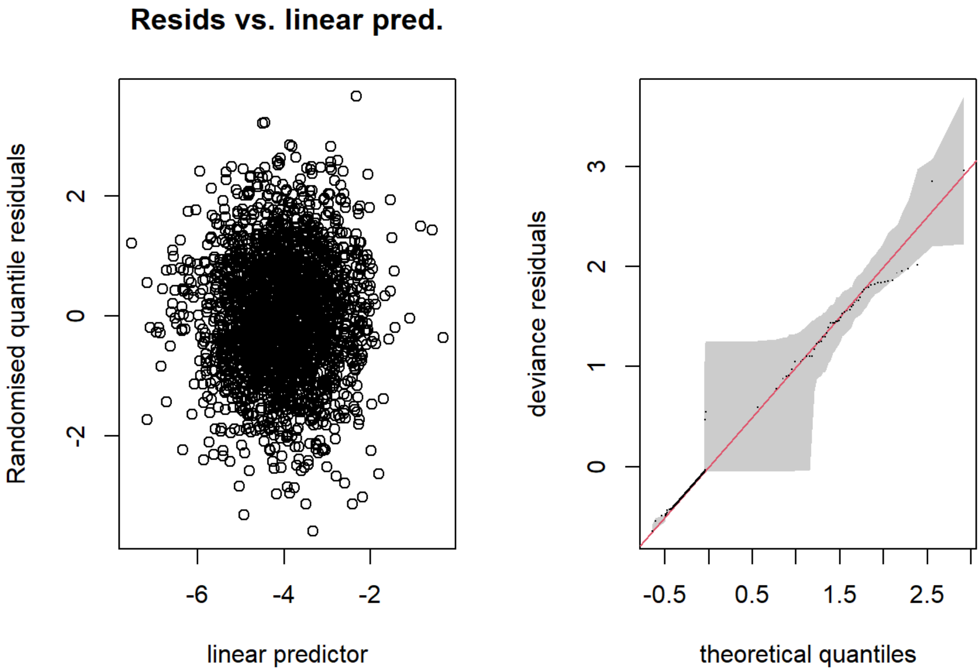

A3.14 Residual and QQ plots from the minke whale prey model for the combined 2005/ 2016 data

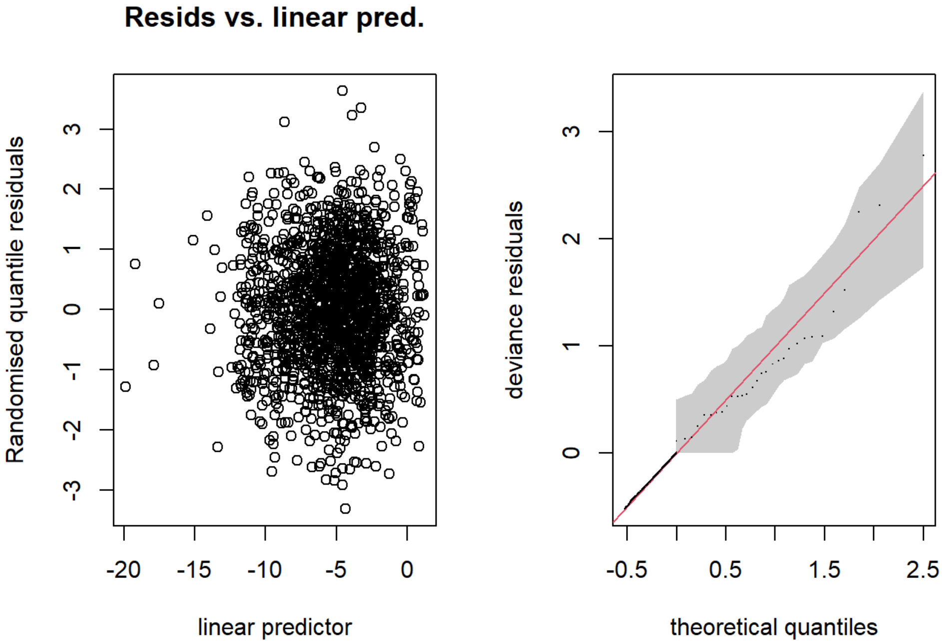

A3.15 Residual and QQ plots from the white-beaked dolphin prey model for the 2016 data

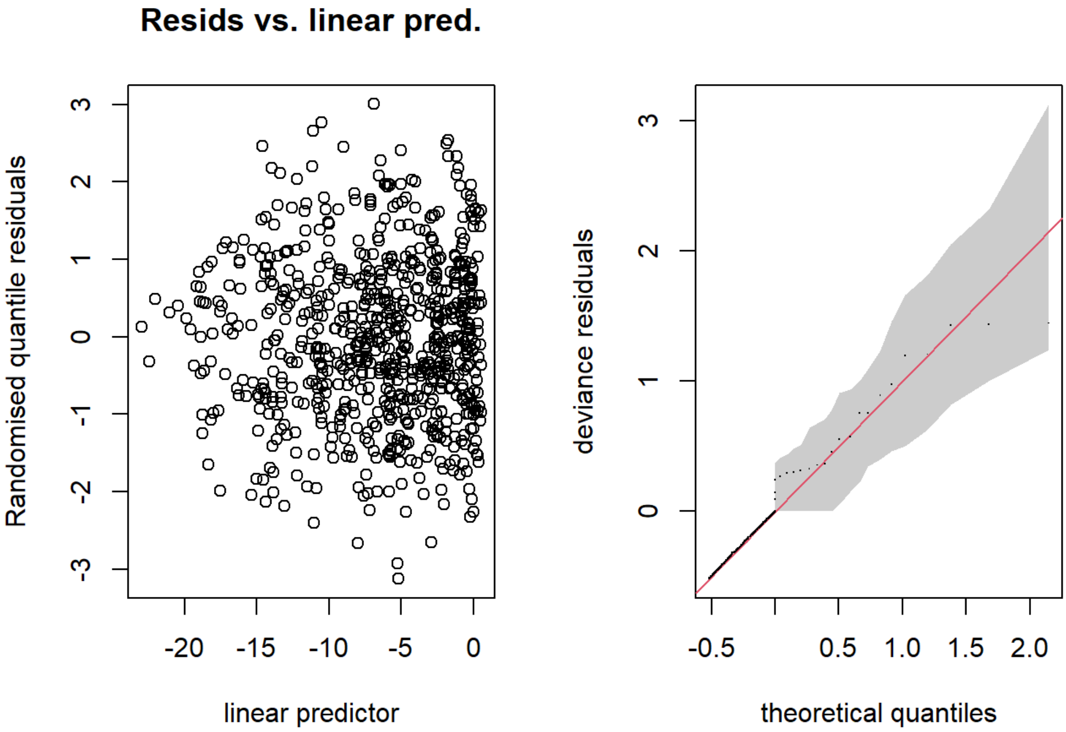

A3.16 Residual and QQ plots from the white-beaked dolphin prey model for the 2005 data

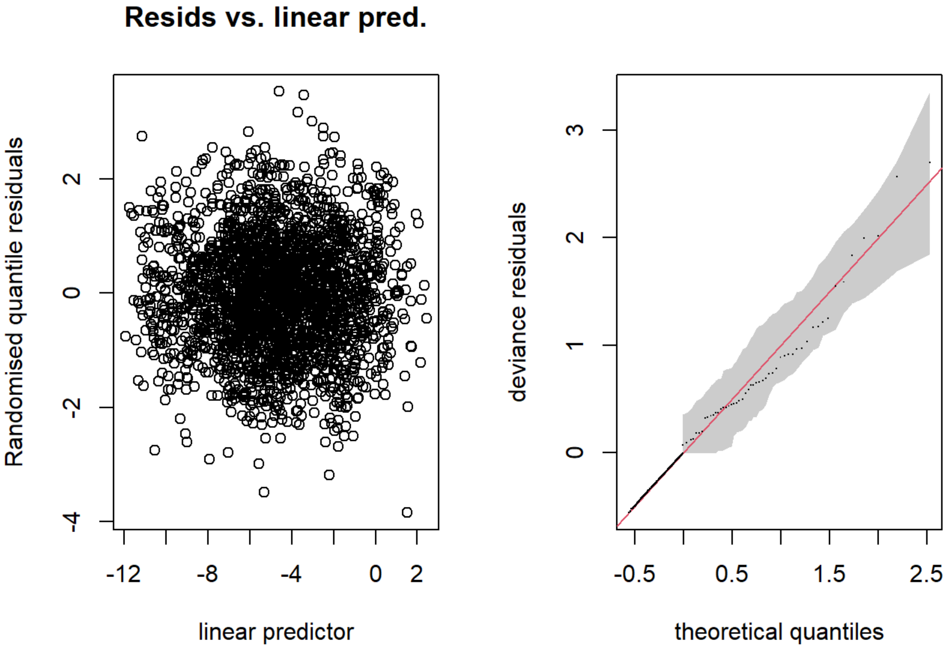

A3.17 Residual and QQ plots from the white-beaked dolphin prey model for the combined 2005/ 2016 data

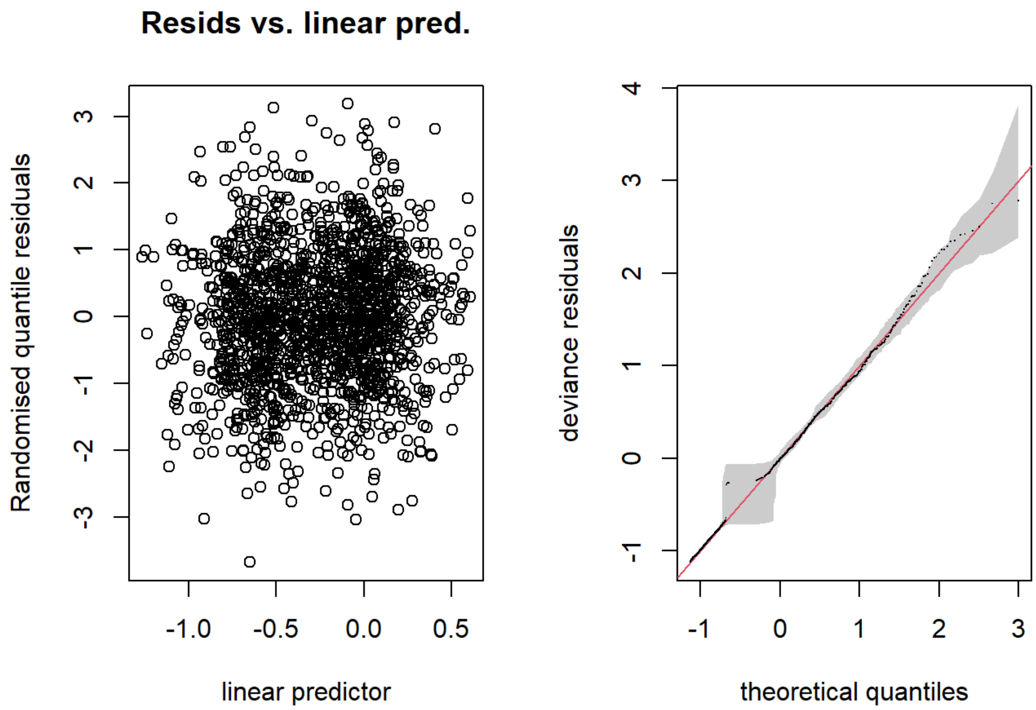

A3.18 Residual and QQ plots from the harbour porpoise prey model for 2016 data

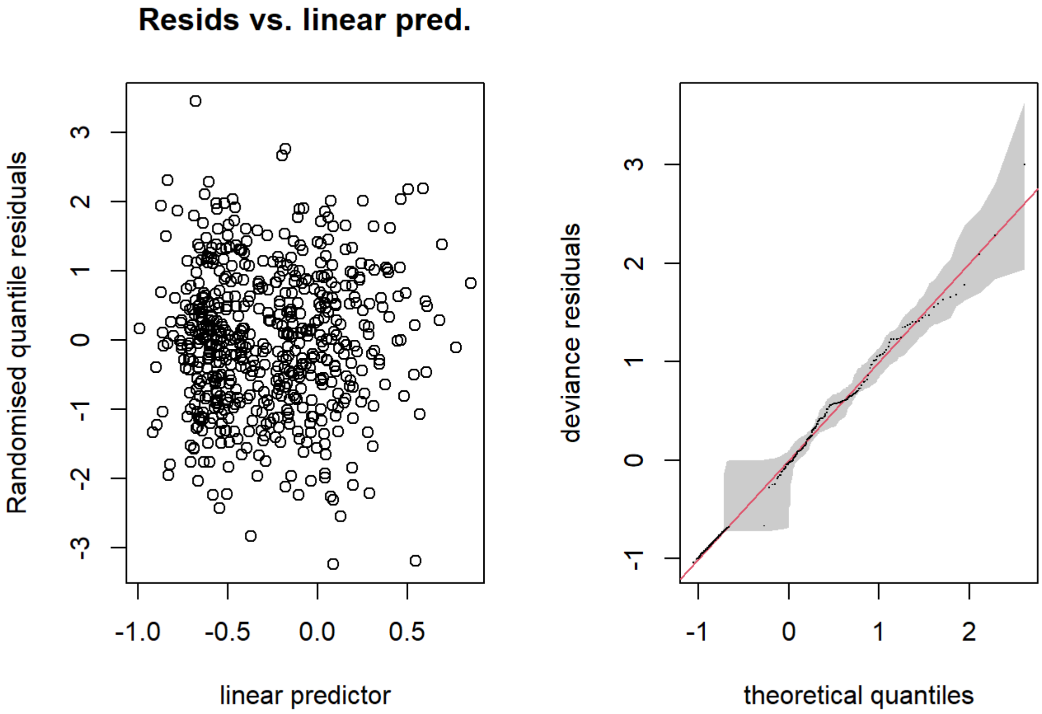

A3.19 Residual and QQ plots from the harbour porpoise prey model for 2005 data

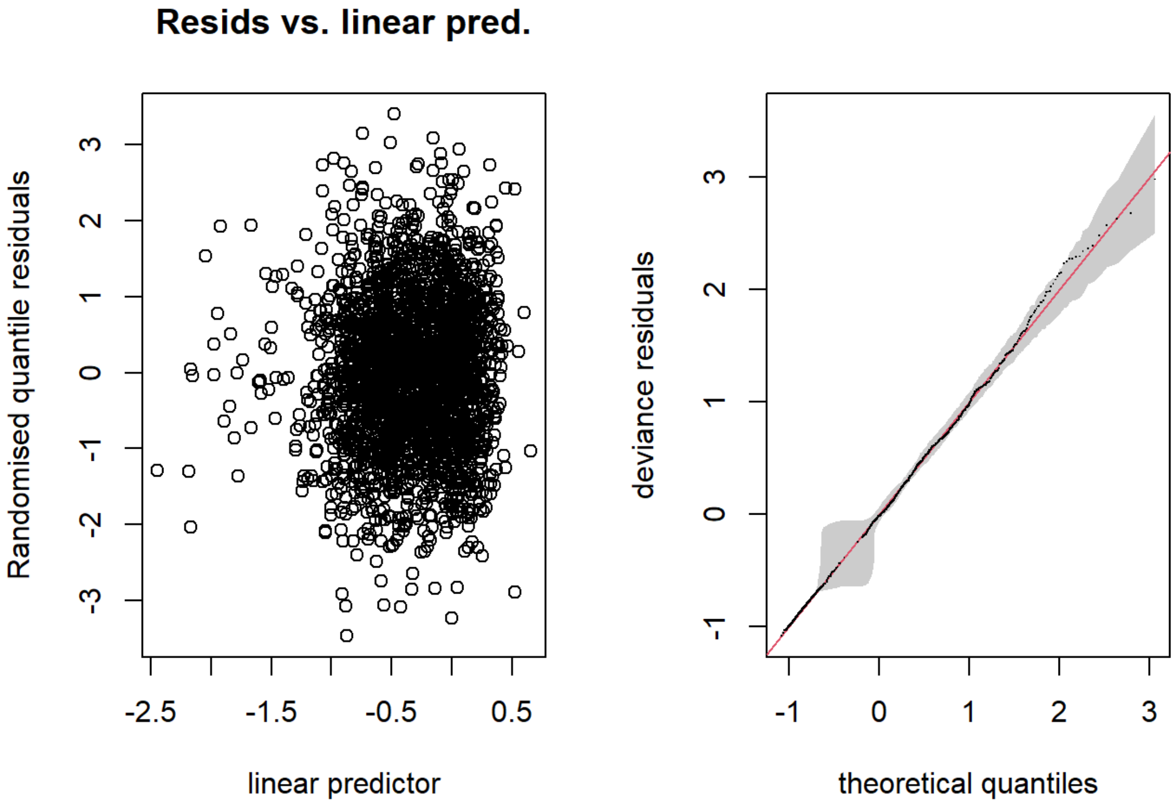

A3.20 Residual and QQ plots from the harbour porpoise prey model for the combined 2005/16 data

Appendix 4 – Appendix for Chapter 5

Residual and QQ plots for models presented in Chapter 5.

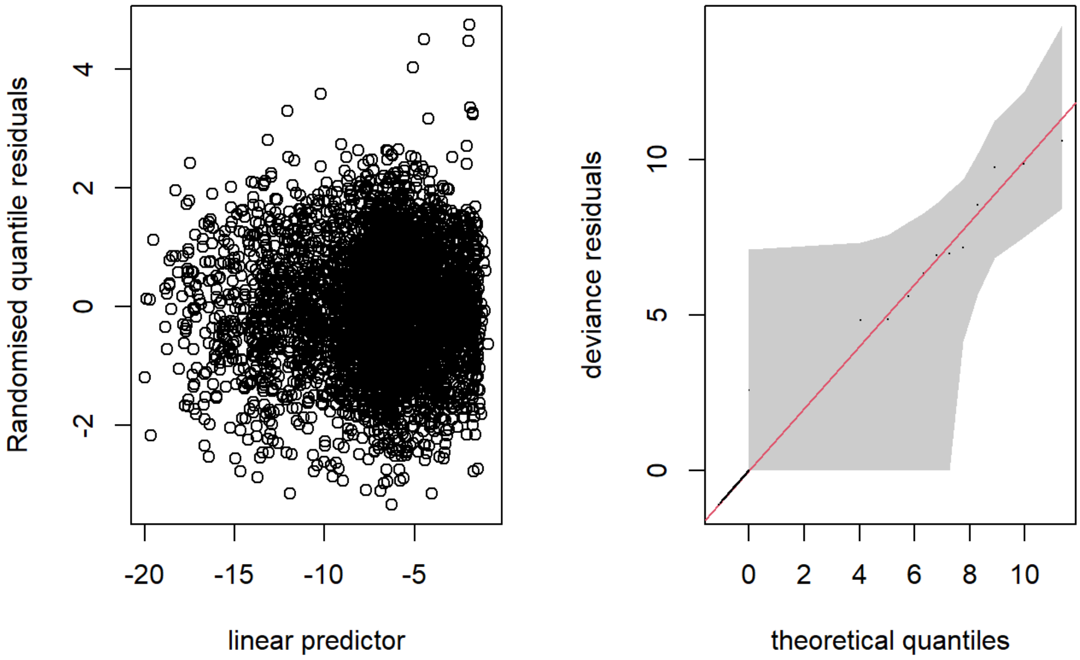

A4.1 Residual and QQ plots from the Atlantic white-sided dolphin model for the combined S3/ObSERVE data

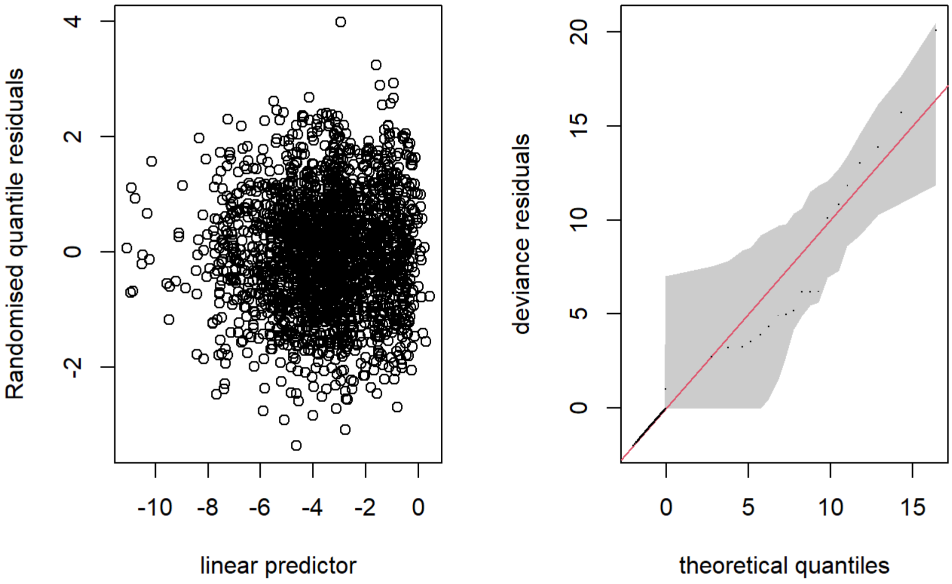

A4.2 Residual vs Linear and QQ plot from the Atlantic white-sided dolphin model for the combined S2/CODA data

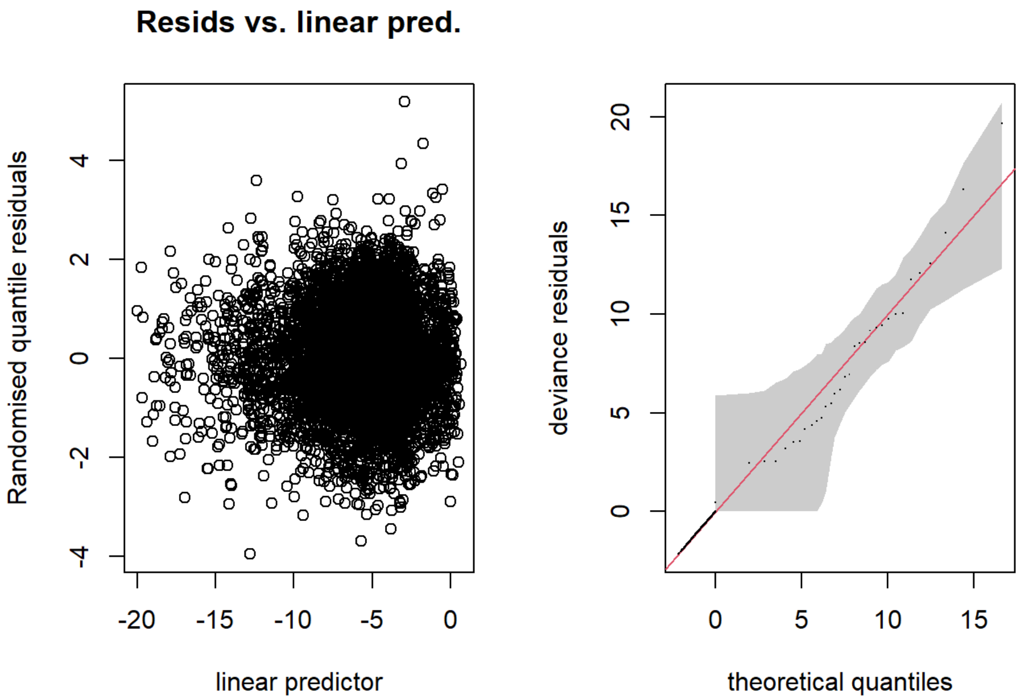

A4.3 Residual vs Linear and QQ plot from the Atlantic white-sided dolphin model for the combined year model

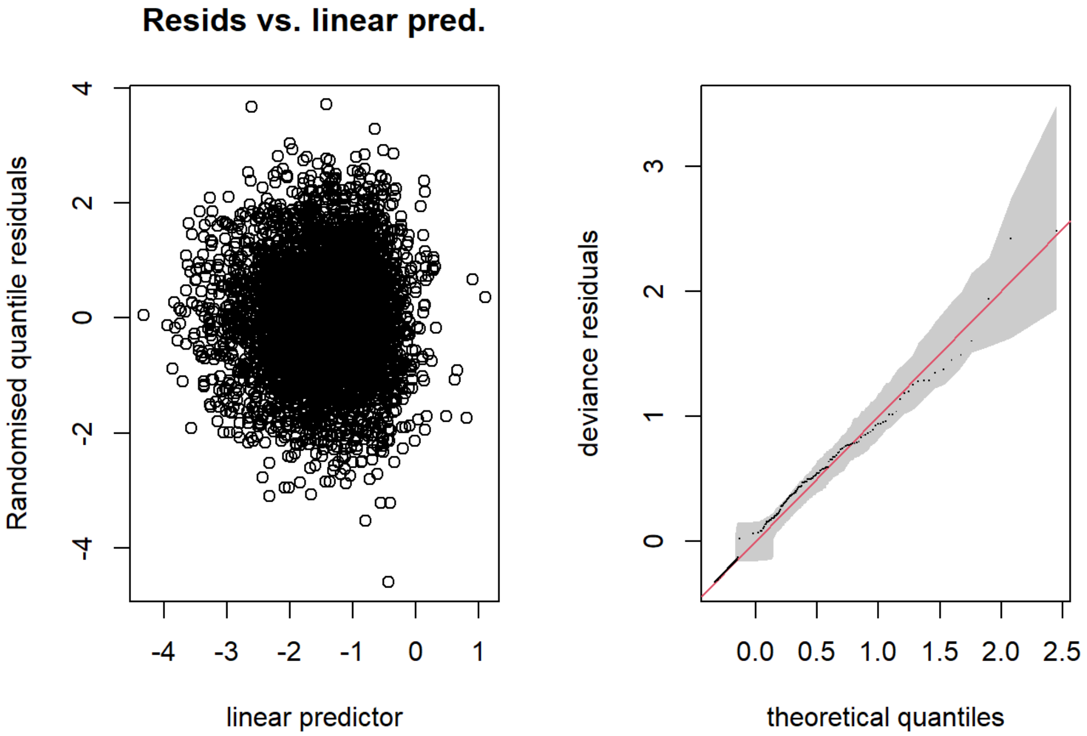

A4.4 Residual vs Linear and QQ plot from the bottlenose dolphin model for the combined S3/ObSERVE data

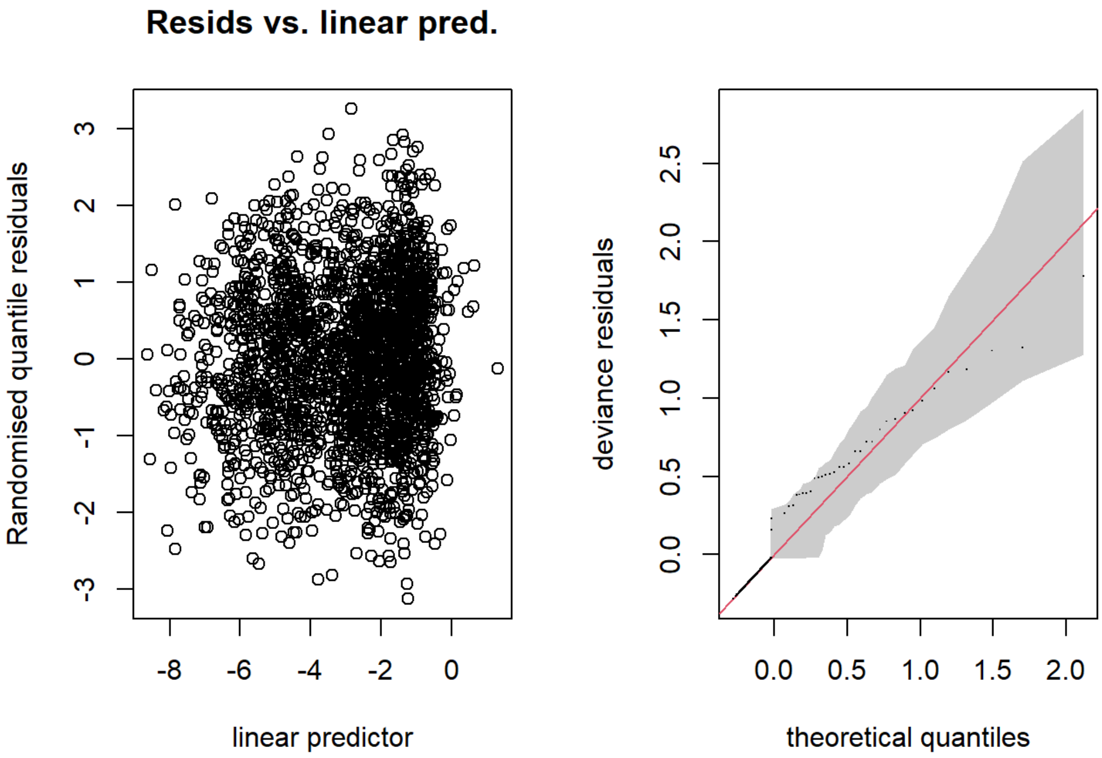

A4.5 Residual vs Linear and QQ plot from the bottlenose dolphin model for the combined S2/CODA data

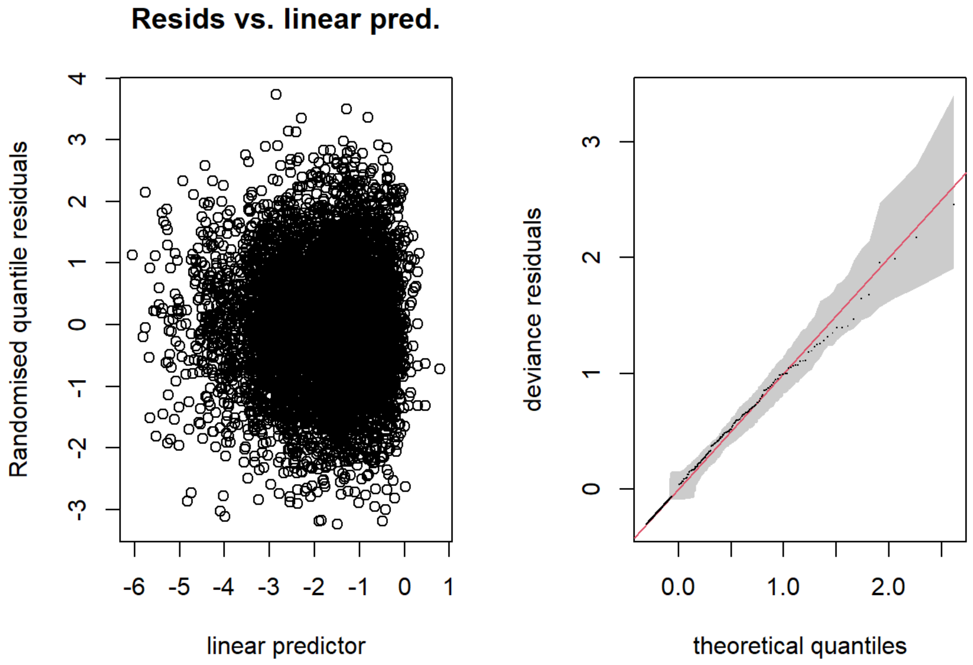

A4.6 Residual vs Linear and QQ plot from the bottlenose dolphin model for the combined year data

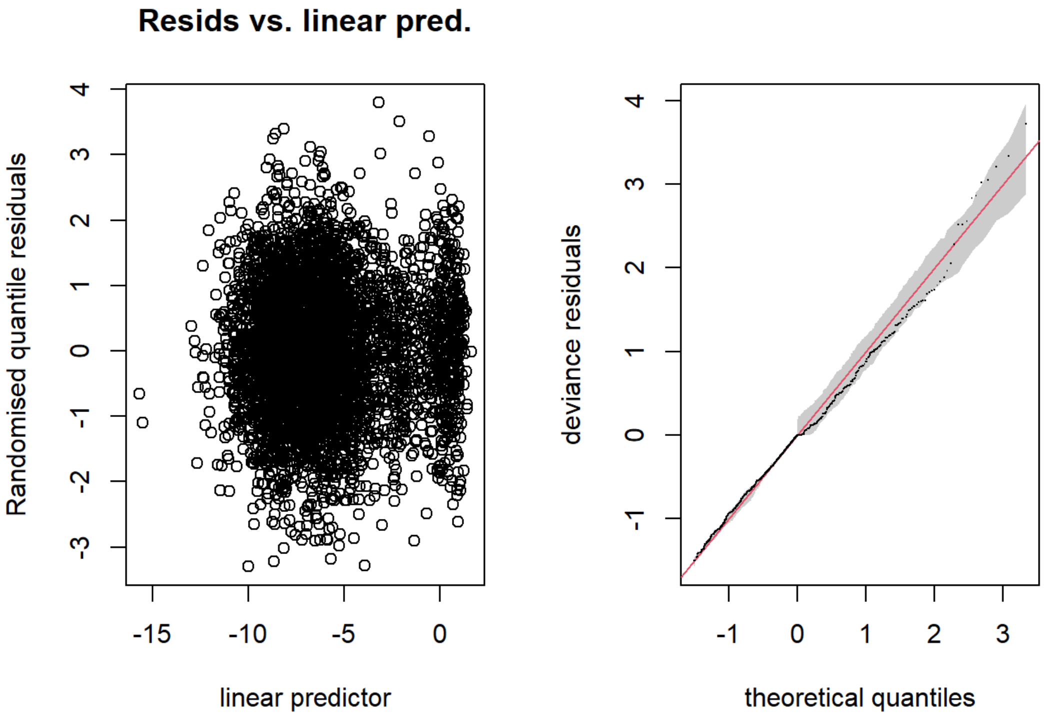

A4.7 Residual vs Linear and QQ plot from the fin whale model for the combined S3/ObSERVE data

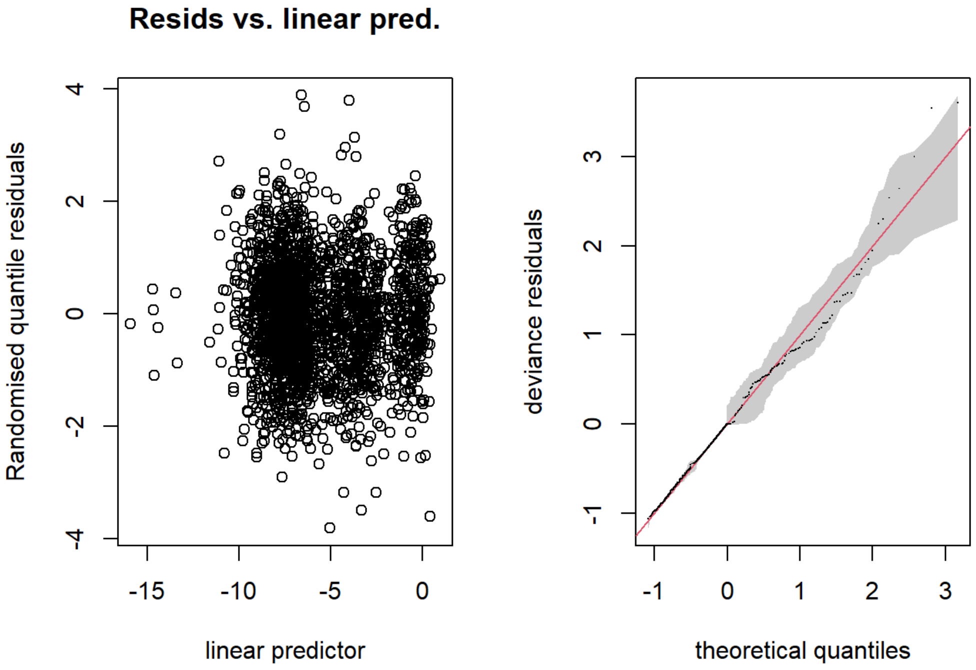

A4.8 Residual vs Linear and QQ plot from the fin whale model for the combined S2/CODA data

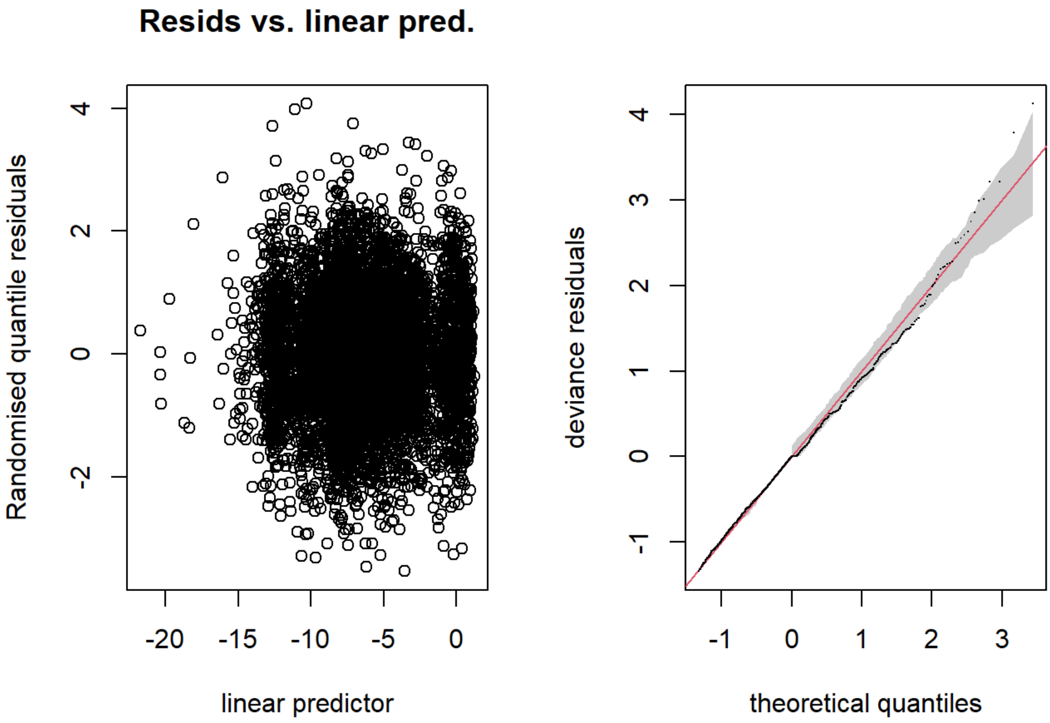

A4.9 Residual vs Linear and QQ plot from the fin whale model for the combined year data

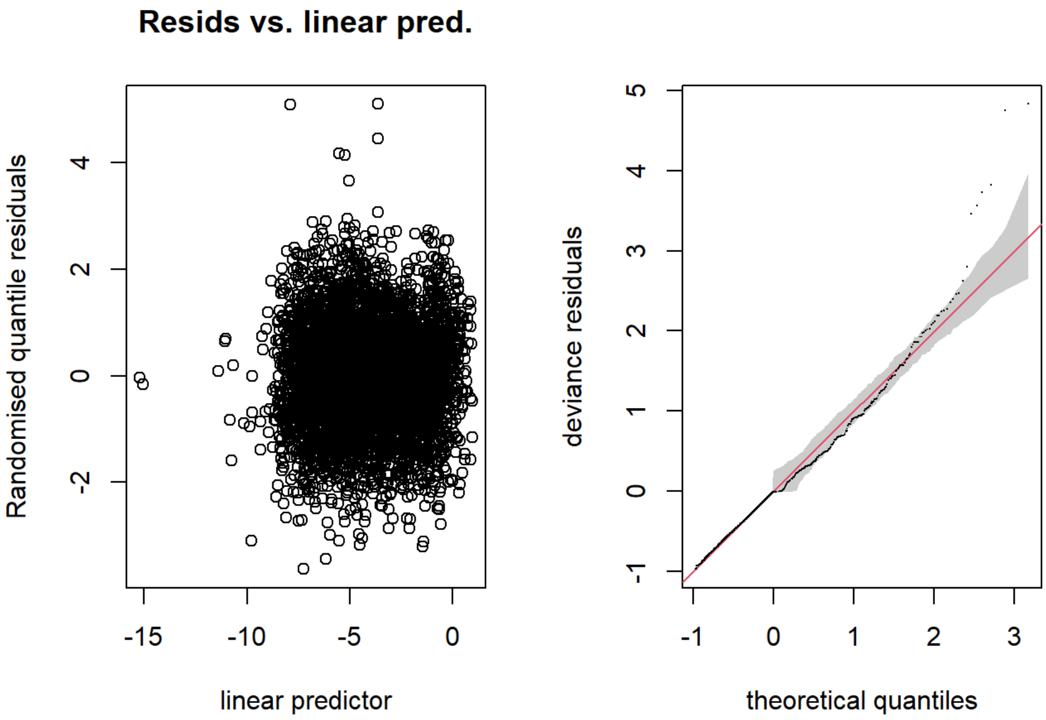

A4.10 Residual vs Linear and QQ plot from the common dolphin model for the combined S3/ObSERVE data

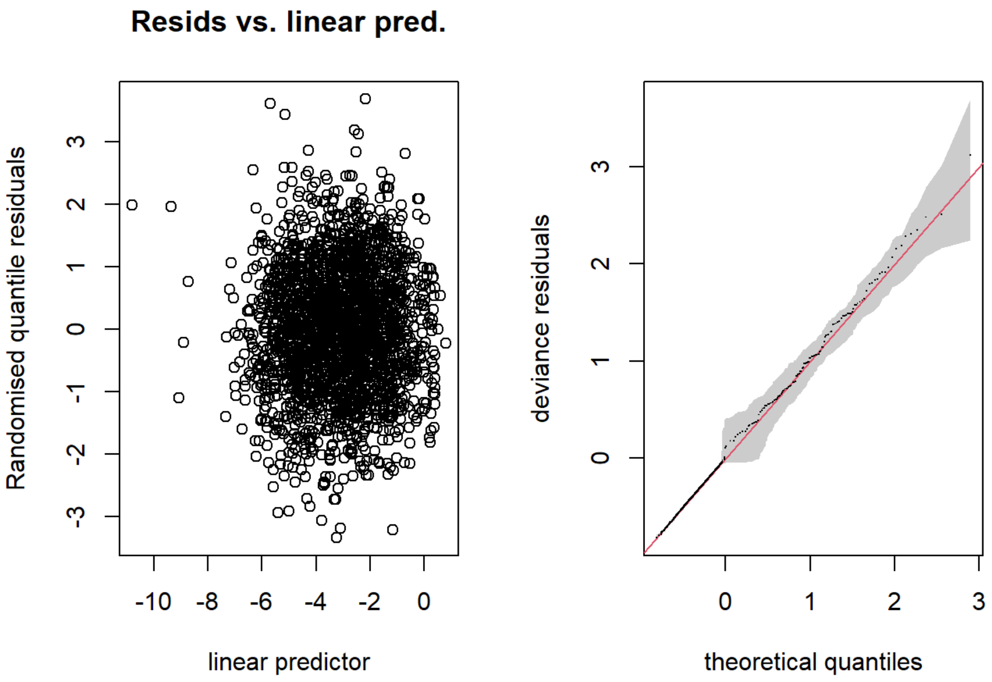

A4.11 Residual vs Linear and QQ plot from the common dolphin model for the combined S2/CODA data

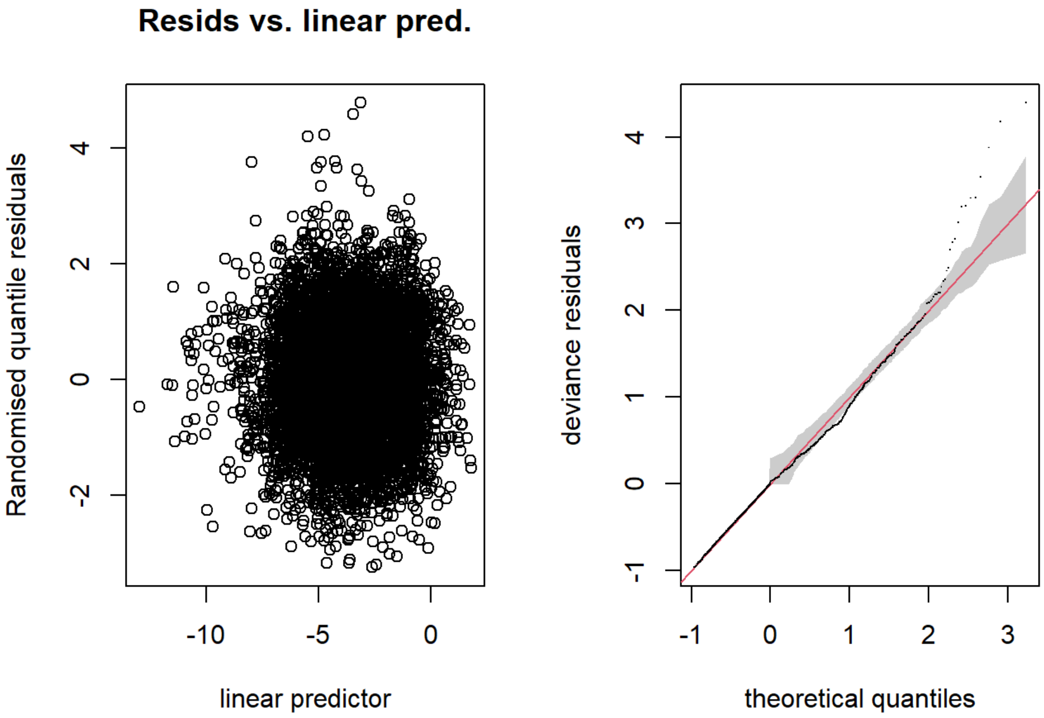

A4.12 Residual vs Linear and QQ plot from the common dolphin model for the combined year data

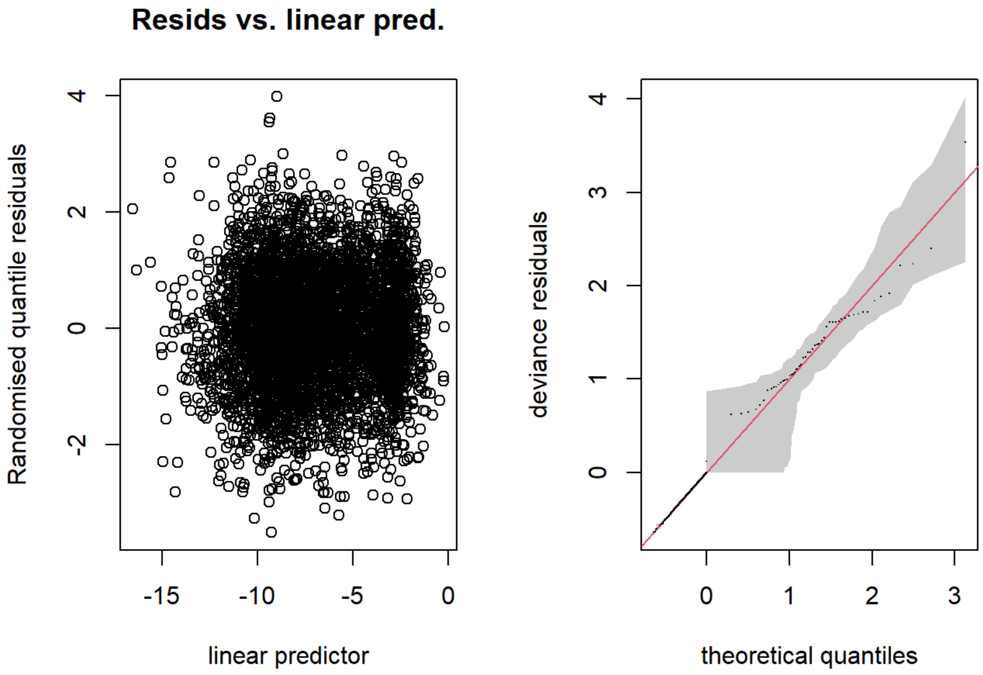

A4.13 Residual vs Linear and QQ plot from the striped dolphin model for the combined S3/ObSERVE data

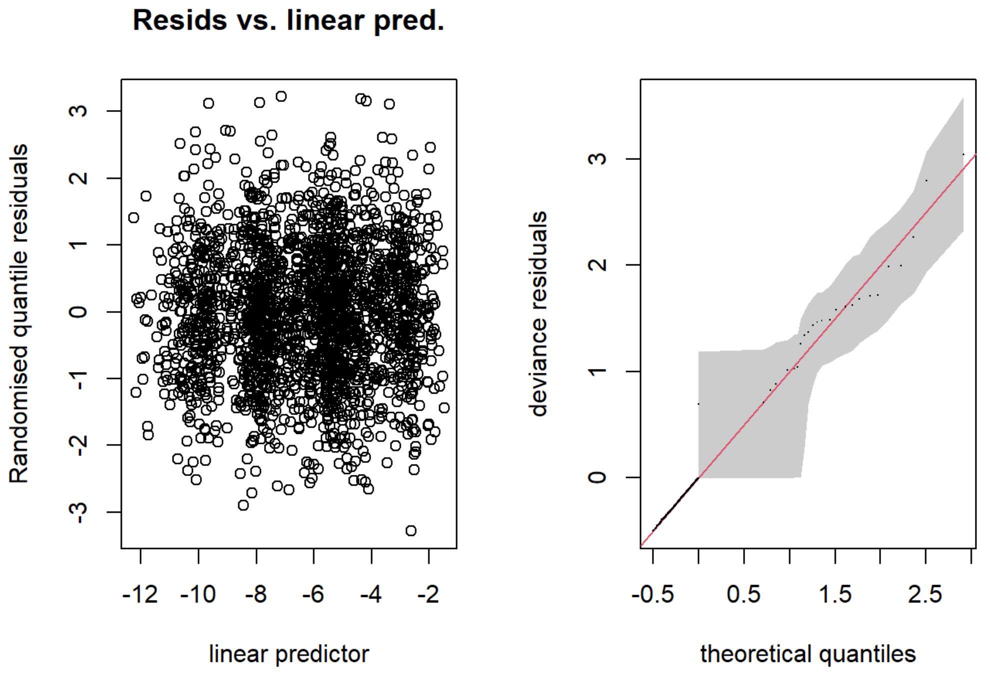

A4.14 Residual vs Linear and QQ plot from the striped dolphin model for the combined S2/CODA data

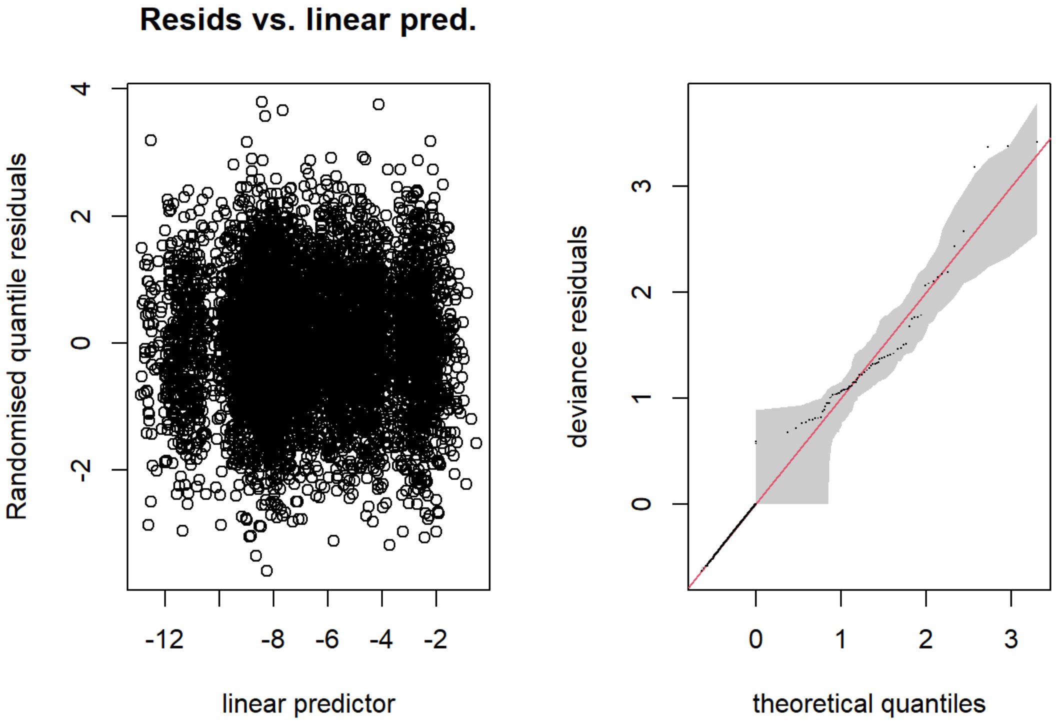

A4.15 Residual vs Linear and QQ plot from the striped dolphin model for the combined year data

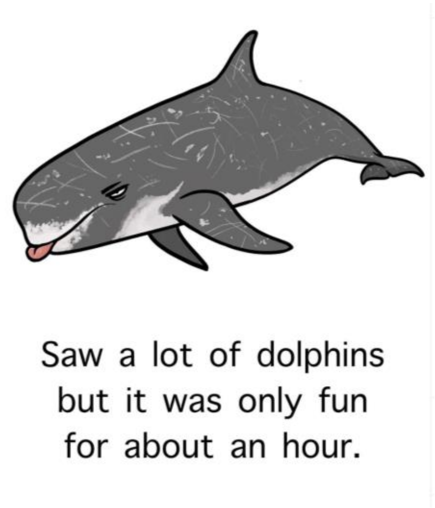

Whalesblow [@whalesblow] “Bad reviews of whale watching – The Truth”. Instagram, December 20, 2021. https://www.instagram.com/p/CXuoBRjFsNg

“Now, bring me that horizon.”

- Pirates of the Caribbean,
Curse of the Black Pearl